improvement of insulin-induced LTD in CA1 hippocampus in the HF-fed female rats.

In the present study, the finding that estrogen could not improve the impairment of insulin-induced LTD in the HF-fed male rats could be due to the difference in the distribution of estrogen receptors in the hippocampus between male and female rats. Estrogen receptors consist of estrogen receptor alpha (ER-α) and estrogen receptor beta (ER-β). Both ER-α and ER-β are found in rat hippocampus, suggesting that this receptor plays an important role in learning and memory (Shughrue and Merchenthaler, 2000). In addition, previous studies have shown that the ERs are important regulators for metabolic disorders such as insulin resistance (Alonso and Gonzalez, 2008; Godsland, 2005; Palin et al., 2001). Furthermore, a previous study has clearly shown gender differences in the ER-β immunoreactivity in rats (Zhang et al., 2002). In that study, the authors found that the expression of ER-β in the hippocampus of female rats is greater than that in male rats. Therefore, the low numbers of ERs in the hippocampus of male rats could be insufficient for estrogen to act to attenuate the neuronal insulin resistance found in male HF rats.

Conclusion

In conclusion, the present study demonstrated that the activation of the estrogen pathway could preserve insulin sensitivity in the peripheral tissue in both male and female rats, whereas it could preserve the neuronal insulin sensitivity only in female rats. With the development of selective ER modulators, future use of the beneficial action of estrogen on neuronal insulin receptor function could be clinically significant and the undesired effects of estrogen could be avoided.

Conflict of interest statement

The authors declare that there is no conflict of interest.

Acknowledgments

The authors wish to thank Prof. M. Kevin O' Carroll, Professor Emeritus, University of Mississippi, USA, and Faculty Consultant, Chiang Mai University, Thailand, for his editorial assistance. This work is supported by grants from the Thailand Research Fund grants TRF-BRG5480003 (SC), TRF-RTA5280006 (NC) and Thailand Research Fund through the Royal Golden Jubilee Ph.D. Program (PHD/0224/2550) to (WP and SC).

References

Alonso A, Gonzalez C. Relationship between non-genomic actions of estrogens and insulin resistace. Infect Disord Drug Targets 2008;8:48–51.
Appleton DJ, Rand JS, Sunvold GD. Basal plasma insulin and homeostasis model assessment (HOMA) are indicators of insulin sensitivity in cats. J Feline Med Surg 2005;7:183–93.
Asthana S, Craft S, Baker LD, Raskind MA, Birnbaum RS, Lofgreen CP, et al. Cognitive and neuroendocrine response to transdermal estrogen in postmenopausal women with Alzheimer's disease: results of a placebo-controlled, double-blind, pilot study. Psychoneuroendocrinology 1999;24:657–77.
Asthana S, Baker LD, Craft S, Stanczyk FZ, Veith RC, Raskind MA, et al. High-dose estradiol improves cognition for women with AD: results of a randomized study. Neurology 2001;57:605–12.
Bryzgalova G, Lundholm L, Portwood N, Gustafsson JA, Khan A, Efendic S, et al. Mechanisms of antidiabetogenic and body weight-lowering effects of estrogen in high-fat diet-fed mice. Am J Physiol Endocrinol Metab 2008;295:E904–12.
Cani PD, Amar J, Iglesias MA, Poggi M, Knauf C, Bastelica D, et al. Metabolic endotoxemia initiates obesity and insulin resistance. Diabetes 2007;56:1761–72.
Chattipakorn SC, McMahon LL. Pharmacological characterization of glycine-gated chloride currents recorded in rat hippocampal slices. J Neurophysiol 2002;87:1515–25.
Daniel JM, Fader AJ, Spencer AL, Dohanich GP. Estrogen enhances performance of female rats during acquisition of a radial arm maze. Horm Behav 1997;32:217–25.
Desrocher M, Rovet J. Neurocognitive correlates of type 1 diabetes mellitus in childhood. Child Neuropsychol 2004;10:36–52.
Godsland IF. Oestrogens and insulin secretion. Diabetologia 2005;48:2213–20.
Gonzalez C, Diaz F, Alonso A. Neuroprotective effects of estrogens: cross-talk between estrogen and intracellular insulin signalling. Infect Disord Drug Targets 2008;8:65–7.
Haffner SM, Miettinen H, Stern MP. The homeostasis model in the San Antonio Heart Study. Diabetes Care 1997;20:1087–92.
Kumagai S, Holmang A, Bjorntorp P. The effects of oestrogen and progesterone on insulin sensitivity in female rats. Acta Physiol Scand 1993;149:91–7.
Louet JF, LeMay C, Mauvais-Jarvis F. Antidiabetic actions of estrogen: insight from human and genetic mouse models. Curr Atheroscler Rep 2004;6:180–5.
Luine VN, Richards ST, Wu VY, Beck KD. Estradiol enhances learning and memory in a spatial memory task and effects levels of monoaminergic neurotransmitters. Horm Behav 1998;34:149–62.
Nuutila P, Knuuti MJ, Maki M, Laine H, Ruotsalainen U, Teras M, et al. Gender and insulin sensitivity in the heart and in skeletal muscles. Studies using positron emission tomography. Diabetes 1995;44:31–6.
Palin SL, Kumar S, Sturdee DW, Barnett AH. HRT in women with diabetes—review of the effects on glucose and lipid metabolism. Diabetes Res Clin Pract 2001;54:67–77.
Pratchayasakul W, Kerdphoo S, Petsophonsakul P, Pongchaidecha A, Chattipakorn N, Chattipakorn SC. Effects of high-fat diet on insulin receptor function in rat hippocampus and the level of neuronal corticosterone. Life Sci 2011;88:619–27.
Riant E, Waget A, Cogo H, Arnal JF, Burcelin R, Gourdy P. Estrogens protect against high-fat diet-induced insulin resistance and glucose intolerance in mice. Endocrinology 2009;150:2109–17.
Shang XL, Zhao JH, Cao YP, Xue YX. Effects of synaptic plasticity regulated by 17beta-estradiol on learning and memory in rats with Alzheimer's disease. Neurosci Bull 2010;26:133–9.
Sherwin BB. Estrogen and memory in women: how can we reconcile the findings? Horm Behav 2005;47:371–5.
Shoelson SE. Banking on ATM as a new target in metabolic syndrome. Cell Metab 2006;4:337–8.
Shughrue PJ, Merchenthaler I. Evidence for novel estrogen binding sites in the rat hippocampus. Neuroscience 2000;99:605–12.
Simpkins JW, Green PS, Gridley KE, Singh M, de Fiebre NC, Rajakumar G. Role of estrogen replacement therapy in memory enhancement and the prevention of neuronal loss associated with Alzheimer's disease. Am J Med 1997;103:19S–25S.
Woolley CS, Wenzel HJ, Schwartzkroin PA. Estradiol increases the frequency of multiple synapse boutons in the hippocampal CA1 region of the adult female rat. J Comp Neurol 1996;373:108–17.
Zhang JQ, Cai WQ, Zhou DS, Su BY. Distribution and differences of estrogen receptor beta immunoreactivity in the brain of adult male and female rats. Brain Res 2002;935:73–80.
Ziomkiewicz A, Ellison PT, Lipson SF, Thune I, Jasienska G. Body fat, energy balance and estradiol levels: a study based on hormonal profiles from complete menstrual cycles. Hum Reprod 2008;23:2555–63.

DOI: 10.1111/j.1540-8175.2011.01499.x

Echocardiography

Effects of Left Ventricular Function on the Exercise Capacity in Patients with Repaired Tetralogy of Fallot

Suchaya Silvilairat, M.D.,* Jatuporn Wongsathikun, Ph.D.,† Rekwan Sittiwangkul, M.D.,* Yupada Pongprot, M.D.,* and Nipon Chattipakorn, M.D., Ph.D.‡

*Department of Pediatrics, Faculty of Medicine, †Department of Physical Therapy, Faculty of Associated Medical Sciences, and ‡Cardiac Electrophysiology Research and Training Center, Chiang Mai University, Chiang Mai, Thailand

Background: Tissue Doppler imaging has been recently used to evaluate ventricular function. Peak oxygen uptake ($V^{\bullet}O_2$peak) has been demonstrated as a predictor for death in adults with repaired tetralogy of Fallot (TOF). The aim of this study was to determine which Doppler parameters correlated with $V^{\bullet}O_2$peak in patients with repaired TOF. Method and Results: Doppler echocardiography, tissue Doppler imaging, and exercise test were performed in 30 patients with TOF after surgical repair. In 30 patients with repaired TOF (median age 14 years, range 9–25 years), 11 patients (37%) were female. Seven patients (median age 12 years) had normal left ventricular diastolic function, whereas the rest of the patients were classified as diastolic dysfunction grade II (median age 15 years; n = 15) and III and IV (median age 18 years; n = 8). The oxygen uptake at anaerobic threshold ($V^{\bullet}O_{2AT}$) and peak exercise in patients with left ventricular diastolic dysfunction was significantly lower than that in those with normal diastolic function. Also, $V^{\bullet}O_{2AT}$ and $V^{\bullet}O_2$peak in patients with diastolic dysfunction grade III and IV were significantly lower than that in those with diastolic dysfunction grade II. Left ventricular early diastolic myocardial velocity was most closely correlated to $V^{\bullet}O_2$peak ($r = 0.51$; $P = 0.005$). Peak early ventricular filling velocity to early diastolic myocardial velocity ratio was significantly correlated with $V^{\bullet}O_2$peak ($r = -0.50$; $P = 0.006$). Conclusion: Left ventricular diastolic dysfunction is correlated with $V^{\bullet}O_2$peak. Left ventricular diastolic function should be a routine echocardiographic assessment in patients with repaired TOF. (Echocardiography 2011;28:1019-1024)

Key words: left ventricular diastolic dysfunction, exercise, repaired tetralogy of Fallot

Tetralogy of Fallot (TOF) is the most common form of cyanotic congenital heart disease occurring in 4–9% of all congenital heart defects.[1] TOF is comprised of the four cardiac findings: large ventricular septal defect (VSD), overriding of the aorta, right ventricular outflow tract obstruction, and right ventricular hypertrophy. The surgical goal is to achieve adequate complete relief of right ventricular outflow obstruction with closure of the VSD. Surgical repair can be performed with low mortality rate and good long-term outcome.[2–11] Nevertheless, the surgical repair leaves the patient with some degree of hemodynamic abnormalities because of residual pulmonary stenosis, pulmonary regurgitation, or myocardial dysfunction. These abnormalities cause no clinical symptom in the majority of patients. However, the careful assessment of exercise capacity demonstrates cardiopulmonary abnormality in some patients.[12–19] Patients repaired at an older age or those followed for a longer time tended to be the most limited.[13] Patients with branch pulmonary stenosis,[14] significant pulmonary regurgitation,[15–21] and left[22,23] or right ventricular dysfunction[24–28] have reduced exercise capacity. New echocardiographic techniques may be promising for early diagnosis of right and left ventricular dysfunction. Tissue Doppler imaging has been recently used to evaluate early myocardial dysfunction. In some patients with myocardial dysfunction, diastolic ventricular dysfunction preceded the onset of systolic impairment.[29] Therefore, in this study, conventional pulse-wave Doppler and tissue Doppler echocardiography were evaluated in patients with repaired TOF. We hypothesized that pulse-wave Doppler and tissue Doppler imaging patterns of diastolic ventricular dysfunction are correlated with exercise intolerance in patients with TOF after a complete repair.

Address for correspondence and reprint requests: Suchaya Silvilairat, M.D., Department of Pediatrics, Faculty of Medicine, Chiang Mai University, Chiang Mai, 50200, Thailand. Fax: +6653-94-6461; E-mail: ssamana@med.cmu.ac.th

Methods:

Study Patients:

We prospectively studied 30 patients with TOF who underwent surgery for total correction at Chiang Mai University Hospital. Echocardiography, electrocardiography, and exercise test were

performed. The study protocol was reviewed and approved by the Chiang Mai University Review Board. All patients or parents had consented to research participation.

Doppler Echocardiography:
Doppler echocardiographic examinations were performed using Philips Sonos 7500 (Philips Medical Systems, Bothell, WA, USA). Doppler echocardiogram and tissue Doppler imaging were performed to evaluate systolic and diastolic ventricular function. Echocardiographic data included left ventricular fractional shortening, pulse-wave Doppler assessment of mitral and pulmonary venous flows, tissue Doppler imaging, the degree of pulmonary stenosis and pulmonary regurgitation, right and left myocardial performance index, and right ventricular fractional area change. Pulse-wave Doppler of mitral valve flow measured peak early ventricular filling velocity (E), peak atrial contraction velocity (A), A-wave duration, and deceleration time. Pulse-wave Doppler of pulmonary venous flow were systolic forward flow velocity, diastolic forward flow velocity, atrial reversal flow velocity, and atrial reversal flow duration. Tissue Doppler imaging signal was obtained from an apical four-chamber view at the right ventricular free wall, ventricular septum, and left ventricular free wall. Tissue Doppler imaging variables included systolic myocardial velocity, early diastolic myocardial velocity (Em), and late diastolic myocardial velocity. Myocardial performance index was calculated by the atrioventricular valve closing to opening time minus ventricular ejection time and divided by the ejection time. Right ventricular fractional area change (ΔFA) was calculated in apical four-chamber views; $\Delta FA = 100 \times (EDA - ESA)/EDA$, where end-diastolic area (EDA) was measured at the maximum ventricular area, coincident with the R-wave of the electrocardiogram, and end-systolic area (ESA) was measured at the minimal area in the same cycle used for EDA. Diastolic left ventricular dysfunction was graded according to pulse-wave Doppler of mitral and pulmonary venous flows and tissue Doppler imaging.[30]

Exercise Test:
Exercise test was performed on an electric cycle ergometer (Corival, Lode, Groningen, The Netherlands). All patients performed a maximal exercise test with a two-minute incremental bicycle protocol with a workload increment of 20 watts for female and 25 watts for male. Electrocardiogram, oxygen saturation, and blood pressure were monitored. Peak oxygen uptake ($V^{\bullet}O_2$peak), carbon dioxide production ($V^{\bullet}CO_2$), minute ventilation ($V^{\bullet}_E$), and respiratory exchange ratio (RER) were measured by using breath-by-breath technique (Ultima CPX, MEDGRAPHICS, St. Paul, MN, USA). The test was terminated according to ACSM guidelines.[31]

Statistical Analysis:
All statistical calculations were assessed using commercially available software (SPSS Version 16, SPSS Inc., Chicago, IL, USA). Comparison of $V^{\bullet}O_2$peak between groups of diastolic ventricular dysfunction was performed using Wilcoxon rank sum. Linear regression analysis was used to assess the correlation between the Doppler parameters and the $V^{\bullet}O_2$peak. A P-value less than 0.05 was considered statistically significant.

Results:
Thirty patients with repaired TOF were studied (median age 14 years, range 9–25 years). Eleven patients (37%) were female. Seven patients (median age 12 years) had normal left ventricular diastolic function, 15 patients (median age 15 years) had diastolic dysfunction grade II, and 8 patients (median age 18 years) had diastolic dysfunction grade III and IV. Baseline clinical characteristics were compared in Table I. The patients with normal diastolic function were younger at the time of operation than the other groups. The patients with diastolic dysfunction grade III and IV had more body surface area and more females than the other groups. However, follow-up time, previous modified Blalock–Taussig shunt, heart rate, and blood pressure were not statistically different among these three groups. The patients had mild residual pulmonary stenosis (median gradient 8 mmHg, range 5–32 mmHg).

Exercise Parameters:
Observed exercise values stratified by left ventricular diastolic function were summarized in Table II. The oxygen uptake at anaerobic threshold ($V^{\bullet}O_{2AT}$) and $V^{\bullet}O_2$peak in patients with left ventricular diastolic dysfunction was significantly lower than that in those with normal diastolic function. Also, $V^{\bullet}O_{2AT}$ and $V^{\bullet}O_2$peak in patients with diastolic dysfunction grade III and IV were significantly lower than that in those with diastolic dysfunction grade II (Fig. 1). However, heart rate, oxygen pulse, $V^{\bullet}_E$, $V^{\bullet}_E/V^{\bullet}CO_2$, RER, and submaximal exercise were not significantly different among these three groups.

Relationship of Pulse-Wave Doppler and Tissue Doppler Data to $V^{\bullet}O_2$ peak:
Results of the relationship between the Doppler data and $V^{\bullet}O_2$peak are graphically displayed in Figure 2. Left ventricular early diastolic myocardial velocity obtained at the left ventricular free wall was most closely correlated to the $V^{\bullet}O_2$peak ($r = 0.51$; $P = 0.005$). Peak early ventricular filling

TABLE I

Demographic and Characteristics of Patients According to Left Ventricular Diastolic Dysfunction (N = 30)

	Normal (N = 7)	Diastolic Dysfunction Grade II (N = 15)	Diastolic Dysfunction Grade III and IV (N = 8)	P Value
Age (years)	12 ± 2	16 ± 4	18 ± 6	0.02
Age at operation (years)	4 ± 1	6 ± 2	8 ± 5	0.04
Follow-up time (years)	8 ± 1	10 ± 3	10 ± 4	0.20
NYHA class (N)				0.06
I	7	14	5	
II	0	1	3	
Modified Blalock–Taussig shunt, N (%)	2 (29%)	2 (13%)	2 (25%)	0.65
BSA (m^2)	1.1 ± 0.2	1.3 ± 0.2	1.4 ± 0.2	0.02
Heart rate at rest (beats/min)	75 ± 10	77 ± 11	84 ± 13	0.40
Systolic BP at rest (mmHg)	98 ± 7	110 ± 14	106 ± 13	0.09
Diastolic BP at rest (mmHg)	59 ± 8	69 ± 13	63 ± 12	0.14
Severity of pulmonary regurgitation, N				0.89
Mild	2	3	1	
Moderate	2	7	4	
Severe	3	5	3	

TABLE II

Comparison of the Exercise Data Stratified by Left Ventricular Diastolic Function

			Exercise	
Parameters	Diastolic Dysfunction	Rest	Anaerobic Threshold	Peak
Heart rate (beats/min)	Normal	86 ± 15	108 ± 10	164 ± 16
	Grade II	85 ± 12	99 ± 14	164 ± 13
	Grade III and IV	89 ± 11	102 ± 11	153 ± 12
$V^{\bullet}O_2$ (mL/kg per min)	Normal	11 ± 2	21 ± 4	41 ± 9
	Grade II	8 ± 2*	16 ± 4*	33 ± 7*
	Grade III and IV	8 ± 1*	12 ± 2*#	25 ± 6*#
$V^{\bullet}O_{2AT}/V^{\bullet}O_2$max (%)	Normal			51 ± 4
	Grade II			49 ± 7
	Grade III and IV			51 ± 13
Oxygen pulse (mL/min per beats)	Normal	3.9 ± 1.3	6.0 ± 1.6	7.6 ± 1.6
	Grade II	4.0 ± 1.1	7.1 ± 2.4	8.8 ± 3.4
	Grade III and IV	4.2 ± 1.1	5.7 ± 1.1	7.7 ± 2.5
Minute ventilation (L/min)	Normal	10 ± 2	19 ± 4	42 ± 8
	Grade II	11 ± 3	19 ± 6	47 ± 16
	Grade III and IV	12 ± 3	15 ± 3	39 ± 14
$V^{\bullet}_E/CO_2$	Normal	38 ± 4	33 ± 5	32 ± 6
	Grade II	36 ± 5	29 ± 5	27 ± 4
	Grade III and IV	40 ± 6	33 ± 5	29 ± 6
Respiratory exchange ratio	Normal	0.8 ± 0.1	0.9 ± 0.1	1.1 ± 0.1
	Grade II	0.9 ± 0.1	0.9 ± 0.1	1.2 ± 0.1
	Grade III and IV	0.8 ± 0.1	0.8 ± 0.1	1.1 ± 0.2
Submaximal exercise, N (%)	Normal			2 (29%)
	Grade II			2 (13%)
	Grade III and IV			1 (13%)

$V^{\bullet}O_2$ = oxygen uptake; $V^{\bullet}O_{2AT}$ = oxygen uptake at anaerobic threshold; $V^{\bullet}_E/CO_2$ = minute ventilation and carbon dioxide production ratio.
*$P < 0.05$ versus normal diastolic function.
#$P < 0.05$ for grade II versus grade III and IV.

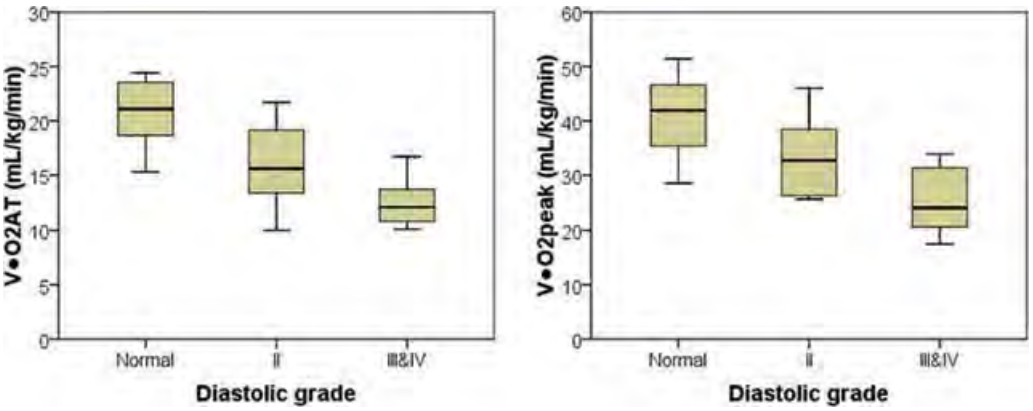

Figure 1. Graphic display comparing the peak oxygen uptake according to grade of left ventricular diastolic function. $V^{\bullet}O_{2AT}$ = oxygen uptake at anaerobic threshold; $V^{\bullet}O_2$peak = peak oxygen uptake.

velocity to early diastolic myocardial velocity ratio (E/Em) significantly correlated with $V^{\bullet}O_2$peak ($r = -0.50$; $P = 0.006$). Left ventricular ejection fraction, myocardial performance index, systolic myocardial velocity, and late diastolic myocardial velocity were not correlated with $V^{\bullet}O_2$peak. Right ventricular echocardiographic parameters including myocardial performance index, fractional area change, and tissue Doppler imaging were not significantly correlated with $V^{\bullet}O_2$peak. Also, pulmonary stenosis gradient and severity of pulmonary regurgitation were not correlated with $V^{\bullet}O_2$peak.

Discussion:

This study supports our hypothesis that pulse-wave Doppler and tissue Doppler patterns of left ventricular diastolic dysfunction correlated with $V^{\bullet}O_2$peak. $V^{\bullet}O_{2AT}$ and $V^{\bullet}O_2$peak in patients with repaired TOF, who have left ventricular diastolic dysfunction, was significantly lower than that in those with normal diastolic left ventricular function. Furthermore, $V^{\bullet}O_{2AT}$ and $V^{\bullet}O_2$peak in patients with diastolic dysfunction grade III and IV was significantly lower than that in those with diastolic dysfunction grade II. Left ventricular early diastolic myocardial velocity obtained at the left ventricular free wall was significantly correlated to $V^{\bullet}O_2$peak. Peak early ventricular filling velocity to early diastolic myocardial velocity ratio also correlated with $V^{\bullet}O_2$peak. In fact, decreased early diastolic myocardial velocity and increased early ventricular filling velocity to early diastolic myocardial velocity ratio are characteristics of diastolic left ventricular dysfunction with increased ventricular end-diastolic pressure and increased left atrial pressure. These findings are of clinical relevance, because tissue Doppler imaging is a readily available tool, and early diastolic myocardial velocity is easier and faster to obtain than exercise capacity testing, especially in young children.

Cheung et al. reported that global left ventricular deformation because of right ventricular dilation was an independent predictor of $V^{\bullet}O_2$peak

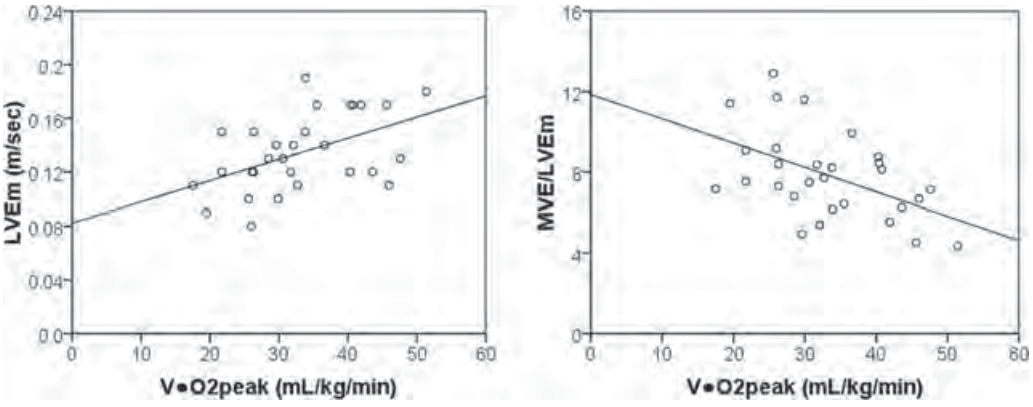

Figure 2. Linear regression analysis comparing the pulse-wave Doppler and tissue Doppler data and peak oxygen uptake in patients with repaired tetralogy of Fallot. LVEm = left ventricular free wall early diastolic myocardial velocity; MVE/LVEm = mitral valve early ventricular filling velocity to left ventricular early diastolic myocardial velocity ratio; $V^{\bullet}O_2$peak = peak oxygen uptake.

in patients with repaired TOF.[32] This study supported this finding that diastolic left ventricular dysfunction was correlated with $V^{\bullet}O_2$peak. Right ventricular dilation might affect the ventricular–ventricular interaction resulting in left ventricular diastolic dysfunction. Norozi et al.[33] and Samman et al.[34] reported that biventricular dysfunction was associated with diminished exercise capacity. $V^{\bullet}O_2$peak was correlated with left ventricular Tei index.[33,34] In fact, Tei index has been shown as an echocardiographic parameter of global systolic and diastolic ventricular function.[35]

Several studies demonstrated right ventricular dysfunction was associated with decreased exercise capacity in adult patients after repaired TOF.[24,25] However, Cheung et al. reported right ventricular function including myocardial performance index, ejection fraction, and tricuspid annular velocity was not a predictor of $V^{\bullet}O_2$peak in adolescents after repaired TOF.[36] Our findings in this study supported their finding that right ventricular function in children and adolescents was not correlated with $V^{\bullet}O_2$peak. Right ventricular function in children and adolescents may be still preserved for pressure and volume overload. We do believe that residual severe pulmonary stenosis and severe pulmonary regurgitation in long-term follow-up might affect right ventricular function, left ventricular diastolic function, and the exercise capacity in adult patients with repaired TOF. The correction of the residual heart defect and medical treatment of left ventricular diastolic function might improve the exercise tolerance in the adult patients after repaired TOF.

The diastolic grading system provides a semiquantitative approach to classify the severity of ventricular function using mitral valve flow, pulmonary venous flow, and tissue Doppler imaging.[30] Ommen et al. demonstrated that the combined parameter of E/Em provided a better estimate of left ventricular filling pressure than other variables.[37] In this study, the grade of diastolic left ventricular function was correlated to $V^{\bullet}O_2$peak. Also, Doppler variables of diastolic dysfunction including left ventricular early diastolic myocardial velocity and increased E/Em ratio were significantly correlated with $V^{\bullet}O_2$peak.

Aortic root dilatation and aortic regurgitation were correlated with reduced left ventricular systolic function in the adult patients with repaired TOF.[38] In this study, five patients had aortic root dilatation. Only two patients had mild aortic regurgitation in children and adolescents with repaired TOF. Therefore, the number of patients is not enough to be correlated with left ventricular function. We believe that these sequelae might have significant impact on left ventricular function in adult patients after repaired TOF.

There is a limitation in our study for evaluation of right ventricular function using echocardiography. Magnetic resonance imaging is the gold standard for evaluation of right ventricular function, but this method is expensive. However, tissue Doppler imaging has been recently used to evaluate right ventricular dysfunction.[24,39,40] Long-term study of the echocardiographic assessment for systolic and diastolic ventricular function in a large number of patients with repaired TOF including older ages is warranted.

Conclusions:

The severity of the left ventricular diastolic dysfunction was inversely correlated with $V^{\bullet}O_2$peak. Left ventricular diastolic dysfunction could be responsible for exercise intolerance. Left ventricular diastolic function should be a routine part of the echocardiographic assessment in patients with repaired TOF. Treatment of left ventricular diastolic dysfunction might improve exercise intolerance in children and adolescents after repaired TOF.

Acknowledgments: This work was supported by the Thailand Research Fund Grants MRG5180103 (S.S.) and RTA5280006 (N.C.).

References

1. Siwik ES, Patel CR, Zahka KG: Tetralogy of fallot. In: Allen HD, Gutgesell HP, Clark EB, Driscoll DJ (eds): *Moss and Adam's heart disease in infants, children, and adolescents including the fetus and young adult*, (*6th Ed*.) Philadelphia, Lippincott Williams & Wilkins, 2001, pp. 880–902.
2. Horneffer PJ, Zahka KG, Rowe SA, et al: Long-term results of total repair of tetralogy of Fallot in childhood. *Ann Thorac Surg* 1990;50(2):179–183.
3. Murphy JG, Gersh BJ, Mair DD, et al: Long-term outcome in patients undergoing surgical repair of tetralogy of Fallot. *N Engl J Med* 1993;329(9):593–599.
4. Reddy VM, Liddicoat JR, McElhinney DB, et al: Routine primary repair of tetralogy of Fallot in neonates and infants less than three months of age. *Ann Thorac Surg* 1995;60(Suppl. VI):S592–S596.
5. Knott-Craig CJ, Elkins RC, Lane MM, et al: A 26-year experience with surgical management of tetralogy of Fallot: Risk analysis for mortality or late reintervention. *Ann Thorac Surg* 1998;66(2):506–511.
6. Pigula FA, Khalil PN, Mayer JE, et al: Repair of tetralogy of Fallot in neonates and young infants. *Circulation* 1999;100(Suppl. XIX):157–161.
7. Caspi J, Zalstein E, Zucker N, et al: Surgical management of tetralogy of Fallot in the first year of life. *Ann Thorac Surg* 1999;68(4):1344–1348.
8. Hirsch JC, Mosca RS, Bove EL: Complete repair of tetralogy of Fallot in the neonate: Results in the modern era. *Ann Thorac Surg* 2000;232(4):508–514.
9. Alexiou C, Mahmoud H, Al-Khaddour A, et al: Outcome after repair of tetralogy of Fallot in the first year of life. *Ann Thorac Surg* 2001;71(2):494–500.
10. Bacha EA, Scheule AM, Zurakowski D, et al: Long-term results after early primary repair of tetralogy of Fallot. *J Thorac Cardiovasc Surg* 2001;122(1):154–161.

11. Cobanoglu A, Schultz JM: Total correction of tetralogy of Fallot in the first year of life: Late results. *Ann Thorac Surg* 2002;74(1):133–138.
12. Sarubbi B, Pacileo G, Pisacane C, et al: Exercise capacity in young patients after total repair of tetralogy of Fallot. *Pediatr Cardiol* 2000;21(3):211–215.
13. Strieder DJ, Aziz K, Zaver AG, et al: Exercise tolerance after repair of tetralogy of Fallot. *Ann Thorac Surg* 1975;19(4):397–405.
14. Rhodes J, Dave A, Pulling MC, et al: Effect of pulmonary artery stenoses on the cardiopulmonary response to exercise following repair of tetralogy of Fallot. *Am J Cardiol* 1998;81(10):1217–1219.
15. Wessel HU, Cunningham WJ, Paul MH, et al: Exercise performance in tetralogy of Fallot after intracardiac repair. *J Thorac Cardiovasc Surg* 1980;80(4):582–593.
16. Rowe SA, Zahka KG, Manolio TA, et al: Lung function and pulmonary regurgitation limit exercise capacity in postoperative tetralogy of Fallot. *J Am Coll Cardiol* 1991;17(2):461–466.
17. Norgard G, Bjorkhaug A, Vik-Mo H: Effects of impaired lung function and pulmonary regurgitation on maximal exercise capacity in patients with repaired tetralogy of Fallot. *Eur Heart J* 1992;13(10):1380–1386.
18. Carvalho JS, Shinebourne EA, Busst C, et al: Exercise capacity after complete repair of tetralogy of Fallot: Deleterious effects of residual pulmonary regurgitation. *Br Heart J* 1992;67(6):470–473.
19. Jonsson H, Ivert T, Jonasson R, et al: Work capacity and central hemodynamics thirteen to twenty-six years after repair of tetralogy of Fallot. *J Thorac Cardiovasc Surg* 1995;110(2):416–426.
20. Helbing WA, Niezen RA, Le Cessie S, et al: Right ventricular diastolic function in children with pulmonary regurgitation after repair of tetralogy of Fallot: Volumetric evaluation by magnetic resonance velocity mapping. *J Am Coll Cardiol* 1996;28(7):1827–1835.
21. Giardini A, Specchia S, Coutsoumbas G, et al: Impact of pulmonary regurgitation and right ventricular dysfunction on oxygen uptake recovery kinetics in repaired tetralogy of Fallot. *Eur J Heart Fail* 2006;8(7):736-743.
22. Mocellin R, Bastanier C, Hofacker W, et al: Exercise performance in children and adolescents after surgical repair of tetralogy of Fallot. *Eur J Cardiol* 1976;4(3):367–374.
23. Kondo C, Nakazawa M, Kusakabe K, et al: Left ventricular dysfunction on exercise long-term after total repair of tetralogy of Fallot. *Circulation* 1995;92(Suppl. IX):250–255.
24. Salehian O, Burwash IG, Chan KL, et al: Tricuspid annular systolic velocity predicts maximal oxygen consumption during exercise in adult patients with repaired tetralogy of Fallot. *J Am Soc Echocardiogr* 2008;21(4):342–346.
25. Singh GK, Greenberg SB, Yap YS, et al: Right ventricular function and exercise performance late after primary repair of tetralogy of Fallot with the transannular patch in infancy. *Am J Cardiol* 1998;81(11):1378–1382.
26. Gatzoulis MA, Norgard G, Redington AN: Biventricular long axis function after repair of tetralogy of Fallot. *Pediatr Cardiol* 1998;19(2):128–132.
27. Harada K, Toyono M, Yamamoto F: Assessment of right ventricular function during exercise with quantitative Doppler tissue imaging in children late after repair of tetralogy of Fallot. *J Am Soc Echocardiogr* 2004;17(8):863–869.
28. D'Andrea A, Caso P, Sarubbi B, et al: Right ventricular myocardial dysfunction in adult patients late after repair of tetralogy of Fallot. *Int J Cardiol* 2004;94 (2-3):213–220.
29. Gharzuddine WS, Kazma HK, Nuwayhid IA, et al: Doppler characterization of left ventricular diastolic function in beta-thalassaemia major. Evidence for an early stage of impaired relaxation. *Eur J Echocardiogr* 2002;3(1):47–51.
30. Silvilairat S, Sittiwangkul R, Pongprot Y, et al: Tissue Doppler echocardiography reliably reflects severity of iron overload in pediatric patients with beta thalassemia. *Eur J Echocardiogr* 2008;9(3):368–372.
31. American College of Sports Medicine, ed. *ACSM's guidelines for exercise testing and prescription. 7th Ed*. Baltimore: Lippincott Williams & Wilkins, 2006. p. 106.
32. Cheung EW, Liang XC, Lam WW, et al: Impact of right ventricular dilation on left ventricular myocardial deformation in patients after surgical repair of tetralogy of fallot. *Am J Cardiol* 2009;104(9):1264–1270.
33. Norozi K, Buchhorn R, Bartmus D, et al: Elevated brain natriuretic peptide and reduced exercise capacity in adult patients operated on for tetralogy of fallot is due to biventricular dysfunction as determined by the myocardial performance index. *Am J Cardiol* 2006;97(9):1377–1382.
34. Samman A, Schwerzmann M, Balint OH, et al: Exercise capacity and biventricular function in adult patients with repaired tetralogy of Fallot. *Am Heart J* 2008;156(1):100–105.
35. Tei C, Ling LH, Hodge DO, et al: New index of combined systolic and diastolic myocardial performance: A simple and reproducible measure of cardiac function-a study in normals and dilated cardiomyopathy. *J Cardiol* 1995;26(6):357–366.
36. Cheung EW, Lam WW, Chiu CS, et al: Plasma brain natriuretic peptide levels, right ventricular volume overload and exercise capacity in adolescents after surgical repair of tetralogy of Fallot. *Int J Cardiol* 2007;121(2):155–162.
37. Ommen SR, Nishimura RA, Appleton CP, et al: Clinical utility of Doppler echocardiography and tissue Doppler imaging in the estimation of left ventricular filling pressures: A comparative simultaneous Doppler-catheterization study. *Circulation* 2000;102(15):1788–1794.
38. Grotenhuis HB, Ottenkamp J, de Bruijn L, et al: Aortic elasticity and size are associated with aortic regurgitation and left ventricular dysfunction in tetralogy of Fallot after pulmonary valve replacement. *Heart* 2009;95(23):1931–1936.
39. Gondi S, Dokainish H. Right ventricular tissue Doppler and strain imaging: Ready for clinical use? *Echocardiography* 2007;24(5):522–532.
40. Cetin I, Tokel K, Varan B, et al: Evaluation of right ventricular function by using tissue Doppler imaging in patients after repair of tetralogy of Fallot. *Echocardiography* 2009;26(8):950–957.

ISSN 0970-9290

Indian Journal of Dental Research

Volume 22 Issue 05 September-October 2011

Contents

Official publication of
Indian Society for Dental Research

Online full text
www.ijdr.in
Medknow Publications

ORIGINAL RESEARCH

Changes in peripheral innervation and nociception in reticular type and erosive type of oral lichen planus

Siriporn Chattipakorn, Jitjiroj Ittichaicharoen, Samreung Rangdaeng[1], Nipon Chattipakorn[2]

Department of Oral Biology and Diagnostic Science, Faculty of Dentistry, [1]Department of Pathology, Faculty of Medicine, [2]Cardiac Electrophysiology Research and Training Center, Faculty of Medicine, Chiang Mai University, Chiang Mai, Thailand

Received : 25-03-10
Review completed : 27-07-10
Accepted : 05-10-10

ABSTRACT

Background: Oral lichen planus (OLP) is a chronic inflammatory lesion in oral mucosa. Reticular (OLP-R) and erosive (OLP-E) types of OLP are the common forms that have been found in dental clinics. The aim of this investigation is to determine the correlation between neurogenic inflammation and nociception associated with OLP-R and OLP-E.

Materials and Methods: The oral mucosal lesions from six patients with OLP-E, four with OLP-R and three with noninflamed oral mucosa, which represent normal mucosa, were identified by morphometric analysis of nerve fibers containing immunoreactive protein gene product (PGP) 9.5. The level of inflammation was measured with hematoxylin and eosin staining and the level of nociception was analyzed with visual analog scale measurement.

Results: We found that 1) an increase in peripheral innervation was related to the size of the area of inflammatory cell infiltration from both OLP-R and OLP-E; 2) the pattern of PGP 9.5-immunoreactivity among OLP-R and OLP-E was not significantly different (P=0.23); and 3) the correlation between nociception and an increase in PGP 9.5-immunoreactivity was not found in OLP-E and in OLP-R.

Conclusions: Our findings suggest that an increase in peripheral innervation may lead to increased inflammation, which is part of the immunopathogenesis of OLP. Differences in nociception between OLP-R and OLP-E arise from the pathogenesis of each lesion, not from the differences in peripheral innervation.

Key words: Neurogenic inflammation, nociception, oral lichen planus

During the past few years, substantial evidence for a relationship between the immune and the nervous systems has been reported. For example, 1) antigen-presenting dendritic cells or immune cells of the epidermis have been shown to be in close contact with cutaneous nerve fibers[1] and 2) neuropeptides, i.e. mediators released by cutaneous nerves, have been demonstrated to influence antigen-presenting cells or immune cells in skin.[2] There is evidence that changes in the skin innervation observed in dermatological diseases contribute to the inflammatory process and to the associated painful sensation. An increase in cutaneous nerve fibers has been reported in itching and painful cutaneous diseases including neurofibroma,[3] nostalgia paraesthetica,[4] prurigo nodularis,[5] vulvodynia[6] and psoriasis.[7,8] In contrast, a reduction of cutaneous nerve fibers can be found in conditions associated with decreased cutaneous nociception, such as diabetic neuropathy,[9] leprosy,[10] or HIV-infected patients suffering from xerosis.[11] The current theory of persistent pain following tissue injury or inflammation is that sensitization involves both the central[12-15] and peripheral nervous systems.[16] A number of studies suggest that the interaction between the inflammation and neural system exists and may lead to painful sensation.[16]

Oral lichen planus (OLP) is a chronic inflammatory disease of the oral mucosa.[17,18] Clinically, OLP is commonly found bilaterally and may present as striated, plaque, atrophic or erosive lesions. OLP is histologically characterized by a well-defined, band-like lymphocytic subepithelial inflammation. OLP usually presents with burning sensation or persistent pain. Although OLP is classified into six types, the reticular type (OLP-R) and erosive type of OLP (OLP-E) are the two most common types. Each type has different clinical features. OLP-R presents without a painful sensation,

Address for correspondence:
Dr. Siriporn C Chattipakorn
E-mail: s.chat@chiangmai.ac.th

Access this article online

Quick Response Code:

Website: www.ijdr.in

DOI: 10.4103/0970-9290.93456

whereas pain is the most commonly found symptom in OLP-E. Although it has been shown that cutaneous innervation or peripheral sensitization is increased following chronic inflammation in dermatological diseases[3-8] and oral lichen planus,[19] information regarding the correlation between neurogenic inflammation and nociception associated with oral mucosal disease such as OLP-R and OLP-E is limited. The present study sought to determine whether 1) two different types of OLP with different levels of nociception, OLP-R and OLP-E, express different patterns of nerve sprouting or peripheral sensitization, and 2) a correlation of an increase of peripheral innervation, inflammatory reaction, and nociception in both OLP lesions exists.

MATERIALS AND METHODS

Patient selection

Thirteen patients with oral mucosal lesions were included in this study. None of the patients had a history of either systemic disease or corticosteriod injections to their lesions. All patients had been treated for Candida infection before biopsy. Clinical details of these patients are shown in Table 1.

All patients were asked to rank the painful sensation of oral lesions before biopsy using a visual analog scale (VAS) system, in which "0" meant no pain at all and "10" meant as painful as imaginable. Biopsies from the oral mucosa of these thirteen patients were obtained. From histological examination, six patients were diagnosed with OLP-E, four with OLP-R and three with noninflamed oral mucosa from the operculum of a third molar after surgical removal of the tooth. The lesions were classified histologically using WHO criteria.[20]

All biopsies came from the buccal mucosa under local anesthesia (2% lidocaine with 1000,000 units norepinephrine). In this study, the biopsy of the OLP-E lesions was performed at the edge of erosive area with the white-striated lesions and the biopsy of the OLP-R lesions was performed at the white-striated area. Some slices of all tissue samples were used for routine histological evaluation including hematoxylin and eosin (H and E) staining. Other slices of all samples were used for protein gene product 9.5 (PGP 9.5) immunohistochemical analysis.

Informed consent was obtained from all patients, and the research plan was accepted by the Ethics Committee of the Faculty of Dentistry, Chiang Mai University, Thailand.

Table 1: Clinical data for patients with OLP-R, OLP-E and noninflamed oral mucosa

	n	Male	Female	Age mean/ range (years)
OLP-R	4	1	3	55/38-76
OLP-E	6	3	3	47/26-63
Noninflamed oral mucosa	3	0	3	30/21-47

OLP-R: Reticular type of oral lichen planus; OLP-E: Erosive type of oral lichen planus

Immunohistochemistry

Three-micron thickness paraffined sections were mounted on 3-aminopropyltriethoxysilane (Dako, Glostrup, Denmark)-coated slides. Sections were deparaffinized with xylene and ethanol and then placed in a boiling solution of freshly prepared citrate buffer (pH 6.0) for 10 min in a pressure cooker before immunostaining. Endogenous peroxidase was inhibited by soaking the sections in 0.3% H_2O_2 in 0.1 M phosphate-buffer saline (PBS) for 30 min at room temperature. The sections were incubated sequentially in a humidified chamber with 1) 3% normal goat serum in 0.1 M PBS (3% NGS, Sigma, St. Louis, MO, USA) as a blocking serum at room temperature for 1 h; 2) primary mouse monoclonal antisera PGP 9.5 (Novacastra Co, Wetzlar, Germany) diluted 1: 20 in 3% normal goat serum overnight at + 4°C; 3) biotinylated goat anti-mouse IgG (Santa Cruz Biotech, Santa Cruz, CA, USA) diluted 1:200 in 0.1 M PBS for 1 h at room temperature; and 4) avidin-biotin-peroxidase complex (Santa Cruz Biotech, Santa Cruz, CA, USA) for 45 min at room temperature. After each step, the sections were rinsed three times in PBS for 5 min. Staining was amplified with the glucose oxidase-3, 3-diaminobenzidine (DAB)-nickel method for 10 min. Sections were washed three times with water for 5 min. The slides were dehydrated in alcohol and xylene, before being mounted in permount (Sigma, St. Louis, MO, USA).

Microscopic evaluation and qualitative assessment

Microscopic examination was performed with an Olympus microscope coupled for morphometric assessment with a digital camera and linked to a semiautomatic Kontron image analysis and processing system. Morphometry of PGP 9.5 immunoreactivity (PGP 9.5-ir) and H and E staining were performed under ×200 magnification. Nerve fiber densities or PGP 9.5-positive fibers (linear intercept number/mm^2 tissue) were performed from the subepithelial area (i.e. an area extending 100 μm deep from the basement membrane area to the lamina propria) in each section as described in a previous study.[19] In each patient, nerve fibers densities were counted in five microscopic fields, in which were covered the whole area in each slide and counted three slides per sample. The epithelium was excluded from the measurement.

Statistical analysis

Results were expressed as the mean ± standard error of the mean (SEM). For comparison between multiple groups, nonparametric analysis with Kruskal–Wallis test and Pearson correlation coefficient were used for data analysis.

RESULTS

Overall innervation as assessed by PGP 9.5-ir as a marker

To determine the pattern of cutaneous innervation of OLP-E, OLP-R and the noninflamed oral mucosa, representing normal mucosa, PGP 9.5-immunoreactivity (PGP 9.5-ir)

was used. The specificity of this primary PGP 9.5 antiserum was previously tested in previous studies.[19,21] An absence of staining was found when the primary antibody was omitted [Figures 1a, c, e and g]. The peripheral nerves visualized by the general neural marker PGP 9.5-ir were easily noticeable. In noninflamed oral mucosa (OM), nerve fibers were located in the deep lamina propria. They were rarely found in close contact with basement membrane. Nerve trunks and rich perivascular innervation appeared in the deeper parts of lamina propria [Figures 1b, d]. However, in both types of OLP, PGP 9.5-positive nerve fibers were concentrated in the superficial subepithelial tissue, and nerve fibers in OLP were found close to the basement membrane [Figures 1f, h]. As shown in Figure 2, the pattern of PGP 9.5-positive nerve fibers in OLP-R and OLP-E was similar. Means of PGP 9.5-positive never fibers per each subepithelial area of OM (1.0 ± 1.0 linear intercept/mm^2), OLP-R lesions (2.4 ± 0.8 linear intercept/mm^2) and OLP-E lesions (3.5 ± 1.2 linear intercept/mm^2) were not significantly different (P=0.39) [Figure 2c]. Furthermore, PGP 9.5-positive nerve fiber density of both types of OLP lesions was high at the superficial subepithelial areas. Underneath this area, i.e. connective tissue layer, high lymphocytic infiltration was seen where no PGP 9.5–positive fibers were found [Figures 3a-d]. By contrast, neither PGP 9.5-positive nerve fibers nor inflammatory infiltration at the superficial subepithelial areas were found in noninflamed oral mucosa tissue [Figures 3e, f]. Hence, the density of PGP 9.5-positive nerve fibers was greatest in the subepithelial inflamed area of both types of OLP lesions, suggesting the existence of a neuroinflammatory process or peripheral sensitization in this disease as in other inflammatory dermatological diseases. In addition, the pattern of peripheral innervation between the two different clinical features of OLP-R and OLP-E were not different.

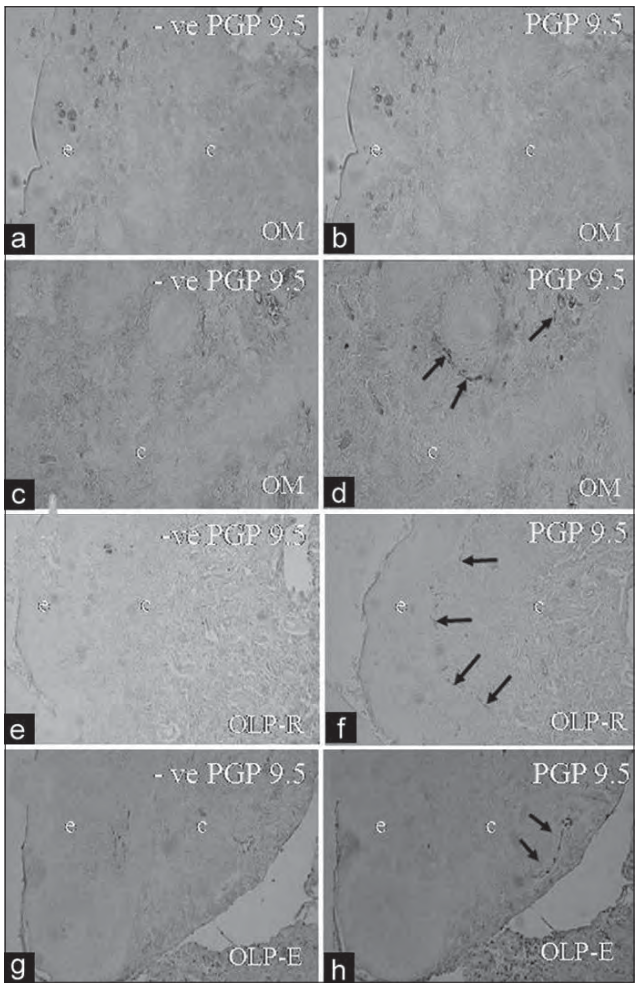

Figure 1: Pattern of overall innervation in noninflamed oral mucosa (OM), reticular type of oral lichen planus (OLP-R) and erosive type of oral lichen planus (OLP-E). Avidin-biotin peroxidase complex (ABC) staining of PGP 9.5 amplified with glucose oxidase-nickel ammonium sulfated methods in all panels (a-h), magnification ×200. a, c, e, f represent the negative control (omitting primary antibody) from adjacent sections of PGP 9.5-positive nerve fibers. No PGP 9.5-positive nerve fibers are seen in any control sections. B and D show the PGP 9.5-positive nerve fibers in noninflamed oral mucosa. Innervation in noninflamed oral mucosa is distributed completely in the deep lamina propria surrounding the blood vessels (arrows) (d). No subepithelial neural network is found (b). OLP-R (f) and OLP-E (h) show a dense subepithelial neural network in OLP (arrows). Nerve fibers are concentrated close to the basement membrane. e: Epithelium; c: Connective tissue

No correlation of innervation and pain levels as assessed by means of VAS in OLP-E and OLP-R

To determine whether correlation between peripheral sensitization or nerve sprouting and nociception exists, VAS

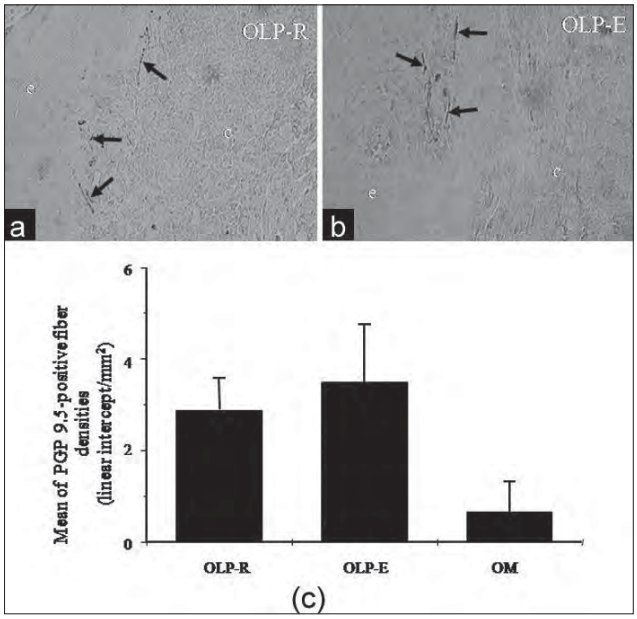

Figure 2: No differences in the pattern of PGP9.5-positive nerve fibers between reticular type of oral lichen planus (OLP-R) and erosive type of oral lichen planus (OLP-E). (a) A sample of PGP 9.5-positive nerve fibers from OLP-R lesions. (b) A sample of PGP9.5-positive nerve fibers from OLP-E lesions. The innervation of both OLP lesions is distributed at the subepithelial networks (arrows). Magnification ×200. (c) A bar graph represents the mean number of PGP 9.5-positive nerve fiber densities in each pathological lesion: Reticular type of oral lichen planus (OLP-R), erosive type of oral lichen planus (OLP-E) and noninflamed oral mucosa (OM)

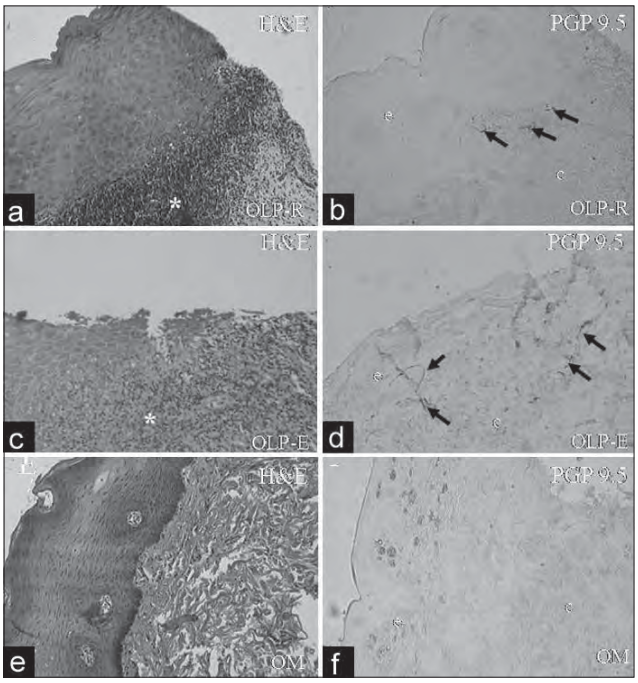

Figure 3: An increase in innervation in the areas of prominent subepithelial lymphocytic infiltration in reticular type of oral lichen planus (OLP-R) and in erosive type of oral lichen planus (OLP-E). H and E staining of OLP-R, OLP-E and noninflamed oral mucosa show in a, c and e, respectively. Avidin-biotin peroxidase complex (abc) staining of PGP 9.5 amplified with glucose oxidase-nickel ammonium sulfated methods from adjacent tissue sections of H and E sections from OLP-R (a), OLP-E (c) and noninflamed oral mucosa: OM (e) presented in b, d and f, respectively. Both PGP9.5-positive nerve fibers (arrows) and lymphocytic infiltration areas (asterisks) are concentrated in the subepithelial areas, in both types of OLP lesions. However, there is no subepithelial innervation with any inflammatory infiltration in noninflamed oral mucosa (e and f). Magnification ×200

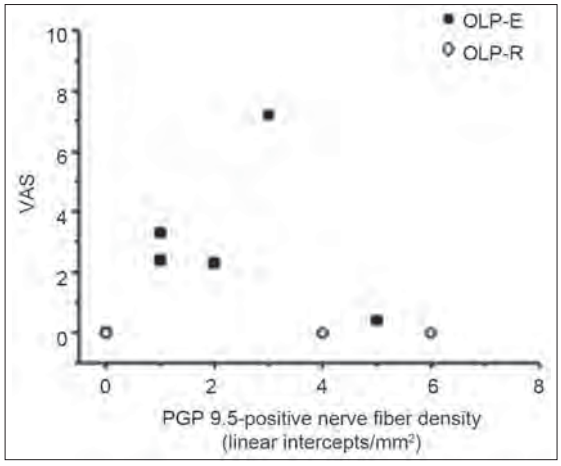

Figure 4: There is no correlation between PGP 9.5-positive nerve fiber densities and nociception in the reticular type of oral lichen planus (OLP-R) or in the erosive type of oral lichen planus (OLP-E). Nociception in each patient is measured with a visual analog scale (VAS) before biopsy

was used as a pain sensation measurement. VAS and PGP 9.5-positive nerve fiber densities were compared in each patient. We found that the average VAS scores in patients with OLP-E (3.12 ± 1.12, n=6) were significantly greater than those in patients with OLP-R (0 ± 0, n=4, P=0.005). However, a correlation between means of PGP 9.5-positive nerve fiber density and VAS scores existed in patients with OLP-R (r=0.0, P=0) and in patients with OLP-E (r=0.21, P=0.7) was not found [Figure 4]. Although an increase in innervation of OLP-E lesions were similar in quality and quantity to that of OLP-R lesions, the pathophysiological changes of epithelial lesions from both types of lesion were different. Loss of epithelium was the characteristic of OLP-E; in contrast, parakeratinized epithelium was distinct in OLP-R. These data imply that it is the epithelial changes in the lesions, not the number of peripheral nerve fibers, which are related to nociception in OLP lesions.

DISCUSSION

Our findings have confirmed the earlier findings that 1) the pattern of innervation in the normal oral mucosa is described as a discontinuous network in the deep lamina propria with no appearance in the superficial lamina propria;[22] 2) the increase in PGP 9.5-positive nerve fibers at the superficial lamina propria was seen in OLP; and 3) the pathophysiological changes in innervation are associated with chronic inflammation.[19] In addition, we have demonstrated that 1) the pattern of innervation in OLP-R and OLP-E is similar, despite the fact that the painful sensations in each is different; and 2) nociception and an increase of nerve sprouting in the superficial lamina propria is not correlated in either OLP-E lesions or in OLP-R lesions.

Nerve sprouting and chronic inflammation in OLP

An increase in PGP 9.5-positive nerve fibers was always observed in both OLP lesions but not in the normal mucosa. These results could be due to both nerve sprouting and collateral formation in OLP lesions. The regeneration of nerve fibers in OLP lesions may occur after tissue injury and may follow angiogenesis of inflamed tissue as demonstrated in previous studies.[23] Sprouting has been demonstrated in other inflammatory models such as: 1) in adjuvant-induced arthritis at the border zone of inflammation[24,25] and 2) in the wound healing of skin lesions from chronic constrictive injury of sciatic nerves or capsaicin-induced depletion of sensory C-fibers in animal models.[26] The induction factors for the existence or elongation of PGP 9.5-positive nerve fibers in lichen planus may be the local mediators secreted by inflammatory cells as reported in previous studies.[24,25] It is also possible that the elongation process of PGP 9.5 positive nerve fibers in lichen planus may act as an attempt at regeneration after chronic inflammation.

The pattern of sprouting from OLP-R and OLP-E was seen to follow the pattern of lymphocytic inflammation. In OLP lesions, the band-like lymphocytic inflammation was found in the subepithelial layers or superficial lamina propria, and

the nerve sprouting was also restricted to the superficial lamina propria. This finding suggests the existence of the reaction between neurogenic and immune systems. In addition, our findings support the theory of neurogenic inflammation in chronic inflammatory diseases.[18,23,27]

Increased peripheral innervation and nociception in OLP

PGP 9.5-immunoreactivity (PGP 9.5-ir) was used to locate single nerve fibers, nerve bundles, and nerves surrounding vessels and innervating muscles and glands.[21] Although PGP 9.5-ir reflects the general innervation pattern of the tissue, several studies have shown that PGP 9.5-positive nerve fibers were correlated with nociception. For example, 1) the increase of PGP 9.5-positive nerve fibers at skin lesions was found with an increase in painful sensation such as thermal hyperalgesia and mechanical allodynia in a chronic constrictive injury in an animal model of painful partial nerve injury;[28,29] 2) loss of cutaneous pain sensation with a reduction of PGP 9.5-positive nerve fibers in leprosy skin lesions[30] and 3) PGP 9.5-positive nerve fibers were reduced in the capsaicin-induced dermal lesion in a rat model, in which capsaicin induces depletion of sensory C-fiber neuropeptides.[26] All of the findings from these previous reports suggest that PGP 9.5 positive nerve fibers are very well correlated with nociceptors. In this study, we found that the mean number of PGP 9.5-positive nerve fibers was not correlated with nociception in OLP-E or in OLP-R. The difference in nociception in both OLP types may be the result of pathophysiological changes in both types of lesion. OLP-E is characterized by loss of mucosal epithelium, which leads to the exposure of lamina propria to the surrounding environment in the oral cavity. OLP-R, however, has parakeratinized epithelium covering the mucosal lesion. Although the pattern and number of PGP 9.5-positive nerve fibers from both lesions are not significantly different, the pathophysiological nature of epithelium from both lesions is totally distinguishable. The epithelial differences in the pathophysiology of OLP-R and OLP-E may be the reason for the difference in pain sensation, because sensory afferents may receive stronger and/or more frequent nociceptive input in OLP-E than in OLP-R. The reason that being no difference in lymphocytic infiltration or PGP 9.5-positive nerve fibers were seen between OLP-E and OLP-R could be due to the fact that extensive lymphocytic inflammation could lead to the loss of nerve fibers in that area, as seen in previous study.[19]

Limitation of this study

Although the pattern of sprouting in OLP lesions in our study was similar to the pattern in a previous study,[19] the number of PGP 9.5-positive nerve fibers was much less than in the previous report.[19] This difference may be due to different techniques used in each study. We used paraffined sections with pressure-cooking techniques as antigen-unmasking techniques, whereas the previous study used frozen sections without antigen-unmasking. Our technique could have led to the loss of some tissue during the immunochemical process.

CONCLUSIONS

Chronic subepithelial inflammation is a diagnostic feature of OLP. Although OLP-E and OLP-R have similar inflammatory responses, the nociception or stressful sensations in patients with the respective OLP lesions are different. The present work suggests that the difference in nociception between both OLP lesion types relates to the structural changes in the epithelium rather than the increase of nerve sprouting from the lesions. In addition, this study supports the relationship between associated neurogenic factors and inflammatory processes in OLP lesions.

ACKNOWLEDGEMENTS

The authors thank Drs. S. Pongsiriwet and S. Krisanaprakornkit for their support in the Oral Medicine Clinic, R. Kitikamdhorn for the technical support, and Professor M. Kevin O Carroll, Professor Emeritus, University of Mississippi School of Dentistry and Faculty Consultant, Faculty of Dentistry, Chiang Mai University, for his editorial assistance during manuscript preparation. This study was supported by the Internal Research Fund of Chiang Mai University (SC) and a grant from the Thailand Research Fund to SC (BRG5480003) and to NC (RTA 5280006).

REFERENCES

1. Hosoi J, Murphy GF, Egan CL, Lerner EA, Grabbe S, Asahina A, *et al.* Regulation of Langerhans cell function by nerves containing calcitonin gene-related peptide. Nature 1993;363:159-63.
2. Lambert RW, Granstein RD. Neuropeptides and Langerhans cells. Exp Dermatol 1998;7:73-80.
3. Vaalasti A, Suomalainen H, Kuokkanen K, Rechardt L. Neuropeptides in cutaneous neurofibromas of von Recklinghausen's disease. J Cutan Pathol 1990;17:371-3.
4. Springall DR, Karanth SS, Kirkham N, Darley CR, Polak JM. Symptoms of notalgia paresthetica may be explained by increased dermal innervation. J Invest Dermatol 1991;97:555-61.
5. Abadia Molina F, Burrows NP, Jones RR, Terenghi G, Polak JM. Increased sensory neuropeptides in nodular prurigo: A quantitative immunohistochemical analysis. Br J Dermatol 1992;127:344-51.
6. Tympanidis P, Terenghi G, Dowd P. Increased innervation of the vulval vestibule in patients with vulvodynia. Br J Dermatol 2003;148:1021-7.
7. Eedy DJ, Shaw C, Johnston CF, Armstrong EP, Buchanan KD. Neuropeptides of the primary sensory neurones in rat skin: An ontogenic study. Regul Pept 1991;33:175-82.
8. Farber EM, Nickoloff BJ, Recht B, Fraki JE. Stress, symmetry, and psoriasis: Possible role of neuropeptides. J Am Acad Dermatol 1986;14:305-11.
9. Levy DM, Terenghi G, Gu XH, Abraham RR, Springall DR, Polak JM. Immunohistochemical measurements of nerves and neuropeptides in diabetic skin: Relationship to tests of neurological function. Diabetologia 1992;35:889-97.
10. Anand P, Pandya S, Ladiwala U, Singhal B, Sinicropi DV, Williams-Chestnut RE. Depletion of nerve growth factor in leprosy. Lancet 1994;344:129-30.

11. Rowe A, Mallon E, Rosenberger P, Barrett M, Walsh J, Bunker CB. Depletion of cutaneous peptidergic innervation in HIV-associated xerosis. J Invest Dermatol 1999;112:284-9.
12. Ji RR, Woolf CJ. Neuronal plasticity and signal transduction in nociceptive neurons: Implications for the initiation and maintenance of pathological pain. Neurobiol Dis 2001;8:1-10.
13. Ren K, Dubner R. Central nervous system plasticity and persistent pain. J Orofac Pain 1999;13:155-63.
14. Urban MO, Gebhart GF. Supraspinal contributions to hyperalgesia. Proc Natl Acad Sci U S A 1999;96:7687-92.
15. Urban MO, Gebhart GF. Central mechanisms in pain. Med Clin North Am 1999;83:585-96.
16. Barnes PJ, Belvisi MG, Rogers DF. Modulation of neurogenic inflammation: Novel approaches to inflammatory disease. Trends Pharmacol Sci 1990;11:185-9.
17. Jungell P. Oral lichen planus: A review. Int J Oral Maxillofac Surg 1991; 20:129-35.
18. Scully C, el-Kom M. Lichen planus: Review and update on pathogenesis. J Oral Pathol 1985;14:431-58.
19. Nissalo S, Hietanen J, Malmstrom M, Hukkanen M, Polak J, Konttinen YT. Disorder-specific changes in innervation in oral lichen planus and lichenoid reactions. J Oral Pathol Med 2000;29:361-9.
20. Pindborg JJ. Histologic typing of cancer and precancer of the oral mucosa. Berlin: Springer-Verlag; 1997.
21. Hilliges M, Hellman M, Ahlstrom U, Johansson O. Immunohistochemical studies of neurochemical markers in normal human buccal mucosa. Histochemistry 1994;101:235-44.
22. Ruokonen H, Hietanen J, Malmström M, Sane J, Häyrinen-Immonen R, Hukkanen M, *et al.* Peripheral nerves and mast cells in normal buccal mucosa. J Oral Pathol Med 1993;22:30-4.
23. Walsh DA, Wharton J, Blake DR, Polak JM. Neural and endothelial regulatory peptides, their possible involvement in inflammation. Int J Tissue React 1992;14:101-11.
24. Imai S, Tokunaga Y, Konttinen YT, Maeda T, Hukuda S, Santavirta S. Ultrastructure of the synovial sensory peptidergic fibers is distinctively altered in different phases of adjuvant induced arthritis in rats: Ultramorphological characterization combined with morphometric and immunohistochemical study for substance P, calcitonin gene related peptide, and protein gene product 9.5. J Rheumatol 1997;24:2177-87.
25. Weihe E, Nohr D, Millan MJ, Stein C, Müller S, Gramsch C, *et al.* Peptide neuroanatomy of adjuvant-induced arthritic inflammation in rat. Agents Actions 1988;25:255-9.
26. Wallengren J, Chen D, Sundler F. Neuropeptide-containing C-fibres and wound healing in rat skin. Neither capsaicin nor peripheral neurotomy affect the rate of healing. Br J Dermatol 1999;140:400-8.
27. Brain SD, Cambridge H, Hughes SR, Wilsoncroft P. Evidence that calcitonin gene-related peptide contributes to inflammation in the skin and joint. Ann N Y Acad Sci 1992;657:412-9.
28. Lindenlaub T, Sommer C. Epidermal innervation density after partial sciatic nerve lesion and pain-related behavior in the rat. Acta Neuropathol (Berl) 2002;104:137-43.
29. Ma W, Bisby MA. Calcitonin gene-related peptide, substance P and protein gene product 9.5 immunoreactive axonal fibers in the rat footpad skin following partial sciatic nerve injuries. J Neurocytol 2000;29:249-62.
30. Facer P, Mathur R, Pandya SS, Ladiwala U, Singhal BS, Anand P. Correlation of quantitative tests of nerve and target organ dysfunction with skin immunohistology in leprosy. Brain 1998;121:2239-47.

How to cite this article: Chattipakorn S, Ittichaicharoen J, Rangdaeng S, Chattipakorn N. Changes in peripheral innervation and nociception in reticular type and erosive type of oral lichen planus. Indian J Dent Res 2011;22:678-83.

Source of Support: Internal Research Fund of Chiang Mai University (SC) and a grant from the Thailand Research Fund to SC (BRG5480003) and to NC (RTA 5280006), **Conflict of Interest:** None declared.

Exp Physiol 96.8 pp 778–789

Research Paper

Effect of rosiglitazone on cardiac electrophysiology, infarct size and mitochondrial function in ischaemia and reperfusion of swine and rat heart

Siripong Palee[1,2], Punate Weerateerangkul[1,2], Sirirat Surinkeaw[1,2], Siriporn Chattipakorn[1,3] and Nipon Chattipakorn[1,2]

[1]*Cardiac Electrophysiology Research and Training Center, Faculty of Medicine,* [2]*Cardiac Electrophysiology Unit, Department of Physiology, Faculty of Medicine and* [3]*Faculty of Dentistry, Chiang Mai University, Chiang Mai, 50200, Thailand*

Rosiglitazone, a peroxisome proliferator-activated receptor γ agonist, has been used to treat type 2 diabetes. Despite debates regarding its cardioprotection, the effects of rosiglitazone on cardiac electrophysiology are still unclear. This study determined the effect of rosiglitazone on ventricular fibrillation (VF) incidence, VF threshold (VFT), defibrillation threshold (DFT) and mitochondrial function during ischaemia and reperfusion. Twenty-six pigs were used. In each pig, either rosiglitazone (1 mg kg^{-1}) or normal saline solution was administered intravenously for 60 min. Then, the left anterior descending coronary artery was ligated for 60 min and released to promote reperfusion for 120 min. The cardiac electrophysiological parameters were determined at the beginning of the study and during the ischaemia and reperfusion periods. The heart was removed, and the area at risk and infarct size in each heart were determined. Cardiac mitochondria were isolated for determination of mitochondrial function. Rosiglitazone did not improve the DFT and VFT during the ischaemia–reperfusion period. In the rosiglitazone group, the VF incidence was increased (58 *versus* 10%) and the time to the first occurrence of VF was decreased (3 ± 2 *versus* 19 ± 1 min) in comparison to the vehicle group ($P < 0.05$). However, the infarct size related to the area at risk in the rosiglitazone group was significantly decreased ($P < 0.05$). In the cardiac mitochondria, rosiglitazone did not alter the level of production of reactive oxygen species and could not prevent mitochondrial membrane potential changes. Rosiglitazone increased the propensity for VF, and could neither increase defibrillation efficacy nor improve cardiac mitochondrial function.

(Received 1 March 2011; accepted after revision 1 June 2011; first published online 10 June 2011)
Corresponding author N. Chattipakorn: Cardiac Electrophysiology Research and Training Center, Faculty of Medicine, Chiang Mai University, Chiang Mai, 50200, Thailand. Email: nchattip@gmail.com

Rosiglitazone is a synthetic agonist of the peroxisome proliferator-activated receptor γ, which has been used to reduce insulin resistance in the treatment of type 2 diabetes (Guo & Tabrizchi, 2006). Rosiglitazone acts as a potent insulin sensitizer by improving glycaemic control (Sauer *et al.* 2006). Data from various studies in the past decade have suggested that rosiglitazone also has cardioprotective effects, such as improvement of cardiac contractile dysfunction (Yue *et al.* 2005), inhibition of the inflammatory response by reducing accumulation of neutrophils and macrophages (Mersmann *et al.* 2008), and protection from myocardial injury during periods of ischaemia–reperfusion in both animal (Yue *et al.* 2001; Khandoudi *et al.* 2002; Molavi *et al.* 2006; Gonon *et al.* 2007; Mersmann *et al.* 2008) and clinical studies (Sidhu *et al.* 2003; Yu *et al.* 2007; Li *et al.* 2008).

Despite these beneficial effects, growing evidence has indicated that rosiglitazone could be harmful to the heart. A recent study in a porcine model demonstrated that treatment with rosiglitazone decreased the time to onset of spontaneous ventricular fibrillation (VF) during ischaemia (Lu *et al.* 2008). Moreover, reports on the effects of rosiglitazone on the reduction of infarct size have been inconsistent (Lautamaki *et al.* 2005; Yue *et al.* 2005; Gonon

DOI: 10.1113/expphysiol.2011.057885

et al. 2007; Graham *et al.* 2010). Growing evidence in clinical trials also indicates possible adverse cardiac effects in patients treated with rosiglitazone (Monami *et al.* 2008; Graham *et al.* 2010; Kaul *et al.* 2010; Loebstein *et al.* 2011), including increased risk of stroke, heart failure and mortality. Regardless of these controversial findings, the effect of rosiglitazone on cardiac electrophysiology, including VF inducibility and defibrillation efficacy during ischaemia–reperfusion periods, is not known.

In the present study, we aimed to determine the effect of rosiglitazone on cardiac electrophysiology during ischaemia–reperfusion periods in swine. The VF threshold (VFT), the incidence of VF occurrence, the defibrillation threshold (DFT) and the effective refractory period (ERP) during periods of ischaemia–reperfusion were determined. We tested the hypothesis that rosiglitazone attenuates the occurrence of VF by increasing the VFT, improves the defibrillation efficacy by decreasing the DFT, and reduces the infarct size during ischaemia–reperfusion periods in swine hearts. We also determined the effect of rosiglitazone on cardiac mitochondria isolated from the ischaemic and remote areas of each heart. We tested the hypothesis that rosiglitazone prevents mitochondrial damage in ischaemia–reperfusion of swine hearts by reducing production of reactive oxygen species (ROS) and preventing mitochondrial membrane potential changes. Moreover, we tested the effects of various concentrations of rosiglitazone on the function of isolated rat cardiac mitochondria exposed to oxidative stress induced by hydrogen peroxide (H_2O_2).

Methods

Ethical approval

All animal study protocols were approved by the Institutional Animal Care and Use Committees of the Faculty of Medicine, Chiang Mai University, Chiang Mai, Thailand.

Animal preparation

Twenty-six domestic pigs (20–25 kg) of either sex were used in this study. Pigs were anaesthetized by intramuscular injection of a combination of atropine (0.04 mg kg^{-1}; T.P. Drug Laboratories Co., Ltd., Bangkok, Thailand), zolitil (5 mg kg^{-1}; Vibbac Laboratories, Carros, France) and xylazine (2.2 mg kg^{-1}; Laboratorios Calier, S.A., Barcelona, Spain), and maintained by 1.5–3.0% isoflurane (Abbott Laboratories Ltd., Queenborough, UK) delivered in 100% oxygen. After cuffed endotracheal intubation, mechanical ventilation (volume controlled, tidal volume = 12 ml kg^{-1}, respiratory rate = 10–15 cycles min^{-1}) was started with pigs in a restrained dorsally recumbent position. Pancuronium (2 mg kg^{-1} loading, 0.5 mg kg^{-1} h^{-1} maintenance) was administered intravenously to minimize skeletal muscle contraction. The vital signs, including the surface electrocardiogram (lead II), femoral arterial blood pressure (BP), heart rate (HR), respiratory rate and core temperature, were continuously monitored. Blood gases and electrolytes were also monitored every 30 min and maintained within acceptable physiological ranges (Kanlop *et al.* 2008). Under fluoroscopic guidance, catheters with 34 and 68 mm platinum-coated titanium coil electrodes (Guidant Corp., St Paul, MN, USA) were inserted into the right ventricular apex and the junction between right atrium and superior vena cava, respectively. These two electrodes were used to deliver the stimulus during VFT and DFT determination (Kanlop *et al.* 2008; Sungnoon *et al.* 2008). The chest was opened through a median sternotomy, and the heart was suspended in a pericardial cradle. The pacing electrodes were affixed to the epicardium at the right ventricle (RV) outflow tract and left ventricle (LV) apex for an ERP and diastolic pacing threshold (DPT) determination. The left anterior descending coronary artery (LAD) was identified and dissected from surrounding tissues.

Study protocol

In the ischaemia–reperfusion study, pigs were divided into two groups. Group I ($n = 12$) received rosiglitazone, and group II ($n = 10$) received normal saline solution. In each pig, the cardiac electrophysiological parameters, including DPT, ERP, corrected QT interval (QTc), VFT and DFT, were determined at the beginning of the study. Then, pigs were randomly assigned to receive either rosiglitazone potassium salt (Cayman Chemical, Ann Arbor, MI, USA; 1 mg kg^{-1} dissolved in 30 ml sterile normal saline solution) or the same volume of sterile normal saline injected intravenously over 60 min. After that, the LAD was ligated with sterile 4–0 silk suture material 5 cm above a distal branch to perform a regional occlusion (Kanlop *et al.* 2011). During the first 20 min of occlusion, if spontaneous VF occurred, the defibrillation shock was delivered to determine the DFT. If VF did not occur within 20 min, VF was electrically induced, and the DFT and VFT were determined using a three-reversal up/down protocol (Kanlop *et al.* 2011). The ischaemic period was sustained for 60 min and then the LAD ligation was released to promote reperfusion for 120 min. All studied parameters were determined again beginning at 60 min after reperfusion.

At the end of experiment, the heart was removed for the determination of the myocardial infarction size. Furthermore, isolated cardiac mitochondria taken from the ischaemic and non-ischaemic areas in each heart were used to determine cardiac mitochondrial function ($n = 4$ in each group). In this study, another group of four pigs without LAD occlusion were also studied for

the electrophysiological effects of rosiglitazone in normal hearts. In this group, haemodynamic parameters as well as the DPT, ERP and DFT were determined before and after rosiglitazone administration.

Diastolic pacing threshold determination

The DPT testing was performed by delivering a train of 10 S1 stimuli of a 5 ms square pulse via the electrode at the tip of the RV catheter at 400 ms intervals. The current was started at 0.1 mA and was increased in 0.1 mA steps until all drive trains elicited a ventricular response (capture). The DPT was defined as the minimal current strength necessary to capture the ventricle (Shinlapawittayatorn *et al.* 2006; Kanlop *et al.* 2008).

Effective refractory period determination

In each train of 10 S1 stimuli, an S2 stimulus (2 × DPT) was introduced in late diastole of the last S1-paced beat (350 ms after the R wave) to elicit a capture. The basic S1–S2 coupling interval was decreased in 10 ms steps until S2 failed to elicit a capture. The ERP was defined as the longest S1–S2 interval at which an S2 stimulus fails to elicit a ventricular response (Kanlop *et al.* 2008).

Ventricular fibrillation threshold determination

The heart was paced three times. The interval between the last S1 and the mid-T wave was determined each time and the average of S1–mid-T wave interval was used as a coupling interval between the last S1 and S2 shock. The VFT testing was performed by delivering S2 shocks which started at 100 V. If this shock induced VF, decrements of 10 V steps were used for each successive shock until VF was no longer induced. If 100 V did not induce VF, increments of 10 V steps were used for each successive shock until VF was induced. The lowest shock strength that could induce VF was the VFT (Kanlop *et al.* 2008).

Defibrillation threshold determination

The defibrillation shock was delivered after 10 s of VF to determine the DFT by using a three-reversal up/down protocol (Kanlop *et al.* 2011). The DFT was defined as the lowest energy required for successful defibrillation of VF after three reversal points, when the next lower setting failed to defibrillate the heart. During the VF event, if the tested shock failed to defibrillate, a rescue shock (600–700 V) was delivered to successfully defibrillate the heart. A period of 4 min was allowed between each VF induction so that the heart could recover (Kanlop *et al.* 2008).

Infarct size and area at risk (AAR) measurement

At the end of each experiment, the heart were removed and irrigated with normal saline to wash out blood from chambers and vessels. The LAD was occluded again at the same site previously done during the ischaemic period. The catheters were inserted into the right and left coronary ostia for Evans Blue dye infusion. The area which could not be infused by Evans Blue was defined as the area of no blood flow during the ischaemic period. The heart was frozen and cut horizontally into 5-mm-thick slices, starting from the apex until 5 mm above the occluding site. Then, each slice was immersed in triphenyltetrazolium chloride for at least 25 min, after which the area with viable tissue could be seen in red. The area that was not stained with Evans Blue was defined as the AAR. The area which demonstrated neither blue nor red was defined as the infarct site (Kanlop *et al.* 2011). The area measurement was performed with Image tool software version 3.0 (The University of Texas Health Science Center at San Antonio, Texas, USA). The infarct size was calculated depending on the weight of each slice as described previously (Kanlop *et al.* 2011).

Table 1. Basic electrophysiological and haemodynamic parameters in normal hearts without left anterior descending coronary artery occlusion

Parameter	Baseline	After rosiglitazone administration
Heart rate (beats min^{-1})	110 ± 9	112 ± 5
Systolic blood pressure (mmHg)	88 ± 3	86 ± 2
Diastolic blood pressure (mmHg)	58 ± 4	57 ± 2
Mean arterial blood pressure (mmHg)	68 ± 4	67 ± 2
Effective refractory period (ms)		
Right ventricular apex (endocardium)	263 ± 19	265 ± 13
Right ventricular outflow tract (epicardium)	265 ± 19	255 ± 13
Left ventricular apex (epicardium)	255 ± 10	255 ± 10
Diastolic pacing threshold (mA)		
Right ventricular apex (endocardium)	0.18 ± 0.05	0.20 ± 0.00
Right ventricular outflow tract (epicardium)	0.18 ± 0.05	0.20 ± 0.08
Left ventricular apex (epicardium)	0.13 ± 0.05	0.15 ± 0.06
Corrected QT interval (ms)	530 ± 68	481 ± 36
QRS duration (ms)	62 ± 9	59 ± 7
Defibrillation threshold		
Peak voltage (V)	340 ± 41	287 ± 32
Total energy (J)	9 ± 2	5 ± 3
Impedance (Ω)	63 ± 6	58 ± 7
Pulse width (ms)	17 ± 1	16 ± 2

Cardiac mitochondrial isolation

Cardiac mitochondria were isolated from the ischaemic and non-ischaemic regions, using the technique described

Table 2. Basic electrophysiological and haemodynamic parameters in hearts during ischaemia–reperfusion protocol

	Saline group			Rosiglitazone group		
Parameter	Baseline	Ischaemia	Reperfusion	Baseline	Ischaemia	Reperfusion
Heart rate (beats min^{-1})	107 ± 7	112 ± 8	117 ± 9	103 ± 17	113 ± 18	116 ± 21
Systolic blood pressure (mmHg)	104 ± 8	97 ± 11	93 ± 10	96 ± 15	91 ± 10	92 ± 14
Diastolic blood pressure (mmHg)	65 ± 7	63 ± 9	55 ± 8	60 ± 8	53 ± 5	53 ± 12
Mean arterial blood pressure (mmHg)	70 ± 25	67 ± 25	61 ± 23	66 ± 23	61 ± 20	60 ± 22
Corrected QT interval (ms)	463 ± 45	492 ± 55	495 ± 33	461 ± 47	455 ± 51	459 ± 48
QRS duration (ms)	55 ± 10	55 ± 9	58 ± 10	61 ± 13	61 ± 8	59 ± 10
Effective refractory period (ms)						
Right ventricular apex (endocardium)	242 ± 17	252 ± 23	246 ± 27	260 ± 13	259 ± 7	248 ± 38
Right ventricular outflow tract (epicardium)	234 ± 28	241 ± 25	240 ± 21	253 ± 16	263 ± 16	257 ± 45
Left ventricular apex (epicardium)	226 ± 22	219 ± 38	238 ± 29	247 ± 20	239 ± 32	257 ± 45
Diastolic pacing threshold (mA)						
Right ventricular apex (endocardium)	0.20 ± 0.05	0.51 ± 0.27	0.52 ± 0.18	0.25 ± 0.16	0.60 ± 0.61	0.60 ± 0.29
Right ventricular outflow tract (epicardium)	0.21 ± 0.14	0.26 ± 0.10	0.24 ± 0.09	0.25 ± 0.12	0.31 ± 0.16	0.32 ± 0.17
Left ventricular apex (epicardium)	0.19 ± 0.09	0.54 ± 0.44	1.03 ± 0.90	0.22 ± 0.13	0.58 ± 0.75	1.13 ± 1.06

Table 3. Ventricular fibrillation threshold and defibrillation threshold

	Saline group			Rosiglitazone group		
Parameter	Baseline	Ischaemia	Reperfusion	Baseline	Ischaemia	Reperfusion
Ventricular fibrillation threshold						
Peak voltage (V)	36 ± 12	30 ± 12	26 ± 5	32 ± 9	40 ± 16	42 ± 22
Total energy (J)	0.10 ± 0.07	0.07 ± 0.07	0.04 ± 0.02	0.04 ± 0.01	0.13 ± 0.11	0.15 ± 0.18
Impedance (Ω)	70 ± 7	65 ± 6	67 ± 6	74 ± 10	72 ± 8	68 ± 5
Pulse width (ms)	16 ± 3	15 ± 2	14 ± 2.65	17 ± 2	17 ± 3	16 ± 3
Defibrillation threshold						
Peak voltage (V)	387 ± 160	382 ± 74	349 ± 92	486 ± 133	470 ± 112	384 ± 125
Total energy (J)	14 ± 7	11 ± 4	10 ± 5	19 ± 10	18 ± 9	12 ± 9
Impedance (Ω)	63 ± 10	61 ± 7	60 ± 8	63 ± 8	62 ± 9	61 ± 9
Pulse width (ms)	17 ± 2	16 ± 1	16 ± 2	17 ± 2	17 ± 2	16 ± 2

previously (Thummasorn *et al.* 2011), and the protein concentration was determined according to bicinchoninic acid assay (Thummasorn *et al.* 2011).

Reactive oxygen species measurement

The fluorescent dye dichlorohydro-fluorescein diacetate (DCFDA) was used to determine the level of ROS production in cardiac mitochondria (Thummasorn *et al.* 2011). The DCFDA could pass through the mitochondrial membrane, and was oxidized by ROS in the mitochondria into DCF. Fluorescence was determined at $\lambda_{excitation}$ 485 nm and $\lambda_{emission}$ 530 nm using a fluorescence microplate reader. The ROS level was expressed as arbitrary units of fluorescence intensity of DCF.

Measurement of mitochondrial membrane potential changes ($\Delta\Psi m$)

The dye 5,5′,6,6′-tetrachloro-1,1′,3,3′-tetraethyl-benzimidazolcarbocyanine iodide (JC-1) was used to determined the change in the mitochondrial membrane potential (Thummasorn *et al.* 2011). JC-1 was characterized as a cation and remained in the mitochondrial matrix as a monomer (green fluorescence) form. However, it could interact with anions in the mitochondrial matrix to form an aggregate (red fluorescence) form. JC-1 monomer fluorescence (green) was excited at 485 nm and the emission detected at 530 nm. JC-1 aggregate fluorescence (red) was excited at 485 nm and the emission fluorescence recorded at 590 nm. Mitochondrial depolarization was indicated by a decrease in the red/green fluorescence intensity ratio.

Isolated rat cardiac mitochondria study protocol

To investigate the dose-dependent effect of rosiglitazone on mitochondrial function, male Wistar rats (300–350 g, ∼2 months old) were used for cardiac mitochondrial isolation. Rats were deeply anesthetized by intraperitonial injection of thiopental (0.5 mg/kg; Research institute of antibiotics and biotransformations, Roztoky, Czech Republic), after which the heart was removed. Cardiac mitochondria were obtained using the differential centrifugation technique as previously described (Thummasorn *et al.* 2011). Isolated cardiac

mitochondrial morphology was confirmed by using an electron microscope. Isolated cardiac mitochondria were divided into eight groups ($n = 5$ in each group) as follows: (1) control group; (2) 2 mM H_2O_2-treated group; (3) 10 μM rosiglitazone pretreated for 15 min; (4) 25 μM rosiglitazone pretreated for 15 min; (5) 50 μM rosiglitazone pretreated for 15 min; (6) 10 μM rosiglitazone pretreated for 15 min, followed by 5 min 2 mM H_2O_2 application; (7) 25 μM rosiglitazone pretreated for 15 min, followed by 5 min 2 mM H_2O_2 application; and (8) 50 μM rosiglitazone pretreated for 15 min, followed by 5 min 2 mM H_2O_2 application. Production of ROS and $\Delta\Psi$m were determined in all groups. The 2 mM H_2O_2 was used because it has been shown to be an optimal dose to cause cardiac mitochondrial dysfunction (Thummasorn *et al.* 2011).

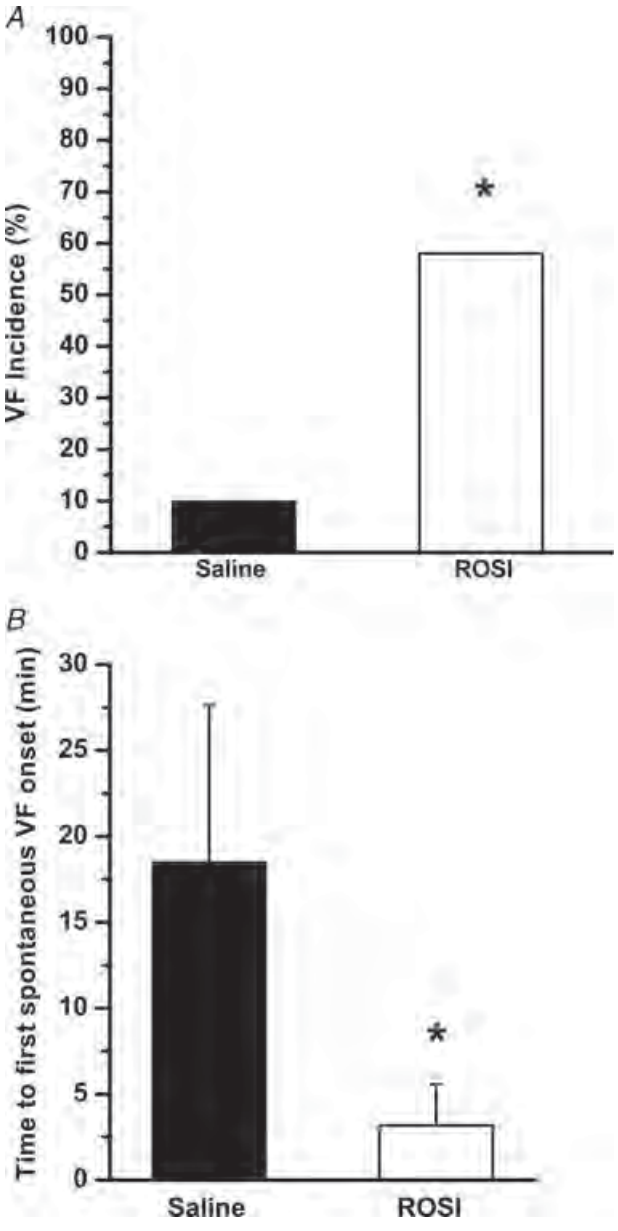

Figure 1. Rosiglitazone (ROSI) and the occurrence of ventricular fibrillation (VF)
Rosiglitazone significantly decreased the time interval from left anterior coronary artery occlusion to the first spontaneous VF onset ($n = 12$; *A*; $^*P < 0.05$ *versus* saline group, Mann–Whitney *U* test) and increased the incidence of VF ($n = 12$; *B*), in comparison with the saline group. $^*P < 0.05$ *versus* saline group (χ^2 test).

Statistical analysis

Data were expressed as means ± SD. Comparisons of variables at baseline, ischaemic and reperfusion periods (comparison within group) were performed using the Wilcoxon signed ranks test. Comparisons among groups were performed using the Mann–Whitney *U* test. Comparisons of the incidence of VF among groups were evaluated by χ^2 test. A value of $P < 0.05$ was considered statistically significant.

Results

The basic electrophysiological and haemodynamic parameters in normal swine heart (i.e. without ischaemia–reperfusion) are shown in Table 1. Acute intravenous administration of rosiglitazone (1.0 mg kg^{-1}) altered neither hemodynamics nor cardiac electrophysiologic parameters.

For the ischaemia–reperfusion experiment, the basic electrophysiological and haemodynamic parameters prior to and during ischaemia–reperfusion are shown in Table 2. Neither saline nor rosiglitazone altered any of the haemodynamic parameters during the ischaemia–reperfusion period. The ERP during the ischaemic phase tended to decrease in the ischaemic region (i.e. LV apex); however, it did not reach statistical significance in either the saline or the rosiglitazone group.

For the VFT, peak voltage and total delivered energy during ischaemic as well as reperfusion periods were not statistically different from the baseline values when treated with rosiglitazone (Table 3). Similar to the VFT, the DFT determined during ischaemic and reperfusion periods were not different compared with the baseline value in both saline- and rosiglitazone-treated groups (Table 3).

The incidence of spontaneous VF was also significantly increased in rosiglitazone-treated pigs (seven of 12 pigs) compared with the saline group (one of 10 pigs; Fig. 1*A*). Moreover, acute intravenous administration of rosiglitazone significantly reduced the time interval from LAD ligation to the onset of the first spontaneous VF occurrence during ischaemia–reperfusion compared with that in the saline group (Fig. 1*B*). However, the dispersion of refractoriness as shown by the standard deviation of the three ERPs measured at three different sites was not different between the saline- and the rosiglitazone-treated group (Fig. 2). Unlike the effect on VF incidence, the areas

of myocardial infarction (i.e. the ratio of infarct size to AAR) in the rosiglitazone group were decreased ($P < 0.05$) compared with the saline group (Fig. 3).

In isolated cardiac mitochondria, rosiglitazone could not prevent mitochondrial membrane potential changes (Fig. 4*A*). Moreover, rosiglitazone could not reduce the level of ROS production in the ischaemic myocardium (Fig. 4*B*).

In rat isolated cardiac mitochondria treated with rosiglitazone at 10, 25 and 50 μM, the drug did not alter cardiac mitochondrial ROS level or membrane potential changes, in comparison to the control group

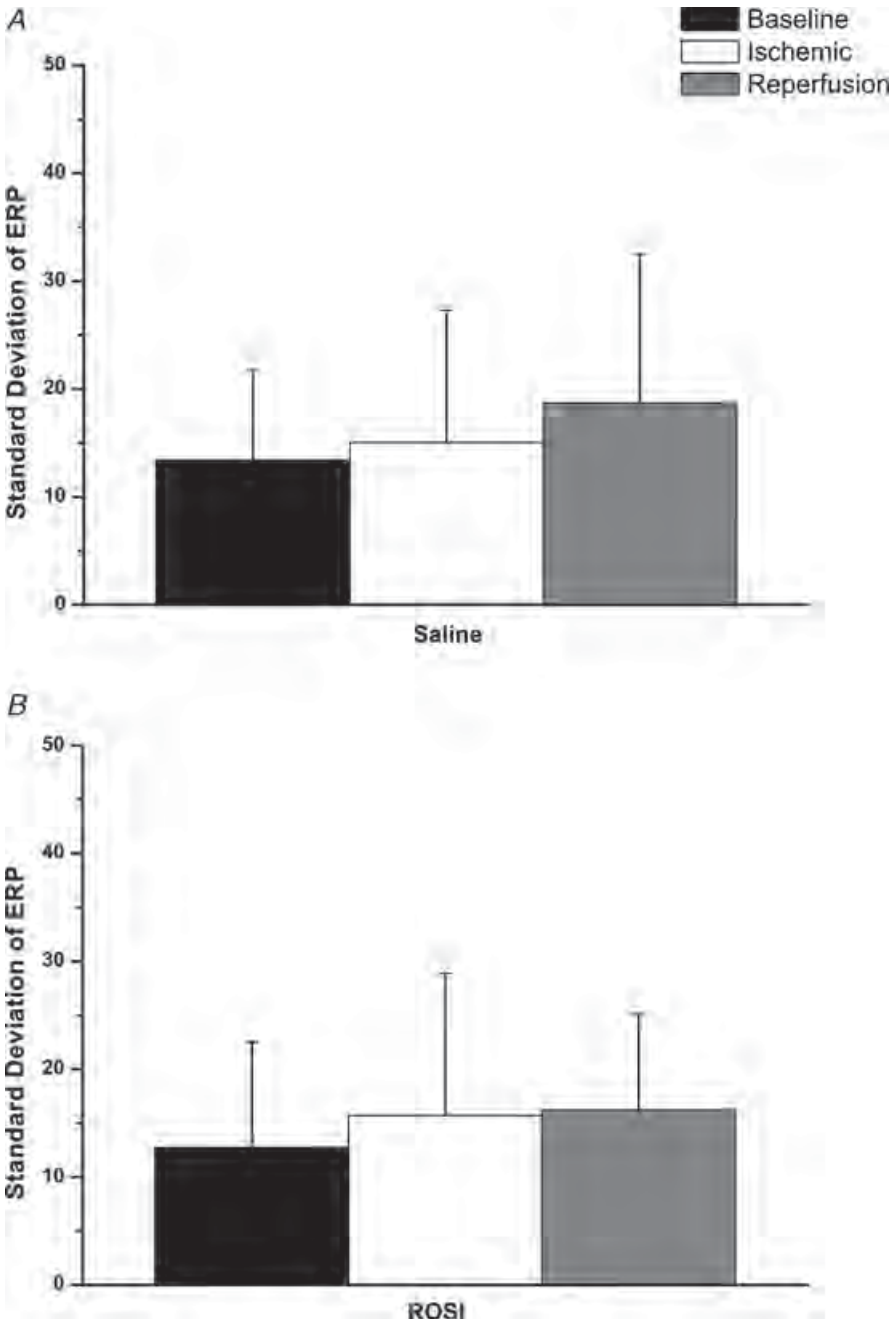

Figure 2. Effect of rosiglitazone on the dispersion of the effective refractory period (ERP) during ischaemia–reperfusion periods
Standard deviation of ERP at baseline and during ischaemia and reperfusion periods was not different in saline group ($n = 10$; *A*) and the rosiglitazone group ($n = 12$; *B*), indicating that rosiglitazone did not cause any change in the dispersion of refractoriness compared with the saline group.

(Fig. 5). When cardiac mitochondria were under severe oxidative stress caused by H_2O_2, i.e. conditions that mimic ischaemia–reperfusion injury, cardiac mitochondrial dysfunction was observed as indicated by a decrease in the red/green fluorescence ratio, indicating cardiac mitochondrial membrane depolarization (Fig. 5*A*) and an increase in ROS level (Fig. 5*B*). None of the three concentrations of rosiglitazone could prevent or attenuate cardiac mitochondrial dysfunction caused by oxidative stress in these isolated cardiac mitochondria (Fig. 5).

Discussion

The major findings of the present study are as follows. In ischaemia–reperfusion of the swine heart, acute intravenous administration of rosiglitazone had the following effects: (1) it facilitated the occurrence of ventricular fibrillation; (2) it reduced the myocardial infarction area; and (3) it failed to prevent cardiac mitochondrial ROS production and mitochondrial depolarization caused by ischaemia–reperfusion injury. Furthermore, acute intravenous administration of rosiglitazone did not alter the basic cardiac electrophysiology and haemodynamic parameters both in normal hearts and in hearts during ischaemia–reperfusion.

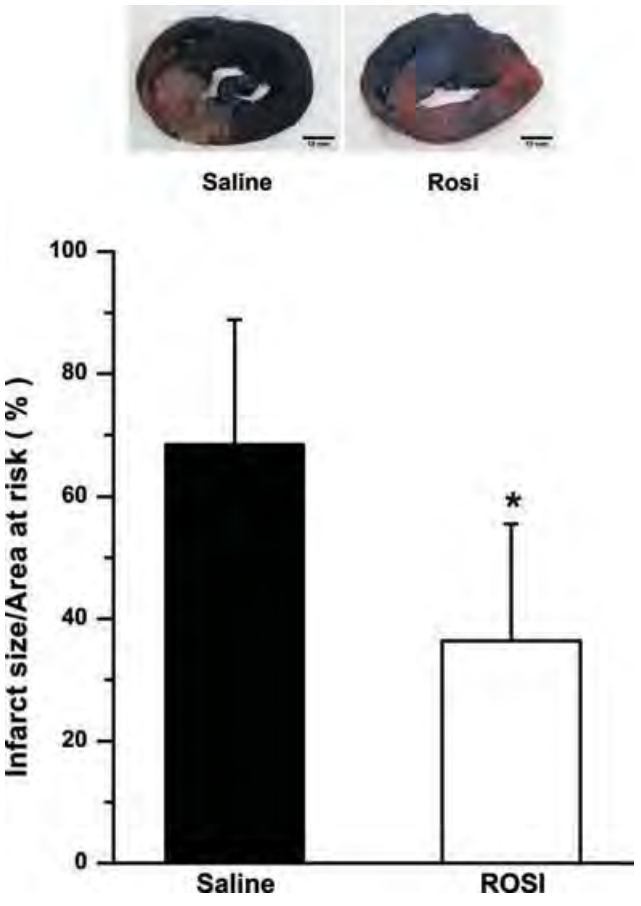

Figure 3. Rosiglitazone and the infarct size
The infarct size in the rosiglitazone group ($n = 12$) was significantly smaller than that in the saline group ($n = 10$). $^{*}P < 0.05$ *versus* saline group (Mann–Whitney *U* test).

In the present study, our finding that acute administration of rosiglitazone did not alter haemodynamic parameters in swine is consistent with a previous report that rosiglitazone did not alter the blood pressure (Lu *et al.* 2008). In addition to haemodynamics, our study also demonstrated for the first time that the basic cardiac electrophysiological parameters as well as the defibrillation efficacy and the VFT were not altered by rosiglitazone in both normal conditions and ischaemia–reperfusion in swine hearts.

During the ischaemic period, our results clearly demonstrated that pigs treated with rosiglitazone had a higher incidence of VF than in the vehicle group. This novel finding indicates that rosiglitazone could facilitate VF initiation in the heart during ischaemia. This adverse effect of rosiglitazone could be responsible for the increased mortality associated with the use of rosiglitazone reported in previous clinical trials (Diamond *et al.* 2007; Nissen & Wolski, 2007; Cobitz *et al.* 2008). Moreover, our results also demonstrated that pigs treated with rosiglitazone also had a shorter time interval from LAD occlusion to the onset of the first spontaneous VF. This latter finding is also consistent with a previous report which demonstrated that rosiglitazone decreased the time to onset of VF during complete coronary occlusion (Lu *et al.* 2008). Both the increased VF incidence and the shorter interval to VF onset suggest that rosiglitazone is proarrhythmic in this model of ischaemia–reperfusion in swine hearts.

It has been proposed that rosiglitazone blocks K_{ATP} channels, and thus alters the action potential shortening during ischaemia and may promote arrhythmia by causing a greater dispersion of refractoriness in myocardial tissue (Janse, 1998). However, our findings do not support this hypothesis, because the dispersion of refractoriness observed in the present study was not different between pigs treated with rosiglitazone and vehicle, suggesting that the profibrillatory effect of rosiglitazone may not be due to facilitating the increased dispersion of ERP during ischaemia.

One possible mechanism of the profibrillatory effect of rosiglitazone could be due to its effects on the cardiac mitochondria. Increased ROS production and oscillation of the mitochondrial membrane potential ($\Delta\Psi m$) have been shown to play an important role in the genesis of cardiac arrhythmias (Aon *et al.* 2009). In the present study, cardiac mitochondria isolated from ischaemic and non-ischaemic areas of swine hearts demonstrated that the clinically relevant dose of rosiglitazone used in this study could not prevent the collapse of $\Delta\Psi m$

and did not reduce the mitochondrial ROS level during ischaemia–reperfusion injury. In rat isolated cardiac mitochondria, our results demonstrated that rosiglitazone at any tested concentrations could neither prevent mitochondrial membrane potential depolarization nor reduce mitochondrial ROS level against oxidative stress caused by H_2O_2, which mimics ischaemia–reperfusion injury. As cardiac mitochondrial ROS production and mitochondrial depolarization have been shown to be responsible for fatal arrhythmias (Aon *et al.* 2009), our findings indicate that rosiglitazone could not prevent the deterioration of mitochondrial function during ischaemia–reperfusion injury.

The only beneficial effect of rosiglitazone found in the present study is that it could significantly reduce the myocardial infarct size. This finding is consistent

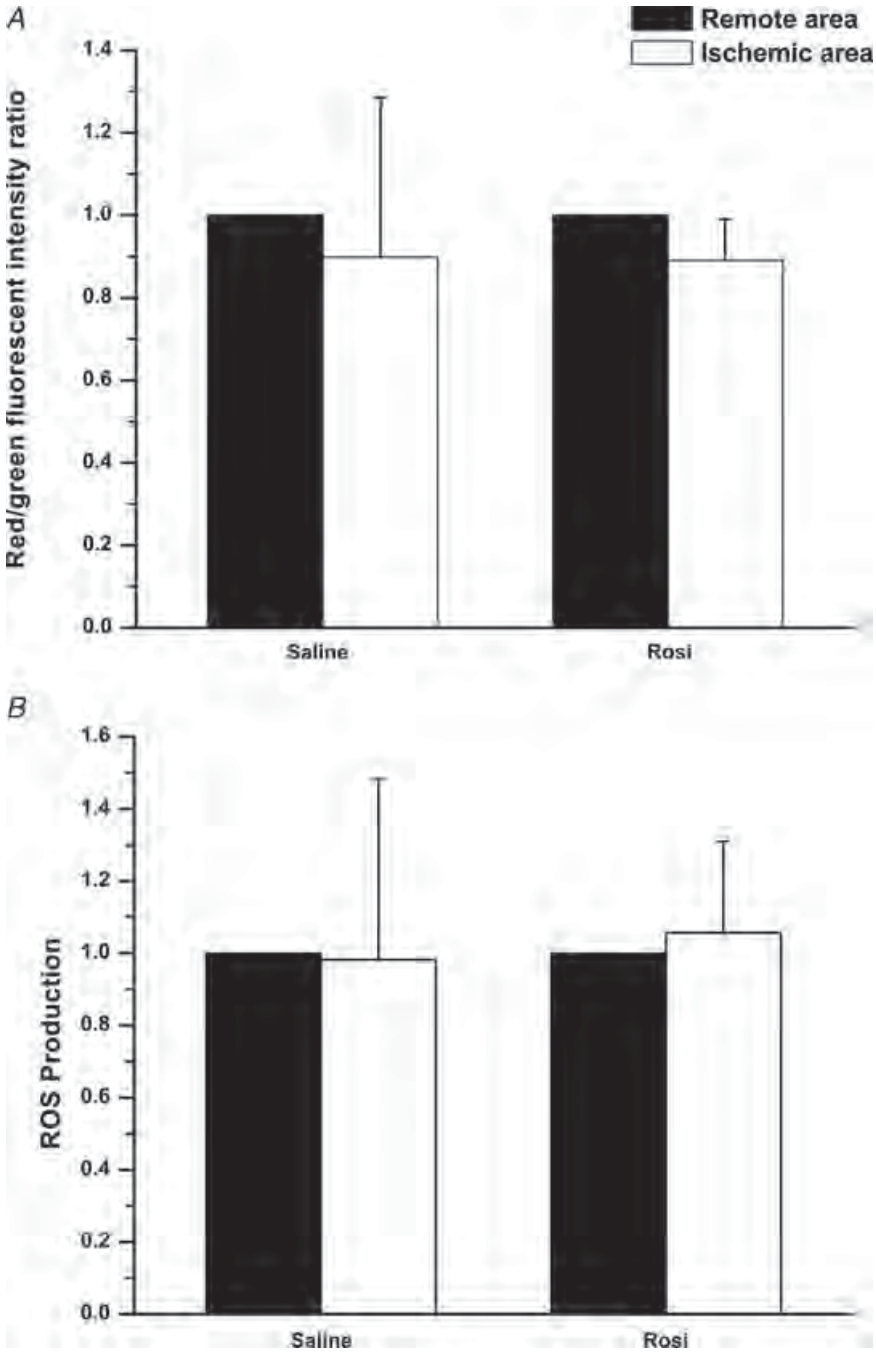

Figure 4. Effect of rosiglitazone on cardiac mitochondria after ischaemia–reperfusion in swine
Rosiglitazone neither prevented mitochondrial membrane depolarization (*A*) nor decreased mitochondrial ROS production (*B*) in the ischaemic myocardium, in comparison to the saline group ($n = 4$).

with previous *in vivo* studies showing that rosiglitazone reduced the ratio of infarct size to the area at risk (Sidell *et al.* 2002; Liu *et al.* 2004; Yue *et al.* 2005; Tao *et al.* 2010; Zhang *et al.* 2010), suggesting that rosiglitazone has an anti-apoptotic effect in myocardium during ischaemia–reperfusion. As mitochondrial ROS production is involved in cell apoptotic pathways (Loor *et al.* 2011) and rosiglitazone could not prevent ROS production, our findings suggest that anti-apoptotic effect of rosiglitazone may not be direct, via the mitochondria, but that it could be involved in the extrinsic apoptotic signalling pathway, which is a mitochondria-independent apoptosis pathway that mediates cellular apoptosis by activating death receptors and transmiting

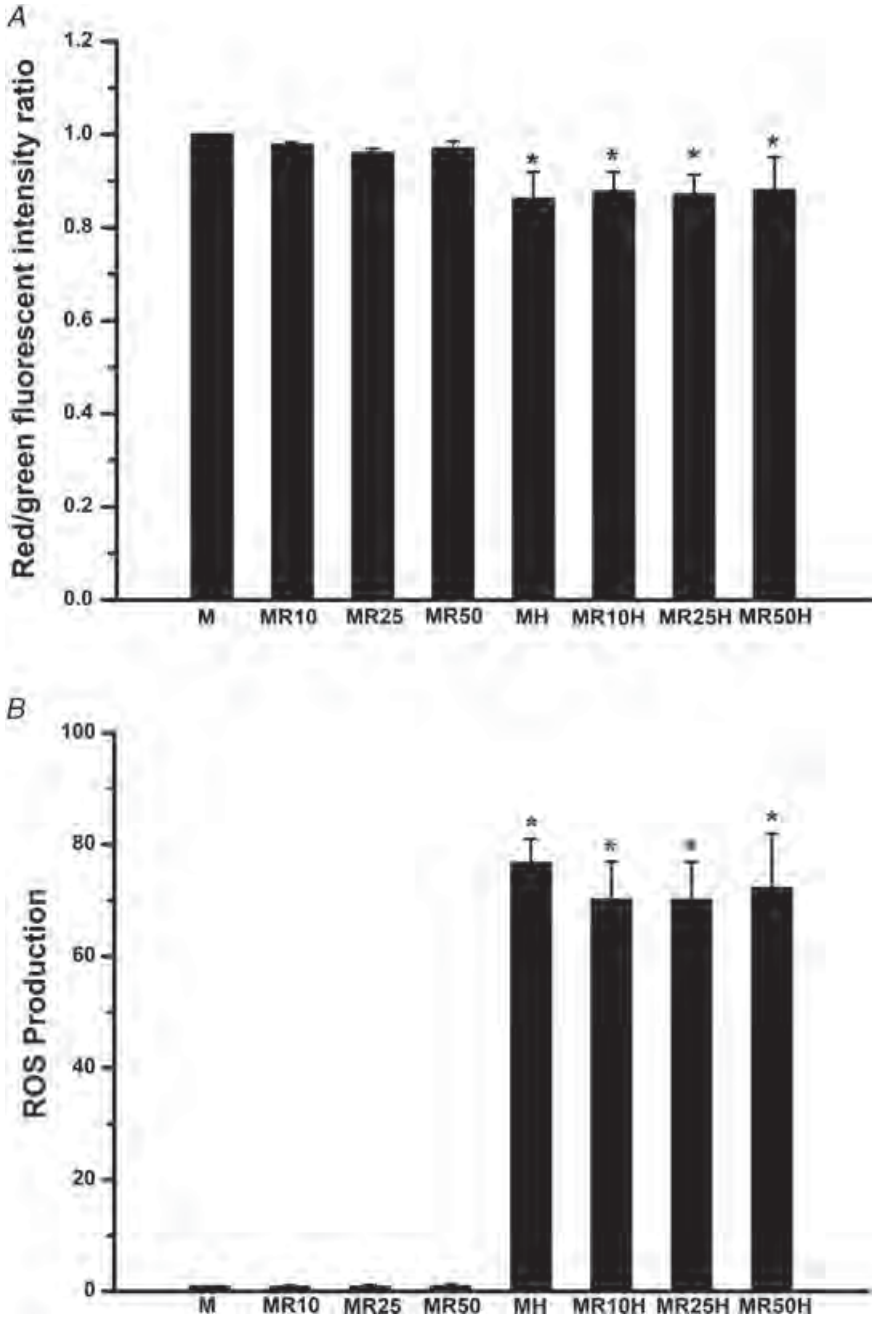

Figure 5. Effect of various concentrations of rosiglitazone on rat isolated cardiac mitochondrial function
Rosiglitazone neither prevented mitochondrial membrane depolarization (*A*) nor decreased mitochondrial ROS production (*B*) under severe oxidative stress induced by H_2O_2, compared with the mitochondrial group. The eight columns in the figure correspond to the eight groups described in the Methods.

apoptotic signals after ligation with specific ligands (Ashe & Berry, 2003; Delhalle *et al.* 2003). However, the inflammatory response could also be responsible for the infarct size reduction observed in this study. Previous studies demonstrated that inflammation could play an important role in myocardial infarction during ischaemia–reperfusion (Werns & Lucchesi, 1987; Bonvini *et al.* 2005); therefore, inhibition of the inflammatory response might reduce myocardial infarct size (Werns & Lucchesi, 1987). As rosiglitazone has been shown to inhibit the inflammatory response by reducing the accumulation of neutrophils and macrophages and the expression of monocyte chemoattractant protein-1 (MCP-1) in the ischaemic heart (Yue *et al.* 2001) and by inhibiting the inflammatory cytokines tumour necrosis factor-α and nuclear factor-κB (Shah *et al.* 2005), the infarct size reduction found in this study could be due to the anti-inflammatory effect of rosiglitazone. Future studies are required to elucidate the anti-apoptotic mechanism of rosiglitazone. Nevertheless, the controversy regarding the cardioprotective effect of rosiglitazone by its ability to decrease the infarct size (Sidell *et al.* 2002; Liu *et al.* 2004; Yue *et al.* 2005; Tao *et al.* 2010; Zhang *et al.* 2010) and the increased mortality with its use (Lygate *et al.* 2003; Lu *et al.* 2008; Blasi *et al.* 2009) have converged into the present study showing that rosiglitazone, despite its infarct size reduction effect, facilitates the occurrence of fatal arrhythmia during ischaemia–reperfusion injury, and could be responsible for increased mortality in patients using this drug, as shown in clinical trials (Diamond *et al.* 2007; Home *et al.* 2007; Lipscombe *et al.* 2007; Nissen & Wolski, 2007).

Study limitation

In the present study, we did not assess the anti-inflammatory signalling, cardiac function or structural changes of cardiomyocytes. However, previous studies demonstrated that rosiglitazone could improve cardiac function during ischaemia–reperfusion (Geng *et al.* 2006; Gonon *et al.* 2007), suggesting that rosiglitazone could influence cardiac function during ischaemia–reperfusion injury.

References

Aon MA, Cortassa S, Akar FG, Brown DA, Zhou L & O'Rourke B (2009). From mitochondrial dynamics to arrhythmias. *Int J Biochem Cell Biol* **41**, 1940–1948.

Ashe PC & Berry MD (2003). Apoptotic signaling cascades. *Prog Neuropsychopharmacol Biol Psychiatry* **27**, 199–214.

Blasi ER, Heyen J, Hemkens M, McHarg A, Ecelbarger CM & Tiwari S (2009). Effects of chronic PPAR-agonist treatment on cardiac structure and function, blood pressure, and kidney in healthy Sprague-Dawley rats. *PPAR Res* **2009**, 237865.

Bonvini RF, Hendiri T & Camenzind E (2005). Inflammatory response post-myocardial infarction and reperfusion: a new therapeutic target? *Eur Heart J Suppl* **7**, I27–I36.

Cobitz A, Zambanini A, Sowell M, Heise M, Louridas B, McMorn S, Semigran M & Koch G (2008). A retrospective evaluation of congestive heart failure and myocardial ischemia events in 14,237 patients with type 2 diabetes mellitus enrolled in 42 short-term, double-blind, randomized clinical studies with rosiglitazone. *Pharmacoepidemiol Drug Saf* **17**, 769–781.

Delhalle S, Duvoix A, Schnekenburger M, Morceau F, Dicato M & Diederich M (2003). An introduction to the molecular mechanisms of apoptosis. *Ann N Y Acad Sci* **1010**, 1–8.

Diamond GA, Bax L & Kaul S (2007). Uncertain effects of rosiglitazone on the risk for myocardial infarction and cardiovascular death. *Ann Intern Med* **147**, 578–581.

Geng DF, Wu W, Jin DM, Wang JF & Wu YM (2006). Effect of peroxisome proliferator-activated receptor γ ligand. Rosiglitazone on left ventricular remodeling in rats with myocardial infarction. *Int J Cardiol* **113**, 86–91.

Gonon AT, Bulhak A, Labruto F, Sjoquist PO & Pernow J (2007). Cardioprotection mediated by rosiglitazone, a peroxisome proliferator-activated receptor gamma ligand, in relation to nitric oxide. *Basic Res Cardiol* **102**, 80–89.

Graham DJ, Ouellet-Hellstrom R, MaCurdy TE, Ali F, Sholley C, Worrall C & Kelman JA (2010). Risk of acute myocardial infarction, stroke, heart failure, and death in elderly Medicare patients treated with rosiglitazone or pioglitazone. *JAMA* **304**, 411–418.

Guo L & Tabrizchi R (2006). Peroxisome proliferator-activated receptor gamma as a drug target in the pathogenesis of insulin resistance. *Pharmacol Ther* **111**, 145–173.

Home PD, Pocock SJ, Beck-Nielsen H, Gomis R, Hanefeld M, Jones NP, Komajda M & McMurray JJ; RECORD Study Group (2007). Rosiglitazone evaluated for cardiovascular outcomes– an interim analysis. *N Engl J Med* **357**, 28–38.

Janse MJ (1998). Vulnerability to ventricular fibrillation. *Chaos* **8**, 149–156.

Kanlop N, Shinlapawittayatorn K, Sungnoon R, Chattipakorn S, Lailerd N & Chattipakorn N (2008). Sildenafil citrate on the inducibility of ventricular fibrillation and upper limit of vulnerability in swine. *Med Sci Monit* **14**, BR205–BR209.

Kanlop N, Thommasorn S, Palee S, Weerateerangkul P, Suwansirikul S, Chattipakorn S & Chattipakorn N (2011). Granulocyte colony-stimulating factor stabilizes cardiac electrophysiology and decreases infarct size during cardiac ischaemic/reperfusion in swine. *Acta Physiol (Oxf)* **202**, 11–20.

Kaul S, Bolger AF, Herrington D, Giugliano RP & Eckel RH (2010). Thiazolidinedione drugs and cardiovascular risks: a science advisory from the American Heart Association and American College Of Cardiology Foundation. *J Am Coll Cardiol* **55**, 1885–1894.

Khandoudi N, Delerive P, Berrebi-Bertrand I, Buckingham RE, Staels B & Bril A (2002). Rosiglitazone, a peroxisome proliferator-activated receptor-γ, inhibits the Jun NH_2-terminal kinase/activating protein 1 pathway and protects the heart from ischemia/reperfusion injury. *Diabetes* **51**, 1507–1514.

Lautamaki R, Airaksinen KE, Seppanen M, Toikka J, Luotolahti M, Ball E, Borra R, Harkonen R, Iozzo P, Stewart M, Knuuti J & Nuutila P (2005). Rosiglitazone improves myocardial glucose uptake in patients with type 2 diabetes and coronary artery disease: a 16-week randomized, double-blind, placebo-controlled study. *Diabetes* **54**, 2787–2794.

Li J, Liu NF & Wei Q (2008). Effect of rosiglitazone on cardiac fibroblast proliferation, nitric oxide production and connective tissue growth factor expression induced by advanced glycation end-products. *J Int Med Res* **36**, 329–335.

Lipscombe LL, Gomes T, Levesque LE, Hux JE, Juurlink DN & Alter DA (2007). Thiazolidinediones and cardiovascular outcomes in older patients with diabetes. *JAMA* **298**, 2634–2643.

Liu HR, Tao L, Gao E, Lopez BL, Christopher TA, Willette RN, Ohlstein EH, Yue TL & Ma XL (2004). Anti-apoptotic effects of rosiglitazone in hypercholesterolemic rabbits subjected to myocardial ischemia and reperfusion. *Cardiovasc Res* **62**, 135–144.

Loebstein R, Dushinat M, Vesterman-Landes J, Silverman B, Friedman N, Katzir I, Kurnik D, Lomnicky Y, Kokia E & Halkin H (2011). Database evaluation of the effects of long-term rosiglitazone treatment on cardiovascular outcomes in patients with type 2 diabetes. *J Clin Pharmacol* **51**, 173–180.

Loor G, Kondapalli J, Iwase H, Chandel NS, Waypa GB, Guzy RD, Vanden Hoek TL & Schumacker PT (2011). Mitochondrial oxidant stress triggers cell death in simulated ischemia–reperfusion. *Biochim Biophys Acta* **1813**, 1382–1394.

Lu L, Reiter MJ, Xu Y, Chicco A, Greyson CR & Schwartz GG (2008). Thiazolidinedione drugs block cardiac K_{ATP} channels and may increase propensity for ischaemic ventricular fibrillation in pigs. *Diabetologia* **51**, 675–685.

Lygate CA, Hulbert K, Monfared M, Cole MA, Clarke K & Neubauer S (2003). The PPARγ-activator rosiglitazone does not alter remodeling but increases mortality in rats post-myocardial infarction. *Cardiovasc Res* **58**, 632–637.

Mersmann J, Tran N, Zacharowski PA, Grotemeyer D & Zacharowski K (2008). Rosiglitazone is cardioprotective in a murine model of myocardial I/R. *Shock* **30**, 64–68.

Molavi B, Chen J & Mehta JL (2006). Cardioprotective effects of rosiglitazone are associated with selective overexpression of type 2 angiotensin receptors and inhibition of p42/44 MAPK. *Am J Physiol Heart Circ Physiol* **291**, H687–H693.

Monami M, Marchionni N & Mannucci E (2008). Winners and losers at the rosiglitazone gamble: a meta-analytical approach at the definition of the cardiovascular risk profile of rosiglitazone. *Diabetes Res Clin Pract* **82**, 48–57.

Nissen SE & Wolski K (2007). Effect of rosiglitazone on the risk of myocardial infarction and death from cardiovascular causes. *N Engl J Med* **356**, 2457–2471.

Sauer WH, Cappola AR, Berlin JA & Kimmel SE (2006). Insulin sensitizing pharmacotherapy for prevention of myocardial infarction in patients with diabetes mellitus. *Am J Cardiol* **97**, 651–654.

Shah RD, Gonzales F, Golez E, Augustin D, Caudillo S, Abbott A, Morello J, McDonough PM, Paolini PJ & Shubeita HE (2005). The antidiabetic agent rosiglitazone upregulates SERCA2 and enhances TNF-α- and LPS-induced NF-κB-dependent transcription and TNF-α-induced IL-6 secretion in ventricular myocytes. *Cell Physiol Biochem* **15**, 41–50.

Shinlapawittayatorn K, Sungnoon R, Chattipakorn S & Chattipakorn N (2006). Effects of sildenafil citrate on defibrillation efficacy. *J Cardiovasc Electrophysiol* **17**, 292–295.

Sidell RJ, Cole MA, Draper NJ, Desrois M, Buckingham RE & Clarke K (2002). Thiazolidinedione treatment normalizes insulin resistance and ischemic injury in the Zucker fatty rat heart. *Diabetes* **51**, 1110–1117.

Sidhu JS, Cowan D & Kaski JC (2003). The effects of rosiglitazone, a peroxisome proliferator-activated receptor-gamma agonist, on markers of endothelial cell activation, C-reactive protein, and fibrinogen levels in non-diabetic coronary artery disease patients. *J Am Coll Cardiol* **42**, 1757–1763.

Sungnoon R, Shinlapawittayatorn K, Chattipakorn SC & Chattipakorn N (2008). Effects of garlic on defibrillation efficacy. *Int J Cardiol* **126**, 143–144.

Tao L, Wang Y, Gao E, Zhang H, Yuan Y, Lau WB, Chan L, Koch WJ & Ma XL (2010). Adiponectin: an indispensable molecule in rosiglitazone cardioprotection following myocardial infarction. *Circ Res* **106**, 409–417.

Thummasorn S, Kumfu S, Chattipakorn S & Chattipakorn N (2011). Granulocyte-colony stimulating factor attenuates mitochondrial dysfunction induced by oxidative stress in cardiac mitochondria. *Mitochondrion* **11**, 457–466.

Werns SW & Lucchesi BR (1987). Inflammation and myocardial infarction. *Br Med Bull* **43**, 460–471.

Yu J, Jin N, Wang G, Zhang F, Mao J & Wang X (2007). Peroxisome proliferator-activated receptor γ agonist improves arterial stiffness in patients with type 2 diabetes mellitus and coronary artery disease. *Metabolism* **56**, 1396–1401.

Yue TL, Bao W, Gu JL, Cui J, Tao L, Ma XL, Ohlstein EH & Jucker BM (2005). Rosiglitazone treatment in Zucker diabetic fatty rats is associated with ameliorated cardiac insulin resistance and protection from ischemia/reperfusion-induced myocardial injury. *Diabetes* **54**, 554–562.

Yue TL, Chen J, Bao W, Narayanan PK, Bril A, Jiang W, Lysko PG, Gu JL, Boyce R, Zimmerman DM, Hart TK, Buckingham RE & Ohlstein EH (2001). In vivo myocardial protection from ischemia/reperfusion injury by the peroxisome proliferator-activated receptor-γ agonist rosiglitazone. *Circulation* **104**, 2588–2594.

Zhang XJ, Xiong ZB, Tang AL, Ma H, Ma YD, Wu JG & Dong YG (2010). Rosiglitazone-induced myocardial protection against ischaemia-reperfusion injury is mediated via a phosphatidylinositol 3-kinase/Akt-dependent pathway. *Clin Exp Pharmacol Physiol* **37**, 156–161.

Acknowledgements

This work was supported by the Faculty of Medicine Endowment Fund (N.C. and S.P.) and grants from the Thailand Research Fund RTA 5280006 (N.C.), BRG 5480003 (S.C.) and the Commission of Higher Education Thailand (S.P. and N.C.).

Mitochondrion 11 (2011) 457–466

Contents lists available at ScienceDirect

Mitochondrion

journal homepage: www.elsevier.com/locate/mito

Granulocyte-colony stimulating factor attenuates mitochondrial dysfunction induced by oxidative stress in cardiac mitochondria

Savitree Thummasorn [a,b], Sirinart Kumfu [a,b], Siriporn Chattipakorn [a,c], Nipon Chattipakorn [a,b,d,*]

[a] Cardiac Electrophysiology Research and Training Center (CERT), Faculty of Medicine, Chiang Mai University, Chiang Mai 50200, Thailand
[b] Cardiac Electrophysiology Unit, Department of Physiology, Faculty of Medicine, Chiang Mai University, Chiang Mai, Thailand
[c] Faculty of Dentistry, Chiang Mai University, Chiang Mai, Thailand
[d] Biomedical Engineering Center, Chiang Mai University, Chiang Mai, Thailand

ARTICLE INFO

Article history:
Received 17 July 2010
Received in revised form 30 November 2010
Accepted 24 January 2011
Available online 1 February 2011

Keywords:
Granulocyte-colony stimulating factor
Mitochondria
Heart
Oxidative stress
Membrane potential
Ischemia

ABSTRACT

During cardiac ischemia–reperfusion injury, reactive oxygen species (ROS) level is markedly increased, leading to oxidative stress and mitochondrial dysfunction. Although granulocyte-colony stimulating factor (G-CSF) is known to be cardioprotective, its effects on cardiac mitochondria during oxidative stress have never been investigated. In this study, we discovered that G-CSF completely prevented mitochondrial swelling and depolarization, and markedly reduced ROS production caused by H_2O_2-induced oxidative stress in isolated cardiac mitochondria. Its effects were similar to those treated with cyclosporine A and 4′-chlorodiazepam. These findings suggest that G-CSF could act directly on cardiac mitochondria to prevent mitochondrial dysfunction caused by oxidative stress.

1. Introduction

Ischemic heart disease has been a major health problem in most countries around the world (Melberg et al., 2010). Pharmacological intervention in ischemic heart disease is one of several means that has been investigated extensively in an attempt to decrease myocardial damage, infarct size, cardiac dysfunction, and fatal arrhythmia. In the heart, mitochondria are known as the principal source of energy as well as reactive oxygen species (ROS) production (Sucher et al., 2009). Under stress condition such as ischemia–reperfusion injury, this condition has been demonstrated to markedly cause severe oxidative stress, an imbalance between the production of reactive oxygen species and a biological system's ability to defend cell damage, leading to mitochondrial dysfunction (Correa et al., 2008). Normally, the defense mechanism is preserved by enzymes that decrease ROS production in cardiac mitochondria. Disturbances in normal oxidative phosphorylation of the electron transport chain during ischemia–reperfusion have been shown to cause toxic effects through the production of ROS that will eventually damage all components of the cells.

A growing body of evidence has demonstrated the important roles of mitochondria in the heart during ischemia–reperfusion injury (Farber et al., 1981; Xiao et al., 2010). During ischemia, the energy production is decreased due to reduced oxidative phosphorylation rate at the inner mitochondrial membrane, causing a rapid increase in ROS production (Niizuma et al., 2009). When ROS produced by the electron-transport chain is accumulated up to a threshold level, it triggers the opening of the inner membrane anion channel (IMAC) (Aon et al., 2003). The opening of the IMAC allows the release of O_2^- from the mitochondrial matrix, resulting in mitochondrial membrane depolarization. Recently, the mitochondrial permeability transition pore (mPTP) has been proposed to have an important role in cell apoptosis and necrosis (Lemasters et al., 1998). The mitochondrial permeability transition (MPT) caused by the opening of mPTP determines not only whether cells will live or die, but also whether cell death occurs by apoptosis or necrosis (Hirsch et al., 1997; Susin et al., 1997). The burst of ROS production could cause further inhibition of oxidative phosphorylation (Nulton-Persson and Szweda, 2001) and increased permeability of the inner mitochondrial membrane via the opening of mPTP (Zoratti and Szabo, 1995). Such events are responsible for the uncoupling of oxidative phosphorylation, mitochondrial membrane potential changes ($\Delta\Psi_m$), and mitochondrial swelling, leading to the release of cytochrome *c*, activation of

Abbreviations: CDP, 4′-chlorodiazepam; CsA, cyclosporine A; G-CSF, Granulocyte-colony stimulating factor; IMAC, inner membrane anion channel; I/R, ischemia–reperfusion; mPTP, mitochondrial permeability transition pore; ROS, reactive oxygen species.

* Corresponding author. Tel.: +66 53 945329; fax: +66 53 945368.
E-mail address: nchattip@med.cmu.ac.th (N. Chattipakorn).

1567-7249/$ – see front matter © 2011 Elsevier B.V. and Mitochondria Research Society. All rights reserved.
doi:10.1016/j.mito.2011.01.008

caspase pathways and cell death by necrosis and/or apoptosis (Petronilli et al., 2001). Because of the deleterious effects of oxidative stress, attempts to find drugs that can attenuate this stress condition and prevent mitochondrial dysfunction have been studied extensively (Aon et al., 2003; Brady et al., 2006; Chen et al., 2008; Cortassa et al., 2004).

Granulocyte-colony stimulating factor (G-CSF) has recently been shown to have cardioprotective effects including improved cardiac function, increased myocardial blood supply, and reduced mortality after cardiac injury under several conditions, including myocardial ischemia (Cheng et al., 2008; Brunner et al., 2008; Okada et al., 2008). Despite these beneficial cardioprotective effects, the effects of G-CSF on cardiac mitochondria under oxidative stress have never been investigated. In the present study, we tested the hypothesis that G-CSF can protect mitochondrial swelling, prevent mitochondrial depolarization, and reduce ROS production under hydrogen peroxide-induced oxidative stress condition in isolated cardiac mitochondria. Isolated cardiac mitochondria were chosen as a study model since the direct effect of pharmacological interventions on the mitochondria could be directly assessed without the interference from intracellular signaling (Bognar et al., 2006; Venditti et al., 2006; Hofer et al., 2009).

2. Materials and methods

2.1. Animal preparation

All animal studies were approved by the Institutional Animal Care and Use Committee at the Faculty of Medicine, Chiang Mai University. Wistar rats (300–350 g) were obtained from the National Laboratory Animal Center, Mahidol University, Bangkok, Thailand. They were housed in a room maintained under constant environmental conditions (temperature 22–25 °C and a constant 12-h light/dark cycle). All animals received standard pelted rat diet and water ad libitum.

2.2. Isolated cardiac mitochondria preparation

Rats were anesthetized using an intraperitoneal injection of thiopental (80 mg/kg). The hearts were removed and homogenized in ice-cold buffer containing (in mmol/l) sucrose 300, TES 5, and EGTA 0.2, pH 7.2 (4 °C). The tissue were finely minced and homogenized by the homogenizer. The homogenate was centrifuged at 800 *g* for 5 min and the supernatant was collected and centrifuged at 8800 *g* for 5 min. Mitochondrial pellets were resuspended in an ice-cold buffer and centrifuged one more time at 8800 *g* for 5 min (Larche et al., 2006). Protein concentration was determined according to Bicinchoninic Acid (BCA) assay (Walker, 1994).

2.3. Experimental protocols

Isolated cardiac mitochondria from rat hearts were used in all experiments. The first protocol investigated the protective effects of G-CSF on oxidative stress-induced mitochondrial dysfunction. Oxidative stress was induced by H_2O_2 application for 5 min in isolated cardiac mitochondria. To test the effectiveness of H_2O_2 in causing mitochondrial damage, H_2O_2 at concentrations of 0.05, 0.1, 0.5, 1.0 and 2.0 mM were used (n = 5/group), and the assessment on mitochondrial swelling, ROS production and mitochondrial membrane potential changes was done according to the experimental protocols listed in Sections 2.5, 2.6 and 2.7.

In the first protocol, cardiac mitochondria were randomly assigned into eight treatment groups: H_2O_2 (2 mM), G-CSF (50 and 200 ng/ml), H_2O_2 (2 mM) pre-treated with G-CSF (25, 50, 100 or 200 ng/ml), and vehicle-treated mitochondria as a control group (n = 8/group, see Fig. 1A). In the second protocol, the mechanism of G-CSF on cardiac mitochondria was investigated. Pharmacological interventions with cyclosporine A (CsA) and 4′-chlorodiazepam (CDP) were used. CsA is the mPTP blocker, whereas CDP is known to inhibit the opening of IMAC. In this protocol, cardiac mitochondria were randomly assigned into 12 groups: control (vehicle), G-CSF (effective dose of G-CSF obtained from the first protocol), CsA (5 μM), CDP (100 μM), H_2O_2, H_2O_2 pre-treated with G-CSF, H_2O_2 pre-treated with CsA, H_2O_2 pre-treated with CDP, H_2O_2 pre-treated with (G-CSF + CsA), H_2O_2 pre-treated with (G-CSF + CDP), H_2O_2 pre-treated with (CsA + CDP), and H_2O_2 pre-treated with (G-CSF + CsA + CDP) (n = 8/group, see Fig. 1B). All groups were studied according to the experimental protocols listed in Sections 2.5, 2.6, and 2.7.

The involvement of the effect of G-CSF on complexes I and III in the electron transport chain was also investigated. Pharmacological interventions with 2-μM rotenone (complex I inhibitor) and 2-μM antimycin A (complex III inhibitor) were used for this study (Fontaine et al., 1998; Marcil et al., 2006). In this protocol, cardiac mitochondria were randomly assigned into eleven treatment groups: control (vehicle), rotenone-treated cardiac mitochondria for 5 min, antimycin A-treated cardiac mitochondria for 5 min, H_2O_2 pre-treated with rotenone, H_2O_2 pre-treated with antimycin A, H_2O_2 (2 mM), H_2O_2 pre-treated with G-CSF, H_2O_2-pretreated with G-CSF and rotenone, respectively, H_2O_2-pretreated with G-CSF and antimycin A, respectively, H_2O_2-pretreated with rotenone and G-CSF, respectively and H_2O_2-pretreated with antimycin A and G-CSF, respectively (n = 8/group, see Fig. 1C). Since the electron transport chain, particularly complexes I and III, is the main source of ROS production, the level of ROS in cardiac mitochondria was determined in this study protocol.

2.4. Identification of cardiac mitochondria with electron microscopy

Electron microscopy was used to identify isolated mitochondria from the hearts (Chelli et al., 2001). Isolated cardiac mitochondria were fixed in 2.5% glutaraldehyde in 0.1 M cacodylate buffer, pH 7.4 at 4°. After rinsing in cacodylate buffer, mitochondrial pellets were postfixed in 1% cacodylate-buffered osmium tetroxide for 2 h at room temperature, and then dehydrated in a graded series of ethanol. Mitochondria were embedded in Epon–Araldite. Ultrathin sections were cut with a diamond knife, placed on copper grids, stained with uranyl acetate and lead citrate, and observed with a transmission electron microscope.

2.5. Effects of pharmacological interventions on cardiac mitochondrial swelling

Cardiac mitochondria from all groups were assessed for mitochondrial swelling. In this study, swelling was assessed by measuring the change in the absorbance of the suspension at 540 nm (*A*540) using a microplate reader (Ruiz-Meana et al., 2006). Mitochondria (0.4 mg/ml) were incubated in respiration buffer (containing 100 mM KCl, 50 mM sucrose, 10 mM HEPES, and 5 mM KH_2PO_4, pH 7.4 at 37 °C) with an addition of 10 mM pyruvate/malate. Mitochondrial swelling was indicated when the absorbance of the suspension decreased.

2.6. Effects of pharmacological interventions on ROS production in cardiac mitochondria

ROS production in mitochondria was measured using a fluorescent microplate reader with dichlorohydro-fluorescein diacetate (DCFDA) (Novalija et al., 2003). Cardiac mitochondria (0.4 mg/ml) were incubated at 25 °C with 2 μM DCFDA for 20 min. The mitochondrial suspension was gently agitated and incubated at room temperature for measurements. DCFDA passed through membranes where it was oxidized in the presence of H_2O_2 to DCF. Fluorescence was determined at λ_{ex} 485 nm and λ_{em} 530 nm

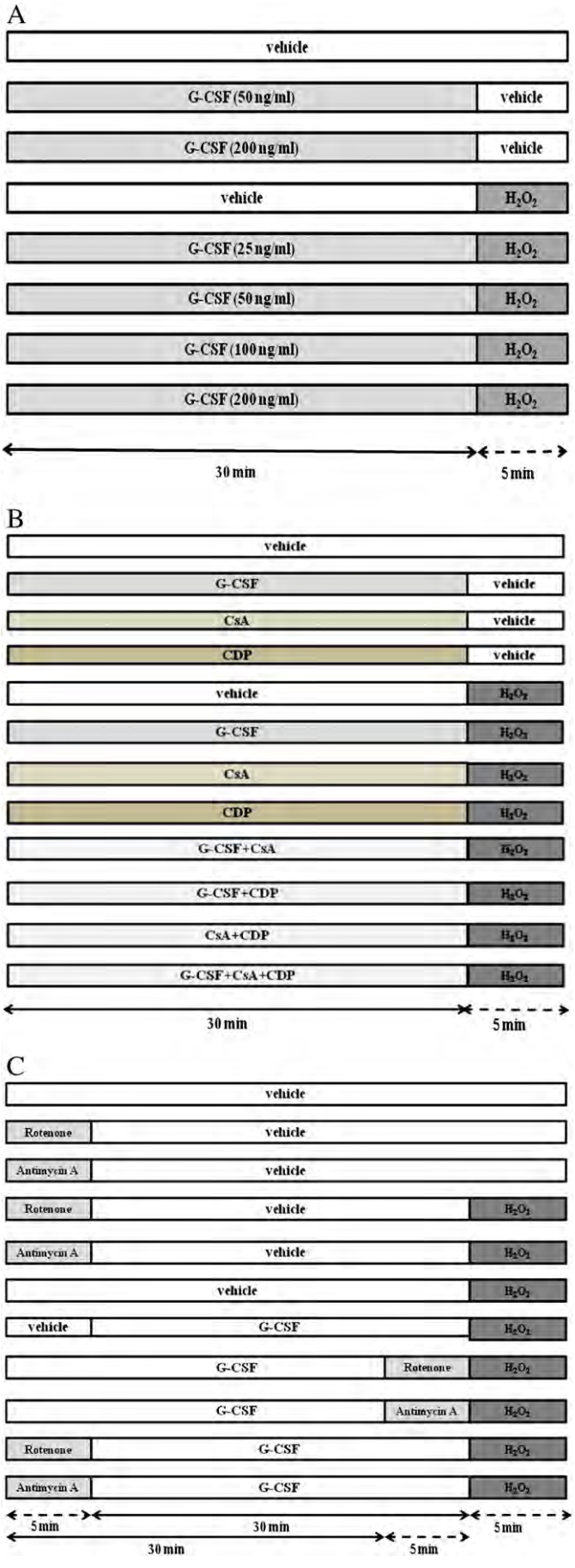

according to the spectral characteristics of DCF. The ROS level was expressed as arbitrary units of fluorescence intensity of DCF.

2.7. Effects of pharmacological interventions on cardiac mitochondrial membrane potential

The changes in mitochondrial membrane potential from all groups of isolated mitochondria were monitored with the dye 5,5′,6,6′-tetrachloro-1,1′,3,3′-tetraethylbenzimidazolcarbocyanine iodide (JC-1) (Tong et al., 2005; Di Lisa et al., 1995). The interaction of JC-1 with mitochondrial membrane components can alter the fluorescence properties associated with the monomer and aggregate. JC-1 has fluorescence properties as cation. When an interaction between JC-1 and anion of O_2^- within mitochondrial matrix occurs, aggregate fluorescence form is seen. However, JC-1 monomer fluorescence form is seen when the JC-1 has no interaction with anion within mitochondrial matrix. The isolated cardiac mitochondria (0.4 mg/ml) were stained with JC-1 (310 nM) at 37 °C for 30 min. The intensity of fluorescence was determined using a fluorescent microplate reader. JC-1 monomer fluorescence (green) was excited at 485 nm and the emission was detected at 530 nm. JC-1 aggregate fluorescence (red) was excited at 485 nm and the emission fluorescence was recorded at 590 nm. Consequently, mitochondrial depolarization was indicated by a decrease in the red/green fluorescence intensity ratio (i.e. $\Delta\Psi m$). The reduction in $\Delta\Psi m$ indicates mitochondrial membrane depolarization.

2.8. Data analysis

All data were presented as means ± SEM. Comparisons were made by one-way ANOVA followed by the Fisher post-hoc test. A P value <0.05 was considered statistically significant.

3. Results

3.1. Effects of H_2O_2 on isolated cardiac mitochondria

H_2O_2 at 0.5 and 1.0 mM could only cause an increase in the ROS level, but did cause neither absorbance (i.e. no mitochondrial swelling) nor membrane potential changes, compared to the control cardiac mitochondria (Fig. 2). However, an application of 2-mM H_2O_2 significantly reduced the absorbance (i.e. mitochondrial swelling), increased ROS level and mitochondrial depolarization (Fig. 2). Since 2-mM H_2O_2 could cause the changes in all determined parameters in isolated cardiac mitochondria, this concentration of H_2O_2 was used in all protocols in this study.

3.2. Effects of G-CSF on mitochondrial swelling

Transmission electron microscope was used to identify the cardiac mitochondria (Fig. 3). The freshly isolated cardiac mitochondria are shown in Fig. 3A. Applying 2-mM H_2O_2 to cardiac mitochondria caused mitochondrial swelling with markedly unfolded cristae (Fig. 3B). When G-CSF at 50 ng/ml was applied to cardiac mitochondria 30 min prior to H_2O_2 application, the morphology of cardiac mitochondria was well preserved (Fig. 3C), indicating the effectiveness of G-CSF in preventing morphological change in cardiac mitochondria from H_2O_2 application. Mitochondrial swelling was quantitatively assessed by reduced absorbance of the mitochondrial suspension. Applying H_2O_2 to mitochondria resulted in decreased

Fig. 1. Diagrams of the study protocols: (A) Effects of G-CSF on H_2O_2-induced mitochondrial damage, (B) Effects of G-CSF, cyclosporine A (CsA), 4′-chlorodiazepam (CDP) on H_2O_2-induced mitochondrial damage, (C) Effects of G-CSF on complexes I and III.

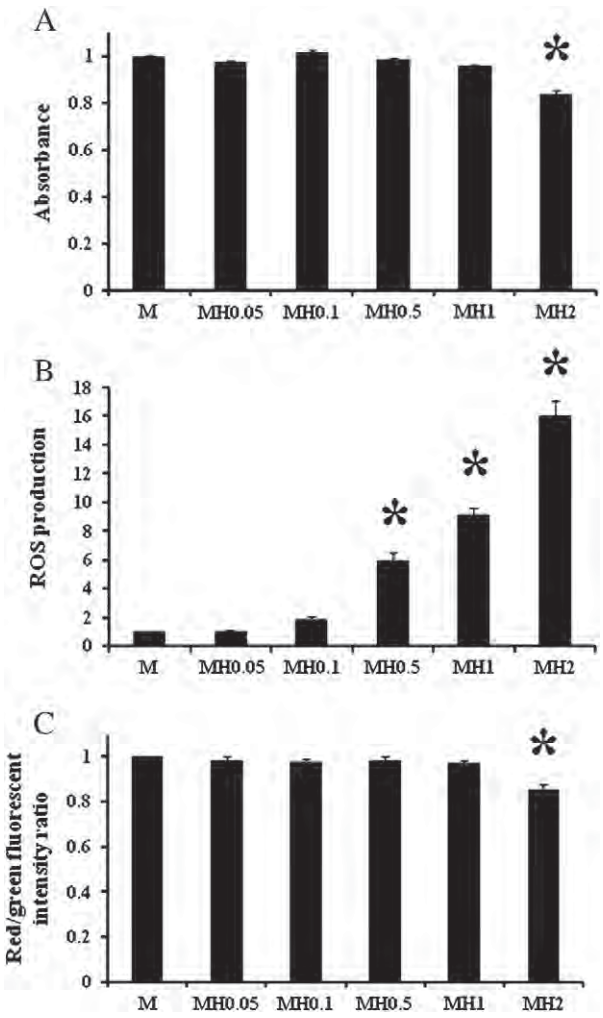

Fig. 2. Effects of H_2O_2 at various concentrations on (A) cardiac mitochondrial swelling, (B) ROS level and (C) mitochondrial membrane potential change. H_2O_2 at 0.5 and 1.0 mM caused an increased ROS level, but neither caused mitochondrial swelling nor membrane potential changes in cardiac mitochondria. However, 2-mM H_2O_2 caused mitochondrial swelling, increased ROS level, and mitochondrial membrane depolarization. M = control, MH(0.05, 0.1, 0.5, 1 and 2) = H_2O_2-treated mitochondria at 0.05, 0.1, 0.5, 1 and 2 mM, respectively. $^*p<0.05$ vs. M group.

absorbance (Fig. 4), suggesting that H_2O_2 can significantly induce mitochondrial swelling. G-CSF at 25 ng/ml did not prevent decreased absorbance, whereas G-CSF at 50, 100, and 200 ng/ml effectively prevented a reduction in the absorbance after H_2O_2 application (Fig. 4). From this kinetic study, a time point of 4 min after H_2O_2 application was chosen to investigate the protective effect of G-CSF. Without H_2O_2, G-CSF itself did not alter the absorbance, compared to the control group (Fig. 5). When G-CSF was applied to cardiac mitochondria prior to H_2O_2 application, G-CSF at concentrations of 50, 100, and 200 ng/ml significantly reduced mitochondrial swelling, compared to the H_2O_2 group. The absorbance measured in these mitochondria pretreated with G-CSF did not differ from that in the control (G0) group (Fig. 5).

3.3. Effects of G-CSF on ROS production

At baseline, ROS levels in cardiac mitochondria in the groups treated with G-CSF (50 and 200 ng/ml) were modestly higher than in the control group (Fig. 6). When H_2O_2 was applied to the mitochondrial suspension, the level of ROS was significantly increased, compared to the control group. However, when G-CSF was applied to cardiac mitochondria prior to H_2O_2 application, G-CSF (25, 50, 100 and 200 ng/ml) significantly reduced ROS level, compared to the H_2O_2 group. Furthermore, G-CSF at 50, 100, and 200 ng/ml decreased ROS levels more than G-CSF at 25 ng/ml. Nevertheless, the ROS levels in cardiac mitochondria pretreated with G-CSF at all concentrations were still higher than that in the control (G0) group.

3.4. Effects of G-CSF on mitochondrial membrane potential changes ($\Delta\Psi m$)

At baseline, the $\Delta\Psi m$ in the G-CSF (50 and 200 ng/ml) groups did not differ from the control group (Fig. 7). When H_2O_2 was added to mitochondrial suspension, mitochondrial depolarization was observed as indicated by a marked decrease in $\Delta\Psi m$. However, when G-CSF was applied to mitochondria prior to H_2O_2 application, G-CSF (50, 100, and 200 ng/ml) significantly attenuated the changes in $\Delta\Psi m$, compared to the H_2O_2 treated group. The $\Delta\Psi m$ in these G-CSF pretreated cardiac mitochondria did not differ from the control (G0) group.

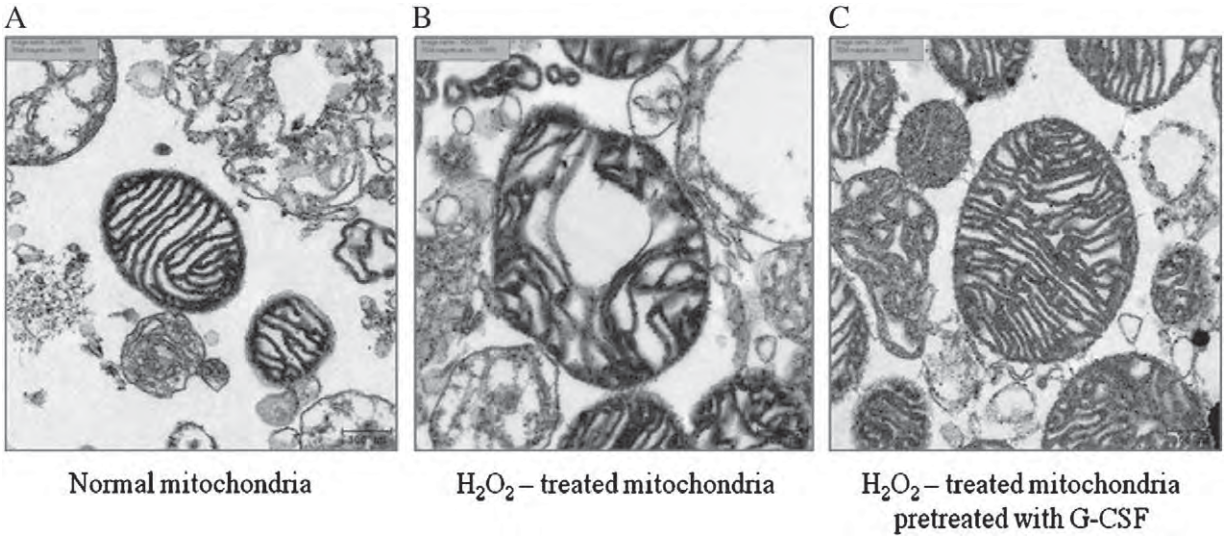

Fig. 3. Identification of the cardiac mitochondria with electron microscopy: (A) normal cardiac mitochondria, (B) cardiac mitochondria treated with 2-mM H_2O_2, (C) cardiac mitochondria pretreated with G-CSF at 50 ng/ml followed by H_2O_2 application.

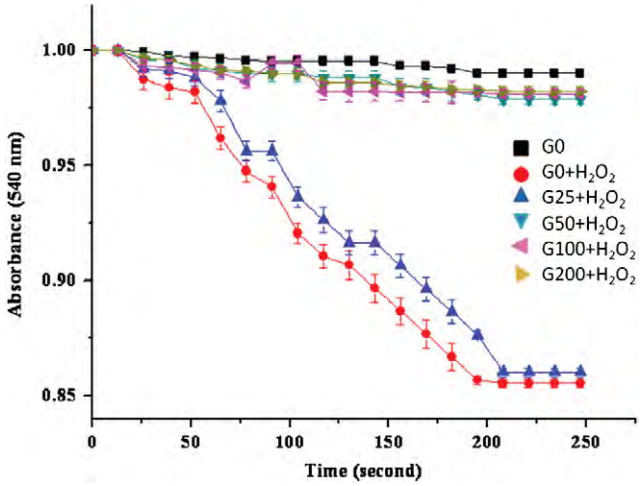

Fig. 4. Kinetic study of the effects of G-CSF on cardiac mitochondrial swelling. Mitochondrial swelling was quantitatively assessed by the reduction in the absorbance of the mitochondrial suspension. G0 = cardiac mitochondria not treated by H_2O_2 or G-CSF, (G0 + H_2O_2) = cardiac mitochondria treated with H_2O_2, (G25, 50, 100, and 200 + H_2O_2) = mitochondria pretreated with G-CSF at 25, 50, 100, and 200 ng/ml followed by H_2O_2 application, respectively.

3.5. Effect of G-CSF, CsA, and CDP on cardiac mitochondrial swelling

At baseline, G-CSF at 50 ng/ml (i.e. G50), CsA, and CDP did not cause any changes in the absorbance of cardiac mitochondria (Fig. 8). G-CSF at 50 ng/ml was chosen since it could effectively prevent absorbance reduction after H_2O_2 application as demonstrated in the previous protocol. When H_2O_2 was applied to mitochondrial suspension, absorbance was markedly decreased compared to the control group. However, pretreating cardiac mitochondria with G-CSF or CsA or CDP prior to H_2O_2 application could attenuate the reduction in the absorbance, compared to the H_2O_2 group. No difference was found among these G-CSF, CsA, and CDP pretreated groups. Furthermore, a combination of (G-CSF + CsA) or (G-CSF + CDP) or (CsA + CDP) or (G-CSF + CsA + CDP) could effectively prevent the absorbance reduction in cardiac mitochondria caused by H_2O_2. The measured absorbance did not differ among these groups, and did not differ from that of the control group (Fig. 8).

3.6. Effects of G-CSF, CsA and CDP on ROS production

At baseline, G-CSF at 50 ng/ml and CsA caused a slight increase in ROS production in isolated cardiac mitochondria (Fig. 9). The ROS level was significantly increased in mitochondria treated with H_2O_2. However, in cardiac mitochondria pretreated with G-CSF or CsA or CDP prior to H_2O_2 application, the ROS level was significantly decreased, compared to the H_2O_2 group. However, the reduction of ROS level among these groups was not equal. CsA prevented ROS production with greatest efficacy, followed by CDP and G-CSF. In addition, when H_2O_2 was added to mitochondria pretreated with (G-CSF + CsA) or (G-CSF + CDP) or (CsA + CDP) or (G-CSF + CsA + CDP), the ROS level was significantly decreased, compared to the H_2O_2 group. However, the level of ROS production did not differ among these combined treatment groups. Furthermore, the reduction in ROS level in these combined treatment groups was similar to that in the (CsA + H_2O_2) group (Fig. 9).

3.7. Effects of G-CSF, CsA, and CDP on mitochondrial membrane potential changes (ΔΨm)

At baseline, G-CSF at 50 ng/ml and CDP alone did not cause any changes in ΔΨm in cardiac mitochondria. However, CsA alone caused a slight decrease in ΔΨm (mitochondrial depolarization) (Fig. 10). When H_2O_2 was added to cardiac mitochondria, ΔΨm was significantly altered, compared to the control group. However, applying H_2O_2 to mitochondria pretreated with G-CSF or CsA or CDP did not alter the ΔΨm. When H_2O_2 was added to mitochondria pretreated with (G-CSF + CsA) or (G-CSF + CDP) or (CsA + CDP) or (G-CSF + CsA + CDP), the ΔΨm was also not altered, compared to the H_2O_2 group. No difference was found for ΔΨm among these combined treatment groups. Furthermore, the ΔΨm in these groups did not differ from that in the control group (Fig. 10).

3.8. Effects of G-CSF on complexes I and III of the electron transport chain

At baseline, rotenone (2 μM) and antimycin A (2 μM) did not cause any change in the ROS level, whereas H_2O_2 caused an increase in the ROS level in cardiac mitochondria (Fig. 11). G-CSF could significantly decrease the ROS level in cardiac mitochondria when it was applied to the mitochondria before the addition of rotenone, antimycin A, and

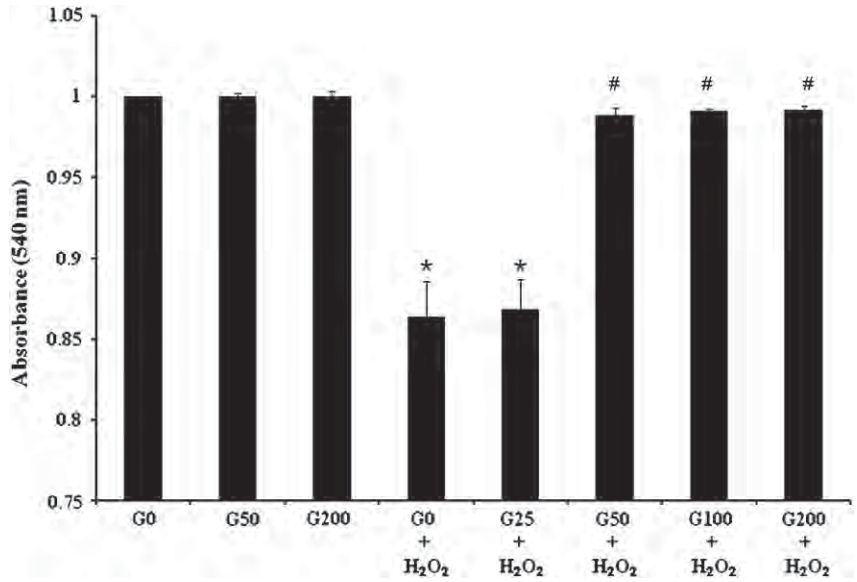

Fig. 5. Effects of G-CSF on cardiac mitochondrial swelling after 4-min H_2O_2 application. G0 = cardiac mitochondria not treated by H_2O_2 or G-CSF, G50 and G200 = cardiac mitochondria treated with G-CSF 50 and 200 ng/ml, respectively, (G0 + H_2O_2) = cardiac mitochondria treated with H_2O_2, (G25, 50, 100, and 200 + H_2O_2) = cardiac mitochondria pretreated with G-CSF at 25, 50, 100, and 200 ng/ml followed by H_2O_2 application, respectively. $^{*}P<0.05$ vs. G0 group, $^{\#}P<0.05$ vs. (G0 + H_2O_2) group.

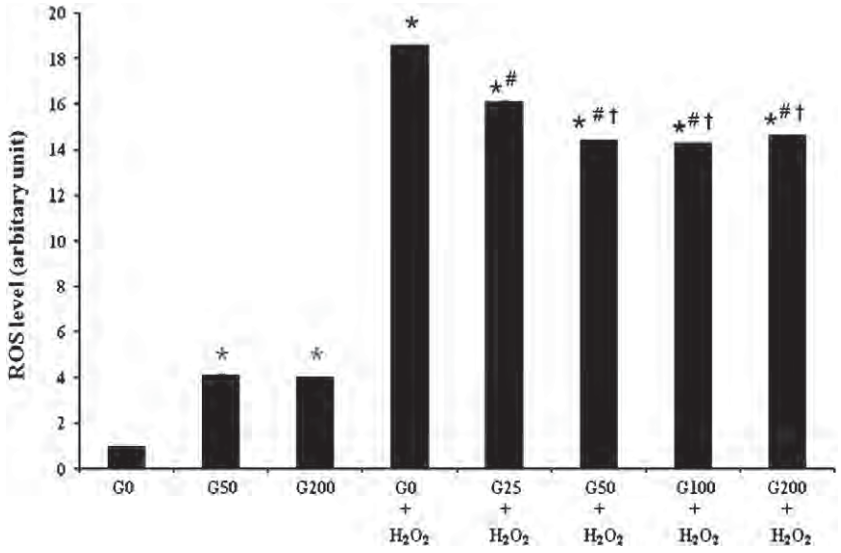

Fig. 6. Effects of G-CSF on ROS level. *$P<0.05$ vs. G0 group, #$P<0.05$ vs. (G0 + H_2O_2) group, † $P<0.05$ vs. (G25 + H_2O_2) group.

H_2O_2 (i.e. ROS level in MG, MGR, and MGA groups was lower than that in the H_2O_2, MRH and MAH groups in Fig. 11). However, the effectiveness of G-CSF in reducing the ROS level was decreased when G-CSF was added to the mitochondria after rotenone and antimycin A application since the ROS levels in MRGH and MAGH were significantly higher than those in the MG, MGRH and MGAH groups.

4. Discussion

Mitochondria have been shown to play a key role in cardiac dysfunction caused by myocardial ischemia (Xiao et al., 2010). A previous study demonstrated that oxidative stress occurring in ischemic myocardium caused an increased ROS production in cardiac mitochondria (Tompkins et al., 2006). The increased ROS level in one or a few mitochondria has been shown to trigger the release of ROS from neighboring mitochondria, a mechanism known as ROS-induced ROS release (Zorov et al., 2006), resulting in a large amount of ROS accumulated in the ischemic myocardium. The increased ROS level could lead to the disruption of the electron transport chain in cardiac mitochondria, causing cardiac mitochondrial dysfunction and eventually leading to myocardial cell death (Tompkins et al., 2006). Pharmacological interventions to attenuate mitochondrial dysfunction have been shown to have cardioprotective effects, including prevention of arrhythmia and reduction of infarct size (Matejikova et al., 2009; Moncada, 2010).

Granulocyte-colony stimulating factor (G-CSF) has recently been shown to improve cardiac function, increase myocardial blood supply, and reduce mortality after cardiac injury under several conditions including ischemic heart (Cheng et al., 2008; Brunner et al., 2008; Okada et al., 2008). However, its effect on cardiac mitochondria undergoing oxidative stress induced by H_2O_2 has never been investigated. In the present study, we found that G-CSF could prevent mitochondrial swelling, decrease ROS level, and attenuate mitochondrial membrane depolarization in cardiac mitochondria under oxidative stress condition.

In the present study, the effective dose of G-CSF (50 ng/ml) could successfully prevent mitochondrial damage. G-CSF at higher concentrations (up to 200 ng/ml) shared equally similar effects to G-CSF at 50 ng/ml. Although G-CSF could completely prevent mitochondrial swelling and $\Delta\Psi m$ changes after oxidative stress induced by H_2O_2, it could only decrease ROS to a certain level, which was still higher than that in the control group. These findings indicate that G-CSF may act

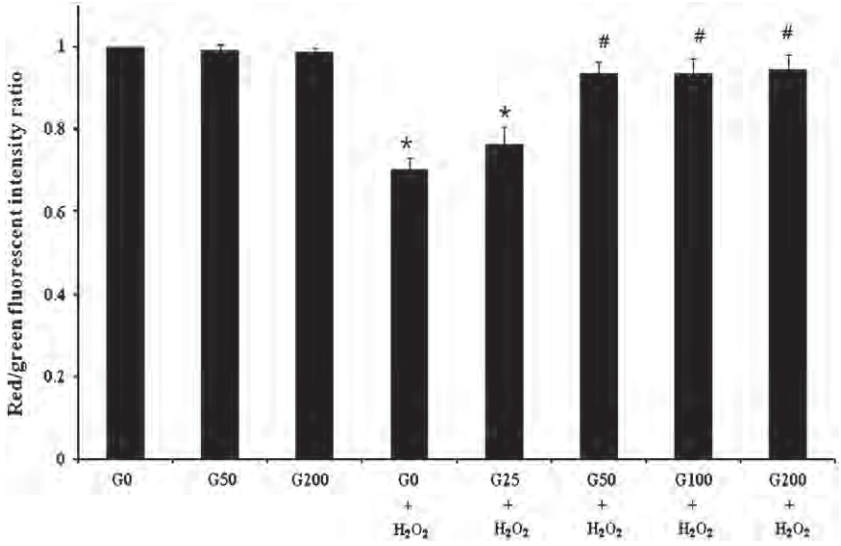

Fig. 7. Effects of G-CSF on cardiac mitochondrial membrane potential changes ($\Delta\Psi m$). *$P<0.05$ vs. G0 group, #$P<0.05$ vs. (G0 + H_2O_2) group.

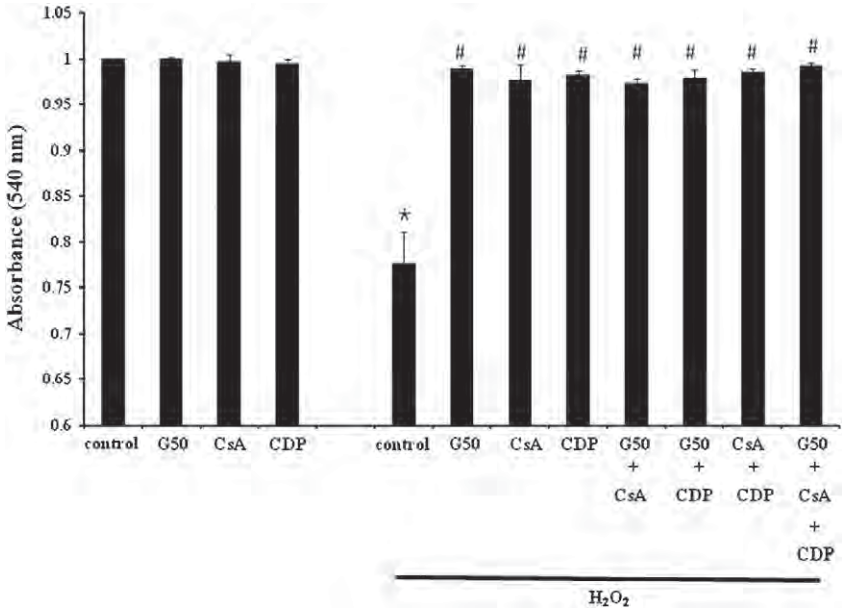

Fig. 8. Effects of G-CSF, CsA, and CDP on cardiac mitochondrial swelling. *$P<0.05$ vs. control group, #$P<0.05$ vs. H_2O_2 group.

more effectively in preventing mitochondrial swelling and mitochondrial depolarization, but less effective in preventing ROS production.

Mitochondrial swelling is described as an increase of mitochondrial volume. The cause of mitochondrial swelling is due to the prolonged opening of mPTP, which causes an increase of permeability to solutes with molecular masses up to 1500 Da. Since mPTP opening can be triggered by the increased ROS level (Hausenloy et al., 2003), the prolonged mPTP opening can lead to free bi-directional movement of low molecular weight molecules across the inner membrane, while proteins remain in the matrix. Consequently, colloidal osmotic pressure increases and causes mitochondrial swelling (the inner membrane cristae unfolded), the rupture of outer mitochondrial membrane, and the release of cytochrome *c* (Azzone and Azzi, 1965; Crompton, 1999). In this study, G-CSF effectively prevented mitochondrial swelling caused by H_2O_2, and this protection is as effective as the effect of the blocker of mPTP opening (CsA). These findings suggested that G-CSF might act on mPTP, thus inhibiting the opening of this pore and leading to the prevention of mitochondrial swelling.

Mitochondria are known as a major organelle for producing ROS in cells. ROS is normally produced at sites of complexes I and III in the electron transport chain (Chen et al., 2008). Under physiological conditions, O_2^- is transported to the electron transport chain for oxidative phosphorylation in the mitochondria and converted into a small amount of H_2O_2 (Chen et al., 2008). However, these ROS are generally degraded by catalase and glutathione peroxidase in the mitochondria. In some pathological conditions such as oxidative stress, ROS production is markedly increased and the ROS degradation process is not sufficiently maintained, resulting in an excess of ROS including O_2^-.

Under physiological conditions, O_2^- can be released across the inner mitochondrial membrane via IMAC, causing mitochondrial membrane depolarization (Brady et al., 2006). The release of ROS via

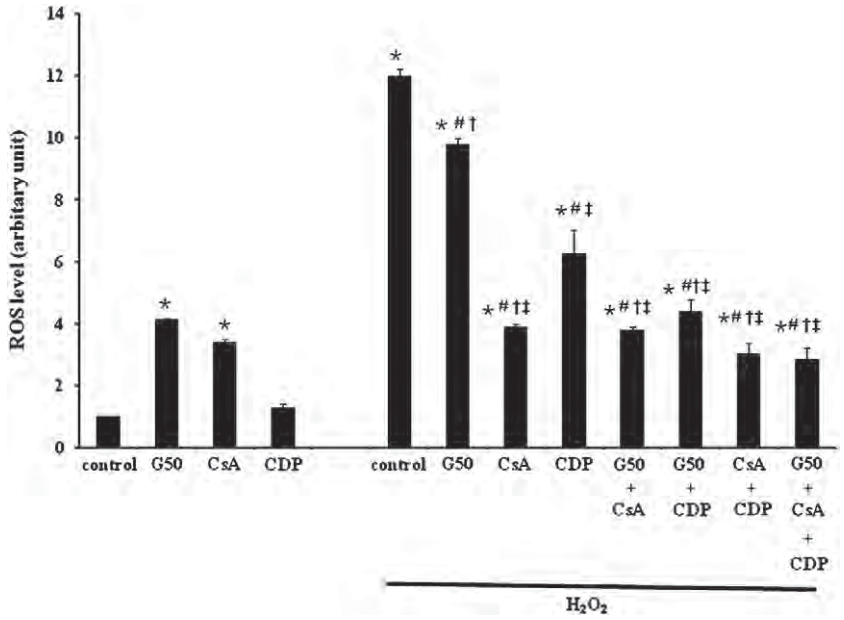

Fig. 9. Effects of G-CSF, CsA, and CDP on ROS level. *$P<0.05$ vs. control group, #$P<0.05$ vs. H_2O_2 group, †$P<0.05$ vs. (CDP + H_2O_2), ‡$P<0.05$ vs. (G-CSF + H_2O_2).

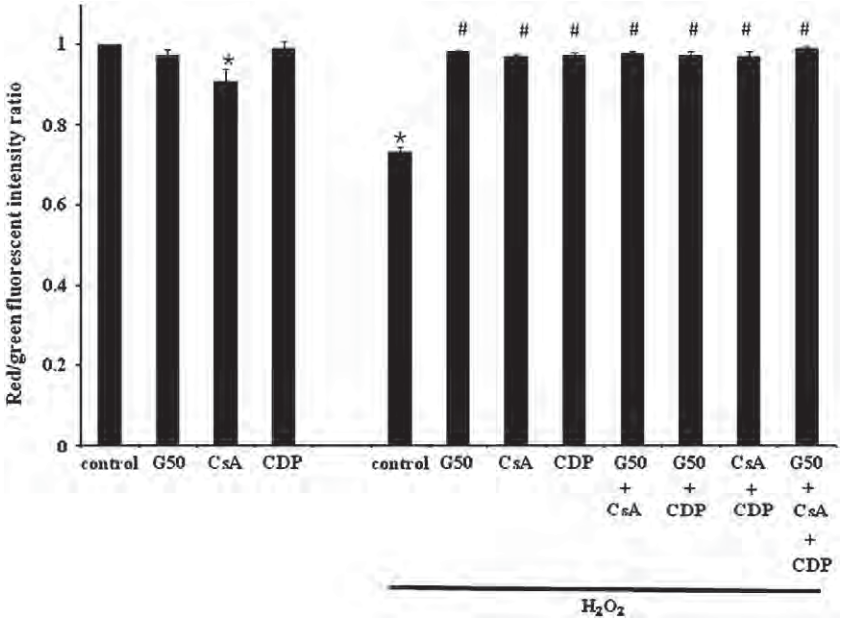

Fig. 10. Effects of G-CSF, CsA, and CDP on cardiac mitochondrial membrane potential changes (ΔΨm). *P<0.05 vs. control group, #P<0.05 vs. H_2O_2 group.

IMAC opening could activate the IMAC of its neighboring mitochondria, resulting in a great increase of ROS (Vanden Hoek et al., 1998). This process is called ROS-induced ROS release mechanism, leading to severe oxidative stress in cells (Zorov et al., 2000). IMAC opening is normally terminated by a reduction of ROS level (i.e. via decreasing ROS production and efflux from the mitochondrial matrix) and ROS scavenging by the antioxidant enzymes (Cortassa et al., 2004). Aon et al. (2003) clearly demonstrated in their excellent study that a certain amount of ROS produced from the electron transport chain is required to accumulate in the mitochondrial matrix up to a critical level in order to trigger the opening of IMAC (Aon et al., 2003). Once the ROS accumulation reaches a point of mitochondrial critical threshold, mitochondrial depolarization is observed and the mitochondrial membrane potential becomes unstable in almost the entire population of mitochondria in the mitochondrial network (Aon et al., 2003).

In the present study, our finding indicated that H_2O_2 used in this study could cause an increased ROS level in cardiac mitochondria, which must be sufficiently high, resulting in the opening of IMAC and eventually leading to a decrease in ΔΨm. Through this mechanism, our findings that G-CSF, CsA, and CDP shared a similar efficacy in the prevention of the mitochondrial depolarization, despite the fact that they had different efficacy in the prevention of ROS production, indicated that these pharmacological interventions can effectively attenuate the ROS level in cardiac mitochondria to a level below the critical threshold required for triggering the IMAC opening. Our findings show that low concentrations of H_2O_2 (0.5 and 1 mM) could increase the ROS level in cardiac mitochondria but did not cause mitochondrial membrane potential changes, whereas high-concentration (2 mM) of H_2O_2 could cause much increase in ROS level and produced mitochondrial membrane depolarization, thus supporting the critical threshold hypothesis.

In the present study, the ROS level was lowest in mitochondria pretreated with CsA, followed by higher levels in the CDP and G-CSF groups. Since the efficacy of G-CSF in preventing mitochondrial

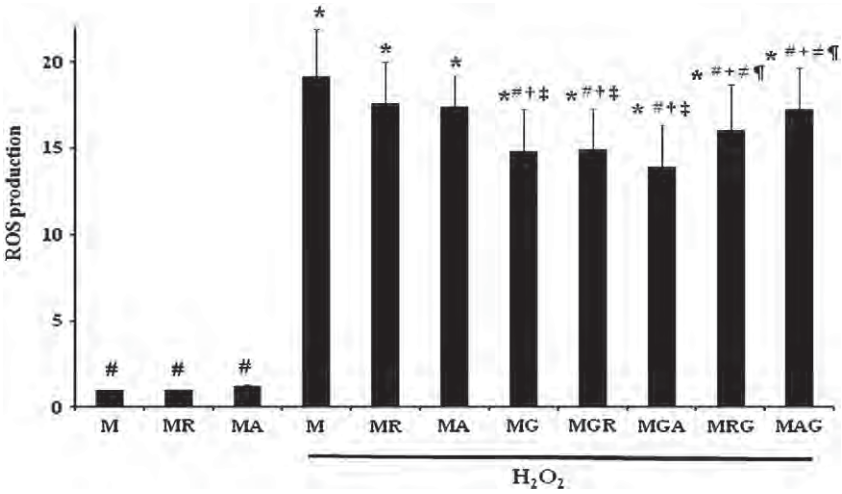

Fig. 11. Effects of G-CSF on complexes I and III. M = healthy cardiac mitochondria, MR = cardiac mitochondria treated with 2-μM rotenone, MA = cardiac mitochondria treated with 2-μM antimycin A, MG = cardiac mitochondria treated with G-CSF 50 ng/ml, MGR = cardiac mitochondria pretreated with G-CSF, followed by rotenone application, respectively, MGA = cardiac mitochondria pretreated with G-CSF, followed by antimycin A application, respectively, MRG = cardiac mitochondria pretreated with rotenone, followed by G-CSF application, respectively, MAG = cardiac mitochondria pretreated with antimycin A, followed by G-CSF application, respectively. *p<0.05 vs. M, # p<0.05 vs. (M + H_2O_2), † p<0.05 vs. MR + H_2O_2, ‡ p<0.05 vs. MA + H_2O_2, + p<0.05 vs. MG + H_2O_2, ≠ p<0.05 vs. MGR + H_2O_2, ¶ p<0.05 vs. MGA + H_2O_2.

depolarization was similar to that of CsA, our findings suggest that the decreased ROS level caused by G-CSF was sufficient to bring the ROS level below the critical threshold. As a result, the trigger of IMAC opening was inhibited, resulting in no change in $\Delta\Psi m$ after H_2O_2 application. All these findings suggest that the accumulation of ROS in cardiac mitochondria up to a critical threshold level could be a key determinant for the cardiac mitochondrial protection.

Without H_2O_2 application, ROS levels in the G-CSF and CsA groups were modestly increased. This could be due to the fact that G-CSF itself can increase ROS production by stimulating the angiogenic factors production (Carrao et al., 2009). In cardiomyocytes, it has been shown that G-CSF can directly stimulate ROS production, which plays a pivotal role in triggering adaptations of the heart to ischemia including growth of the coronary collaterals (Carrao et al., 2009). However, the ROS level caused by G-CSF alone was not sufficient to cause the opening of the IMAC.

Our results also showed that applying CsA alone could modestly raise the ROS level in cardiac mitochondria. CsA is known to effectively block the mPTP opening, therefore the release of ROS from mitochondria can be blocked inside the matrix at some degree. Our study also showed that CsA alone can cause a modest decrease in $\Delta\Psi m$, compared to the control group. This evidence suggests that under physiological condition, mPTP flickering (i.e. opening and closing) is essential for the exchange of metabolites between cardiac mitochondria and cytosol, thus maintaining cardiac mitochondrial membrane potential (Kroemer et al., 2007). Therefore, blocking the opening of mPTP by CsA could prevent this exchange process, resulting in a slight change in $\Delta\Psi m$.

In the present study, CsA had the highest efficacy in preventing ROS production in cardiac mitochondria. The lower efficacy of CDP than CsA in preventing ROS production could be due to the fact that blocking IMAC only prevents the release of ROS from the mitochondrial matrix, while the remaining ROS could still be released from the intermembrane space and out of the mitochondria via mPTP. Thus, ROS-induced ROS release mechanism could still occur within the mitochondrial network, resulting in a higher level of ROS in the CDP group. Since combined treatment with G-CSF and CDP could effectively decrease ROS level to a similar degree as that in CsA, these findings suggested that G-CSF may act as a blocker of mPTP opening, but with less efficacy than CsA in preventing ROS production.

In the present study, our results indicated that the protective effect of G-CSF on mitochondria could involve complexes I and III on the electron transport chain. Complexes I and III are known as the main sources of ROS production in the mitochondria (Andrukhiv et al., 2006). In a previous study, Chen et al. reported that rotenone did not alter net ROS generation in intact mitochondria (Chen et al., 2003). However, under the pathological condition such as myocardial ischemia, administration of rotenone could decrease the production of ROS in mitochondria (Becker et al., 1999). Our results were consistent with these previous reports. In the present study, although rotenone has a tendency to decrease ROS production in cardiac mitochondria pretreated with rotenone prior to H_2O_2 application, compared to mitochondria treated with H_2O_2, it did not reach statistical significance. Antimycin A is previously reported that it can increase ROS production (Chen et al., 2008). In the present study, antimycin A-treated cardiac mitochondria under the H_2O_2-induced oxidative stress condition can increase ROS production compared to the control group. Similar to rotenone, antimycin A did not alter ROS level in normal cardiac mitochondria, and did not change ROS level when H_2O_2 was applied. However, the ROS level measured in the groups in which G-CSF was administered prior to the application of rotenone and antimycin A was significantly lower than that in the groups in which G-CSF was administered after rotenone and antimycin A. This finding indicated that the effect of G-CSF on mitochondria could involve complexes I and III activity in the electron transport chain. It is also important to note that although these findings indicate that G-CSF could affect complexes I and III activity, future studies are needed to elucidate the definite mechanism of G-CSF as well as its involvement on complexes IV and V in the electron transport chain.

5. Conclusions

Under oxidative stress, G-CSF can effectively prevent mitochondrial swelling, mitochondrial membrane potential changes, and ROS production in cardiac mitochondria. Its mechanism could be due to the inhibition of mPTP opening and could involve the complexes I and III activity on the electron transport chain. These beneficial effects of G-CSF may be used to prevent cardiac mitochondrial damage under oxidative stress conditions.

Disclosures

The authors have no conflict of interest to declare.

Acknowledgements

We would like to thank Punate Weerateerangkul from Cardiac Electrophysiology Research and Training Center (CERT), Faculty of Medicine, Chiang Mai University, for his technical assistance. This study was supported by Thailand Research Fund grants RTA 5280006 (N.C.) and RMU 5180007 (S.C.).

References

Andrukhiv, A., Costa, A.D., West, I.C., Garlid, K.D., 2006. Opening mitoKATP increases superoxide generation from complex I of the electron transport chain. Am. J. Physiol. Heart Circ. Physiol. 291, H2067–H2074.

Aon, M.A., Cortassa, S., Marban, E., O'Rourke, B., 2003. Synchronized whole cell oscillations in mitochondrial metabolism triggered by a local release of reactive oxygen species in cardiac myocytes. J. Biol. Chem. 278, 44735–44744.

Azzone, G.F., Azzi, A., 1965. Volume changes in liver mitochondria. Proc. Natl. Acad. Sci. U. S. A. 53, 1084–1089.

Becker, L.B., vanden Hoek, T.L., Shao, Z.H., Li, C.Q., Schumacker, P.T., 1999. Generation of superoxide in cardiomyocytes during ischemia before reperfusion. Am. J. Physiol. 277, H2240–H2246.

Bognar, Z., Kalai, T., Palfi, A., Hanto, K., Bognar, B., Mark, L., Szabo, Z., Tapodi, A., Radnai, B., Sarszegi, Z., Szanto, A., Gallyas Jr., F., Hideg, K., Sumegi, B., Varbiro, G., 2006. A novel SOD-mimetic permeability transition inhibitor agent protects ischemic heart by inhibiting both apoptotic and necrotic cell death. Free Radic. Biol. Med. 41, 835–848.

Brady, N.R., Hamacher-Brady, A., Westerhoff, H.V., Gottlieb, R.A., 2006. A wave of reactive oxygen species (ROS)-induced ROS release in a sea of excitable mitochondria. Antioxid. Redox Signal. 8, 1651–1665.

Brunner, S., Huber, B.C., Fischer, R., Groebner, M., Hacker, M., David, R., Zaruba, M.M., Vallaster, M., Rischpler, C., Wilke, A., Gerbitz, A., Franz, W.M., 2008. G-CSF treatment after myocardial infarction: impact on bone marrow-derived vs cardiac progenitor cells. Exp. Hematol. 36, 695–702.

Carrao, A.C., Chilian, W.M., Yun, J., Kolz, C., Rocic, P., Lehmann, K., van den Wijngaard, J.P., van Horssen, P., Spaan, J.A., Ohanyan, V., Pung, Y.F., Buschmann, I., 2009. Stimulation of coronary collateral growth by granulocyte stimulating factor: role of reactive oxygen species. Arterioscler. Thromb. Vasc. Biol. 29, 1817–1822.

Chelli, B., Falleni, A., Salvetti, F., Gremigni, V., Lucacchini, A., Martini, C., 2001. Peripheral-type benzodiazepine receptor ligands: mitochondrial permeability transition induction in rat cardiac tissue. Biochem. Pharmacol. 61, 695–705.

Chen, Q., Vazquez, E.J., Moghaddas, S., Hoppel, C.L., Lesnefsky, E.J., 2003. Production of reactive oxygen species by mitochondria: central role of complex III. J. Biol. Chem. 278, 36027–36031.

Chen, Q., Moghaddas, S., Hoppel, C.L., Lesnefsky, E.J., 2008. Ischemic defects in the electron transport chain increase the production of reactive oxygen species from isolated rat heart mitochondria. Am. J. Physiol. Cell Physiol. 294, C460–C466.

Cheng, Z., Ou, L., Liu, Y., Liu, X., Li, F., Sun, B., Che, Y., Kong, D., Yu, Y., Steinhoff, G., 2008. Granulocyte colony-stimulating factor exacerbates cardiac fibrosis after myocardial infarction in a rat model of permanent occlusion. Cardiovasc. Res. 80, 425–434.

Correa, F., Garcia, N., Robles, C., Martinez-Abundis, E., Zazueta, C., 2008. Relationship between oxidative stress and mitochondrial function in the post-conditioned heart. J. Bioenerg. Biomembr. 40, 599–606.

Cortassa, S., Aon, M.A., Winslow, R.L., O'Rourke, B., 2004. A mitochondrial oscillator dependent on reactive oxygen species. Biophys. J. 87, 2060–2073.

Crompton, M., 1999. The mitochondrial permeability transition pore and its role in cell death. Biochem. J. 341, 233–249.

Di Lisa, F., Blank, P.S., Colonna, R., Gambassi, G., Silverman, H.S., Stern, M.D., Hansford, R.G., 1995. Mitochondrial membrane potential in single living adult rat cardiac myocytes exposed to anoxia or metabolic inhibition. J. Physiol. 486, 1–13.

Farber, J.L., Chien, K.R., Mittnacht Jr., S., 1981. Myocardial ischemia: the pathogenesis of irreversible cell injury in ischemia. Am. J. Pathol. 102, 271–281.

Fontaine, E., Eriksson, O., Ichas, F., Bernardi, P., 1998. Regulation of the permeability transition pore in skeletal muscle mitochondria. Modulation by electron flow through the respiratory chain complex I. J. Biol. Chem. 273, 12662–12668.

Hausenloy, D.J., Duchen, M.R., Yellon, D.M., 2003. Inhibiting mitochondrial permeability transition pore opening at reperfusion protects against ischaemia–reperfusion injury. Cardiovasc. Res. 60, 617–625.

Hirsch, T., Marchetti, P., Susin, S.A., Dallaporta, B., Zamzami, N., Marzo, I., Geuskens, M., Kroemer, G., 1997. The apoptosis–necrosis paradox. Apoptogenic proteases activated after mitochondrial permeability transition determine the mode of cell death. Oncogene 15, 1573–1581.

Hofer, T., Servais, S., Seo, A.Y., Marzetti, E., Hiona, A., Upadhyay, S.J., Wohlgemuth, S.E., Leeuwenburgh, C., 2009. Bioenergetics and permeability transition pore opening in heart subsarcolemmal and interfibrillar mitochondria: effects of aging and lifelong calorie restriction. Mech. Ageing Dev. 130, 297–307.

Kroemer, G., Galluzzi, L., Brenner, C., 2007. Mitochondrial membrane permeabilization in cell death. Physiol. Rev. 87, 99–163.

Larche, J., Lancel, S., Hassoun, S.M., Favory, R., Decoster, B., Marchetti, P., Chopin, C., Neviere, R., 2006. Inhibition of mitochondrial permeability transition prevents sepsis-induced myocardial dysfunction and mortality. J. Am. Coll. Cardiol. 48, 377–385.

Lemasters, J.J., Nieminen, A.L., Qian, T., Trost, L.C., Elmore, S.P., Nishimura, Y., Crowe, R.A., Cascio, W.E., Bradham, C.A., Brenner, D.A., Herman, B., 1998. The mitochondrial permeability transition in cell death: a common mechanism in necrosis, apoptosis and autophagy. Biochim. Biophys. Acta 1366, 177–196.

Marcil, M., Bourduas, K., Ascah, A., Burelle, Y., 2006. Exercise training induces respiratory substrate-specific decrease in Ca2+-induced permeability transition pore opening in heart mitochondria. Am. J. Physiol. Heart Circ. Physiol. 290, H1549–H1557.

Matejikova, J., Ravingerova, T., Pancza, D., Carnicka, S., Kolar, F., 2009. Mitochondrial KATP opening confers protection against lethal myocardial injury and ischaemia-induced arrhythmias in the rat heart via PI3K/Akt-dependent and -independent mechanisms. Can. J. Physiol. Pharmacol. 87, 1055–1062.

Melberg, T., Burman, R., Dickstein, K., 2010. The impact of the 2007 ESC-ACC-AHA-WHF Universal definition on the incidence and classification of acute myocardial infarction: a retrospective cohort study. Int. J. Cardiol. 139, 228–233.

Moncada, S., 2010. Mitochondria as pharmacological targets. Br. J. Pharmacol. 160, 217–219.

Niizuma, K., Endo, H., Chan, P.H., 2009. Oxidative stress and mitochondrial dysfunction as determinants of ischemic neuronal death and survival. J. Neurochem. 109, 133–138.

Novalija, E., Kevin, L.G., Eells, J.T., Henry, M.M., Stowe, D.F., 2003. Anesthetic preconditioning improves adenosine triphosphate synthesis and reduces reactive oxygen species formation in mitochondria after ischemia by a redox dependent mechanism. Anesthesiology 98, 1155–1163.

Nulton-Persson, A.C., Szweda, L.I., 2001. Modulation of mitochondrial function by hydrogen peroxide. J. Biol. Chem. 276, 23357–23361.

Okada, H., Takemura, G., Li, Y., Ohno, T., Li, L., Maruyama, R., Esaki, M., Miyata, S., Kanamori, H., Ogino, A., Nakagawa, M., Minatoguchi, S., Fujiwara, T., Fujiwara, H., 2008. Effect of a long-term treatment with a low-dose granulocyte colony-stimulating factor on post-infarction process in the heart. J. Cell. Mol. Med. 12, 1272–1283.

Petronilli, V., Penzo, D., Scorrano, L., Bernardi, P., Di Lisa, F., 2001. The mitochondrial permeability transition, release of cytochrome c and cell death. Correlation with the duration of pore openings in situ. J. Biol. Chem. 276, 12030–12034.

Ruiz-Meana, M., Garcia-Dorado, D., Miro-Casas, E., Abellan, A., Soler-Soler, J., 2006. Mitochondrial Ca2+ uptake during simulated ischemia does not affect permeability transition pore opening upon simulated reperfusion. Cardiovasc. Res. 71, 715–724.

Sucher, R., Gehwolf, P., Kaier, T., Hermann, M., Maglione, M., Oberhuber, R., Ratschiller, T., Kuznetsov, A.V., Bosch, F., Kozlov, A.V., Ashraf, M.I., Schneeberger, S., Brandacher, G., Ollinger, R., Margreiter, R., Troppmair, J., 2009. Intracellular signaling pathways control mitochondrial events associated with the development of ischemia/reperfusion-associated damage. Transpl. Int. 22, 922–930.

Susin, S.A., Zamzami, N., Castedo, M., Daugas, E., Wang, H.G., Geley, S., Fassy, F., Reed, J.C., Kroemer, G., 1997. The central executioner of apoptosis: multiple connections between protease activation and mitochondria in Fas/APO-1/CD95- and ceramide-induced apoptosis. J. Exp. Med. 186, 25–37.

Tompkins, A.J., Burwell, L.S., Digerness, S.B., Zaragoza, C., Holman, W.L., Brookes, P.S., 2006. Mitochondrial dysfunction in cardiac ischemia–reperfusion injury: ROS from complex I, without inhibition. Biochim. Biophys. Acta 1762, 223–231.

Tong, V., Teng, X.W., Chang, T.K., Abbott, F.S., 2005. Valproic acid II: effects on oxidative stress, mitochondrial membrane potential, and cytotoxicity in glutathione-depleted rat hepatocytes. Toxicol. Sci. 86, 436–443.

Vanden Hoek, T.L., Becker, L.B., Shao, Z., Li, C., Schumacker, P.T., 1998. Reactive oxygen species released from mitochondria during brief hypoxia induce preconditioning in cardiomyocytes. J. Biol. Chem. 273, 18092–18098.

Venditti, P., Pamplona, R., Portero-Otin, M., De Rosa, R., Di Meo, S., 2006. Effect of experimental and cold exposure induced hyperthyroidism on H_2O_2 production and susceptibility to oxidative stress of rat liver mitochondria. Arch. Biochem. Biophys. 447, 11–22.

Walker, J.M., 1994. The bicinchoninic acid (BCA) assay for protein quantitation. Methods Mol. Biol. 32, 5–8.

Xiao, J., Liang, D., Zhang, H., Liu, Y., Li, F., Chen, Y.H., 2010. 4′-chlorodiazepam, a translocator protein (18 kDa) antagonist, improves cardiac functional recovery during postischemia reperfusion in rats. Exp. Biol. Med. (Maywood) 235, 478–486.

Zoratti, M., Szabo, I., 1995. The mitochondrial permeability transition. Biochim. Biophys. Acta 1241, 139–176.

Zorov, D.B., Filburn, C.R., Klotz, L.O., Zweier, J.L., Sollott, S.J., 2000. Reactive oxygen species (ROS)-induced ROS release: a new phenomenon accompanying induction of the mitochondrial permeability transition in cardiac myocytes. J. Exp. Med. 192, 1001–1014.

Zorov, D.B., Juhaszova, M., Sollott, S.J., 2006. Mitochondrial ROS-induced ROS release: an update and review. Biochim. Biophys. Acta 1757, 509–517.

ACTA PHYSIOLOGICA

Acta Physiol 2011, **202**, 11–20

Granulocyte colony-stimulating factor stabilizes cardiac electrophysiology and decreases infarct size during cardiac ischaemic/reperfusion in swine

N. Kanlop,[1,2,*] S. Thommasorn,[1,2,*] S. Palee,[1,2,*] P. Weerateerangkul,[1,2] S. Suwansirikul,[3] S. Chattipakorn[2,4] and N. Chattipakorn[1,2,5]

1 *Cardiac Electrophysiology Unit, Department of Physiology, Chiang Mai University, Chiang Mai, Thailand*

2 *Cardiac Electrophysiology Research and Training Center, Chiang Mai University, Chiang Mai, Thailand*

3 *Department of Pathology, Faculty of Medicine, Chiang Mai University, Chiang Mai, Thailand*

4 *Department of Oral Biology, Faculty of Dentistry, Chiang Mai University, Chiang Mai, Thailand*

5 *Biomedical Engineering Center, Chiang Mai University, Chiang Mai, Thailand*

Received 18 October 2010,
revision requested 5 November 2010,
final revision received 12 January 2011,
accepted 20 January 2011

Correspondence: N. Chattipakorn, MD, PhD, Cardiac Electrophysiology Research and Training Center, Faculty of Medicine, Chiang Mai University, Chiang Mai 50200, Thailand.
E-mail: nchattip@gmail.com
*These authors contributed equally in this work.

Abstract

Aim: Effects of granulocyte colony-stimulating factor (G-CSF) on cardiac electrophysiology during ischaemic/reperfusion (I/R) period are unclear. We hypothesized that G-CSF stabilizes cardiac electrophysiology during I/R injury by prolonging the effective refractory period (ERP), increasing the ventricular fibrillation threshold (VFT) and decreasing the defibrillation threshold (DFT), and that the cardioprotection of G-CSF is via preventing cardiac mitochondrial dysfunction.

Methods: In intact-heart protocol, pigs were infused with either G-CSF or vehicle (n = 7 each group) without I/R induction. In I/R protocol, pigs were infused with G-CSF (0.33 μg kg^{-1} min^{-1}) or vehicle (n = 8 each group) for 30 min prior to a 45-min left anterior descending artery occlusion and at reperfusion. Diastolic pacing threshold (DPT), ERP, VFT and DFT were determined in all pigs before and during I/R period. Rat's isolated cardiac mitochondria were used to test the protective effect of G-CSF (100 nM) in H_2O_2-induced mitochondrial oxidative damage.

Results: Neither G-CSF nor vehicle altered any parameter in intact-heart pigs. During ischaemic period, G-CSF significantly increased the DPT, ERP and VFT without altering the DFT. During reperfusion, G-CSF continued to increase the DPT without altering other parameters. The infarct size was significantly decreased in the G-CSF group, compared to the vehicle. G-CSF could also prevent cardiac mitochondrial swelling, decrease ROS production, and prevent mitochondrial membrane depolarization.

Conclusion: G-CSF increases the DPT, ERP and VFT and reduces the infarct size, thus stabilizing the myocardial electrophysiology, and preventing fatal arrhythmia during I/R. The protective mechanism could be via its effect in preventing cardiac mitochondrial dysfunction.

Keywords granulocyte colony-stimulating factor, ischaemic/reperfusion injury, mitochondria, oxidative stress, ventricular fibrillation.

Myocardial infarction remains the major problem in many countries throughout the world. Previous studies have demonstrated that myocardial injury during the ischaemic-reperfusion injury could facilitate spontaneous ventricular fibrillation (VF), decrease the VF threshold (VFT) and increase the defibrillation

threshold (DFT) (Qin *et al.*, 2002, Anastasiou-Nana *et al.* 2005). The association between arrhythmic events and the infarct size during ischaemic/reperfusion (I/R) has been demonstrated in which the reduction of the infarct size could significantly ameliorate arrhythmic events from myocardial ischaemia (Sobel *et al.* 1972, Xiao *et al.* 2008).

Granulocyte colony-stimulating factor (G-CSF) is a drug known to promote the proliferation, survival and differentiation of haematopoietic cells, and has been used as an adjuvant drug for stem cell therapy in the treatment of acute and chronic myocardial infarction (Fujita *et al.* 2007, Kastrup *et al.*, 2006). Although previous studies have shown that the combination of G-CSF and stem cell therapy enhanced the regeneration of myocardium and improved reperfusion function, thus reducing the adverse events from myocardial ischaemia (Fujita *et al.*, 2007, Kastrup *et al.* 2006), recent studies have demonstrated that G-CSF can exert its own potential effects on the heart (Yagi *et al.* 2008, Abdel-Latif *et al.* 2008). It has been shown that treating acute MI patients with G-CSF resulted in improved left ventricular function and decreased VF incidence (Baldo *et al.*, 2008, Engelmann *et al.* 2008). Despite these potential benefits, some clinical reports demonstrated otherwise (Ripa *et al.* 2006, Zohlnhofer *et al.* 2006, 2008). Nevertheless, the direct effect of G-CSF on the susceptibility of VF induction and defibrillation efficacy during ischaemia/reperfusion period has never been investigated.

Growing evidence indicates the important role of mitochondria in protection against arrhythmia. Cardiac mitochondrial membrane potential dissipation has been shown to be associated with cardiac arrhythmias, and drugs that could prevent depolarization of mitochondrial membrane potential has been demonstrated to prevent cardiac arrhythmia in the heart under various stress conditions (Aon *et al.* 2008, O'Rourke *et al.* 2007, Akar *et al.*, 2005, Aon *et al.*, 2009). In cardiac ischaemia/reperfusion (I/R) injury, reactive oxygen species (ROS) have been shown to be mainly responsible for cardiac and mitochondrial dysfunction (O'Rourke *et al.* 2007, Aon *et al.*, 2006, Akar *et al.*, 2005). A recent study also demonstrated that G-CSF could protect cardiac mitochondrial damage during the early phase of myocardial injury(Hiraumi *et al.* 2009).

In this study, the effects of G-CSF on cardiac electrophysiology as well as the incidence of VF during I/R period were investigated in swine. We hypothesized that G-CSF increases the VFT and decreases the DFT, leading to arrhythmia prevention and improved defibrillation efficacy. We also tested the hypothesis that G-CSF protects the heart during I/R injury by preventing cardiac mitochondrial dysfunction. Isolated rat's cardiac mitochondria were used to test this hypothesis. H_2O_2 was used to mimic the I/R injury by causing oxidative damage in cardiac mitochondria (Yang and Cortopassi, 1998).

Methods

Thirty domestic pigs (25–30 kg) of either sex were used in this study. This study has been carried out in accordance with the Guide for the Care and Use of Laboratory Animal as adopted and promulgated by the US National Institutes of Health and has been approved by the Institutional Animal Care and Use Committees of the Faculty of Medicine, Chiang Mai University. The pigs were anesthetized by a combination of atropine (0.04 mg kg^{-1}), telazol (4.4 mg kg^{-1}), and xylazine (2.2 mg kg^{-1}), and maintained by 1.5–3.0% isoflurane delivered in 100% oxygen. The vital signs including femoral arterial blood pressure (BP), heart rates (HR), lead II electrocardiogram, respiratory rate and core temperature were continuously monitored for the entire study. The PaO_2, end-tidal CO_2 and blood gases were measured and maintained under physiologic condition. Under artificial respiration, a 34-mm platinum coated titanium coil electrode catheter (Guidant Corp., St Paul, MN, USA) was inserted into the right ventricular apex and a 68-mm electrode catheter at the junction between right atrium and superior vena cava (Chattipakorn *et al.*, 2006, Kanlop *et al.* 2008, Shinlapawittayatorn *et al.*, 2006, Sungnoon *et al.* 2008). These two electrodes were used to deliver strong stimulus during VFT and DFT determination. Median sternotomy was done and the heart was suspended in a pericardial cradle. The left anterior descending coronary artery (LAD) was dissected from its surrounding tissues.

Two protocols were performed in this study; one in pigs with normal hearts without ischaemia (n = 14) and another in pigs with I/R hearts (n = 16). In each experimental model, pigs were divided equally into two groups; G-CSF and vehicle. In each pig, cardiac electrophysiological parameters, including diastolic pacing threshold (DPT), effective refractory period (ERP), VFT and DFT were determined at the beginning of the study. G-CSF (0.33 μg kg^{-1} min^{-1}) (Takahama *et al.*, 2006) and vehicle (normal saline solution of similar amount) were administered intravenously for 30 min in G-CSF and vehicle groups, respectively. In the intact-heart model, the cardiac electrophysiological parameters were determined before and after the drug or vehicle administration. In the I/R model, the LAD was ligated at 5 cm above a distal branch of LAD to perform a complete regional occlusion. The ischaemic period was sustained for 45 min and then the LAD was reperfused (Krug *et al.* 1966). During the first 20 min of occlusion, defibrillation shock would be delivered to terminate VF if VF spontaneously occurred. The time

interval for the first VF to occur after LAD occlusion was determined in each pig. Once the spontaneous VF disappeared or did not occur within 20 min, VF would be electrically induced for the VFT determination (Qin *et al.* 2002a). The DFT was also determined simultaneously with VFT determination. At the time of reperfusion, G-CSF or vehicle was infused again and all parameters were determined at 30 min after the reperfusion (Chattipakorn *et al.*, 2006, Kanlop *et al.*, 2008). Illustration of the study in the ischaemic-reperfusion protocol is shown in Figure 1.

A train of 10 S1 stimuli (square, 5-ms pulse width, 500-ms interval) was delivered from the tip of RV pacing electrode to determine the DPT. The pacing current was initially at 0.1 mA and increased in 0.1-mA steps until all stimuli exerted their ventricular responses. This pacing current was defined as the DPT. The ERP was determined by delivering an S2 stimulus after the last S1. The S1–S2 interval was initially set at 350 ms and was decremented in 10-ms steps until an S2 stimulus could not elicit a ventricular response. The last S1–S2 interval that elicited a ventricular response was defined as an ERP (Kanlop *et al.*, 2008).

VFT and DFT determination protocol: VF was induced by delivering a stimulus during the vulnerable period (T-wave of lead II ECG). The coupling interval for VF induction was determined by delivering a train of 10 S1s for three times and the interval between the last S1 and the peak-T wave from each train was determined. The average value of these intervals was used as a coupling interval to deliver an S2 stimulus for VF induction (Kanlop *et al.*, 2008, Chattipakorn *et al.* 2000a,b,c). A biphasic S2 shock (Ventak ECD, Guidant Corp.) was delivered through shocking electrodes for VFT and DFT determination. For VFT determination, the S2 shock strength was initially at 100 V. This strength was reduced or increased in 10-V steps depending on whether VF induction was successful or failed, respectively (Kanlop *et al.*, 2008). The lowest shock strength required for inducing VF was defined as the VFT (Kanlop *et al.*, 2008). There was a minimum interval of 4 min between each VF episode to allow the hemodynamic status to return to physiological conditions (Sungnoon *et al.*, 2008). The DFT was determined using a three-reversal up/down protocol (Chattipakorn *et al.*, 2006, Shinlapawittayatorn *et al.*, 2006). In brief, the defibrillation shock was initially at 400 V and delivered after 10 s of VF. The shock strength was decreased or increased in 80-V steps depending on whether the shock succeeded or failed to terminate VF, respectively. This process was repeated with an increment or decrement of 40-V and 20-V steps. The lowest shock strength required for successful defibrillation after the third reversal was defined as the DFT (Chattipakorn *et al.* 2006, Shinlapawittayatorn *et al.* 2006).

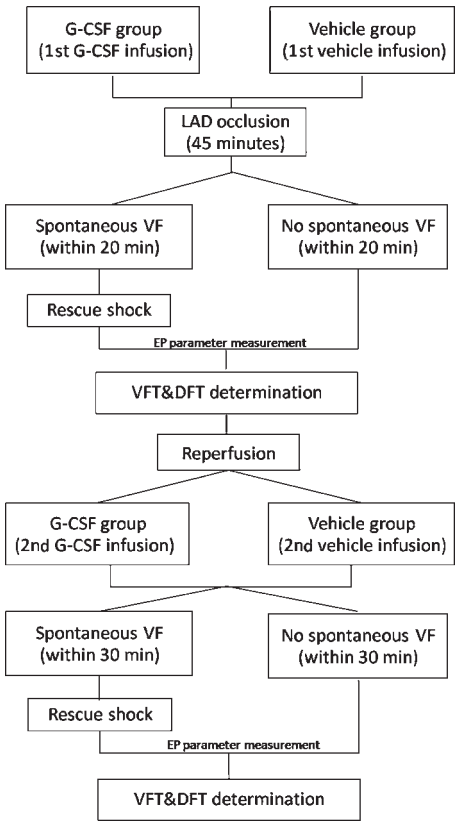

Figure 1 Illustrated diagram of the ischaemic-reperfusion protocol in swine.

G-CSF preparation

G-CSF (Neupogen®, Thousand Oaks, CA, USA) was used for intravenous infusion. A vial of Neupogen® of 1.0 mL contains 30 MU (=300 μg) of filgrastim. G-CSF 1.0 mL was diluted in 9 mL dextrose saline solution (30 μg mL^{-1}) and intravenously infused for 30 min at the rate of 0.011 mL kg^{-1}min^{-1} (0.33 μg kg^{-1} min^{-1}) (Takahama *et al.*, 2006).

Infarct size and area at risk (AAR) measurement

At the end of each experiment, the heart was removed and irrigated with normal saline to wash out blood from chambers and vessels. The LAD was occluded again at the same site previously done during the ischaemic period. The catheters were inserted into the right and left coronary ostia for Evan blue infusion. The area which could not be infused by Evan blue was defined as area of no blood flow during ischaemic period. The heart was frozen and cut horizontally into 5-mm thick slices, starting from the apex until 5 mm above the occluding site. Then, each slice was immersed in Triphenyltetrazolium chloride (TTC) at least 25 min

(Takahama *et al.*, 2006, Khalil *et al.* 2006), after which the area with viable tissue was seen in red. The area that was not stained with Evan blue was defined as area at risk (AAR). The area which demonstrated neither blue nor red was defined as the infarct site. The area measurements were performed with IMAGE tool software version 3.0 (University of Texas Health Sciences Center, San Antonio, TX, USA). The infarct site was calculated depending on the weight of each slice according to the formula of Riess *et al.* (2009):

$$\text{Total infarct size} = \frac{\sum[(\text{Infarct size of slice n}/\text{total area}) \times \text{weight of slice n}]}{\text{Total weight of slices}}$$

$$\text{Total AAR} = \frac{\sum[(\text{AAR of slice n}/\text{total area}) \times \text{weight of slice n}]}{\text{Total weight of slices}}$$

Cardiac mitochondria study protocol

In this protocol, cardiac mitochondria were isolated from the hearts of Wistar rats using the technique described previously (Larche *et al.* 2006), and the protein concentration was determined according to bicinchoninic acid (BCA) assay (Walker 1994). The morphology of the isolated cardiac mitochondria was confirmed using the electron microscope. In this protocol, H_2O_2 (2 mM) was used to mimic the oxidative stress condition occurring during I/R injury (Yang & Cortopassi 1998a). Cardiac mitochondria were divided into three treatment groups ($n = 5$ in each group): (1) a control group, (2) H_2O_2 treated group, (3) G-CSF (100 nM) plus H_2O_2 treated group. In group 2, cardiac mitochondria were incubated with H_2O_2 for 5 min, whereas in group 3 cardiac mitochondria were pre-treated with G-CSF (100 nM) for 30 min followed by H_2O_2 application for another 5 min. At the end-point, cardiac mitochondria in each group were determined for mitochondrial swelling, mitochondrial ROS production, and mitochondrial membrane potential changes.

Determination of cardiac mitochondrial swelling

The change in the absorbance of the mitochondrial suspension (0.4 mg mL^{-1}) at 540 nm ($A540$) was determined using a microplate reader (Ruiz-Meana *et al.* 2006). The decrease in the absorbance of the mitochondrial suspension indicated mitochondrial swelling.

Determination of cardiac mitochondrial ROS production

The dye dichlorohydro-fluorescein diacetate (DCFDA) was used to determine the level of ROS production in cardiac mitochondria (Novalija *et al.* 2003). DCFDA could pass through the mitochondrial membrane, and was oxidized by ROS in the mitochondria into DCF. Fluorescence was determined at λ_{ex} 485 nm and λ_{em} 530 nm using a fluorescence microplate reader. The ROS level was expressed as arbitrary units of fluorescence intensity of DCF.

Determination of cardiac mitochondrial membrane potential changes

The dye 5,5′,6,6′-tetrachloro-1,1′,3,3′-tetraethylbenzimidazolcarbocyanine iodide (JC-1) was used to determine the change in the mitochondrial membrane potential (Di Lisa *et al.* 1995, Tong *et al.* 2005). JC-1 was characterized as a cation and remained in the mitochondrial matrix as a monomer (green fluorescence) form. However, it could interact with anions in the mitochondrial matrix to form an aggregate (red fluorescence) form. JC-1 monomer fluorescence (green) was excited at 485 nm and the emission was detected at 530 nm. JC-1 aggregate fluorescence (red) was excited at 485 nm and the emission fluorescence was recorded at 590 nm. Mitochondrial depolarization was indicated by a decrease in the red/green fluorescence intensity ratio.

Statistical analysis

Values were expressed as mean ± SD. Analysis of covariance (ANCOVA) was used to assess whether the inequality of the baseline values affected the results after the treatment. Comparisons of variables before and after the drugs or vehicle administration (comparison within group) were performed individually in each group using the paired, two-tailed student's *t*-test. Comparisons among treatments of cardiac mitochondria were made by one-way ANOVA followed by the Fisher *post-hoc* test. $P < 0.05$ was considered statistically significant.

Results

In the intact-heart model, the baseline parameters such as the DPT, ERP, HR, systolic BP and diastolic BP between G-CSF and vehicle groups were not significantly different. Neither G-CSF nor saline administration altered the HR, systolic BP and diastolic BP (data not shown). The DPT was not changed after G-CSF or saline infusion. The ERP was slightly increased in the G-CSF group, however, it was not statistically significant (Table 1). For the VFT and DFT measurements, all determined parameters including the peak voltage, total energy, pulse width and impedance after G-CSF or saline infusion were not changed from their baseline values (Table 1).

Table 1 Electrophysiological parameters in the *normal-heart* pigs without ischaemia/reperfusion induction protocol

Parameters	G-CSF group (n = 7)	Vehicle group (n = 7)
Baseline		
Peak voltage (V) of VFT	47 ± 8	47 ± 8
Total energy (J) of VFT	0.2 ± 0.06	0.2 ± 0.06
Peak voltage (V) of DFT	518 ± 77	518 ± 77
Total energy (J) of DFT	21 ± 7	20 ± 7
DPT (mA)	0.3 ± 0.1	0.3 ± 0.1
ERP (ms)	284 ± 53	282 ± 53
After drug administration		
Peak voltage (V) of VFT	48 ± 6	46 ± 6
Total energy (J) of VFT	0.2 ± 0.04	0.2 ± 0.04
Peak voltage (V) of DFT	514 ± 57	502 ± 57
Total energy (J) of DFT	21 ± 5	20 ± 5
DPT (mA)	0.3 ± 0.2	0.3 ± 0.2
ERP (ms)	301 ± 36	285 ± 40

VFT, ventricular fibrillation threshold; DFT, defibrillation threshold; DPT, diastolic pacing threshold; ERP, effective refractory period.

Table 2 Electrophysiological and hemodynamic parameters at the baseline, ischaemia and reperfusion phases during the G-CSF or vehicle administration in the *ischaemia/reperfusion* protocol

Parameters	G-CSF group (n = 8)	Vehicle group (n = 8)
Pre-occlusion (baseline)		
DPT (mA)	0.2 ± 0.1	0.2 ± 0.1
ERP (ms)	253 ± 15	247 ± 17
HR (beats min^{-1})	95 ± 7	90 ± 10
Systolic pressure (mmHg)	100 ± 10	113 ± 10
Diastolic pressure (mmHg)	66 ± 10	73 ± 13
Occlusion (ischaemia)		
DPT (mA)	0.5 ± 0.2*	0.5 ± 0.2*
ERP (ms)	276 ± 18*	254 ± 15
HR (beats min^{-1})	92 ± 16	98 ± 14
Systolic pressure (mmHg)	85 ± 16*	96 ± 13*
Diastolic pressure (mmHg)	59 ± 14	62 ± 8*
Reperfusion		
DPT (mA)	0.7 ± 0.2*†	0.5 ± 0.1*
ERP (ms)	245 ± 31†	250 ± 20
HR (beats min^{-1})	96 ± 13	96 ± 8
Systolic pressure (mmHg)	66 ± 4*	73 ± 5*
Diastolic pressure (mmHg)	55 ± 9	60 ± 12*

DPT, diastolic pacing threshold; ERP, effective refractory period; HR, heart rate.
*P < 0.05 vs. the baseline in each group, $^{\dagger}P$ < 0.05 vs. ischaemic phase in each group.

In the I/R model, the baseline parameters such as the DPT, ERP, HR, systolic BP and diastolic BP between G-CSF and vehicle groups were not significantly different (Table 2). In the G-CSF group, the DPT and ERP were increased (P < 0.05) and the systolic BP was decreased (P < 0.05) during LAD occlusion, compared to the baseline. During reperfusion, the DPT was significantly increased from that at the baseline and ischaemic phase. The ERP which was significantly increased from the baseline during the occlusion period was returned to the baseline during the reperfusion phase (Table 2). The systolic BP was still significantly decreased (P < 0.05), compared to the baseline.

In the vehicle group, the DPT were increased (P < 0.05) and the systolic and diastolic BP were decreased (P < 0.05) during LAD occlusion, compared to the baseline. The ERP was not changed from the baseline during this phase. During reperfusion, the DPT was not increased from its value at ischaemic phase, but was still significantly higher than the DPT at the baseline (Table 2). Similar to the ischaemic phase, the ERP was not changed from the baseline during reperfusion.

During LAD occlusion, the incidence of VF between G-CSF (5/8) and vehicle group (4/8) were not significantly different. The time interval from the LAD occlusion to the first VF occurrence of the G-CSF (15 ± 2 min) and vehicle (19 ± 4 min) groups were not significantly different.

For the VFT measurement during the ischaemic period, both peak voltage and total energy of the VFT in the G-CSF group were significantly increased from the baseline (Fig. 2). During reperfusion, both peak voltage and total energy of the VFT in the G-CSF group were significantly decreased from the VFT during ischaemia and were not significantly different from the baseline. In the vehicle group, both peak voltage and total energy of the VFT were not significantly changed from the baseline throughout the entire study. The pulse width and impedance for the VFT were neither changed for the entire period of the study in both groups (data not shown).

For the DFT determination, all parameters including peak voltage, total energy (Fig. 3), pulse width and impedance during occlusion and reperfusion were not significantly different from the baseline parameters in both experimental groups.

The area at risk in this study was not different between the G-CSF-treated group and the vehicle-treated group (P = 0.15, Fig. 4a). However, the size of the infarct myocardium was significantly larger in the vehicle-treated group than in the G-CSF-treated group (Fig. 4b).

For cardiac mitochondrial study, H_2O_2 significantly caused cardiac mitochondrial swelling, increased mitochondrial ROS level, and depolarized mitochondrial

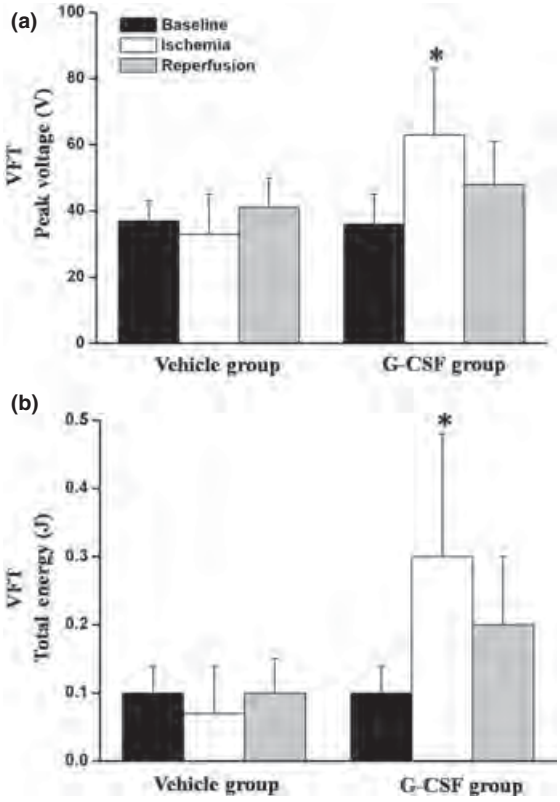

Figure 2 Effects of G-CSF and vehicle on the ventricular fibrillation threshold (VFT) at the baseline and during ischaemic and reperfusion periods. The peak voltage (a) and total energy (b) after G-CSF infusion was significantly elevated, compared to the baseline values. Vehicle did not alter the VFT. $^*P < 0.05$ compared to the baseline value.

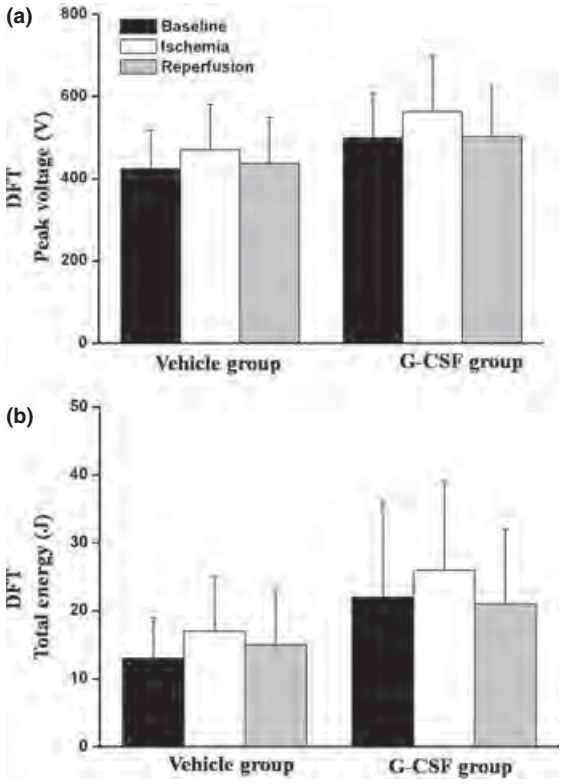

Figure 3 Effects of G-CSF and vehicle on the defibrillation threshold (DFT). The peak voltage (a) and total energy (b) after either G-CSF or vehicle infusion were not significantly altered, compared to the baseline values.

membrane potential (Fig. 5). When cardiac mitochondria were pre-treated with G-CSF, it could protect H_2O_2-induced mitochondrial swelling, decreased mitochondrial ROS level, and prevented mitochondrial depolarization (Fig. 5).

Discussion

The major findings of this study are as follows: (1) In intact heart, G-CSF did not affect any measured electrophysiologic parameter, (2) The DPT was significantly and progressively increased from the baseline during ischaemic and reperfusion phases in the G-CSF group, (3) During the ischaemic period, the ERP and the VFT in the G-CSF group were significantly increased from the baseline, but returned to the baseline value during reperfusion, (4) The DFT during ischaemia and reperfusion was not altered from the baseline in both G-CSF and vehicle groups, (5) G-CSF significantly decreased the infarct size, and (6) G-CSF protected cardiac mitochondrial swelling, decreased ROS level, and prevented mitochondrial depolarization caused by oxidative stress.

Previous clinical trials and a recent meta-analysis found that when G-CSF was used as a purpose to mobilize stem cell in patients with acute myocardial infarction, no significant differences on cardiac function or infarct size were found between G-CSF and Placebo groups (Ripa *et al.* 2006, Zohlnhofer *et al.* 2006, 2008). However, the effects of acute G-CSF administration on cardiac electrophysiology during cardiac ischaemia/reperfusion have never been investigated. Our study is the first study investigated the direct effects of G-CSF on the cardiac electrophysiology and the infarct size during cardiac I/R in a swine model. The aim was to investigate the effect of G-CSF directly on the electrophysiology and infarct size of the heart under acute I/R condition, and without stem cell therapy for myocardial recovery.

Several studies that directly investigated the direct effect of G-CSF on the heart have reported that G-CSF prevents adverse effects of acute myocardial infarction such as ventricular arrhythmia and heart failure, and improves cardiac function (Baldo *et al.* 2008, Ince *et al.* 2005, Kuhlmann *et al.* 2006). The proposed cardioprotective mechanisms of G-CSF against I/R injury include its ability to limit the infarct size (Takahama

Acta Physiologica © 2011 Scandinavian Physiological Society, doi: 10.1111/j.1748-1716.2011.02259.x

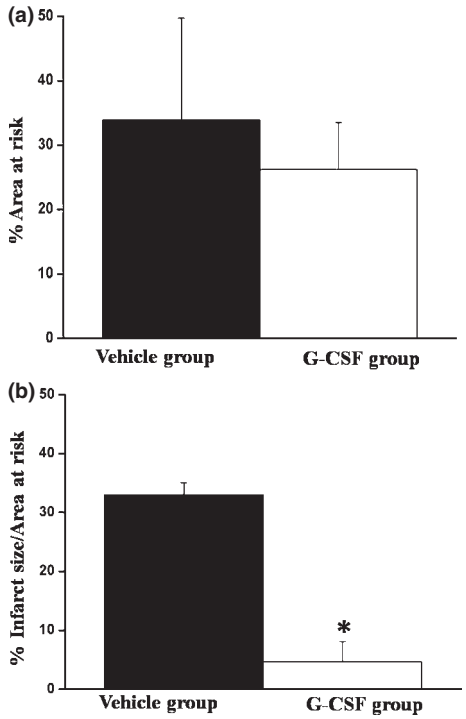

Figure 4 Effects of G-CSF and vehicle on the infarct size and area at risk (AAR). The infarct size was prominent in the vehicle group, whereas it was much smaller in the G-CSF group. The AAR was not different between the two groups. $^{*}P < 0.05$ compared to the vehicle group.

et al., 2006). Thus, consistent with a previous report in canine (Takahama *et al.*, 2006), our results clearly indicated that in this short period of acute myocardial ischaemia, G-CSF could markedly reduce the infarct size in the swine model.

In this study, the DPT was increased after LAD occlusion in both G-CSF and saline groups. However, in the former group, the DPT was further increased even after reperfusion, whereas it was not changed in the vehicle group. This finding indicates that G-CSF could have electrophysiologically stabilized the myocardium during I/R event by raising the DPT, thus preventing the heart from arrhythmia susceptibility from this ischaemia/reperfusion injury. Furthermore, the ERP was prolonged significantly during myocardial ischaemia in the G-CSF treated groups. It is known that VF induction can be facilitated by ERP shortening, and that ERP prolongation could decrease the dispersion of refractoriness in the heart, thus impeding the VF induction (Maass *et al.* 2009). Although the incidence of VF and time interval from LAD occlusion to the first observed VF between the G-CSF and vehicle groups were not different in this study, the VFT was significantly increased during the ischaemic period in the G-CSF group. Since the VFT could effectively represent the susceptibility of the heart to ventricular arrhythmia induction, increased VFT by G-CSF suggested that ischaemic myocardium had low susceptibility to VF

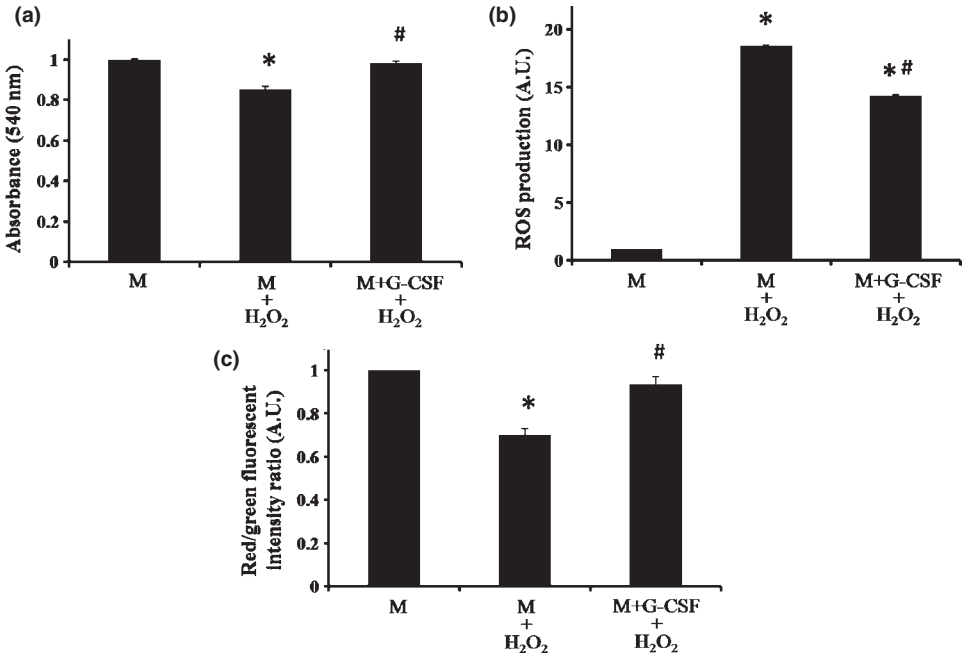

Figure 5 Effects of G-CSF on cardiac mitochondria. G-CSF could effectively prevent cardiac mitochondrial swelling (a), decrease mitochondrial ROS level (b), as well as prevent mitochondrial depolarization (c) caused by H_2O_2-induced oxidative damage. M, cardiac mitochondria; M + H_2O_2, cardiac mitochondria treated with H_2O_2; M + G-CSF + H_2O_2, cardiac mitochondria pre-treated with G-CSF, followed by H_2O_2 treatment. $^{*}P < 0.05$ vs. M, $^{\#}P < 0.05$ vs. M + H_2O_2.

induction. Also, the VF incidence in our study is different from a previous report that demonstrated a reduction in VF incidence after G-CSF administration (Takahama *et al.* 2006). This difference could be due to the different sites of LAD occlusion since the AAR in this study was 23 ± 0.9%, whereas the AAR in the previous study was ~40% (Takahama *et al.*, 2006).

Mitochondria are vital organelles in many organs including the heart. Previous studies demonstrated that it played a vital role in determining cardiac arrhythmia and cell death (Aon *et al.* 2008, O'Rourke *et al.* 2007, Akar *et al.* 2005, Aon *et al.* 2009). During ischaemia/reperfusion in the heart, ROS is known to be a major cause of cardiac dysfunction and lethal arrhythmia (O'Rourke *et al.* 2007, Aon *et al.* 2006, Akar *et al.*, 2005). In this study, we demonstrated that G-CSF could protect cardiac mitochondrial damage during H_2O_2-induced oxidative stress, by protecting cardiac mitochondrial swelling, decreasing mitochondrial ROS production, and preventing cardiac mitochondrial depolarization. It is important to note that G-CSF could completely protect the cardiac mitochondria against swelling (Fig. 5a) and membrane depolarization (Fig. 5c) caused by oxidative stress in this study since no statistical differences were found between cardiac mitochondria in the control group (group 1) and cardiac mitochondria pre-treated with G-CSF followed by H_2O_2 treatment (group 3). All of these beneficial effects could result in preserving cardiac mitochondrial function during severe oxidative stress condition as seen in the heart during ischaemia/reperfusion injury. Therefore, this role of G-CSF in preserving cardiac mitochondrial function could be responsible for its cardioprotection against ischaemia/reperfusion injury as seen in a swine model in this study. Since species differences could play an important role in the effect of G-CSF, future studies including a direct investigation on the role of cardiac mitochondria in the acute I/R model are needed to verify this hypothesis. Furthermore, future investigations on the role of G-CSF administered after the occlusion are required to warrant its clinical benefits in acute myocardial infarction.

Conclusion

G-CSF increases the DPT, ERP and the VFT, thus stabilizing the myocardial electrophysiology during acute myocardial ischaemia. However, the VF incidence and the time to VF onset are not affected by G-CSF administration. G-CSF also decreases the infarct size. Since G-CSF could protect cardiac mitochondrial dysfunction caused by oxidative damage, this beneficial effect could be responsible for its cardioprotection during I/R injury.

Conflict of interest

The authors declare that there are no conflicts of interest.

We thank Ms Rodjana Tawan and Ms Chontichaporn Tejamai for their technical assistance. The funding was supported by the Thailand Research Fund grants RTA 5280006 (NC), RMU 5180007 (SC), the Faculty of Medicine Endowment Fund, Chiang Mai University (NK, NC), and the Commission of Higher Education Thailand (SP, NC).

References

Abdel-Latif, A., Bolli, R., Zuba-Surma, E.K., Tleyjeh, I.M., Hornung, C.A. & Dawn, B. 2008. Granulocyte colony-stimulating factor therapy for cardiac repair after acute myocardial infarction: a systematic review and meta-analysis of randomized controlled trials. *Am Heart J* **156**, 216–226.

Akar, F.G., Aon, M.A., Tomaselli, G.F. & O'Rourke, B. 2005. The mitochondrial origin of postischemic arrhythmias. *J Clin Invest* **115**, 3527–3535.

Anastasiou-Nana, M.I., Tsagalou, E.P., Charitos, C., Siafakas, K.X., Drakos, S., Terrovitis, J.V., Ntalianis, A., Doufas, A., Mavrikakis, J. & Nanas, J.N. 2005. Effects of transient myocardial ischemia on the ventricular defibrillation threshold. *Pacing Clin Electrophysiol* **28**, 97–101.

Aon, M.A., Cortassa, S., Akar, F.G. & O'Rourke, B. 2006. Mitochondrial criticality: a new concept at the turning point of life or death. *Biochim Biophys Acta* **1762**, 232–240.

Aon, M.A., Cortassa, S. & O'Rourke, B. 2008. Mitochondrial oscillations in physiology and pathophysiology. *Adv Exp Med Biol* **641**, 98–117.

Aon, M.A., Cortassa, S., Akar, F.G., Brown, D.A., Zhou, L. & O'Rourke, B. 2009. From mitochondrial dynamics to arrhythmias. *Int J Biochem Cell Biol* **41**, 1940–1948.

Baldo, M.P., Davel, A.P., Nicoletti-Carvalho, J.E., Bordin, S., Rossoni, L.V. & Mill, J.G. 2008. Granulocyte colony-stimulating factor reduces mortality by suppressing ventricular arrhythmias in acute phase of myocardial infarction in rats. *J Cardiovasc Pharmacol* **52**, 375–380.

Chattipakorn, N., Fotuhi, P.C., Sreenan, C.M., White, J.B. & Ideker, R.E. 2000a. Pacing after shocks stronger than the upper limit of vulnerability: impact on fibrillation induction. *Circulation* **101**, 1337–1343.

Chattipakorn, N., Fotuhi, P.C., Zheng, X. & Ideker, R.E. 2000b. Left ventricular apex ablation decreases the upper limit of vulnerability. *Circulation* **101**, 2458–2460.

Chattipakorn, N., Rogers, J.M. & Ideker, R.E. 2000c. Influence of postshock epicardial activation patterns on initiation of ventricular fibrillation by upper limit of vulnerability shocks. *Circulation* **101**, 1329–1336.

Chattipakorn, N., Shinlapawittayatorn, K., Sungnoon, R. & Chattipakorn, S.C. 2006. Effects of n-3 polyunsaturated fatty acid on upper limit of vulnerability shocks. *Int J Cardiol* **107**, 299–302.

Di Lisa, F., Blank, P.S., Colonna, R., Gambassi, G., Silverman, H.S., Stern, M.D. & Hansford, R.G. 1995. Mitochondrial

membrane potential in single living adult rat cardiac myocytes exposed to anoxia or metabolic inhibition. *J Physiol* **486**, 1–13.

Engelmann, M.G., Theiss, H.D., Theiss, C., Huber, A., Wintersperger, B.J., Werle-Ruedinger, A.E., Schoenberg, S.O., Steinbeck, G. & Franz, W.M. 2008. G-CSF in patients suffering from late revascularized ST elevation myocardial infarction: analysis on the timing of G-CSF administration. *Exp Hematol* **36**, 703–709.

Fujita, J., Mori, M., Kawada, H., Ieda, Y., Tsuma, M., Matsuzaki, Y., Kawaguchi, H., Yagi, T., Yuasa, S., Endo, J. *et al.* 2007. Administration of granulocyte colony-stimulating factor after myocardial infarction enhances the recruitment of hematopoietic stem cell-derived myofibroblasts and contributes to cardiac repair. *Stem Cells* **25**, 2750–2759.

Hiraumi, Y., Iwai-Kanai, E., Baba, S., Yui, Y., Kamitsuji, Y., Mizushima, Y., Matsubara, H., Watanabe, M., Watanabe, K., Toyokuni, S., Matsubara, H., Nakahata, T. & Adachi, S. 2009. Granulocyte colony-stimulating factor protects cardiac mitochondria in the early phase of cardiac injury. *Am J Physiol Heart Circ Physiol* **296**, H823–H832.

Ince, H., Petzsch, M., Kleine, H.D., Eckard, H., Rehders, T., Burska, D., Kische, S., Freund, M. & Nienaber, C.A. 2005. Prevention of left ventricular remodeling with granulocyte colony-stimulating factor after acute myocardial infarction: final 1-year results of the Front-Integrated Revascularization and Stem Cell Liberation in Evolving Acute Myocardial Infarction by Granulocyte Colony-Stimulating Factor (FIRSTLINE-AMI) Trial. *Circulation* **112**, I73–I80.

Kanlop, N., Shinlapawittayatorn, K., Sungnoon, R., Chattipakorn, S., Lailerd, N. & Chattipakorn, N. 2008. Sildenafil citrate on the inducibility of ventricular fibrillation and upper limit of vulnerability in swine. *Med Sci Monit* **14**, BR205–BR209.

Kastrup, J., Ripa, R.S., Wang, Y. & Jorgensen, E. 2006. Myocardial regeneration induced by granulocyte-colony-stimulating factor mobilization of stem cells in patients with acute or chronic ischaemic heart disease: a non-invasive alternative for clinical stem cell therapy? *Eur Heart J* **27**, 2748–2754.

Khalil, P.N., Siebeck, M., Huss, R., Pollhammer, M., Khalil, M.N., Neuhof, C. & Fritz, H. 2006. Histochemical assessment of early myocardial infarction using 2,3,5-triphenyltetrazolium chloride in blood-perfused porcine hearts. *J Pharmacol Toxicol Methods* **54**, 307–312.

Krug, A., Du Mesnil, d.R. & Korb, G. 1966. Blood supply of the myocardium after temporary coronary occlusion. *Circ Res* **19**, 57–62.

Kuhlmann, M.T., Kirchhof, P., Klocke, R., Hasib, L., Stypmann, J., Fabritz, L., Stelljes, M., Tian, W., Zwiener, M., Mueller, M., Kienast, J., Breithardt, G. & Nikol, S. 2006. G-CSF/SCF reduces inducible arrhythmias in the infarcted heart potentially via increased connexin43 expression and arteriogenesis. *J Exp Med* **203**, 87–97.

Larche, J., Lancel, S., Hassoun, S.M., Favory, R., Decoster, B., Marchetti, P., Chopin, C. & Neviere, R. 2006. Inhibition of mitochondrial permeability transition prevents sepsis-induced myocardial dysfunction and mortality. *J Am Coll Cardiol* **48**, 377–385.

Maass, K., Chase, S.E., Lin, X. & Delmar, M. 2009. Cx43 CT domain influences infarct size and susceptibility to ventricular tachyarrhythmias in acute myocardial infarction. *Cardiovasc Res* **84**, 361–367.

Novalija, E., Kevin, L.G., Eells, J.T., Henry, M.M. & Stowe, D.F. 2003. Anesthetic preconditioning improves adenosine triphosphate synthesis and reduces reactive oxygen species formation in mitochondria after ischemia by a redox dependent mechanism. *Anesthesiology* **98**, 1155–1163.

O'Rourke, B., Cortassa, S., Akar, F. & Aon, M. 2007. Mitochondrial ion channels in cardiac function and dysfunction. *Novartis Found Symp* **287**, 140–151.

Qin, H., Walcott, G.P., Killingsworth, C.R., Rollins, D.L., Smith, W.M. & Ideker, R.E. 2002. Impact of myocardial ischemia and reperfusion on ventricular defibrillation patterns, energy requirements, and detection of recovery. *Circulation* **105**, 2537–2542.

Riess, M.L., Rhodes, S.S., Stowe, D.F., Aldakkak, M. & Camara, A.K. 2009. Comparison of cumulative planimetry versus manual dissection to assess experimental infarct size in isolated hearts. *J Pharmacol Toxicol Methods* **60**, 275–280.

Ripa, R.S., Jorgensen, E., Wang, Y., Thune, J.J., Nilsson, J.C., Sondergaard, L., Johnsen, H.E., Kober, L., Grande, P. & Kastrup, J. 2006. Stem cell mobilization induced by subcutaneous granulocyte-colony stimulating factor to improve cardiac regeneration after acute ST-elevation myocardial infarction: result of the double-blind, randomized, placebo-controlled stem cells in myocardial infarction (STEMMI) trial. *Circulation* **113**, 1983–1992.

Ruiz-Meana, M., Garcia-Dorado, D., Miro-Casas, E., Abellan, A. & Soler-Soler, J. 2006. Mitochondrial Ca2+ uptake during simulated ischemia does not affect permeability transition pore opening upon simulated reperfusion. *Cardiovasc Res* **71**, 715–724.

Shinlapawittayatorn, K., Sungnoon, R., Chattipakorn, S. & Chattipakorn, N. 2006. Effects of sildenafil citrate on defibrillation efficacy. *J Cardiovasc Electrophysiol* **17**, 292–295.

Sobel, B.E., Bresnahan, G.F., Shell, W.E. & Yoder, R.D. 1972. Estimation of infarct size in man and its relation to prognosis. *Circulation* **46**, 640–648.

Sungnoon, R., Kanlop, N., Chattipakorn, S.C., Tawan, R. & Chattipakorn, N. 2008. Effects of garlic on the induction of ventricular fibrillation. *Nutrition* **24**, 711–716.

Takahama, H., Minamino, T., Hirata, A., Ogai, A., Asanuma, H., Fujita, M., Wakeno, M., Tsukamoto, O., Okada, K., Komamura, K., Takashima, S., Shinozaki, Y., Mori, H., Mochizuki, N. & Kitakaze, M. 2006. Granulocyte colony-stimulating factor mediates cardioprotection against ischemia/reperfusion injury via phosphatidylinositol-3-kinase/Akt pathway in canine hearts. *Cardiovasc Drugs Ther* **20**, 159–165.

Tong, V., Teng, X.W., Chang, T.K. & Abbott, F.S. 2005. Valproic acid II: effects on oxidative stress, mitochondrial membrane potential, and cytotoxicity in glutathione-depleted rat hepatocytes. *Toxicol Sci* **86**, 436–443.

Walker, J.M. 1994. The bicinchoninic acid (BCA) assay for protein quantitation. *Methods Mol Biol* **32**, 5–8.

Xiao, Y.F., Sigg, D.C., Ujhelyi, M.R., Wilhelm, J.J., Richardson, E.S. & Iaizzo, P.A. 2008. Pericardial delivery of omega-3 fatty acid: a novel approach to reducing myocardial infarct sizes and arrhythmias. *Am J Physiol Heart Circ Physiol* **294**, H2212–H2218.

Yagi, T., Fukuda, K., Fujita, J., Endo, J., Hisaka, Y., Suzuki, Y., Tamura, M. & Ogawa, S. 2008. G-CSF augments small vessel and cell density in canine myocardial infarciton. *Keio J Med* **57**, 139–149.

Yang, J.C. & Cortopassi, G.A. 1998. Induction of the mitochondrial permeability transition causes release of the apoptogenic factor cytochrome c. *Free Radic Biol Med* **24**, 624–631.

Zohlnhofer, D., Ott, I., Mehilli, J., Schomig, K., Michalk, F., Ibrahim, T., Meisetschlager, G., von Wedel, J., Bollwein, H., Seyfarth, M., Dirschinger, J., Schmitt, C., Schwaiger, M., Kastrati, A. & Schomig, A. 2006. Stem cell mobilization by granulocyte colony-stimulating factor in patients with acute myocardial infarction: a randomized controlled trial. *JAMA* **295**, 1003–1010.

Zohlnhofer, D., Dibra, A., Koppara, T., de Waha, A., Ripa, R.S., Kastrup, J., Valgimigli, M., Schomig, A. & Kastrati, A. 2008. Stem cell mobilization by granulocyte colony-stimulating factor for myocardial recovery after acute myocardial infarction: a meta-analysis. *J Am Coll Cardiol* **51**, 1429–1437.

Life Sciences 88 (2011) 619–627

Contents lists available at ScienceDirect

Life Sciences

journal homepage: www.elsevier.com/locate/lifescie

Effects of high-fat diet on insulin receptor function in rat hippocampus and the level of neuronal corticosterone

Wasana Pratchayasakul [a], Sasiwan Kerdphoo [a], Petnoi Petsophonsakul [a], Anchalee Pongchaidecha [a], Nipon Chattipakorn [a], Siriporn C. Chattipakorn [a,b,*]

[a] Cardiac Electrophysiology Research and Training Center, Department of Physiology, Faculty of Medicine, Chiang Mai University, Chiang Mai 50200, Thailand
[b] Department of Odontology and Oral Pathology, Faculty of Dentistry, Chiang Mai University, Chiang Mai 50200, Thailand

ARTICLE INFO

Article history:
Received 15 September 2010
Accepted 20 January 2011

Keywords:
High-fat diet
Insulin resistance
Hippocampus
Insulin-mediated LTD

ABSTRACT

Aim: Chronic consumption of a high-fat (HF) diet contributes to peripheral insulin resistance and elevated plasma corticosterone. However, the effect of HF consumption on the neurofunctional insulin receptors and neuronal corticosterone level is unclear. We tested the hypothesis that HF consumption can lead to peripheral insulin resistance, elevated neuronal corticosterone, and impaired neuronal responses to insulin.
Main methods: Male Wistar rats were fed with normal diet or HF diet for 4, 8 or 12 weeks. At the end of each dietary period, plasma was collected for investigating peripheral insulin resistance parameters and corticosterone. Brains were then rapidly removed for studying the function of neuronal insulin receptors (IRs) by extracellular recording in CA1 hippocampus, neuronal IR signaling by immunoblot technique and neuronal corticosterone.
Key findings: Elevated plasma corticosterone level was initially seen in 4-week HF-fed rats. Peripheral insulin resistance developed at 8-week HF-fed rats. However, the elevated neuronal corticosterone level was found at 12-week HF consumption. The neuronal IR response demonstrated by insulin-mediated long-term depression in CA1 hippocampus was diminished in 12-week HF-fed rats. The phosphorylation levels of neuronal IR, IR substrate 1 and Akt/PKB were decreased in 12-week HF-fed rats with no change in these proteins. There was a correlation among peripheral insulin resistance, neuronal stress (elevated neuronal corticosterone), and neuronal insulin resistance in HF group.
Significance: Our findings suggest that HF consumption can lead to the elevation of corticosterone and peripheral insulin resistance, which could contribute to neuronal insulin resistance and neuronal stress.

Introduction

Insulin has been shown to play a role in synaptic plasticity by facilitating clathrin-dependent internalization of alpha-amino-3 hydroxy-5-methylisoxazole-4-propionic acid (AMPA) receptors, causing long-term depression (LTD) in hippocampal CA1 neurons (Ahmadian et al., 2004; Man et al., 2000). That evidence indicates that the neurofunctional IRs in the CA1 hippocampus is insulin-mediated LTD. Moreover, the activation of insulin receptors turns on the protein kinase activity of the IR, which triggers cascades of signal transduction through its downstream substrate molecules. Several insulin receptor signaling pathways activated by IRs include insulin receptor substrate-1 (IRS-1) (Olefsky, 1990). It has been demonstrated that rats trained in a spatial learning task showed the learning-specific increase in IRS-1 in the hippocampal synaptic membrane (Morris et al., 2004). These findings suggest that IR signaling plays a role in learning and memory by modulating activities of synaptic plasticity such as insulin-mediated LTD and by triggering signal transduction cascades such as IR, IRS-1 and serine/threonine-specific protein kinase/protein kinase B (Akt/PKB).

In hamsters with insulin resistance induced by fructose feeding, it has been shown that hippocampal synaptic plasticity, an important biological mechanism of learning and memory, was impaired (Mielke et al., 2005). Excessive fat consumption has also been shown to play an important part in the development of insulin resistance and type2 diabetes (Zierath et al., 1998). Several studies suggest that consumption of a diet rich in fat for 3 months can develop peripheral insulin resistance and impede cognitive performance (Greenwood and Winocur, 2005; Kalmijn et al., 2004). These findings suggest that the development of insulin resistance can mediate the cognitive deficit associated with HF diet. However, the effect of HF diet on the neurofunctional IRs is still unclear. In addition, the effects of time-course of HF diet consumption on the neurofunctional IRs have never been investigated. Therefore, in this study we tested the hypothesis that HF consumption for a specific period of time can cause peripheral

* Corresponding author at: Department of Odontology and Oral Pathology, Faculty of Dentistry, Chiang Mai University, Chiang Mai 50200, Thailand. Tel.: +66 53 944 451; fax: +66 53 222 844.
E-mail address: s.chat@chiangmai.ac.th (S.C. Chattipakorn).

0024-3205/$ – see front matter © 2011 Elsevier Inc. All rights reserved.
doi:10.1016/j.lfs.2011.02.003

insulin resistance and can lead to impaired neuronal response to insulin (or neuronal insulin resistance). We used an electrophysiological study to investigate whether the neuronal responses to insulin (insulin-mediated LTD) are altered by HF consumption at different time course in order to detect the earliest stage of the disruption of the neurofunctional IRs. We also examined the alteration of biochemical activity of insulin receptor pathways: IR, IRS-1 and Akt/PKB, in the brain following each time course of HF consumption.

Glucocorticoid participates in the control of homeostasis and stress. Previous studies demonstrated that adrenal corticosteroid level was increased in rodents with diabetes (Chan et al., 2005; Langley and York, 1990). In addition, Stranahan and colleagues demonstrated that diabetes could impair hippocampal function via glucocorticoid effects (Stranahan et al., 2008a,b). Despite these findings, the correlation among peripheral and neuronal insulin resistance, and the level of corticosterone following HF consumption has not yet been investigated. In this study, we also determined whether the neuronal insulin resistance can develop with neuronal stress after HF consumption by using the amount of neuronal corticosterone as an indicator of neuronal stress.

Materials and methods

Animals and dietary protocols

All experiments were conducted in accordance with an approved protocol from the Faculty of Medicine, Chiang Mai University Institutional Animal Care and Use Committee, in compliance with NIH guidelines. Male Wistar rats weighing ~200 g were obtained from the National Animal Center, Salaya Campus, Mahidol University, Thailand. All animals were individually housed in a temperature-controlled environment with a 12:12 light–dark cycle. One week after arrival, rats were randomly assigned to one of the two dietary groups ($n = 43$ in high-fat diet group and $n = 44$ in normal diet group). The normal-diet (ND) group received a standard laboratory chow, in which 19.7% of total energy (%E) was from fat, with energy content calculated at 4.02 kcal/g (Mouse Feed Food No.082, C.P. Company, Bangkok, Thailand). The HF group consumed a diet containing fat, mostly from lard (59.3% E), with energy content calculated at 5.35 kcal/g, for 12 weeks. The animals were maintained in individual cages with unrestricted access to food and water. Body weight and food intake were recorded daily. Blood samples were collected from the tail at weeks 4, 8 and 12 after fasting for at least 5 h. Plasma was separated and stored at −80 °C for subsequent biochemical analyses. At the end of each experimental period (4, 8 and 12 weeks) of both dietary regimens, animals were deeply anesthetized and decapitated. The brain was rapidly removed for brain slice preparation and one lobe of liver as well as visceral fat were removed, weighed and stored at −80 °C for further biochemical analysis.

The oral glucose tolerance test (OGTT) was investigated in the 12-week HF diet and 12-week ND group. After rats being on the dietary for 12 weeks, animals were fast for 12 h before they were used in the OGTT. An OGTT consisted of 2 g/kg body weight glucose feeding by gavage. Blood was collected from a small cut at the tip of the tail immediately before and at 15, 30, 60 and 120 min after glucose feeding. The plasma was stored at −80 °C until it was used for glucose analysis with a commercially available kit (Biotech, Bangkok, Thailand).

Analytical procedure for the level of glucose, triglyceride, insulin and corticosterone in plasma and neuronal corticosterone

Fasted plasma glucose and triglyceride concentrations were determined by colorimetric assay using commercially available kits (Biotech, Bangkok, Thailand). Fasted plasma insulin level was measured by Sandwich ELISA kits (LINCO Research, Missouri, USA). Neuronal corticosterone levels from brain homogenate samples and fasted plasma corticosterone levels were measured using an enzyme imunoassay kit (Assay Designs Inc, Ann Arbor, MI, USA).

Determination of insulin resistance (HOMA index)

Insulin resistance was assessed by Homeostasis Model Assessment (HOMA) (Appleton et al., 2005; Haffner et al., 1997) as a mathematical model describing the degree of insulin resistance, calculated from fasting plasma insulin and fasting plasma glucose concentration. A higher HOMA index indicates a higher degree of insulin resistance.

Analysis of liver triglyceride concentration

Tissue homogenates were prepared for triglyceride assay by a modification of the method of Frayn and Maycock (Frayn et al., 1980). The triglyceride concentration was analyzed with a commercially available kit (Biotech, Bangkok, Thailand).

Brain slice preparation

At the end of weeks 4, 8 and 12, the animals were anesthetized with isoflurane after fasting for at least 5 h. Brain slice preparation was following our previous study (Chattipakorn and McMahon, 2002). Hippocampal slices were used for the extracellular recordings, immunoprecipitation and immunoblotting.

Extracellular recording of hippocampal slices

To investigate insulin-induced long-term depression (LTD), the hippocampal slices were transferred to a submersion recording chamber and continuously perfused at 3–4 ml/min with standard aCSF warmed to 25–28 °C. Field excitatory postsynaptic potentials (fEPSPs) were evoked by stimulating the Schaffer collateral–commissural pathway with a bipolar tungsten electrode, while recordings were gathered from the stratum radiatum of the hippocampal CA1 region with micropipettes (3 Mohm) filled with 2 M NaCl. Stimulus frequency was 0.033 Hz. The stimulus intensity was adjusted to yield a fEPSP of 0.8–1.0 mV in amplitude. Hippocampal slices were perfused with aCSF (as baseline condition) for 10 min and then perfused with aCSF plus 500 nM insulin (as insulin stimulation) for 10 min, after which the hippocampal slices were perfused with aCSF again (wash out) and recorded for the next 30 min.

To investigate that the reduction of insulin-mediated LTD was the result of an alteration of neuronal insulin signaling and not a non-specific alteration of synaptic transmission following neuronal insulin resistance, we examined the characterized form of synaptic plasticity that may not depend upon insulin signaling, by measuring paired pulse facilitation (PPF) and carbachol-induced LTD (mLTD). PPF is a measurement of short-term potentiation, which may occur at the presynaptic sites (Zucker and Regehr, 2002). PPF occurs following two identical stimulations, separated by 50-msec, applied to the Schaffer collateral. To investigate mLTD, the protocol was as following. The stable 10-min baseline of CA1 fEPSPs was recorded by stimulating the Schaffer collateral–commisural pathway with bipolar tungsten electrode. Stimulus frequency was 0.1 Hz and stimulus intensity was adjusted to yield fEPSPs of 0.8–1.0 mV amplitude. The cholinergic agonist, carbachol 50 μM (Calbiochem, San Diego, CA, USA), was superfused for 10 min to induce mLTD after which the carbachol was washed out and recorded for the next 30 min.

All data were filtered at 3 kHz, digitized at 10 kHz, and stored on a computer using pClamp 9.2 software (Axon Instruments, Foster City, CA, USA). The initial slope of the fEPSPs was measured and plotted vs. time using Origin 8.0 software.

Preparation of brain homogenates for immunoprecipitation, immunoblotting and neuronal corticosterone measurement

To examine the alteration of neuronal insulin-mediated phosphorylation of the IR, the IRS-1 and the Akt/PKB following 4, 8 and 12 weeks of two dietary regimens, six brain slices per animal were placed into either aCSF or aCSF plus 500 nM insulin (Humelin R, Eli Lilly, Giessen, Germany) for 5 min. Then, three brain slices in each conditioned group were homogenized in 500 μl of ice-cold brain slice lysis buffer [1 mM EDTA, 1 mM EGTA, 1% NP-40, 1% Triton X-100 and supplemented with a protease inhibitor cocktail, Roche complete mini-tablets, (Roche Molecular Biochemicals, Indianapolis, IN, USA)]. Next, the homogenates were centrifuged at 9000 *g* for 30 min at 4 °C and the protein concentration was measured using the Bio-Rad DC Protein assay kit (Bio-Rad Laboratories, Hercules, CA, USA). These homogenates were then stored at −80 °C for further biochemical analysis of the tyrosine phosphorylation of IR, IRS-1 and Akt/PKB.

To determine the level of IR, IRS-1 and Akt/PKB protein expression as well as the level of neuronal corticosterone in the brain, another set of three brain slices in aCSF was homogenized over ice in non-ionizing lysis buffer containing: 100 mM NaCl, 25 mM EDTA, 10 mM Tris, 1% Triton X-100, and 1% NP-40 supplemented with a protease inhibitor cocktail (Roche Molecular Biochemicals). Then, homogenates were stored at −80 °C for further western blot analysis of IR, IRS-1, Akt/PKB and biochemical analysis of neuronal corticosterone levels.

Immunoprecipitation and immunoblotting

IRS-1 protein and tyrosine phosphorylation of IR and IRS-1 were immunoprecipitated from brain homogenates with polyclonal antibodies against each protein (1 μg antibody/500 μg total lysate). Rabbit anti-IR and rabbit anti-IRS-1 (Santa Cruz Biotechnology, Santa Cruz, CA, USA) with protein A agarose beads were used to prepare each protein for immunoprecipitation as previously described (Mielke et al., 2005). Then, the proteins were separated by electrophoresis with SDS-Page on 10% polyacrylamide gels (Bio-Rad Laboratories) and transferred to nitrocellulose membranes and immunoblotting was conducted with anti IRS-1 rabbit and phosphotyrosine antibody (rabbit polyclonal, 1:600 in TBST, Santa Cruz Biotechnology) to determine the changes in IRS-1 level and insulin-mediated tyrosine phosphorylation of the IR and IRS-1, respectively.

Akt/PKB in both serine 473 and threonine 308 kinases phosphorylation were electrophoresed and immunoblotted with rabbit antibodies Akt/PKB both serine 473 and threonine 308. Examination of the levels of IRβ and Akt/PKB protein was conducted with homogenates prepared from another set of three brain slices. Both proteins were resolved by the immunoprecipitation and immunoblot assay conducted with rabbit anti-IR and rabbit anti-Akt/PKB (1:1000 in TBST, Santa Cruz Biotechnology). For loading control, immunoblotting for each membrane was completed incubation with anti-β-actin (1:400; rabbit polyclonal; Sigma, Missouri, USA).

All membranes for visualizing the phosphorylation and the protein levels of IR, IRS-1 and Akt/PKB were incubated with secondary goat anti-rabbit antibody conjugated with horseradish peroxidase (1:8000 in TBST, Bio-Rad Laboratories) and Amersham ECL western blotting detection reagents (GE Healthcare, Buckinghamshire, UK). Band intensities were quantified by Scion Image and the results were shown in average signal intensity (arbitrary) units.

Statistical analysis

Data were presented as means ± SE. All statistical analyses were performed using the program SPSS (version 16; SPSS, Chicago, IL, USA). The significance of the difference between the means was calculated by Student's *t*-test with $p<0.05$ for the OGTT test and two-way ANOVA between treatment and time following with post-hoc analysis for remaining parameters. Pearson's correlation analysis was used to determine the relationship among the plasma parameters, liver triglyceride content, visceral fat, body weight, and neuronal corticosterone in hippocampus and the percentages of insulin-mediated LTD in all animals.

Results

Peripheral insulin resistance developed in rats after 8-week HF feeding

The initial animal body weight was not different among experimental groups. Animals fed with HF for 4 weeks had an increased in body weight compared to rats fed with ND (Table 1). However, the level of glucose, triglyceride, and insulin in plasma and HOMA index did not differ between both dietary groups.

Animals in the 8-week and 12-week HF group had a significant increase in body weight, visceral fat, fasted plasma glucose, plasma insulin, liver triglyceride content and HOMA index compared to those with ND feeding ($p<0.05$, Table 1). However, plasma triglyceride and free fatty acid level were not significantly different between both dietary groups.

In addition, we found that body weight, visceral fat and plasma glucose level were increased in a time-dependent manner in both dietary groups. However, the HOMA index was increased in a time-dependent manner only in the HF group. The glucose responses during the OGTT in the 12-week HF group was markedly increased at 15-, 30- and 60 min time points, compared to those in the ND group ($p<0.05$). The total area under the glucose curve (AUCg) was also significantly increased in the 12-week HF group (26.3 ± 9.3 g/dl × min vs. 21.2 ± 5.7 g/dl × min of ND, $p<0.05$).

Rats fed with the HF diet consumed less food per day than those on the ND ($p<0.05$). However, when the consumed food weights were converted to caloric intake, rats fed with HF consumed more calories per day than rats fed with ND ($p<0.01$).

HF feeding for 12 weeks reduced the ability of insulin to induce LTD in hippocampal CA1 circuits

In all time courses (4-, 8- and 12-week) of ND-fed rats, we found that insulin application to hippocampal slices reduced the size of the fEPSP responses at 2–3 min after the start of insulin infusion with maximum effects appearing over the following 10–15 min, and the depression of fEPSPs was prominent and long lasted for 30–40 min (Figs. 1 and 2A). In our set-up, 500 nM insulin added to the infusion line required approximately 1 min to reach the slices.

In HF animals, the degree of insulin-mediated LTD observed from slices of 4-week and 8-week HF animals was not significantly reduced compared to the 4-week and 8-week ND animals ($n=6$–8 independent slices per group, $n=6$ animals/group, Fig. 1). In the 12-week HF-fed group, the amount of insulin-mediated LTD was significantly diminished ($p<0.05$ vs. ND group, Fig. 2A). At 30-minute post-insulin stimulation, the percentage reduction of the normalized fEPSP slope from 12-week ND was 73.60 ± 4.18% of the average slope recording during the baseline level ($n=16$ independent slices, $n=14$ animals/group), while the percentage reduction of fEPSPs of 12-week HF slices was 9.34 ± 3.09% of the values recorded before insulin application ($n=17$ independent slices, $n=13$ animals/group) (Fig. 2A). Furthermore, we found that the average degree of insulin-mediated LTD at all time courses of both dietary groups was significantly correlated with several peripheral insulin resistance parameters ($p<0.01$; as shown in Table 2).

We found no significant difference in the pair-pulsed facilitation (PPF), which is a ratio of fEPSP slope$_2$/fEPSP slope$_1$, of slices recorded at the baseline between both dietary groups at all time courses ($p>0.05$). To confirm whether the impairment of the insulin-mediated LTD in 12-week HF group could occur without the

Table 1
Effect of 4-, 8- and 12-week HF diet feeding on body weight, visceral fat, fasted plasma glucose, triglyceride, free fatty acid, insulin, liver triglyceride and HOMA index. *, $p<0.05$ compared to ND group in each time course; [a], $p<0.05$ compared to 4-week group of the same dietary regimen; [b], $p<0.05$ compared to 8-week group of the same dietary regimen.

Parameters	4 weeks		8 weeks		12 weeks	
	ND	HF	ND	HF	ND	HF
Body weight (g)	354.62 ± 5.35	394.60 ± 6.82 *	427.50 ± 5.93 [a]	501.67 ± 7.31 *,[a]	460.18 ± 8.37 [a,b]	546.25 ± 8.32 *,[a,b]
Visceral fat (g)	16.67 ± 1.21	31.00 ± 3.97 *	17.68 ± 2.94	47.02 ± 5.43 *,[a]	25.19 ± 1.96 [a]	45.47 ± 2.01 *,[a]
Glucose (mg/dl)	130.88 ± 3.49	123.13 ± 3.10	130.03 ± 4.21	150.03 ± 5.70 *,[a]	149.41 ± 4.39 [a]	153.42 ± 2.95 [a]
Triglyceride (mg%)	87.44 ± 4.75	72.33 ± 7.43	72.28 ± 3.94	65.70 ± 4.24	84.89 ± 6.85	76.84 ± 5.48
Free fatty acid (mM)	0.63 ± 0.06	0.53 ± 0.06	0.66 ± 0.07	0.54 ± 0.09	0.83 ± 0.13	0.77 ± 0.08
Insulin (ng/ml)	2.42 ± 0.53	2.79 ± 0.34	2.02 ± 0.35	3.73 ± 0.73*	2.14 ± 0.54	4.23 ± 0.59*
Liver triglyceride (mg/g tissue)	21.15 ± 2.21	170.52 ± 19.00*	18.51 ± 1.94	171.10 ± 27.11*	17.50 ± 1.50	173.40 ± 6.99*
HOMA index	17.15 ± 4.51	17.10 ± 3.72	16.35 ± 3.56	31.42 ± 7.10*,[a]	20.05 ± 5.57	39.69 ± 5.69*,[a]

interruption of other forms of plasticity, the experiment of carbachol-induced LTD was performed. We found that the degree of carbachol-induced LTD in CA1 hippocampus of both 12-week HF and ND groups was similar (Fig. 2B).

Depressed phosphorylation of insulin receptor (IR), insulin receptor substrate-1 (IRS-1) and Akt/PKB levels in brain slices after 12-week HF consumption

In order to compare neuronal insulin receptor signaling within 4-, 8- and 12-week time courses between HF and ND rats, we investigated whether the protein levels of IR, IRS-1 and Akt/PKB were down-regulated in relation to the reduction of the ability of insulin-mediated LTD in CA1 hippocampus. We found that the levels of the IR, IRS-1 and Akt/PKB from 4-, 8- and 12-week HF brain slices were not significantly different from 4-, 8- and 12-week ND brains (Fig. 3, n = 4–8 animals/group).

Interestingly, the IRS-1 protein levels in the 12-week HF group revealed a 20% reduction from those slices observed in the 12-week ND group, however, it was not significantly different ($p = 0.1$, n = 8/group, Fig. 3B). Although, there is no significant difference in the expression of IRS-1 protein in both dietary groups at each time-course, we found that the longer time of high-fat diet consumption leads to the reduction of IRS-1 expression ($p<0.05$, Fig. 3B).

The phosphorylation status of IR, IRS-1 and Akt/PKB in the acutely prepared brain slices under basal condition following the insulin stimulation is illustrated in Fig. 4. The basal (non-insulin stimulated) phosphorylation levels of IR and IRS-1 from the 4-, 8- and 12-week ND and from the 4-, 8- and 12-week HF groups were weakly variable detected by immunoprecipitation and phosphotyrosine immunoblotting. The possible explanation of the variability of basal phosphorylation levels is that the different endogenous insulin levels in the brainslices, could stimulate the phosphorylation of IR, IRS-1 and Akt/PKB, even though there was no exogenous insulin application onto the brainslices. However, insulin stimulation resulted in the strong observable phosphorylation of IR, IRS-1 and Akt/PKB levels in 4-, 8- and 12-week ND and 12-week HF groups (Fig. 4A–D). In 4-, 8- and 12-week ND-fed rats, the exposure to insulin stimulation resulted in an increase in IR, IRS-1 and Akt/PKB phosphorylation, compared to their own basal condition. Interestingly, at 12-week feeding, the insulin-stimulated IR phosphorylation was significantly lower in the HF group (0.96 ± 0.03) than in the ND group (1.28 ± 0.06), accounting for ~25% reduction ($p<0.01$, n = 11/group, Fig. 4A). We also found that the reduction of the insulin-stimulated IR phosphorylation in only high-fat diet consumption group was a time-dependent manner ($p<0.05$, Fig. 4A). Similarly, the insulin-stimulated IRS-1 phosphorylation was significantly lower in the 12-week HF group (1.02 ± 0.04) than in the 12-week ND group (1.20 ± 0.03), accounting for ~15% reduction ($p<0.01$, Fig. 4B). From the brain slices of the 12-week HF group, Akt/PKB phosphorylation of serine 473 was significantly decreased, compared to that in the ND group ($p<0.05$, Fig. 4C), and the Akt/PKB phosphorylation of threonine 308 was slightly decreased but did not reach a statistical significance ($p = 0.05$, Fig. 4D).

Increased plasma and neuronal corticosterone levels following HF consumption

Lin and colleagues have shown that increased plasma corticosterone level could induce peripheral insulin resistance (Lin et al., 2000; Stranahan et al., 2008a,b). In the present study, we also found that the levels of plasma corticosterone in HF-fed rats were significantly higher than those in the ND rats starting from 4-week HF consumption and remained higher throughout the course of the study ($p<0.05$, Fig. 5A). The increased level of plasma corticosterone in these HF-fed

Table 2
Correlation among peripheral insulin resistance parameters, % change of fEPSP slope in response to 500 nM insulin and neuronal corticosterone in rats that received normal diet or high-fat diet for 4, 8 and 12 weeks. *, correlation is significant at the 0.05 level; **, correlation is significant at the 0.01 level.

Parameters	% change of fEPSP slope in response to 500 nM insulin	Body weight (g)	Visceral fat (g)	Plasma glucose (mg/dl)	Plasma insulin (ng/ml)	Liver triglyceride content (mg/g tissue)	HOMA index	Plasma corticosterone (ng/ml)	Neuronal corticosterone (ng/mg protein)
% change of fEPSP slope in response to 500 nM insulin	1	−0.808**	−0.622**	0.553**	−0.440**	−0.593	−0.634	−0.746**	−0.652**
Body weight (g)	−0.808**	1	0.775**	0.581**	0.532**	0.677**	0.684**	0.759**	0.452*
Visceral Fat (g)	−0.622**	0.775**	1	0.553**	0.470**	0.791**	0.626**	0.725**	0.497**
Plasma glucose (mg/dl)	−0.500**	0.581**	0.553**	1	0.201	0.412*	0.600**	0.571**	0.363
Plasma insulin (ng/ml)	−0.440**	0.532**	0.470**	0.201	1	0.608**	0.589**	0.414*	0.475*
Liver triglyceride content (mg/g tissue)	−0.593**	0.677**	0.791**	0.412*	0.608**	1	0.679**	0.697**	0.470*
HOMA index	−0.634**	0.684**	0.626**	0.600**	0.589**	0.679**	1	0.585**	0.547**
Plasma corticosterone (ng/ml)	−0.746**	0.759**	0.725**	0.571**	0.414**	0.697**	0.585**	1	0.387
Neuronal corticosterone (ng/mg protein)	−0.652**	0.452**	0.497**	0.363	0.475*	0.471*	0.547**	0.387	1

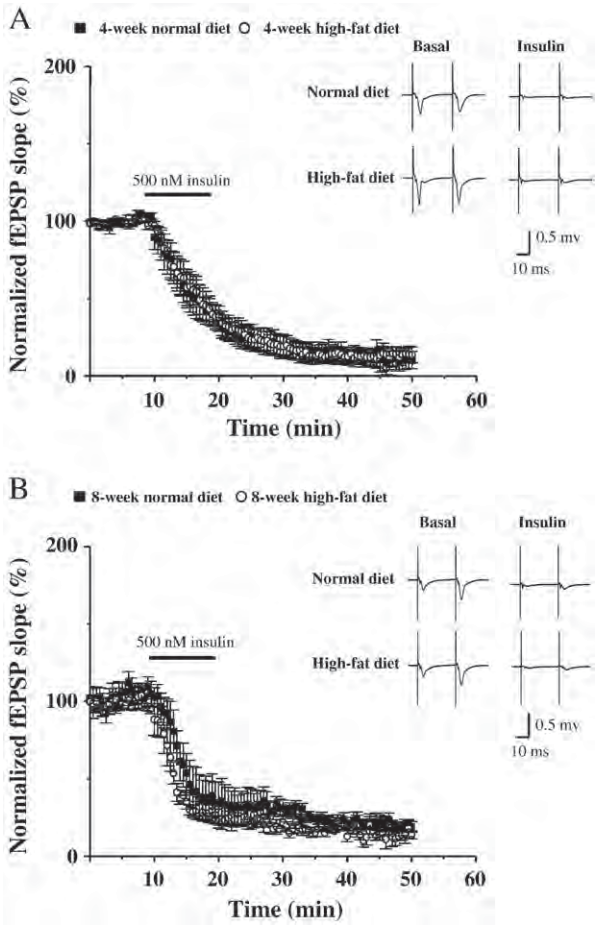

Fig. 1. Four- and eight-week HF diet feeding had no effects on the ability of insulin-mediated long-term depression (LTD) on fEPSPs in hippocampal CA1 regions. Panels A and B represent responses before and after insulin stimulation in brain slices from ND and HF groups. *Panel A*: Average normalized fEPSPs (fEPSPt/fEPSPo with fEPSPs being points at which fEPSP slopes stabilized) from 4-week-ND-fed (n = 6–8 independent slices per 6 animals) and 4-week-HF-fed (n = 6–8 independent slices per 6 animals) brain slices *Panel B*: Average normalized fEPSPs from 8-week-ND-fed (n = 6–8 independent slices per 6 animals) and 8-week-HF-fed (n = 6–8 independent slices per 6 animals) brain slices. Both 4-week and 8-week HF diets had no effect on the ability of insulin to depress fEPSPs. Examples of averages of 20 consecutive traces taken from a slice treated with aCSF (basal) and with 500 nM (insulin) are shown in the insets of Panels A and B.

rats was in a time-dependent manner. Unlike plasma corticosterone, the level of neuronal corticosterone was significantly greater than that in the ND group only in the 12-week HF-fed rats (Fig. 5B, $p < 0.01$). Our results also demonstrated that the decrease in neuronal insulin receptor function was correlated well among an increase of all parameters of peripheral insulin resistance, plasma corticosterone and neuronal corticosterone (Table 2).

Discussion

The major findings in the present study are that in the HF fed rats, 1) elevated plasma corticosterone level was observed after 4-week HF feeding; 2) peripheral insulin resistance was developed after 8-week HF feeding; and 3) increased neuronal corticosterone level and the occurrence of neuronal insulin resistance were observed after 12-week HF feeding.

Earlier works found that HF diet causes insulin resistance characterized by hyperinsulinemia, hyperlipidemia, elevated corticosteroids and decreased insulin sensitivity (Hummel et al., 1966; Manco et al., 2004; Riccardi et al., 2004). In both basic and clinical studies, it has been shown that the development of insulin resistance is associated with HF consumption and is linked to cognitive deficits (Greenwood and Winocur, 2005; Riccardi et al., 2004; Winocur and Greenwood, 2005). While considerable research has examined both the consequences and mechanisms of a diminished insulin response in various peripheral tissues, only a few studies have investigated the effects of this metabolic disruption within the CNS, particularly the metabolic disturbance following the consumption of HF diets. In addition, although much evidence suggests that neuronal insulin signaling might play a role in neuronal plasticity (Park et al., 2001; Wickelgren, 1998; Zhao and Alkon, 2001), the number of available reports in an area of HF diet consumption and neuronal insulin resistance is still limited.

Growing evidence demonstrates the influence of time-course effects on the learning and memory processes caused by HF diet. Previous studies demonstrated that rats fed with HF diet for 3 months had cognitive impairment (Greenwood and Winocur, 1996), while rats fed with HF diet for 8 months exhibited impaired learning ability and reduced hippocampal synaptic plasticity (Stranahan et al., 2008a, b). Despite these reports, the neurofunctional insulin resistance in hippocampus in different time-course of HF consumption has not

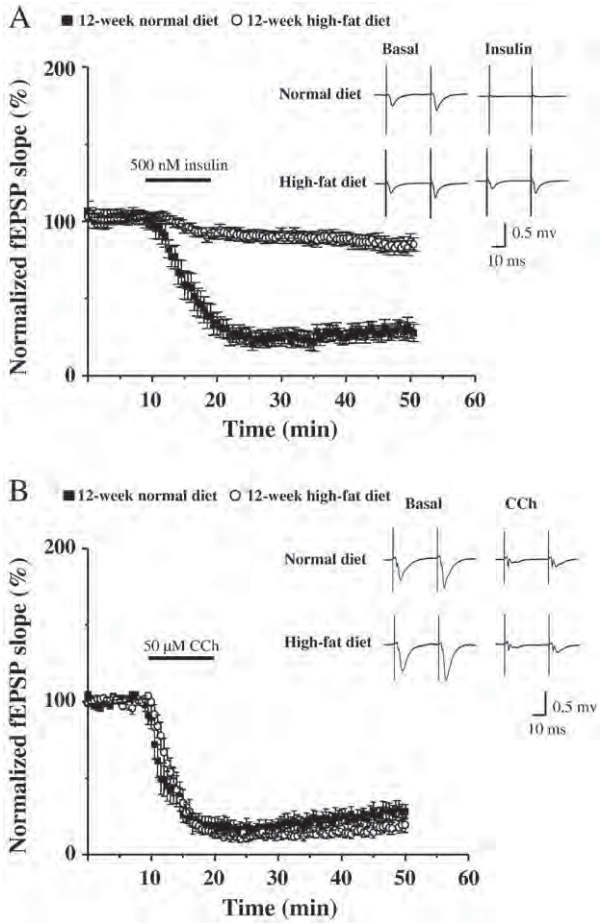

Fig. 2. *Panel A*: Twelve-week-HF diet feeding significantly diminished the ability of insulin-mediated long term depression (LTD) in CA1 hippocampus. A summary of averages of 16–17 experiments (n = 16–17 independent slices, n = 13–14 animals/group) shows that bath application of 500 nM insulin for 10 min produced a depression of fEPSPs in 12-week-ND brain slices and the fEPSPs did not fully recover after washout of insulin. However, 500 nM insulin-mediated LTD was significantly attenuated by 12-week-HF diets. *Panel B*: Average normalized fEPSPs (fEPSPt/fEPSPo with fEPSPs being points at which fEPSP slopes stabilized) from 12-week-ND-fed (n = 17 independent slices, n = 14 animals/group) and 12-week-HF-fed (n = 16 independent slices, n = 13 animals/group) brain slices. Representative traces were indicated for 12-week ND group and 12-week HF group (in upper panel). Carbachol-induced LTD (mLTD) recorded from CA1 hippocampal slices harvested from 12-week ND and 12-week HF diet, suggested no difference in mLTD occurring during the neuronal insulin resistance. CCh, carbachol.

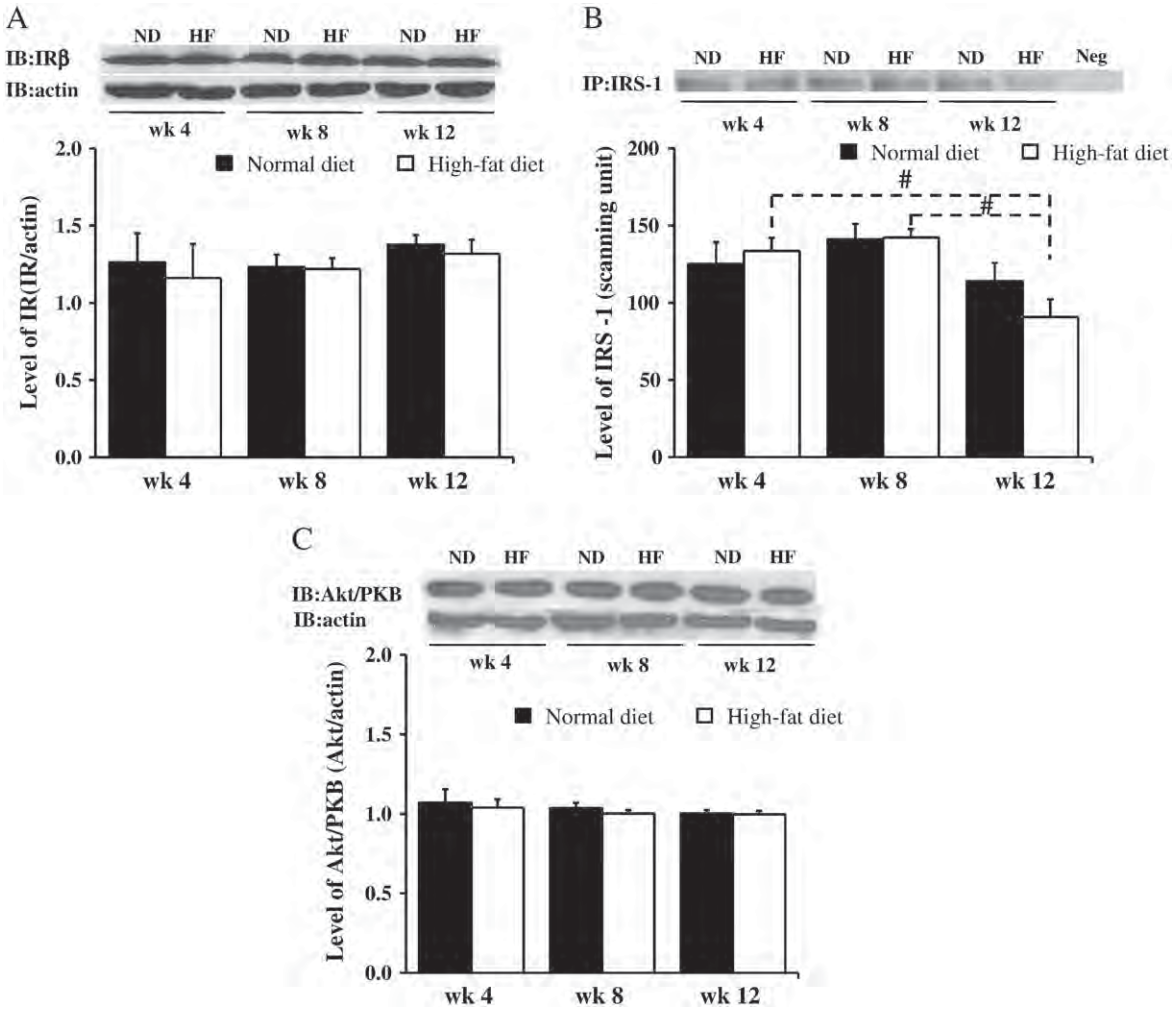

Fig. 3. The protein levels of IR, IRS-1 and Akt/PKB were not changed following 4-, 8- and 12- week HF diet feeding. *Panels A–C*: Representive immunoblots indicate that the total cellular amount of the IR (A), IRS-1 (B) and Akt/PKB (C) proteins were unchanged in the 4-, 8- and 12-week HF rat brain slices compared to the 4-, 8- and 12-week ND slices, and the densitometric quantitation of blots from both groups was not different. All immunoblotting lanes were loaded with equal amounts of protein (40 μg/lane). #, $p<0.05$ compared to 12-week group of the same dietary regimen. ND, normal diet fed group; HF, high-fat fed group; Negative (Neg), no proteins had been loaded.

been investigated. To determine the existence of neurofunctional insulin resistance in the brain following HF diet consumption, we determined the efficacy of the neurofunctional insulin receptor characterized as insulin-mediated LTD in CA1 hippocampus and the stimulated phosphorylation status of IR, IRS-1 and Akt/PKB in brain slices harvested from control and HF fed rats. We demonstrated a significant reduction of the insulin-mediated LTD in CA1 hippocampal slices and the insulin-mediated phosphorylation of IR, IRS-1 and Akt/PKB in 12-week HF-fed rats. Our findings suggest that the consumption of HF diet for only 12 weeks can down-regulate the neuronal insulin receptor sensitivity as well as the peripheral insulin sensitivity. A previous study on hamsters with peripheral insulin resistance resulting from a 6-week high-fructose diet has shown a reduction of IR, IRS-1 and Akt/PKB phosphorylation in the brain and insulin-mediated LTD in the hippocampus (Mielke et al., 2005). Our study demonstrates that the development of neuronal insulin resistance after HF consumption required a longer time than that after fructose consumption.

Insulin has been shown to regulate the endocytosis of AMPA receptors through calcium-dependent clathrin mediated internalization of AMPA receptors at the postsynaptic sites, which causes the depression of excitatory synaptic transmission (Ahmadian et al., 2004; Beattie et al., 2000; Huang et al., 2004; Lin et al., 2000; Man et al., 2000). In the present study, a significant reduction of insulin-mediated LTD in hippocampal slices from the 12-week HF group was observed. The reduction of insulin-mediated LTD was well correlated with other peripheral insulin resistance such as an increase in visceral fat, weight, plasma glucose, insulin level and liver triglyceride content. These results suggest that changes in metabolic system are linked to the neuronal function. The weakening of insulin-mediated LTD indicated one of the functional consequences of impaired neuronal insulin signaling. The reduced LTD induction could be due to the significant decrease in insulin-induced phosphorylation of the insulin receptor signaling: IR, IRS-1 and Akt/PKB in brain slices of the 12-week HF group as seen in the present study (Fig. 4). Previous studies demonstrated that the phosphorylation of Akt/PKB contributed to an increase in the level of intracellular calcium (Sun et al., 2006; Viard et al., 2004; Worrall and Olefsky, 2002). Thus, the reduction in Akt/PKB phosphorylation of neuronal IR found in the present study could lead to the decreased intracellular calcium and contributes to impair calcium dependent clathrin-mediated internalization of AMPARs, resulting in the decline of insulin-induced LTD in the 12-week HF feeding rats.

Although it is possible that the diminished insulin-mediated LTD in the HF group could be due to changes in synaptic transmission in CA1 hippocampus caused by HF, the unaltered PPF hippocampal CA1 regions in both dietary treatments suggested that HF feeding did not affect presynaptic responses to electrical stimulation. Therefore, it may be concluded that 12 weeks of HF feeding only significantly affects the neuronal insulin receptor signaling function at the post-

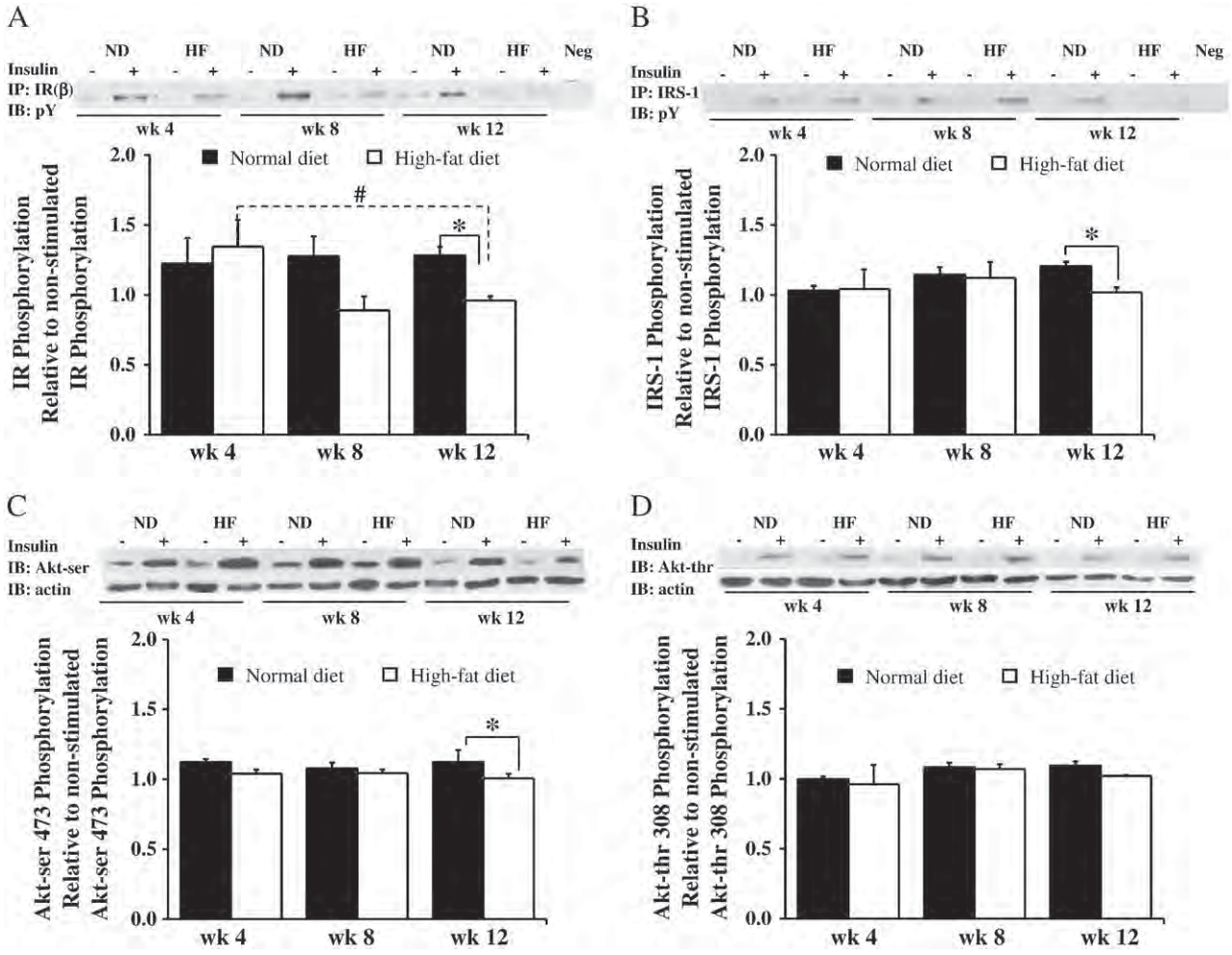

Fig. 4. Insulin-induced tyrosine phosphorylation of both neuronal insulin receptor β subunit (IR), the substrate protein IRS-1 and Akt/PKB was weakened in the 12-week HF-fed group. *Panels A–D*: Representive blots of tyrosine phosphorylation illustrated a marked decrease in the ability of insulin to stimulate IR (A), IRS-1 (B), serine 473 kinase of Akt/PKB (C) and threonine 308 kinase of Akt/PKB (D) phosphorylation in brain slices harvested from the 4-, 8- and 12-week HF-fed group compared to the 4-, 8- and 12-week ND-fed group. Densitometric quantitation of blots from insulin stimulated IR, IRS-1 and Akt/PKB was significantly greater in the 12-week ND-fed group than that in the 12-week HF-fed group. All immunoblotting lanes were loaded with equal amounts of protein (20 μg/lane). *, $p<0.05$ compared to ND group in each time course; #, $p<0.05$ compared to 12-week group of the same dietary regimen; ND, normal diet fed group; HF, high-fat fed group; Negative (Neg), no proteins had been loaded; -, no insulin stimulation; +, insulin stimulation.

synaptic sites, but not at the pre-synaptic release in CA1 hippocampus. Carbachol-induced LTD or muscarinic LTD (mLTD) in CA1 hippocampus, characterized as the other form of synaptic plasticity (Scheiderer et al., 2006), is believed to be a substrate of learning and memory at the molecular level (Scheiderer et al., 2006). We demonstrated in this study that the reduction of neuronal insulin response in the 12-week HF group was unaffected in mLTD, suggesting that this form of synaptic plasticity may not require neuronal insulin signaling. Our finding was similar to previous reports, showing that the weakening of insulin-mediated LTD has no effect upon the induction and maintenance of the LTP via a high-frequency stimulation (Mielke et al., 2005, 2006), but was different from the other previous study (Stranahan et al., 2008a,b). In that study, Stranahan and colleague demonstrated that rats fed with high-fat, high glucose for 8 months reduced LTP at schaffer-CA1 synapse (Stranahan et al., 2008a,b). The differences in the results between Stranahan study and our study may depend upon the differences in dietary regimen and time-course of HF consumption.

In the present study, the phosphorylation of IR, IRS-1 and Akt/PKB in brain slices was diminished at 12 weeks, whereas the levels of IR, IRS-1 and Akt/PKB in brain slices were not altered by 4-, 8- and 12-week HF diet feeding (see Fig. 4). These changes in phosphorylation of neuronal insulin signaling confirm the impairment of insulin receptor function in the brain following 12-week HF feeding. The unchanged levels of IR, IRS-1 and Akt/PKB proteins in the brain following HF diet consumption in the present study are consistent with those previously reported in the liver (Hahn-Obercyger et al., 2009), in the skeletal muscle (Youngren et al., 2001) and in the hippocampus (Banas et al., 2009). Furthermore, the impairment of IR, IRS-1 and Akt/PKB protein kinase activity has been demonstrated in the skeletal muscle (Barnard et al., 1992), fat (Boyd et al., 1990) and liver tissues (Watarai et al., 1988) in 10–12 week consumption of HF diets. All of these findings indicate that HF diet could cause defective neuronal insulin receptor function, but not at the level of protein expression.

In addition to the weakening of neurofunctional insulin receptors and neuronal insulin signaling, our results demonstrated that the level of plasma corticosterone was increased prior to the development of peripheral insulin resistance in HF fed rats. It had been previously described that corticosterone influences insulin sensitivity and that enhancement of peripheral corticosterone could contribute to the development of peripheral insulin resistance (Reynolds and Walker, 2003). Furthermore, it is known that the basal level of corticosteroids physiologically protects neuronal damage, whereas the stress or high level of corticosteroids can contribute to neuronal damage (McEwen, 2007). Several studies demonstrated that chronic exposure to high level of corticosteroids can produce neuronal stress and neuronal loss in CA3 pyramidal neurons of rodents (Sapolsky et al., 1985) and

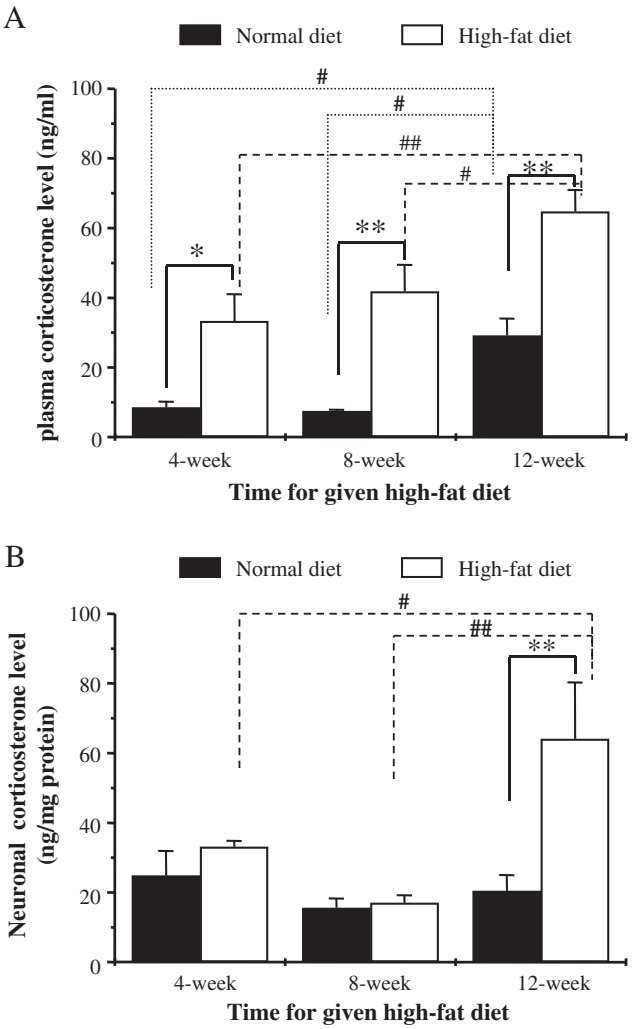

Fig. 5. Increased plasma and neuronal corticosterone levels following HF diet feeding. *Panel A*: Plasma corticosterone level following 4-, 8- and 12-week feeding of both ND and HF diet. *Panel B*: Neuronal corticosterone level following 4-, 8- and 12-week feeding of both ND and HF diet. *, $p<0.05$ compared to ND group in each time course; **, $p<0.01$ compared to ND group in each time course; #, $p<0.05$ compared to 12-week group of the same dietary regimen; ##, $p<0.01$ compared to 12-week group of the same dietary regimen.

primates (Sapolsky et al., 1990; Uno et al., 1989). In addition, a previous study demonstrated that corticosterone could induce insulin resistance in the skeletal muscles (Zhao et al., 2009). Thus, the elevation of neuronal corticosterone level found in our study could also promote neuronal insulin resistance. Our findings suggest that obesity following HF diet consumption could lead to neuronal insulin resistance and neuronal stress as shown by an increased release of neuronal corticosterone (Stranahan et al., 2008a,b).

Study limitation

The limitation of this study is that the morphological data on the integrity of dendritic spines and terminals in the CA1 region of the hippocampus were not investigated. However, the present study demonstrated that the amount of insulin receptor was not different between the high-fat fed and normal diet fed rats, suggesting that the reduction of insulin-induced LTD in high-fat fed rats was due to the decreased function of insulin signaling, as supported by the decreased phosphorylated IR, IRS and Akt/PKB levels in the high-fat fed rats.

Conclusion

The present study demonstrates that a significant modification of important neuronal insulin receptor signaling can be induced by a fat-enriched diet. Fed for 12 weeks, the HF diet clearly induces neuronal insulin resistance, which is identified as a significant reduction in the ability of insulin to induce LTD, and a reduction in the stimulated phosphotyrosine activity of IR, IRS-1 and Akt/PKB in brain slices. Twelve-week HF feeding not only causes neuronal insulin resistance, but also leads to neuronal stress, as indicated by increased neuronal corticisterone level. Since the defective insulin receptor signaling has been shown to associate with the pathogenesis of Alzheimer's disease (Watson and Craft, 2004), cognitive impairment (Greenwood and Winocur, 1990, 1996, 2005; Winocur and Greenwood, 2005) and the presence of cognitive impairment in patients with type II diabetes (Gispen and Biessels, 2000), the neuronal insulin resistance developing after 12-week HF consumption could be responsible for the impairment of cognition through the glucocorticoid-mediated effect in this animal model.

Conflict of interest statement

The authors declare that there are no conflicts of interest.

Acknowledgments

The authors wish to thank Prof. M. Kevin O' Carroll, Professor Emeritus, University of Mississippi School of Dentistry, USA, and Faculty Consultant, Faculty of Dentistry, Chiang Mai University, Thailand, for his editorial assistance. This work is supported by the Thailand Research Fund grants: TRF-RMU5180007 (SC), TRF-RTA5280006 (NC), TRF through the Royal Golden Jubilee PhD Program (PHD/0224/2550) to WP and SC, Thailand National Research Council grant (SC) and the Faculty of Medicine Endowment Fund, Chiang Mai University (WP, AP, NC and SC).

References

Ahmadian G, Ju W, Liu L, Wyszynski M, Lee SH, Dunah AW, et al. Tyrosine phosphorylation of GluR2 is required for insulin-stimulated AMPA receptor endocytosis and LTD. EMBO J 2004;23:1040–50.
Appleton DJ, Rand JS, Sunvold GD. Basal plasma insulin and homeostasis model assessment (HOMA) are indicators of insulin sensitivity in cats. J Feline Med Surg 2005;7:183–93.
Banas SM, Rouch C, Kassis N, Markaki EM, Gerozissis K. A dietary fat excess alters metabolic and neuroendocrine responses before the onset of metabolic diseases. Cell Mol Neurobiol 2009;29:157–68.
Barnard RJ, Lawani LO, Martin DA, Youngren JF, Singh R, Scheck SH. Effects of maturation and aging on the skeletal muscle glucose transport system. Am J Physiol 1992;262:619–26.
Beattie EC, Carroll RC, Yu X, Morishita W, Yasuda H, von Zastrow M, et al. Regulation of AMPA receptor endocytosis by a signaling mechanism shared with LTD. Nat Neurosci 2000;3:1291–300.
Boyd JJ, Contreras I, Kern M, Tapscott EB, Downes DL, Frisell WR, et al. Effect of a high-fat-sucrose diet on in vivo insulin receptor kinase activation. Am J Physiol 1990;259:111–6.
Chan O, Inouye K, Akirav EM, Park E, Riddell MC, Matthews SG, et al. Hyperglycemia does not increase basal hypothalamo–pituitary–adrenal activity in diabetes but it does impair the HPA response to insulin-induced hypoglycemia. Am J Physiol Regul Integr Comp Physiol 2005;289:235–46.
Chattipakorn SC, McMahon LL. Pharmacological characterization of glycine-gated chloride currents recorded in rat hippocampal slices. J Neurophysiol 2002;87:1515–25.
Frayn KN, Little RA, Threlfall CJ. Protein metabolism after unilateral femoral fracture in the rat, and comparison with sham operation. Br J Exp Pathol 1980;61:474–8.
Gispen WH, Biessels GJ. Cognition and synaptic plasticity in diabetes mellitus. Trends Neurosci 2000;23:542–9.
Greenwood CE, Winocur G. Learning and memory impairment in rats fed a high saturated fat diet. Behav Neural Biol 1990;53:74–87.
Greenwood CE, Winocur G. Cognitive impairment in rats fed high-fat diets: a specific effect of saturated fatty-acid intake. Behav Neurosci 1996;110:451–9.
Greenwood CE, Winocur G. High-fat diets, insulin resistance and declining cognitive function. Neurobiol Aging 2005;26:42–5.
Haffner SM, Miettinen H, Stern MP. The homeostasis model in the San Antonio Heart Study. Diab Care 1997;20:1087–92.

Hahn-Obercyger M, Graeve L, Madar Z. A high-cholesterol diet increases the association between caveolae and insulin receptors in rat liver. J Lipid Res 2009;50:98-107.
Huang CC, Lee CC, Hsu KS. An investigation into signal transduction mechanisms involved in insulin-induced long-term depression in the CA1 region of the hippocampus. J Neurochem 2004;89:217–31.
Hummel KP, Dickie MM, Coleman DL. Diabetes, a new mutation in the mouse. Science 1966;153:1127–8.
Kalmijn S, van Boxtel MP, Ocke M, Verschuren WM, Kromhout D, Launer LJ. Dietary intake of fatty acids and fish in relation to cognitive performance at middle age. Neurology 2004;62:275–80.
Langley SC, York DA. Effects of antiglucocorticoid RU 486 on development of obesity in obese fa/fa Zucker rats. Am J Physiol 1990;259:539–44.
Lin JW, Ju W, Foster K, Lee SH, Ahmadian G, Wyszynski M, et al. Distinct molecular mechanisms and divergent endocytotic pathways of AMPA receptor internalization. Nat Neurosci 2000;3:1282–90.
Man HY, Lin JW, Ju WH, Ahmadian G, Liu L, Becker LE, et al. Regulation of AMPA receptor-mediated synaptic transmission by clathrin-dependent receptor internalization. Neuron 2000;25:649–62.
Manco M, Calvani M, Mingrone G. Effects of dietary fatty acids on insulin sensitivity and secretion. Diab Obes Metab 2004;6:402–13.
McEwen BS. Physiology and neurobiology of stress and adaptation: central role of the brain. Physiol Rev 2007;87:873–904.
Mielke JG, Nicolitch K, Avellaneda V, Earlam K, Ahuja T, Mealing G, et al. Longitudinal study of the effects of a high-fat diet on glucose regulation, hippocampal function, and cerebral insulin sensitivity in C57BL/6 mice. Behav Brain Res 2006;175:374–82.
Mielke JG, Taghibiglou C, Liu L, Zhang Y, Jia Z, Adeli K, et al. A biochemical and functional characterization of diet-induced brain insulin resistance. J Neurochem 2005;93: 1568–78.
Morris MC, Evans DA, Bienias JL, Tangney CC, Wilson RS. Dietary fat intake and 6-year cognitive change in an older biracial community population. Neurology 2004;62: 1573–9.
Olefsky JM. The insulin receptor. A multifunctional protein. Diabetes 1990;39:1009–16.
Park JG, Bose A, Leszyk J, Czech MP. PYK2 as a mediator of endothelin-1/G alpha 11 signaling to GLUT4 glucose transporters. J Biol Chem 2001;276:47751–4.
Reynolds RM, Walker BR. Human insulin resistance: the role of glucocorticoids. Diab Obes Metab 2003;5:5-12.
Riccardi G, Giacco R, Rivellese AA. Dietary fat, insulin sensitivity and the metabolic syndrome. Clin Nutr 2004;23:447–56.
Sapolsky RM, Krey LC, McEwen BS. Prolonged glucocorticoid exposure reduces hippocampal neuron number: implications for aging. J Neurosci 1985;5:1222–7.
Sapolsky RM, Uno H, Rebert CS, Finch CE. Hippocampal damage associated with prolonged glucocorticoid exposure in primates. J Neurosci 1990;10:2897–902.
Scheiderer CL, McCutchen E, Thacker EE, Kolasa K, Ward MK, Parsons D, et al. Sympathetic sprouting drives hippocampal cholinergic reinnervation that prevents loss of a muscarinic receptor-dependent long-term depression at CA3–CA1 synapses. J Neurosci 2006;26:3745–56.
Stranahan AM, Arumugam TV, Cutler RG, Lee K, Egan JM, Mattson MP. Diabetes impairs hippocampal function through glucocorticoid-mediated effects on new and mature neurons. Nat Neurosci 2008a;11:309–17.
Stranahan AM, Norman ED, Lee K, Cutler RG, Telljohann RS, Egan JM, et al. Diet-induced insulin resistance impairs hippocampal synaptic plasticity and cognition in middle-aged rats. Hippocampus 2008b;18:1085–8.
Sun H, Kerfant BG, Zhao D, Trivieri MG, Oudit GY, Penninger JM, et al. Insulin-like growth factor-1 and PTEN deletion enhance cardiac L-type Ca2+ currents via increased PI3Kalpha/PKB signaling. Circ Res 2006;98:1390–7.
Uno H, Tarara R, Else JG, Suleman MA, Sapolsky RM. Hippocampal damage associated with prolonged and fatal stress in primates. J Neurosci 1989;9:1705–11.
Viard P, Butcher AJ, Halet G, Davies A, Nurnberg B, Heblich F, et al. PI3K promotes voltage-dependent calcium channel trafficking to the plasma membrane. Nat Neurosci 2004;7:939–46.
Watarai T, Kobayashi M, Takata Y, Sasaoka T, Iwasaki M, Shigeta Y. Alteration of insulin-receptor kinase activity by high-fat feeding. Diabetes 1988;37:1397–404.
Watson GS, Craft S. Modulation of memory by insulin and glucose: neuropsychological observations in Alzheimer's disease. Eur J Pharmacol 2004;490:97-113.
Wickelgren I. Tracking insulin to the mind. Science 1998;280:517–9.
Winocur G, Greenwood CE. Studies of the effects of high fat diets on cognitive function in a rat model. Neurobiol Aging 2005;26:46–9.
Worrall DS, Olefsky JM. The effects of intracellular calcium depletion on insulin signaling in 3T3-L1 adipocytes. Mol Endocrinol 2002;16:378–89.
Youngren JF, Paik J, Barnard RJ. Impaired insulin-receptor autophosphorylation is an early defect in fat-fed, insulin-resistant rats. J Appl Physiol 2001;91:2240–7.
Zhao JP, Lin H, Jiao HC, Song ZG. Corticosterone suppresses insulin- and NO-stimulated muscle glucose uptake in broiler chickens (*Gallus gallus domesticus*). Comp Biochem Physiol C Toxicol Pharmacol 2009;149:448–54.
Zhao WQ, Alkon DL. Role of insulin and insulin receptor in learning and memory. Mol Cell Endocrinol 2001;177:125–34.
Zierath JR, Livingston JN, Thorne A, Bolinder J, Reynisdottir S, Lonnqvist F, et al. Regional difference in insulin inhibition of non-esterified fatty acid release from human adipocytes: relation to insulin receptor phosphorylation and intracellular signalling through the insulin receptor substrate-1 pathway. Diabetologia 1998;41:1343–54.
Zucker RS, Regehr WG. Short-term synaptic plasticity. Annu Rev Physiol 2002;64: 355–405.

ELSEVIER

Canadian Journal of Cardiology 27 (2011) 262.e3–262.e13 www.onlinecjc.ca

Review

Roles of Mitochondrial Benzodiazepine Receptor in the Heart

Sirirat Surinkaew, BSc, Siriporn Chattipakorn, DDS, PhD, and Nipon Chattipakorn, MD, PhD

Cardiac Electrophysiology Unit, Department of Physiology, Cardiac Electrophysiology Research and Training Center, Faculty of Medicine and Faculty of Dentistry, Chiang Mai University, Chiang Mai, Thailand

ABSTRACT

Mitochondrial benzodiazepine receptor (mBzR) is a type of peripheral benzodiazepine receptor that is located in the outer membrane of mitochondria. It is an 18-kDa protein that can form a multimeric complex with voltage-dependent anion channel (32 kDa) and adenine nucleotide translocator (30 kDa). mBzR is found in various species and abundantly distributed in peripheral tissues, including the cardiovascular system. The mitochondria are well known as the site of energy production, and the heart is the organ that highly requires this energy supply. In the past decades, it has been shown that mBzR plays a critical role in regulating mitochondrial and heart functions. A growing body of evidence demonstrates that mBzR is associated with regulation of mitochondrial respiration, mitochondrial membrane potential, apoptosis, and reactive oxygen species production. Moreover, mBzR has been suggested to play a role in alteration of physiological effects in the heart such as contractility and heart rate. mBzR is involved in the pathologic condition such as ischemia/reperfusion injury, responses to stress, and changes in electrophysiological properties and arrhythmogenesis. In this review, evidence of the roles of mBzR in the heart under both physiological and pathologic conditions is presented. Clinical studies regarding the use of pharmacologic intervention involving mBzR in the heart are also discussed as a possible target for the treatment of electrical and mechanical dysfunction in the heart.

RÉSUMÉ

Le récepteur mitochondrial des benzodiazépines (mBzR) est un type de récepteur périphérique des benzodiazépines situé dans la membrane externe de la mitochondrie. C'est une protéine 18 kDa qui peut former un complexe multimérique avec le canal anionique voltage-dépendant (32 kDa) et le translocateur des nucléotides adényliques (30 kDa). Le mBzR se retrouve dans différentes espèces et est abondamment distribué dans les tissus périphériques, incluant le système cardiovasculaire. Les mitochondries sont bien connues comme étant le site de production d'énergie, et le cœur est l'organe qui requiert le plus grand approvisionnement énergétique. Au cours des dernières décennies, il a été démontré que le mBzR joue un rôle critique dans la régulation mitochondriale et les fonctions du cœur. Un nombre croissant de preuves démontrent que le mBzR est associé à la régulation de la respiration mitochondriale, au potentiel de la membrane mitochondriale, à l'apoptose et à la production d'espèces réactives de l'oxygène. De plus, le mBzR semble jouer un rôle dans les modifications physiologiques du cœur comme la contractilité et la fréquence cardiaque. Le mBzR est impliqué dans des pathologies tels les lésions d'ischémie-reperfusion, les réponses au stress, et les changements dans les propriétés électrophysiologiques et l'arythmogenèse. Dans cette revue, les rôles du mBzR sur le cœur sont mis en évidence tant dans des conditions physiologiques que pathologiques. Des études cliniques au sujet de l'utilisation d'interventions pharmacologiques impliquant le mBzR pour le cœur sont aussi discutées comme un objectif possible dans le traitement des dysfonctions électriques et mécaniques du cœur.

Peripheral benzodiazepine receptor (PBR) is a receptor found in peripheral tissues such as adrenal, kidney, and brain in various species and is found in abundance in cardiovascular system.[1-3] Initially discovered in rat peripheral tissues by Braestrup and Squires during 1970s[4] as benzodiazepine binding site, it is distinct from the central benzodiazepine receptors, which are localized solely to neuronal cells in the central nervous system. The majority of PBRs are located in the mitochondrial outer membrane and arenormally recognized as mitochondrial benzodiazepine receptors (mBzRs).[5,6] However, several studies demonstrated that PBRs are also located outside the mitochondria, such as in the nuclear fractions[7] and plasma membrane[8] of various cell types). PBR is an 18-kDa protein consisting of 169 amino acids[9] that can form a protein complex with voltage-dependent anion channel (VDAC; 32 kDa) at the outer membrane and adenine nucleotide translocator (ANT; 30 kDa) at the inner membrane.[6] Recently, PBR has been renamed "translocator protein 18 kDa" (TSPO) by a group of scientists to represent a specific structure and molecular function of PBR.[10] The name indicates the location of proteins:

Received for publication March 26, 2010. Accepted June 2, 2010.

Corresponding author: Dr Nipon Chattipakorn, Cardiac Electrophysiology Research and Training Center, Faculty of Medicine, Chiang Mai University, Chiang Mai, 50200, Thailand. Tel.: +66-53-945329; fax.: +66-53-945368.

E-mail: nchattip@med.cmu.ac.th

See page 262.e11 for disclosure information.

doi:10.1016/j.cjca.2010.12.023

mitochondrial translocator protein (mitoTSPO) and nuclear translocator protein (nucTSPO). To date, "PBR" is also widely accepted among the scientific community.

A growing body of evidence indicates that mBzR could play vital regulatory and protective roles for cellular and organ functions in various organs.[11] These roles include cardioprotective effects in the heart, steroidogenesis in the adrenal glands, astrocyte and microglia activation in the brain, and heme biosynthesis in the liver.[12-15] Under cardiac ischemia/reperfusion (I/R) condition, it has been reported that mBzR plays an important role in the regulation of cardiac cell under this pathologic condition. The abnormality at the level of organelle such as mitochondria in this condition can tremendously affect cardiac electrophysiology as well as an excitation-contraction coupling process in cardiomyocytes.

In this review, the roles of mBzR in the heart under physiological conditions and during I/R injury are mainly discussed, with a focus on its effects on cardioprotection, electrophysiological alterations, reactive oxygen species (ROS) production, and the undesired effect caused by mBzR stimulation in the heart during I/R injury. The disputed findings regarding the effects of mBzR ligands on cardiac electrophysiology under a variety of stresses as well as several clinical studies available at this time are also presented with the hope that they will encourage further studies to help elucidate the mechanism of mBzR in the heart and to warrant its clinical usefulness as a potential therapeutic target for the treatment of ischemic heart disease in the near future.

Cardiac Mitochondrial Benzodiazepine Receptor

The mitoTSPO, or mBzR, is located on the mitochondrial outer membrane of a cardiac cell and has a structure similar to that found in the other peripheral tissues. mBzR is a 18-kDa protein that can form a multimeric complex with VDAC and ANT. mBzR itself has minimal function in the interaction with some ligands, but the forming of mBzR and other proteins has been shown to drive drug-binding properties and functions. In the heart, mBzR has been shown to be involved in many critical cellular controls, including apoptotic cell death, mitochondrial membrane potential ($\Delta\Psi_m$) changes, mitochondrial permeability, mitochondrial respiration, and intracellular calcium overload and responses to stress.[12] Endogenous ligands such as protophophyrin IX, diazepam binding inhibitor, triakontatetraneuropeptide, and phospholipase A_2 have been shown to affect mBzR in these processes.[12] In the past decades, a number of exogenous ligands have been synthesized and were specific to mBzR. These include PK11195 [1-(2-chlorophenyl)-*N*-methyl-*N*-(1-methyl-propyl)-3-isoquinoline carboxamide], 4′-chlorodiazepam (4′-Cl-DZP) or Ro5-4864 [7-chloro-5-(4-chlorophenyl)-1,3-dihydro-1-methy-2*H*-1,4-benzodiazepin-2-one], SSR180575 (7-chloro-*N,N*,5-trimethyl-4-oxo-3-phenyl-3, 5-dihydro-4*H*-pyridazino[4,5-**b**]indole-1-acetamide), FGIN-1-27 [*N,N*-di-*n*-hexyl 2-(4-fluorophenyl)indole-3-acetamide], pyrrolo[2,1-**d**][1,5] benzodiazepine derivative, and AHN086 [1-(2-isothiocyanatoethyl)-7-chloro-1,3-dihydro-5-(4-chloro-phenyl)-2*H*-1 and 4-benzodiazepine-2-one HCl]. These ligands have been extensively investigated for their cellular effects on mBzR in the heart.[12,16,17]

In thyroidectomized Holtzman adult male rats, it has been shown that the mBzR binding sites with exogenous ligand (4′-Cl-DZP) from cardiac ventricular homogenate were decreased, whereas its affinity was increased.[18] However, in the heart of male mice after copulation, cardiac mBzR binding sites were increased and its affinity was not altered.[19] Stress has been shown to influence mBzR binding affinity in the heart. In cardiac membrane of rats, 2 and 4 hours after an 80-minute session of inescapable tail shock–induced experiment, stress has been shown to reduce mBzR levels.[20] In mouse ventricles, the density of mBzR was upregulated after an acute stress but was downregulated after a repeated stressor.[21,22] In a study using stress induced by 6 and 12 hours of noise exposure, mBzR binding sites were significantly decreased in the right atrial "crude membranes" and "mitochondrial fractions."[23] This change was related to the duration of noise stress without any change in affinity. However, in this stress-induced condition, mBzR reduction could be prevented by the administration of mBzR ligands PK11195, 4′-Cl-DZP, and diazepam.[23]

In summary, mBzR levels could be increased after acute stress, whereas they were downregulated after prolonged stimulation. However, under myocardial I/R injury in rats, cardiac mBzR binding sites and affinity were not altered.[24] The proposed mechanisms of mBzR density and affinity alterations in the heart have been due mainly to hormonal and stress conditions.[25] However, the existence and the role of mBzR in the cardiac innervations remain unknown and require further investigation. The conditioning effects on mBzR levels and affinity are summarized in Table 1.

Physiological Effects of Mitochondrial Benzodiazepine Receptor Activation in the Heart

A number of studies have demonstrated that mBzR has strong physiological effects on the heart.[12,26-36] Specific synthetic mBzR ligands such as benzodiazepines have been shown to affect cardiac chronotropy and inotropy.[27-36] A possible interaction between mBzR and voltage-gated Ca^{2+} channel has been reported and has been proposed to be responsible for the alteration in cardiac action potential duration (APD) and contractility.[27] However, a definite mechanism of mBzR activation on the physiological effects in the heart remains controversial because discrepancies in findings still largely exist.

Negative inotropic effect was observed with the use of mBzR ligands (ie, 4′-Cl-DZP) in various models including papillary muscle from right and left ventricles of guinea pigs, isolated perfused rats and rabbit hearts, and isolated canine right atrium.[27-32] Despite these findings, Weissman et al.[35] and Leeuwin et al.[33] reported otherwise. The former study demonstrated that 4′-Cl-DZP augmented the increase in inotropic response that is initially induced by BAY K8644, a Ca^{2+} channel activator, by 2-fold, whereas it did not have an inotropic effect by itself.[35] The latter study found that 4′-Cl-DZP had a dose-dependent positive inotropic effect and increased coronary blood flow in the isolated perfused rat hearts.[33] These responses were abolished in the presence of PK11195, the mBzR ligand.[33] However, Grupp et al. demonstrated that 4′-Cl-DZP had no effects on inotropic response but induced a dose-dependent increase of coronary flow rate in the isolated perfused rat heart.[34] These inconsistent findings, either positive, negative, or unchanged effects on inotropic response of mBzR ligands, have not been elucidated. It could be due to the differences in 4′-Cl-DZP doses, experimental models, and species used in those studies. This effect is summarized in Table 2.

Table 1. Conditioning effects on mBzR levels and affinity

Conditions	Models	mBzR ligands	mBzR levels	mBzR affinity	Reference
Thyroidectomized	Cardiac ventricular homogenate of Holtzman adult male rats	[^{3}H]Ro5-4864	↓	↑	Kragie and Smiehorowski[18]
Copulation	Male mice hearts	[^{3}H]Ro5-4864	↑	↔	Saano et al.[19]
Inescapable tail shock	Rat cardiac membrane	[^{3}H]Ro5-4864	↓	—	Drugan et al.[20]
Inescapable tail shock	Mouse cardiac ventricles	[^{3}H]Ro5-4864	↑/↓	↔	Drugan et al.[21]
Acute maximum extra shock	Mouse cardiac ventricles	[^{3}H]Ro5-4864	↑	↔	Basile et al.[22]
In vivo 6-, 12-hr noise stress	Atrial crude membrane and cardiac mitochondrial fractions	[^{3}H]PK11195	↓	↔	Salvetti et al.[23]
Ischemia/reperfusion	Mitochondria of Wistar rat hearts	[^{3}H]PK11195	↔	↔	Obame et al.[24]
Fearfulness	Maudsley reactive rat (a high level of fearfulness) hearts	[^{3}H]Ro5-4864	↓	—	Drugan et al.[25]

↓, Decrease; ↑, increase; ↔, no change; ↑/↓, increase then decrease; —, not studied.

Although PK11195 and 4′-Cl-DZP seem to act differently, they display the same affinity as that of mBzR.[37] PK11195 does not change either inotropic effect or coronary flow rate by itself, but it antagonized the negative inotropic response in papillary muscle and abolished positive inotropic response caused by 4′-Cl-DZP in isolated perfused rat heart.[28,33] These responses indicated that the effects of PK11195 may be dependent on the actions of 4′-Cl-DZP. However, Edoute et al.[30] demonstrated in an isolated perfused rat heart model that PK11195 was a more potent depressant in heart functions than 4′-Cl-DZP in decreasing aortic flow, dP/dt_{max}, end-systolic pressure, and stroke work. Furthermore, the differences in the findings between the two mBzR ligands 4′-Cl-DZP and PK11195 could be attributed to the nature of the ligand-receptor interactions, which are enthalpy and entropy driven, the basis of thermodynamic parameters for the binding equilibrium.[37] 4′-Cl-DZP has been classified as agonist and PK11195 has been classified as antagonist. However, this classification was ambiguous,[24,30,34,38,39] as in some physiological conditions, these two ligands have been shown to have similar effects. Furthermore, in the past few years, the mBzR ligands that caused adverse effects in the heart have been identified as agonist, whereas mBzR ligands that were shown to have protective effects have been identified as antagonist.[39,40]

Although mBzR ligands have been shown to have no effect on heart rate at low concentrations,[30,34,35] several studies have demonstrated that negative chronotropic could be found at high concentrations (Table 2).[31,32,36] In canine isolated right atrium, 4′-Cl-DZP injected into sinus node decreased both atrial rate and contractile force at the concentration of 100-1000 μg.[31] Using positron emission tomography technique in canine living heart, Charbonneau et al.[36] demonstrated that the injection of 4′-Cl-DZP induced a significant drop in heart rate. Recently, Brown et al. [32] reported that in intact isolated perfused rabbit heart, high concentration of 4′-Cl-DZP (ie, >24 μM) led to a negative chronotropic effect.

Table 2. Physiological effects of mBzR ligands in the heart

Ligands	Properties	Concentration	Models	Species	Physiological effects		References
					Contractility	Heart rate	
4′-Cl-DZP	mBzR antagonist	3 nM-3 μM	Papillary muscle	Guinea pig	↓	—	Mestre et al.,[27, 28]
		≥3 μM	Papillary muscle	Guinea pig	↓	—	Holck and Osterrieder[29]
		≤10 μM	Isolated perfused heart	Sprague-Dawley rat	↔	↔	Grupp et al.34
		10 μM	Isolated perfused heart	Sprague-Dawley rat	↓	↔	Edoute et al.[30]
		10 μM	Isolated atrium	Guinea pig	↔	↔	Weissman et al.[35]
		24 μM	Isolated perfused heart	Rabbit	↓	↓	Brown et al.[32]
		20-400 μM	Isolated perfused heart	Wistar rat	↑	—	Leeuwin et al.[33]
		100-1000 μg/kg	Isolated right atrium	Canine	↓	↓	Saegusa et al.[31]
		≥200 μg/kg	In vivo heart	Canine	—	↓	Charbonneau et al.[36]
PK11195	mBzR agonist	<3 μM	Papillary muscle	Guinea pig	↔	—	Mestre et al.[27,28]
		1 nM-10 μM	Isolated perfused heart	Sprague-Dawley rat	↔	↔	Grupp et al.[34]
		0.1 μM	Isolated perfused heart	Sprague-Dawley rat	↓	↔	Edoute et al.[30]
		50 μM	Isolated perfused heart	Wistar rat	↔	—	Leeuwin et al.[33]
		Excess	In vivo heart	Canine	—	↔	Charbonneau et al.[36]
PK11195 + 4′-Cl-DZP		PK (30 nM-3 μM) 4′ (3 nM-3 μM)	Papillary muscle	Guinea pig	↑	—	Mestre et al.[28]
		PK (1 μM-50 μM), 4′ (20-400 μM)	Isolated perfused heart	Wistar rat	↓	—	Leeuwin et al.[33]

↓, Decrease; ↑, increase; ↔, no change; ↑ / ↓, increase then decrease; —, not studied.

Furthermore, there are pieces of evidence to show that mBzR ligands affect ion currents in the isolated cardiomyocytes, as detailed in the following paragraph. Therefore, the decrease in heart rate may be due to a reduction in net inward current during phase 4 of the pacemaker cell, leading to a hyperpolarization of the resting membrane potential.[41]

Because peripheral-type benzodiazepine binding sites are pharmacologic receptors coupled to calcium channels, it has been proposed that the binding of ligands to mBzR may play a role in transportation of calcium in and out of the cell.[27] This hypothesis is supported by studies in isolated guinea pig and rabbit ventricular myocytes.[29,32] In a study by Holck and Osterrieder,[29] 4′-Cl-DZP at concentration >3 μM reduced inward Ca^{2+} current and rectified K^+ current in isolated guinea pig cardiac myocytes. Brown et al. also demonstrated that 4′-Cl-DZP (24 μM) decreased Ca^{2+} inward current during phase 2 of action potential in rabbit cardiomyocytes.[32] In cardiomyocytes, pyrrolo[2,1-**d**][1,5]benzodiazepine derivatives, an mBzR ligand, decreased Ca^{2+} current.[17] The decrease in Ca^{2+} current then diminished the trigger for Ca^{2+} release from the sarcoplasmic reticulum, which explains the negative inotropic effect of the compound. However, in Leeuwin et al.'s[33] finding, the positive inotropic effect of 4′-Cl-DZP was not clearly explained.

Table 2 summarizes the physiologic effects of mBzR activation reported to date. A high concentration of 4′-Cl-DZP (≥10 μM) was found to induce negative inotropic effect in isolated perfused rat and rabbit hearts,[30,32] except for one study.[33] In contrast, a low concentration of <10 μM did not affect the contractility in either isolated perfused rat heart or isolated atrium models.[34,35] Despite these reports, inconsistent results derived from studies using the same model and the same species still exist.[27-29] Mestre et al. demonstrated that 4′-Cl-DZP of <3 μM reduced contractility in papillary muscle,[27,28] whereas Holck and Osterrieder reported that it did not alter the contractility, the inward calcium current nor the inwardly rectifying potassium current in isolated cardiac ventricular myocytes.[27-29] It is important to note that the negative chronotropic effect of mBzR ligand 4′-Cl-DZP has been shown only in the moderate-sized to large animal models (ie, canine[31,36] and rabbit[32]), whereas no chronotropic effect was found in rats[30,34] and guinea pig.[35]

In summary, mBzR plays an important physiological role in the heart. Findings from previous studies strongly indicate that the physiological roles of mBzR in the heart differ in different species, suggesting that its effects in the human heart could be similar or different from those found in basic studies and will need further validation in future studies.

Mitochondrial Benzodiazepine Receptor and Ischemia/Reperfusion Injury

During myocardial I/R, mitochondria are known to be involved in apoptotic or necrotic cell death. In the apoptosis pathway, I/R injury causes mitochondrial swelling and release of cytochrome c to the cytoplasm.[42] The release of cytochrome c and induction of apoptotic cell death have been shown to involve in the opening of mitochondrial permeability transition pore (mPTP).[43] mPTP is a multiprotein complex that can form large nonselective pores in the mitochondrial inner membrane. Opening of this pore allows free passage of any molecules up to 1.5 kDa and also disrupts the permeability barrier of the inner membrane. The major components of the mPTP involve VDAC, ANT, and cycloplilin D, whereas mBzR, hexokinase, creatine kinase, and Bcl2 have been shown to play regulatory roles with this complex.[44] Since a multimeric complex of mBzRs has structurally linked to mPTP, it is believed that both of them could play a role together in cardioprotective effects.[9]

During I/R, the energy production is decreased due to the reduced oxidative phosphorylation rate at the inner mitochondrial membrane. This event also rapidly induces ROS production.[45,46] ROS that is generated from the electron transport chain and released to cytosol from any mitochondria can destabilize its neighboring mitochondrial membrane by inducing the release of ROS from these neighboring mitochondria. This mechanism is known as ROS-induced ROS release.[47] These events lead to $\Delta\Psi_m$ and metabolic mitochondrial oscillation. The loss of $\Delta\Psi_m$ causes a rapid mitochondrial dysfunction and leads to apoptotic and necrotic cell death.[48]

mBzR-mediated Cardioprotection Against Ischemia/Reperfusion Injury

In I/R injury, the mBzR ligands 4′-Cl-DZP, SSR180575, and PK11195 have been shown to improve cardiac functions and reduce the incidence of arrhythmias.[24,32,39,49,50] As shown in Table 3, in both in vivo and ex vivo ischemia models, pretreatment with 4′-Cl-DZP before ischemia induction or at the onset of reperfusion improved left ventricular developed pressure (LVDP) and reduced apoptosis, infarct size, and postischemic arrhythmias.[24,32,39,49] Leducq et al. found that the new, potent, and selective mBzR ligand SSR180575[51,52] was able to restore the left ventricular function after it was impaired during reperfusion in low-flow and regional ischemia in rat and rabbit models, respectively. The restoration behaved in a dose-dependent manner, without changing the baseline values.[49] Interestingly, although PK11195 has been shown previously to antagonize the effects of 4′-Cl-DZP in intact isolated perfused heart,[33] it has been demonstrated to improve LVDP and dP/dt_{max} and reduce infarct size under a pathologic condition (ie, in isolated global ischemic rat heart).[24] These cardioprotective effects of PK11195 were similar to those with the administration of 4′-Cl-DZP alone, with co-treatment with 4′-Cl-DZP, and with ischemic preconditioning.[24] Moreover, in an ischemic phase induced by coronary artery ligation in dog, the administration of PK11195 significantly increased the heart rate and decreased the mean arterial blood pressure.[50]

The loss of mitochondrial integrity that resulted from calcium overload has been shown to induce mPTP opening, leading to massive swelling of mitochondria, membrane rupture, release of cytochrome c from mitochondria, and activation of proapoptotic Bcl-2 family member proteins such as Bax. These effects eventually cause cell death.[53,54] In an in vivo rat model of occlusion/reperfusion, the levels of cytosolic cytochrome c and caspase-9 were significantly increased in a time-dependent manner during reperfusion. In addition, the level of the reactive 10- to 15-kDa form of Bax was increased in mitochondrial extract with its sudden drop in cytosolic levels during reperfusion.[42] The activation of Bax that is translocated into the mitochondria triggers mitochondrial membrane permeability, regulates the release of cytochrome c, and supports the apop-

Table 3. Effects of mBzR ligands on ischemia/reperfusion heart

Ligands	Properties	Models	Type of Ischemia	Effects of I/R					Reference
				Infarct size	Apoptosis	Improved LVDP	dP/dt_{max}	Arrhythmias	
4′-Cl-DZP	mBzR antagonist	Isolated rabbit hearts	Global ischemia	—	—	Yes	—	↓	Brown et al.[32]
		Isolated Wistar rat hearts	Global ischemia	↓	—	Yes	↑	—	Obame et al.[24]
		Wistar rats	LAD occlusion	↓	↓	—	—	—	Obame et al.[24]
		Isolated guinea pig hearts	Global ischemia	—	—	—	—	↓	Akar et al.[39]
		Isolated Sprague-Dawley rat hearts	Low-flow I/R	—	—	Yes	—	—	Laducq et al.[49]
		Isolated Sprague-Dawley rat hearts	Low-flow I/R	—	—	—	—	↓	Li et al.[40]
SSR180575	mBzR antagonist	Isolated Sprague-Dawley rat hearts	Low-flow I/R	—	—	Yes	—	—	Laducq et al.[49]
		Rabbit	LAD occlusion	↓	—	Yes	↑	—	Laducq et al.[49]
		Wistar rat	LAD occlusion	↓	—	—	—	—	Laducq et al.[49]
PK11195	mBzR agonist	Dog	LAD occlusion	—	—	—	—	↓	Steenbergen et al.[50]
		Isolated Wistar rat hearts	Global ischemia	↓	—	Yes	↑	—	Obame et al.[24]
PK11195 + 4′-Cl-DZP		Isolated Wistar rat hearts	Global ischemia	↓	—	Yes	↑	—	Obame et al.[24]
FGIN-1-27	mBzR agonist	Isolated guinea pig hearts	Global ischemia	—	—	—	—	↑	Akar et al.[39]
		Isolated Sprague-Dawley rat hearts	Low flow I/R	—	—	—	—	↑	Li et al.[40]

I/R, Ischemia/reperfusion; LAD, left anterior descending coronary artery; LVDP, left ventricular developed pressure; ↓, decrease; ↑, increase; —, not studied.

tosome formation and apoptotic process during cardiac reperfusion. Recently, 4′-Cl-DZP has been shown to limit apoptosis by reducing the release of apoptosis inducing factor and cytochrome c from intermembrane space of mitochondria. These resulted in the prevention of the redistribution of the Bcl-2 family proteins and reduction of the 10-kDa form of Bax during I/R period.[24] In addition, 4′-Cl-DZP administered before ischemia or during reperfusion was able to reduce infarct size in isolated myocardium and the effect was similar to that of ischemic preconditioning.[24] Hence, it is possible that the protective effects against I/R injury induced by the mBzR ligands and preconditioning could share common signaling pathways.[24]

It has been shown that the rise in end-diastolic pressure, particularly during the ischemic phase, involves the combination of calcium overload and the depletion of ATP.[55] Stabilizing effects of 4′-Cl-DZP on mitochondrial function have been shown to maintain energy supply by improving oxidative phosphorylation and maintaining mitochondrial yields during I/R in rats.[24] This protection against I/R was associated with an increase in respiratory control ratio related to the increase in the state 3 respiratory rate.[24,56] Furthermore, the administration of cyclosporin A (CsA), the mPTP blocker, did not change the respiratory rate, indicating that the mitochondrial inner membrane was not affected, thus confirming that mPTP opening was not involved in this process.[24] The effects of mBzR ligands on I/R injury are summarized in Table 3. It is clear that the definite mechanism regarding the role of mBzR and mPTP on I/R injury process is still debated. Studies in mitochondria isolated from I/R rat hearts showed that the administration of CsA blocked Ca^{2+}-induced mitochondrial swelling, whereas 4′-Cl-DZP had no effect.[24] However, previous studies demonstrated that mBzR ligands such as 4′-Cl-DZP, PK11195, and ANH086 by themselves could induce mPTP opening in a dose-dependent manner and could induce mitochondrial Ca^{2+} release in rat cardiac mitochondrial fraction, and that these effects were abolished by CsA or other mPTP inhibitors.[24,53,57,58] Further studies are needed to resolve these discrepancies.

In summary, mBzR antagonists such as 4′-Cl-DZP demonstrated its protection against I/R injury, whereas mBzR agonists demonstrated opposite results. These effects include improved cardiac function, reduced infarct size, and arrhythmia prevention. The proposed mechanism of this protection of mBzR antagonist against I/R injury is thought to be partly due to its antiapoptotic effects, as well as its ability to stabilize mitochondrial function.

mBzR and Cardiac Electrophysiological Alterations

Cardiac arrhythmias are known to frequently occur during myocardial I/R process.[39] Growing evidence indicated that mBzR plays an important role in this phenomenon.[32,39,40,50] In isolated hearts with global ischemia, administration of 4′-Cl-DZP either before ischemia induction or prior to reperfusion can reduce the incidence of postischemic arrhythmias.[32,39] Moreover, it has been shown that PK11195, the specific mBzR ligand, protected dogs from early and delayed ventricular arrhythmias after 20 minutes of ischemia by left anterior descending coronary artery (LAD) occlusion and significantly prevented ventricular fibrillation after reperfusion.[50]

Under physiological condition, 4′-Cl-DZP has been shown to decrease APD in a dose-dependent manner in guinea pig papillary muscle[27,28] and in isolated cardiomyocytes.[29,32] However, in intact perfused rat heart, 4′-Cl-DZP had no effect on sarcolemma ion channel and did not alter the action potential.[39] Under pathologic conditions (ie, ischemia or flash-induced stress), 4′-Cl-DZP rapidly prevented APD shortening, facilitated normal action potential morphology, and prevented postischemic tachyarrhythmias.[39] Furthermore, when the bolus dose was administered at the onset of reperfusion, 4′-Cl-DZP could stabilize the action potential and completely prevented arrhythmias.[39] These effects of mBzR ligands on the incidence of arrhythmias and cardiac electrophysiology are summarized in Tables 3 and 4.

Although mBzR has a functional link with Ca^{2+} channels, its effects can be seen beyond the Ca^{2+} channels. It has been shown that the cardioprotective properties of Ca^{2+} channel blockers were effective only when given as preischemic treatment; they were not effective when administered at the onset of reperfusion.[59,60] However, the administration of mBzR antagonist 4′-Cl-DZP as a pretreatment or a bolus at the onset of reperfusion could successfully reduce the incidence of both arrhythmia and mechanical dysfunction.[32,39] Previous studies demonstrated that mBzR was associated with the activation of 2 important channels at mitochondrial membrane—these were mPTP, which was shown to be opened during reperfusion but not during ischemia,[61] and mitochondrial inner membrane anion channel (IMAC), which might be activated during ischemia and early reperfusion.[39] Furthermore, these 2 channels have been implicated in $\Delta\Psi_m$ depolarization. Huser et al.[62] showed that $\Delta\Psi_m$ fluctuation in individual cardiac mitochondria was caused by repetitive opening and closing of the mPTP, oxidative stress, and/or cellular Ca^{2+} overload. These events initially triggered pore openings at shorter duration followed by prolonged openings, resulting in the dissipation of $\Delta\Psi_m$ as efflux of large solutes coincide with swelling of mitochondrial and loss of $\Delta\Psi_m$.[62] O'Rourke[63] demonstrated that IMAC was involved in $\Delta\Psi_m$ oscillation induced by substrate deprivation and suggested that IMAC may be activated under metabolic stress in intact cardiomyocytes. Still, the functional link between mBzR and mPTP or IMAC is unclear. In a patch-clamp study of isolated mitoplasts, 4′-Cl-DZP has been shown to inhibit mPTP and IMAC opening at nanomolar concentration.[64] Nevertheless, previous studies have suggested that mPTP was not involved in the arrhythmogenesis of I/R myocardium. It has been shown that the mPTP blocker CsA could well preserve rat cardiac mitochondria from Ca^{2+}-induced mPTP opening[23,53] but did not prevent the loss of $\Delta\Psi_m$ and did not completely reduce the incidence of postischemic arrhythmias.[32,39,65] Furthermore, it has been suggested that IMAC activation during ischemia and early reperfusion could be a precursor to the activation of mPTP.[39,66]

In summary, inactivation of mBzR can prevent mitochondrial dysfunction and cardiac electrophysiology alterations under stresses such as I/R injury by stabilized $\Delta\Psi_m$, preserved cardiac action potential in both duration and morphology, and prevented postischemic arrhythmias. The proposed mechanism of these actions has been related to IMAC and mPTP inactivation, leading to the prevention of cellular deterioration from I/R injury.

mBzR and ROS in the Heart

It is known that mitochondria, a vital source of energetic pool in the cell during oxidative phosphorylation, are the main source of ROS production.[67] In cardiac cell, the population of mitochondria in cytoplasm is >50% of the cell volume. A small amount (1%-5%) of electrons that flow through the electron transport chain in the mitochondria and leak into the cytoplasm and mitochondrial matrix contributes to ROS production.[66,68] ROS has been shown to play an important role as the determinant of cell survival in ischemia.[69-71] It has been shown that ROS release during ischemic preconditioning can act as signaling molecules that may activate protein kinase C and mitochondrial ATP-sensitive potassium channels (mitoK$_{ATP}$). This results in the protection of cardiomyocytes against injury.[69,70,72-74] Despite that, an increase in ROS production in postischemic hearts shows different effects. Under physiological conditions, there is a balance between ROS production and the intracellular ROS scavenging capacity.[71] However, such a balance is upset under pathologic conditions. It has been shown that oxidative stress is induced by an increase in ROS production or a depletion of ROS scavengers or the depletion of cytosolic reduced glutathione (GSH).[75] These ROS may lead to mitochondrial dysfunction, apoptotic cell death, and persistent contractile dysfunction.[45,66,67,76]

In models of metabolic stress induction in the form of substrate deprivation[77,78] or localized ROS generations by laser flash–induced stress,[66,79] ROS was found to trigger cellwide oscillations and collapse of $\Delta\Psi_m$ in the entire mitochondrial network of isolated cardiomyocytes. Aon et al.[66] demonstrated that the effects of ROS generation triggered by the flash on cellwide mitochondrial oscillation were not abolished by either acute addition or the preincubation of 1 μM CsA, the inhibitor of mPTP. These suggest that mPTP was not involved in this process. Previous studies demonstrated that ROS can trigger the opening of IMAC.[39,66] Aon et al.[66] found that PK11195, which is one of several classes of amphipathic inhibitors of IMAC, could prevent the cellwide synchronized mitochondrial oscillations and ROS bursts after a flash. Although matrix ROS was found to increase markedly in the flash region of the cell during mitochondrial depolarization, these ROS did not dissipate to other regions, confirming that PK11195 could prevent ROS-induced ROS release in these cells.[66] Consistently, 4′-Cl-DZP has been shown to suppress the entire cell oscillation of $\Delta\Psi_m$, eliminate APD oscillation in isolated cardiomyocytes,[39] and improve mitochondrial phosphorylation rate.[24,49]

In summary, a high level of ROS following reperfusion can greatly destabilize the system and produce changes in the cardiac action potential, which may contribute to the genesis of arrhythmia. Because these effects were abolished by mBzR antagonists, it was proposed that mBzR activates IMAC, the precursor of mPTP opening, to release ROS and leads to neighboring mitochondrial instability, known as ROS-induced ROS release mechanism (Fig. 1). This process is the primary cause of mitochondrial oscillation in the whole cell and cardiac physiology alterations. Nevertheless, the modulations of mBzR on mitochondrial ion channels and other proteins are still unclear and need further investigation.

Table 4. Electrophysiological effects of mBzR in the heart

Ligands	Properties	Concentration	Models	Species	Electrophysiological effects			ROS production	Reference
					APD	$[Ca^{2+}]_i$	Oscillation of $\Delta\Psi_m$ depolarization		
4′-Cl-DZP	mBzR antagonist	0.03-3.0 μM	Papillary muscle	Guinea pig	↓	—	—	—	Mestre et al.[28]
		3 μM	Papillary muscle	Guinea pig	↓	—	—	—	Mestre et al.[27]
		<3 μM	Isolated cardiomyocytes	Guinea pig	↔	μ	—	—	Holck and Osterrieder[29]
		≥3 μM	Isolated cardiomyocytes	Guinea pig	↓	↓	—	—	Holck and Osterrieder[29]
		24 μM	Isolated cardiomyocytes	Rabbit	↓	↓	—	—	Brown et al.[32]
		32 μM	Isolated cardiomyocytes; flash-induced	Guinea pig	↑	—	No	—	Akar et al.[39]
		32-100 μM	Intact perfused heart	Guinea pig	↔	—	—	—	Akar et al.[39]
		32-100 μM	Global ischemia	Guinea pig	↑	—	—	—	Akar et al.[39]
		64 μM	Isolated cardiomyocytes; flash-induced	Guinea pig	—	—	No	—	Aon et al.[66]
PK11195	mBzR agonist	3 nM-3 μM	Papillary muscle	Guinea pig	↔	—	—	—	Mestre et al.[28]
		3 μM	Papillary muscle	Guinea pig	↔	—	—	—	Mestre et al.[27]
		50-200 μM	Isolated cardiac mitochondrial	Sprague-Dawley rat	—	—	Yes	—	Li et al.[57]
		50 μM	Isolated cardiomyocytes; flash-induced	Guinea pig	—	—	No	↓	Aon et al.[66]
PK11195 + 4′-Cl-DZP		PK (30-300 nM), PK (3 nM-3 μM),	Papillary muscle	Guinea pig	↑	—	—	—	Mestre et al.[28]
FGIN-1-27	mBzR agonist	4.6 μM	Global ischemia	Guinea pig	↓	—	—	—	Akar et al.[39]
		4.6 μM	Isolated cardiomyocytes	Sprague-Dawley rat	—	↓	—	—	Li et al.[40]
		92 μM	Isolated cardiomyocytes; flash-induced	Guinea pig	—	—	No	—	Aon et al.[66]

↓, Decrease; ↑, increase; ↔, no change; —, not studied.

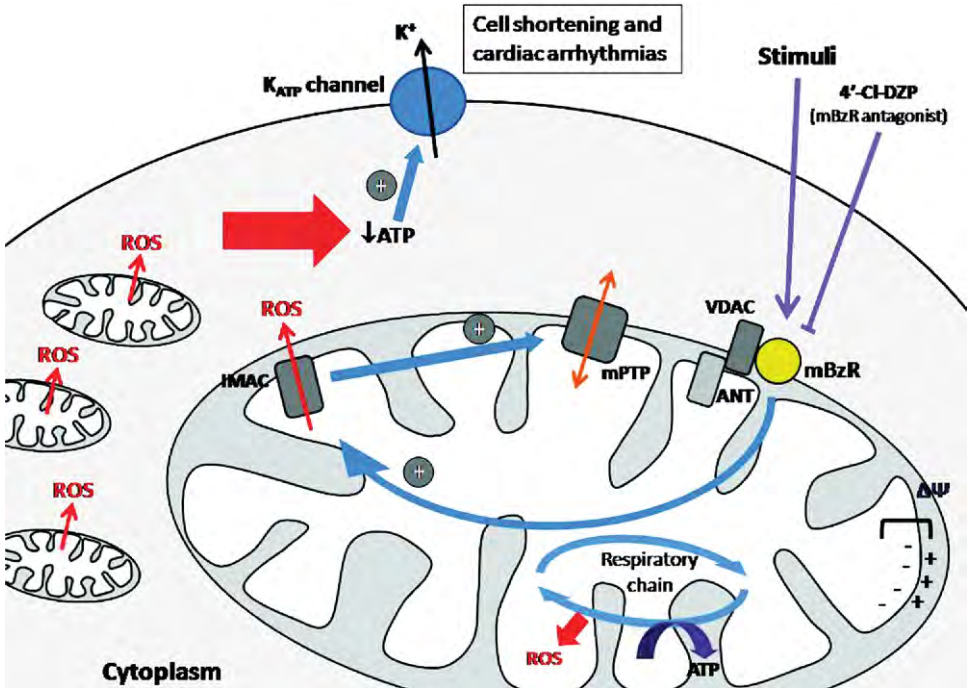

Figure 1. Hypothetical scheme of mitochondrial benzodiazepine receptor (mBzR) and other mitochondrial ion channels on the effect of reactive oxygen species (ROS)-induced ROS release mechanism and the cardiac physiology alterations. Under stress condition, ROS is increased from respiratory chain, and activation of mBzR leads to the opening of mitochondrial inner membrane anion channel (IMAC) and mitochondrial permeability transition pore (mPTP). These processes result in the oscillation or collapse of mitochondrial membrane potential ($\Delta\Psi_m$) and ROS-induced ROS release mechanism. The loss of mitochondria membrane integrity leads to the decrease of energy supply and activates sarcolemma adenosine triphosphate (ATP)-sensitive potassium channel (K_{ATP}) channel, resulting in the change in cardiac action potential, and finally leads to fatal arrhythmias. mBzR antagonists such as 4′-Cl-DZP that could inhibit $\Delta\Psi_m$ depolarization and prevent postischemic electrical dysfunction are used for protective effect against arrhythmia. ANT, adenine nucleotide translocator; VDAC, voltage-dependent anion channel.

Adverse Effect of mBzR Stimulation in I/R Heart

With the use of mBzR agonists, important findings have been reported regarding the adverse effects of mBzR stimulation in the heart that underwent I/R injury. FGIN-1-27 is the mBzR agonist that bound with high affinity to mBzR but not to the central benzodiazepine receptors.[80] It has been demonstrated that adding FGIN-1-27 to the perfusate worsened the effect of I/R on the heart, because an increased incidence of arrhythmias was observed.[39] Furthermore, hearts pretreated with FGIN-1-27 have been shown to accelerate the APD shortening; reduce action potential amplitude (APA), upstroke velocity (dF/dt), and time for the onset of inexcitability; and eventually lead to arrhythmias.[39] These findings have led to a novel proposed mechanism of arrhythmogenesis in the myocardium.[39] At the mitochondria level, mBzR has been shown to be involved in the oscillations of $\Delta\Psi_m$ in which 4′-Cl-DZP abolished the flash-induced $\Delta\Psi_m$ oscillation, whereas FGIN-1-27 caused permanent $\Delta\Psi_m$ depolarization.[66] It has been proposed that the mechanism of arrhythmogenesis involves the loss of $\Delta\Psi_m$, which induces mitochondrial network interaction, uncoupling of metabolism, and whole-cell electrical and mechanical dysfunction and results in the reentry of cardiac arrhythmias in postischemic heart. This mechanism, proposed by Akar et al. and called "metabolic sink/block,"[39] is a block of electrical propagation that is distinct from other existing conduction blocks (ie, gap junction block, anatomic block, and dynamic functional block). Here, metabolic sink/block is dependent on the formation of areas undergoing regional or temporal changes in $\Delta\Psi_m$. The loss of $\Delta\Psi_m$ induced by mBzR agonist may lead to postischemic arrhythmias.[39] Furthermore, to investigate the correlation between $\Delta\Psi_m$ and APD, Akar et al.[39] demonstrated that glibenclamide, the ATP-sensitive potassium channel (K_{ATP}) inhibitor, blunted the effects of FGIN-1-27, which initially reduced APA and dF/dt in an isolated ischemic rat heart study. This indicates that K_{ATP} activation was responsible for the ischemia-induced electrophysiological changes in the hearts.

In summary, mitochondrial stress such as that under ischemia can lead to mitochondrial depolarization, failure of oxidative phosphorylation, and depletion in energetic pool, resulting in an activation of sarcolemma K_{ATP} channels and changes in the duration of cardiac action potential in individual cells or myocardium, and leads to fatal arrhythmias. The mBzR antagonist 4′-Cl-DZP could blunt these effects through the inhibition of $\Delta\Psi_m$ depolarization, which has been shown to be more effective in preventing postischemic electrical dysfunction by preserving energy depletion and inhibition of sarcolemmal K_{ATP} channels, whereas FGIN-1-27, an mBzR stimulator, shows adverse effects (see Fig. 1).

Clinical Studies of Mitochondrial Benzodiazepine Receptor in the Heart

Characterization and localization of mBzR in human using noninvasive method had been reported in several studies. In a report by Charbonneau et al.,[36] ^{11}C-PK11195, the highly spe-

cific activity and short-lived cyclotron isotope, was injected into 7 normal male subjects, and positron emission tomography was used to locate the distribution of the isotope. ^{11}C-PK11195 was found to be concentrated in the myocardium. In an in vivo evaluation of biodistribution, displacement, and metabolization, [^{123}I]iodo-PK11195 has been shown to rapidly decay into 2 polar metabolites on high-performance liquid chromatography, in plasma samples of healthy volunteers.[81,82] These results were similar to those in mice in which 2 polar metabolites were found in the blood.[81] Unlike in the blood, only original radioactive compounds were found in the hearts of healthy humans.[81] These findings has led to the hypothesis that either no metabolism of this isotope occurs in the heart or metabolites of [^{123}I]iodo-PK11195 that were found in the blood do not enter the heart.[81]

In patients with coronary heart disease who were treated intravenously with PK11195 at the concentration of 20 mg, no hemodynamic changes or anti-ischemic effects were observed.[83] These findings were different from those reported in animal models, suggesting that the effects of this ligand could vary among different species. Although the effects of other mBzR ligands such as 4′-Cl-DZP have been shown to have cardioprotective effects in various animal models in I/R injury, none has been investigated in humans. This is partly due to the fact that most studies were performed in in vitro or small animal models, without the supporting data from any preclinical studies. It is known that the physiological roles of mBzR could vary from species to species; therefore, future studies performed in human-like animal models are needed prior to clinical studies to validate findings from previous studies. If the results warrant its cardioprotective effects, clinical studies can be the next step to investigate the effects of mBzR ligands, which have been proved to have cardioprotective benefits in those animal models to warrant the possibility of their clinical usefulness.

Conclusion

A growing body of evidence demonstrates the ability of mBzR ligands to improve cardiac functions via mitochondrial functions, despite some discrepancies in results. The improvements were achieved by mBzR ligands maintaining energy supply, reducing calcium overload, preventing the mitochondrial ROS-induced ROS release, and restoring normal electrical activity in the heart. Given the important clinical implications of these mBzR ligands, they may represent novel therapeutic strategies for preventing electrical and mechanical dysfunctions at the mitochondrial level in the heart in the near future.

Funding Sources

This work was supported by the Thailand Research Fund grants RTA5280006 (to N.C.) and RMU5180007 (to S.C.).

Disclosures

The authors have no conflicts of interest to disclose.

References

1. Awad M, Gavish M. Binding of [3H]Ro 5-4864 and [3H]PK 11195 to cerebral cortex and peripheral tissues of various species: species differences and heterogeneity in peripheral benzodiazepine binding sites. J Neurochem 1987;49:1407-14.
2. Le Fur G, Guilloux F, Rufat P, et al. Peripheral benzodiazepine binding sites: effect of PK 11195, 1-(2-chlorophenyl)-N-methyl-(1-methylpropyl)-3 isoquinolinecarboxamide. II. In vivo studies. Life Sci 1983;32:1849-56.
3. Le Fur G, Perrier ML, Vaucher N, et al. Peripheral benzodiazepine binding sites: effect of PK 11195, 1-(2-chlorophenyl)-N-methyl-N-(1-methylpropyl)-3-isoquinolinecarboxamide. I. In vitro studies. Life Sci 1983;32:1839-47.
4. Braestrup C, Squires RF. Specific benzodiazepine receptors in rat brain characterized by high-affinity (3H)diazepam binding. Proc Natl Acad Sci U S A 1977;74:3805-9.
5. Anholt RR, Pedersen PL, De Souza EB, Snyder SH. The peripheral-type benzodiazepine receptor. Localization to the mitochondrial outer membrane. J Biol Chem 1986;261:576-83.
6. McEnery MW, Snowman AM, Trifiletti RR, Snyder SH. Isolation of the mitochondrial benzodiazepine receptor: association with the voltage-dependent anion channel and the adenine nucleotide carrier. Proc Natl Acad Sci U S A 1992;89:3170-4.
7. Hardwick M, Fertikh D, Culty M, Li H, Vidic B, Papadopoulos V. Peripheral-type benzodiazepine receptor (PBR) in human breast cancer: correlation of breast cancer cell aggressive phenotype with PBR expression, nuclear localization, and PBR-mediated cell proliferation and nuclear transport of cholesterol. Cancer Res 1999;59:831-42.
8. Woods MJ, Williams DC. Multiple forms and locations for the peripheral-type benzodiazepine receptor. Biochem Pharmacol 1996;52:1805-14.
9. Casellas P, Galiegue S, Basile AS. Peripheral benzodiazepine receptors and mitochondrial function. Neurochem Int 2002;40:475-86.
10. Papadopoulos V, Baraldi M, Guilarte TR, et al. Translocator protein (18kDa): new nomenclature for the peripheral-type benzodiazepine receptor based on its structure and molecular function. Trends Pharmacol Sci 2006;27:402-9.
11. Chen MK, Guilarte TR. Translocator protein 18 kDa (TSPO): molecular sensor of brain injury and repair. Pharmacol Ther 2008;118:1-17.
12. Veenman L, Gavish M. The peripheral-type benzodiazepine receptor and the cardiovascular system. Implications for drug development. Pharmacol Ther 2006;110:503-24.
13. Besman MJ, Yanagibashi K, Lee TD, Kawamura M, Hall PF, Shively JE. Identification of des-(Gly-Ile)-endozepine as an effector of corticotropin-dependent adrenal steroidogenesis: stimulation of cholesterol delivery is mediated by the peripheral benzodiazepine receptor. Proc Natl Acad Sci U S A 1989;86:4897-901.
14. Alho H, Varga V, Krueger KE. Expression of mitochondrial benzodiazepine receptor and its putative endogenous ligand diazepam binding inhibitor in cultured primary astrocytes and C-6 cells: relation to cell growth. Cell Growth Differ 1994;5:1005-14.
15. Taketani S, Kohno H, Furukawa T, Tokunaga R. Involvement of peripheral-type benzodiazepine receptors in the intracellular transport of heme and porphyrins. J Biochem 1995;117:875-80.
16. James ML, Selleri S, Kassiou M. Development of ligands for the peripheral benzodiazepine receptor. Curr Med Chem 2006;13:1991-2001.
17. Campiani G, Fiorini I, De Filippis MP, et al. Cardiovascular characterization of pyrrolo[2,1-d][1,5]benzothiazepine derivatives binding selectively to the peripheral-type benzodiazepine receptor (PBR): from dual PBR affinity and calcium antagonist activity to novel and selective calcium entry blockers. J Med Chem 1996;39:2922-38.

18. Kragie L, Smiehorowski R. Altered peripheral benzodiazepine receptor binding in cardiac and liver tissues from thyroidectomized rats. Life Sci 1994;55:1911-8.

19. Saano V, Rago L, Tupala E, Airaksinen MM. Changes in GABA-benzodiazepine receptor complex and in peripheral benzodiazepine receptors in male mice after copulation. Pharmacol Biochem Behav 1995;51:529-33.

20. Drugan RC, Basile AS, Crawley JN, Paul SM, Skolnick P. Characterization of stress-induced alterations in [3H] Ro5-4864 binding to peripheral benzodiazepine receptors in rat heart and kidney. Pharmacol Biochem Behav 1988;30:1015-20.

21. Drugan RC, Basile AS, Crawley JN, Paul SM, Skolnick P. Inescapable shock reduces [3H]Ro 5-4864 binding to "peripheral-type" benzodiazepine receptors in the rat. Pharmacol Biochem Behav 1986;24:1673-7.

22. Basile AS, Weissman BA, Skolnick P. Maximal electroshock increases the density of [3H]Ro 5-4864 binding to mouse cerebral cortex. Brain Res Bull 1987;19:1-7.

23. Salvetti F, Chelli B, Gesi M, et al. Effect of noise exposure on rat cardiac peripheral benzodiazepine receptors. Life Sci 2000;66:1165-75.

24. Obame FN, Zini R, Souktani R, Berdeaux A, Morin D. Peripheral benzodiazepine receptor-induced myocardial protection is mediated by inhibition of mitochondrial membrane permeabilization. J Pharmacol Exp Ther 2007;323:336-45.

25. Drugan RC, Basile AS, Crawley JN, Paul SM, Skolnick P. "Peripheral" benzodiazepine binding sites in the Maudsley reactive rat: selective decrease confined to peripheral tissues. Brain Res Bull 1987;18:143-5.

26. Gavish M, Katz Y, Bar-Ami S, Weizman R. Biochemical, physiological, and pathological aspects of the peripheral benzodiazepine receptor. J Neurochem 1992;58:1589-601.

27. Mestre M, Carriot T, Belin C, et al. Electrophysiological and pharmacological evidence that peripheral type benzodiazepine receptors are coupled to calcium channels in the heart. Life Sci 1985;36:391-400.

28. Mestre M, Carriot T, Belin C, et al. Electrophysiological and pharmacological characterization of peripheral benzodiazepine receptors in a guinea pig heart preparation. Life Sci 1984;35:953-62.

29. Holck M, Osterrieder W. The peripheral, high affinity benzodiazepine binding site is not coupled to the cardiac Ca^{2+} channel. Eur J Pharmacol 1985;118:293-301.

30. Edoute Y, Giris J, Ben-Haim SA, et al. Ro 5-4864 and PK 11195, but not diazepam, depress cardiac function in an isolated working rat heart model. Pharmacology 1993;46:224-30.

31. Saegusa K, Furukawa Y, Ogiwara Y, Takeda M, Chiba S. Pharmacologic basis of responses to midazolam in the isolated, cross-perfused, canine right atrium. Anesth Analg 1987;66:711-8.

32. Brown DA, Aon MA, Akar FG, et al. Effects of 4′-chlorodiazepam on cellular excitation-contraction coupling and ischaemia-reperfusion injury in rabbit heart. Cardiovasc Res 2008;79:141-9.

33. Leeuwin RS, Zeegers A, van Hamme J, van Wilgenburg H. Modification of cardiac actions of RO 05-4864 by PK 11195 and flumazenil in the perfused rat heart. Life Sci 1997;61:1631-42.

34. Grupp IL, French JF, Matlib MA. Benzodiazepine Ro 5-4864 increases coronary flow. Eur J Pharmacol 1987;143:143-7.

35. Weissman BA, Bolger GT, Chiang PK. Interactions between nitrogen oxide-containing compounds and peripheral benzodiazepine receptors. FEBS Lett 1990;260:169-72.

36. Charbonneau P, Syrota A, Crouzel C, et al. Peripheral-type benzodiazepine receptors in the living heart characterized by positron emission tomography. Circulation 1986;73:476-83.

37. Le Fur G, Vaucher N, Perrier ML, et al. Differentiation between two ligands for peripheral benzodiazepine binding sites, [3H]RO5-4864 and [3H]PK 11195, by thermodynamic studies. Life Sci 1983;33:449-57.

38. Mukhin AG, Papadopoulos V, Costa E, Krueger KE. Mitochondrial benzodiazepine receptors regulate steroid biosynthesis. Proc Natl Acad Sci U S A 1989;86:9813-6.

39. Akar FG, Aon MA, Tomaselli GF, O'Rourke B. The mitochondrial origin of postischemic arrhythmias. J Clin Invest 2005;115:3527-35.

40. Li J, Xiao J, Liu Y, et al. Mitochondrial benzodiazepine receptors mediate cardioprotection of estrogen against ischemic ventricular fibrillation. Pharmacol Res 2009;60:61-7.

41. Mangoni ME, Marger L, Nargeot J. If current inhibition: cellular basis and physiology. Adv Cardiol 2006;43:17-30.

42. Lundberg KC, Szweda LI. Initiation of mitochondrial-mediated apoptosis during cardiac reperfusion. Arch Biochem Biophys 2004;432:50-7.

43. Petronilli V, Penzo D, Scorrano L, Bernardi P, Di Lisa F. The mitochondrial permeability transition, release of cytochrome c and cell death. Correlation with the duration of pore openings in situ. J Biol Chem 2001; 276:12030-4.

44. Weiss JN, Korge P, Honda HM, Ping P. Role of the mitochondrial permeability transition in myocardial disease. Circ Res 2003;93:292-301.

45. Bolli R, Patel BS, Jeroudi MO, Lai EK, McCay PB. Demonstration of free radical generation in "stunned" myocardium of intact dogs with the use of the spin trap alpha-phenyl N-tert-butyl nitrone. J Clin Invest 1988;82: 476-85.

46. Zweier JL, Flaherty JT, Weisfeldt ML. Direct measurement of free radical generation following reperfusion of ischemic myocardium. Proc Natl Acad Sci U S A 1987;84:1404-7.

47. Zorov DB, Filburn CR, Klotz LO, Zweier JL, Sollott SJ. Reactive oxygen species (ROS)-induced ROS release: a new phenomenon accompanying induction of the mitochondrial permeability transition in cardiac myocytes. J Exp Med 2000;192:1001-14.

48. Das A, Xi L, Kukreja RC. Phosphodiesterase-5 inhibitor sildenafil preconditions adult cardiac myocytes against necrosis and apoptosis. Essential role of nitric oxide signaling. J Biol Chem 2005;280:12944-55.

49. Leducq N, Bono F, Sulpice T, et al. Role of peripheral benzodiazepine receptors in mitochondrial, cellular, and cardiac damage induced by oxidative stress and ischemia-reperfusion. J Pharmacol Exp Ther 2003;306: 828-37.

50. Mestre M, Bouetard G, Uzan A, et al. PK 11195, an antagonist of peripheral benzodiazepine receptors, reduces ventricular arrhythmias during myocardial ischemia and reperfusion in the dog. Eur J Pharmacol 1985; 112:257-60.

51. Vin V, Leducq N, Bono F, Herbert JM. Binding characteristics of SSR180575, a potent and selective peripheral benzodiazepine ligand. Biochem Biophys Res Commun 2003;310:785-90.

52. Ferzaz B, Brault E, Bourliaud G, et al. SSR180575 (7-chloro-N,N,5-trimethyl-4-oxo-3-phenyl-3,5-dihydro-4H-pyridazino[4,5-b]i ndole-1-acetamide), a peripheral benzodiazepine receptor ligand, promotes neuronal survival and repair. J Pharmacol Exp Ther 2002;301:1067-78.

53. Chelli B, Falleni A, Salvetti F, et al. Peripheral-type benzodiazepine receptor ligands: mitochondrial permeability transition induction in rat cardiac tissue. Biochem Pharmacol 2001;61:695-705.

54. Yang JC, Cortopassi GA. Induction of the mitochondrial permeability transition causes release of the apoptogenic factor cytochrome c. Free Radic Biol Med 1998;24:624-31.

55. Steenbergen C, Murphy E, Watts JA, London RE. Correlation between cytosolic free calcium, contracture, ATP, and irreversible ischemic injury in perfused rat heart. Circ Res 1990;66:135-46.

56. Moreno-Sanchez R, Hogue BA, Bravo C, et al. Inhibition of substrate oxidation in mitochondria by the peripheral-type benzodiazepine receptor ligand AHN 086. Biochem Pharmacol 1991;41:1479-84.

57. Li J, Wang J, Zeng Y. Peripheral benzodiazepine receptor ligand, PK11195 induces mitochondria cytochrome c release and dissipation of mitochondria potential via induction of mitochondria permeability transition. Eur J Pharmacol 2007;560:117-22.

58. Moreno-Sanchez R, Bravo C, Gutierrez J, Newman AH, Chiang PK. Release of Ca2+ from heart and kidney mitochondria by peripheral-type benzodiazepine receptor ligands. Int J Biochem 1991;23:207-13.

59. Balasubramaniam R, Chawla S, Mackenzie L, et al. Nifedipine and diltiazem suppress ventricular arrhythmogenesis and calcium release in mouse hearts. Pflugers Arch 2004;449:150-8.

60. Baxter GF, Yellon DM. Attenuation of reperfusion-induced ventricular fibrillation in the rat isolated hypertrophied heart by preischemic diltiazem treatment. Cardiovasc Drugs Ther 1993;7:225-31.

61. Griffiths EJ, Halestrap AP. Mitochondrial non-specific pores remain closed during cardiac ischaemia, but open upon reperfusion. Biochem J 1995;307 (Pt 1):93-8.

62. Huser J, Blatter LA. Fluctuations in mitochondrial membrane potential caused by repetitive gating of the permeability transition pore. Biochem J 1999;343 Pt 2:311-7.

63. O'Rourke B. Pathophysiological and protective roles of mitochondrial ion channels. J Physiol 2000;529 Pt 1:23-36.

64. Kinnally KW, Zorov DB, Antonenko YN, et al. Mitochondrial benzodiazepine receptor linked to inner membrane ion channels by nanomolar actions of ligands. Proc Natl Acad Sci U S A 1993;90:1374-8.

65. Berkich DA, Salama G, LaNoue KF. Mitochondrial membrane potentials in ischemic hearts. Arch Biochem Biophys 2003;420:279-86.

66. Aon MA, Cortassa S, Marban E, O'Rourke B. Synchronized whole cell oscillations in mitochondrial metabolism triggered by a local release of reactive oxygen species in cardiac myocytes. J Biol Chem 2003;278: 44735-44.

67. Ambrosio G, Zweier JL, Duilio C, et al. Evidence that mitochondrial respiration is a source of potentially toxic oxygen free radicals in intact rabbit hearts subjected to ischemia and reflow. J Biol Chem 1993;268: 18532-41.

68. Kowaltowski AJ, Vercesi AE. Mitochondrial damage induced by conditions of oxidative stress. Free Radic Biol Med 1999;26:463-71.

69. Vanden Hoek TL, Becker LB, Shao Z, Li C, Schumacker PT. Reactive oxygen species released from mitochondria during brief hypoxia induce preconditioning in cardiomyocytes. J Biol Chem 1998;273:18092-8.

70. Baines CP, Goto M, Downey JM. Oxygen radicals released during ischemic preconditioning contribute to cardioprotection in the rabbit myocardium. J Mol Cell Cardiol 1997;29:207-16.

71. Hess ML, Manson NH. Molecular oxygen: friend and foe. The role of the oxygen free radical system in the calcium paradox, the oxygen paradox and ischemia/reperfusion injury. J Mol Cell Cardiol 1984;16:969-85.

72. Sasaki N, Sato T, Ohler A, O'Rourke B, Marban E. Activation of mitochondrial ATP-dependent potassium channels by nitric oxide. Circulation 2000;101:439-45.

73. Sato T, O'Rourke B, Marban E. Modulation of mitochondrial ATP-dependent K+ channels by protein kinase C. Circ Res 1998;83:110-4.

74. Sundaresan M, Yu ZX, Ferrans VJ, Irani K, Finkel T. Requirement for generation of H2O2 for platelet-derived growth factor signal transduction. Science 1995;270:296-9.

75. Aon MA, Cortassa S, Maack C, O'Rourke B. Sequential opening of mitochondrial ion channels as a function of glutathione redox thiol status. J Biol Chem 2007;282:21889-900.

76. Von Harsdorf R, Li PF, Dietz R. Signaling pathways in reactive oxygen species-induced cardiomyocyte apoptosis. Circulation 1999;99:2934-41.

77. O'Rourke B, Ramza BM, Marban E. Oscillations of membrane current and excitability driven by metabolic oscillations in heart cells. Science 1994;265:962-6.

78. Romashko DN, Marban E, O'Rourke B. Subcellular metabolic transients and mitochondrial redox waves in heart cells. Proc Natl Acad Sci U S A 1998;95:1618-23.

79. on MA, Cortassa S, O'Rourke B. Percolation and criticality in a mitochondrial network. Proc Natl Acad Sci U S A 2004;101:4447-52.

80. Romeo E, Auta J, Kozikowski AP, et al. 2-Aryl-3-indoleacetamides (FGIN-1): a new class of potent and specific ligands for the mitochondrial DBI receptor (MDR). J Pharmacol Exp Ther 1992;262:971-8.

81. Dumont F, De Vos F, Versijpt J, et al. In vivo evaluation in mice and metabolism in blood of human volunteers of [123I]iodo-PK11195: a possible single-photon emission tomography tracer for visualization of inflammation. Eur J Nucl Med 1999;26:194-200.

82. Versijpt J, Dumont F, Thierens H, et al. Biodistribution and dosimetry of [123I]iodo-PK 11195: a potential agent for SPET imaging of the peripheral benzodiazepine receptor. Eur J Nucl Med 2000;27:1326-33.

83. Drobinski G, Lechat P, Eugene L, Grosgogeat Y. [Absence of an antiischemic effect of the peripheral benzodiazepine receptor antagonist PK 11195. Study by atrial stimulation in man]. Therapie 1989;44:263-7.

© Med Sci Monit, 2011; 17(2): RA44-52
PMID: 21278703

WWW.MEDSCIMONIT.COM
Review Article

Received: 2010.04.07
Accepted: 2010.10.05
Published: 2011.02.01

Roles of the nitric oxide signaling pathway in cardiac ischemic preconditioning against myocardial ischemia-reperfusion injury

Punate Weerateerangkul[1,2], Siriporn Chattipakorn[2,3], Nipon Chattipakorn[1,2,4]

[1] Cardiac Electrophysiology Unit, Department of Physiology, Faculty of Medicine, Chiang Mai University, Chiang Mai, Thailand
[2] Cardiac Electrophysiology Research and Training Center, Faculty of Medicine, Chiang Mai University, Chiang Mai, Thailand
[3] Faculty of Dentistry, Chiang Mai University, Chiang Mai, Thailand
[4] Biomedical Engineering Center, Chiang Mai University, Chiang Mai, Thailand

Source of support: Thailand Research Fund grants RTA5280006 (NC) and RMU5180007 (SC), the Office of the Higher Education Commission of Thailand (PW, NC), and the Biomedical Engineering Center (NC), Chiang Mai University, Chiang Mai, Thailand

Summary

Nitric oxide (NO), a vasoactive gas that can freely diffuse into the cell, has many physiological effects in various cell types. Since 1986, numerous studies of ischemic preconditioning against ischemia-reperfusion (I/R) injury have been undertaken and the roles of the NO signaling pathway in cardioprotection have been explored. Many studies have confirmed the effect of NO and that its relative signaling pathway is important for preconditioning of the cardioprotective effect. The NO signaling against I/R injury targeted on the mitochondria is believed to be the end-target for cardioprotection. If the NO signaling pathway is disrupted or inhibited, cardioprotection by preconditioning disappears. During preconditioning, signaling is initiated from the sarcolemmal membrane, and then spread into the cytoplasm via many series of enzymes, including nitric oxide synthase (NOS), the NO-producing enzyme, soluble guanylyl cyclase (sGC), and protein kinase G (PKG). Finally, the signal is transmitted into the mitochondria, where the cardioprotective effect occurs. It is now well established that mitochondria act to protect the heart against I/R injury via the opening of the mitochondrial ATP-sensitive K^+ channel and the inhibition of mitochondrial permeability transition (MPT). This knowledge may be useful in developing novel strategies for clinical cardioprotection from I/R injury.

key words: **nitric oxide • ischemic preconditioning • ischemia/reperfusion injury • heart**

Full-text PDF: http://www.medscimonit.com/fulltxt.php?ICID=881385
Word count: 5164
Tables: 1
Figures: 1
References: 93

Author's address: Nipon Chattipakorn, Cardiac Electrophysiology Research and Training Center, Faculty of Medicine, Chiang Mai University, Chiang Mai 50200, Thailand, e-mail: nchattip@gmail.com

Background

Acute myocardial infarction (MI) is one of the major causes of death worldwide [1]. Acute MI occurs when the large epicardial coronary artery is occluded by a thrombotic blood clot or lipid accumulation. When the occlusion lasts over 20–40 minutes, ischemic tissues become irreversibly damaged, resulting in infarction [2]. The precise time to the development of infarction varies between species. For example, faster development is observed in small rodents with a high heart rate and low collateral blood flow, and slower development is found in larger animals [3]. The progressive and irreversible damage incurred during myocardial ischemia can only be stopped by an immediate reperfusion. Despite this fact, severe and irreversible myocardium damage during the ischemic phase could be caused by reperfusion itself, referred to as reperfusion injury [4]. Irreversible reperfusion injury is defined as an injury caused by reperfusion after the ischemic episode, and results in the death and loss of cells that had only been reversibly injured and primed for death during the preceding ischemic episode [2].

During ischemia, the cardiomyocytes become depleted of oxygen and energy. Higher CO_2 and lactate production in the cell is associated with greater acidosis. The increased acidosis that is produced by anaerobic metabolism increases the influx of Na^+ via the Na^+/H^+ exchanger and the depletion of ATP for Na^+/K^+ ATPase activity, which in turn inhibits the eradication of Na^+ from the cell. This results in the accumulation of Na^+ in cytoplasm [5]. The large amount of Na^+ in cytoplasm drives the reverse mode of the Na^+/Ca^{2+} exchanger, leading to the overload of Ca^{2+}. Finally, the elevated cytosolic Ca^{2+} levels contribute to the opening of a mitochondrial permeability transition pore (mPTP) and result in the death of cells [6]. Large infarct size and failure of infarct tissues to perform a physiological function may lead to heart failure. Protecting the heart from these harmful consequences of coronary occlusion has been the goal of ongoing research by a number of investigators for many decades [7–12]. In recent years, cardiac ischemic preconditioning (i.e., the brief sequences of coronary occlusion and reperfusion before prolonged occlusion) has been extensively studied and found to be cardioprotective against ischemia/reperfusion (I/R) injury. Its various roles in cardioprotection involve many factors, including the nitric oxide signaling pathways [13]. In this review, factors involving the cardioprotective process of ischemic preconditioning, particularly nitric oxide (NO), are presented, the mechanisms of this process are explained, and clinical implications for future therapeutic approaches involving the role of nitric oxide (NO) are discussed.

Ischemic Preconditioning

Ischemic preconditioning (IPC) is the induction of a brief episode of ischemia and reperfusion in myocardium to markedly reduce tissue damage induced by prolonged ischemia [7]. Ischemic preconditioning as a potent cardioprotective method against I/R injury was first reported by Murry et al. in 1986 [8]. In their study using dogs, four sequential episodes of 5-minute occlusion each followed by 5-minute reperfusion were induced in the left circumflex coronary artery, preceding a sustained 40-minute prolonged occlusion period. Another group of dogs were left on a prolonged coronary ligation without IPC. After 4 days of reperfusion, the infarction generated in the former group was reduced by 75% compared to that of the latter group. In their study there was no significant difference in the collateral blood flows of both groups. These results suggested that the tolerance of cardiac tissue to I/R injury is not related to the change of regional blood flow. This remarkable cardioprotection process has also been demonstrated in various species of experimental animals, including rats, mice, rabbits, chicken, and swine [9–13].

Although many investigations have documented preconditioning as an intervention capable of protecting the heart against I/R injury, the cardioprotective effect of IPC is relatively short-lived and the underlying mechanism is not completely understood. More recently it was found that the fundamental processes and the end-target of cardioprotection of IPC mechanisms are related to the prevention of mitochondrial permeability transition (MPT) [1]. Any drug that blocks MPT, such as cyclosporine A, is able to mimic the IPC effect [6]. The MPT and intramitochondrial signaling against I/R injury will be described later in this review.

Even after IPC was first described by Murry et al. in 1986, its mechanisms remained largely unknown for several years. The only clue at the time from studies in various species was that IPC was not involved in the coronary blood flow through the damaged area [14]. However, in 1991 Liu et al. discovered that stimulation of cardiac G_i-coupled adenosine receptor type 1 (A_1) was necessary for the preconditioning effect [14]. The study also showed that IPC's protection could be attenuated by an adenosine receptor antagonist, whereas the infusion of adenosine, or the A_1-specific agonist N6-1-(phenyl-2R-isopropyl) adenosine (R-PIA), could reduce the infarct size. Therefore, cardioprotection of IPC was achieved as ischemic myocardium rapidly degraded ATP to adenosine, which then accumulated in this area [7].

Bradykinin and opioid receptors are also involved in the IPC process [15–17]. During the preconditioning ischemia, bradykinin and endogenous opioid are released from the heart, together with the production of adenosine as a result of metabolic breakdown of ATP [7]. These 3 ligands activate their respective G-protein coupled receptors (GPCRs), which work on the other pathways to protect the heart from ischemic conditions [7]. Nevertheless, the protection of IPC could not be completely blocked if 1 of these 3 receptors is inhibited. On the other hand, it was suggested that combining 2 or more of these receptors produces an incremental cardioprotective effect against I/R injury of IPC [18]. Further research has shown that increasing the number of preconditioning cycles leads to greater resistance of the heart to I/R injury [19]. It was proposed that the additional brief I/R cycles produced more of the trigger substances, and more activities of these receptors could be observed [19]. In addition to these substances and receptors, nitric oxide (NO) has been shown to play an important role in the cardioprotective process of IPC during myocardial ischemia, which will be described later in this review.

Nitric Oxide in the Heart

NO is a signaling molecule that affects the cardiovascular system as a vasodilatator [20]. In hypertensive patients the level of NO metabolites (nitrite and nitrate) are found to be attenuated from their normal levels and inversely correlated

with blood pressure [21]. In the heart, NO is known to be an important regulator of cardiac contractility in physiological condition [22]. In cardiomyocytes all 3 isozymes of NO synthase (NOS) are expressed – neuronal NOS (nNOS, NOS1), inducible NOS (iNOS, NOS2) and endothelial NOS (eNOS, NOS3) [22]. Despite the fact that NO is a highly diffusible signaling molecule that can diffuse freely across the membranes, many studies have shown that the regulation of nNOS and eNOS are localized due to their compartmentalization. nNOS is located in the sarcoplasmic reticulum (SR), whereas eNOS is located in the caveolae of the sarcolemma [22]. Each type of NOS performs a different cardiac contraction modulation. While nNOS signaling potentiates the response of β-adrenergic stimulation [23], eNOS signaling depresses the functional regulation of β-adrenergic stimulation [24]. Although nNOS and eNOS are membrane-bound enzymes and regulate cardiomyocytes under physiological condition, iNOS is a soluble enzyme and produces less expression in physiological condition [24]. Many factors appear to be involved in the regulation of iNOS induction in response to cytokines or cardiac stress [25].

NOS produces NO from the conversion of L-arginine into citruline, using a large number of cofactors, including nicotinamide adenine dinucleotide phosphate (NADPH) and flavin mononucleotide (FMN) [25]. Then, the activation of soluble guanylyl cyclase (sGC) by NO leads to the formation of cGMP from the nucleotide GTP [25]. cGMP-dependent protein kinase (PKG) is further activated, initiating numerous physiological regulations in cardiomyocytes. As a result, L-type Ca^{2+} channel (LTCC) activity is depressed by NO via cGMP-dependent pathways [26–28]. Moreover, a phosphorylation of α_{1C} subunit at position Ser^{533} of LTCC can be developed by the activated PKG, causing an inhibition of L-type Ca^{2+} current ($I_{Ca,L}$) [26]. The rate of Ca^{2+} reuptake into SR, by the increased phosphorylation of phospholamban, can be increased by NO signaling [29]. NO that is released from nNOS when it binds with the superoxide anion, can form peroxynitrite, which exerts this specific effect on phospholamban [29]. Apart from the studies of the effects of NO and cGMP on the Ca^{2+} channel, other cardiac ion channels have also been shown to be regulated by this pathway. The ATP-sensitive K^+ channel is activated by NO donors, and this involves both activation of PKG and the cGMP-independent effect [30,31]. The hyperpolarization-activated pacemaker current (I_f) is also activated by NO and the cGMP-dependent pathway in isolated guinea pig sinoatrial node cells and in human right atrial appendage cells [32,33].

Role of Nitric Oxide Signaling Pathway in the Cytosolic Signaling of IPC

NO and its signaling pathway have been shown to be important in cardioprotection against I/R injury [1]. Numerous studies have shown the cardioprotective effect of both endogenous and exogenous NO on IPC (Table 1). In 1995 it was shown for the first time that NO has a cardioprotective effect against I/R injury, but another report in the same year showed the opposite result [34,35]. Williams et al. reported that endogenous NO plays a critical role in the reduction of infarct size after a 30-minute period of ischemia and a 120-minute period of reperfusion in rabbit hearts in an *in vivo* model [34]. Using L-nitro-arginine (L-NA), a non-specific NOS inhibitor, to treat one group before coronary occlusion and another group during reperfusion (with the same dose administered in each group), increased infarct areas in both groups were observed, compared to a vehicle-treated group. In addition, there was no significant difference in infarct sizes between the L-NA-treated groups before and after coronary occlusion [34]. Despite this result, Woolfson et al. reported that when the isolated rabbit heart was perfused with N (G)-nitro-L-arginine methyl ester (L-NAME), the non-specific NOS inhibitor, at 10 min before the coronary occlusion and continued for 15 min of reperfusion period in 45 min of ischemia and 180 min of reperfusion episode, the infarct size was decreased compared to the untreated group [35]. These inconsistent findings could be due to use of different study models as well as differences in the duration of the treatment with NOS inhibitors and/or the duration of I/R episodes. Moreover, NO is claimed to be a pro-apoptotic factor when it reacts with superoxide anion to form peroxynitrite [36]. This result may be the cause of the myocardial injury in I/R condition found by Woolfson et al. [35], who also found that the NOS inhibitor could reduce infarct size in non-preconditioned hearts after I/R injury [35]. Nevertheless, the mechanisms of NO in the heart are still unclear and need to be investigated further.

The cardioprotective effect of NO on I/R injury was also supported by Zhao et al. in 1997 [37], who suggested that monophosphoryl lipid A (MLA) has an IPC-mimetic effect due to an increase in iNOS activity after coronary occlusion and reperfusion in rabbit hearts [37], as well as discovering the important role of iNOS in the cardioprotective effect against I/R injury when aminoguanidine (AMG), the specific-iNOS inhibitor, was used. In groups treated with AMG alone or with MLA, the infarct size was significantly increased compared to the MLA-only treated group and was not different from the vehicle-treated group [37]. These results suggested that when iNOS is inhibited, the cardioprotective effect of MLA disappears. In a pacing-induced preconditioning model of the rat heart, N^G-nitro-L-arginine (L-NNA), a non-specific NOS inhibitor, increased the release of lactate dehydrogenase, a marker of necrotic cell death, from the coronary-occluded ischemic area [38]. Yang et al. found that L-NAME could abolish the cardioprotective effect of adenosine receptor agonist 5'-(N-ethylcarboxamido) adenosine (NECA) or bradykinin in the I/R model in rabbit hearts [39]. Prendes et al. demonstrated in 2007 that IPC increased cardiac contractility after global ischemia and reperfusion in isolated rat hearts [40]; however, the effect of IPC disappeared when treated with L-NAME [40]. All of these studies demonstrated the cardioprotective effect of NO against I/R injury.

The role of exogenous NO in cardioprotection during ischemia was demonstrated by Nakano et al. [41], who found that S-nitroso-N-acetylpenicillamine (SNAP), an NO donor that serves as the resource of exogenous NO, was able to mimic preconditioning by decreasing infarct size in rabbit hearts after a long period of I/R without IPC, compared to those without SNAP infusion. The study also reported that protein kinase C (PKC) and free radicals or reactive oxygen species (ROS) were important for cardioprotection of the preconditioning-mimetic effect of exogenous NO. When chelerythrine, an inhibitor of PKC, or N-(2-mercaptopropionyl)-glycine (MPG), a ROS scavenger, were combined with SNAP,

Table 1. Effects of sources of NO in cardioprotection against ischemia-reperfusion injury.

Source of NO	Model of I/R	Animal Models	Effect of NO	References
Endogenous	Isolated heart (coronary ligation) Isolated heart (global ischemia)	Rabbit	Reduce infarct size (in both models of I/R injury)	[34]
Endogenous	Cultured embryonic ventricular myocyte	Chick	Decrease cell death	[58]
Endogenous	Isolated heart (coronary ligation)	Rat	Decrease cell death by decreasing of lactate dehydrogenase released	[38]
Endogenous	Isolated heart (global ischemia)	Rat	Improve cardiac function but do not change in cell viability	[40]
Endogenous	*In vivo* (coronary ligation)	Rabbit	Reduce infarct size	[62]
iNOS	*In vivo* (coronary ligation)	Rabbit	Reduce infarct size	[37]
iNOS	Isolated heart (global ischemia)	Mouse	Reduce infarct size	[44]
iNOS	*In vivo* (coronary ligation)	Mouse	Reduce infarct size	[82]
iNOS, eNOS	Isolated heart (global ischemia) Isolated cardiomyocyte	Rat	Reduce infarct size Decrease cell death	[61]
eNOS, iNOS and exogenous	Isolated heart (global ischemia)	Mouse	Reduce infarct size	[43]
eNOS	Isolated heart (global ischemia)	Mouse	No response	[48]
eNOS	Isolated heart (global ischemia)	Mouse	Reduce infarct size	[50]
Exogenous	Isolated heart (coronary ligation)	Rat	Reduce infarct size	[59]
Exogenous	Heart slice	Rat	Decrease necrosis and apoptosis	[60]
Exogenous	Cultured neonatal cardiomyocyte	Rat	Decrease cell death	[85]
Exogenous	Isolated heart (coronary ligation)	Rabbit	Reduce infarct size	[41]
Exogenous	Isolated heart (coronary ligation)	Rat	Reduce infarct size	[42]

the cardioprotective effect of SNAP was eliminated, as shown by the enlargement of infarct size as compared to the SNAP-only treated group [41].

The cardioprotective effects of NO have also been supported by other studies [42,43]. Kanno et al. in 2000 showed that iNOS was overexpressed in eNOS knockout mice after 30 minutes of ischemia followed by 60 minutes of reperfusion; however, nitrite formation and infract area were not different from that of wild type mice [43]. The role of iNOS was also reported by Zhao et al. in 2000 [44], who found that an increase in iNOS expression could be induced by treating with 2-chloro-N^6-cyclopentyladenosine (CCPA), an adenosine A_1 receptor agonist, while the effect disappeared when treated with 8-cyclopentyl-1,3-dipropylxanthine (DPCPX), an adenosine A_1 receptor antagonist [44]. CCPA was also found to reduce infarct size after I/R, while DPCPX or S-methylisothiourea (SMT), a specific iNOS inhibitor, cancelled this effect [44]. Results of a study by Wang et al. in 2002 supported the dominant effect of iNOS in preconditioning [45]. It was discovered that IPC, with a sequence of 6 cycles of 4-minute coronary occlusion and 4-minute reperfusion, increased the expressions of iNOS mRNA and protein at 3 hours after the last cycle of IPC [45]; however, the expression of eNOS remained unchanged [45]. Although iNOS has been shown to protect the heart against myocardial injury after I/R, in 2008 Heinzel et al. found that the treatment of iNOS inhibitor aminoguanidine (AG) in the sustained moderate regional ischemia by a reduction in coronary artery pressure to ~45 mmHg for 6 h in miniswine, AG caused an increase in the cell shortening compared to a non-treated group combination with L-arginine in an isolated cardiomyocyte model [46]. This result suggests the role of iNOS in the attenuation of cardiac function after hypoperfused ischemia [46]. The role of iNOS in the late phase of IPC was also observed. Guo et al. found that iNOS knockout mice had larger infarct size than wild-type mice after being subjected to 30-min coronary occlusion and 24-h reperfusion in the presence of IPC (6 episodes of 4-min occlusion and 4-min reperfusion cycles) [47]. Moreover, at 24 h after I/R, wild-type mice with IPC had smaller infarct size than both non-IPC wild-type and iNOS knockout mice at 24 h after IPC [47]. This cardioprotective effect of iNOS was supported by the increased level of iNOS expression in the IPC group compared to the non-IPC group at 24 h after IPC [47].

The significance of eNOS on cardioprotection against I/R injury has also been investigated. Bell et al. reported that the infarct size in eNOS knockout mice was not different from that of wild-type mice after IPC [48]. This finding is consistent with a 2008 study by Guo et al., which reported that both eNOS-knockout mice and wild-type mice have a

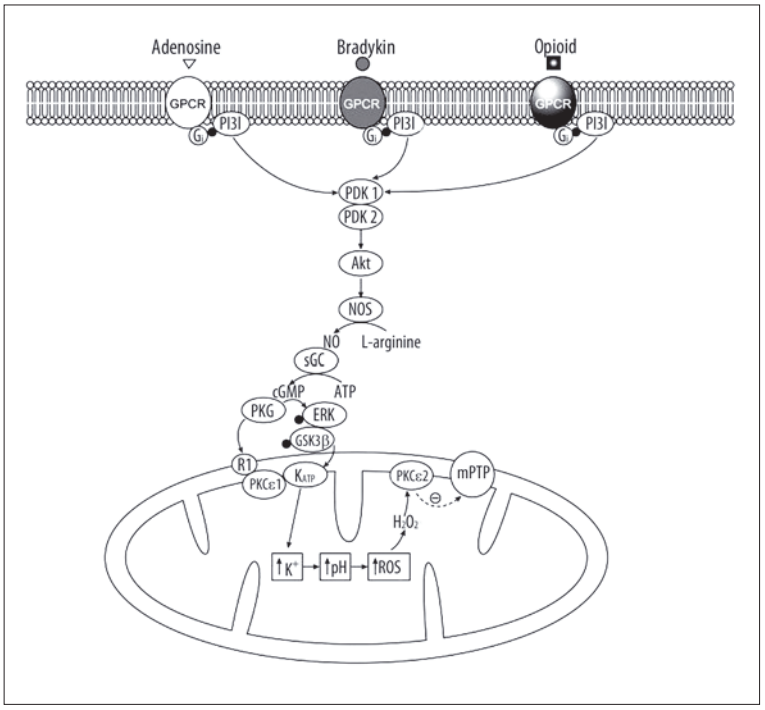

Figure 1. The schematic diagram represents the ischemic preconditioning pathway in cardiomyocytes. IPC induces cardiomyocytes to release adenosine, bradykinin and endogenous opioid which occupy their specific G-protein coupled receptors. After that, the signal will pass into the cytosol via the activation of the enzyme series including PI3K, PDKs, Akt and NOS. The latter enzyme produces NO which acts as signaling molecule to activate sGC and resulted in the cGMP formation. Then, cGMP activates PKG which has the separated mechanism on the mitochondria, the direct and indirect mechanism. The direct mechanism of PKG is on the R1 protein on outer mitochondrial membrane which then activates the opening of mitoK$_{ATP}$ channel on the inner mitochondrial membrane via the phosphorylation of PKCε1. The indirect mechanism of PKG is the phosphorylation of ERK and GSK3β which then act on mitoK$_{ATP}$ channel. However, the mechanism of how GSK3β activates the opening of mitoK$_{ATP}$ channel is still unclear. After the mitoK$_{ATP}$ channel opening, K^+ then enters the mitochondrial matrix and H^+ is ejected out of the matrix to balance the positive charge. When H^+ level decreases, the electron transport chain is interrupted and leads to the formation of superoxide anion and then H_2O_2. Finally, H_2O_2 will act as signaling molecule to activate PKCε2 which then inhibits the opening of mitochondrial permeable transition pore (mPTP). This inhibition of mPTP opening helps to protect mitochondrial damage during I/R injury. (Modified with permission from [63]).

similar infarct size after I/R injury in the non-preconditioned state [49]. In eNOS knockout mice, these findings suggested that the role of eNOS in preconditioning is less prominent than that of iNOS. Although the infarct size was reduced in the overexpressed eNOS compared to wild type mice, du Toit et al. found that there was no difference in the infarct size between IPC and non-IPC in this overexpressed eNOS mouse model [50]. It has been proposed that the heart with eNOS overexpression may be already maximally protected against I/R injury by elevated endogenous NO levels produced by eNOS in this model [50]. Nevertheless, it is not known whether exogenous NO would be beneficial in overexpressed eNOS mice, and further studies are needed to investigate this possibility.

In biological systems, NO has also been found to be produced from enzyme-independent generation [51]. Under acidic conditions, such as intracellular acidosis from ischemia, NO can be generated in the tissues from the reduction of nitrite, NO_2^- [52]. Zweier et al. found that although all NOS isoforms in the heart were totally blocked by L-NAME, the NO formation was partially inhibited in the hearts after 30 min of ischemia [53]. They also reported that in the I/R condition of 30-min ischemia followed by 45-min reperfusion, the time course of the recovery of rate pressure product in L-NAME-treated hearts were higher than in the untreated group; however, when L-NAME was combined with nitrite, the time course of the recovery of rate pressure product decreased [53]. This finding suggested that nitrite can reverse the inhibitory effect of NOS inhibitor, indicating the enzyme-independent generation of NO as a possible mechanism protecting against myocardial I/R injury.

The cardioprotective mechanisms of NO beyond the cGMP/PKG-dependent pathway have also been reported. Since NO can modify the structure of protein through the mechanism called S-nitrosylation, some recent studies have also demonstrated the cardioprotective effect of NO via this mechanism [54,55]. S-nitrosylation occurs when NO, from NO sources such as NOS, acts through the post-translational modification of cysteine thiol on the targeted proteins that colocalized with it to form S-nitrosothiol (SNO), resulting in a change in their protein functions [56,57]. A study by Sun et al. in 2007 reported that when treated with S-nitrosoglutathione (GSNO) (i.e., the exogenous source of NO for S-nitrosylation), the infarct area was smaller than in the untreated group after 20 min of no-flow ischemia and 20 min of reperfusion in isolated mouse hearts [54]. Lin et al. in 2009, using female ovariectomized mice, demonstrated that 17β-estradiol (E2) and the estrogen receptor-β-selective agonist 2,2-bis(4-hydroxyphenyl)-proprionitrite (DPN) decreased the infarct size in the heart after being subjected to 20 min of ischemia followed by 30 min of reperfusion [55]. Proteomic analysis also demonstrated that an increase in S-nitrosylation of a number of proteins could be found in the DPN- and E2-treated hearts, as well as in the preconditioning group [55]. This finding suggests that the increased SNO protein from DPN and E2 treatment after

I/R could lead to cardioprotection against myocardial injury [55]. Therefore, the S-nitrosylation by NO could be one of the major targets for cardioprotection against I/R injury.

Nitric Oxide and Intramitochondrial Signaling of IPC

A growing body of evidence demonstrates the important relationship among NO, ROS, and ischemic preconditioning[41,58–62]. In 2003 Lebuffe et al. found that H_2O_2 and NO were important for preconditioning-like cardioprotection [58]. Furthermore, when the mitochondrial ATP-sensitive K^+ (mitoK_{ATP}) channel was inhibited by 5-hydroxydecanoate (5-HD) in the IPC model, the cardioprotective effect of IPC disappeared [58], suggesting the importance of the mitoK_{ATP} channel in cardioprotection against I/R injury.

Recent research on the mechanisms of IPC suggests that during a brief episode of ischemia, 3 ligands are released from the cardiomyocytes, and long sequences of activities are found here [7]. These ligands (bradykinin, endogenous opioid, and adenosine), occupying their respective G-protein coupled receptors (GPCRs), result in activations of phosphatidylinositol 3-kinase (PI_3K) and series of phospholipid-dependent kinase (PDK) (Figure 1). PDK causes phosphorylation and activation of Akt, where the latter induces further phosphorylation onto NOS, causing NO to be generated. After that, sGC, activated by NO, transforms GTP into cGMP, in which PKG is finally activated. In the last step of cytosolic signaling, PKG then reacts on mitochondria, resulting in the opening of the mitoK_{ATP} channel (Figure 1) [63]. The opening of the mitoK_{ATP} channel leads to the inhibition of the mitochondrial permeability transition pore (mPTP), resulting in the protection of mitochondria from damage during ischemia. Thus, a cGMP-dependent mechanism has been proposed as the main pathway to activate the mitoK_{ATP} channel via phosphorylation by PKG [60,62].

In mitochondria, the mPTP has also been shown to play a critical role in I/R injury. The mPTP is the megachannel that is the formation of 3 specific components, including the voltage-dependent anion channel (VDAC), the adenosine nucleotide transporter (ANT), and cyclophilin D [64]. Currently, the molecular structure of this pore is still under debate [64]. A high concentration of calcium, including calcium overload due to myocardial ischemia, has been shown to trigger the opening of mPTP [65]. Previous studies demonstrated that cyclosporine A, the mPTP inhibitor, could protect the heart from myocardial I/R injury [66,67]. In 2002, Hausenloy et al. proposed that the inhibition of mPTP opening could be the end-target of IPC [68]. Therefore, if mPTP opening is inhibited or interrupted by the process of mitoK_{ATP} channel opening, mitochondrial damage from I/R injury could be prevented, resulting in cardioprotection against I/R injury.

Exogenous NO by SNAP can increase ROS generation in isolated rat cardiomyocytes [59]. However, when SNAP was co-incubated with 5-HD, the ROS production decreased. On the other hand, when treated with diazoxide, the mitoK_{ATP} channel opener, without the treatment of SNAP, the ROS production was instead increased [59]. These findings suggested a relationship between NO, mitoK_{ATP} channel, and ROS production, in which ROS production via the opening of mitoK_{ATP} channel is activated by NO.

Growing evidence supports the proposed hypothesis that the NO-cGMP-PKG pathway causes the mitoK_{ATP} channel opening [58,60,62,69,70]. In this pathway, PKG was proposed as the last step in the signaling process before the involvement of mitochondria (Figure 1). This hypothesis was established when it was shown that exogenous PKG plus cGMP, when added to the isolated mitochondria, causes the increase of mitochondrial matrices due to the opening of the mitoK_{ATP} channel [71]. Furthermore, this effect could be reversed by several substances such as KT5823 (the specific PKG inhibitor), 5-HD or glibenclamide (the mitoK_{ATP} channel inhibitors), and εV_{1-2} (the protein kinase C ε isoform [PKCε]-specific inhibitor) [71].

The mitoK_{ATP} channel is located in the mitochondrial inner membrane (MIM); however, PKG is a cytosolic enzyme that is unable to cross the mitochondrial outer membrane (MOM). Therefore, how PKG interacts with the mitoK_{ATP} channel remains unknown. It has been proposed that phosphorylation of serine or threonine by an unknown protein called R1, located on MOM, is a necessary step taken by PKG (Figure 1) [63]. The PKG-dependent mitoK_{ATP} channel opening seems to require the intact MOM, and is reversed by Ser/Thr phosphatase PP2A [63]. The phosphorylation of this unknown protein R1 causes the signal to be transmitted to PKCε on the MIM, leading to phosphorylation and opening of the mitoK_{ATP} channel (Figure 1).

The confirmation of the presence of R1 was demonstrated by Costa and Garlid in 2008 [72], who used mitochondria and mitoplast (mitochondria without MOM) to test the effects of many specific activators and inhibitors on intramitochondrial signaling [72]. By using phorbol 12-myristate-13-acetate (PMA), a PKCε activator that can cross the MOM, they found that it caused mitochondria matrix swelling due to the opening of the mitoK_{ATP} channel in both mitochondria and mitoplast. However, when treated with isolated PKG, the swelling was observed in mitochondria but not in mitoplast [72]. Both the effects of PMA and PKG, nonetheless, could be removed when treated with the PKCε phosphatase PP2A [72]. This clearly shows that the specific protein R1 located in MOM has the ability to interact with PKG, as well as the ability to open the mitoK_{ATP} channel. PKG itself does not directly open the mitoK_{ATP} channel, and does not cause the mitochondrial matrix swelling in the mitoplast [72].

Another mechanism by which PKG mediates the opening of the mitoK_{ATP} channel was demonstrated by Das et al. in 2008 and 2009 [73,74]. The 2008 study demonstrated that the expression of ERK and GSK3β protein in the ischemia-reoxygenation condition was increased in mouse cardiomyocytes treated with sildenafil citrate, the phosphodiesterase type 5 (PDE-5) inhibitor [73]. They also demonstrated that when treated with the combination of PD98059, an ERK inhibitor, and sildenafil citrate, the level of necrosis and apoptosis increased compared to sildenafil citrate treated alone in ischemia-reoxygenation cardiomyocytes [73]. In 2009, their subsequent study demonstrated that after treatment with sildenafil citrate for 24 h, the phosphorylation of ERK and GSK3β increased in the intact mouse heart [74]; however, when treated with PD98059, the phosphorylation of ERK and GSK3β decreased and were not different from the control. These findings suggested that GSK3β is downstream

of ERK [74], and led the researchers to propose a mechanism downstream from PKG, in which ERK and GSK3β protect the heart against I/R injury via the opening of the mitoK$_{ATP}$ channel (Figure 1).

GSK3β, a multifunctional Ser/Thr kinase, is one of the main target signaling cascades in cardioprotection against I/R injury [75]. This protein was originally found to be involved in the disruption of glycogen synthesis via the inhibition of glycogen synthase, and was named glycogen synthase kinase (GSK) [75,76]. The role of GSK3β phosphorylation in the inhibition of mPTP opening in the heart was first reported by Juhaszova et al. in 2004 [77], showing that the threshold for mPTP opening was increased when GSK3β was knockdown via RNAi in isolated neonatal rat cardiomyocytes [77]. The GSK3β inhibitors were also reported to have a cardioprotective effect against I/R injury [78]. A 2002 study by Tong et al. demonstrated that pretreatment with lithium as well as SB216763, the GSK3β inhibitors, could decrease the infarct size after 20-min global ischemia and 30-min reperfusion in isolated rat hearts [78]. A 2006 *in vivo* study in rats by Nishihara et al. also supports the hypothesis that the GSK3β inhibitor SB216763 can limit infarct size after 20-min LAD occlusion and 40-min reperfusion in a dose-dependent manner [79]. Moreover, a study by Gross et al. in 2004 found that SB216763 and another GSK3β inhibitor, SB415286, when administered for 10 min before ischemia or 5 min before reperfusion, could decrease infarct size, and that infarct size was not different between pre- and post-treatment in 30-min ischemia and 2-hr reperfusion in rats [80]. In 2008, Obame et al. demonstrated that the cardioprotective effect of the GSK3β inhibitor against I/R injury was related to the inhibition of mPTP opening [81].

In mitochondria, the opening of the mitoK$_{ATP}$ channel leads to an increase in K^+ influx, causing swelling and alkalinization of the mitochondrial matrix. The increased K^+ influx then replaces H^+ in the electron transport chain, and as a result, superoxide anion, the first ROS that appears in the mitochondria, is produced [63]. The superoxide anion then reacts with H_2O to form H_2O_2, which directly activates PKCε on the MIM. Two isoforms of PKCε are found in MIM – PKCε1 and PKCε2 [63]. PKCε1, located close to the mitoK$_{ATP}$ channel, causes the phosphorylation and opening of the mitoK$_{ATP}$ channel. The other isoform, PKCε2, is located close to mPTP, and its activation causes the inhibition of mPTP opening [63]. A growing body of evidence currently supports this cardioprotective effect against I/R injury by the ROS production in mitochondria from the opening of the mitoK$_{ATP}$ channel [72,82,83]. The end-target effect of mPTP inhibition allows cells to survive due to an inhibition of the released apoptotic signal from mitochondria by the MPT process (the summarized diagram of the pathway is shown in Figure 1) [1,84]. Moreover, the irreversible mPTP opening can lead to the reduction of ATP production by abolishing mitochondrial membrane potential, which finally results in necrotic cell death from energy depletion [69]. Despite the inhibition of MPT by the opening of mitoK$_{ATP}$ channels, a 2008 study by Rickover et al. demonstrated that exogenous NO from SNP decreased intracellular Ca^{2+} overload in cardiomyocytes after ischemia-reoxygenation [85]. Since the intracellular Ca^{2+} overload can directly activate mPTP opening, the reduction of intracellular Ca^{2+} could attenuate the activation of mPTP in I/R condition [86].

Research Translation of Nitric Oxide against I/R Injury

NO-mediated signaling is intimately involved in the pathway that triggers protection against I/R injury. The preconditioning pathway initiates on the sarcolemmal membrane of cardiomyocytes, and carries messages to intracellular enzyme cascading, and, finally, to mitochondria. During the IPC process, myocardial resistance to hypoxic conditions can occur as a result of a brief ischemia before the reperfusion episode. Unfortunately, IPC is not feasible in patients presenting at the hospital with an acute MI. The goal of effective treatment of acute MI in humans, therefore, is to induce an IPC-like effect that can help myocardium to survive the prolonged ischemic process, similar to that in preconditioning.

Enhancing the NO signaling pathway could become a widely accepted method for mimicking the preconditioning effect, as this signaling plays an important role in both physiological and pathological conditions. Drugs such as NO donor or PDE-5 inhibitor are widely used to interrupt the NO signaling pathway. Many studies have found that sildenafil citrate, the PDE-5 inhibitor used for treatment of erectile dysfunction, has abilities to attenuate ischemic cardiomyopathy and reduce cell death from hypoxic conditions [87–90]. Ockaili et al. demonstrated that sildenafil citrate was able to decrease infarct size after coronary artery occlusion in rabbits, and that the effect was blocked by inhibiting mitoK$_{ATP}$ channel (5-HD) [87]. Another study by this team showed that the expression of iNOS and eNOS mRNA and protein in isolated mouse hearts could be increased by sildenafil citrate [88]. The level of eNOS mRNA increased transiently and peaked at 45 minutes after the sample was treated with the drug [88]. The rate of iNOS mRNA expression was slower, but the peak was higher than that of eNOS. Moreover, a significant increase in iNOS and eNOS proteins was detected 24 hours after treatment with sildenafil citrate. The cardioprotective effect against I/R injury induced by sildenafil citrate was eliminated by 1400W, the specific iNOS inhibitor [88]. Das et al. demonstrated that, in an isolated ventricular myocyte, necrosis and apoptosis were reduced, whereas the expression of iNOS and eNOS was elevated, when sildenafil citrate was applied after an ischemia-reoxygenation [89].

Conclusions

Since sildenafil citrate and other PDE-5 inhibitors have been approved by the U.S. Food and Drug Administration (FDA) as a vasoactive drug for the treatment of erectile dysfunction, the drugs may be useful for cardioprotection against I/R injury. Moreover, other pharmacological agents that are related to the NO signaling pathway, including NO donors such as nitroglycerin or drugs that have been shown to have positive effects on NO signaling in β-blockers such as nebivolol, could also impart the NO-related cardioprotection against ischemic cell death [91,92]. According to our understanding of the IPC mechanism, the drugs that regulate some parts of its cascade, including adenosine, bradykinin, opioid agonists, or PI3K-Akt activators, could be applied in clinical practice as possible cardioprotective agents against I/R injury [93]. However, clinical trials of these agents against I/R injury have not yet been conducted. Future demonstration

of the cardioprotective effect of pharmacological IPC in patients should be explored, and this could have an enormous impact on development of drugs for clinical application of pharmacological preconditioning.

REFERENCES:

1. Downey JM, Davis AM, Cohen MV: Signaling pathways in ischemic preconditioning. Heart Fail Rev, 2007; 12(3–4): 181–88
2. Skyschally A, Schulz R, Heusch G: Pathophysiology of myocardial infarction: protection by ischemic pre- and postconditioning. Herz, 2008; 33(2): 88–100
3. Schaper W, Gorge G, Winkler B, Schaper J: The collateral circulation of the heart. ProgCardiovasc Dis, 1988; 31(1): 57–77
4. Matsumura K, Jeremy RW, Schaper J, Becker LC: Progression of myocardial necrosis during reperfusion of ischemic myocardium. Circulation, 1998; 97(8): 795–804
5. Ladilov YV, Siegmund B, Piper HM: Protection of reoxygenated cardiomyocytes against hypercontracture by inhibition of Na+/H+ exchange. Am J Physiol, 1995; 268(4 Pt 2): H1531–39
6. Crompton M: The mitochondrial permeability transition pore and its role in cell death. Biochem J, 1999; 341(Pt 2): 233–49
7. Cohen MV, Baines CP, Downey JM: Ischemic preconditioning: from adenosine receptor to KATP channel. Annu Rev Physiol, 2000; 62: 79–109
8. Murry CE, Jennings RB, Reimer KA: Preconditioning with ischemia: a delay of lethal cell injury in ischemic myocardium. Circulation, 1986; 74(5): 1124–36
9. Liu Y, Downey JM: Ischemic preconditioning protects against infarction in rat heart. Am J Physiol, 1992; 263(4 Pt 2): H1107–12
10. Guo Y, Wu WJ, Qiu Y et al: Demonstration of an early and a late phase of ischemic preconditioning in mice. Am J Physiol, 1998; 275(4 Pt 2): H1375–87
11. Cohen MV, Liu GS, Downey JM: Preconditioning causes improved wall motion as well as smaller infarcts after transient coronary occlusion in rabbits. Circulation, 1991; 84(1): 341–49
12. Strickler J, Jacobson KA, Liang BT: Direct preconditioning of cultured chick ventricular myocytes. Novel functions of cardiac adenosine A2a and A3 receptors. J Clin Invest, 1996; 98(8): 1773–79
13. Stefano G, Esch T, Bilfinger T, Kream R: Proinflammation and preconditioning protection are part of a common nitric oxide mediated process. Med Sci Monit, 2010; 16(6): RA125–30
14. Liu GS, Thornton J, Van Winkle DM et al: Protection against infarction afforded by preconditioning is mediated by A1 adenosine receptors in rabbit heart. Circulation, 1991; 84(1): 350–56
15. Wall TM, Sheehy R, Hartman JC: Role of bradykinin in myocardial preconditioning. J Pharmacol Exp Ther, 1994; 270(2): 681–89
16. Schultz JE, Rose E, Yao Z, Gross GJ: Evidence for involvement of opioid receptors in ischemic preconditioning in rat hearts. Am J Physiol, 1995; 268(5 Pt 2): H2157–61
17. Stefano GB, Neenan K, Cadet P et al: Ischemic preconditioning - an opiate constitutive nitric oxide molecular hypothesis. Med Sci Monit, 2001; 7(6): 1357–75
18. Goto M, Liu Y, Yang XM et al: Role of bradykinin in protection of ischemic preconditioning in rabbit hearts. Circ Res, 1995; 77(3): 611–21
19. Baker JE, Holman P, Gross GJ: Preconditioning in immature rabbit hearts: role of KATP channels. Circulation, 1999; 99(9): 1249–54
20. Hanafy KA, Krumenacker JS, Murad F: NO, nitrotyrosine, and cyclic GMP in signal transduction. Med Sci Monit, 2001; 7(4): 801–19
21. Lyamina NP, Dolotovskaya PV, Lyamina SV et al: Nitric oxide production and intensity of free radical processes in young men with high normal and hypertensive blood pressure. Med SciMonit, 2003; 9(7): CR304–10
22. Ziolo MT, Bers DM: The real estate of NOS signaling: location, location, location. Circ Res, 2003; 92(12): 1279–81
23. Barouch LA, Harrison RW, Skaf MW et al: Nitric oxide regulates the heart by spatial confinement of nitric oxide synthase isoforms. Nature, 2002; 416(6878): 337–39
24. Massion PB, Balligand JL: Modulation of cardiac contraction, relaxation and rate by the endothelial nitric oxide synthase (eNOS): lessons from genetically modified mice. J Physiol, 2003; 546(Pt 1): 63–75
25. Bruckdorfer R: The basics about nitric oxide. Mol Aspects Med, 2005; 26(1–2): 3–31
26. Jiang LH, Gawler DJ, Hodson N et al: Regulation of cloned cardiac L-type calcium channels by cGMP-dependent protein kinase. J BiolChem, 2000; 275(9): 6135–43
27. Wang H, Kohr MJ, Wheeler DG, Ziolo MT: Endothelial nitric oxide synthase decreases beta-adrenergic responsiveness via inhibition of the L-type Ca^{2+} current. Am J Physiol Heart Circ Physiol, 2008; 294(3): H1473–80
28. Wang H, Kohr, MJ, Traynham CJ, Ziolo MT: Phosphodiesterase 5 restricts NOS3/Soluble guanylatecyclase signaling to L-type Ca^{2+} current in cardiac myocytes. J Mol Cell Cardiol, 2009; 47: 304–14
29. Wang H, Kohr MJ, Traynham CJ et al: Neuronal nitric oxide synthase signaling within cardiac myocytes targets phospholamban. Am J Physiol Cell Physiol, 2008; 294(6): C1566–75
30. Han J, Kim N, Joo H et al: ATP-sensitive K(+) channel activation by nitric oxide and protein kinase G in rabbit ventricular myocytes. Am J Physiol Heart Circ Physiol, 2002; 283(4): H1545–54
31. Sasaki N, Sato T, Ohler A et al: Activation of mitochondrial ATP-dependent potassium channels by nitric oxide. Circulation, 2000; 101(4): 439–45
32. Herring N, Rigg L, Terrar DA, Paterson DJ: NO-cGMP pathway increases the hyperpolarisation-activated current, I(f), and heart rate during adrenergic stimulation. Cardiovasc Res, 2001; 52(3): 446–53
33. Lonardo G, Cerbai E, Casini Set al: Atrial natriuretic peptide modulates the hyperpolarization-activated current (If) in human atrial myocytes. Cardiovasc Res, 2004; 63(3): 528–36
34. Williams MW, Taft CS, Ramnauth S et al: Endogenous nitric oxide (NO) protects against ischaemia-reperfusion injury in the rabbit. Cardiovasc Res, 1995; 30(1): 79–86
35. Woolfson RG, Patel VC, Neild GH, Yellon DM: Inhibition of nitric oxide synthesis reduces infarct size by an adenosine-dependent mechanism. Circulation, 1995; 91(5): 1545–51
36. Rakhit RD, Marber MS: Nitric oxide: an emerging role in cardioprotection? Heart, 2001; 86: 368–72
37. Zhao L, Weber PA, Smith JR et al: Role of inducible nitric oxide synthase in pharmacological "preconditioning" with monophosphoryl lipid A. J Mol Cell Cardiol, 1997; 29(6): 1567–76
38. Ferdinandy P, Szilvassy Z, Horvath LI et al: Loss of pacing-induced preconditioning in rat hearts: role of nitric oxide and cholesterol-enriched diet. J Mol Cell Cardiol, 1997; 29(12): 3321–33
39. Yang XM, Krieg T, Cui L et al: NECA and bradykinin at reperfusion reduce infarction in rabbit hearts by signaling through PI3K, ERK, and NO. J Mol Cell Cardiol, 2004; 36: 411–21
40. Marina Prendes MG, Gonzalez M, Savino EA, Varela A: Role of endogenous nitric oxide in classic preconditioning in rat hearts. Regul Pept, 2007; 139(1–3): 141–45
41. Nakano A, Liu GS, Heusch G et al: Exogenous nitric oxide can trigger a preconditioned state through a free radical mechanism, but endogenous nitric oxide is not a trigger of classical ischemic preconditioning. J Mol Cell Cardiol, 2000; 32(7): 1159–67
42. Lochner A, Marais E, Genade S, Moolman JA: Nitric oxide: a trigger for classic preconditioning? Am J Physiol Heart Circ Physiol, 2000; 279(6): H2752–65
43. Kanno S, Lee PC, Zhang Y et al: Attenuation of myocardial ischemia/reperfusion injury by superinduction of inducible nitric oxide synthase. Circulation, 2000; 101(23): 2742–48
44. Zhao T, Xi L, Chelliah J et al: Inducible nitric oxide synthase mediates delayed myocardial protection induced by activation of adenosine A(1) receptors: evidence from gene-knockout mice. Circulation, 2000; 102(8): 902–7
45. Wang Y, Guo Y, Zhang SX et al: Ischemic preconditioning upregulates inducible nitric oxide synthase in cardiac myocyte. J Mol Cell Cardiol, 2002; 34(1): 5–15
46. Heinzel FR, Gres P, Boengler K et al: Inducible nitric oxide synthase expression and cardiomyocyte dysfunction during sustained moderate ischemia in pigs. Circ Res, 2008; 103: 1120–27
47. Guo Y, Jones WK, Xuan YT et al: The late phase of ischemic preconditioning is abrogated by targeted disruption of the inducible NO synthase gene. Proc Natl Acad Sci USA, 1998: 96(20): 11507–12
48. Bell RM, Yellon DM: The contribution of endothelial nitric oxide synthase to early ischaemic preconditioning: the lowering of the preconditioning threshold. An investigation in eNOS knockout mice.Cardiovasc Res, 2001; 52(2): 274–80
49. Guo Y, Li Q, Wu WJ et al: Endothelial nitric oxide synthase is not necessary for the early phase of ischemic preconditioning in the mouse. J Mol Cell Cardiol, 2008; 44: 496–501

50. du Toit EF, Genade S, Carlini S et al: Efficacy of ischaemic preconditioning in the eNOS overexpressed working mouse heart model. Eur J Pharmacol, 2007; 556(1–3): 115–20
51. Samouilov A, Kuppusamy P, Zweier JL: Evaluation of the magnitude and rate of nitric oxide production from nitrite in biological systems. Arch Biochem Biophys, 1998; 357(1): 1–7
52. Zweier JL, Wang P, Samouilov A, Kuppusamy P: Enzyme independent formation of nitric oxide in biological tissues. Nat Med, 1995; 1: 1796–801
53. Zweier JL, Samouilov A, Kuppusamy P: Non-enzymatic nitric oxide synthesis in biological systems. Biochim Biophys Acta, 1999; 250–62
54. Sun J, Morgan M, Shen RF et al: Mitochondrial energetics and calcium transport preconditioning results in S-nitrosylation of proteins involved in regulation of mitochondrial energetics and calcium transport. Circ Res, 2007; 101: 1155–63
55. Lin J, Steenbergen C, Murphy E, Sun J: Estrogen receptor-β activation results in S-nitrosylation of proteins involved in cardioprotection. Circulation, 2009; 120: 245–54
56. Foster MW, Stamler JS: New insight into protein S-nitrosylation: Mitochondria as a model system. J BiolChem, 2004; 279(24): 25891–97
57. Sun J: Protein S-nitrosylation: A role of nitric oxide signaling in cardiac ischemic preconditioning. Acta Physiol Sin, 2007; 59(5): 544–52
58. Lebuffe G, Schumacker PT, Shao ZH et al: ROS and NO trigger early preconditioning: relationship to mitochondrial KATP channel. Am J Physiol Heart Circ Physiol, 2003; 284(1): H299–308
59. Xu Z, Ji X, Boysen PG: Exogenous nitric oxide generates ROS and induces cardioprotection: involvement of PKG, mitochondrial KATP channels, and ERK. Am J Physiol Heart Circ Physiol, 2004; 286(4): H1433–40
60. Cuong DV, Kim N, Youm JB et al: Nitric oxide-cGMP-protein kinase G signaling pathway induces anoxic preconditioning through activation of ATP-sensitive K+ channels in rat hearts. Am J Physiol Heart Circ Physiol, 2006; 290(5): H1808–17
61. Cuong DV, Warda M, Kim N et al: Dynamic changes in nitric oxide and mitochondrial oxidative stress with site-dependent differential tissue response during anoxic preconditioning in rat heart. Am J Physiol Heart Circ Physiol, 2007; 293(3): H1457–65
62. Oldenburg O, Qin Q, Krieg T et al: Bradykinin induces mitochondrial ROS generation via NO, cGMP, PKG, and mitoKATP channel opening and leads to cardioprotection. Am J Physiol Heart Circ Physiol, 2004; 286(1): H468–76
63. Costa AD, Pierre SV, Cohen MV et al: cGMP signalling in pre- and postconditioning: the role of mitochondria. Cardiovasc Res, 2008; 77(2): 344–52
64. Javadov S, Karmazyn M, Escobales N: Mitochondrial permeability transition pore opening as a promising therapeutic target in cardiac diseases. J Pharmacol Exp Ther, 2009; 330(3): 670–78
65. Halestrap AP: A pore way to die: the role of mitochondria in reperfusion injury and cardioprotection. Biochem Soc Trans, 2010; 38(4): 841–60
66. Crompton M, Andreeva L: On the involvement of a mitochondrial pore in reperfusion injury. Basic Res Cardiol, 1993; 88: 513–23
67. Griffiths EJ, Halestrap AP: Protection by Cyclosporin A of ischemia/reperfusion-induced damage in isolated rat hearts. J Mol Cell Cardiol, 1993; 25: 1461–69
68. Hausenloy DJ, Maddock HL, Baxter GF, Yellon DM: Inhibiting mitochondrial permeability transition pore opening: a new paradigm for myocardial preconditioning? Cardiovasc Res, 2002; 55: 534–43
69. Cuong DV, Kim N, Joo H et al: Subunit composition of ATP-sensitive potassium channels in mitochondria of rat hearts. Mitochondrion, 2005; 5(2): 121–33
70. Ljubkovic M, Shi Y, Cheng Q et al: Cardiac mitochondrial ATP-sensitive potassium channel is activated by nitric oxide *in vitro.* FEBS Lett, 2007; 581(22): 4255–59
71. Costa AD, Garlid KD, West IC et al: Protein kinase G transmits the cardioprotective signal from cytosol to mitochondria. Circ Res, 2005; 97(4): 329–36
72. Costa AD, Garlid KD: Intramitochondrial signaling: interactions among mitoKATP, PKCepsilon, ROS, and MPT. Am J Physiol Heart Circ Physiol, 2008; 295(2): H874–82
73. Das A, Xi L, Kukreja RC: Protein kinase G-dependent cardioprotective mechanism of phosphodiesterase-5 inhibition involves phosphorylation of ERK and GSK3beta. J Biol Chem, 2008; 283(43): 29572–85
74. Das A, Salloum FN, Xi L, Rao YJ, Kukreja RC: ERK phosphorylation mediates sildenafil-induced myocardial protection against ischemia-reperfusion injury in mice. Am J Physiol Heart Circ Physiol, 2009; 296(5): H1236–43
75. Miura T, Tanno M: Mitochondria and GSK-3β in cardioprotection against ischemia/reperfusion injury. Cardiovasc Drugs Ther, 2010, DOI 10.1007/s10557-010-6234-z
76. Fenger M, Haugaard SB, Andersen O et al: Is glycogen synthase kinase-3β an ultraconserved kernel enzyme? Gene Exp Genet Genomics, 2009; 2: 1–27
77. Juhaszova M, Zorov DB, Kim S-H et al: Glycogen synthase kinase-3β mediates convergence of protection signaling to inhibit the mitochondrial permeability transition pore. J Clin Invest, 2004; 113: 1535–49
78. Tong H, Imahashi K, Steenbergen C, Murphy E: Phosphorylation of glycogen synthase kinase-3beta during preconditioning through a phosphatidylinositol-3-kinase-dependent pathway is cardioprotective. Circ Res, 2002; 90: 377–79
79. Nishihara M, Miura T, Miki T et al: Erythropoietin affords additional cardioprotection to preconditioned hearts by enhanced phosphorylation of glycogen synthase kinase-3β. Am J Physiol Heart Circ Physiol, 2006; 291: H748–55
80. Gross ER, Hsu AK, Gross GJ: Opioid-induced cardioprotection occurs via glycogen synthase kinase beta inhibition during reperfusion in intact rat hearts. Circ Res, 2004; 94: 960–66
81. Obame FN, Plin-Mercier C, Assaly R et al: Cardioprotective effect of morphine and a blocker of glycogen synthase kinase 3 beta, SB216763 [3-(2, 4-dichlorophenyl)-4(1-methyl-1H-indol-3-yl)-1H-pyrrole-2, 5-dione], via inhibition of the mitochondrial permeability transitionpore. J Pharmacol Exp Ther, 2008; 326: 252–58
82. West MB, Rokosh G, Obal D et al: Cardiac myocyte-specific expression of inducible nitric oxide synthase protects against ischemia/reperfusion injury by preventing mitochondrial permeability transition. Circulation, 2008; 118(19): 1970–78
83. Andrukhiv A, Costa AD, West IC, Garlid KD: Opening mitoKATP increases superoxide generation from complex I of the electron transport chain. Am J Physiol Heart Circ Physiol, 2006; 291(5): H2067–74
84. Gomez L, Paillard M, Thibault H et al: Inhibition of GSK3beta by postconditioning is required to prevent opening of the mitochondrial permeability transition pore during reperfusion. Circulation, 2008; 117(21): 2761–68
85. Rickover O, Zinman T, Kaplan D, Shainberg A: Exogenous nitric oxide triggers classic ischemic preconditioning by preventing intracellular Ca2+ overload in cardiomyocytes. Cell Calcium, 2008; 43(4): 324–33
86. Lemasters JJ, Theruvath TP, Zhong Z, Nieminen AL: Mitochondrial calcium and the permeability transition in cell death. Biochim Biophys Acta, 2009; 1787(11): 1395–401
87. Ockaili R, Salloum F, Hawkins J, Kukreja RC: Sildenafil (Viagra) induces powerful cardioprotective effect via opening of mitochondrial K(ATP) channels in rabbits. Am J Physiol Heart Circ Physiol, 2002; 283(3): H1263–69
88. Salloum F, Yin C, Xi L, Kukreja RC: Sildenafil induces delayed preconditioning through inducible nitric oxide synthase-dependent pathway in mouse heart. Circ Res, 2003; 92(6): 595–97
89. Das A, Xi L, Kukreja RC: Phosphodiesterase-5 inhibitor sildenafil preconditions adult cardiac myocytes against necrosis and apoptosis. Essential role of nitric oxide signaling. J Biol Chem, 2005; 280(13): 12944–55
90. Salloum FN, Abbate A, Das A et al: Sildenafil (Viagra) attenuates ischemic cardiomyopathy and improves left ventricular function in mice. Am J Physiol Heart Circ Physiol, 2008; 294(3): H1398–406
91. Hu CP, Li YJ, Deng HW: The cardioprotective effects of nitroglycerin-induced preconditioning are mediated by calcitonin gene-related peptide. Eur J Pharmacol, 1999; 369(2): 189–94
92. Mercanoglu G, Safran N, Gungor M et al: The effects of nebivolol on apoptosis in a rat infarct model. Circ J, 2008; 72(4): 660–70
93. Granfeldt A, Lefer DJ, Vinten-Johansen J: Protective ischaemia in patients: preconditioning and postconditioning. Cardiovasc Res, 2009; 83(2): 234–46

Review article

Effects of cilostazol in the heart

Natnicha Kanlop[a,b], Siriporn Chattipakorn[b,c] and Nipon Chattipakorn[a,b,d]

Cilostazol is a selective phosphodiesterase 3 (PDE3) inhibitor approved by the Food and Drug Administration for treatment of intermittent claudication. It has also been used in bradyarrhythmic patients to increase heart rates. Recently, cilostazol has been shown to prevent ventricular fibrillation in patients with Brugada syndrome. Cilostazol is hypothesized to suppress transient outward potassium (I_{to}) current and increase inward calcium current, thus, maintaining the dome (phase 2) of action potential, decreasing transmural dispersion of repolarization and preventing ventricular fibrillation. Although many PDE3 inhibitors have been shown to increase cardiac arrhythmia in heart failure, cilostazol has presented effects that are different from other PDE3 inhibitors, especially adenosine uptake inhibition. Owing to this effect, cilostazol could be an effective cardioprotective drug, with its beneficial effects in preventing arrhythmia. In this review, the cardiac electrophysiological effects of cilostazol are presented and its possible cardioprotective effects, particularly in preventing ventricular fibrillation, are discussed, with emphasis on the need to further verify its clinical benefits. *J Cardiovasc Med* **12:88–95 © 2011 Italian Federation of Cardiology.**

Journal of Cardiovascular Medicine 2011, **12**:88–95

Keywords: arrhythmia, Brugada syndrome, cilostazol, heart, ventricular fibrillation

[a]Cardiac Electrophysiology Unit, Department of Physiology, [b]Cardiac Electrophysiology Research and Training Center, Faculty of Medicine, [c]Department of Oral Biology and Diagnostic Science, Faculty of Dentistry and [d]Biomedical Engineering Center, Chiang Mai University, Chiang Mai, Thailand

Correspondence to Nipon Chattipakorn, MD, PhD, Cardiac Electrophysiology Research and Training Center, Faculty of Medicine, Chiang Mai University, Chiang Mai 50200, Thailand
Tel: +66 53 945329; fax: +66 53 945368; e-mail: nchattip@gmail.com

Received 8 July 2010 **Revised** 30 November 2010
Accepted 9 December 2010

Introduction

Cilostazol (PLETAL or PLETAAL) is a quinolinone derivative and a selective phosphodiesterase 3 (PDE3) inhibitor. In humans, the PDE3 isoenzyme is mainly found in platelets, in vascular smooth muscle, in the liver, in the smooth muscle of the airway, in T lymphocytes, in adipose tissue and in cardiac tissue [1]. Because of its potent vasodilation effect and antiplatelet aggregation, cilostazol has been approved by the US Food and Drug Administration (FDA) for claudication treatment to relieve leg pain symptoms, allowing greater tolerance in patients with chronic arterial occlusion [2,3]. Although cilostazol has been used mainly in intermittent claudication (chronic arterial occlusion), it has been shown to be useful in preventing embolic stroke in arrhythmic patients [4], and could decrease the wall thickness of coronary arteries in type 2 diabetic patients [5]. In addition, it has been found that cilostazol could affect the automaticity of the heart and also increase heart rate, leading to an improvement of bradyarrhythmias [4], including bradycardic atrial fibrillation, atrioventricular block and sick sinus syndrome (SSS) [6–11]. Recently, a case report of Brugada syndrome patients showed that the oral administration of cilostazol at therapeutic dose could prevent the frequency of ventricular fibrillation in these patients [12]. The report suggested that, in addition to its vasodilating effect, cilistazol could potentially have antiarrhythmic effects.

In recent decades, PDE3 inhibitors such as milrinone and vesnarinone have been shown to be arrhythmogenic and to increase mortality rate in heart failure patients [13,14]. The proposed mechanism for this undesirable effect was the drug's effects in increasing the cyclic AMP (cAMP) level [13,14]. Thus, according to the FDA, all PDE3 inhibitors, including cilostazol, are contraindicated in chronic heart failure patients of any severity because of the recognition that they increased the mortality rates in this group of patients [15]. Despite the fact that cilostazol is a PDE3 inhibitor, it is important to note that its roles in the heart are different from those of other PDE3 inhibitors. Cilostazol has been demonstrated to not only inhibit PDE3 but also to inhibit adenosine uptake, resulting in a reduction of cyclic adenosine monophosphate (cAMP) level [16–19]. Therefore, unlike other PDE3 inhibitors, these actions of cilostazol may be beneficial in cardioprotection [16–19].

Although the vasodilation and antiplatelet aggregation effects of cilostazol have been extensively investigated and reviewed [20–23], it is still unclear whether cilostazol would have beneficial or adverse effects on the heart. As cilostazol is currently of interest to many investigators and because it could have different effects on the heart compared with other PDE3 inhibitors, this review will present the roles of this PDE3 inhibitor and its arrhythmogenic effect on the heart. The electrophysiological

1558-2027 © 2011 Italian Federation of Cardiology DOI:10.2459/JCM.0b013e3283439746

and cardioprotective effects of cilostazol, on the basis of its cellular mechanism, which is different from that of other PDE3 inhibitory drugs, will be discussed. The mechanisms of cilostazol on arrhythmogenic prevention, particularly its role on ventricular fibrillation prevention in Brugada syndrome, will also be presented. With increasing knowledge and understanding of its mechanisms, cilostazol may be clinically useful for arrhythmia prevention in the future. Finally, the ultimate goal of this review is to provide the pathophysiological basis for future investigations to comprehend the rationale of the study design that verifies the effects of cilostazol in a heart failure model.

Phosphodiesterase 3 inhibitor and the heart

PDE is the enzyme that hydrolyses cAMP and cyclic guanosine monophosphate (cGMP) to their inactive state, thus regulating levels of intracellular cAMP and cGMP. PDE has been classified into 11 isoenzymes, depending on the differences of the affinity for cAMP, cGMP and the physiochemical and pharmacological properties of PDE [1,24]. Generally, once adenylate cyclase and guanylate cyclase pathways are generated by the induction of extracellular signals, ATP and GTP are then changed to cAMP and cGMP, respectively, depending on their corresponding pathways. cAMP and cGMP are the second messengers that mediate biological responses. The active forms of both cAMP and cGMP are converted to their inactive forms by PDE [1,24].

PDE3 belongs to the PDE family that has high affinity for both cAMP and cGMP [1]. As the binding of cGMP at the active site of PDE3 can competitively inhibit cAMP hydrolysis, this enzyme is also defined as cGMP-inhibited PDE [1]. However, the amount of cAMP that is hydrolyzed by PDE3 is 10 times greater than that of cGMP [1]. The increased level of intracellular cAMP could activate cAMP-dependent protein kinase A (PK-A), leading to phosphorylation of important proteins or receptors in the heart, which involve a diversity of cellular functions (Fig. 1). In a sinoatrial node, cAMP enables a signal transduction involving the activated PK-A, the L-type Ca^{2+}channel (I_{CaL}), and a component of a delay rectifier potassium channel (I_{Ks}). Therefore, drugs that block PDE3 pathways would cause a positive chronotropic effect [6,8,9,11].

PDE3 is primarily associated with the regulation of contractile function in the heart. When the activity of PK-A in the myocardium is raised by the increased intracellular cAMP from the PDE3 inhibitor, phosphorylation of I_{CaL} channels in sarcolemmal membrane and ryanodine receptor (RyR) occurs. The Ca^{2+} influx through I_{CaL} channels trigger a release of Ca^{2+} from sarcoplasmic reticulum via RyR. The binding of this increased cytoplasmic Ca^{2+}concentration to troponin C activates actin–myosin cross-bridge formation, thus, eliciting the contractile function [25]. In many studies, the benefits of inotropic action of PDE3 inhibitors such as amrinone, enoximone and milrinone in chronic heart failure patients have been demonstrated, for example, the reduction of left ventricular end-diastolic pressure and the increase in ejection fraction and stroke volume [26–31]. It has been observed that the use of PDE3 inhibitors actually produce desirable effects in the short term, however, deleterious effects arise over time [26–28].

Undesirable effects of phosphodiesterase 3 inhibitors in the heart

The adverse effects of PDE3 inhibitors on the heart have been demonstrated, especially the acceleration of the progression of heart failure and the induction of ventricular tachyarrhythmia [13,14,32,33]. The remarkable clinical studies that demonstrated the significant increase in cardiovascular mortality were the Prospective Randomized Milrinone Survival Evaluation (PROMISE) [14] and the Vesnarinone trial (VEST) [13] studies, which reported increased cardiovascular mortality due to PDE3 inhibitor administration. In the latter study, 120 mg of vesnarinone was suddenly withdrawn due to its severe adverse effect. These reports were consistent with the data of the randomized controlled trial that investigated the effects of PDE3 inhibitors versus placebo in chronic heart failure patients [32].

As the deleterious effects of PDE3 inhibitors could be due to the exertion of cAMP, it is interesting to explore the signal pathway that causes changes in the level of cAMP. The β-adrenergic agonist, which shows undesirable effects, including mortality rates and progressive heart failure, also behaves in a manner similar to the PDE3 inhibitors [34,35]. It has been shown that the β-adrenergic antagonist can decrease intracellular cAMP content in cardiac myocytes by decreasing the transmembrane signal, hence, improving the symptoms and the survival rate in heart failure. The studies of PDE3 inhibitors adjuvant to the β-adrenergic antagonist have shown an improvement of the ejection fraction and functional status in patients with dilated cardiomyopathy and chronic heart failure [36–39].

Previous studies have demonstrated that the level of cAMP was lower in failing hearts than in normal hearts, which could be an adaptive body response to protect myocardial cells from further injury [32]. Several studies demonstrated that cAMP could be the substrate that caused adverse effects on the failing heart [32,34,35]. The reduction of cAMP in heart failure may be caused by the downregulation of β-adrenoreceptors, enhanced expression of G_i-protein or increased β-adrenoreceptor kinase [40]. In heart failure, there are disturbances of Ca^{2+} modulation in which abnormal expression and function of a sarco/endoplasmic reticulum ATPase (SERCA) plays an important role [41]. Schmidt *et al.*

Fig. 1

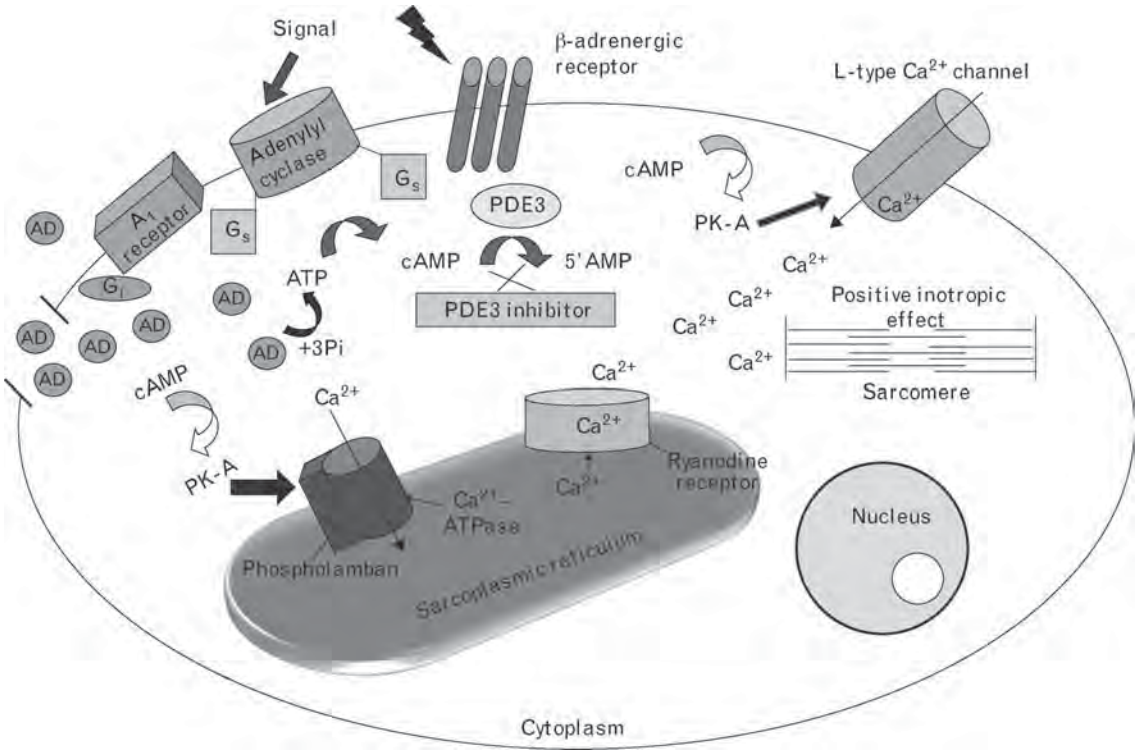

Effect of phosphodiesterase 3 (PDE3) inhibitors in cardiomyocytes. The pathway can be directly activated by signals through adenylyl cyclase or the β-adrenergic receptor. The myocardium uptakes adenosines (ADs) to synthesize ATP. Then, the adenylate cyclase enzyme converts ATP to cyclic AMP (cAMP). The increasing of cAMP can lead to many physiological responses via the activation of cAMP-dependent protein kinase A (PK-A). This PK-A can phosphorylate L-type Ca^{2+}channels and ryanodine receptors to stimulate Ca^{2+}-induced Ca^{2+}-release mechanism, leading to cardiac contraction. During the cardiac relaxation period, the phosphorylation of phospholamban by PK-A can elicit Ca^{2+} reuptake through Ca^{2+}-ATPase on the sarcoplasmic reticulum. Under physiological condition, cAMP is hydrolyzed to an inactive product (5′AMP) by PDE3 enzyme. Therefore, inhibition of PDE3 (i.e. by PDE3 inhibitors) can cause an increased cAMP level, thus enhancing the cAMP action, especially the positive inotropic effect. In heart failure, this is an undesired effect caused by PDE3 inhibitors.

[42] demonstrated that an impaired SERCA function in human end-stage heart failure patients could be due to the reduction of cAMP-dependent phosphorylation of the phospholamban. These situations altered intracellular Ca^{2+} homeostasis by reducing systolic peak Ca^{2+}, increasing diastolic Ca^{2+} and sustaining diastolic Ca^{2+} sequestration, thus producing electrophysiological abnormality in the heart [42].

As a result of intracellular cAMP and Ca^{2+} dynamic disturbances, PDE3 inhibitors can cause ventricular arrhythmia by several mechanisms. First, the increased intracellular cAMP, which triggers early and delayed afterdepolarizations (DADs), could provoke a slow conduction and alter refractoriness in depolarized tissues [43]. Second, an abnormal Ca^{2+} homeostasis due to the increased intracellular cAMP, that is, an abnormal increase in RyR2 opening probability during diastole, which is induced by chronic PK-A-mediated hyperphosphorylation in failing hearts [43,44]. This condition can promote the occurrence of DAD via transient activation of a Ca^{2+}-dependent inward current [43,44]. Third, the higher myocardial oxygen consumption due to the inotropic effect of these PDE3 inhibitors can increase the frequency of arrhythmias [33,45]. One should be aware of these adverse effects of PDE3 inhibitors if they are to be used as inotropic drugs, particularly in heart failure patients [13,33,34,46–48].

Cilostazol and its dual inhibitory effect in the heart

Cilostazol is a quinolinone derivative that selectively inhibits PDE3. Because of its potent vasodilating and antithrombotic effects, cilostazol has been used for effective treatment of intermittent claudication, a manifestation of chronic arterial occlusive disease. As cilostazol is a PDE3 inhibitor, it falls into the same category as the other PDE3 inhibitors whose use the FDA prohibits with heart failure patients [2]. Currently, there is no study that directly investigates the effect of cilostazol in heart failure.

Growing evidence has demonstrated that cilostazol could have many potential benefits on the heart and that the

prohibition of its use should be reinvestigated and reconsidered [4,6,8–11,16,21,23,46,49,50]. This is due to the findings that although cilostazol is a PDE3 inhibitor, its effects on the heart could be different from other PDE3 inhibitors (Fig. 2) [16,17]. One such piece of evidence is the finding that the positive inotropic effect caused by cilostazol was much less than that caused by milrinone [16,19,21]. It has been shown that cilostazol has a dual inhibitory effect, in which it not only selectively inhibits PDE3 but also inhibits adenosine uptake into cardiac myocytes [17]. The latter mechanism is only found in cilostozol and not in other PDE3 inhibitors [17].

In the myocardium, adenosine acts on the A_1 receptor which then activates G_i-protein. As a result, the adenylate cyclase pathway is inhibited by adenosine through the adenosine A_1-receptor, thus, attenuating the positive inotropy. In addition, the inhibitory effect of cilostazol on adenosine uptake could lead to low intracellular adenosine level, resulting in decreased cAMP level [17,19]. Thus, this effect could attenuate the inotropic effect, compared with other PDE3 inhibitors (Fig. 2). However, this effect is different in pacemaker cells, in which the ATP and adenine derivatives potentially enhance the negative chronotropic effect [51]. Therefore, cilostazol could cause a positive chronotropic effect due to its inhibitory effect on adenosine uptake. Furthermore, if adenosine uptake into cardiomyocytes is inhibited, adenosine in the interstitial space and blood circulation will be increased, resulting in an activation of adenosine A2-receptors in platelets and vascular smooth muscle and causing vasodilation and antiplatelet aggregation [16,19,21]. Therefore, unlike other PDE3 inhibitors that have been shown to cause an increase in mortality rate in heart failure patients and induced tachyarrhythmia via cAMP [19,32,33,52], cilostazol may provide the beneficial effects of PDE3 inhibitors, without needing to be overconcerned about its adverse effects in heart failure patients, due to its mechanism as described above. It is important to note that current evidence regarding cilostazol and tachyarrhythmia is still limited and unclear. Nevertheless, recent evidence has indicated that cilostazol could lower, at least not increase, major cardiovascular events in patients with coronary artery or peripheral artery disease [53–56].

Cilostazol and bradyarrhythmia

For symptomatic bradycardia, the implantation of a cardiac pacemaker is the first-line regimen of treatment [57,58]. Nevertheless, the overuse of hospitalization and long bed rest is still a cost burden. Therefore, alternative therapies have been proposed, especially in terms of medication use. Recently, theophylline, a

Fig. 2

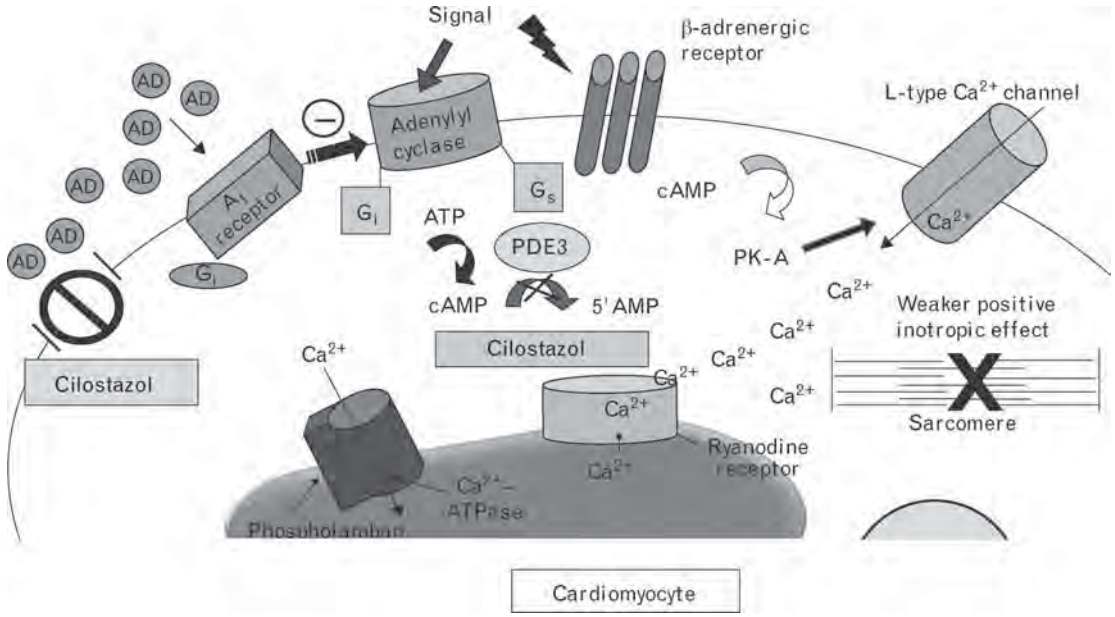

Effects of cilostazol in cardiomyocytes. Unlike other phosphodiesterase 3 (PDE3) inhibitors, cilostazol has a dual inhibitory effect. In addition to inhibition of PDE3, cilostazol also inhibits cellular adenosine uptake. As the intracellular adenosines (ADs) are reduced, the cAMPs would be decreased. Although adenylate cyclase can still function normally when the PDE3 is inhibited, the cyclic AMP (cAMP) level will not be sufficiently increased in this case. Furthermore, cAMP signaling can be attenuated due to the accumulation of adenosines outside the cell, resulting in the attenuation of the adenylate cyclase activity pathway through the G_i-protein of the A_1-receptor. This dual inhibitory effect of cilostazol may be responsible for diminished inotropic effect, compared with other PDE3 inhibitors. PK-A, cAMP-dependent protein kinase A.

nonselective PDE inhibitor, had been shown to have clinical efficacy in bradyarrhythmia treatment [4]. However, it had produced adverse reactions in which it increased the number and degree of ventricular arrhythmias. Previous studies also demonstrated that amrinone, a PDE3 inhibitor, decreased the effective refractory period of the right atrium and functional refractory period of the atrioventricular node [4,33,59,60]. In studies using milrinone, there was a trend toward a lower corrected sinus-node recovery time and maximal 1:1 atrioventricular conduction [33]. These findings suggested that PDE3 inhibitors could have positive chronotropic and dromotropic effects.

Atarashi *et al.* [4] demonstrated that cilostazol increased heart rates and improved the symptoms in patients with bradyarrhythmia, bradycardic atrial fibrillation, SSS and Wenckebach-type atrioventricular block. In patients with third-degree atrioventricular block, cilostazol also increased heart rates and additionally increased ventricular escape rate, without abolishment of atrioventricular block or change in the frequency of premature ventricular beats [6]. Furthermore, cilostazol has been shown to decrease atrial natriuretic peptide and brain natriuretic peptide concentration [6,7], the hormones that are present in atrioventricular asynchrony and heart failure patients [61].

Investigations of the roles of cilostazol on heart rate variability (HRV) have shown that cilostazol significantly improved the slow heart rate, the frequency domain in SSS and bradycardic atrial fibrillation patients [9,11]. Although the mechanism underlying the chronotropic effect of PDE3 inhibitors has been clarified, the direct mechanism of cilostazol is still unclear, as there is no cardiac electrophysiological study regarding the effect of cilostazol. Nevertheless, the positive chronotropic effect of cilostazol has been proposed to be due to several mechanisms. Cilostazol causes an increased coronary blood flow and blood supply to the sinus node or the atrioventricular node in patients who have bradyarrhythmia arising from the ischemic process [4]. Cilostazol also antagonizes ATP, which is a factor causing sinus bradyarrhythmia and atrioventricular delays [4]. It is known that ATP and adenosine produce a negative chronotropic effect by causing a hyperpolarization of maximum diastolic potential. The hyperpolarization occurs when adenosine or ATP induces a time-dependent inwardly rectifying outward K^+ current [61]. It has also been proposed that adenosine inhibits noradrenaline release [51,61]. Furthermore, cilostazol can inhibit the adenosine uptake, resulting in a strong positive chronotropic effect (Fig. 2). It has been shown that the increase of cAMP in nodal cells caused by cilostazol could also cause adrenergic stimulation [4]. In addition, it is known that cilostazol causes systemic vasodilatation, thus producing a reflex adrenergic stimulation [4]. Although the positive dromotropic effect of PDE3 inhibitors is still unclear, it is possible that the negative dromotropic effect of adenosine is antagonized by cilostazol [62]. Despite the fact that cilostazol has a positive chronotropy and some evidence has suggested its possible undesired tachyarrhythmic effect [8,63–65], recent reports and meta-analysis have indicated that it could either lower the incidence of cardiac death and major cardiac events or, at least, that it did not increase major cardiovascular events or mortality in patients treated for coronary artery disease and peripheral vascular disease [53–56].

Cilostazol and ventricular tachyarrhythmia

Brugada syndrome is another cardiac electrophysiological abnormality caused by an abnormal *SCN5A* gene [66]. It causes a decreased sodium current and gives prominent transient outward potassium current (I_{to}) in the epicardium rather than in the endocardium, wherein this imbalance of current induces a prominent notch in phase 1 of the action potential. Consequently, the loss of the dome of action potential in the ventricular epicardium, but not endocardium, produces ST elevation and develops transmural dispersion of repolarization, which is vulnerable to ventricular fibrillation induction [66–72].

In a recent case report of Brugada syndrome patients who experienced several episodes of ventricular fibrillation and retained implantable cardioverter defibrillators (ICDs), it was found that the ventricular fibrillation episode was completely abolished after being treated with cilostazol at 200 mg/day [12]. However, when cilostazol was discontinued, ventricular fibrillation recurred even when being treated at 100 mg/day. After 200 mg/day of cilostazol was readministered, ventricular fibrillation disappeared. In a 1-year follow-up in three ICD implanted patients, no ventricular fibrillation was observed with cilostazol treatment [12]. This report strongly indicates the need for further investigation regarding the beneficial effects of cilostazol in preventing ventricular tachyarrhythmia. Supporting this notion is a recent report by Kanlop *et al.* [73] who demonstrated in swine that intravenous administration of cilostazol (6 mg/kg) could increase the ventricular fibrillation threshold, as well as improve defibrillation efficacy.

Several mechanisms have been proposed to explain the effects of cilostazol in preventing ventricular fibrillation in those cases with Brugada syndrome. Cilostazol has the ability to accelerate heart rate, which can suppress the transient outward K^+ channel (I_{to}) [12]. If I_{to} is suppressed, other channels that always open following the I_{to} will be decelerated. This effect can prolong the action potential duration. Also, cilostazol can increase intracellular cAMP, which can lead to an increase in intracellular Ca^{2+}. This effect could preserve the dome of an action potential and normalizes the ST segment, thus preventing arrhythmia [12].

The sympatovagal imbalance during a nocturnal period indicated by an increased vagal tone and a decreased sympathetic tone has been proposed as a major factor in aggravating arrhythmia in Brugada patients [74,75]. HRV in Brugada patients demonstrated a nocturnal standard deviation of averaged *N–N* intervals (SDANN), an ultra-low-frequency (ULF) and a low-frequency component were lowered, whereas a high-frequency component was increased in patients who showed deleterious symptoms [74,75]. The results also demonstrated the association between a ST segment elevation following ventricular fibrillation events and an increased vagal activity [74,75]. It is possible that the inhibition of adenosine uptake by cilostazol could prevent vagal hyperactivity in Brugada syndrome. Furthermore, the PDE3 inhibitory effects of cilostazol could improve the sympathetic tone through the adenylate cyclase pathway by increasing cAMP levels. These dual mechanisms could, therefore, maintain a sympatovagal balance in Brugada syndrome. However, the hypothesis that cilostazol can improve HRV in Brugada patients needs to be validated in future studies.

In contrast to the report by Tsuchiya [12], Abud *et al.* [76] have demonstrated that cilostazol failed to prevent ventricular fibrillation in Brugada patients. As the ventricular tachyarrhythmia in Brugada syndrome could originate in the ventricle or in the atrium, as atrial fibrillation precipitating ventricular fibrillation [77], it is possible that the different genotypes of Brugada syndrome, as presenting with or without atrial fibrillation [76,78], might affect the result of cilostazol treatment in different ways. Therefore, it may be concluded that cilostazol could be useful for treating ventricular fibrillation in Brugada syndrome if the arrhythmia originates in the ventricle. However, in atrial fibrillation-precipitated ventricular fibrillation cases, cilostazol may not prevent the occurrence of ventricular fibrillation [76].

Conclusion

Cilostazol has been shown to affect cardiac electrophysiological properties by increasing inward Ca^{2+} current and decreasing outward potassium current (I_{to}), thus, minimizing the ventricular arrhythmia induction. Cilostazol increases intracellular cAMP in myocardial cells to a lesser degree, compared with other PDE3 inhibitors, and inhibits adenosine uptake in myocardial cells. It has also been shown to be beneficial in bradyarrhythmias. Furthermore, despite its positive chronotropic effect, recent reports have indicated that it did not increase major cardiovascular events when used in patients with coronary artery or peripheral artery diseases. All of these effects of cilostazol could be beneficial in arrhythmia prevention, even in heart failure. Future investigations on the effects of cilostazol in the heart failure model are needed to warrant its possible clinical benefits.

Acknowledgements

This work was supported by the Thailand Research Fund grants RTA 5280006 (N.C.), RMU 5180007 (S.C.), and a grant from the Biomedical Engineering Center, Chiang Mai University (N.C.).

References

1 Manganiello VC, Murata T, Taira M, Belfrage P, Degerman E. Diversity in cyclic nucleotide phosphodiesterase isoenzyme families. *Arch Biochem Biophys* 1995; **322**:1–13.
2 Dawson DL, Cutler BS, Meissner MH, Strandness DE Jr. Cilostazol has beneficial effects in treatment of intermittent claudication: results from a multicenter, randomized, prospective, double-blind trial. *Circulation* 1998; **98**:678–686.
3 Pratt CM. Analysis of the cilostazol safety database. *Am J Cardiol* 2001; **87**:28D–33D.
4 Atarashi H, Endoh Y, Saitoh H, Kishida H, Hayakawa H. Chronotropic effects of cilostazol, a new antithrombotic agent, in patients with bradyarrhythmias. *J Cardiovasc Pharmacol* 1998; **31**:534–539.
5 Katakami N, Kim YS, Kawamori R, Yamasaki Y. The phosphodiesterase inhibitor cilostazol induces regression of carotid atherosclerosis in subjects with type 2 diabetes mellitus: principal results of the Diabetic Atherosclerosis Prevention by Cilostazol (DAPC) study – a randomized trial. *Circulation* 2010; **121**:2584–2591.
6 Kodama-Takahashi K, Kurata A, Ohshima K, Yamamoto K, Uemura S, Watanabe S, *et al.* Effect of cilostazol on the ventricular escape rate and neurohumoral factors in patients with third-degree atrioventricular block. *Chest* 2003; **123**:1161–1169.
7 Madias JE. Cilostazol: an 'intermittent claudication' remedy for the management of third-degree AV block. *Chest* 2003; **123**:979–982.
8 Gamssari F, Mahmood H, Ho JS, Villareal RP, Liu B, Rasekh A, *et al.* Rapid ventricular tachycardias associated with cilostazol use. *Tex Heart Inst J* 2002; **29**:140–142.
9 Toyonaga S, Nakatsu T, Murakami T, Kusachi S, Mashima K, Tominaga Y, *et al.* Effects of cilostazol on heart rate and its variation in patients with atrial fibrillation associated with bradycardia. *J Cardiovasc Pharmacol Ther* 2000; **5**:183–191.
10 Kishida M, Watanabe K, Tsuruoka T. Effects of cilostazol in patients with bradycardiac atrial fibrillation. *J Cardiol* 2001; **37**:27–33.
11 Ueda H, Nakatsu T, Murakami T, Kusachi S, Tominaga Y, Yamane S, *et al.* Effects of cilostazol on heart rate and its variability in patients with sick sinus syndrome. *Clin Drug Invest* 2001; **21**:605–612.
12 Tsuchiya T, Ashikaga K, Honda T, Arita M. Prevention of ventricular fibrillation by cilostazol, an oral phosphodiesterase inhibitor, in a patient with Brugada syndrome. *J Cardiovasc Electrophysiol* 2002; **13**:698–701.
13 Feldman AM, Bristow MR, Parmley WW, Carson PE, Pepine CJ, Gilbert EM, *et al.* Effects of vesnarinone on morbidity and mortality in patients with heart failure. Vesnarinone Study Group. *N Engl J Med* 1993; **329**:149–155.
14 Packer M, Carver JR, Rodeheffer RJ, Ivanhoe RJ, Di Bianco R, Zeldis SM, *et al.* Effect of oral milrinone on mortality in severe chronic heart failure. The PROMISE Study Research Group. *N Engl J Med* 1991; **325**:1468–1475.
15 Hiatt WR, Money SR, Brass EP. Long-term safety of cilostazol in patients with peripheral artery disease: the CASTLE study (Cilostazol: a study in long-term effects). *J Vasc Surg* 2008; **47**:330–336.
16 Cone J, Wang S, Tandon N, Fong M, Sun B, Sakurai K, *et al.* Comparison of the effects of cilostazol and milrinone on intracellular cAMP levels and cellular function in platelets and cardiac cells. *J Cardiovasc Pharmacol* 1999; **34**:497–504.
17 Liu Y, Shakur Y, Yoshitake M, Kambayashi JJ. Cilostazol (pletal): a dual inhibitor of cyclic nucleotide phosphodiesterase type 3 and adenosine uptake. *Cardiovasc Drug Rev* 2001; **19**:369–386.
18 Shakur Y, Fong M, Hensley J, Cone J, Movsesian MA, Kambayashi J, *et al.* Comparison of the effects of cilostazol and milrinone on cAMP-PDE activity, intracellular cAMP and calcium in the heart. *Cardiovasc Drugs Ther* 2002; **16**:417–427.
19 Wang S, Cone J, Fong M, Yoshitake M, Kambayashi J, Liu Y. Interplay between inhibition of adenosine uptake and phosphodiesterase type 3 on cardiac function by cilostazol, an agent to treat intermittent claudication. *J Cardiovasc Pharmacol* 2001; **38**:775–783.
20 Hayashi S, Morishita R, Matsushita H, Nakagami H, Taniyama Y, Nakamura T, *et al.* Cyclic AMP inhibited proliferation of human aortic vascular smooth muscle cells, accompanied by induction of p53 and p21. *Hypertension* 2000; **35**:237–243.

21 Kambayashi J, Liu Y, Sun B, Shakur Y, Yoshitake M, Czerwiec F. Cilostazol as a unique antithrombotic agent. *Curr Pharm Des* 2003; **9**:2289–2302.
22 Kim MJ, Park KG, Lee KM, Kim HS, Kim SY, Kim CS, *et al.* Cilostazol inhibits vascular smooth muscle cell growth by downregulation of the transcription factor E2F. *Hypertension* 2005; **45**:552–556.
23 Watanabe K, Ikeda S, Komatsu J, Inaba S, Suzuki J, Sueda S, *et al.* Effect of cilostazol on vasomotor reactivity in patients with vasospastic angina pectoris. *Am J Cardiol* 2003; **92**:21–25.
24 Smith VB, Spina D, Page CP. Phosphodiesterase inhibitors. *Br J Pharmacol* 2006; **147**:S252–S257.
25 Phrommintikul A, Chattipakorn N. Roles of cardiac ryanodine receptor in heart failure and sudden cardiac death. *Int J Cardiol* 2006; **112**:142–152.
26 Baim DS, McDowell AV, Cherniles J, Monrad ES, Parker JA, Edelson J, *et al.* Evaluation of a new bipyridine inotropic agent – milrinone – in patients with severe congestive heart failure. *N Engl J Med* 1983; **309**:748–756.
27 Benotti JR, Grossman W, Braunwald E, Davolos DD, Alousi AA. Hemodynamic assessment of amrinone. A new inotropic agent. *N Engl J Med* 1978; **299**:1373–1377.
28 Jaski BE, Fifer MA, Wright RF, Braunwald E, Colucci WS. Positive inotropic and vasodilator actions of milrinone in patients with severe congestive heart failure. Dose-response relationships and comparison to nitroprusside. *J Clin Invest* 1985; **75**:643–649.
29 Murali S, Uretsky BF, Valdes AM, Kolesar JA, Reddy PS. Acute hemodynamic and hormonal effects of CI-930, a new phosphodiesterase inhibitor, in severe congestive heart failure. *Am J Cardiol* 1987; **59**:1356–1360.
30 Rauch B, Zimmermann R, Kapp M, Haass M, Von Molitor S, Smolarz A, *et al.* Hemodynamic and neuroendocrine response to acute administration of the phosphodiesterase inhibitor BM14.478 in patients with congestive heart failure. *Clin Cardiol* 1991; **14**:386–395.
31 Sinoway LS, Maskin CS, Chadwick B, Forman R, Sonnenblick EH, Le Jemtel TH. Long-term therapy with a new cardiotonic agent, WIN 47203: drug-dependent improvement in cardiac performance and progression of the underlying disease. *J Am Coll Cardiol* 1983; **2**:327–331.
32 Amsallem E, Kasparian C, Haddour G, Boissel JP, Nony P. Phosphodiesterase III inhibitors for heart failure. *Cochrane Database Syst Rev* 2005:CD002230.
33 Naccarelli GV, Goldstein RA. Electrophysiology of phosphodiesterase inhibitors. *Am J Cardiol* 1989; **63**:35A–40A.
34 Movsesian MA. PDE3 inhibition in dilated cardiomyopathy: reasons to reconsider. *J Card Fail* 2003; **9**:475–480.
35 Movsesian MA. Beta-adrenergic receptor agonists and cyclic nucleotide phosphodiesterase inhibitors: shifting the focus from inotropy to cyclic adenosine monophosphate. *J Am Coll Cardiol* 1999; **34**:318–324.
36 Carceles MD, Aleixandre F, Fuente T, Lopez-Vidal J, Laorden ML. Combined phosphodiesterase inhibition and beta-blockade in the GI104313, decreases ischemia-induced arrhythmias in the rat. *Can J Anaesth* 2001; **48**:486–492.
37 Hauptman PJ, Woods D, Prirzker MR. Novel use of a short-acting intravenous beta blocker in combination with inotropic therapy as a bridge to chronic oral beta blockade in patients with advanced heart failure. *Clin Cardiol* 2002; **25**:247–249.
38 Kumar A, Choudhary G, Antonio C, Just V, Jain A, Heaney L, *et al.* Carvedilol titration in patients with congestive heart failure receiving inotropic therapy. *Am Heart J* 2001; **142**:512–515.
39 Shakar SF, Abraham WT, Gilbert EM, Robertson AD, Lowes BD, Zisman LS, *et al.* Combined oral positive inotropic and beta-blocker therapy for treatment of refractory class IV heart failure. *J Am Coll Cardiol* 1998; **31**:1336–1340.
40 Hambleton R, Krall J, Tikishvili E, Honeggar M, Ahmad F, Manganiello VC, *et al.* Isoforms of cyclic nucleotide phosphodiesterase PDE3 and their contribution to cAMP hydrolytic activity in subcellular fractions of human myocardium. *J Biol Chem* 2005; **280**:39168–39174.
41 Frank KF, Bolck B, Brixius K, Kranias EG, Schwinger RH. Modulation of SERCA: implications for the failing human heart. *Basic Res Cardiol* 2002; **97 (Suppl 1)**:I72–I78.
42 Schmidt U, Hajjar RJ, Kim CS, Lebeche D, Doye AA, Gwathmey JK. Human heart failure: cAMP stimulation of SR Ca(2+)-ATPase activity and phosphorylation level of phospholamban. *Am J Physiol* 1999; **277**:H474–H480.
43 Rubart M, Zipes DP. Mechanism of sudden cardiac death. *J Clin Invest* 2005; **115**:2305–2315.
44 Morgan JP, Erny RE, Allen PD, Grossman W, Gwathmey JK. Abnormal intracellular calcium handling, a major cause of systolic and diastolic dysfunction in ventricular myocardium from patients with heart failure. *Circulation* 1990; **81**:III21–III32.
45 Sunderdiek U, Korbmacher B, Gams E, Schipke JD. Myocardial efficiency in stunned myocardium. Comparison of Ca(2+)-sensitization and PDE III-inhibition on energy consumption. *Eur J Cardiothorac Surg* 2000; **18**:83–89.
46 Feldman AM, McNamara DM. Reevaluating the role of phosphodiesterase inhibitors in the treatment of cardiovascular disease. *Clin Cardiol* 2002; **25**:256–262.
47 Goldstein RA, Geraci SA, Gray EL, Rinkenberger RL, Dougherty AH, Naccarelli GV. Electrophysiologic effects of milrinone in patients with congestive heart failure. *Am J Cardiol* 1986; **57**:624–628.
48 Lalukota K, Cleland JG, Ingle L, Clark AL, Coletta AP. Clinical trials update from the Heart Failure Society of America: EMOTE, HERB-CHF, BEST genetic sub-study and RHYTHM-ICD. *Eur J Heart Fail* 2004; **6**:953–955.
49 Tsuchikane E, Fukuhara A, Kobayashi T, Kirino M, Yamasaki K, Kobayashi T, *et al.* Impact of cilostazol on restenosis after percutaneous coronary balloon angioplasty. *Circulation* 1999; **100**:21–26.
50 Tsuchiya T. Role of pharmacotherapy in Brugada syndrome. *Indian Pacing Electrophysiol J* 2004; **4**:26–32.
51 Versprille A. The chronotropic effect of adenine- and hypoxanthine derivatives on isolated rat hearts before and after removing the sino-auricular node. *Pflugers Arch Gesamte Physiol Menschen Tiere* 1966; **291**:261–267.
52 Lubbe WF, Nguyen T, West EJ. Modulation of myocardial cyclic AMP and vulnerability to fibrillation in the rat heart. *Fed Proc* 1983; **42**:2460–2464.
53 Ahn Y, Jeong MH, Jeong JW, Kim KH, Ahn TH, Kang WC, *et al.* Randomized comparison of cilostazol vs clopidogrel after drug-eluting stenting in diabetic patients: clilostazol for diabetic patients in drug-eluting stent (CIDES) trial. *Circ J* 2008; **72**:35–39.
54 Uchiyama S, Demaerschalk BM, Goto S, Shinohara Y, Gotoh F, Stone WM, *et al.* Stroke prevention by cilostazol in patients with atherothrombosis: meta-analysis of placebo-controlled randomized trials. *J Stroke Cerebrovasc Dis* 2009; **18**:482–490.
55 Robless P, Mikhailidis DP, Stansby GP. Cilostazol for peripheral arterial disease. *Cochrane Database Syst Rev* 2008:CD003748.
56 Park KH, Jeong MH, Lee MG, Ko JS, Lee SE, Kang WY, *et al.* Efficacy of triple anti-platelet therapy including cilostazol in acute myocardial infarction patients undergoing drug-eluting stent implantation. *Korean Circ J* 2009; **39**:190–197.
57 Furman S. Cardiac pacing and pacemaker. I: Indications for pacing bradyarrhythmias. *Am Heart J* 1977; **93**:523–530.
58 Knight BP, Gersh BJ, Carlson MD, Friedman PA, McNamara RL, Strickberger SA, *et al.* Role of permanent pacing to prevent atrial fibrillation: science advisory from the American Heart Association Council on Clinical Cardiology (Subcommittee on Electrocardiography and Arrhythmias) and the Quality of Care and Outcomes Research Interdisciplinary Working Group, in collaboration with the Heart Rhythm Society. *Circulation* 2005; **111**:240–243.
59 Goldstein RA, Gray EL, Dougherty AH, Naccarelli GV. Electrophysiologic effects of amrinone. *Am J Cardiol* 1985; **56**:25B–28B.
60 Naccarelli GV, Gray EL, Dougherty AH, Hanna JE, Goldstein RA. Amrinone: acute electrophysiologic and hemodynamic effects in patients with congestive heart failure. *Am J Cardiol* 1984; **54**:600–604.
61 Belardinelli L, Giles WR, West A. Ionic mechanisms of adenosine actions in pacemaker cells from rabbit heart. *J Physiol* 1988; **405**:615–633.
62 Martynyuk AE, Zima A, Seubert CN, Morey TE, Belardinelli L, Dennis DM. Potentiation of the negative dromotropic effect of adenosine by rapid heart rates: possible ionic mechanism. *Basic Res Cardiol* 2002; **97**:295–304.
63 Sanganalmath SK, Barta J, Takeda N, Kumamoto H, Dhalla NS. Antiplatelet therapy mitigates cardiac remodeling and dysfunction in congestive heart failure due to myocardial infarction. *Can J Physiol Pharmacol* 2008; **86**:180–189.
64 Shinohara Y, Katayama Y, Uchiyama S, Yamaguchi T, Handa S, Matsuoka K, *et al.* Cilostazol for prevention of secondary stroke (CSPS 2): an aspirin-controlled, double-blind, randomised non-inferiority trial. *Lancet Neurol* 2010; **9**:959–968.
65 Barta J, Sanganalmath SK, Kumamoto H, Takeda N, Edes I, Dhalla NS. Antiplatelet agents sarpogrelate and cilostazol affect experimentally-induced ventricular arrhythmias and mortality. *Cardiovasc Toxicol* 2008; **8**:127–135.
66 Alings M, Wilde A. 'Brugada' syndrome: clinical data and suggested pathophysiological mechanism. *Circulation* 1999; **99**:666–673.
67 Shimizu W. The Brugada syndrome: an update. *Intern Med* 2005; **44**:1224–1231.
68 Francis J, Antzelevitch C. Brugada syndrome. *Int J Cardiol* 2005; **101**:173–178.
69 Miyoshi S, Mitamura H, Fukuda Y, Tanimoto K, Hagiwara Y, Kanki H, *et al.* Link between SCN5A mutation and the Brugada syndrome ECG phenotype: simulation study. *Circ J* 2005; **69**:567–575.

70 Khan IA, Nair CK. Brugada and long QT-3 syndromes: two phenotypes of the sodium channel disease. *Ann Noninvasive Electrocardiol* 2004; **9**:280–289.
71 Antzelevitch C. Brugada syndrome: overview. In: Antzelevitch C, Brugada P, Brugada J, Brugada R, editors. *The Brugada syndrome: from bench to bedside*. Oxford: Blackwell-Futula; 2005. pp. 1–22.
72 Antzelevitch CP, Fish JMD, Di Diego JMM. Cellular mechanisms underlying the Brugada syndrome. In: Antzelevitch C, Brugada P, Brugada J, Brugada R, editors. *The Brugada syndrome: from bench to bedside*. Oxford: Blackwell-Futura; 2005. pp. 52–77.
73 Kanlop N, Shinlapawittayatorn K, Sungnoon R, Weerateerangkul P, Chattipakorn S, Chattipakorn N. Cilostazol attenuates ventricular arrhythmia induction and improves defibrillation efficacy in swine. *Can J Physiol Pharmacol* 2010; **88**:422–428.
74 Krittayaphong R, Veerakul G, Nademanee K, Kangkagate C. Heart rate variability in patients with Brugada syndrome in Thailand. *Eur Heart J* 2003; **24**:1771–1778.
75 Hermida JS, Leenhardt A, Cauchemez B, Denjoy I, Jarry G, Mizon F, *et al.* Decreased nocturnal standard deviation of averaged NN intervals. An independent marker to identify patients at risk in the Brugada syndrome. *Eur Heart J* 2003; **24**:2061–2069.
76 Abud A, Bagattin D, Goyeneche R, Becker C. Failure of cilostazol in the prevention of ventricular fibrillation in a patient with Brugada syndrome. *J Cardiovasc Electrophysiol* 2006; **17**:210–212.
77 Borggrefe MMP, Schimpf RM, Gaita FM, Eckardt LM, Wolpert CM. Atrial tachyarrhythmias in Brugada syndrome. In: Antzelevitch C, Brugada P, Brugada J, Brugada R, editors. *The Brugada syndrome: from bench to bedside*. Oxford: Blackwell-Futura; 2005. pp. 178–83.
78 Morita H, Kusano-Fukushima K, Nagase S, Fujimoto Y, Hisamatsu K, Fujio H, *et al.* Atrial fibrillation and atrial vulnerability in patients with Brugada syndrome. *J Am Coll Cardiol* 2002; **40**:1437–1444.

World Journal of Cardiology

Online Submissions: http://www.wjgnet.com/1949-8462office
wjc@wjgnet.com
doi:10.4330/wjc.v3.i5.144

World J Cardiol 2011 May 26; 3(5): 144-152
ISSN 1949-8462 (online)

PPARγ activator, rosiglitazone: Is it beneficial or harmful to the cardiovascular system?

Siripong Palee, Siriporn Chattipakorn, Arintaya Phrommintikul, Nipon Chattipakorn

Siripong Palee, Nipon Chattipakorn, Cardiac Electrophysiology Unit, Department of Physiology, Faculty of Medicine, Chiang Mai University, Chiang Mai, 50200, Thailand
Siripong Palee, Siriporn Chattipakorn, Arintaya Phrommintikul, Nipon Chattipakorn, Cardiac Electrophysiology Research and Training Center, Faculty of Medicine, Chiang Mai University, Chiang Mai, 50200, Thailand
Siriporn Chattipakorn, Faculty of Dentistry, Chiang Mai University, Chiang Mai, 50200, Thailand
Arintaya Phrommintikul, Department of Medicine, Faculty of Medicine, Chiang Mai University, Chiang Mai, 50200, Thailand
Author contributions: All authors contributed equally to this review.
Supported by Grants from the Thailand Research Fund RTA 5280006 (NC), BRG (SC), MRG5280169 (AP) and the Commission of Higher Education Thailand (SP, NC)
Correspondence to: Nipon Chattipakorn, MD, PhD, Cardiac Electrophysiology Research and Training Center, Faculty of Medicine, Chiang Mai University, Chiang Mai, 50200, Thailand. nchattip@gmail.com
Telephone: +66-53-945329 Fax: +66-53-945368
Received: March 17, 2011 Revised: April 4, 2011
Accepted: April 11, 2011
Published online: May 26, 2011

Abstract

Rosiglitazone is a synthetic agonist of peroxisome proliferator-activated receptor γ which is used to improve insulin resistance in patients with type Ⅱ diabetes. Rosiglitazone exerts its glucose-lowering effects by improving insulin sensitivity. Data from various studies in the past decade suggest that the therapeutic effects of rosiglitazone reach far beyond its use as an insulin sensitizer since it also has other benefits on the cardiovascular system such as improvement of contractile dysfunction, inhibition of the inflammatory response by reducing neutrophil and macrophage accumulation, and the protection of myocardial injury during ischemic/reperfusion in different animal models. Previous clinical studies in type Ⅱ diabetes patients demonstrated that rosiglitazone played an important role in protecting against arteriosclerosis by normalizing the metabolic disorders and reducing chronic inflammation of the vascular system. Despite these benefits, inconsistent findings have been reported, and growing evidence has demonstrated adverse effects of rosiglitazone on the cardiovascular system, including increased risk of acute myocardial infarction, heart failure and chronic heart failure. As a result, rosiglitazone has been recently withdrawn from EU countries. Nevertheless, the effect of rosiglitazone on ischemic heart disease has not yet been firmly established. Future prospective clinical trials designed for the specific purpose of establishing the cardiovascular benefit or risk of rosiglitazone would be the best way to resolve the uncertainties regarding the safety of rosiglitazone in patients with heart disease.

Key words: Rosiglitazone; Ischemic reperfusion injury; Heart disease; Type Ⅱ diabetic; Thiazolidinediones

Peer reviewer: Antigone Lazou, Professor of Physiology, Lab of Animal Physiology, Sch of Biology,Aristotle University of Thessaloniki, Thessaloniki 54124, Greece

Palee S, Chattipakorn S, Phrommintikul A, Chattipakorn N. PPARγ activator, rosiglitazone: Is it beneficial or harmful to the cardiovascular system? *World J Cardiol* 2011; 3(5): 144-152 Available from: URL: http://www.wjgnet.com/1949-8462/full/v3/i5/144.htm DOI: http://dx.doi.org/10.4330/wjc.v3.i5.144

INTRODUCTION

Type Ⅱ diabetes mellitus (T2DM) is a disease whose incidence is dramatically increasing and requires continuing medical management in many countries[1,2]. T2DM is characterized by insulin resistance and impaired glucose tolerance[3]. The development of T2DM involves 3 metabolic defects that include insulin resistance, alterations in hepatic glucose production and β-cell deficiency[4]. The

earliest defect seen in the development of T2DM is insulin resistance[4]. In this state, the β-cells produce large amounts of insulin reaching a supraphysiologic level as a compensatory response to peripheral tissue insulin resistance. If insulin resistance is left untreated, the β-cells begin to fail to produce insulin, resulting in a state of relative insulin deficiency[4]. T2DM is known to develop after this phase. T2DM patients have a 2- to 4-fold increased risk of developing coronary artery disease, unstable angina and myocardial infarction (MI)[5,6]. Furthermore, T2DM patients have been shown to have a worse prognosis than non-diabetic patients after a cardiovascular event[7,8].

Thiazolidinediones (TZDs) are an oral medication developed to reduce insulin resistance in T2DM patients and have been used since 1997[9]. TZDs exert their properties by stimulating a nuclear hormone receptor, the peroxisome proliferator-activated receptor γ (PPARγ)[10]. Troglitazone was the first drug developed but was withdrawn from the market due to liver toxicity[9]. Currently, pioglitazone and rosiglitazone are the only compounds that are available for clinical use[9]. However, the effects of rosiglitazone have been controversial regarding cardiovascular effects in both animal and clinical studies[11-59]. On the positive side, rosiglitazone has been shown to exert its potent insulin sensitization by improving insulin resistance in T2DM[10,60]. Various studies demonstrated that the therapeutic effects of rosiglitazone could reach far beyond its action as an insulin sensitizer because it has other therapeutic effects on many organs especially in the cardiovascular system in both animal models and humans[11-59]. Nevertheless, in the past decade growing evidence from both basic and clinical studies indicates that rosiglitazone could be harmful to the heart[11-25]. Because of its serious undesired effects, rosiglitazone has been recently withdrawn from the EU market[61], and is under close monitoring by the US Food and Drug Administration[62,63].

In this review, we aim to summarize and discuss the overall benefits as well as the adverse effects of rosiglitazone on the heart from both pre-clinical and clinical reports. Understanding the inconsistent findings as well as the limitations found in each study using rosiglitazone should allow investigators to carefully design future studies that hopefully can clarify previous inconsistent findings, and to indicate whether rosiglitazone should be used in patients.

BENEFICIAL EFFECTS OF ROSIGLITAZONE ON THE CARDIOVASCULAR SYSTEM

Previous studies reported that rosiglitazone had beneficial effects on the cardiovascular system in *in vitro*, *in vivo* and clinical studies. These beneficial effects of rosiglitazone are summarized in Table 1. In rat models of ischemic/reperfusion (I/R) injury, pretreatment with rosiglitazone reduced the infarct size and improved ischemia/reperfusion-induced myocardial contractile dysfunction[26,46,48]. Rosiglitazone treatment also improved left ventricular (LV) systolic pressure and positive and negative maximal values of the first derivative of LV pressure (dP/dt) during I/R injury[32,46]. In addition, in both obese and normal rats rosiglitazone could decrease systolic blood pressure, improve contractile function and normalize the insulin level[31,44,45]. These findings suggested that rosiglitazone could prevent the development of hypertension associated with insulin resistance. This notion was supported by the finding that rosiglitazone treatment could enhance nitric oxide (NO)-mediated arteriolar dilation[28]. Furthermore the accumulation of neutrophils and macrophages and expression of monocyte chemoattractant factor (MCP)-1 in the ischemic heart was diminished by rosiglitazone[46]. Likewise, rosiglitazone treatment in diabetic rat and mouse models reduced the blood levels of glucose, triglycerides, and free fatty acids, and enhanced cardiac glucose oxidation in the ischemic myocardium[26,50]. Rosiglitazone treatment also reduced myocardial apoptosis and infarction size post I/R injury by restoring the balance between the pro-apoptotic and anti-apoptotic mitogen-activated protein kinase (MAPK) signaling pathway, increasing phosphatidylinositol-3-kinase-Akt phosphorylation, and inhibiting p42/44 MAPK[26,35,38,41,59].

In *in vitro* studies, incubation of a rat cardiomyoblast cell line with rosiglitazone demonstrated cardioprotective effects against oxidative stress, and the antioxidant enzyme heme oxygenase 1 was upregulated in these cells after rosiglitazone treatment[40]. Furthermore, rosiglitazone could inhibit cardiac fibroblast proliferation, increase connective tissue growth factor expression and decrease NO production induced by advanced glycation endproducts in cultured neonatal rat cardiac fibroblasts[37]. In addition, rosiglitazone could prevent cardiac hypertrophy by inhibiting angiotensin Ⅱ[27,32,54].

Many clinical studies reported that the beneficial effects of rosiglitazone on the cardiovascular system were similar to those from animal studies. Rosiglitazone therapy has been shown to reduce cardiovascular complications associated with T2DM[47,49,58]. Data from preliminary studies in patients who underwent coronary angioplasty and stent implantation demonstrated that rosiglitazone treatment for 6 mo led to a lower occurrence of restenosis and a lower degree of stenosis of the luminal diameter after angioplasty[64]. Furthermore, a study in patients with T2DM demonstrated that treatment with 4 mg/d of rosiglitazone for 12 wk decreased not only insulin resistance but also pulse wave velocity, which is a direct parameter of arterial stiffness in patients with diabetes and coronary arteries disease (CAD)[58]. Rosiglitazone has been shown to reduce plasma levels of C-reactive protein[5,51,56,58], matrix metalloproteinase-9 and MCP-1[58] in T2DM patients, suggesting that rosiglitazone plays an important role in protecting against arteriosclerosis by normalizing metabolic disorders and reducing chronic inflammation of the vascular system. Rosiglitazone treat-

Table 1 Reports of the beneficial effects of rosiglitazone on the cardiovascular system in pre-clinical and clinical studies

Models	Dose of rosiglitazone	Major findings	Interpretation	Ref.
Cultured neonatal rat cardiomyocytes	5 μmol/L; pretreated for 30 min before stimulation with Ang Ⅱ (1 μmol/L) for 48 h	Inhibited Ang Ⅱ-induced upregulation of skeletal α-actin and ANP genes, and prevent an increase in cell surface area	Rosiglitazone involved in the inhibition of cardiac hypertrophy	[27]
Isolated and cultured neonatal rat ventricular myocytes	1, 5, 10 μmol/L; pretreated for 48 h	Accelerated Ca^{2+} transient decay rates Increased SERCA2 mRNA levels Upregulation of IL-6 secretion Enhanced TNF-α- and lipopolysaccharide-induced NF-κB-dependent transcription	Cardioprotective effects of rosiglitazone may be mediated *via* NF-κB	[43]
Isolated and cultured adult rat ventricular myocytes	10^{-8}-10^{-5} mol; pretreated for 24 h	Did not increase protein synthesis Did not attenuate hypertrophic response to noradrenaline, phorbol-12-myristate13-acetate and endothelin-1	Rosiglitazone did not directly induce cardiomyocyte hypertrophy in cardiomyocytes	[30]
Cultured neonatal rat ventricular myocytes	10 μmol/L; pretreated for 24 h	Inhibited the endothelin-1-induced increase in protein synthesis, surface area, calcineurin enzymatic activity, and protein expression Inhibited the nuclear translocation of NFATc4 Enhanced the association between PPARγ and calcineurin/nuclear factor of activated T-cells	Rosiglitazone inhibited endothelin-1-induced cardiac hypertrophy *via* calcineurin/nuclear factor of activated T-cells pathway	[29]
Cultured rat cardiomyoblast cell line H9c2(2-1)	100 μmol/L; pretreated for 24 h	Increased expression of heme oxygenase 1 Increased cell viability under oxidative stress induced by H_2O_2	Rosiglitazone had cardioprotective effects against oxidative stress	[40]
Cultured neonatal rat cardiac fibroblasts	0.1, 1, 10 μmol/L pretreated for 48 h	Inhibited cardiac fibroblast proliferation Increased connective tissue growth factor expression Decreased nitric oxide production induced by advanced glycation endproducts	Rosiglitazone could prevent myocardial fibrosis	[37]
Cultured neonatal rat ventricular myocytes	1 μmol/L; pretreated for 30 min prior to H_2O_2 treatment	Decrease cell apoptosis Increase Bcl-2 protein content	Rosiglitazone protected cells from oxidative stress through upregulating Bcl-2 expression	[42]
Cultured neonatal rat cardiac myocytes	0.1, 1, 3, 10, 30 μmol/L; pretreated for 30 min before hypoxia	Decreased cytoplasmic accumulation of histone-associated DNA fragments Increased reoxygenation-induced rephosphorylation of Akt Did not alter phosphorylation of the MAP kinases ERK1/2 and c-Jun N-terminal kinase	Rosiglitazone protected cardiac myocytes against I/R injury by facilitating Akt rephosphorylation	[35]
Fatty Zucker rats	7-7.5 μmol/L per kilogram po; 9-12 wk	Decreased systolic blood pressure Decreased fasting hyperinsulinemia Improved mesenteric arteries contraction and relaxation	Rosiglitazone prevented the development of HT and endothelial dysfunction associated with insulin resistance	[45]
Rats with I/R injury	3 mg/kg per day po; pretreated for 7 d; 1 and 3 mg/kg iv given during I/R	Improved left ventricular systolic pressure, dP/dt_{max} and dP/dt_{min} Reduced neutrophils and macrophages accumulation Reduced the infarct size Downregulation of CD11b/CD18 Upregulation of L-selectin on neutrophils and monocytes	Rosiglitazone decreased infarct size and improved contractile dysfunction during I/R possibly *via* inhibition of the inflammatory response	[46]
Fatty Zucker rats with I/R injury (*Ex vivo* model)	3 mg/kg po; 7 or 14 d prior to isolated perfuse heart study	Normalized the insulin resistance Restored GLUT4 protein levels Improved contractile function Prevented greater loss of ATP	Rosiglitazone protected obese rat heart from I/R injury	[44]
I/R injury in isolated perfused normal and STZ- induced diabetic rat hearts (*Ex vivo* model)	1 μmol/L given prior to ischemia; 10 μmol/kg per day po after STZ injection for 4 wk	Inhibited activating protein-1 DNA-binding activity Inhibited of Jun NH_2-terminal kinase phosphorylation Reduced lactate levels and lactate dehydrogenase activity	Rosiglitazone attenuated postischemic myocardial injury in isolated rat heart	[34]
Sprague-Dawley rats	5 mg/kg per day po; 7 d	Reduced systolic blood pressure reduced vascular DNA synthesis, expression of cyclin D1 and cdk4, AT_1 receptors, vascular cell adhesion molecule-1, and platelet and endothelial cell adhesion molecule, and NF-κB activity	Rosiglitazone prevented the development of hypertension and endothelial dysfunction	[31]
T2DM mice	3 mg/kg per day po; 7 d	Did not affect serum glucose and insulin Increased serum 8-isoprostane and dihydroethydine-detectable superoxide production Enhanced catalase and reduced NAD(P)H oxidase activity Did not affect SOD activity	Rosiglitazone enhanced nitric oxide mediation of coronary arteriolar dilations *via* attenuating oxidative stress in T2DM mice	[28]

Hypercholesterolemic New Zealand rabbits with I/R injury	3 mg/kg per day po; 5 wk prior to I/R	Attenuated postischemic myocardial nitrative stress Restored a beneficial balance between pro- and anti-apoptotic MAPK signaling Reduced postischemic myocardial apoptosis Improved cardiac functional recovery	Rosiglitazone attenuated arteriosclerosis and prevented I/R-induced myocardial apoptosis	[38]
Zucker diabetic fatty rats with I/R injury	3 mg/kg per day po; 8 d prior to I/R	Reduced blood glucose, triglycerides, and free fatty acids levels Enhanced cardiac glucose oxidation Increased Akt phosphorylation (Akt-pS473) and its downstream targets (glycogen synthase kinase-3β and FKHR-pS256) (forkhead transcription factor) Reduced apoptotic cardiomyocytes and myocardial infarct size	Rosiglitazone protected heart against I/R injury	[26]
Sprague-Dawley rats with I/R injury	3 mg/kg per day po; 7 d prior to I/R	Reduced infarct size Decreased myocardial expression of AT_1 receptors Increased AT_2 mRNA and protein expression Inhibited p42/44 MAPK Did not alter Akt1 expression	Rosiglitazone attenuated myocardial I/R injury possibly *via* increase expression of AT_2 and inhibition of p42/44 MAPK	[41]
Sprague-Dawley rats with I/R injury	3 mg/kg per day po for 8 wk prior to I/R	Improved left ventricular dP/dt_{max} and dP/dt_{min} Inhibited myocardial angiotensin Ⅱ and aldosterone No significant effects on myocardial AT_1 and AT_2 mRNA	Rosiglitazone had a beneficial effect on post-infarct ventricular remodeling, but had a neutral effect on mortality	[32]
WT and eNOS knockout mice with I/R injury	3 mg/kg ip; pretreated for 45 min prior to I/R	WT mice: increased the recovery of left ventricular function and coronary flow following ischemia eNOS knockout mice: suppressed the recovery of myocardial function following ischemia	Rosiglitazone protected the heart against I/R injury *via* nitric oxide by phosphorylation of eNOS	[48]
Isolated perfused hearts from T2DM mice	23 mg/kg per day po; pretreated for 5 wk	Normalized plasma glucose and lipid concentrations Restored rates of cardiac glucose and fatty acid oxidation Improved cardiac efficiency due to decrease in unloaded myocardial oxygen consumption Improved functional recovery after low-flow ischemia	Rosiglitazone improved cardiac efficiency and ventricular function	[50]
WT and APN knockdown/knockout mice with myocardial infarction	20 mg/kg per day po; pretreated 72 h prior to MI and continuously treated until 7 and 14 d	Improved the postischemic survival rate of WT mice at 14 d of treatment Increased adipocyte APN expression Elevated plasma APN levels Reduced infarct size Decreased apoptosis and oxidative stress Improved cardiac function	APN was crucial for cardioprotective effects of rosiglitazone in myocardial infarction	[57]
Hypercholesterolemic rats	4 mg/kg per day po; pretreated for 5 mo	Reduced Ang Ⅱ level Upregulated AT_2 Improved lipid metabolism	Rosiglitazone protected the heart against cardiac hypertrophy *via* improved lipid profile, reduced Ang-Ⅱ and increase AT_2 expression	[54]
Mice with I/R injury	3 mg/kg per day po; pretreated for 14 d prior to I/R	Reduced ratio of infarct size to ischemic area (area at risk) Reduced the occurrence ventricular fibrillation Attenuated cardiac apoptosis Increased levels of p-Akt and p-GSK-3α	Cardioprotective effects of rosiglitazone against I/R injury were mediated *via* a PI3K/Akt/GSK-3α-dependent pathway	[59]
T2DM patients (n = 21)	4 mg/d; 6 mo	Weight loss (first 12 wk) Decreased waist circumference Decreased systolic and diastolic blood pressure Reduced HbA1c	Rosiglitazone amplified some of the positive benefits of lifestyle intervention	[55]
Randomized, double-blind, placebo-controlled study in T2DM (n = 357)	4 or 8 mg/d; 26 wk	Reduced C-reactive protein, matrix metalloproteinase-9 and white blood cell levels Did not alter interleukin-6 level	Rosiglitazone had beneficial effects on overall cardiovascular risk	[49]
Randomized, double-blind in CAD patients without diabetes (n = 40, control = 44)	4 mg/d for 8 wk followed by 8 mg/d for 4 wk	Reduced E-selectin Reduced von Willebrand Reduced C-reactive protein & fibrinogen Reduced homeostasis model of insulin resistance index Elevation of LDL and triglyceride level	Rosiglitazone reduces markers of endothelial cell activation and levels of acute-phase reactants in CAD patients without DM	[56]
Randomized, double-blind, placebo-controlled study in T2DM with CAD patients (n = 54)	4-8 mg/d; 16 wk	Improved glycemic control and whole-body insulin sensitivity Increased myocardial glucose uptake in both ischemic and non-ischemic regions	Rosiglitazone facilitated myocardial glucose storage and utilization in T2DM with CAD patients	[36]
Randomized controlled trial in patients with impaired glucose tolerance (n = 2365, control = 2634)	8 mg/d; 3 yr	Facilitated normoglycemic Did not alter cardiovascular event	Rosiglitazone reduced incidence of T2DM and increased normoglycemia	[47]

Randomized, double-blind, placebo-controlled trial in patients with T2DM (n = 70, control =16)	8 mg/d; 6 mo	Decreased plasma glucose and HbA1c with a trend to decrease HOMA index Decreased C-peptide and fasting insulin Reduced C-reactive protein Improved endothelium-dependent dilation	Rosiglitazone improved endothelial function and C-reactive protein in patients with T2DM	[51]
Randomized, controlled trial in patient with T2DM with CAD (Rosiglitazone; n = 25)	4 mg/d; 12 wk	Decreased insulin resistance Decreased pulse wave velocity Reduced plasma levels of C-reactive protein and monocyte chemoattractant protein 1	Rosiglitazone prevented arteriosclerosis by normalizing metabolic disorders and reducing chronic inflammation of the vascular system	[58]
Prospective and cross-sectional study in T2DM (Rosiglitazone; n = 22, metformin/ rosiglitazone; n = 100)	Treated with rosiglitazone 6 mo	Decreased endotoxin Increased adiponectin levels	Lower endotoxin and higher adiponectin in the groups treated with rosiglitazone may be responsible for the improved insulin sensitivity	[39]
Comprehensive meta-analysis of randomized clinical trials (n = 42922, control = 45483)	Results of 164 trials with duration > 4 wk	The OR for all-cause and cardiovascular mortality with rosiglitazone was 0.93 and 0.94, respectively The OR for nonfatal MI and heart failure with rosiglitazone was 1.14 (0.9-1.45) and 1.69 (1.21-2.36), respectively The risk of heart failure was higher when rosiglitazone was administered as add-on therapy to insulin	Rosiglitazone did not increase risk of MI or cardiovascular mortality	[52]

Ang: Angiotensin; ANP: Atrial natriuretic peptide; OR: Odds ratio; T2DM: Type 2 diabetes mellitus; Hb: Hemoglobin; HOMA: Homeostatic Model of Insulin Resistance; CAD: Coronary artery disease; WT: Wild-type; APN: Adiponectin; eNOS: Endothelial nitric oxide synthase; GSK: Glycogen synthase kinase; LDL: Low density lipoprotein; AT: Angiotensin receptor type; SOD: Superoxide dismutase; MAPK: Mitogen-activated protein kinase; PI3K: Phosphatidyl inositol-3-kinase; STZ: Streptozotocin; I/R: Ischemia/reperfusion; TNF: Tumor necrosis factor; IL: Interleukin; NF: Nuclear factor; SERCA: sarcoendoplasmic reticulum calcium ATPase; HT: Hypertension; NFAT: nuclear factor of activated T cells; ERK: Extracellular signal-regulated kinase; PPAR: Peroxisome proliferator-activated receptor; MI: Myocardial infarction.

ment in patients with T2DM with/without CAD has also been shown to improve myocardial glucose uptake and utilization[36,47]. Rosiglitazone decreased both systolic and diastolic pressure[53,55], suggesting that this drug could improve systolic and diastolic function. All of these findings indicate that in addition to improving insulin resistance in T2DM patients, rosiglitazone also has the beneficial effects on overall cardiovascular risk.

ADVERSE EFFECTS OF ROSIGLITAZONE ON THE CARDIOVASCULAR SYSTEM

Despite these previously mentioned beneficial effects of rosiglitazone on the cardiovascular system, growing evidence indicates other adverse cardiovascular outcomes. The effect of rosiglitazone in increasing mortality in post-MI rats was first reported by Lygate *et al*[21] in 2003. Later, more studies, including clinical trials, demonstrated undesirable effects of rosiglitazone on the cardiovascular system. These findings suggested that rosiglitazone treatment may be harmful and should be used with caution in cardiovascular patients. A summary of reports on the adverse effects of rosiglitazone in various models as well as clinical studies are shown in Table 2.

Rosiglitazone treatment has been shown to induce apoptotic cell death in cultured vascular smooth muscle cell by increasing caspase 3 activity and the cytoplasmic histone-associated DNA fragmentation *via* the proapoptotic extracellular signal-regulated kinase 1/2-independent pathway[17]. Likewise, in an *in vivo* I/R injury model, it has been demonstrated that rosiglitazone therapy for 8 wk in non-diabetic rats with MI did not reduce either LV infarct size or LV hypertrophy, and increased mortality rate after I/R injury[21]. These findings suggested that rosiglitazone did not have cardioprotective effects in myocardial I/R injury. Furthermore, rosiglitazone treatment has been shown to increase cardiac phosphorylation of the p38MAPK signaling pathway[15], suggesting that rosiglitazone could facilitate cardiomyocyte apoptosis. In addition, rosiglitazone has been shown to be associated with an increased incidence of cardiac hypertrophy due to the increased expression of atrial natriuretic peptide, B-type natriuretic peptide, collagen I and Ⅲ and fibronectin[16], leading to cardiac hypertrophy. The deterioration in cardiac function was also found in mice and rats when treated with rosiglitazone[12,24].

In a large animal model, which is more similar to a human, a recent study in swine has demonstrated that intravenous administration of rosiglitazone at clinically relevant doses attenuated epicardial monophasic action potential shortening during ischemia, possibly *via* blockade of cardiac ATP-sensitive potassium channels, and increased the propensity for ventricular fibrillation[20].

Growing evidence from recent clinical trials suggest that rosiglitazone could have serious harmful effects on the cardiovascular system[11,13,14,18,19,22,23,65]. The meta-analysis by Nissen *et al*[11] was the first report raising concerns about the cardiovascular safety profile of rosiglitazone. In a meta-analysis, Nissen *et al*[11] demonstrated that T2DM patients who received rosiglitazone treatment had a significantly increased risk of MI, heart failure and cardiovascular mortality. Although the method and statistical analysis used in this study have been criticized[14,52,66], the subsequent meta-analyses showed similar concerns

Table 2 Reports of the adverse effects of rosiglitazone on the cardiovascular system in pre-clinical and clinical studies

Model	Dose of rosiglitazone	Major findings	Interpretation	Ref.
Isolated and cultured vascular smooth muscle cells	1-10 μmol/L; incubated for 24 h	Induced cell death in a concentration-dependent manner Increased caspase 3 activity and the cytoplasmic histone-associated DNA fragmentation PD98059 (MAPKK inhibitor) did not abolish rosiglitazone induced ERK1/2 activation (proapoptotic effects)	Rosiglitazone induced apoptotic cell death through an ERK1/2-independent pathway	[17]
Rats with I/R injury	3 mg/kg per day po; pretreated for 14 d prior to I/R	Did not reduce left ventricular infarct size or hypertrophy Increased mortality rate Improved ejection fraction and prevented an increase left ventricular end diastolic pressure	Rosiglitazone did not prevent left ventricular remodeling, but was associated with increased mortality after myocardial infarction	[21]
Swine with I/R injury	3 mg/kg per day po; pretreated for 8 d prior to I/R	Increased expression of PPARγ Had no effect on myocardial contractile function Did not alter substrate uptake and proinflammatory cytokines expression	Rosiglitazone had no cardioprotective effects in a swine model of myocardial I/R injury	[25]
PPARγ-knockout (CM-PGKO) mouse	10 mg/kg per day po; 4 wk	Increased phosphorylation of p38 mitogen-activated protein kinase Induced phosphorylation of extracellular signal-related kinase 1/2 Did not affect phosphorylation of c-Jun N-terminal kinases Induced cardiac hypertrophy	Rosiglitazone caused cardiac hypertrophy at least partially independent of PPARγ in cardiomyocytes	[15]
Wild type and PPARγ overexpression mice	10 mg/kg per day po; 15 d	Increased lipid accumulation Increased size of the heart Decreased fractional shortening Increased CD36 expression	Rosiglitazone and PPARγ overexpression could be harmful to cardiac function	[24]
Swine with I/R injury	0.1, 1.0 10 mg/kg iv; pretreated for 60 min	Attenuated MAP shortening during ischemia by blocking cardiac KATP channels Increased propensity for ventricular fibrillation during myocardial ischemia	Rosiglitazone promoted onset of ventricular fibrillation during cardiac ischemia	[20]
Sprague-Dawley rats	15 mg/kg per day po; 21 d	Induced eccentric heart hypertrophy associated with increased expression of ANP, BNP, collagen Ⅰ and Ⅲ and fibronectin Reduced heart rate and increased stroke volume Increased heart glycogen content, myofibrillar protein content and turnover Reduced glycogen phosphorylase expression and activity	Rosiglitazone induced cardiac hypertrophy *via* the mTOR pathway	[16]
Meta-analysis in T2DM (n = 15565, control = 12282)	Received rosiglitazone more than 24 wk	Increased the risk of myocardial infarction Increased cardiovascular death incidence	Rosiglitazone increased in the risk of myocardial infarction and borderline increased in risk of cardiovascular death	[11]
RECORD study (n = 4447)	Received rosiglitazone with mean follow-up time of 3.75 yr	Increased the risk of heart failure	Rosiglitazone increased risk of heart failure, but did not increase the risk of cardiovascular death or all cause mortality	[18]
RECORD study (n = 4447)	Received rosiglitazone with mean follow-up time of 5.5 yr	Increased the risk of heart failure	Rosiglitazone increased risk of heart failure Suggestion of contraindication for rosiglitazone to be used in patients developing symptomatic heart failure	[65]
Case-control analysis of a retrospective cohort study (n = 159026)	Treated with TZDs at least 1 yr	Increased risk of heart failure Increased mortality Increased risk of acute myocardial infarction	Rosiglitazone was associated with risk of heart failure, acute myocardial infarction, and mortality	[19]
Retrospective, double-blind, randomized clinical studies with rosiglitazone (n = 14237)	Received rosiglitazone 24-52 wk	Increased heart failure incidence Increased events of myocardial ischemia	Rosiglitazone increased the risk of heart failure and myocardial infarction	[13]
A meta-analysis of randomized controlled trials (n = 6421, control = 7870)	Received rosiglitazone at least 12 mo	Increased risk of myocardial infarction and heart failure No increased risk of cardiovascular mortality	Rosiglitazone increased risk of myocardial infarction and heart failure, without increased risk of cardiovascular mortality	[23]

I/R: Ischemia/reperfusion; PPAR: Peroxisome proliferator-activated receptor; T2DM: Type 2 diabetes mellitus; RECORD: Rosiglitazone Evaluated for Cardiac Outcomes and Regulation of Glycaemia in Diabetes; ANP: Atrial natriuretic peptide; BNP: B-type natriuretic peptide; ERK: Extracellular signal-regulated kinase; TZD: Thiazolidinedione; mTOR: Mammalian Target of Rapamycin pathway

regarding MI and heart failure, but not cardiovascular mortality[23,52,65].

Lipscombe *et al*[19] also demonstrated that rosiglitazone therapy in patients with T2DM was associated with a significantly increased risk of congestive heart failure, acute MI, and death. Similarly, results from a meta-analysis demonstrated that rosiglitazone treatment for at least 12 mo was associated with a significantly increased risk of MI and heart failure[23]. A retrospective analysis also suggested that rosiglitazone may increase the risk of heart failure[13]. These data from the clinical trials and meta-analysis in recent years strongly indicated that rosiglitazone could have adverse effects on the cardiovascular outcome due to increased risk of MI and heart failure, resulting in increased mortality in patients treated over a long period with rosiglitazone[14,18,22,23]. A meta-analysis demonstrated that patients treated with both rosiglitazone and pioglitazone had a 1.7-fold increase in risk of congestive heart failure with a slightly greater increase in risk with rosiglitazone than with pioglitazone (1.3-fold)[67].

The association between TZDs and heart failure is well recognized as a class effect. An increased plasma volume rather than direct effects on cardiac function is thought to be the mechanism responsible for heart failure[12]. Fluid retention is mediated through increased sodium reabsorption of the renal PPARγ-dependent pathway in the collecting tubules[68].

Unlike the mechanism responsible for heart failure, the mechanism of increased MI risk of rosiglitazone is still controversial. An unfavorable effect of the lipid profile has been proposed, in which rosiglitazone increases low density lipoprotein cholesterol to a greater extent than pioglitazone, and decreases the triglyceride level to a smaller extent than pioglitazone[69].

DISCREPANCY IN FINDINGS FROM ROSIGLITAZONE USE

As summarized in Table 1 for the beneficial effects and Table 2 for the adverse effects of rosiglitazone, these controversial reports are still debated. Although each side for and against the use of rosiglitazone has its own supporting documentation, the growing number of reports of serious adverse cardiovascular effects cannot be taken lightly. It is possible that the controversy on the cardiovascular effects of rosiglitazone could be due to differences in species which could have different drug metabolism, different experimental models, different drug administration methods as well as different time intervals of drug treatment which relates to the effects of the drug. The differences in patients' clinical characteristics may also contribute to the differences in outcomes, in which older patients with preexisting cardiovascular disease are more likely to have serious cardiovascular events.

Regardless of this controversy, since evidence from clinical reports indicated potential cardiovascular risks of rosiglitazone, the European Medicines Agency suggested that the anti-diabetes drug rosiglitazone (Avandia®) should be suspended from the EU market due to its excessive cardiovascular risk[61,70]. As a result, rosiglitazone has been withdrawn from the EU market[61]. However, rosiglitazone is still available in the US but remains under close monitoring from the US Food and Drug Administration[61-63,71].

CONCLUSION

Rosiglitazone is a potent agent in the treatment of hyperglycemia in patients with T2DM because it is an insulin sensitizer and improves glucose uptake. Despite previous reports on its beneficial effects, growing evidence indicates that rosiglitazone increases cardiovascular risks in patients taking this drug. Although this drug has been withdrawn from the EU market, it is still can be used elsewhere. It is important that future large clinical trials should be done to evaluate the definitive cardiovascular outcome of the drug and the interplay between rosiglitazone and other available anti-hyperglycemic agents. In addition, large meta-analyses are also essential and must be carefully interpreted in order to elucidate the effects of rosiglitazone on cardiovascular risks and outcomes.

REFERENCES

1 **Quinn CE**, Hamilton PK, Lockhart CJ, McVeigh GE. Thiazolidinediones: effects on insulin resistance and the cardiovascular system. *Br J Pharmacol* 2008; **153**: 636-645
2 Standards of medical care in diabetes--2008. *Diabetes Care* 2008; **31** Suppl 1: S12-S54
3 **Jay MA**, Ren J. Peroxisome proliferator-activated receptor (PPAR) in metabolic syndrome and type 2 diabetes mellitus. *Curr Diabetes Rev* 2007; **3**: 33-39
4 **Dumasia R**, Eagle KA, Kline-Rogers E, May N, Cho L, Mukherjee D. Role of PPAR- gamma agonist thiazolidinediones in treatment of pre-diabetic and diabetic individuals: a cardiovascular perspective. *Curr Drug Targets Cardiovasc Haematol Disord* 2005; **5**: 377-386
5 **Haffner SM**, Lehto S, Rönnemaa T, Pyörälä K, Laakso M. Mortality from coronary heart disease in subjects with type 2 diabetes and in nondiabetic subjects with and without prior myocardial infarction. *N Engl J Med* 1998; **339**: 229-234
6 **Huang PL**. Unraveling the links between diabetes, obesity, and cardiovascular disease. *Circ Res* 2005; **96**: 1129-1131
7 **Rosamond W**, Flegal K, Furie K, Go A, Greenlund K, Haase N, Hailpern SM, Ho M, Howard V, Kissela B, Kittner S, Lloyd-Jones D, McDermott M, Meigs J, Moy C, Nichol G, O' Donnell C, Roger V, Sorlie P, Steinberger J, Thom T, Wilson M, Hong Y. Heart disease and stroke statistics--2008 update: a report from the American Heart Association Statistics Committee and Stroke Statistics Subcommittee. *Circulation* 2008; **117**: e25-146
8 **Timmer JR**, Ottervanger JP, Thomas K, Hoorntje JC, de Boer MJ, Suryapranata H, Zijlstra F. Long-term, cause-specific mortality after myocardial infarction in diabetes. *Eur Heart J* 2004; **25**: 926-931
9 **Day C**. Thiazolidinediones: a new class of antidiabetic drugs. *Diabet Med* 1999; **16**: 179-192
10 **Guo L**, Tabrizchi R. Peroxisome proliferator-activated receptor gamma as a drug target in the pathogenesis of insulin resistance. *Pharmacol Ther* 2006; **111**: 145-173
11 **Nissen SE**, Wolski K. Effect of rosiglitazone on the risk of myocardial infarction and death from cardiovascular causes. *N Engl J Med* 2007; **356**: 2457-2471

12 Effects of Chronic PPAR-Agonist Treatment on Cardiac Structure and Function, Blood Pressure, and Kidney in Healthy Sprague-Dawley Rats. *PPAR Res* 2009; **2009**: 237865
13 **Cobitz A**, Zambanini A, Sowell M, Heise M, Louridas B, McMorn S, Semigran M, Koch G. A retrospective evaluation of congestive heart failure and myocardial ischemia events in 14,237 patients with type 2 diabetes mellitus enrolled in 42 short-term, double-blind, randomized clinical studies with rosiglitazone. *Pharmacoepidemiol Drug Saf* 2008; **17**: 769-781
14 **Diamond GA**, Bax L, Kaul S. Uncertain effects of rosiglitazone on the risk for myocardial infarction and cardiovascular death. *Ann Intern Med* 2007; **147**: 578-581
15 **Duan SZ**, Ivashchenko CY, Russell MW, Milstone DS, Mortensen RM. Cardiomyocyte-specific knockout and agonist of peroxisome proliferator-activated receptor-gamma both induce cardiac hypertrophy in mice. *Circ Res* 2005; **97**: 372-379
16 **Festuccia WT**, Laplante M, Brûlé S, Houde VP, Achouba A, Lachance D, Pedrosa ML, Silva ME, Guerra-Sá R, Couet J, Arsenault M, Marette A, Deshaies Y. Rosiglitazone-induced heart remodelling is associated with enhanced turnover of myofibrillar protein and mTOR activation. *J Mol Cell Cardiol* 2009; **47**: 85-95
17 **Gouni-Berthold I**, Berthold HK, Weber AA, Ko Y, Seul C, Vetter H, Sachinidis A. Troglitazone and rosiglitazone induce apoptosis of vascular smooth muscle cells through an extracellular signal-regulated kinase-independent pathway. *Naunyn Schmiedebergs Arch Pharmacol* 2001; **363**: 215-221
18 **Home PD**, Pocock SJ, Beck-Nielsen H, Gomis R, Hanefeld M, Jones NP, Komajda M, McMurray JJ. Rosiglitazone evaluated for cardiovascular outcomes--an interim analysis. *N Engl J Med* 2007; **357**: 28-38
19 **Lipscombe LL**, Gomes T, Lévesque LE, Hux JE, Juurlink DN, Alter DA. Thiazolidinediones and cardiovascular outcomes in older patients with diabetes. *JAMA* 2007; **298**: 2634-2643
20 **Lu L**, Reiter MJ, Xu Y, Chicco A, Greyson CR, Schwartz GG. Thiazolidinedione drugs block cardiac KATP channels and may increase propensity for ischaemic ventricular fibrillation in pigs. *Diabetologia* 2008; **51**: 675-685
21 **Lygate CA**, Hulbert K, Monfared M, Cole MA, Clarke K, Neubauer S. The PPARgamma-activator rosiglitazone does not alter remodeling but increases mortality in rats post-myocardial infarction. *Cardiovasc Res* 2003; **58**: 632-637
22 **Psaty BM**, Furberg CD. The record on rosiglitazone and the risk of myocardial infarction. *N Engl J Med* 2007; **357**: 67-69
23 **Singh S**, Loke YK, Furberg CD. Long-term risk of cardiovascular events with rosiglitazone: a meta-analysis. *JAMA* 2007; **298**: 1189-1195
24 **Son NH**, Park TS, Yamashita H, Yokoyama M, Huggins LA, Okajima K, Homma S, Szabolcs MJ, Huang LS, Goldberg IJ. Cardiomyocyte expression of PPARgamma leads to cardiac dysfunction in mice. *J Clin Invest* 2007; **117**: 2791-2801
25 **Xu Y**, Gen M, Lu L, Fox J, Weiss SO, Brown RD, Perlov D, Ahmad H, Zhu P, Greyson C, Long CS, Schwartz GG. PPAR-gamma activation fails to provide myocardial protection in ischemia and reperfusion in pigs. *Am J Physiol Heart Circ Physiol* 2005; **288**: H1314-H1323
26 **Yue TL**, Bao W, Gu JL, Cui J, Tao L, Ma XL, Ohlstein EH, Jucker BM. Rosiglitazone treatment in Zucker diabetic Fatty rats is associated with ameliorated cardiac insulin resistance and protection from ischemia/reperfusion-induced myocardial injury. *Diabetes* 2005; **54**: 554-562
27 **Asakawa M**, Takano H, Nagai T, Uozumi H, Hasegawa H, Kubota N, Saito T, Masuda Y, Kadowaki T, Komuro I. Peroxisome proliferator-activated receptor gamma plays a critical role in inhibition of cardiac hypertrophy in vitro and in vivo. *Circulation* 2002; **105**: 1240-1246
28 **Bagi Z**, Koller A, Kaley G. PPARgamma activation, by reducing oxidative stress, increases NO bioavailability in coronary arterioles of mice with Type 2 diabetes. *Am J Physiol Heart Circ Physiol* 2004; **286**: H742-H748
29 **Bao Y**, Li R, Jiang J, Cai B, Gao J, Le K, Zhang F, Chen S, Liu P. Activation of peroxisome proliferator-activated receptor gamma inhibits endothelin-1-induced cardiac hypertrophy via the calcineurin/NFAT signaling pathway. *Mol Cell Biochem* 2008; **317**: 189-196
30 **Bell D**, McDermott BJ. Effects of rosiglitazone and interactions with growth-regulating factors in ventricular cell hypertrophy. *Eur J Pharmacol* 2005; **508**: 69-76
31 **Diep QN**, El Mabrouk M, Cohn JS, Endemann D, Amiri F, Virdis A, Neves MF, Schiffrin EL. Structure, endothelial function, cell growth, and inflammation in blood vessels of angiotensin II-infused rats: role of peroxisome proliferator-activated receptor-gamma. *Circulation* 2002; **105**: 2296-2302
32 **Geng DF**, Wu W, Jin DM, Wang JF, Wu YM. Effect of peroxisome proliferator-activated receptor gamma ligand. Rosiglitazone on left ventricular remodeling in rats with myocardial infarction. *Int J Cardiol* 2006; **113**: 86-91
33 **Graham DJ**, Ouellet-Hellstrom R, MaCurdy TE, Ali F, Sholley C, Worrall C, Kelman JA. Risk of acute myocardial infarction, stroke, heart failure, and death in elderly Medicare patients treated with rosiglitazone or pioglitazone. *JAMA* 2010; **304**: 411-418
34 **Khandoudi N**, Delerive P, Berrebi-Bertrand I, Buckingham RE, Staels B, Bril A. Rosiglitazone, a peroxisome proliferator-activated receptor-gamma, inhibits the Jun NH(2)-terminal kinase/activating protein 1 pathway and protects the heart from ischemia/reperfusion injury. *Diabetes* 2002; **51**: 1507-1514
35 **Kilter H**, Werner M, Roggia C, Reil JC, Schäfers HJ, Kintscher U, Böhm M. The PPAR-gamma agonist rosiglitazone facilitates Akt rephosphorylation and inhibits apoptosis in cardiomyocytes during hypoxia/reoxygenation. *Diabetes Obes Metab* 2009; **11**: 1060-1067
36 **Lautamäki R**, Airaksinen KE, Seppänen M, Toikka J, Luotolahti M, Ball E, Borra R, Härkönen R, Iozzo P, Stewart M, Knuuti J, Nuutila P. Rosiglitazone improves myocardial glucose uptake in patients with type 2 diabetes and coronary artery disease: a 16-week randomized, double-blind, placebo-controlled study. *Diabetes* 2005; **54**: 2787-2794
37 **Li J**, Liu NF, Wei Q. Effect of rosiglitazone on cardiac fibroblast proliferation, nitric oxide production and connective tissue growth factor expression induced by advanced glycation end-products. *J Int Med Res* 2008; **36**: 329-335
38 **Liu HR**, Tao L, Gao E, Lopez BL, Christopher TA, Willette RN, Ohlstein EH, Yue TL, Ma XL. Anti-apoptotic effects of rosiglitazone in hypercholesterolemic rabbits subjected to myocardial ischemia and reperfusion. *Cardiovasc Res* 2004; **62**: 135-144
39 **Al-Attas OS**, Al-Daghri NM, Al-Rubeaan K, da Silva NF, Sabico SL, Kumar S, McTernan PG, Harte AL. Changes in endotoxin levels in T2DM subjects on anti-diabetic therapies. *Cardiovasc Diabetol* 2009; **8**: 20
40 **Mersmann J**, Tran N, Zacharowski PA, Grotemeyer D, Zacharowski K. Rosiglitazone is cardioprotective in a murine model of myocardial I/R. *Shock* 2008; **30**: 64-68
41 **Molavi B**, Chen J, Mehta JL. Cardioprotective effects of rosiglitazone are associated with selective overexpression of type 2 angiotensin receptors and inhibition of p42/44 MAPK. *Am J Physiol Heart Circ Physiol* 2006; **291**: H687-H693
42 **Ren Y**, Sun C, Sun Y, Tan H, Wu Y, Cui B, Wu Z. PPAR gamma protects cardiomyocytes against oxidative stress and apoptosis via Bcl-2 upregulation. *Vascul Pharmacol* 2009; **51**: 169-174
43 **Shah RD**, Gonzales F, Golez E, Augustin D, Caudillo S, Abbott A, Morello J, McDonough PM, Paolini PJ, Shubeita HE. The antidiabetic agent rosiglitazone upregulates SERCA2 and enhances TNF-alpha- and LPS-induced NF-kappaB-dependent transcription and TNF-alpha-induced IL-6 secretion in ventricular myocytes. *Cell Physiol Biochem* 2005; **15**: 41-50

44 **Sidell RJ**, Cole MA, Draper NJ, Desrois M, Buckingham RE, Clarke K. Thiazolidinedione treatment normalizes insulin resistance and ischemic injury in the zucker Fatty rat heart. *Diabetes* 2002; **51**: 1110-1117

45 **Walker AB**, Chattington PD, Buckingham RE, Williams G. The thiazolidinedione rosiglitazone (BRL-49653) lowers blood pressure and protects against impairment of endothelial function in Zucker fatty rats. *Diabetes* 1999; **48**: 1448-1453

46 **Yue Tl TL**, Chen J, Bao W, Narayanan PK, Bril A, Jiang W, Lysko PG, Gu JL, Boyce R, Zimmerman DM, Hart TK, Buckingham RE, Ohlstein EH. In vivo myocardial protection from ischemia/reperfusion injury by the peroxisome proliferator-activated receptor-gamma agonist rosiglitazone. *Circulation* 2001; **104**: 2588-2594

47 **Gerstein HC**, Yusuf S, Bosch J, Pogue J, Sheridan P, Dinccag N, Hanefeld M, Hoogwerf B, Laakso M, Mohan V, Shaw J, Zinman B, Holman RR. Effect of rosiglitazone on the frequency of diabetes in patients with impaired glucose tolerance or impaired fasting glucose: a randomised controlled trial. *Lancet* 2006; **368**: 1096-1105

48 **Gonon AT**, Bulhak A, Labruto F, Sjöquist PO, Pernow J. Cardioprotection mediated by rosiglitazone, a peroxisome proliferator-activated receptor gamma ligand, in relation to nitric oxide. *Basic Res Cardiol* 2007; **102**: 80-89

49 **Haffner SM**, Greenberg AS, Weston WM, Chen H, Williams K, Freed MI. Effect of rosiglitazone treatment on nontraditional markers of cardiovascular disease in patients with type 2 diabetes mellitus. *Circulation* 2002; **106**: 679-684

50 **How OJ**, Larsen TS, Hafstad AD, Khalid A, Myhre ES, Murray AJ, Boardman NT, Cole M, Clarke K, Severson DL, Aasum E. Rosiglitazone treatment improves cardiac efficiency in hearts from diabetic mice. *Arch Physiol Biochem* 2007; **113**: 211-220

51 **Kelly AS**, Thelen AM, Kaiser DR, Gonzalez-Campoy JM, Bank AJ. Rosiglitazone improves endothelial function and inflammation but not asymmetric dimethylarginine or oxidative stress in patients with type 2 diabetes mellitus. *Vasc Med* 2007; **12**: 311-318

52 **Mannucci E**, Monami M, Di Bari M, Lamanna C, Gori F, Gensini GF, Marchionni N. Cardiac safety profile of rosiglitazone: a comprehensive meta-analysis of randomized clinical trials. *Int J Cardiol* 2010; **143**: 135-140

53 **Nilsson PM**, Hedblad B, Donaldson J, Berglund G. Rosiglitazone reduces office and diastolic ambulatory blood pressure following 1-year treatment in non-diabetic subjects with insulin resistance. *Blood Press* 2007; **16**: 95-100

54 **Ren L**, Li Y, Li Y, Tang R, Hu D, Sheng Z, Liu N. The inhibitory effects of rosiglitazone on cardiac hypertrophy through modulating the renin-angiotensin system in diet-induced hypercholesterolemic rats. *Cell Biochem Funct* 2010; **28**: 58-65

55 **Reynolds LR**, Konz EC, Frederich RC, Anderson JW. Rosiglitazone amplifies the benefits of lifestyle intervention measures in long-standing type 2 diabetes mellitus. *Diabetes Obes Metab* 2002; **4**: 270-275

56 **Sidhu JS**, Cowan D, Kaski JC. The effects of rosiglitazone, a peroxisome proliferator-activated receptor-gamma agonist, on markers of endothelial cell activation, C-reactive protein, and fibrinogen levels in non-diabetic coronary artery disease patients. *J Am Coll Cardiol* 2003; **42**: 1757-1763

57 **Tao L**, Wang Y, Gao E, Zhang H, Yuan Y, Lau WB, Chan L, Koch WJ, Ma XL. Adiponectin: an indispensable molecule in rosiglitazone cardioprotection following myocardial infarction. *Circ Res* 2010; **106**: 409-417

58 **Yu J**, Jin N, Wang G, Zhang F, Mao J, Wang X. Peroxisome proliferator-activated receptor gamma agonist improves arterial stiffness in patients with type 2 diabetes mellitus and coronary artery disease. *Metabolism* 2007; **56**: 1396-1401

59 **Zhang XJ**, Xiong ZB, Tang AL, Ma H, Ma YD, Wu JG, Dong YG. Rosiglitazone-induced myocardial protection against ischaemia-reperfusion injury is mediated via a phosphatidylinositol 3-kinase/Akt-dependent pathway. *Clin Exp Pharmacol Physiol* 2010; **37**: 156-161

60 **Sauer WH**, Cappola AR, Berlin JA, Kimmel SE. Insulin sensitizing pharmacotherapy for prevention of myocardial infarction in patients with diabetes mellitus. *Am J Cardiol* 2006; **97**: 651-654

61 **European Medicines Agency**. European Medicines Agency recommends suspension of Avandia, Avandamet and Avaglim. Press release, September 23, 2010

62 **The US Food and Drug Administration**. Decision on continued marketing of rosiglitazone (Avandia, Avandamet, Avandaryl). September 22, 2010

63 **The US Food and Drug Administration**. FDA significantly restricts access to the diabetes drug Avandia. September 23, 2010

64 **Choi D**, Kim SK, Choi SH, Ko YG, Ahn CW, Jang Y, Lim SK, Lee HC, Cha BS. Preventative effects of rosiglitazone on restenosis after coronary stent implantation in patients with type 2 diabetes. *Diabetes Care* 2004; **27**: 2654-2660

65 **Komajda M**, McMurray JJ, Beck-Nielsen H, Gomis R, Hanefeld M, Pocock SJ, Curtis PS, Jones NP, Home PD. Heart failure events with rosiglitazone in type 2 diabetes: data from the RECORD clinical trial. *Eur Heart J* 2010; **31**: 824-831

66 **Bilous RW**. Rosiglitazone and myocardial infarction: cause for concern or misleading meta-analysis? *Diabet Med* 2007; **24**: 931-933

67 **Lago RM**, Singh PP, Nesto RW. Congestive heart failure and cardiovascular death in patients with prediabetes and type 2 diabetes given thiazolidinediones: a meta-analysis of randomised clinical trials. *Lancet* 2007; **370**: 1129-1136

68 **Zhang H**, Zhang A, Kohan DE, Nelson RD, Gonzalez FJ, Yang T. Collecting duct-specific deletion of peroxisome proliferator-activated receptor gamma blocks thiazolidinedione-induced fluid retention. *Proc Natl Acad Sci USA* 2005; **102**: 9406-9411

69 **Goldberg RB**, Kendall DM, Deeg MA, Buse JB, Zagar AJ, Pinaire JA, Tan MH, Khan MA, Perez AT, Jacober SJ. A comparison of lipid and glycemic effects of pioglitazone and rosiglitazone in patients with type 2 diabetes and dyslipidemia. *Diabetes Care* 2005; **28**: 1547-1554

70 **Blind E**, Dunder K, de Graeff PA, Abadie E. Rosiglitazone: a European regulatory perspective. *Diabetologia* 2011; **54**: 213-218

71 **Woodcock J**, Sharfstein JM, Hamburg M. Regulatory action on rosiglitazone by the U.S. Food and Drug Administration. *N Engl J Med* 2010; **363**: 1489-1491

S- Editor Cheng JX **L- Editor** Cant MR **E- Editor** Zheng XM

World Journal of Cardiology

Online Submissions: http://www.wjgnet.com/1949-8462office
wjc@wjgnet.com
doi:10.4330/wjc.v3.i7.215

World J Cardiol 2011 July 26; 3(7): 215-218
ISSN 1949-8462 (online)

Calcium channels and iron uptake into the heart

Nipon Chattipakorn, Sirinart Kumfu, Suthat Fucharoen, Siriporn Chattipakorn

Nipon Chattipakorn, Sirinart Kumfu, Department of Physiology, Cardiac Electrophysiology Unit, Faculty of Medicine, Chiang Mai University, Chiang Mai 50200, Thailand
Nipon Chattipakorn, Sirinart Kumfu, Siriporn Chattipakorn, Cardiac Electrophysiology Research and Training Center, Faculty of Medicine, Chiang Mai University, Chiang Mai 50200, Thailand
Suthat Fucharoen, The Institute of Molecular Biosciences, Mahidol University, Bangkok 73170, Thailand
Siriporn Chattipakorn, Faculty of Dentistry, Chiang Mai University, Chiang Mai 50200, Thailand
Author contributions: All authors contributed equally to this work.
Supported by Thailand Research Fund grants RTA5280006 (Chattipakorn N), BRG5480003 (Chattipakorn S), the National Research Council of Thailand (Chattipakorn N), and the Thailand Research Fund Royal Golden Jubilee project (Kumfu S and Chattipakorn N)
Correspondence to: Nipon Chattipakorn, MD, PhD, Cardiac Electrophysiology Research and Training Center, Faculty of Medicine, Chiang Mai University, Chiang Mai 50200, Thailand. nchattip@gmail.com
Telephone: +66-53-945329 Fax: +66-53-945368
Received: April 19, 2011 Revised: July 4, 2011
Accepted: July 11, 2011
Published online: July 26, 2011

Abstract

Iron overload can lead to iron deposits in many tissues, particularly in the heart. It has also been shown to be associated with elevated oxidative stress in tissues. Elevated cardiac iron deposits can lead to iron overload cardiomyopathy, a condition which provokes mortality due to heart failure in iron-overloaded patients. Currently, the mechanism of iron uptake into cardiomyocytes is still not clearly understood. Growing evidence suggests L-type Ca^{2+} channels (LTCCs) as a possible pathway for ferrous iron (Fe^{2+}) uptake into cardiomyocytes under iron overload conditions. Nevertheless, controversy still exists since some findings on pharmacological interventions and those using different cell types do not support LTCC's role as a portal for iron uptake in cardiac cells. Recently, T-type Ca^{2+} channels (TTCC) have been shown to play an important role in the diseased heart. Although TTCC and iron uptake in cardiomyocytes has not been investigated greatly, a recent finding indicated that TTCC could be an important portal in thalassemic hearts. In this review, comprehensive findings collected from previous studies as well as a discussion of the controversy regarding iron uptake mechanisms into cardiomyocytes *via* calcium channels are presented with the hope that understanding the cellular iron uptake mechanism in cardiomyocytes will lead to improved treatment and prevention strategies, particularly in iron-overloaded patients.

Key words: Cardiomyocytes; L-type calcium channel; T-type calcium channels; Iron overload; Thalassemia

Peer reviewers: Morten Grunnet, PhD, Professor, Head of Drug Discovery Portfolio Management, NeuroSearch A/S, 2750 Ballerup, Denmark; Mohamed Chahine, PhD, Professeur Titulaire, Le Centre de Recherche Université Laval Robert-Giffard, Local F-6539, 2601 chemin de la Canardière, Québec G1J 2G3, Canada

Chattipakorn N, Kumfu S, Fucharoen S, Chattipakorn S. Calcium channels and iron uptake into the heart. *World J Cardiol* 2011; 3(7): 215-218 Available from: URL: http://www.wjgnet.com/1949-8462/full/v3/i7/215.htm DOI: http://dx.doi.org/10.4330/wjc.v3.i7.215

INTRODUCTION

Iron (Fe) is an essential element for all living organisms and plays a central role in many Fe-containing proteins such as in iron storage proteins (ferritin and hemosiderin), energy metabolism (cytochromes, mitochondrial aconitase and Fe-S proteins of the electron transport chain), cellular respiration (hemoglobin and myoglobin), and DNA synthesis (ribonucleotide reductase)[1-3]. However, under iron overload conditions the regulatory mechanism which keeps the balance between iron uptake

and iron excretion could be disrupted, causing an elevation of non-transferrin bound iron (NTBI) in the plasma of iron-overloaded patients[4,5]. NTBI is toxic and participates in the production of harmful hydroxyl radicals, which could cause severe cellular damage and organ dysfunction[1,2,6,7].

An excess of plasma iron can lead to iron accumulation in many organs including the heart[5]. Excessive iron accumulation in the heart can cause cardiac cellular damage known as iron-overload cardiomyopathy. This cardiac complication causes 71% of all deaths in thalassemia major patients[8]. Although iron chelation therapy is widely used for treating iron overload patients, iron overload cardiomyopathy is still the most common cause of mortality in these patients[9,10]. Even though the fundamental mechanisms for excessive iron uptake in the heart have been investigated for decades, the precise mechanism underlying cardiomyocyte dysfunction induced by iron overload is not clearly understood. Although several NTBI transporters have been proposed and are responsible for cellular iron uptake, recent evidence suggests that calcium channels may play an important role as a portal for cardiac iron uptake[11].

In this review, the role of L-type Ca^{2+} channels (LTCC) as well as T-type Ca^{2+} channels (TTCC) as iron transporters into the heart are presented. The consistent findings as well as discrepancies of results among various studies on iron uptake into cardiomyocytes *via* these calcium channels under various conditions are comprehensively reviewed and discussed.

LTCCS AS A PORTAL FOR IRON UPTAKE INTO CARDIOMYOCYTES

The L-type Ca^{2+} channel is a voltage-gated ion channel that plays a central role in cardiac and smooth muscle contraction[12]. LTCCs are heterotetrameric polypeptide complexes that are composed of $\alpha1$, $\alpha2/\delta$, β, and, in some tissues, γ subunits[12]. The Ca^{2+} channel $\alpha1$ subunit (170-240 ku) is organized into four homologous motifs (I -IV), with six transmembrane segments (S1-S6)[12]. Recently, 10 $\alpha1$ subunit genes have been identified including $Ca_V1.1$ ($\alpha1S$), 1.2 ($\alpha1C$), 1.3 ($\alpha1D$), 1.4 ($\alpha1F$), $Ca_V2.1$ ($\alpha1A$), 2.2 ($\alpha1B$), 2.3 ($\alpha1E$), $Ca_V3.1$ ($\alpha1G$), 3.2 ($\alpha1H$), and 3.3 ($\alpha1I$). For LTCCs, these can be divided into 4 classes: $Ca_V1.1$ ($\alpha1S$), 1.2 ($\alpha1C$), 1.3 ($\alpha1D$), and 1.4 ($\alpha1F$). In cardiac muscles, only the $\alpha1C$ (dihydropyridine-sensitive) subunit is expressed in high levels and is also called a high-voltage-activated channel[12]. LTCCs can be found in the heart and are primarily used for Ca^{2+} transport as well as playing an important role in the electrical activity of the heart. However, previous studies have shown that LTCCs can also transport other divalent cations including Fe^{2+}[13-15].

Several findings have been shown to support the role of LTCC in myocardial iron transport[11,15]. A study in an iron loaded perfused rat heart showed that iron uptake was increased by the LTCC agonist, Bay K 8644 and iron uptake was inhibited by the LTCC blocker, nifedipine[15]. Oudit *et al*[16] demonstrated that treatments with LTCC blockers such as amlodipine and verapamil could lead to the inhibition of LTCC current in cardiomyocytes, reduced myocardial iron accumulation, decreased oxidative stress and improved survival in iron-loaded mice. In addition, iron overloaded transgenic mice with cardiac-specific overexpression of LTCC were shown to have increased myocardial iron accumulation and oxidative stress, resulting in impaired cardiac function in comparison with control mice[16]. Furthermore, since the LTCC does not contain iron responsive elements (IREs) in the LTCC mRNA, it is not regulated by cellular iron levels under an iron overload condition. As a result, L-type Ca^{2+} currents were not decreased in iron overload conditions[16], confirming that the expression of LTCC was not regulated by the IRE. Furthermore, it has been shown in iron overloaded rats that the LTCC blocker diazepam could reduce mortality from iron overload without inhibition of iron absorption or urinary iron excretion[17].

In addition to the heart, a previous study also demonstrated that LTCC blockers verapamil and amlodipine did not decrease iron accumulation in the liver of mice with iron overload, and hypothesized that this was due to the fact that hepatocytes express minimal levels of LTCC[16]. However, a recent study by Ludwiczek and colleagues demonstrated that the LTCC blocker nifedipine could reduce iron accumulation in the liver of wild-type mice, but had no effect in divalent metal transporter 1 (DMT1) deficient mice, suggesting that this effect of nifedipine-mediated modulation of iron transport is *via* DMT1[18]. Nevertheless, these findings suggest that nifedipine could possibly be beneficial in iron overload cardiomyopathy.

DISCREPANCIES IN FINDINGS ON IRON UPTAKE INTO CARDIOMYOCYTES *VIA* LTCC

It is important to realize that not all reports regarding the mechanisms of iron uptake *via* LTCC are consistent. Despite strong evidence supporting the role of LTCC as a route for NTBI transport in the heart, Parkes and colleagues demonstrated otherwise[19]. In cultured rat neonatal myocytes, they demonstrated that LTCC blockers (nifedipine, verapamil, and diltiazem) did not alter iron uptake in these cells[19]. Our recent findings also demonstrated that the LTCC blocker verapamil could not prevent iron uptake into cultured adult mouse cardiomyocytes[20].

Several reasons to explain these inconsistent results may be drawn from previous reports. Most studies that support the role of LTCC for iron uptake in cardiomyocytes used freshly prepared cardiomyocytes taken from isolated perfused hearts[15] or *in vivo*[16]. However, a report that failed to show the role of LTCC in iron uptake into cardiomyocytes used cultured cardiomyocytes[19,20].

In cultured cardiomyocytes, it is possible that LTCC

may not fully develop compared with isolated cardiomyocytes obtained from the heart. If fully developed, it is also possible that the LTCC in cultured cardiomyocytes may not function properly. Furthermore, the ages of cultured cardiomyocytes could have played a role in this discrepancy.

In the light of these inconsistent findings, it is possible that cardiomyocytes obtained from different methods may have different cellular characteristics and properties. All of these proposed hypotheses have not been tested and will need to be further investigated to elucidate the definite mechanism of iron uptake into the heart and resolve these existing discrepancies.

TTCC AS A PORTAL FOR IRON UPTAKE INTO CARDIOMYOCYTES

TTCC have three isoforms: $Ca_v3.1$ (α1G), 3.2 (α1H), and 3.3 (α1I) that are localized to the brain, kidney, and heart and are also called low-voltage-activated channels[21]. It has been shown that only $Ca_v3.1$ and $Ca_v3.2$ are expressed in the heart[21]. TTCCs have been reported to be functionally expressed only in embryonic hearts and disappear in adults[22]. TTCC can be found abundantly only in sinoatrial pacemaker cells and Purkinje fibers of many species in adult hearts and are important for the maintenance of pacemaker activity[21,23]. However, TTCC currents and expression have been demonstrated to reappear and play an important pathological role in diseased hearts with conditions such as ventricular hypertrophy[21,24,25] and post-myocardial infarction[26]. The increased TTCC expression has been shown to contribute to the progression of heart failure[21].

Growing evidence indicates that TTCC blockers could be beneficial in diseased hearts. Recently, Horiba and colleagues demonstrated that the blockade of Ca^{2+} entry into cardiomyocytes *via* TTCC using the TTCC blocker efonidipine could block signal transduction involved in cardiac hypertrophy[27]. In addition, a study in a mouse model of dilated cardiomyopathy has shown that a TTCC blocker could restore the resting membrane potential, and reduce the number of premature ventricular contractions and ventricular tachycardia, thus reducing the incidence of sudden death in these mice[28]. These findings suggest that TTCC blockade may be potentially useful for the prevention of sudden death in patients with heart failure[28]. It is known that iron overload conditions can lead to increased iron uptake into cardiomyocytes, resulting in cardiac hypertrophy and failure[29-32]. However, it is not known if TTCC blockers could be cardioprotective in this type of cardiomyopathy.

Recently, our study using cultured cardiomyocytes taken from the heart of thalassemic mice demonstrated that intracellular iron accumulation in cultured ventricular myocytes of thalassemic mice was significantly higher than in wild type (WT) cells[20]. These findings suggest that thalassemic cardiomyocytes could have pathways which can greatly uptake iron into the cells more than that in WT cells. In addition, under an iron overloaded condition, our results demonstrated that the TTCC blocker, efonidipine, could prevent iron uptake into cultured thalassemic cardiomyocytes[20]. Although efonidipine is not a selective TTCC blocker and could also block LTCC, its efficacy in blocking TTCC is greater than that of LTCC[21]. In that study, since verapamil could not prevent iron uptake when efonidipine could, these findings suggested that TTCC could play a significant role in iron uptake into cardiomyocytes in this thalassemic cardiomyocyte model[20]. Moreover, our microarray data demonstrated that the TTCC genes were up-regulated in thalassemic hearts, which is well correlated with the iron uptake results, suggesting that TTCCs could play an important role in iron uptake in thalassemic hearts, and that their re-expression could be due to the pathological state of a thalassemic heart itself or from the iron-overloaded condition, or both.

Since iron overload patients can develop cardiomyopathy and heart failure[33-35], it is important that the association between iron overload, TTCC expression/function and cardiac complications be determined. Future studies in both basic and clinical research are needed to warrant the clinical usefulness of TTCC blockers in the prevention and treatment of iron overload cardiomyopathy particularly in thalassemia patients.

CONCLUSION

Iron overload is a serious and fatal complication in many diseases including iron-overload cardiomyopathy in thalassemia patients. Although pathways for cellular iron uptake have been investigated for many decades, its mechanism is still not clearly understood. In the past few years, findings regarding new possible pathways for cellular iron uptake have been suspected, including LTCC and TTCC. However, their definite roles as iron transporters in cardiomyocytes are still debated. Understanding the mechanism by which iron enters cardiac cells is very important, since it will provide us with the knowledge to be used in developing better treatment and prevention strategies in iron overloaded patients.

REFERENCES

1 **Andrews NC.** Disorders of iron metabolism. *N Engl J Med* 1999; **341**: 1986-1995
2 **Hentze MW,** Muckenthaler MU, Andrews NC. Balancing acts: molecular control of mammalian iron metabolism. *Cell* 2004; **117**: 285-297
3 **Napier I,** Ponka P, Richardson DR. Iron trafficking in the mitochondrion: novel pathways revealed by disease. *Blood* 2005; **105**: 1867-1874
4 **Esposito BP,** Breuer W, Sirankapracha P, Pootrakul P, Hershko C, Cabantchik ZI. Labile plasma iron in iron overload: redox activity and susceptibility to chelation. *Blood* 2003; **102**: 2670-2677
5 **Templeton DM,** Liu Y. Genetic regulation of cell function in response to iron overload or chelation. *Biochim Biophys Acta* 2003; **1619**: 113-124
6 **Gutteridge JM,** Rowley DA, Griffiths E, Halliwell B. Low-molecular-weight iron complexes and oxygen radical reac-

tions in idiopathic haemochromatosis. *Clin Sci* (Lond) 1985; **68**: 463-467
7 **Gao X,** Qian M, Campian JL, Marshall J, Zhou Z, Roberts AM, Kang YJ, Prabhu SD, Sun XF, Eaton JW. Mitochondrial dysfunction may explain the cardiomyopathy of chronic iron overload. *Free Radic Biol Med* 2010; **49**: 401-407
8 **Wood JC,** Enriquez C, Ghugre N, Otto-Duessel M, Aguilar M, Nelson MD, Moats R, Coates TD. Physiology and pathophysiology of iron cardiomyopathy in thalassemia. *Ann N Y Acad Sci* 2005; **1054**: 386-395
9 **Modell B,** Khan M, Darlison M. Survival in beta-thalassaemia major in the UK: data from the UK Thalassaemia Register. *Lancet* 2000; **355**: 2051-2052
10 **Li CK,** Luk CW, Ling SC, Chik KW, Yuen HL, Li CK, Shing MM, Chang KO, Yuen PM. Morbidity and mortality patterns of thalassaemia major patients in Hong Kong: retrospective study. *Hong Kong Med J* 2002; **8**: 255-260
11 **Oudit GY,** Trivieri MG, Khaper N, Liu PP, Backx PH. Role of L-type Ca2+ channels in iron transport and iron-overload cardiomyopathy. *J Mol Med* (Berl) 2006; **84**: 349-364
12 **Catterall WA.** Structure and regulation of voltage-gated Ca2+ channels. *Annu Rev Cell Dev Biol* 2000; **16**: 521-555
13 **Lansman JB,** Hess P, Tsien RW. Blockade of current through single calcium channels by Cd2+, Mg2+, and Ca2+. Voltage and concentration dependence of calcium entry into the pore. *J Gen Physiol* 1986; **88**: 321-347
14 **Hess P,** Lansman JB, Tsien RW. Calcium channel selectivity for divalent and monovalent cations. Voltage and concentration dependence of single channel current in ventricular heart cells. *J Gen Physiol* 1986; **88**: 293-319
15 **Tsushima RG,** Wickenden AD, Bouchard RA, Oudit GY, Liu PP, Backx PH. Modulation of iron uptake in heart by L-type Ca2+ channel modifiers: possible implications in iron overload. *Circ Res* 1999; **84**: 1302-1309
16 **Oudit GY,** Sun H, Trivieri MG, Koch SE, Dawood F, Ackerley C, Yazdanpanah M, Wilson GJ, Schwartz A, Liu PP, Backx PH. L-type Ca2+ channels provide a major pathway for iron entry into cardiomyocytes in iron-overload cardiomyopathy. *Nat Med* 2003; **9**: 1187-1194
17 **Fassos FF,** Berkovitch M, Daneman N, Koren L, Cameron R, Klein J, Falcitelli C, St Louis P, Daneman R, Koren G. The efficacy of diazepam in the treatment of acute iron overload in rats. *Can J Physiol Pharmacol* 1998; **76**: 895-899
18 **Ludwiczek S,** Theurl I, Muckenthaler MU, Jakab M, Mair SM, Theurl M, Kiss J, Paulmichl M, Hentze MW, Ritter M, Weiss G. Ca2+ channel blockers reverse iron overload by a new mechanism via divalent metal transporter-1. *Nat Med* 2007; **13**: 448-454
19 **Parkes JG,** Olivieri NF, Templeton DM. Characterization of Fe2+ and Fe3+ transport by iron-loaded cardiac myocytes. *Toxicology* 1997; **117**: 141-151
20 **Kumfu S,** Chattipakorn S, Srichairatanakool S, Settakorn J, Fucharoen S, Chattipakorn N. T-type calcium channel as a portal of iron uptake into cardiomyocytes of beta-thalassemic mice. *Eur J Haematol* 2011; **86**: 156-166
21 **Vassort G,** Talavera K, Alvarez JL. Role of T-type Ca2+ channels in the heart. *Cell Calcium* 2006; **40**: 205-220
22 **Lory P,** Bidaud I, Chemin J. T-type calcium channels in differentiation and proliferation. *Cell Calcium* 2006; **40**: 135-146
23 **Niwa N,** Yasui K, Opthof T, Takemura H, Shimizu A, Horiba M, Lee JK, Honjo H, Kamiya K, Kodama I. Cav3.2 subunit underlies the functional T-type Ca2+ channel in murine hearts during the embryonic period. *Am J Physiol Heart Circ Physiol* 2004; **286**: H2257-H2263
24 **Nuss HB,** Houser SR. T-type Ca2+ current is expressed in hypertrophied adult feline left ventricular myocytes. *Circ Res* 1993; **73**: 777-782
25 **Martínez ML,** Heredia MP, Delgado C. Expression of T-type Ca(2+) channels in ventricular cells from hypertrophied rat hearts. *J Mol Cell Cardiol* 1999; **31**: 1617-1625
26 **Huang B,** Qin D, Deng L, Boutjdir M, E1-Sherif N. Reexpression of T-type Ca2+ channel gene and current in post-infarction remodeled rat left ventricle. *Cardiovasc Res* 2000; **46**: 442-449
27 **Horiba M,** Muto T, Ueda N, Opthof T, Miwa K, Hojo M, Lee JK, Kamiya K, Kodama I, Yasui K. T-type Ca2+ channel blockers prevent cardiac cell hypertrophy through an inhibition of calcineurin-NFAT3 activation as well as L-type Ca2+ channel blockers. *Life Sci* 2008; **82**: 554-560
28 **Kinoshita H,** Kuwahara K, Takano M, Arai Y, Kuwabara Y, Yasuno S, Nakagawa Y, Nakanishi M, Harada M, Fujiwara M, Murakami M, Ueshima K, Nakao K. T-type Ca2+ channel blockade prevents sudden death in mice with heart failure. *Circulation* 2009; **120**: 743-752
29 **Hausse AO,** Aggoun Y, Bonnet D, Sidi D, Munnich A, Rötig A, Rustin P. Idebenone and reduced cardiac hypertrophy in Friedreich's ataxia. *Heart* 2002; **87**: 346-349
30 **Wood JC,** Otto-Duessel M, Gonzalez I, Aguilar MI, Shimada H, Nick H, Nelson M, Moats R. Deferasirox and deferiprone remove cardiac iron in the iron-overloaded gerbil. *Transl Res* 2006; **148**: 272-280
31 **Yang T,** Brittenham GM, Dong WQ, Levy MN, Obejero-Paz CA, Kuryshev YA, Brown AM. Deferoxamine prevents cardiac hypertrophy and failure in the gerbil model of iron-induced cardiomyopathy. *J Lab Clin Med* 2003; **142**: 332-340
32 **Yang T,** Dong WQ, Kuryshev YA, Obejero-Paz C, Levy MN, Brittenham GM, Kiatchoosakun S, Kirkpatrick D, Hoit BD, Brown AM. Bimodal cardiac dysfunction in an animal model of iron overload. *J Lab Clin Med* 2002; **140**: 263-271
33 **Olivieri NF,** Nathan DG, MacMillan JH, Wayne AS, Liu PP, McGee A, Martin M, Koren G, Cohen AR. Survival in medically treated patients with homozygous beta-thalassemia. *N Engl J Med* 1994; **331**: 574-578
34 **Olivieri NF.** The beta-thalassemias. *N Engl J Med* 1999; **341**: 99-109
35 **Brittenham GM,** Griffith PM, Nienhuis AW, McLaren CE, Young NS, Tucker EE, Allen CJ, Farrell DE, Harris JW. Efficacy of deferoxamine in preventing complications of iron overload in patients with thalassemia major. *N Engl J Med* 1994; **331**: 567-573

S- Editor Cheng JX **L- Editor** O'Neill M **E- Editor** Zheng XM

European Journal of Haematology 86 (156–166)

ORIGINAL ARTICLE

T-type calcium channel as a portal of iron uptake into cardiomyocytes of beta-thalassemic mice

Sirinart Kumfu[1], Siriporn Chattipakorn[1,2], Somdet Srichairatanakool[1], Jongkolnee Settakorn[1], Suthat Fucharoen[3], Nipon Chattipakorn[1,4]

[1]Cardiac Electrophysiology Research and Training Center, Department of Physiology, Faculty of Medicine, Chiang Mai University, Chiang Mai; [2]Department of Oral Biology and Diagnostic Science, Faculty of Dentistry, Chiang Mai University, Chiang Mai; [3]Thalassemia Research Center, Mahidol University, Bangkok; [4]Biomedical Engineering Center, Chiang Mai University, Chiang Mai, Thailand

Abstract

Objectives: Iron-overload condition can be found in β-thalassemic patients with regular blood transfusion, leading to iron deposition in various organs including the heart. Elevated cardiac iron causes iron-overload cardiomyopathy, a condition that provokes mortality because of heart failure in patients with thalassemia. Previous studies demonstrated that myocardial iron uptake may occur via L-type calcium channels (LTCCs). However, direct evidence regarding the claimed pathway in thalassemic cardiomyocytes has never been investigated. *Methods:* Hearts from genetic-altered β-thalassemic mice and adult wild-type mice were used for cultured ventricular cardiomyocytes. Blockers for LTCC, T-type calcium channel (TTCC), transferrin receptor1 (TfR1), and divalent metal transporter1 (DMT1) were used, and quantification of cellular iron uptake under various iron loading conditions was performed by Calcein-AM fluorescence assay. Microarray analysis was performed to investigate gene expressions in the hearts of these mice. *Results:* This study demonstrated that iron uptake under iron-overload conditions in the cultured ventricular myocytes of thalassemic mice was greater than that of wild-type cells ($P < 0.01$). TTCC blocker, efonidipine, and an iron chelator, deferoxamine, could prevent iron uptake into cultured cardiomyocytes, whereas blockers of TfR1, DMT1, and LTCC could not. Microarray analysis from thalassemic hearts demonstrated highly up-regulated genes of TTCC, zinc transporter, and transferrin receptor2. *Conclusions:* Our findings indicated that iron uptake mechanisms in cultured thalassemic cardiomyocytes are mainly mediated by TTCC, suggesting that TTCC is the important pathway for iron uptake in this cultured thalassemic cardiomyocyte model.

Key words cardiomyocytes; T-type calcium channel; L-type calcium channel; iron overload; thalassemia

Correspondence Nipon Chattipakorn, MD, PhD, Cardiac Electrophysiology Research and Training Center, Faculty of Medicine, Chiang Mai University, Chiang Mai 50200, Thailand. Tel: +66 53 945329; Fax: +66 53 945368; e-mail: nchattip@gmail.com

This work was supported by grants from the Thailand Research Fund RTA 5280006 (N.C.), RMU 5180007 (S.C.), TRF (S.F.) and the National Research Council of Thailand (N.C.).

Accepted for publication 1 November 2010 doi:10.1111/j.1600-0609.2010.01549.x

Iron overload conditions can be found in patients with thalassemia who receive regular blood transfusion (1, 2). Under physiologic condition, plasma transferrin binds to plasma iron, resulting in iron uptake into cells via endocytosis of transferrin–transferrin receptor pathway, thus reducing plasma free-iron level (3). Under iron excess condition, non-transferrin-bound iron (NTBI) can be found in plasma and can lead to iron accumulation in various organs (4–6). In the heart, iron deposit can lead to iron overload cardiomyopathy, a condition that is mainly responsible for cardiac dysfunction and mortality in patients with thalassemia (5–7). Although pathways of iron entry into the heart have been investigated for decades, the precise mechanisms by which NTBI gets into cardiomyocytes under iron overload conditions are still not clearly understood.

Several cellular iron transporters such as divalent metal transporter-1 (DMT1) and transferrin receptor

(TfR1) have been shown to be portals for iron transport into cells such as enterocytes and hepatocytes (3). However, in the heart, it has been shown that under iron-loading conditions, TfR1 or DMT1 mRNA and protein expressions were suppressed (8–11), suggesting that they may not be the major portals for iron entry in cardiomyocytes under iron-overload conditions. However, its role in thalassemic cardiomyocytes is not known.

In the past decades, L-type calcium channels (LTCC) has been proposed as a possible portal for iron uptake in cardiomyocytes (12, 13). The role of LTCC in mediating iron uptake into cardiomyocytes has been demonstrated using LTCC agonist to increase iron uptake in isolated perfused rat heart (12) and LTCC blockers to reduce intracellular myocardial iron accumulation in an *in vivo* model (13). Despite this evidence regarding the role of LTCC as an iron portal, inconsistent findings exist that failed to demonstrate LTCC as a portal for iron uptake into cardiomyocytes (14). Furthermore, NTBI transportation via LTCC into thalassemic cardiomyocytes has never been investigated.

In the heart, T-type Ca^{2+} channels (TTCC) have been reported to exist and contribute to cardiac electrical activity during early embryonic state (15). However, under physiologic condition, they normally disappear shortly after birth and cannot be found in the cardiomyocytes (16). However, TTCC current has been shown to reappear in ventricular myocytes under some pathological processes such as ventricular hypertrophy (17) and postmyocardial infarction (18). However, the re-expression of TTCC in thalassemic hearts as well as the role of TTCC as a portal for iron uptake in ventricular thalassemic cardiomyocytes has never been investigated.

It is not known whether iron uptake mechanism in thalassemic cardiomyocytes would be similar or different than that in normal cardiomyocytes. Therefore, in this study, we sought to determine the iron uptake mechanisms using cultured thalassemic cardiomyocytes prepared from the hearts of adult β-thalassemic mice. We investigated the effects of LTCC and TTCC blockers, TfR1 blocker, DMT1 blocker, and iron chelator on iron uptake into thalassemic cardiomyocytes. Iron uptake was determined under various iron-loaded concentrations. In addition, microarray analysis on thalassemic hearts was performed to identify the up-regulation and down-regulation of genes that regulate iron transport and cardiac ion channels, compared to the wild-type hearts.

Materials and methods

Animal models

All animal studies were approved by the Institutional Animal Care and Use Committee (IACUC) of the Faculty of Medicine, Chiang Mai University (No. 44/2552) in compliance with NIH guidelines. The investigation conforms with the *Guide for the Care and Use of Laboratory Animals* published by the US National Institutes of Health (NIH Publication No. 85-23, revised 1996). Three types of adult C57/BL6 mice (9–12 months old): wild type (mu$\beta^{+/+}$, WT, $n = 42$), heterozygous β^{KO} type (mu$\beta^{th\text{-}3/+}$, HT, $n = 43$), and double heterozygous β^{KO} with HbE (hu$\beta^{E/+}$, mu$\beta^{Th\text{-}3/+}$, DH, $n = 38$), were used in this study (19, 20). All animals were housed in temperature- and humidity-controlled rooms with 12-h light/dark cycles. We have shown previously that HT mice had reduced hemoglobin level, increased serum iron (SI), increased reactive oxygen species (ROS) production, and depressed heart rate variability (HRV) (21), the clinical pictures that are similar to thalassemia intermedia in patients with thalassemia. Furthermore, our previous study demonstrated that the DH mice with depressed HRV had normal hemoglobin level, SI, and ROS production, indicating the altered cardiac autonomic control (21). Each mouse was genetically characterized prior to its entry into the study (19, 20).

Cultured cardiomyocytes

Primary cultured cardiomyocytes were obtained from HT, DH, and WT adult C57/BL6 mice at 9–12 months of age. Each mouse was anesthetized with isoflurane (Abbott Laboratories, Chicago, IL, USA) and the heart was removed. The ventricles were cut and incubated in Ca^{2+}-Mg^{2+} free Hank's balanced salt solution containing 2 mg/ml collagenase type 2 (PAA Laboratories, New Bedford, MA, USA) for 15 min. Cardiomyocytes were isolated by incubation with 0.25% trypsin–EDTA (Sigma-Aldrich, St. Louis, MO, USA) for 15 min. The cell suspension was centrifuged at 521 ***g*** for 5 min. After the centrifugation, the cell pellets were mixed and resuspended in completed M199 medium containing 20% fetal bovine serum with 1% penicillin–streptomycin (22). The cell suspension was plated on culture flask and incubated at 37°C in a humidified atmosphere with 5% CO_2 for 10 d. Although these 10-d-old cardiomyocytes have been shown to undergo a morphological transformation and increase cell size, their cardiac phenotype is well preserved (23–25).

Immunocytochemistry methods

To identify the cardiomyocytes in cultured cells, the immunocytochemistry methods were used (26). All genotypes of cultured cardiomyocytes (WT, HT, and DH) were trypsinized, washed, and centrifuged at 3000 ***g*** for 5 min at 25°C. Then, the cells were plated on coverslip overnight, before they were fixed with 4% paraformaldehyde for 30 min and kept frozen until they were used for

immunocytochemistry. The cells were washed three times with Tris-buffered saline (TBS) and incubated for 1 h with blocking solution (BS) containing 1.5% normal goat serum in TBS. To identify the cardiomyocytes, those fixed cells were subject to immunostaining with primary antibodies directed against myosin light chain-2 (MLC-2) (Santa Cruz Biotechnology, Santa Cruz, CA, USA) and GATA-binding protein-4 (GATA-4) (Santa Cruz Biotechnology). Both MLC-2 and GATA-4 have been shown to be the markers for cardiomyocytes (27).

Iron treatment of the cardiomyocytes

Ferric ammonium citrate (FAC) at various concentrations ranging from 0 to 2284.8 μM (0–160 μg/ml) co-administered with 1 mM ascorbic acid (AA), which represents ascorbate-reduced form of iron (Fe^{2+}), was added to the culture medium of all types of cardiomyocytes for 48 h. The amount of iron uptake into cultured cells was detected using Calcein-AM fluorescence assay (28, 29).

Pharmacological interventions of iron uptake into cardiomyocytes

To determine the effect of iron chelator desferoxamine (DFO: Novartis Ltd., East Hanover, CA, USA) on iron-loaded cardiomyocytes, the cells were loaded with a combination of 285.6 μM FAC + 1 mM AA (or 20 μg/ml Fe^{2+}), i.e. a concentration similar to the plasma iron level in patients with thalassemia (8), and DFO at concentrations of 142.8 and 285.6 μM for 48 h (11, 14).

To determine the roles of LTCC, TTCC, TfR1, and DMT1 on iron uptake, the cells were exposed to (i) various concentrations of LTCC blocker (verapamil) (Sigma-Aldrich) ranging from 0 to 80 μM and (ii) various concentrations of TTCC blocker (efonidipine) (Sigma-Aldrich) ranging from 0 to 20 μM. Although efonidipine can block both LTCC and TTCC, it has been shown that efonidipine could block TTCC more effectively than LTCC (30). Comparisons between the effects of verapamil and efonidipine on iron uptake would allow us to differentiate the effects of these two calcium channel blockers, (iii) anti-TfR1 antibody (Santa Cruz Biotechnology) at 5 and 10 μg/ml and (iv) ebselen [DMT1 blocker (31)] at 12.5 and 25 μM, for 60 min, before loaded with FAC + 1 mM AA, which represents Fe^{2+}, at 285.6 μM for 48 h (14). Then, the cells were analyzed for the iron uptake into cardiomyocytes by using Calcein-AM fluorescence assay (28, 29).

Cell viability determination with methyl thiazol tetrazolium (MTT) assay

In the present study, MTT assay was used to determine the viability of cells and the toxicity of all substances used in cultured cardiomyocytes (32). After the cardiomyocytes had been plated in a multiwell microtiter plate at 5000 cells/well and incubated at 37°C for 24 h, they were treated with FAC + 1 mM AA solutions at various concentrations of 0–2284.8 μM (Fe^{2+}, 0–160 μg/ml), or iron chelator solutions (DFO) at concentrations of 0–285.6 μM, or LTCC blocker solutions (verapamil) at concentrations of 0–80 μM, or TTCC blocker solutions (efonidipine) at concentrations of 0–20 μM, or anti-TfR1 antibody at 5–10 μg/ml, or ebselen at 12.5–25 μM, and plated at 37°C for 48 h. After each treatment, cultured cardiomyocytes were treated with MTT reagents to investigate the cell viability. The MTT reagent at 5 mg/ml (15 μL) was added to the treated cells and further incubated for 4 h. The reaction product, blue-colored formazan, was extracted with dimethyl sulphoxide (DMSO) (200 μL), and the absorbance was read at 540/630 nm using a microtiter plate reader (Synergy HT BIO-TEK, Winooski, VT, USA). Viable cells reduced MTT [3-(4,5-dimethylthiazol-2-yl)-2,5-diphenyl tetrazolium bromide] from a yellow water-soluble dye to an insoluble formazan product of dark blue color (32). The number of viable cells was normalized and compared with untreated cells, and the data were expressed as percentage of cell viability (32). All samples were assayed in triplicate, and the mean for each experiment was determined.

Calcein-AM fluorescence assay

To determine the amount of iron uptake into cardiomyocytes, the Calcein-AM fluorescence assay was used (28, 29). Calcein-AM could easily diffuse into the cell through the cell membrane of viable cells owing to its enhanced hydrophobicity compared to Calcein. After Calcein-AM permeated into the cytoplasm, it was hydrolyzed by esterases to become Calcein, which remained inside the cell. Fluorescence intensity of Calcein was quenched by labile iron inside the cell (28, 29). If the labile iron level inside the cells was high, the fluorescence intensity would be low and *vice versa*. After the iron-loaded treatments, cells were washed with phosphate-buffered saline (PBS) and incubated with the fluorescent metal sensor, calcein-AM (5 μM) (Sigma-Aldrich), at 37°C for 30 min. Cells were washed with PBS and were measured for the fluorescence intensity with fluorescence plate reader at 485-nm excitation and 530-nm emission filters (28, 29). Calcein-loaded cells that were shown in the form of fluorescence intensity (FI) were inversely correlated with intracellular iron. During the assay, cell viability was always greater than 95% and was unchanged throughout the process.

RNA isolation for microarray analysis

The heart samples of HT ($n = 5$) and WT ($n = 4$) mice were removed. The RNeasy RNA isolation kit (Qiagen, Valencia, CA, USA) was used to obtain total heart RNA, and the RNase-free DNase (Qiagen) was used to remove the residual DNA from the sample. The optical density (OD) measurements at 260 and 280 nm were used to determine RNA concentration and purity (33). All samples had an OD260/OD280 ratio of 1.80 or higher.

Microarray studies were performed by Codelink™ Expression Bioarray System (Amersham Biosciences, Buckinghamshire, UK). Heart specimens derived from HT and WT C57BL/6 mice were subject to total RNA extraction. In each sample, 100 ng of total RNA was amplified using the Codelink Expression Assay Reagent kit (Amersham Biosciences), following the manufacturer's instructions. The *in vitro* transcription reaction was conducted with labeling of the cRNA by biotinylation. The labeled and amplified cRNA was hybridized to Codelink Uniset Mouse 20K I Bioarray slide (20 000 genes, Amersham Biosciences) at 37°C for 18 h, according to Codelink hybridization protocol. The arrays were washed and then stained with 2 μg/ml cyanine5-streptavidin (Amersham Biosciences). The GenePix Array Scanner (Molecular Devices, Sunnyvale, CA, USA) was used to scan the arrays. Samples were analyzed using Wayne State University Intelligent Biosystems Software (Department of Computer Science, Wayne State University, MI, USA).

Statistical analysis

All iron uptake experiments were performed in triplicate. Data were reported as the mean ± standard error of mean (SEM) and were processed using SPSS (Statistical Package for Social Sciences, Chicago, IL, USA) release 13.0 for Windows. One-way ANOVA analyses and Student's *t*-test were performed for group comparisons. *P*-value < 0.05 was considered statistical significance.

Results

Identification of cardiomyocytes and effects of iron overload in cardiomyocytes

Positive staining of both MLC-2 and GATA-4 was found in all types (WT, HT, and DH) of cultured cells, indicating that these cells were cardiomyocytes (Fig. 1). Negative control without primary antibody incubation was also performed and demonstrated that no positive staining was observed. At the baseline level, intracellular iron accumulation in the cultured ventricular myocytes of thalassemic (both HT and DH) mice was significantly higher than those of WT cells (Fig. 2). Under iron-overload condition, iron uptake into all types of cardiomyocytes was in a dose-dependent manner (Fig. 2).

Effects of iron chelator, deferoxamine (DFO), on iron uptake in cardiomyocytes

When DFO was added, it could chelate ascorbate-reduced form of iron from culture medium and led to an increase in Calcein fluorescence intensity, indicating that DFO treatment could decrease iron entry into cultured cardiomyocytes (Fig. 3). This effect of DFO was also in a dose-dependent manner. This finding suggested that DFO could inhibit ascorbate-reduced form of iron uptake into all types of cultured cardiomyocytes and confirmed that the Calcein-AM method used in this study is an appropriate method for measuring intracellular labile iron in thalassemic cardiomyocytes.

Effect of LTCC blocker, verapamil, on iron uptake in cardiomyocytes

To investigate whether LTCC was a possible portal for iron uptake into cardiomyocytes in this cultured cardiomyocyte model, verapamil, the LTCC blocker, co-administered with FAC + AA was added to all types of cultured cardiomyocytes. Our results demonstrated that verapamil, at various concentrations, could not prevent ascorbate-reduced form of iron uptake into any types of cardiomyocytes (Fig. 4). These findings suggested that iron uptake mechanisms in cultured cardiomyocytes were not mainly mediated by LTCC.

Effects of TfR1 and DMT1 on iron uptake into cardiomyocytes

Although previous studies demonstrated that TfR1 and DMT1 expressions in the heart were limited under iron-overload condition (8–11), those studies were carried in normal cardiomyocytes. Their roles in thalassemic cardiomyocytes have never been tested. To test whether TfR1 and DMT1 are involved in iron uptake into thalassemic cardiomyocytes, anti-TfR1 antibody and ebselen (DMT1 blocker) (34) were used to determine the roles of TfR1 and DMT1 for iron uptake into iron-loaded cardiomyocytes. Our results demonstrated that anti-TfR1 antibody at concentrations of 5 and 10 μg/ml and ebselen at concentration of 12.5 and 25 μM could not prevent iron uptake into any types of cardiomyocytes (Fig. 5). These findings indicate that TfR1 and DMT1 were not the common pathways for iron uptake into cultured cardiomyocytes under iron-overload condition.

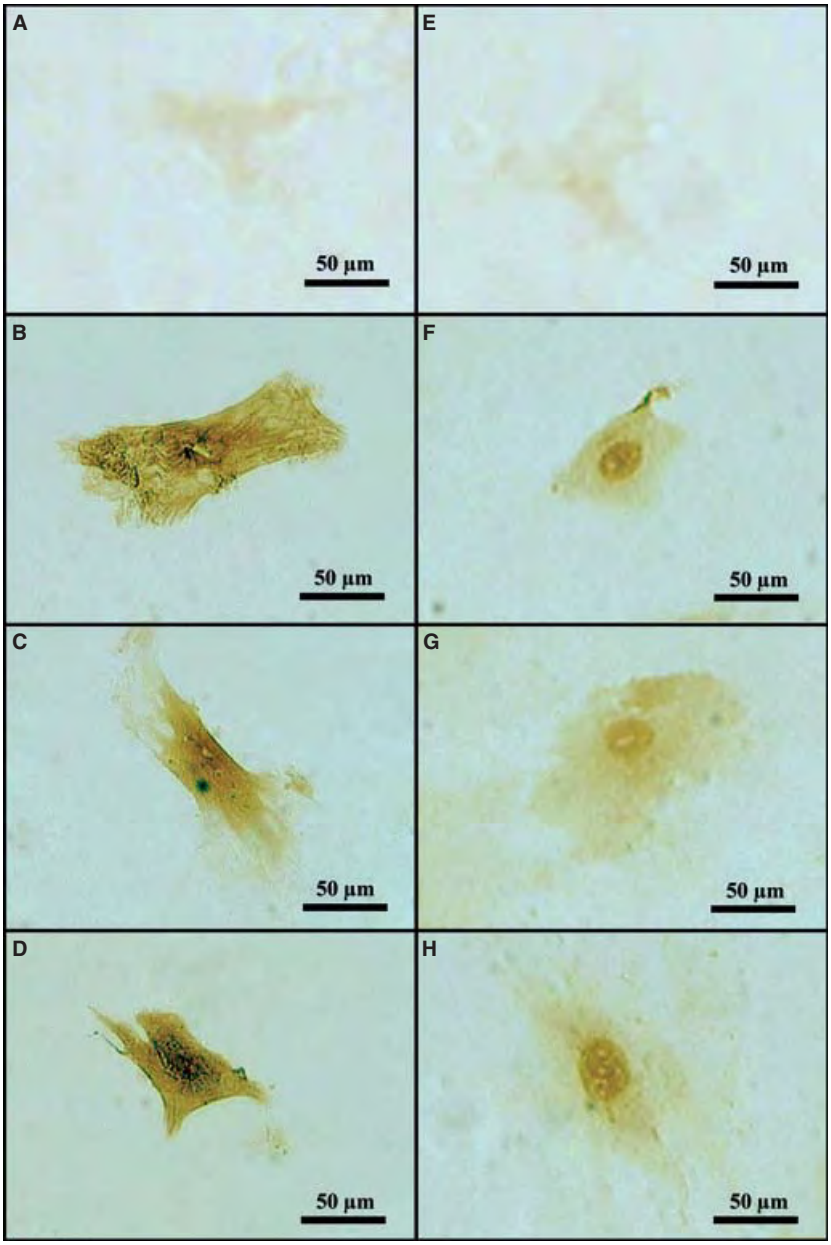

Figure 1 Immunoperoxidase staining of cultured cardiomyocytes. Negative control without primary antibody for myosin light chain 2 (MLC-2) is shown in (A). Positive MLC-2 staining can be seen in the cytoplasm of cardiomyocytes taken from (B) wild type (WT), (C) double heterozygous β^{KO} with HbE (DH), and (D) heterozygous β^{KO} type (HT). Negative control without primary antibody for GATA-binding protein 4 (GATA-4) is shown in (E). Positive GATA-4 staining can be seen in the nucleus of cardiomyocytes taken from WT (F), DH (G), and HT (H).

Effects of TTCC blocker, efonidipine, on iron uptake in cardiomyocytes

The role of TTCC on ascorbate-reduced form of iron transportation in ventricular thalassemic cardiomyocytes has never been investigated. Therefore, we further investigated whether TTCC was a possible portal for iron uptake in this cultured cardiomyocyte model. To test this hypothesis, efonidipine, the TTCC blocker, co-administered with FAC + AA was added to all types of cultured cardiomyocytes. Our results demonstrated that efonidipine, at all tested concentrations, could prevent ascorbate-reduced form of iron uptake into all types of cardiomyocytes ($P < 0.05$) (Fig. 6). Moreover, efonidipine at 20 μM could prevent iron uptake into HT cardiomyocytes greater than that in DH and WT cells ($P < 0.05$). Furthermore, efonidipine at 10 μM could prevent iron uptake into HT cells greater than that in WT cells ($P < 0.05$). These findings suggested that iron uptake mechanisms in cultured thalassemic cardiomyocytes were mainly mediated by TTCC.

Cytotoxic effects of treated reagents in cardiomyocytes

The cytotoxic effect of all reagents used in this study (FAC + AA, DFO, verapamil, efonidipine, anti-TfR1

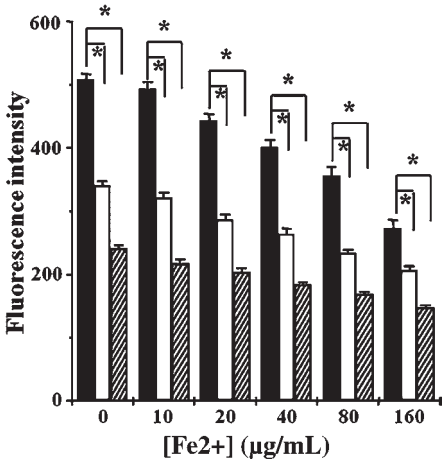

Figure 2 Iron uptake into cardiomyocytes (n = 9/group). Cardiomyocytes from WT (black bar), DH (white bar), and HT (dashed bar) were plated and loaded with various concentrations of ferric ammonium citrates with 1 mM ascorbic acid (FAC ± AA) for 48 h. Iron uptake into cardiomyocytes was determined using Calcein-AM fluorescence assay. Data were presented as mean ± SEM. $^{*}P < 0.01$ vs. WT cells.

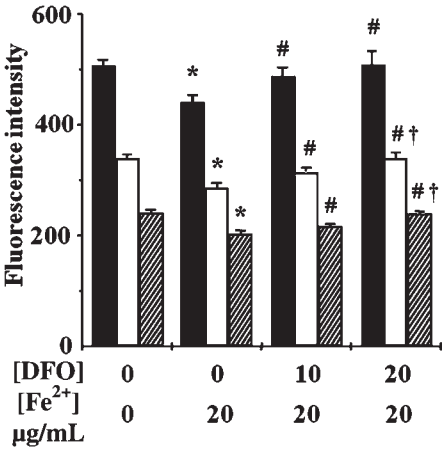

Figure 3 Effects of an iron chelator, desferoxamine (DFO), on iron uptake into cardiomyocytes (n = 9/group). Cardiomyocytes from WT (black bar), DH (white bar), and HT (dashed bar) were plated and loaded with the combination of 285.6 μM (20 μg/ml) ferric ammonium citrate with 1 mM ascorbic acid (FAC ± AA) and various concentrations of DFO (0–285.6 μM) for 48 h. Cellular iron uptake into cardiomyocytes was determined using Calcein-AM fluorescence assay. Data were presented as mean ± SEM. $^{*}P < 0.05$ vs. control (non-iron-treated group) of the same cell type, $^{\#}P < 0.05$ vs. iron-treated group of the same cell type without DFO, $^{\dagger}P < 0.01$ vs. DFO 10-μg/ml group of the same cell type.

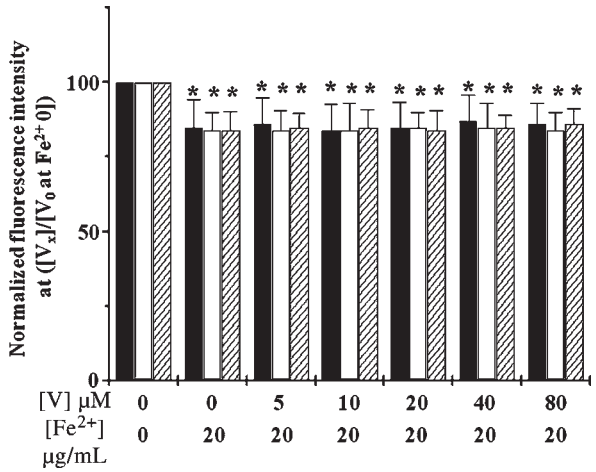

Figure 4 Effects of LTCC blocker, verapamil (V), on iron uptake into cardiomyocytes (n = 9/group). Cardiomyocytes from WT (black bar), DH (white bar), and HT (dashed bar) were plated and exposed to various concentrations of verapamil (0–80 μM) for 60 min before loaded with 285.6 μM (20 μg/ml) ferric ammonium citrate with 1 mM ascorbic acid (FAC ± AA) for 48 h. Cellular iron uptake was determined using Calcein-AM fluorescence assay. Data were presented as mean ± SEM. $^{*}P < 0.05$ vs. control (non-iron-treated group) of the same cell type.

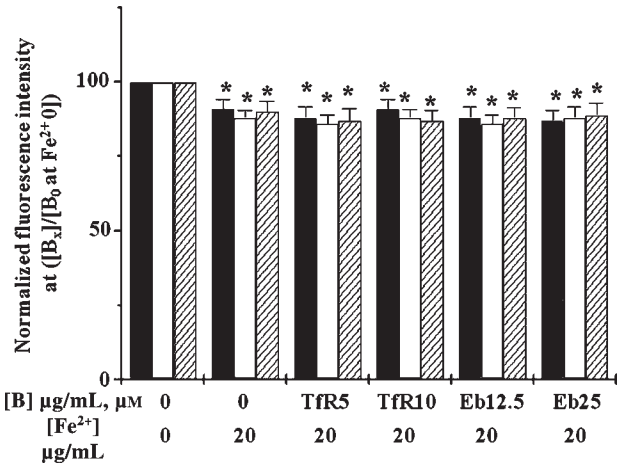

Figure 5 Effects of anti-TfR1 antibody and divalent metal transporter1 (DMT1) blocker on iron uptake into cardiomyocytes (n = 6/group). Cardiomyocytes from WT (black bar), DH (white bar), and HT (dashed bar) were plated and the cells were exposed to various concentrations of anti-TfR1 antibody (aTfR, 5 and 10 μg/ml) or Ebselen (DMT1 blocker, 12.5 and 25 μM) for 60 min, before loaded with 285.6 μM (20 μg/ml) ferric ammonium citrate with 1 mM ascorbic acid (FAC ± AA) for 48 h. Cellular iron uptake was determined using Calcein-AM fluorescence assay. Data were presented as mean ± SEM. $^{*}P < 0.05$ vs. control (non-iron-treated group) of the same cell type.

antibody, and ebselen) on cardiomyocytes was tested by the MTT assay. We found that cell viability of cardiomyocytes was greater than 95% in all treatments, indicating that there was no cytotoxic effect on cultured cardiomyocytes treated with various concentrations of reagents used in this study.

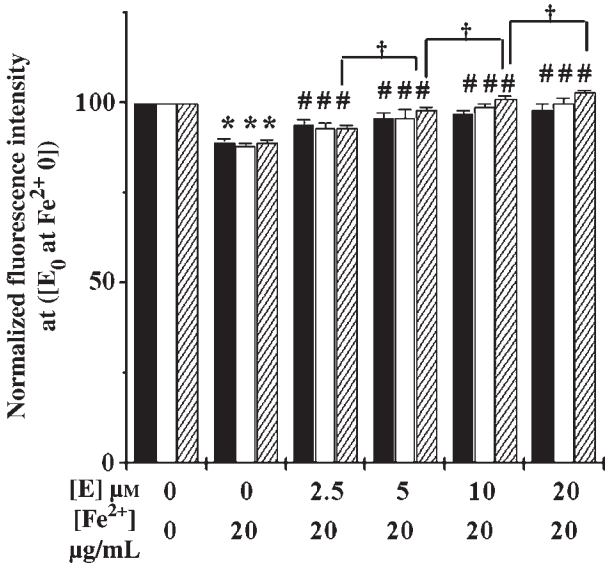

Figure 6 Effects of T-type calcium channel blocker, efonidipine (E), on iron uptake into cardiomyocytes (n = 5/group). Cardiomyocytes from WT (black bar), DH (white bar), and HT (dashed bar) were plated and exposed to various concentrations of efonidipine (0–20 μM) for 60 min, before loaded with 285.6 μM (20 μg/ml) ferric ammonium citrate with 1 mM ascorbic acid (FAC ± AA) for 48 h. Cellular iron uptake was determined using Calcein-AM fluorescence assay. Data were presented as mean ± SEM. $^{*}P < 0.05$ vs. control (non-iron-treated group) of the same cell type. $^{\#}P < 0.05$ vs. iron-treated group of the same cell type without efonidipine. $^{\dagger}P < 0.01$ vs. the other efonidipine concentration of the same cell-type group.

Identification and validation of changes in gene expressions in thalassemic hearts

Microarray study was performed to investigate gene expressions in the heart tissues of the HT thalassemic mice, compared to those in WT mice. In the HT hearts, a number of transporters and ion channels were up-regulated (Table 1). Up-regulations of different subunits of calcium channel were demonstrated in the HT hearts. These include up-regulated TTCC genes such as voltage-dependent T-type alpha 1G subunit (Cacna1g) and voltage-dependent T-type alpha 1H subunit (Cacna1h) calcium channels, which were increased in the HT hearts, compared to those in WT. However, LTCC genes in HT hearts were not different from those in WT hearts. In addition, the up-regulations of zinc transporter such as solute carrier family 39 (zinc transporter) member 5 (Slc39a5), solute carrier family 39 (zinc transporter) member 3 (Slc39a3), solute carrier family 30 (zinc transporter) member 6 (Slc30a6), and solute carrier family 39 (zinc transporter) member 8 (Slc39a8) were found. Transferrin receptor2 (TfR2) and musculus mRNA for transferrin receptor were also up-regulated in HT hearts, compared to those in the WT hearts.

Table 1 Genes with up-regulated expression in HT heart tissues, compared to WT

Gene name	Accession	Fold change
Calcium channel mRNA	AF217002.1	1.519295
Calcium channel, voltage-dependent, T-type, alpha 1G subunit (Cacna1g)	NM_009783.1	1.463021
Calcium channel, voltage-dependent, T-type, alpha 1H subunit (Cacna1h)	NM_021415.2	1.281072
Calcium channel, voltage-dependent, alpha 2/delta subunit 2 (Cacna2d2)	NM_020263.2	2.391459
Solute carrier family 30 (zinc transporter), member 6 (Slc30a6)	NM_144798.2	1.675099
Solute carrier family 39 (zinc transporter), member 5 (Slc39a5)	NM_028051.1	2.159819
Solute carrier family 39 (zinc transporter), member 8 (Slc39a8)	NM_026228.2	1.753658
Solute carrier family 39 (zinc transporter), member 3 (Slc39a3)	NM_134135.1	1.787308
Musculus mRNA for transferrin receptor	X57349.1	1.557613
Transferrin receptor 2 (Trfr2)	NM_015799.2	1.602854

Table 2 Genes with down-regulated expression in HT heart tissues, compared to WT

Gene name	Accession	Fold change
Calcium channel, voltage-dependent, gamma subunit 3 (Cacng3)	NM_019430.1	−6.718658
Calcium channel, voltage-dependent, gamma subunit 7 (Cacng7)	NM_133189.1	−5.312569
Solute carrier family 11 [proton-coupled divalent metal ion transporters (DMT)], member 1 (Slc11a1)	NM_013612.1	−1.491265
Solute carrier family 11 [proton-coupled divalent metal ion transporters (DMT)], member 2 (Slc11a2)	NM_008732.1	−1.693117
Solute carrier family 30 (zinc transporter), member 7 (Slc30a7)	NM_023214.3	−2.242076
Solute carrier family 40 [iron-regulated transporter (ferroportin)], member 1 (Slc40a1)	NM_016917.1	−1.421172

DMT, divalent metal transporter.

Down-regulations of DMT family were observed in the HT hearts (Table 2), such as solute carrier family 11 (proton-coupled DMT), member 1 (Slc11a1), and solute carrier family 11 (proton-coupled DMT), member 2 (Slc11a2). These down-regulations of DMT genes agreed well with our data, showing that DMT1 blocker could not prevent iron uptake into thalassemic cardiomyocytes. Furthermore, we also found the down-regulation of iron exporter ferroportin or solute carrier family 40 [iron-regulated transporter (ferroportin)], member 1 (Slc40a1) in the HT hearts.

Discussion

Iron-overload cardiomyopathy has been responsible for cardiovascular morbidity and mortality in patients with thalassemia for many decades (1, 2). Currently, the definite mechanism of iron entry into cardiomyocytes is not clearly understood. The precise mechanism of iron uptake into the heart is crucial as it could provide new approaches for the treatment of iron-overloaded patients. Although a number of studies have been carried out to investigate the iron uptake mechanism in the heart, they were performed in normal hearts. It is not known whether iron entry into cardiac cells is similar or different in thalassemic cardiomyocytes. Our study is the first study that a mouse model of β-thalassemia, in which the HT mice showed a pathophysiology resembling that of human patients with β-thalassemia intermedia (19, 20, 35), was used to investigate the possible pathways of iron uptake into thalassemic cardiomyocytes.

In the present study, the major findings are that (i) iron accumulation at the baseline in the cultured ventricular cardiomyocytes of thalassemic mice was significantly higher than that of WT cells; (ii) DFO could prevent iron uptake into the cells; (iii) the iron uptake into cardiomyocytes could not be blocked by LTCC blocker (verapamil), anti-TfR1 antibody nor DMT1 blocker; (iv) the iron uptake into cardiomyocytes could be prevented by TTCC blocker, efonidipine; and (v) up-regulated genes of TTCC, zinc transporter, and TfR2 were found in thalassemic cardiomyocytes.

We previously demonstrated that HT mice had a significant increase in serum iron, compared to the DH and WT mice (21). In the present study, the baseline of iron accumulation in HT cardiomyocytes which was greater than that in WT could be directly attributed to the high level of serum iron and high iron accumulation in heart tissue (36). Under the normal condition, iron uptake (iron accumulation) into the cultured ventricular cardiomyocytes of both types of thalassemic mice was significantly greater than that of WT cells. These findings suggest that thalassemic cardiomyocytes could have pathways that can greatly uptake iron into the cells more than that in the WT cells. To confirm that iron is uptaken into all types of cultured cardiomyocytes, iron chelator DFO was used and the results showed that DFO could block iron uptake into all types of cultured cardiomyocytes.

Verapamil did not block iron uptake in cultured thalassemic cardiomyocytes

Calcium channel blockers have been widely used to treat cardiovascular diseases for many decades (37, 38). Recent evidence demonstrated that, under the conditions of iron overload, LTCC may be a critical transporter of iron into cardiomyocytes (12, 13). In the present study, by using the LTCC blocker, our results demonstrated that verapamil could not block iron uptake into any types of cultured cardiomyocytes. These findings suggested that an iron uptake mechanism in cultured cardiomyocytes is not mainly via LTCC and indicated that it may be mediated through other pathways rather than LTCC. Our findings were consistent with a previous study in providing evidence for ascorbate-reduced form of iron transport in the heart (14). Parkes *et al.* (14) demonstrated that the applications of LTCC blockers (nifedipine, verapamil, diltiazem) failed to alter the iron uptake rates in cultured rat neonatal myocytes. However, several studies using isolated perfused hearts (12) or *in vivo* heart models (13) demonstrated that LTCC is a possible pathway for iron uptake in the heart. The discrepancy in findings regarding the effects of LTCC blocker on iron uptake between ours and others could be attributed to the different experimental models used in those studies. It is also possible that the function or activity in transporting iron of LTCC in our cultured cardiomyocytes could be different than that in the *in vivo* or isolated cardiomyocyte models reported in the previous studies (12, 13).

TfR1 and DMT1 were not the main portals for iron uptake in cultured thalassemic cardiomyocytes

Because LTCC blocker could not prevent iron uptake into cardiomyocytes, free excess iron should enter the cells via other pathways. The two most common and possible pathways are via DMT1 and TfR1. In the hearts, previous studies demonstrated the evidence that both DMT1 and TfR1 were not the portals for iron uptake in the heart under iron-overload condition (8, 9). However, their role as iron transporters in thalassemic cardiomyocytes has never been investigated. In the present study, anti-TfR1 antibody and ebselen, i.e. DMT1 blocker, were used to prevent iron uptake via TfR1 and DMT1. The results showed that neither anti-TfR1 antibody nor ebselen could block iron uptake into any types of cultured cardiomyocytes. These findings suggested that TfR1 and DMT1 did not play a major role in iron uptake into cultured cardiomyocytes under iron-overload conditions. These findings were consistent with a previous study which demonstrated that TfR1 and/or DMT1 mRNA as well as their protein expressions were suppressed in cultured neonatal rat cardiomyocytes (8) and in normal adult rat hearts (9) under iron-loaded conditions. Supporting these findings is also from our microarray data which demonstrated that DMT1 and 2 mRNA expressions in the HT heart were down-regulated, compared to that in the WT hearts.

Efonidipine could prevent iron uptake in cultured thalassemic cardiomyocytes

TTCCs are abundantly expressed in the embryonic cardiomyocytes, but their expression is suppressed in the adult cells (16). However, TTCC has been shown to re-express in pathologic hearts such as hypertrophied and failing ventricles, and the resultant T-type Ca^{2+} currents ($I_{Ca,T}$) are thought to be involved in the pathological process (17, 18). In our cultured cardiomyocyte model, the results showed that TTCC blocker, efonidipine, could prevent iron uptake into cultured cardiomyocytes, with most effectiveness in HT cardiomyocytes. Although efonidipine is not a selective TTCC blocker and could also block LTCC, its efficacy in blocking TTCC is greater than that of LTCC (30). Because verapamil could not prevent iron uptake when efonidipine could, these findings suggested that TTCC could play a significant role in iron uptake into cardiomyocytes in this model. Moreover, our microarray data demonstrated that the TTCC genes were up-regulated in the HT hearts, which is well correlated with iron uptake result, suggesting that TTCCs play an important role in iron uptake in thalassemic hearts, and that their re-expression could be attributed to the pathological state of thalassemic hearts itself or from the iron-overload condition, or both.

Microarray findings indicate other possible iron uptake pathways

As our study demonstrated that TTCC was the main portal for iron uptake in cultured thalassemic cardiomyocytes, we used the microarray assay to investigate the changes of genes of all possible iron transporters in the hearts of thalassemic mice, especially the TTCC genes. Despite enormous amount of information obtained from the microarray assay, we found that several iron transporters in the hearts, including TTCC, TfR2, and zinc transporter, were markedly up-regulated in the HT hearts, whereas ferroportin was down-regulated in the HT hearts. The findings that TTCC genes were upregulated in the thalassemic hearts correlated well with the pharmacological study in the present study that TTCC blocker could prevent iron uptake into the hearts and may well explain the greater amount of iron uptake found in cultured thalassemic cardiomyocytes, compared to the wild-type cells. In addition to TTCC up-regulated genes, microarray data also provided other possible pathways for iron uptake into these cultured thalassemic cardiomyocytes. These include the up-regulated zinc transporter and TfR2 genes. With these valuable data from microarray analysis, future studies are required to investigate the roles of zinc transporter and TfR2 in cellular iron uptake in both normal and thalassemic hearts.

Study limitation

Our finding that TTCC was a major portal for iron entry in the cultured ventricular myocytes of thalassemic mice could be a disease- and species-specific finding and that it could be different in a different study model. Furthermore, because our findings were based on the *in vitro* study, it is possible that similar or different results can be observed in an *in vivo* model. Future *in vivo* studies are needed to warrant the findings obtained from our *in vitro* model.

Conclusion

This study demonstrated that iron uptake under iron-overload condition in the cultured ventricular myocytes of thalassemic mice was greater than that of wild-type cells. TTCC could be one of the main portals for iron uptake into cultured thalassemic cardiomyocytes, as demonstrated by the prevention of iron uptake by TTCC blocker and the up-regulated genes of TTCC from thalassemic mouse hearts. However, microarray data also provide other possible pathways such as zinc transporter and TfR2, as indicated by an up-regulation of these genes in thalassemic hearts. Future studies are required to investigate the possible roles of these transporters in iron uptake mechanisms in thalassemic hearts.

Conflicts of interest statement

The authors declare that there are no conflicts of interest.

References

1. Andrews NC. Disorders of iron metabolism. *N Engl J Med* 1999;**341**:1986–95.
2. Weatherall DJ, Clegg JB. Thalassemia – a global public health problem. *Nat Med* 1996;**2**:847–9.
3. Hentze MW, Muckenthaler MU, Andrews NC. Balancing acts: molecular control of mammalian iron metabolism. *Cell* 2004;**117**:285–97.
4. Breuer W, Shvartsman M, Cabantchik ZI. Intracellular labile iron. *Int J Biochem Cell Biol* 2008;**40**:350–4.
5. Lekawanvijit S, Chattipakorn N. Iron overload thalassemic cardiomyopathy: iron status assessment and mechanisms of mechanical and electrical disturbance due to iron toxicity. *Can J Cardiol* 2009;**25**:213–8.
6. Wood JC, Enriquez C, Ghugre N, Otto-Duessel M, Aguilar M, Nelson MD, Moats R, Coates TD. Physiology and pathophysiology of iron cardiomyopathy in thalassemia. *Ann N Y Acad Sci* 2005;**1054**:386–95.
7. Rutjanaprom W, Kanlop N, Charoenkwan P, Sittiwangkul R, Srichairatanakool S, Tantiworawit A, Phrommintikul A, Chattipakorn S, Fucharoen S,

Chattipakorn N. Heart rate variability in beta-thalassemia patients. *Eur J Haematol* 2009;**83**:483–9.
8. Liu Y, Parkes JG, Templeton DM. Differential accumulation of non-transferrin-bound iron by cardiac myocytes and fibroblasts. *J Mol Cell Cardiol* 2003;**35**:505–14.
9. Ke Y, Chen YY, Chang YZ, Duan XL, Ho KP, Jiang DH, Wang K, Qian ZM. Post-transcriptional expression of DMT1 in the heart of rat. *J Cell Physiol* 2003;**196**:124–30.
10. Rodriguez A, Hilvo M, Kytomaki L, Fleming RE, Britton RS, Bacon BR, Parkkila S. Effects of iron loading on muscle: genome-wide mRNA expression profiling in the mouse. *BMC Genomics* 2007;**8**:379.
11. Parkes JG, Liu Y, Sirna JB, Templeton DM. Changes in gene expression with iron loading and chelation in cardiac myocytes and non-myocytic fibroblasts. *J Mol Cell Cardiol* 2000;**32**:233–46.
12. Tsushima RG, Wickenden AD, Bouchard RA, Oudit GY, Liu PP, Backx PH. Modulation of iron uptake in heart by L-type Ca2+ channel modifiers: possible implications in iron overload. *Circ Res* 1999;**84**:1302–9.
13. Oudit GY, Sun H, Trivieri MG, *et al*. L-type Ca2+ channels provide a major pathway for iron entry into cardiomyocytes in iron-overload cardiomyopathy. *Nat Med* 2003;**9**:1187–94.
14. Parkes JG, Olivieri NF, Templeton DM. Characterization of Fe2+ and Fe3+ transport by iron-loaded cardiac myocytes. *Toxicology* 1997;**117**:141–51.
15. Niwa N, Yasui K, Opthof T, Takemura H, Shimizu A, Horiba M, Lee JK, Honjo H, Kamiya K, Kodama I. Cav3.2 subunit underlies the functional T-type Ca2+ channel in murine hearts during the embryonic period. *Am J Physiol Heart Circ Physiol* 2004;**286**:H2257–63.
16. Yasui K, Niwa N, Takemura H, *et al*. Pathophysiological significance of T-type Ca2+ channels: expression of T-type Ca2+ channels in fetal and diseased heart. *J Pharmacol Sci* 2005;**99**:205–10.
17. Martinez ML, Heredia MP, Delgado C. Expression of T-type Ca(2+) channels in ventricular cells from hypertrophied rat hearts. *J Mol Cell Cardiol* 1999;**31**:1617–25.
18. Huang B, Qin D, Deng L, Boutjdir M, N E-S. Reexpression of T-type Ca2+ channel gene and current in post-infarction remodeled rat left ventricle. *Cardiovasc Res* 2000;**46**:442–9.
19. Jamsai D, Zaibak F, Khongnium W, Vadolas J, Voullaire L, Fowler KJ, Gazeas S, Fucharoen S, Williamson R, Ioannou PA. A humanized mouse model for a common beta0-thalassemia mutation. *Genomics* 2005;**85**:453–61.
20. Jamsai D, Zaibak F, Vadolas J, Voullaire L, Fowler KJ, Gazeas S, Peters H, Fucharoen S, Williamson R, Ioannou PA. A humanized BAC transgenic/knockout mouse model for HbE/beta-thalassemia. *Genomics* 2006;**88**:309–15.
21. Incharoen T, Thephinlap C, Srichairatanakool S, Chattipakorn S, Winichagoon P, Fucharoen S, Vadolas J, Chattipakorn N. Heart rate variability in beta-thalassemic mice. *Int J Cardiol* 2007;**121**:203–4.
22. Song W, Lu X, Feng Q. Tumor necrosis factor-alpha induces apoptosis via inducible nitric oxide synthase in neonatal mouse cardiomyocytes. *Cardiovasc Res* 2000;**45**:595–602.
23. Dyntar D, Eppenberger-Eberhardt M, Maedler K, Pruschy M, Eppenberger HM, Spinas GA, Donath MY. Glucose and palmitic acid induce degeneration of myofibrils and modulate apoptosis in rat adult cardiomyocytes. *Diabetes* 2001;**50**:2105–13.
24. Dyntar D, Sergeev P, Klisic J, Ambuhl P, Schaub MC, Donath MY. High glucose alters cardiomyocyte contacts and inhibits myofibrillar formation. *J Clin Endocrinol Metab* 2006;**91**:1961–7.
25. Eppenberger HM, Zuppinger C. In vitro reestablishment of cell-cell contacts in adult rat cardiomyocytes. Functional role of transmembrane components in the formation of new intercalated disk-like cell contacts. *FASEB J* 1999;**13**(Suppl):S83–9.
26. Li Z, Gu TX, Zhang YH. Hepatocyte growth factor combined with insulin like growth factor-1 improves expression of GATA-4 in mesenchymal stem cells cocultured with cardiomyocytes. *Chin Med J (Engl)* 2008;**121**:336–40.
27. Fukuda K. Use of adult marrow mesenchymal stem cells for regeneration of cardiomyocytes. *Bone Marrow Transplant* 2003;**32**(Suppl 1):S25–7.
28. Glickstein H, El RB, Link G, Breuer W, Konijn AM, Hershko C, Nick H, Cabantchik ZI. Action of chelators in iron-loaded cardiac cells: accessibility to intracellular labile iron and functional consequences. *Blood* 2006;**108**:3195–203.
29. Shvartsman M, Kikkeri R, Shanzer A, Cabantchik ZI. Non-transferrin-bound iron reaches mitochondria by a chelator-inaccessible mechanism: biological and clinical implications. *Am J Physiol Cell Physiol* 2007;**293**:C1383–94.
30. Vassort G, Talavera K, Alvarez JL. Role of T-type Ca2+ channels in the heart. *Cell Calcium* 2006;**40**:205–20.
31. Wetli HA, Buckett PD, Wessling-Resnick M. Small-molecule screening identifies the selanazal drug ebselen as a potent inhibitor of DMT1-mediated iron uptake. *Chem Biol* 2006;**13**:965–72.
32. Mosmann T. Rapid colorimetric assay for cellular growth and survival: application to proliferation and cytotoxicity assays. *J Immunol Methods* 1983;**65**:55–63.
33. Kitagawa-Sakakida S, Fukushima N, Sawa Y, Horiguchi K, Doi T, Shirakura R, Matsuda H. Microarray-based gene expression profiling of retransplanted rat cardiac allografts that develop cardiac allograft vasculopathy. *J Heart Lung Transplant* 2005;**24**:2068–74.
34. Davis MT, Bartfay WJ. Ebselen decreases oxygen free radical production and iron concentrations in the hearts of chronically iron-overloaded mice. *Biol Res Nurs* 2004;**6**:37–45.
35. Yang B, Kirby S, Lewis J, Detloff PJ, Maeda N, Smithies O. A mouse model for beta 0-thalassemia. *Proc Natl Acad Sci U S A* 1995;**92**:11608–12.

36. Thephinlap C, Phisalaphong C, Fucharoen S, Porter JB, Srichairatanakool S. Efficacy of curcuminoids in alleviation of iron overload and lipid peroxidation in thalassemic mice. *Med Chem* 2009;**5**:474–82.
37. Pepine CJ, Handberg EM, Cooper-DeHoff RM, *et al*. A calcium antagonist vs a non-calcium antagonist hypertension treatment strategy for patients with coronary artery disease. The International Verapamil-Trandolapril Study (INVEST): a randomized controlled trial. *JAMA* 2003;**290**:2805–16.
38. Julius S, Kjeldsen SE, Weber M, *et al*. Outcomes in hypertensive patients at high cardiovascular risk treated with regimens based on valsartan or amlodipine: the VALUE randomised trial. *Lancet* 2004;**363**:2022–31.

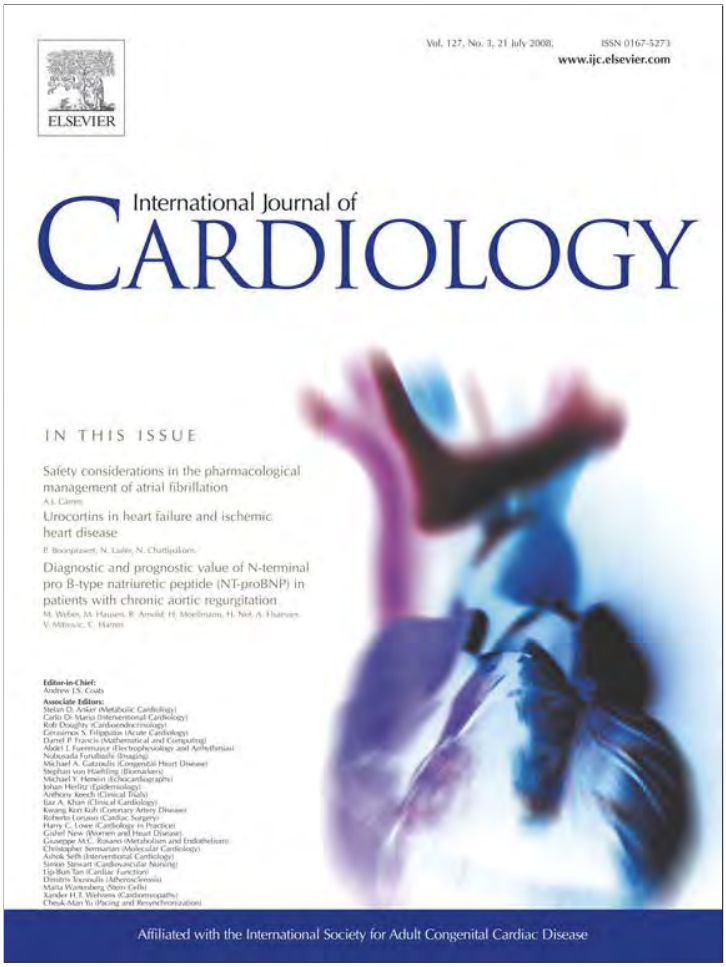

ELSEVIER

International Journal of Cardiology 127 (2008) 307–312

International Journal of Cardiology

www.elsevier.com/locate/ijcard

Review

Urocortins in heart failure and ischemic heart disease ☆

Phitsanu Boonprasert [a,c], Narissara Lailerd [b,c], Nipon Chattipakorn [b,c,d,*]

[a] *Department of Internal Medicine, Faculty of Medicine, Chiang Mai University, Chiang Mai, Thailand*
[b] *Cardiac Electrophysiology Unit, Department of Physiology, Faculty of Medicine, Chiang Mai University, Chiang Mai, Thailand*
[c] *Cardiac Electrophysiology Research and Training Center, Faculty of Medicine, Chiang Mai University, Chiang Mai, Thailand*
[d] *Biomedical Engineering Center, Chiang Mai University, Chiang Mai, Thailand*

Received 30 August 2007; accepted 17 November 2007
Available online 3 January 2008

Abstract

Urocortins, a novel member of the corticotrophin-releasing factor (CRF) family, have been shown in animal and human studies to possess several beneficial effects in stress, cardiovascular and renal function, and inflammatory responses via CRF receptors. In the heart, urocortins have been demonstrated to produce cardioprotective effects during ischemia and reperfusion injury. Urocortins have also exerted effects on hemodynamic, endocrine and renal parameters in experimental animal heart failure models. In humans, plasma urocortin levels have been shown to significantly increase in systolic heart failure patients. This growing evidence suggests that urocortins may have a prognostic value as well as being a potential therapeutic treatment for heart failure and myocardial infarction patients. Currently, only a few clinical studies on urocortins are available. In this review article, the role of urocortins in the heart has been summarized. Their possible beneficial roles in heart failure and myocardial infarction have been discussed, based on relevant published articles from both basic and clinical studies available to date.

Keywords: Urocortins; Corticotropin-releasing factor; CRF receptor; Heart failure; Myocardial infarction; Ischemia–reperfusion injury

1. Introduction

Heart failure and ischemic heart disease are common cardiac syndromes, in which an increased incidence has been shown in most nations around the world. The progress of these clinical syndromes can lead to left ventricular dysfunction; including systolic and diastolic dysfunction, and sudden cardiac death. To prevent the progression of the diseases, their identification at an early stage is crucial, since late stage heart failure has been shown to have poor prognosis with high mortality [1]. In past decades, several cardiac markers were shown to have a predictive value regarding the progression and prognosis in myocardial infarction and heart failure patients. These markers included NT-proBNP [2], cardiac troponin [3], hs-CRP [4], and creatine kinase [5]. Recently, the novel cardioprotective peptides, "urocortins", have been demonstrated to possess potential value as an early diagnostic marker in heart failure [6]. In this review article, the roles of urocortins as an early cardiac marker as well as their effects in heart failure and ischemic heart disease from animal and clinical studies are presented. In addition, the roles of urocortins, which point to a future clinical research and therapeutic application, are also discussed.

2. Urocortins

Urocortins, 40 amino acid peptides, are a member of the hypothalamic corticotropin-releasing factor (CRF) family. The CRF family consists of CRF, fish urotensin I, frog sauvagine, urocortin I, urocortin II (stresscopin-related peptide, SRP), and

☆ Supported by the Biomedical Engineering Center research grant, Chiang Mai University (NC, NL) and the Thailand Research Fund grant, RMU 4980001(NC) and MRG 4980165 (NL).
* Corresponding author. Cardiac Electrophysiology Research and Training Center, Faculty of Medicine, Chiang Mai University, Chiang Mai, Thailand. Tel.: +66 53 945329; fax: +66 53 945368.
E-mail address: nchattip@mail.med.cmu.ac.th (N. Chattipakorn).

0167-5273/$ - see front matter © 2007 Elsevier Ireland Ltd. All rights reserved.
doi:10.1016/j.ijcard.2007.11.026

urocortin III (stresscopin, SCP) [7–10]. The actions of the CRF family peptides are mediated via CRF receptors that are derived from two distinct genes; CRF type1 receptor and CRF type2 receptor [11,12]. Rat urocortin I was first discovered in 1995 from a discrete midbrain region [9]. Its structure is related to urotensin (65% sequence identified) and corticotropin-releasing factor (CRF) (45% sequence identified) [9]. Human urocortin I was identified later by the molecular cloning technique [10]. Regarding its sequence, it was 63% identical to fish urotensin I and 43% identical to CRF at the amino acid level. In rat, the rank orders of mRNA expression of CRF and urocortin I as well as their receptors in each of the tissue types have been shown as follows: the majority of CRF mRNA was found in the brain, whereas the majority of urocortin I mRNA was found in both the heart and brain [13]. Recently, new members of this family, urocortin II and urocortin III, have been identified from human libraries and the genome database [23]. Urocortin II and urocortin III have approximately 20–40% homology with CRF and urocortin I. The homology between urocortin II and urocortin III is approximately 40%. In 2001, human versions of these novel urocortins were also isolated, including a stresscopin-related peptide, which is equivalent to urocortin II, and a stresscopin that is equivalent to urocortin III [7,8,14].

Although urocortins share moderate sequence identity with one another and with CRF, each urocortin has a unique anatomical distribution under the control of different genes. In humans, urocortin I is detected in the brain, placenta, gastrointestinal tract, synovial tissue, lymphocytes, adipose tissue, endothelial cells, immunological tissues, and heart [15–21]. In the brain, urocortin I was detectable at the Edinger–Wesphal nucleus, the lateral superior olive, the supraoptic nucleus (SON), the lateral hypothalamic area, and most caudal part of several brainstem and spinal cord motoneuron nuclei [12,22]. In the nervous system, urocortin I has been shown to enhance anxiety and suppress appetite via the CRF type1 receptor [23]. The finding of urocortin mRNA expression in synovium tissues in rheumatoid arthritis and osteoarthritis patients suggests that urocortin may also act as an immune-inflammatory mediator [19]. Urocortin I activates the pituitary–adrenal axis inducing the release of adrenocorticotropic hormone (ACTH), and increasing plasma cortisol, and atrial natriuretic peptide in animal models [24–27]. In humans, the biological effects of urocortin I infusion in healthy males include increased plasma level of ACTH and cortisol. These effects of urocortin I are mediated via the CRF type1 receptor [28]. Similar to urocortin I, urocortin II is expressed in the heart and discrete areas of the central nervous system of rats, including stress-related cell groups in the hypothalamus, brainstem and spinal cord [8,29]. Urocortin III is also expressed in the brain and peripheral tissues such as gastro-intestinal tract, pancreas, and skin. However, the expression of urocortin III is considerably lower than that of urocortin II [7,30–32]. In humans, urocortin III was present in both the ventricles and atria [33]. However, the highest levels were found in all regions of the pituitary and hypothalamus [32]. Urocortin III was also distributed in other tissues, such as the lung, pancreas, liver, spleen and skeletal muscle, and present in human plasma and urine [33].

3. CRF receptors for urocortins

CRF receptors consist of two types of seven-transmembrane-spanning G-protein receptors, which are coupled to adrenylyl cyclase: CRF type1 and CRF type2 receptors. The CRF type1 receptor is found predominantly in the pituitary and brain regions, whereas the CRF type2 receptor is highly expressed in peripheral tissues including the heart [8,13,29,34]. The CRF type1 receptor has a single functional form: CRF type1 (alpha) receptor, whereas the CRF type2 receptor has three isoforms: CRF type2 (alpha) receptor, CRF type2 (beta) receptor and CRF type2 (gamma) receptor [11,35,36]. The CRF type1 receptor implicates in adrenocorticotropic hormone (ACTH) release and anxiety-like effect, while the CRF type2 receptor contributes to anxiolysis, appetite-inhibition, vasodilatation, positive inotropic action on the myocardium, and dearousal effects [12]. CRF and urocortin I can bind to both CRF type1 and type2 receptors [9]. Urocortin II and urocortin III bind to only the CRF type2 receptor [7,8]. The CRF type2 receptor binds to urocortin I, urocortin II and urocortin III, with approximately 40-fold greater affinity than CRF [9].

CRF type2 receptors have different tissue distributions. In rats, the CRF type2 (alpha) receptor is highly expressed in the brain, while the CRF type2 (beta) receptor is expressed in the brain, heart, lung, gastrointestinal tract, and skeletal muscle [37]. The CRF type2 (gamma) receptor has only been detected in the brain [38]. The cDNA sequence in the protein-coding region of rat tissue is 94% identical to the CRF type2 (beta) receptor [39,40]. The CRF type2 (beta) receptor has 10-fold higher affinity to urocortin than CRF in rat models [9], whereas the CRF type1 receptor shows little ligand selectivity for urocortin [10]. In the rat's heart, only the CRF type2 (beta) receptor is found. The high level of urocortin mRNA detected in the heart was related to the high expression of CRF type2 (beta) receptor coupling in the heart tissue of rats [13]. In the human heart, however, only the alpha type of CRF type2 receptor is found [41,42].

4. Urocortins and the heart

Kimura et al. reported that urocortins and the CRF type2 (alpha) receptor were detected in all chambers of four human hearts, and detected with highest intensity in the left ventricle, whereas CRF was not detected in cardiac myocytes [17]. In their study, detection of the CRF type1 receptor was weak in the left atrium, left ventricle and right ventricle [17]. Since the CRF type2 (alpha) receptor was detected predominantly in the left ventricle, it has been suggested that urocortins, not CRF, may have an important role on cardiac function [17]. By using radioligand binding techniques, Wiley and Davenport

demonstrated that urocortins have a high affinity to the CRF type2 (alpha) receptor in human left ventricular myocardium, intramyocardial blood vessels and within the medial layer of internal mammary arteries [43].

Currently, urocortins are overwhelmingly shown to affect cardiovascular physiology in normal animals, and pacing-induced heart failure in animal models and clinical studies [26,27,44,45]. The cardiovascular effects of urocortins include a dose-dependent increase in heart rate, cardiac output, and coronary blood flow [26]. Interestingly, urocortins have been shown to possess an anti-apoptotic effect in myocardium that has undergone ischemia–reperfusion injury [26,44,45]. Urocortin and CRF also exerted coronary vasodilatation and positive inotropic effect. These physiological effects of urocortin have been shown to last longer than the action of CRF [46].

The high dose administration of urocortin I in rats has been reported to decrease arterial pressure via vasodilatation, as revealed by a decrease in total peripheral resistance and slightly increased cardiac output [47]. The dilator action of urocortin I is mostly manifested in the heart and stomach [48]. In mice, urocortin I increases cardiac contractility, heart rate, and vasodilatation [46]. However, these effects were not found in CRF type2 receptor-deficient mice [49,50]. These data indicate that actions of urocortin I in peripheral tissues are expressed via the CRF type2 receptor. Urocortin I has also been shown to enhance cardiac output, protect myocytes from ischemia–reperfusion injury, stimulate cardiac natriuretic peptide secretion, induce vasodilatation, especially in the coronary arteries of normal and heart failure models [26,27,44–46,51–54], and decrease left atrial pressure and peripheral vascular resistance [27,27,47].

Urocortin II exerts positive inotropic effect via CRF type2 receptor-mediated stimulation and enhances contractility of rabbit ventricular myocytes [55]. Urocortin III causes an increase in cardiac output and a decrease in peripheral resistance and left atrial pressure in heart failure sheep [56]. Since these cardiovascular effects are beneficial in reducing preload and afterload to the heart, researchers are currently investigating the roles of urocortins in heart failure using animal models as well as heart failure patients [6,27,47,56,57].

5. Urocortins and heart failure

Rademaker et al. investigated the effects of urocortin administration in both normal and pacing-induced heart failure sheep [27,47,56,57]. Urocortin I, urocortin II and urocortin III induced an immediate increase in cardiac output and a decrease in peripheral resistance and left atrial pressure. In normal sheep, however, only slight changes in peripheral resistance and atrial pressure were found. Interestingly, urocortin I, urocortin II and urocortin III caused a dose-dependent decrease in plasma vasopressin, endothelin-1, renin, aldosterone, epinephrine, plasma atrial and brain natriuretic peptide levels in heart failure sheep, whereas adrenocorticotropic hormone and cortisol levels were increased. These urocortins also increased urine output, sodium excretion, and creatinine clearance [47,56,57]. Urocortin infusion in normal sheep resulted in a similar rise in cortisol and vasopressin, a decrease in aldosterone, and no significant effects on plasma renin activity and natriuretic peptides. Nevertheless, long-term peripheral and central administration of urocortin caused an increase in arterial pressure and heart rate in 15 normal ewes [58]. Furthermore, Mackay et al. also demonstrated that urocortin II caused a reduction in arterial pressure and increased heart rate in fifty adult heart failure rats [59]. These reports, using animal models, support the role of urocortins in arterial pressure and intravascular volume homeostasis in heart failure.

Currently, there are only a few clinical studies of urocortin available. In a cross-sectional study by Ng et al., investigation was carried out on plasma urocortin in 119 patients with systolic heart failure and 212 healthy individuals (LVEF > 50%) [6]. They reported that urocortin was elevated in systolic heart failure (LVEF ≤ 45%), especially in NYHA functional classes I–II [6]. The relative increase in plasma urocortin level was greater in males than in females, but the level decreased with increasing age, especially in heart failure groups. The decreased urocortin levels, with increasing NYHA class, were reinforced by a significant correlation between urocortin and ejection fraction in heart failure patients. From these findings, it was suggested that the urocortin level complemented NT-proBNP in the early diagnosis of mild clinical heart failure [6]. An increased plasma urocortin level in mild stage systolic heart failure, and the reduced level when heart failure progresses, could have potential clinical benefits if warranted, since these findings may be used for the diagnosis of early heart failure and as a prognostic indicator for heart failure progression. Recently, Davis et al. investigated the effects of urocortin II infusion in 8 healthy unmedicated men [60]. They found that urocortin II induced an increase in cardiac output, heart rate, and left ventricular ejection fraction, while decreasing systemic vascular resistance. These effects also increased plasma renin activity, angiotensin II and norepinephrine [60]. Although the clinical benefits of urocortins are still unclear, due to the small number of clinical studies, the growing body of evidence indicates the need to warrant their clinical significance by performing more clinical studies in the future, including those that investigate the plasma profile of urocortin in heart failure patients with long-term follow up.

6. Urocortins and myocardial ischemia

Apoptosis is known to implicate the pathogenesis of cardiovascular diseases such as myocardial infarction [61]. It causes the loss of cardiac myocytes and worsens the cardiac function. While hypoxia induces both necrotic and apoptotic forms of cell death in cardiac myocytes, the degree of cardiac dysfunction after ischemia–reperfusion injury reflects the level of myocardial injury and cell death [62].

In experimental studies, the increased urocortin level had been expressed when cardiac cells were exposed to thermal shock and ischemia [63,64]. Brar et al. studied urocortin

against the damaging effects of ischemia–reperfusion injury in rat hearts [44]. They demonstrated that exogenous urocortin caused increased cardiac contractility and vasodilatation, especially in coronary arteries, and protected the heart during ischemia by reducing the number of cell deaths induced by hypoxia [44]. Urocortin prevented neonatal rat myocytes from cell death when it was administered prior to stimulated hypoxia/ischemia, and at the point of reoxygenation after stimulated hypoxia/ischemia [44]. It acted via a p42/p44 MAPK-dependent signaling pathway in *in vitro* and *in vivo* adult rat hearts with ischemia–reperfusion injury [54]. In cardiac myocytes of rats, Okosi et al. demonstrated that the urocortin mRNA level was increased by thermal shock and that exogenous urocortin protected cardiac myocytes from cell death induced by hypoxia [64]. Exogenous urocortin also protected cardiac myocytes against necrotic cell death from a reduction in LDH release [64]. Other protective roles of urocortin in ischemia–reperfusion injury include inhibiting free radical activities, preventing mitochondrial damage, and activating the phosphatidylinositol 3-OH kinase and PKC-epsilon in mice [65–69]. The infarction size and mean arterial pressure were significantly decreased in rat hearts that received urocortin [54,69].

Urocortin increased interleukin-6 levels from peripheral blood mononuclear cells [19]. In mice, it reduced lipopolysaccharide-induced serum TNF-alpha and interleukin-1 beta levels [19,70]. Honjo et al. demonstrated that urocortin mRNA expression is also upregulated by TNF-alpha and IFN-gamma [18], suggesting that urocortin could have an anti-oxidative effect against oxidative stress in inflammatory lesions [18]. Urocortin has also been shown to reduce necrotic and apoptotic cell death in isolated rat hearts exposed to ischemia–reperfusion injury, and partially prevent the depletion of cellular energy stores, with enhancement of ventricular function [62].

In murine hearts, Brar et al. demonstrated that urocortin II and urocortin III protected murine cardiomyocytes from ischemia–reperfusion injury and reduced the percentage of infarct size [29]. These effects have been demonstrated to act via the ERK1/2-p42 signaling pathway and CRF type2 receptor mediated in the heart [29].

7. Future role and clinical application of urocortins

Previous studies have demonstrated the beneficial effects of urocortin, including coronary vasodilatation, increased cardiac contractility, coronary blood flow and conductance, cardiac output, and heart rate as well as protection against ischemia–reperfusion injury [26,27,29,44,45,47,56,57,63,64]. Theoretically, these effects are useful in the treatment of cardiovascular disorders, particularly heart failure and conditions associated with ischemia–reperfusion such as myocardial infarction. Practically, the role of urocortins in heart failure and ischemic heart disease is still unclear. Therefore, caution should be taken despite growing evidence of the beneficial effects of urocortins. For example, exogenous urocortin I could cause undesired effects when treating ischemia–reperfusion injury, since it could increase the plasma ACTH level via CRF type1 receptor activation [28]. Since most reports were performed in experimental animal models, with only a few clinical studies, large prospective clinical studies with long-term follow up are needed to warrant the clinical significance of urocortins.

References

[1] Minino AM, Arias E, Kochanek KD, Murphy SL, Smith BL. Deaths: final data for 2000. Natl Vital Stat Rep 2002;50:1–119.
[2] Cowie MR, Struthers AD, Wood DA, et al. Value of natriuretic peptides in assessment of patients with possible new heart failure in primary care. Lancet 1997;350:1349–53.
[3] Mair J. Cardiac troponin I and troponin T: are enzymes still relevant as cardiac markers. Clin Chim Acta 1997;257:99–115.
[4] Rifai N, Ridker PM. High-sensitivity C-reactive protein: a novel and promising marker of coronary heart disease. Clin Chem 2001;47:403–411.
[5] Adams JE, Abendschein DR, Jaffe AS. Biochemical markers of myocardial injury. Is MB creatine kinase the choice for the 1990s. Circulation 1993;88:750–63.
[6] Ng LL, Loke IW, O'Brien RJ, Squire IB, Davies JE. Plasma urocortin in human systolic heart failure. Clin Sci (Lond) 2004;106:383–8.
[7] Lewis K, Li C, Perrin MH, et al. Identification of urocortin III, an additional member of the corticotropin-releasing factor (CRF) family with high affinity for the CRF2 receptor. Proc Natl Acad Sci U S A 2001;98:7570–5.
[8] Reyes TM, Lewis K, Perrin MH, et al. Urocortin II: a member of the corticotropin-releasing factor (CRF) neuropeptide family that is selectively bound by type 2 CRF receptors. Proc Natl Acad Sci U S A 2001;98:2843–8.
[9] Vaughan J, Donaldson C, Bittencourt J, et al. Urocortin, a mammalian neuropeptide related to fish urotensin I and to corticotropin-releasing factor. Nature 1995;378:287–92.
[10] Donaldson CJ, Sutton SW, Perrin MH, et al. Cloning and characterization of human urocortin. Endocrinology 1996;137:2167–70.
[11] Lovenberg TW, Liaw CW, Grigoriadis DE, et al. Cloning and characterization of a functionally distinct corticotropin-releasing factor receptor subtype from rat brain. Proc Natl Acad Sci U S A 1995;92:836–40.
[12] Skelton KH, Owens MJ, Nemeroff CB. The neurobiology of urocortin. Regul Pept 2000;93:85–92.
[13] Baigent SM, Lowry PJ. mRNA expression profiles for corticotrophin-releasing factor (CRF), urocortin, CRF receptors and CRF-binding protein in peripheral rat tissues. J Mol Endocrinol 2000;25:43–52.
[14] Scarabelli TM, Knight R, Stephanou A, et al. Clinical implications of apoptosis in ischemic myocardium. Curr Probl Cardiol 2006;31:181–264.
[15] Seres J, Bornstein SR, Seres P, et al. Corticotropin-releasing hormone system in human adipose tissue. J Clin Endocrinol Metab 2004;89:965–970.
[16] Bamberger CM, Wald M, Bamberger AM, Ergun S, Beil FU, Schulte HM. Human lymphocytes produce urocortin, but not corticotropin-releasing hormone. J Clin Endocrinol Metab 1998;83:708–711.
[17] Kimura Y, Takahashi K, Totsune K, et al. Expression of urocortin and corticotropin-releasing factor receptor subtypes in the human heart. J Clin Endocrinol Metab 2002;87:340–346.
[18] Honjo T, Inoue N, Shiraki R, et al. Endothelial urocortin has potent antioxidative properties and is upregulated by inflammatory cytokines and pitavastatin. J Vasc Res 2006;43:131–138.
[19] Kohno M, Kawahito Y, Tsubouchi Y, et al. Urocortin expression in synovium of patients with rheumatoid arthritis and osteoarthritis: relation to inflammatory activity. J Clin Endocrinol Metab 2001;86:4344–4352.
[20] Petraglia F, Florio P, Gallo R, et al. Human placenta and fetal membranes express human urocortin mRNA and peptide. J Clin Endocrinol Metab 1996;81:3807–3810.

[21] Takahashi K, Totsune K, Sone M, et al. Regional distribution of urocortin-like immunoreactivity and expression of urocortin mRNA in the human brain. Peptides 1998;19:643–647.
[22] Bittencourt JC, Vaughan J, Arias C, Rissman RA, Vale WW, Sawchenko PE. Urocortin expression in rat brain: evidence against a pervasive relationship of urocortin-containing projections with targets bearing type 2 CRF receptors. J Comp Neurol 1999;415:285–312.
[23] Scarabelli T, Knight R. Urocortins: take them to heart. Curr Med Chem Cardiovasc Hematol Agents 2004;2:335–342.
[24] Holmberg BJ, Morrison CD, Keisler DH. Endocrine responses of ovariectomized ewes to i.c.v. infusion of urocortin. J Endocrinol 2001;171:517–524.
[25] Ikeda K, Tojo K, Sato S, et al. Urocortin, a newly identified corticotropin-releasing factor-related mammalian peptide, stimulates atrial natriuretic peptide and brain natriuretic peptide secretions from neonatal rat cardiomyocytes. Biochem Biophys Res Commun 1998;250: 298–304.
[26] Parkes DG, Vaughan J, Rivier J, Vale WW, May CN. Cardiac inotropic actions of urocortin in conscious sheep. Am J Physiol 1997;272: H2115–22.
[27] Rademaker MT, Charles CJ, Espiner EA, et al. Beneficial hemodynamic, endocrine, and renal effects of urocortin in experimental heart failure: comparison with normal sheep. J Am Coll Cardiol 2002;40: 1495–1505.
[28] Davis ME, Pemberton CJ, Yandle TG, et al. Urocortin-1 infusion in normal humans. J Clin Endocrinol Metab 2004;89:1402–1409.
[29] Brar BK, Jonassen AK, Egorina EM, et al. Urocortin-II and urocortin-III are cardioprotective against ischemia reperfusion injury: an essential endogenous cardioprotective role for corticotropin releasing factor receptor type 2 in the murine heart. Endocrinology 2004;145: 24–35.
[30] Hsu SY, Hsueh AJ. Human stresscopin and stresscopin-related peptide are selective ligands for the type 2 corticotropin-releasing hormone receptor. Nat Med 2001;7:605–611.
[31] Li C, Chen P, Vaughan J, et al. Urocortin III is expressed in pancreatic beta-cells and stimulates insulin and glucagon secretion. Endocrinology 2003;144:3216–3224.
[32] Li C, Vaughan J, Sawchenko PE, Vale WW. Urocortin III-immunoreactive projections in rat brain: partial overlap with sites of type 2 corticotrophin-releasing factor receptor expression. J Neurosci 2002;22:991–1001.
[33] Takahashi K, Totsune K, Murakami O, et al. Expression of urocortin III/stresscopin in human heart and kidney. J Clin Endocrinol Metab 2004;89:1897–1903.
[34] Iino K, Sasano H, Oki Y, et al. Urocortin expression in the human central nervous system. Clin Endocrinol (Oxf) 1999;50:107–114.
[35] Chang CP, Pearse RV, O'Connell S, Rosenfeld MG. Identification of a seven transmembrane helix receptor for corticotropin-releasing factor and sauvagine in mammalian brain. Neuron 1993;11:1187–1195.
[36] Kishimoto T, Pearse RV, Lin CR, Rosenfeld MG. A sauvagine/corticotropin-releasing factor receptor expressed in heart and skeletal muscle. Proc Natl Acad Sci U S A 1995;92:1108–1112.
[37] Lovenberg TW, Chalmers DT, Liu C, de Souza EB. CRF2 alpha and CRF2 beta receptor mRNAs are differentially distributed between the rat central nervous system and peripheral tissues. Endocrinology 1995;136:4139–4142.
[38] Kostich WA, Chen A, Sperle K, Largent BL. Molecular identification and analysis of a novel human corticotropin-releasing factor (CRF) receptor: the CRF2gamma receptor. Mol Endocrinol 1998;12: 1077–1085.
[39] Liaw CW, Lovenberg TW, Barry G, Oltersdorf T, Grigoriadis DE, de Souza EB. Cloning and characterization of the human corticotropin-releasing factor-2 receptor complementary deoxyribonucleic acid. Endocrinology 1996;137:72–77.
[40] Nishikimi T, Miyata A, Horio T, et al. Urocortin, a member of the corticotropin-releasing factor family, in normal and diseased heart. Am J Physiol Heart Circ Physiol 2000;279:H3031–9.
[41] Chen R, Lewis KA, Perrin MH, Vale WW. Expression cloning of a human corticotropin-releasing-factor receptor. Proc Natl Acad Sci U S A 1993;90:8967–8971.
[42] Stenzel P, Kesterson R, Yeung W, Cone RD, Rittenberg MB, Stenzel-Poore MP. Identification of a novel murine receptor for corticotropin-releasing hormone expressed in the heart. Mol Endocrinol 1995;9: 637–45.
[43] Wiley KE, Davenport AP. CRF2 receptors are highly expressed in the human cardiovascular system and their cognate ligands urocortins 2 and 3 are potent vasodilators. Br J Pharmacol 2004;143:508–14.
[44] Brar BK, Jonassen AK, Stephanou A, et al. Urocortin protects against ischemic and reperfusion injury via a MAPK-dependent pathway. J Biol Chem 2000;275:8508–14.
[45] Charles CJ, Rademaker MT, Richards AM. Urocortins: putative role in cardiovascular disease. Curr Med Chem Cardiovasc Hematol Agents 2004;2:43–7.
[46] Terui K, Higashiyama A, Horiba N, Furukawa KI, Motomura S, Suda T. Coronary vasodilation and positive inotropism by urocortin in the isolated rat heart. J Endocrinol 2001;169:177–83.
[47] Rademaker MT, Charles CJ, Espiner EA, Frampton CM, Lainchbury JG, Richards AM. Four-day urocortin-I administration has sustained beneficial haemodynamic, hormonal, and renal effects in experimental heart failure. Eur Heart J 2005;26:2055–62.
[48] Abdelrahman AM, Pang CC. Regional haemodynamic effects of urocortin in the anaesthetized rat. Eur J Pharmacol 2003;466:317–21.
[49] Bale TL, Picetti R, Contarino A, K oob GF, Vale WW, Lee KF. Mice deficient for both corticotropin-releasing factor receptor 1 (CRFR1) and CRFR2 have an impaired stress response and display sexually dichotomous anxiety-like behavior. J Neurosci 2002;22:193–9.
[50] Coste SC, Kesterson RA, Heldwein KA, et al. Abnormal adaptations to stress and impaired cardiovascular function in mice lacking corticotropin-releasing hormone receptor-2. Nat Genet 2000;24:403–9.
[51] Gordon JM, Dusting GJ, Woodman OL, Ritchie RH. Cardioprotective action of CRF peptide urocortin against simulated ischemia in adult rat cardiomyocytes. Am J Physiol Heart Circ Physiol 2003;284:H330–6.
[52] Huang Y, Chan FL, Lau CW, et al. Urocortin-induced endothelium-dependent relaxation of rat coronary artery: role of nitric oxide and K^+ channels. Br J Pharmacol 2002;135:1467–76.
[53] Latchman DS. Urocortin protects against ischemic injury via a MAPK-dependent pathway. Trends Cardiovasc Med 2001;11:167–9.
[54] Schulman D, Latchman DS, Yellon DM. Urocortin protects the heart from reperfusion injury via upregulation of p42/p44 MAPK signaling pathway. Am J Physiol Heart Circ Physiol 2002;283:H1481–8.
[55] Yang LZ, Kockskamper J, Heinzel FR, et al. Urocortin II enhances contractility in rabbit ventricular myocytes via CRF(2) receptor-mediated stimulation of protein kinase A. Cardiovasc Res 2006;69: 402–11.
[56] Rademaker MT, Cameron VA, Charles CJ, Richards AM. Urocortin 3: haemodynamic, hormonal, and renal effects in experimental heart failure. Eur Heart J 2006;27:2088–98.
[57] Rademaker MT, Cameron VA, Charles CJ, Richards AM. Integrated hemodynamic, hormonal, and renal actions of urocortin 2 in normal and paced sheep: beneficial effects in heart failure. Circulation 2005;112:3624–32.
[58] Weisinger RS, Blair-West JR, Burns P, et al. Cardiovascular effects of long-term central and peripheral administration of urocortin, corticotropin-releasing factor, and adrenocorticotropin in sheep. Endocrinology 2004;145:5598–5604.
[59] Mackay KB, Stiefel TH, Ling N, Foster AC. Effects of a selective agonist and antagonist of CRF2 receptors on cardiovascular function in the rat. Eur J Pharmacol 2003;469:111–115.
[60] Davis ME, Pemberton CJ, Yandle TG, et al. Urocortin 2 infusion in healthy humans: hemodynamic, neurohormonal, and renal responses. J Am Coll Cardiol 2007;49:461–471.
[61] Hausenloy DJ, Yellon DM. New directions for protecting the heart against ischaemia–reperfusion injury: targeting the Reperfusion Injury Salvage Kinase (RISK)-pathway. Cardiovasc Res 2004;61:448–460.

[62] Scarabelli TM, Pasini E, Stephanou A, et al. Urocortin promotes hemodynamic and bioenergetic recovery and improves cell survival in the isolated rat heart exposed to ischemia/reperfusion. J Am Coll Cardiol 2002;40:155–161.
[63] Brar BK, Stephanou A, Okosi A, et al. CRH-like peptides protect cardiac myocytes from lethal ischaemic injury. Mol Cell Endocrinol 1999;158:55–63.
[64] Okosi A, Brar BK, Chan M, et al. Expression and protective effects of urocortin in cardiac myocytes. Neuropeptides 1998;32:167–171.
[65] Brar BK, Stephanou A, Knight R, Latchman DS. Activation of protein kinase B/Akt by urocortin is essential for its ability to protect cardiac cells against hypoxia/reoxygenation-induced cell death. J Mol Cell Cardiol 2002;34:483–492.
[66] Garcia-Villalon AL, Amezquita YM, Monge L, et al. Mechanisms of the protective effects of urocortin on coronary endothelial function during ischemia–reperfusion in rat isolated hearts. Br J Pharmacol 2005;145:490–494.
[67] Lawrence KM, Kabir AM, Bellahcene M, et al. Cardioprotection mediated by urocortin is dependent on PKCepsilon activation. FASEB J 2005;19:831–833.
[68] Lawrence KM, Townsend PA, Davidson SM, et al. The cardioprotective effect of urocortin during ischaemia/reperfusion involves the prevention of mitochondrial damage. Biochem Biophys Res Commun 2004;321:479–486.
[69] Liu CN, Yang C, Liu XY, Li S. In vivo protective effects of urocortin on ischemia–reperfusion injury in rat heart via free radical mechanisms. Can J Physiol Pharmacol 2005;83:459–465.
[70] Agnello D, Bertini R, Sacco S, Meazza C, Villa P, Ghezzi P. Corticosteroid-independent inhibition of tumor necrosis factor production by the neuropeptide urocortin. Am J Physiol 1998;275:E757–E762.

Cilostazol attenuates ventricular arrhythmia induction and improves defibrillation efficacy in swine

Natnicha Kanlop, Krekwit Shinlapawittayatorn, Rattapong Sungnoon, Punate Weerateerangkul, Siriporn Chattipakorn, and Nipon Chattipakorn

Abstract: Previous reports demonstrated that cilostazol, a phosphodiesterase 3 inhibitor, affected cellular electrophysiology and reduced episodes of ventricular fibrillation (VF) in patients with Brugada syndrome. However, its effects on VF induction and defibrillation efficacy have never been investigated. We tested the hypothesis that cilostazol increases the VF threshold (VFT) and decreases the upper limit of vulnerability (ULV) and the defibrillation threshold (DFT). A total of 48 pigs were randomly assigned to defibrillation and VF induction studies. The diastolic pacing threshold (DPT), VFT, ULV, DFT, and effective refractory period were determined before and after the infusion of cilostazol at 6 mg/kg, 3 mg/kg, or vehicle. The DPT was significantly increased after administration of 3 and 6 mg/kg cilostazol. The ULV and DFT were significantly decreased after administration of 6 mg/kg cilostazol only. The ULV in the 6 mg/kg group had 12% lower peak voltage and 25% lower total energy, and the DFT had 13% lower peak voltage and 25% lower total energy. The VFT was not altered in any experimental group. This study shows that cilostazol administration significantly increased the DPT, which was associated with significantly reduced DFT and ULV.

Key words: cilostazol, phosphodiesterase 3, ventricular fibrillation threshold, defibrillation threshold, upper limit of vulnerability, arrhythmia inducibility.

Résumé : Des rapports antérieurs ont démontré que le cilostazol, un inhibiteur de la phosphodiestérase III, influe sur l'électrophysiologie cellulaire et réduit les épisodes de fibrillation ventriculaire (FV) dans le syndrome de Brugada. Toutefois ses effets sur l'induction de la FV et l'efficacité de la défibrillation n'ont jamais été examinés. Nous avons vérifié l'hypothèse que le cilostazol augmente le seuil de FV (SFV), et diminue la limite maximale de vulnérabilité (LMV) et le seuil de défibrillation (SDF). Nous avons réparti 48 porcs au hasard dans des groupes d'induction de fibrillation ventriculaire et de défibrillation. Nous avons déterminé le seuil de stimulation diastolique (SSD), la période réfractaire efficace, le SVF, la LMV et le SDF, avant et après la perfusion 6 mg/kg de cilostazol, de 3 mg/kg, ou d'un véhicule. L'administration de cilostazol a augmenté le SDF de manière significative. La perfusion de 6 mg/kg a augmenté significativement la LMV et le SDF. La LSV du groupe 6 mg/kg a eu une tension de crête de 12 % inférieure et une énergie totale de 25 % inférieure. Le SDF de ce groupe a eu une tension de crête de 13 % inférieure et une énergie totale de 25 % inférieure. Le SFV est demeuré stable chez tous les groupes expérimentaux. Ainsi, l'administration de cilostazol a augmenté significativement le SSD, ce qui a été associé à une réduction significative du SDF et de la LMV.

Mots-clés : cilostazol, phosphodiestérase 3, seuil de fibrillation ventriculaire, défibrillation, limite maximale de vulnérabilité, inductibilité d'arythmies.

[Traduit par la Rédaction]

Received 19 March 2009. Accepted 4 November 2009. Published on the NRC Research Press Web site at cjpp.nrc.ca on 20 April 2010.

N. Kanlop, K. Shinlapawittayatorn, R. Sungnoon, and P. Weerateerangkul. Cardiac Electrophysiology Unit, Department of Physiology, and Cardiac Electrophysiology Research and Training Center, Faculty of Medicine, Chiang Mai University, Chiang Mai, Thailand.
S. Chattipakorn. Faculty of Dentistry, and Cardiac Electrophysiology Research and Training Center, Faculty of Medicine, Chiang Mai University, Chiang Mai, Thailand.
N. Chattipakorn.[1] Cardiac Electrophysiology Unit, Department of Physiology; Cardiac Electrophysiology Research and Training Center, Faculty of Medicine; and Biomedical Engineering Center, Chiang Mai University, Chiang Mai, Thailand.

[1]Corresponding author (e-mail: nchattip@gmail.com).

Introduction

Cilostazol is a selective phosphodiesterase 3 (PDE3) inhibitor (Cone et al. 1999). Because of its potent effect on vasodilatation and antiplatelet aggregation, cilostazol was approved by the US Food and Drug Administration for claudication treatment (Dawson et al. 1998). The antiarrhythmic effects of cilostazol were first presented in atrial bradyarrhythmia (Atarashi et al. 1998). Previous studies demonstrated that cilostazol affected the automaticity of the heart by increasing heart rates in patients and improving symptoms in bradycardic atrial fibrillation, sick sinus syndrome, and Wenckebach type atrioventricular (AV) block (Madias 2003). In patients with third-degree AV block, cilostazol increased heart rates and increased the ventricular escape rate without the abolishment of AV block or a change in the fre-

quency of premature ventricular beats (Kodama-Takahashi et al. 2003). Also, cilostazol has been shown to decrease atrial natriuretic peptide (ANP) and brain natriuretic peptide (BNP) concentrations (Madias 2003), hormones presenting in AV asynchrony and heart failure (Mair et al. 2001).

In a recent case report on Brugada syndrome patients, it was shown that ventricular fibrillation (VF) episodes were completely abolished after oral administration of cilostazol at 200 mg/day (Tsuchiya et al. 2002). However, VF recurred when cilostazol was discontinued or reduced to 100 mg/day. In a 1-year follow-up of 3 patients with implanted cardioverter defibrillators, no VF occurred during cilostazol treatment (Tsuchiya et al. 2002). Recently, cilostazol has been shown to directly activate mitochondrial Ca^{2+}-activated K^+ channels, thus protecting the myocardium from ischemic and (or) reperfusion injury.(Fukasawa et al. 2008).

Despite this possible beneficial effect, direct investigation has never been tested regarding the effects of cilostazol on VF induction and defibrillation. In the present study, we tested the hypotheses that (*i*) cilostazol decreases VF inducibility by increasing VF threshold (VFT) and decreasing the upper limit of vulnerability (ULV), and that (*ii*) cilostazol improves defibrillation efficacy by decreasing the defibrillation threshold (DFT).

Materials and methods

Animal preparation and electrode placement

Forty-eight male and female Landrace pigs (25–30 kg) were used in this study. The animals were cared for in accordance with the *Guide to the Care and Use of Experimental Animals* (Olfert et al. 1993) and with the Institutional Animal Care and Use Committees of the Faculty of Medicine, Chiang Mai University. In each pig, anesthesia was induced with a combination of atropine (0.04 mg/kg), telazol (4.4 mg/kg), and xylazine (2.2 mg/kg) and maintained with 1.5%–3.0% isoflurane delivered in 100% oxygen (Shinlapawittayatorn et al. 2006). The surface electrocardiogram (lead II), arterial oxygen tension (Pa_{O_2}), end-tidal CO_2, femoral arterial blood pressure (BP), core temperature, respiratory rate, blood gases, and electrolytes were monitored throughout the study. Under artificial respiration, a catheter with a 34 mm platinum-coated titanium coil electrode (Guidant) was inserted into the right ventricular (RV) apex. A 68 mm electrode catheter was placed at the junction between the right atrium and the superior vena cava (Chattipakorn et al. 2000*a*). These 2 electrodes were used for shock delivery. The acute experiments were divided into 2 series: a VF induction study (series 1, $n = 24$) and a defibrillation study (series 2, $n = 24$). Pigs were randomly designated to 1 of these 2 series. In each series, the pigs were divided into 3 groups ($n = 8$ each). All parameters in the VF induction and defibrillation studies were determined before and after cilostazol or vehicle administration. In these cases, both BP and heart rate (HR) were determined from the data recorded before VFT, ULV, and DFT determination before drug or saline administration. The drug was infused for 50 min. At the end of the infusion, we waited for another 20 min before the determination of electrophysiological parameters (i.e., BP and HR) began.

Diastolic pacing threshold and effective refractory period measurement

A train of 10 S1 stimuli was delivered through a pacing electrode with a stimulation pulse of 5 ms at the tip of an RV catheter, beginning at 0.1 mA, with 500 ms intervals. The pacing current was increased in 0.1 mA increments until all S1 stimuli elicited a ventricular response. This current was defined as the diastolic pacing threshold (DPT). The effective refractory period (ERP) was determined by delivering an S2 stimulus after the last S1 stimulus. The S1–S2 interval was initially set at 350 ms and was reduced in 10 ms steps until an S2 stimulus was unable to elicit a ventricular response. This S1–S2 interval was defined as an ERP (Kanlop et al. 2008).

VF induction and ULV determination protocol

The interval between the last S1 and the peak T wave was determined 3 times from the lead II electrocardiogram. The average of these intervals was used as a coupling interval to deliver an S2 stimulus (S1–S2 coupling interval) (Chattipakorn et al. 2000*b*, 2000*c*, 2006; Rodríguez and Trayanova 2003; Swerdlow et al. 2003). The S2 shock was biphasic and was delivered by shocking electrodes with a Ventak external cardioverter-defibrillator (ECD) (Guidant). The initial shock strength was set at 100 V. If the shock induced VF, the shock strength was decreased in 10 V steps until VF was not induced (Compos et al. 1997; Malkin and Hoffmeister 2000). If the shock did not induce VF, the strength was increased in 10 V steps until VF was induced (Compos et al. 1997; Malkin and Hoffmeister 2000). The lowest shock strength required to induce VF is defined as the VFT (Lakkireddy et al. 2006).

For ULV determination, the coupling interval between the last S1 and the peak T wave was determined again. An S2 stimulus was then delivered at an initial shock strength of 400 V. The shock strength was increased or decreased after a 3-reversal up/down protocol (Chattipakorn et al. 2000*b*) The lowest shock strength above the VFT that was unable to induce VF was defined as the ULV. There was a minimum interval of 4 min between VF episodes to allow the heart to return to physiological conditions (Sungnoon et al. 2008).

Defibrillation protocol

VF was induced by delivering a 60 Hz AC current through the tip of the RV electrode. Defibrillation shocks were delivered with defibrillation electrodes after VF was induced for 10 s. For episodes in which defibrillation was unsuccessful, a rescue shock was delivered to restore sinus rhythm. A minimum interval of 4 min was allowed between VF episodes. The defibrillation shock strength was initially set at 400 V and was increased or decreased after the 3-reversal up/down protocol (Chattipakorn et al. 2000*a*). The lowest shock strength required for successful defibrillation after the third reversal was defined as the DFT.

Cilostazol preparation

Cilostazol solution was prepared as an aqueous stock solution (Hakaim et al. 1999; Saitoh et al. 1993). A 50 mg cilostazol (Pletal) tablet was dissolved in normal saline just before the experiment to form a concentration

Table 1. Electrophysiological and hemodynamic parameters measured before and after drug or saline administration in Landrace pigs.

	Group I, cilostazol 6 mg/kg		Group II, cilostazol 3 mg/kg		Group III, control	
	Before	After	Before	After	Before	After
Diastolic pacing threshold, mA	0.40±0.06	1.40±0.20**	0.40±0.07	0.90±0.08**	0.40±0.07	0.6±0.07
Effective refractory period, ms	273±9	293±9	233±8	253±12	234±8	246±6
S1–S2 coupling interval, ms	308±11	324±14	262±8	265±15	258±10	266±11
Systolic blood pressure, mm Hg	121±6	113±5	122±7	120±5	120±5	123±9
Diastolic blood pressure, mm Hg	78±6	79±6	82±6	78±3	74±5	77±8
Heart rate, beats/min	86±3	86±5	99±5	106±4	99±5	103±3

Note: The control group received 100 mL saline (vehicle). Values are means of 8 animals per group. **, Significant at $p = 0.01$ vs. before drug administration (within group).

of 0.5 mg/mL. The solution was then filtered using Whatman No. 1 filter paper until a clear solution was obtained.

A previous study reported that the pharmacological effects were demonstrated with an infusion of cilostazol 3 mg/kg body weight in the in vivo model (Hakaim et al. 1999). Therefore, in the present study, we started by intravenously administering cilostazol at a dose of 6 mg/kg, 3 mg/kg, or vehicle (100 mL saline) in groups I, II, and III, respectively, over 50 min, to investigate their effects on fibrillation induction and defibrillation efficacy.

Statistical analysis

Values are expressed as means ± SE in both VF induction and defibrillation studies. Analysis of covariance (ANCOVA) was used to assess whether the inequality of the baseline values affected the results after treatment. Comparisons of variables before and after drug or saline administration (within-group comparison) were performed individually in each group by using the paired 2-tailed Student's t test. Values of $p < 0.05$ were considered statistically significant.

Results

The basic cardiac electrophysiological and hemodynamic parameters (DPT, ERP, S1–S2 coupling interval, HR, systolic BP (SBP), and diastolic BP (DBP)) in all experimental groups are shown in Table 1. After the drug administration in groups I (cilostazol 6 mg/kg) and II (cilostazol 3 mg/kg), the DPT (tested DPT) was significantly higher ($p = 0.01$ in both groups) than the DPT before drug administration (control DPT). In group III, vehicle (saline) did not change the DPT compared with baseline. The ERPs were not different in any of the experimental groups. The S1–S2 coupling interval before and after drug administration was not different in any of the groups. Both concentrations of cilostazol and vehicle administration did not change systolic BP, diastolic BP, or HR.

In the VF induction study, the number of VF episodes requiring defibrillation shocks before drug administration was 7.4 ± 0.5, 6.8 ± 0.4, and 7.0 ±0.3 episodes in groups I, II, and III, respectively, and after drug administration was 6.3 ± 0.3, 7.0 ± 0.6, and 7.1 ± 0.3 episodes, respectively. It has been shown that the VF episodes were not significantly different in any of the groups. The peak voltage, total energy, impedance, and pulse width of VFT before and after drug or vehicle administration were not changed in any of the experimental groups (Fig. 1). From the analysis of covariance, the tested ULV was found to be affected by the baseline ULV. Despite this effect, the tested ULV was still significantly ($p < 0.05$) decreased after 6 mg/kg cilostazol administration (Figs. 2A, 2B). In the 6 mg/kg group, peak voltage was reduced by 12% and total energy was reduced by 25%. The impedance and pulse width were not significantly changed in any of the experimental groups (Figs. 2C, 2D). Furthermore, in group I, the ULV – VFT window width, calculated by subtracting the VFT from the ULV, was shown to significantly decrease compared with the ULV – VFT window width before drug administration. This effect was not shown in groups II or III. (Table 2)

In the defibrillation study, before drug administration, VF was induced 7.1 ± 0.6, 7.5 ± 1.0, and 9.1 ± 0.5 episodes in groups I, II, and III, respectively; after drug administration, VF was induced 6.9 ± 1.0, 6.9 ± 0.6, and 9.0 ± 0.5 episodes, respectively. It has been shown that the VF episodes were not significantly different in any of the groups. The tested DFT was affected by the baseline DFT. However, 6 mg/kg cilostazol significantly decreased the DFT from the baseline.(Figs. 3A, 3B). In the 6 mg/kg group, peak voltage was reduced by approximately 13% and total energy was reduced by approximately 25%. The peak voltage and total energy for the DFT before and after drug or saline administration were not different in groups II or III. The impedance and pulse width were not significantly changed in any of the groups (Figs. 3C, 3D).

Discussion

The major findings of this study are as follows: (*i*) administration of both 3 and 6 mg/kg cilostazol significantly increased the DPT; and (*ii*) a 6 mg/kg cilostazol infusion significantly decreased the ULV and the DFT.

Effects of cilostazol on myocardial stabilization

In the past, there was disagreement over the use of PDE3 inhibitors in patients with cardiac disease, since the inhibitors facilitate the incidence of arrhythmia in this group of patients (Feldman et al. 1993; Packer et al. 1991). Previous studies investigated the effects of PDE3 inhibitors, such as amrinone, milrinone, and enoximone, on cardiac electrophysiological parameters by measuring HR, QT_c (corrected QT interval), and atrial or ventricular ERP (Goldstein et al. 1986; Miles et al. 1989; Naccarelli et al. 1984). However, the effects of cilostazol on the DPT and ERP have never been investigated.

It is known that PDE3 has many isoforms, and that PDE3 inhibitory drugs demonstrate different effects depending on

Fig. 1. Effects of cilostazol on electrophysiological parameters for the ventricular fibrillation threshold before and after drug administration (n = 8 pigs per group).

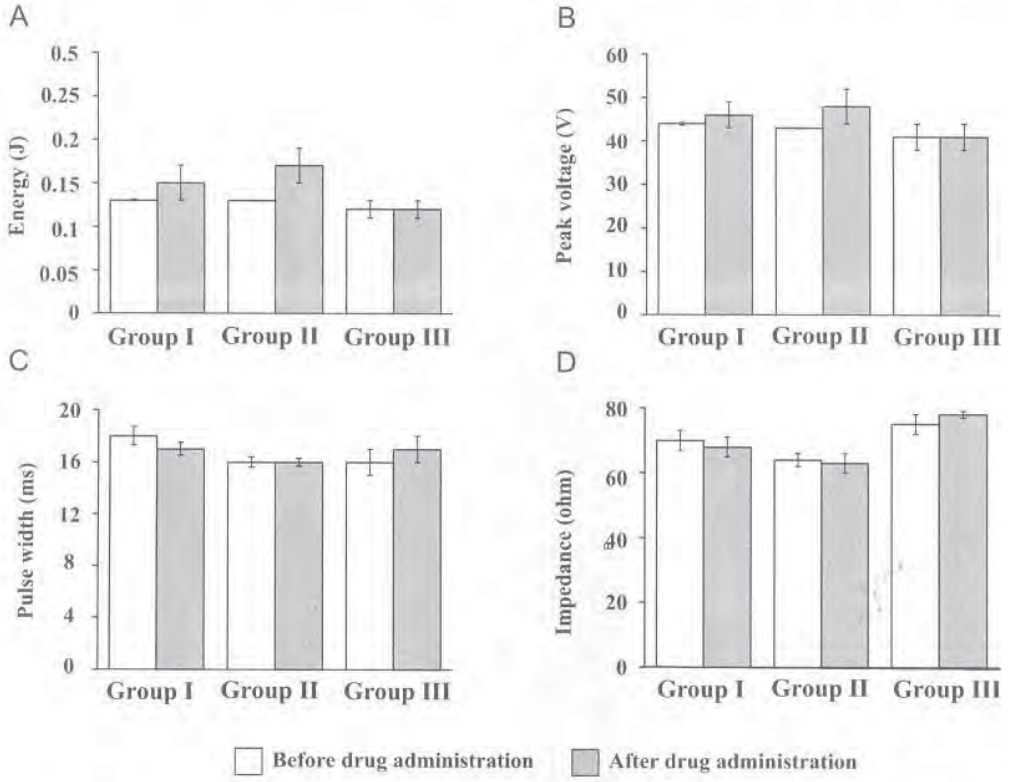

Fig. 2. Effects of cilostazol on electrophysiological parameters for the upper limit of vulnerability before and after drug administration. *, Significant at $p < 0.05$ vs. before drug administration (within group, n = 8).

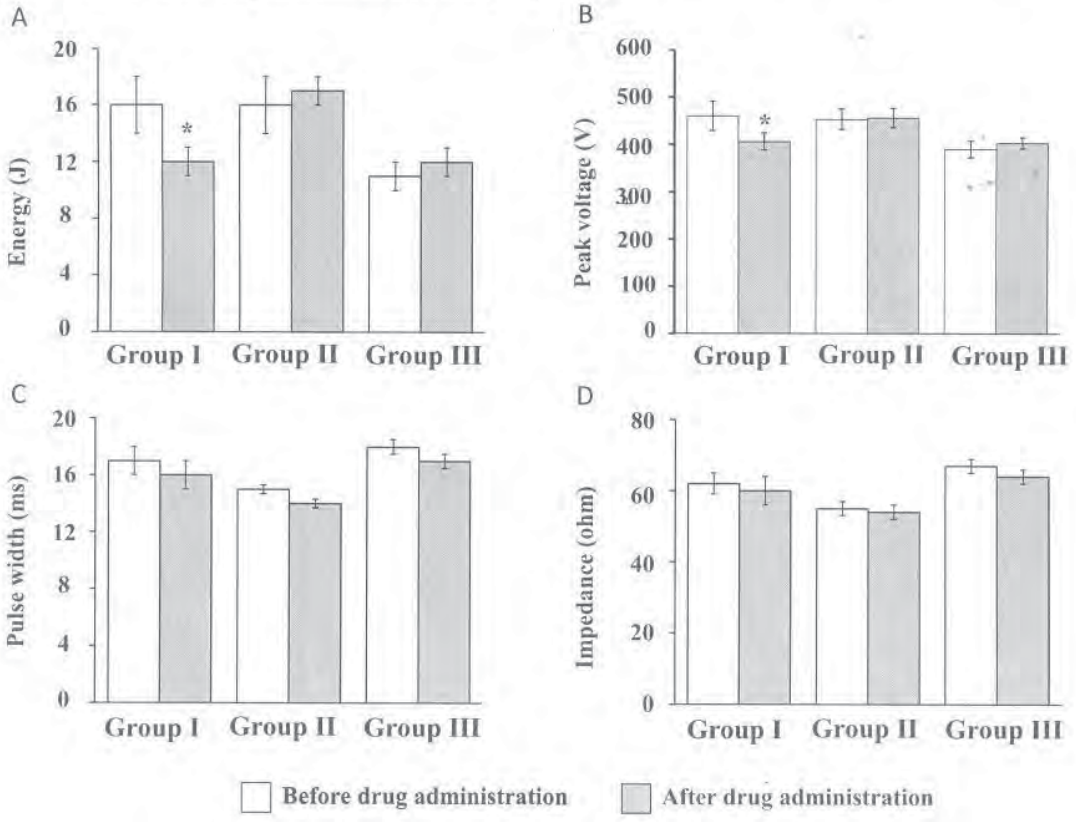

Table 2. The mean ventricular fibrillation induction window width (ULV–VFT) in the 3 treatment groups.

	Group I, cilostazol 6 mg/kg		Group II, cilostazol 3 mg/kg		Group III, control	
	Before	After	Before	After	Before	After
Voltage, V	416±31	360±16*	410±22	407±20	349±19	362±13
Energy, J	16±2	12±1*	17±1	17±1	11±3	12±2

Note: ULV, upper limit of vulnerability; VFT, ventricular fibrillation threshold. Values are means of 8 animals per group.
*, Significant at $p < 0.05$ vs. before drug administration (within group).

Fig. 3. Effects of cilostazol on electrophysiologic parameters for the defibrillation threshold before and after drug administration. *, Significant at $p < 0.05$ vs. before drug administration (within group, $n = 8$).

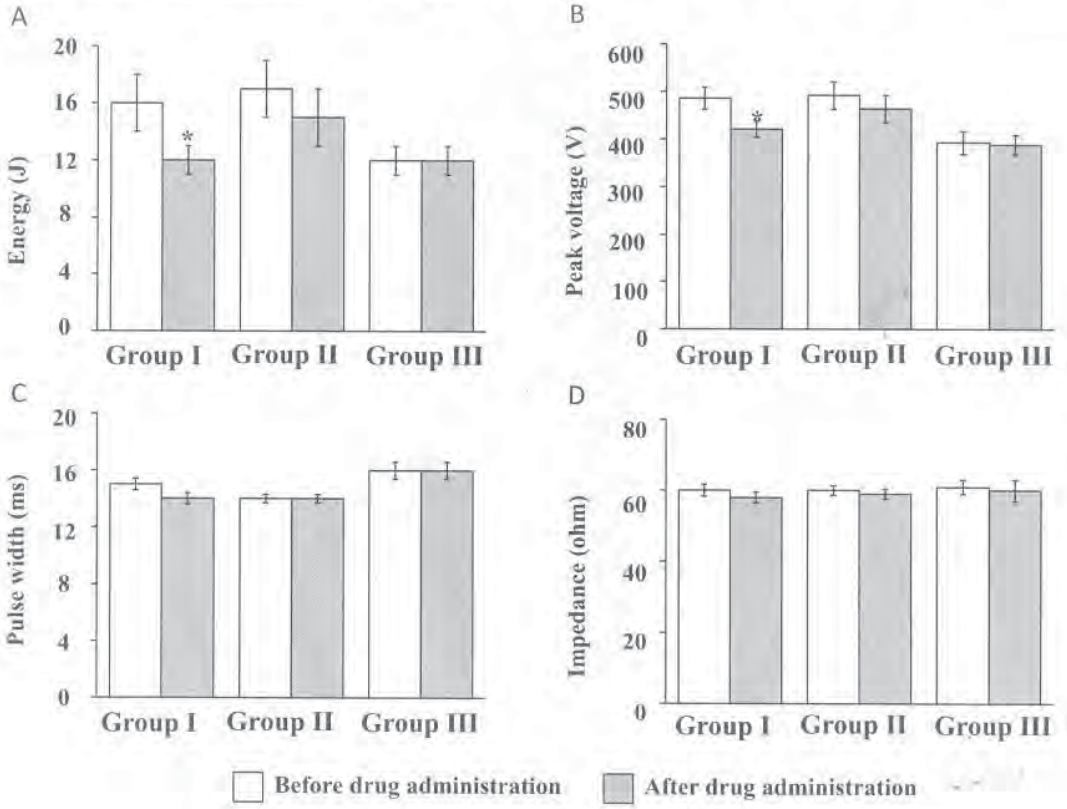

the PDE3 isoform they inhibit (Atarashi et al. 1998; Cone et al. 1999; Hambleton et al. 2005). In this study, ERP was not changed from baseline after cilostazol administration. This finding is similar to that reported previously using other PDE3 inhibitors (Goldstein et al. 1986; Miles et al. 1989; Naccarelli et al. 1984). However, the effect of a PDE3 inhibitor on the DPT has never been investigated. In our study, cilostazol increased the DPT. It is possible that the effect of cilostazol on the DPT is similar to or different from previously tested PDE3 inhibitors, because of the different isoforms that each drug inhibits. This hypothesis remains to be tested.

Recently, Fukasawa and colleagues (2008) demonstrated that cilostazol promotes the electrical stability of myocardium in ischemic and (or) reperfusion injury in isolated hearts by directly activating mitochondrial Ca^{2+}-activated K^+ ($mitoK_{Ca}$) channels, leading to an attenuation of Ca^{2+} overload in mitochondria and the stabilization of Ca^{2+} homeostasis. Furthermore, in normal hearts, cilostazol is known to activate L-type Ca^{2+} channels using a cAMP-activated protein kinase A pathway (Verde et al. 1999).

Effects of cilostazol on defibrillation efficacy

In this study, we demonstrated that cilostazol 6 mg/kg increased defibrillation efficacy by significantly decreasing the DFT. The DFT was not significantly changed after the infusion of cilostazol 3 mg/kg. Since uniform dispersion of refractoriness is an important determinant of successful defibrillation, one possible explanation for this observation is that cilostazol decreases the degree of dispersion of refractoriness in a dose-dependent manner. Future studies are needed to test this hypothesis.

Effects of cilostazol on VF induction

In the present study, the administration of cilostazol 6 mg/kg significantly decreased the ULV, and the proportion of ULV reduction was similar to the proportion of DFT reduction. Previous studies have demonstrated a close correlation between

the ULV and the DFT (Green et al. 2003; Rodríguez and Trayanova 2003). Our study has shown that both dosages of cilostazol increased the DPT. It is possible that the DPT increased by cilostazol decreases the sensitivity of the myocardium to any premature stimulus. According to the ULV hypothesis for defibrillation, shocks weaker than the ULV fail to defibrillate because they fall into the vulnerable period, thus reinitiating VF (Chen et al. 1986). Our results are consistent with such reports. Regarding the reentrant mechanism, the important factors for VF initiation and sustained VF are the initiation of new wave fronts, an increased dispersion of refractoriness that leads to unidirectional block, and a decreased conduction velocity (Rodríguez and Trayanova 2003).

Study limitations

This study was performed in normal pig hearts. The effects of cilostazol on VF induction or defibrillation may be different in diseased hearts, such as those in patients with Brugada syndrome or myocardial infarction. Also, it is possible that cilostazol 6 mg/kg increases the VFT, but that the VFT protocol used in our study was not sensitive enough (10 V steps) to detect it. This may explain why VFT did not significantly change after cilostazol administration. Since the plasma level of cilostazol was not measured, the relationship between plasma concentration and the observed effects remains to be investigated. The definite mechanism responsible for this dose-dependent effect of cilostazol on the ULV and the DFT was not elucidated in this study because of technical limitations. Our DPT and ERP results do not predict total electrical stability, since they were determined at only a single site. Although it is possible that DPT increases with time because of electrode contact changes or tissue damage, it is likely that the increase in DPT by cilostazol in our study was due to the effect of the drug itself because saline did not change the DPT. Furthermore, the vascular effect of cilostazol was not observed in this study. It is possible that these effects were masked by the effects of the deep general anesthesia with fluid maintenance that was used to keep the animal under physiological conditions throughout the study.

Conclusion

Cilostazol alters cardiac electrophysiology by increasing the DPT and decreasing the ULV and DFT. These findings indicate that cilostazol can decrease VF inducibility by reducing the ULV and can improve defibrillation efficacy by reducing the shock energy required to successfully defibrillate the heart.

Acknowledgments

This study was supported by the Young Investigator Research Fund, Chiang Mai University (N.K.); the Faculty of Medicine Endowment Fund, Chiang Mai University (N.K.); and the Thailand Research Fund, grants RTA5280006 (N.C.) and RMU5180007 (S.C.).

References

Atarashi, H., Endoh, Y., Saitoh, H., Kishida, H., and Hayakawa, H. 1998. Chronotropic effects of cilostazol, a new antithrombotic agent, in patients with bradyarrhythmias. J. Cardiovasc. Pharmacol. **31**(4): 534–539. doi:10.1097/00005344-199804000-00010. PMID:9554801.

Chattipakorn, N., Fotuhi, P.C., and Ideker, R.E. 2000*a*. Prediction of defibrillation outcome by epicardial activation patterns following shocks near the defibrillation threshold. J. Cardiovasc. Electrophysiol. **11**(9): 1014–1021. doi:10.1111/j.1540-8167.2000.tb00174.x. PMID:11021472.

Chattipakorn, N., Fotuhi, P.C., Zheng, X., and Ideker, R.E. 2000*b*. Left ventricular apex ablation decreases the upper limit of vulnerability. Circulation, **101**(21): 2458–2460. PMID:10831517.

Chattipakorn, N., Rogers, J.M., and Ideker, R.E. 2000*c*. Influence of postshock epicardial activation patterns on initiation of ventricular fibrillation by upper limit of vulnerability shocks. Circulation, **101**(11): 1329–1336. PMID:10725295.

Chattipakorn, N., Shinlapawittayatorn, K., Sungnoon, R., and Chattipakorn, S.C. 2006. Effects of n-3 polyunsaturated fatty acid on upper limit of vulnerability shocks. Int. J. Cardiol. **107**(3): 299–302. doi:10.1016/j.ijcard.2005.03.032. PMID:16503251.

Chen, P.S., Shibata, N., Dixon, E.G., Martin, R.O., and Ideker, R.E. 1986. Comparison of the defibrillation threshold and the upper limit of ventricular vulnerability. Circulation, **73**(5): 1022–1028. PMID:3698224.

Compos, A.T., Malkin, R.A., and Ideker, R.E. 1997. An up-down Bayesian, defibrillation efficacy estimator. Pacing Clin. Electrophysiol. **20**(5 Pt 1): 1292–1300. doi:10.1111/j.1540-8159.1997.tb06782.x. PMID:9170129.

Cone, J., Wang, S., Tandon, N., Fong, M., Sun, B., Sakurai, K., et al. 1999. Comparison of the effects of cilostazol and milrinone on intracellular cAMP levels and cellular function in platelets and cardiac cells. J. Cardiovasc. Pharmacol. **34**(4): 497–504. doi:10.1097/00005344-199910000-00004. PMID:10511123.

Dawson, D.L., Cutler, B.S., Meissner, M.H., and Strandness, D.E., Jr. 1998. Cilostazol has beneficial effects in treatment of intermittent claudication: results from a multicenter, randomized, prospective, double-blind trial. Circulation, **98**(7): 678–686. PMID:9715861.

Feldman, A.M., Bristow, M.R., Parmley, W.W., Carson, P.E., Pepine, C.J., Gilbert, E.M., et al.Vesnarinone Study Group. 1993. Effects of vesnarinone on morbidity and mortality in patients with heart failure. N. Engl. J. Med. **329**(3): 149–155. doi:10.1056/NEJM199307153290301. PMID:8515787.

Fukasawa, M., Nishida, H., Sato, T., Miyazaki, M., and Nakaya, H. 2008. 6-[4-(1-Cyclohexyl-1H-tetrazol-5-yl)butoxy]-3,4-dihydro-2-(1H)quinolinone (cilostazol), a phosphodiesterase type 3 inhibitor, reduces infarct size via activation of mitochondrial $Ca2^{+}$-activated K^{+} channels in rabbit hearts. J. Pharmacol. Exp. Ther. **326**(1): 100–104. doi:10.1124/jpet.108.136218. PMID:18381926.

Goldstein, R.A., Geraci, S.A., Gray, E.L., Rinkenberger, R.L., Dougherty, A.H., and Naccarelli, G.V. 1986. Electrophysiologic effects of milrinone in patients with congestive heart failure. Am. J. Cardiol. **57**(8): 624–628. doi:10.1016/0002-9149(86)90847-7. PMID:3953448.

Green, U.B., Garg, A., Al-Kandari, F., Ungab, G., Tone, L., and Feld, G.K. 2003. Successful implantation of cardiac defibrillators without induction of ventricular fibrillation using upper limit of vulnerability testing. J. Interv. Card. Electrophysiol. **8**(1): 71–75. doi:10.1023/A:1022304417889. PMID:12652181.

Hakaim, A.G., Cunningham, L., White, J.L., and Hoover, K. 1999. Selective type III phosphodiesterase inhibition prevents elevated compartment pressure after ischemia/reperfusion injury. J. Trauma, **46**(5): 869–872. doi:10.1097/00005373-199905000-00016. PMID:10338405.

Hambleton, R., Krall, J., Tikishvili, E., Honeggar, M., Ahmad, F.,

Manganiello, V.C., and Movsesian, M.A. 2005. Isoforms of cyclic nucleotide phosphodiesterase PDE3 and their contribution to cAMP hydrolytic activity in subcellular fractions of human myocardium. J. Biol. Chem. **280**(47): 39168–39174. doi:10.1074/jbc.M506760200. PMID:16172121.

Kanlop, N., Shinlapawittayatorn, K., Sungnoon, R., Chattipakorn, S., Lailerd, N., and Chattipakorn, N. 2008. Sildenafil citrate on the inducibility of ventricular fibrillation and upper limit of vulnerability in swine. Med. Sci. Monit. **14**(10): BR205–BR209. PMID:18830184.

Kodama-Takahashi, K., Kurata, A., Ohshima, K., Yamamoto, K., Uemura, S., Watanabe, S., and Iwata, T. 2003. Effect of cilostazol on the ventricular escape rate and neurohumoral factors in patients with third-degree atrioventricular block. Chest, **123**(4): 1161–1169. doi:10.1378/chest.123.4.1161. PMID:12684307.

Lakkireddy, D., Wallick, D., Ryschon, K., Chung, M.K., Butany, J., Martin, D., et al. 2006. Effects of cocaine intoxication on the threshold for stun gun induction of ventricular fibrillation. J. Am. Coll. Cardiol. **48**(4): 805–811. doi:10.1016/j.jacc.2006.03.055. PMID:16904553.

Madias, J.E. 2003. Cilostazol: an "intermittent claudication" remedy for the management of third-degree AV block. Chest, **123**(4): 979–982. doi:10.1378/chest.123.4.979. PMID:12684279.

Mair, J., Hammerer-Lercher, A., and Puschendorf, B. 2001. The impact of cardiac natriuretic peptide determination on the diagnosis and management of heart failure. Clin. Chem. Lab. Med. **39**(7): 571–588. doi:10.1515/CCLM.2001.093. PMID:11522102.

Malkin, R.A., and Hoffmeister, B.K. 2000. Hemodynamic collapse, geometry, and the rapidly paced upper limit of ventricular vulnerability to fibrillation by T-wave stimulation. J. Electrocardiol. **33**(3): 279–286. doi:10.1054/jelc.2000.7663. PMID:10954381.

Miles, W.M., Heger, J.J., Minardo, J.D., Klein, L.S., Prystowsky, E.N., and Zipes, D.P. 1989. The electrophysiologic effects of enoximone in patients with preexisting ventricular tachyarrhythmias. Am. Heart J. **117**(1): 112–121. doi:10.1016/0002-8703(89)90664-9. PMID:2521415.

Naccarelli, G.V., Gray, E.L., Dougherty, A.H., Hanna, J.E., and Goldstein, R.A. 1984. Amrinone: acute electrophysiologic and hemodynamic effects in patients with congestive heart failure. Am. J. Cardiol. **54**(6): 600–604. doi:10.1016/0002-9149(84)90257-1. PMID:6475780.

Olfert, O.D., Cross, B.M., and McWilliam, A.A. (*Editors*). 1993. Guide to the care and use of experimental animals. 2nd ed. Canadian Council on Animal Care, Ottawa, Canada.

Packer, M., Carver, J.R., Rodeheffer, R.J., Ivanhoe, R.J., DiBianco, R., Zeldis, S.M., et al.; The PROMISE Study Research Group. 1991. Effect of oral milrinone on mortality in severe chronic heart failure. N. Engl. J. Med. **325**(21): 1468–1475. PMID:1944425.

Rodríguez, B., and Trayanova, N. 2003. Upper limit of vulnerability in a defibrillation model of the rabbit ventricles. J. Electrocardiol. **36**(Suppl): 51–56. doi:10.1016/j.jelectrocard.2003.09.066. PMID:14716592.

Saitoh, S., Saito, T., Otake, A., Owada, T., Mitsugi, M., Hashimoto, H., and Maruyama, Y. 1993. Cilostazol, a novel cyclic AMP phosphodiesterase inhibitor, prevents reocclusion after coronary arterial thrombolysis with recombinant tissue-type plasminogen activator. Arterioscler. Thromb. **13**(4): 563–570. PMID:8385480.

Shinlapawittayatorn, K., Sungnoon, R., Chattipakorn, S., and Chattipakorn, N. 2006. Effects of sildenafil citrate on defibrillation efficacy. J. Cardiovasc. Electrophysiol. **17**(3): 292–295. doi:10.1111/j.1540-8167.2006.00348.x. PMID:16643403.

Sungnoon, R., Kanlop, N., Chattipakorn, S.C., Tawan, R., and Chattipakorn, N. 2008. Effects of garlic on the induction of ventricular fibrillation. Nutrition, **24**(7–8): 711–716. doi:10.1016/j.nut.2008.03.003. PMID:18456459.

Swerdlow, C., Shivkumar, K., and Zhang, J. 2003. Determination of the upper limit of vulnerability using implantable cardioverter-defibrillator electrograms. Circulation, **107**(24): 3028–3033. doi:10.1161/01.CIR.0000074220.19414.18. PMID:12810611.

Tsuchiya, T., Ashikaga, K., Honda, T., and Arita, M. 2002. Prevention of ventricular fibrillation by cilostazol, an oral phosphodiesterase inhibitor, in a patient with Brugada syndrome. J. Cardiovasc. Electrophysiol. **13**(7): 698–701. doi:10.1046/j.1540-8167.2002.00698.x. PMID:12139296.

Verde, I., Vandecasteele, G., Lezoualc'h, F., and Fischmeister, R. 1999. Characterization of the cyclic nucleotide phosphodiesterase subtypes involved in the regulation of the L-type Ca^{2+} current in rat ventricular myocytes. Br. J. Pharmacol. **127**(1): 65–74. doi:10.1038/sj.bjp.0702506. PMID:10369457.

Indian J Med Res 131, March 2010, pp 411-417

Reversible acetylcholinesterase inhibitory effect of *Tabernaemontana divaricata* extract on synaptic transmission in rat CA1 hippocampus

Wasana Pratchayasakul, Anchalee Pongchaidecha, Nipon Chattipakorn & Siriporn C. Chattipakorn*

*Department of Physiology, Faculty of Medicine & *Department of Odontology & Oral Pathology, Faculty of Dentistry, Chiang Mai University, Chiang Mai, Thailand*

Received November 17, 2008

***Background & objectives*: Acetylcholinesterase inhibitors (AChE-Is) are used for the treatment of Alzheimer's disease (AD). These drugs including galanthamine have been shown to modulate synaptic activity in hippocampus and improve memory processes. Although *Tabernaemontana divaricata* extract (TDE) has been used as traditional medicine for various pharmacological effects, its effect in enhancing cholinergic activity provides additional benefit to its known effects. We investigated whether TDE can modulate the synaptic function in hippocampus and compared its effects to those of galanthamine.**

***Methods*: Hippocampal slices were prepared from male Wistar rats, functional effects of TDE were characterized by using pharmacological tools and extracellular recordings of field excitatory postsynaptic potentials (fEPSPs).**

***Results*: TDE significantly reduced fEPSPs. The fEPSPs reduction was prevented by atropine, but not pancuronium. These TDE effects were similar to those of galanthamine.**

***Interpretation & conclusions*: Our findings indicate that TDE can effectively modulate synaptic responses in the hippocampus similar to galanthamine, suggesting that this traditional medicine could be beneficial in ageing with ACh deprivation in the brain.**

Key words Acetylcholinesterase inhibitor - field excitatory postsynaptic potentials- hippocampus - *Tabernaemontana divaricata*

Acetylcholine (ACh), acting through neuronal muscarinic acetylcholine receptors (mAChRs) and nicotinic acetylcholine receptors (nAChRs), is an important modulator of electrical activity in the brain. It is involved in numerous cellular processes underlying cognition including development, synaptic transmission, neuronal excitability and systems-level rhythmicity[1-3]. Stimulation of cholinergic inputs to the hippocampus demonstrates a decrease in the size of synaptic responses in glutamatergic projections in different regions of the hippocampus[1,4-8]. An acetylcholinesterase inhibitor (AChE-I), physostigmine, has been shown to enhance cholinergic transmission and depress glutamate release in hippocampal pathways[9]. Modulation of the synaptic strength of excitatory glutamate synapses in the hippocampus is believed to be involved in memory processing[10].

The loss of cholinergic function, particularly in the hippocampus, has been implicated in Alzheimer's

disease (AD)[11]. Current treatment is mainly based on the use of AChE-Is. Although some beneficial effects of these drugs on cognition have been reported, these are costly and have undesirable side effects[12]. Several drugs commonly used today for AD treatment were developed from local and traditional medicine, such as galanthamine, an AChE-I which was developed from alkaloids in 'Snowdrop'[13].

Tabernaemontana divaricata (L.) R. Br. Ex Roem. & Schult (*T. divaricata*), a garden plant in tropical countries, is a rich source of alkaloids with various pharmacological properties[14]. *T. divaricata* has been used in the folk medicine for anti-infection, anti-inflammation, analgesic effect, anti-tumour effect, antioxidative effect and the effect in neuronal activity[15]. Ingkaninan *et al*[16] have shown *in vitro* that ethanol extracts from *T. divaricata* root (TDE) at a concentration of 0.1 mg/ml inhibit >90 per cent of AChE activity. Recently, we have demonstrated that TDE acts as a reversible neuronal AChE-I in rats[17]. These findings suggest that this traditional medicine could possibly help to improve memory, particularly in ageing with ACh deprivation in the brain. Despite this advancement in our understanding of the effects of TDE, its functional effect in the hippocampus, a brain region critical for learning and memory, has never been investigated. Therefore, in the present study we tested whether TDE can modulate dendritic field excitatory postsynaptic potentials (fEPSPs), which indicate the neuronal synaptic function, in *Cornu Ammonis* 1 (CA1) hippocampal slices of normal rats as found in current AChE-I drugs used for AD therapy. We also compared the effects of TDE with galanthamine, a well-known AChE-I drug used to treat AD patients.

Material & Methods

Plant materials and T. divaricata extract: *T. divaricata* (collection no. Changwijit 0020 at the PBM herbarium, Fac. Pharmaceutical Sciences, Mahidol University, Thailand) was collected from Phitsanulok, Thailand. Roots were extracted as described previously[17]. To validate the quality of TDE in each experiment, each lot was analyzed for inhibitory effects of AChE activity *in vitro* and *in vivo* before being used.

Hippocampal slice preparation: The study protocol was approved from the Faculty of Medicine, Chiang Mai University Institutional Animal Care and Use Committee. Hippocampal slices (400 μm) were prepared from 4-5 wk old male Wistar rats obtained from the National Animal Center, Salaya Campus, Mohidol University, Thailand (n=23) using standard methods. Rats were anaesthetized with halothane, decapitated, and the brain removed and placed in ice-cold "high sucrose" artificial CSF (aCSF) containing (mM): NaCl 85; KCl 2.5; $MgSO_4$ 4; $CaCl_2$ 0.5; NaH_2PO_4 1.25; $NaHCO_3$ 25; glucose 25; sucrose 75; kynurenic acid 2; ascorbate 0.5, saturated with 95 per cent O_2/5 per cent CO_2 (pH 7.4). This solution enhanced neuronal survival during the slicing procedure. Hippocampal slices were cut using a vibratome (Vibratome Company, St. Louis, MO, USA). Following a 30-min post-slice incubation in high sucrose aCSF, slices were transferred to a standard aCSF solution containing (mM): NaCl 119; KCl 2.5; $CaCl_2$ 2.5; $MgSO_4$ 1.3; NaH_2PO_4 1; $NaHCO_3$ 26; and glucose 10, saturated with 95 per cent O_2/5 per cent CO_2 (pH 7.4) for an additional 30 min. For recordings, the slices were transferred to a submersion recording chamber and continuously perfused at 3-4 ml/min with standard aCSF warmed to 25-28°C.

Stimulation and recording: CA1 fEPSPs were recorded (Axopatch 200B, Axon Instruments, CA, USA) using standard methods described previously[18]. A stainless steel bipolar stimulating electrode (FHC, Bowdoinham, ME, USA) was placed in stratum radiatum to stimulate the Schaffer collaterals. A glass microelectrode (Sutter Instrument, Novato, CA, USA) filled with 2M of NaCl (Sigma, St. Louis, MO, USA) was placed in CA1 stratum radiatum to record fEPSPs. The stimulus frequency was 0.1 Hz. The stimulus intensity was adjusted to yield a fEPSP of 0.8-1.0mV in amplitude and produce ~50 per cent of maximal fEPSP responses. The delivery of two stimuli in rapid succession (50 msec interstimulus interval) elicited paired-pulse facilitation (PPF).

Drug application: Substances used in this experiment included TDE (dissolved in ethanol), atropine, ACh and galanthamine (dissolved in ddH_2O). Appropriate concentrations of specific substances in solution were determined experimentally[17]. In baseline and wash conditions, hippocampal slices were perfused with standard aCSF. The same amount of ethanol was added to standard aCSF in baseline and wash conditions as was used for dissolving TDE. All chemicals were applied to the slices in a bath chamber via gravity perfusion. All chemicals were obtained from Sigma, St. Louis, MO, USA.

Data analysis: Data were filtered at 3 kHz, digitized at 10 kHz, and stored on a computer using pClamp 9.2 software (Axon Instruments, CA, USA). The initial slope of the fEPSP was measured and plotted vs. time. The initial slope is the first slope of the field

potential detected following stimulus artifact and fiber valley. The initial slope is used for measurement of synaptic strength in the synaptic experiment. Statistical significance between the groups was determined with the Student's t-test. Only experiments with less than a 10 per cent change in the original baseline were included in the analysis.

Results

TDE's effect on fEPSPs was recorded in the stratum radiatum of the CA1 hippocampus, in response to stimulation of Schaffer collaterals. Paired-pulse facilitation (PPF), in response to paired stimulation pulses, was used to clarify Schaffer collateral pathways (Fig. 1A). TDE (60 µg/ml) reduced the size of the responses beginning 2-3 min after the start of infusion, with maximum effects appearing over the following 5-7 min. In our set-up, compounds added to the infusion line required approximately 1 min to reach the slices. The fEPSP depression was prominent and did not appear to be accompanied by distortion of waveform (Fig. 1A, inset). The fEPSP responses returned to the same level as baseline responses after 15 min of washout (Fig. 1A). The mean depression of fEPSPs following the application of 60 µg/ml of TDE was 47 ± 4 per cent (n=7, Fig. 1B). We used 60 µg/ml of TDE in this study since this concentration demonstrated maximum effect on the depression of fEPSPs in this study. TDE with concentrations higher than 10 µg/ml transiently reduced synaptic responses. The range of fEPSP depression in TDE concentrations of 10-100 µg/ml was 46-75 per cent (n=5 per dose, the dose response curve of TDE was not shown).

The effects of 60 µg/ml of TDE were completely blocked by 10 µM atropine, an mAChR antagonist (Fig. 2A and 2B), suggesting that the TDE effect was mediated by mAChRs. We used a high concentration of atropine (10 µM) since it can completely block the TDE effect on reducing synaptic response in all hippocampal slices. To investigate whether the nAChRs were involved in the synaptic modulation of TDE, pancuronium

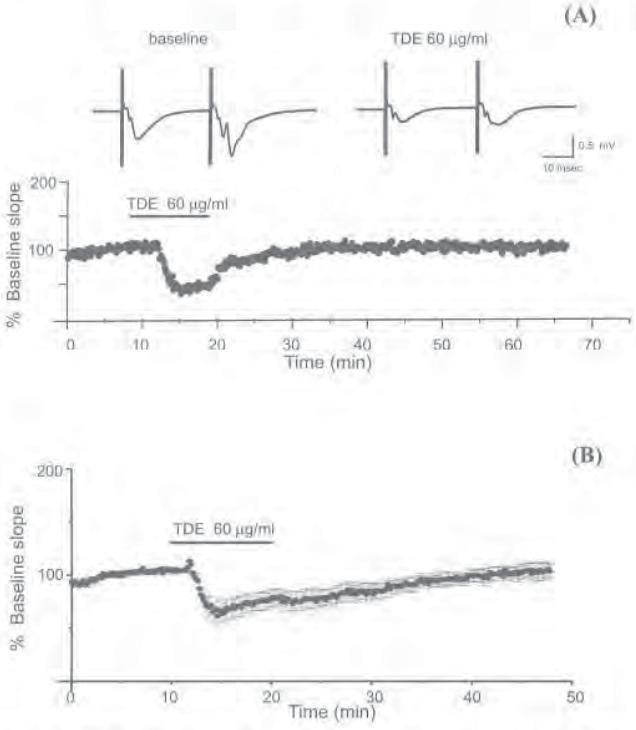

Fig. 1. TDE effects on CA1 hippocampal responses. **(A)** TDE-induced depression of synaptic responses. Traces were obtained from the experiment shown in 1A (inset). Each trace shows the average of 20 consecutive sweeps, recorded 2 min before (baseline) and during TDE application (TDE 60 µg/ml). **(B)** Average of 7 TDE applications shown as mean ± SEM.

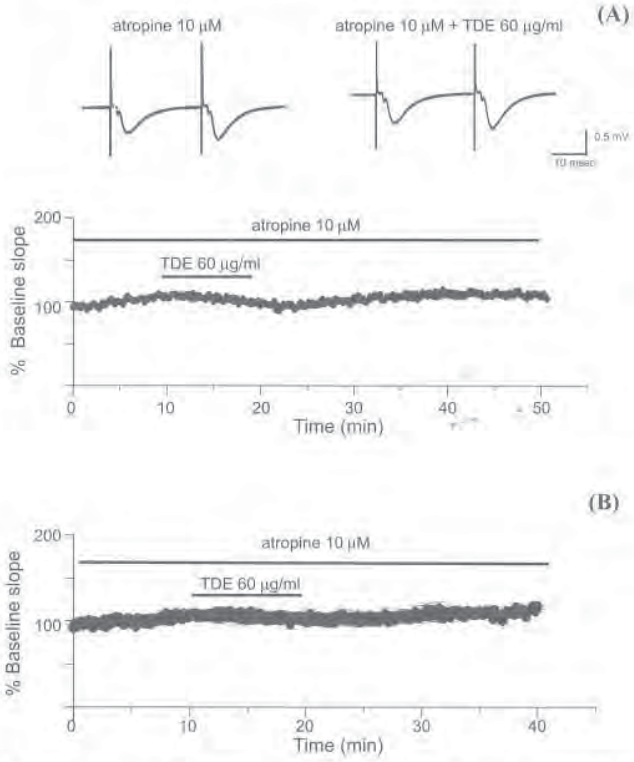

Fig. 2. The non selective muscarinic antagonist, atropine (10 µM), completely blocked the acute synaptic depression caused by TDE. **(A)** Atropine blocked the TDE-induced synaptic depression. Traces were obtained from the experiment shown in 2A (inset). Each trace shows the average of 20 consecutive sweeps, recorded 2 min before the application of TDE (atropine 10 µM) and during the application of TDE (atropine 10 µM + TDE 60 µg/ml application). **(B)** Average of 7 TDE applications shown as mean ± SEM.

bromide, a non selective nAChR antagonist, was used. In contrast to the effect of atropine, the TDE-induced reduction in Schaffer collateral fEPSPs persisted despite pretreatment of the slices with pancuronium bromide (100 μM). The mean depression of fEPSPs following the application of 60 μg/ml of TDE with and without 100 μM pancuronium was not significantly different (n=6). We used a high concentration of pancuronium (100 μM, the dose response curve of pancuronium with 60 μg/ml was not shown in this study) to completely block all subtypes of nAChR in hippocampal regions without having any effects on synaptic transmission[19].

The TDE effect of fEPSPs that we observed in CA1 was similar to the effect of galanthamine, a reversible AChE-I, and of ACh. One μM galanthamine application transiently depressed fEPSPs (Fig. 3). The mean fEPSP depression following the application of 1μM galanthamine was 42 ± 8 per cent (Fig. 3B, n=4). We used 1 μM galanthamine in this study since it has been shown to modulate glutamatergic synaptic transmission[20]. The effect of galanthamine in suppressing fEPSPs was also completely blocked by 10 μM atropine (Fig. 3A). Our findings suggest that TDE acts to suppress CA1 synaptic responses as same as galanthamine does.

Ach (1 mm) transiently depressed fEPSPs, similar to that of TDE application (Fig. 4). The ACh effect in suppressing fEPSPs was also completely blocked by 10 μM atropine (Fig. 4A). The mean fEPSP depression following the application of 1 mM ACh was 77 ± 3 per

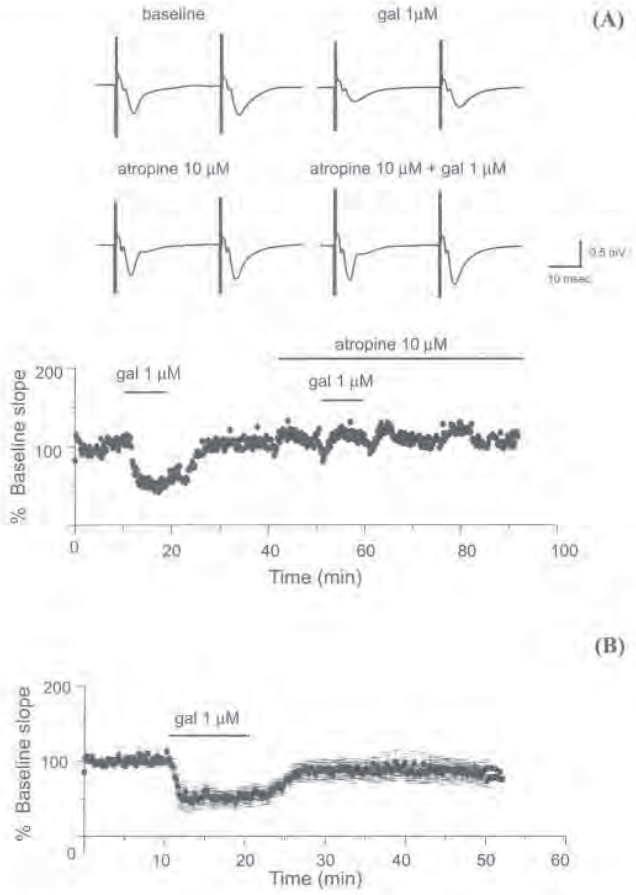

Fig. 3. Effect of 1 μM galanthamine (gal) on CA1 hippocampal responses. **(A)** Galanthamine-induced depression of synaptic responses. Depression was blocked by atropine (10 μM). Traces were obtained from the experiment shown in 3A (inset). Each trace shows the average of 20 consecutive sweeps. **(B)** Average of 4 galanthamine applications shown as mean ± SEM.

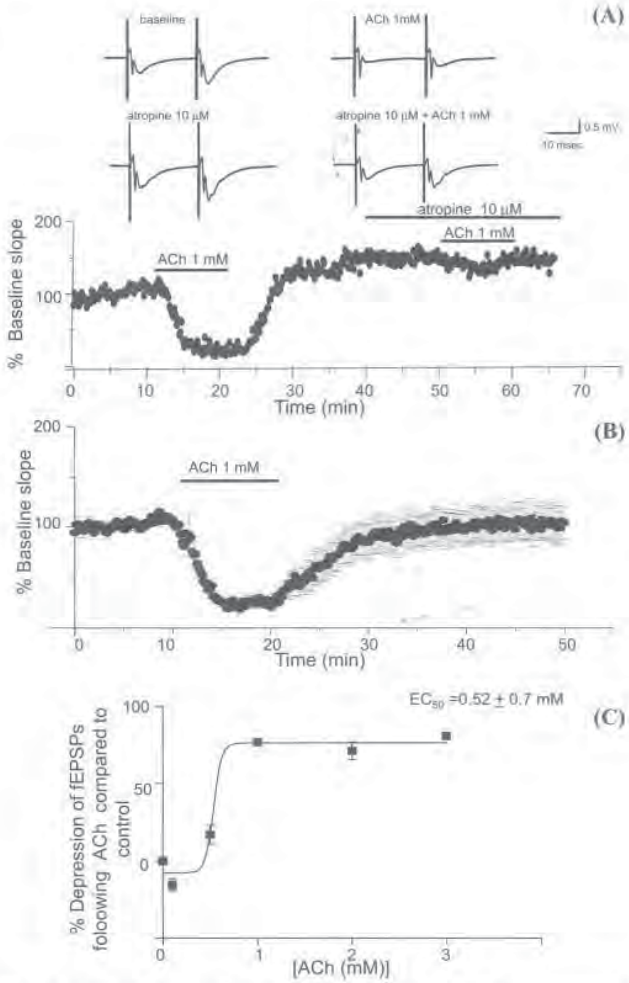

Fig. 4. Acetylcholine (ACh) caused a large depression of hippocampal synaptic response. Its effect was blocked by atropine. **(A)** ACh-induced depression of synaptic responses. ACh effect was blocked by atropine. Traces were obtained from the experiment shown in 4A (inset). Each trace shows an average of 20 consecutive sweeps. **(B)** Average of 7 ACh applications shown as mean ± SEM. **(C)** The dose response of ACh in depressing synaptic responses (n=5).

cent (n=7, Fig. 4B). We used 1 mM ACh since it had maximal effect on fEPSPs depression (Fig. 4C). The depression of fEPSPs by ACh was dose-dependent and the EC_{50} in fEPSPs depression occurred at 0.52 ± 0.7 mM of ACh (n=5 per dose, Fig. 4C).

The depression of synaptic transmission caused by both TDE and galanthamine application was less and slower than that by ACh (Fig. 5A). This finding suggests that TDE depresses fEPSPs in a similar way to galanthamine and TDE might not directly suppress fEPSPs in the same fashion as ACh application. Fig. 5B demonstrates the paired-pulse facilitation (PPF), a simple and sensitive measure of changes in presynaptic neurotransmitter release probability. We used PPF to test the hypothesis that TDE, galanthamine and ACh reduce synaptic responses by presynaptically depressing glutamatergic release. Mean paired-pulse facilitation of the CA1 hippocampus was increased during the application of TDE (60 µg/ml), galanthamine (1 µM) and ACh (1 mM) (Fig. 5B). Mean facilitation of the response slope with 60 µg/ml of TDE during infusion was 11 ± 4 per cent greater than that before TDE infusion ($P<0.05$). Mean facilitation of the response slope with 1µM galanthamine during infusion was 13 ± 1 per cent greater than before galanthamine infusion ($P<0.05$). The increase of the PPF response slope with 1 mM ACh during infusion was 35 ± 6 per cent greater than that before ACh infusion ($P<0.01$).

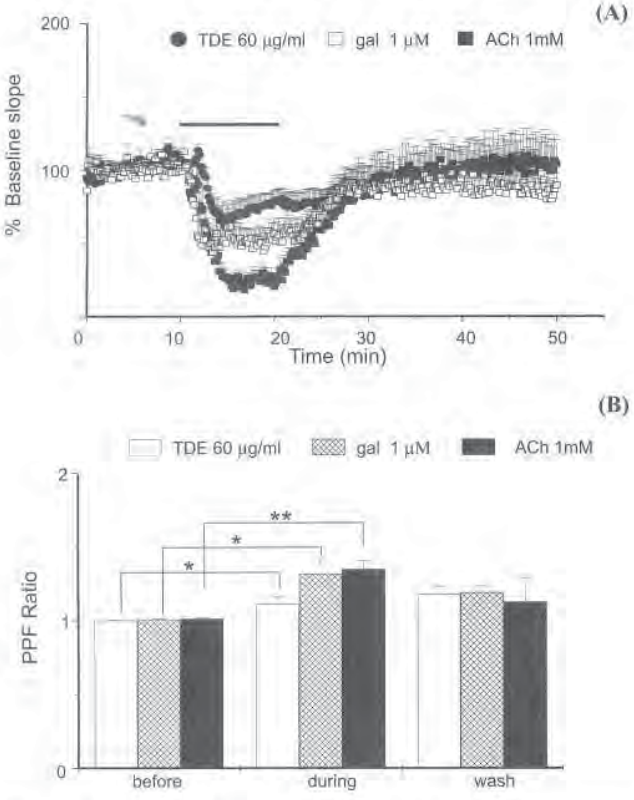

Fig. 5. Comparison of average depression of synaptic responses between 60 µg/ml of TDE, 1 µM galanthamine (gal) and 1 mM of ACh. **(A)** TDE- and galanthamine-induced suppression of CA1 hippocampal synaptic responses appeared to be less and slower than ACh-induced suppression. **(B)** TDE, galanthamine and ACh significantly increased paired-pulse facilitation (PPF) (*$P<0.05$, **$P<0.01$ before comparison during TDE, galanthamine or ACh application).

Discussion

The major finding of this study was that TDE suppressed synaptic transmission at hippocampal CA1 synapse. We demonstrated that TDE-enhanced cholinergic transmission in hippocampal circuits affected synaptic glutamatergic transmission by depressing neurotransmitter release in a similar manner to galanthamine and ACh. In this study, the TDE effect was blocked by atropine, but not pancuronium, suggesting that TDE may modulate synaptic transmission via the muscarinic cholinergic function.

A massive glutamatergic input from the cortex depends on a collection of afferents releasing neurotransmitters other than glutamate for synchronizing rhythms in the hippocampus. ACh is one of powerful presynaptic modulators at the glutamatergic synapses[6,21]. The cholinergic innervation in the hippocampus is provided from the medial septal nucleus[22]. Stimulation of cholinergic innervation in different regions of the hippocampus reduces glutamatergic synaptic transmission[1,4-8,23]. Much evidence has been provided on cholinergic interaction with glutamatergic transmission[11,24]. A study showed that coincident glutamatergic and cholinergic inputs transiently depress glutamatergic release at the CA1 synapse[3]. The interaction between cholinergic and glutamatergic transmission was suggested to be important in memory processing[23].

We have shown that TDE acts as a reversible AChE-I and is capable of increasing neuronal activity in the cerebral cortex, possibly by increasing cholinergic function[17]. In this study, we showed that TDE caused a transient depression of synaptic transmission in Schaffer collateral pathways of the CA1 response. The modulation of synaptic response by TDE was similar to the effect of galanthamine and ACh. These findings suggest that TDE possibly elevates the endogenous ACh level at the cholinergic synapses in hippocampal circuits. The synaptic

modulation of TDE may occur via cholinergic regulation of neurotransmission. This possibility is supported by our findings where the transient depression resulting from TDE application was prevented by mAChRs blockade. Atropine alone had no effect on hippocampal synaptic transmission. Also, TDE effects were similar to those of galanthamine, as demonstrated in this study, and those of physostigmine in a previous study[9].

Changes in a paired-pulse ratio by drug typically indicate a presynaptic mechanism of drug action[25,26]. TDE acutely reduces the fEPSPs slope and the depression is accompanied by an increase in the paired-pulse ratio, suggesting that TDE transiently depressed synaptic transmission by decreasing neurotransmitter release at the presynaptic site. This effect is similar to those observed in physostigmine application[9]. TDE's effect on the paired-pulse ratio was similar to those of galanthamine and ACh. The paired-pulse results provide insights into the functional changes arising from cholinergic suppression of glutamatergic synapses by TDE. The different fEPSPs depression and PPF effects between ACh and TDE/galanthamine found in this study could be due to the fact that TDE and galanthamine caused an increase in the endogenous ACh level at the synaptic sites. However, the increased amount of ACh in the synaptic regions caused by TDE and galanthamine application was less than the high-concentration exogenous ACh application in our study.

In conclusion, the present findings demonstrated that TDE showed similar effects to those of galanthamine. This important evidence indicates that consumption of this natural product (TDE) could be beneficial in slowing the process of learning and memory loss particularly in old age people or Alzheimer's patients. Our findings also suggest that TDE could possibly be used to develop a new acetylcholinesterase inhibitor for the treatment of Alzheimer's disease. Further, our findings support the beneficial effects of TDE and demonstrate the additional benefits of this traditional medicine on the learning and memory process with future clinical significance.

Acknowledgment

The authors thank Drs K. Ingkaninan for providing the TDE extract and MKO Carroll for editorial assistance. This work was supported by Thailand Research Fund: TRF-RMU4880013 and RMU5180007 (SC), TRF-RTA 5280006 (NC) and Faculty of Medicine Endowment Fund CMU (AP, SC and NC).

References

1. Hasselmo ME, Fehlau BP. Differences in time course of ACh and GABA modulation of excitatory synaptic potentials in slices of rat hippocampus. *J Neurophysiol* 2001; *86* : 1792-802.
2. Levin ED. Nicotinic receptor subtypes and cognitive function. *J Neurobiol* 2002; *53* : 633-40.
3. Volpicelli LA, Levey AI. Muscarinic acetylcholine receptor subtypes in cerebral cortex and hippocampus. *Prog Brain Res* 2004; *145* : 59-66.
4. Foster TC, Deadwyler SA. Acetylcholine modulates averaged sensory evoked responses and perforant path evoked field potentials in the rat dentate gyrus. *Brain Res* 1992; *587* : 95-101.
5. Gipson KE, Yeckel MF. Coincident glutamatergic and cholinergic inputs transiently depress glutamate release at rat schaffer collateral synapses. *J Neurophysiol* 2007; *97* : 4108-19.
6. Kahle JS, Cotman CW. Carbachol depresses synaptic responses in the medial but not the lateral perforant path. *Brain Res* 1989; *482* : 159-63.
7. Konopacki J, MacIver MB, Bland BH, Roth SH. Theta in hippocampal slices: relation to synaptic responses of dentate neurons. *Brain Res Bull* 1987; *18* : 25-7.
8. Yamamoto C, Kawai N. Presynaptic action of acetylcholine in thin sections from the guinea pig dentate gyrus *in vitro*. *Exp Neurol* 1967; *19* : 176-87.
9. Colgin LL, Kramar EA, Gall CM, Lynch G. Septal modulation of excitatory transmission in hippocampus. *J Neurophysiol* 2003; *90* : 2358-66.
10. Bliss TV, Collingridge GL. A synaptic model of memory: long-term potentiation in the hippocampus. *Nature* 1993; *361* : 31-9.
11. Terry AV Jr, Buccafusco JJ. The cholinergic hypothesis of age and Alzheimer's disease-related cognitive deficits: recent challenges and their implications for novel drug development. *J Pharmacol Exp Ther* 2003; *306* : 821-7.
12. Giacobini E. Cholinesterase inhibitors: new roles and therapeutic alternatives. *Pharmacol Res* 2004; *50* : 433-40.
13. Heinrich M, Lee TH. Galanthamine from snowdrop - the development of a modern drug against Alzheimer's disease from local Caucasian knowledge. *J Ethnopharmacol* 2004; *92* : 147-62.
14. van Beek TA, Verpoorte R, Svendsen AB, Leeuwenberg AJ, Bisset NG. *Tabernaemontana* L. (Apocynaceae): a review of its taxonomy, phytochemistry, ethnobotany and pharmacology. *J Ethnopharmacol* 1984; *10* : 1-156.
15. Pratchayasakul W, Pongchaidecha A, Chattipakorn N, Chattipakorn S. Ethnobotany & ethnopharmacology of *Tabernaemontana divaricata*. *Indian J Med Res* 2008; *127* : 317-35.
16. Ingkaninan K, Temkitthawon P, Chuenchom K, Yuyaem T, Thongnoi W. Screening for acetylcholinesterase inhibitory activity in plants used in Thai traditional rejuvenating and neurotonic remedies. *J Ethnopharmacol* 2003; *89* : 261-4.
17. Chattipakorn S, Pongpanparadorn A, Pratchayasakul W, Pongchaidacha A, Ingkaninan K, Chattipakorn N.

Tabernaemontana divaricata extract inhibits neuronal acetylcholinesterase activity in rats. *J Ethnopharmacol* 2007 1; *110* : 61-8.

18. McMahon LL, Kauer JA. Hippocampal interneurons express a novel form of synaptic plasticity. *Neuron* 1997; *18* : 295-305.
19. Chiodini FC, Tassonyi E, Fuchs-Buder T, Fathi M, Bertrand D, Muller D. Effects of neuromuscular blocking agents on excitatory transmission and gamma-aminobutyric acidA-mediated inhibition in the rat hippocampal slice. *Anesthesiology* 1998; *88* : 1003-13.
20. Santos MD, Alkondon M, Pereira EF, Aracava Y, Eisenberg HM, Maelicke A, *et al*. The nicotinic allosteric potentiating ligand galantamine facilitates synaptic transmission in the mammalian central nervous system. *Mol Pharmacol* 2002; *61* : 1222-34.
21. Hasselmo ME. Neuromodulation: acetylcholine and memory consolidation. *Trends Cogn Sci* 1999; *3* : 351-9.
22. Dutar P, Bassant MH, Senut MC, Lamour Y. The septohippocampal pathway: structure and function of a central cholinergic system. *Physiol Rev* 1995; *75* : 393-427.
23. Hasselmo ME, Schnell E, Barkai E. Dynamics of learning and recall at excitatory recurrent synapses and cholinergic modulation in rat hippocampal region CA3. *J Neurosci* 1995; *15* : 5249-62.
24. Aigner TG. Pharmacology of memory: cholinergic-glutamatergic interactions. *Curr Opin Neurobiol* 1995; *5* : 155-60.
25. Creager R, Dunwiddie T, Lynch G. Paired-pulse and frequency facilitation in the CA1 region of the *in vitro* rat hippocampus. *J Physiol* 1980; *299* : 409-24.
26. Wu LG, Saggau P. Presynaptic calcium is increased during normal synaptic transmission and paired-pulse facilitation, but not in long-term potentiation in area CA1 of hippocampus. *J Neurosci* 1994; *14* : 645-54.

Reprint requests: Dr Siriporn Chattipakorn, Department of Odontology & Oral Pathology, Faculty of Dentistry, Chiang Mai University
Chiang Mai, 50200, Thailand
e-mail: s.chat@chiangmai.ac.th

European Journal of Haematology 83 (483–489)

ORIGINAL ARTICLE

Heart rate variability in beta-thalassemia patients

Wasarut Rutjanaprom[1,2], Natnicha Kanlop[1,2], Pimlak Charoenkwan[3], Rekwan Sittiwangkul[3], Somdet Srichairatanakool[2,4], Adisak Tantiworawit[5], Arintaya Phrommintikul[5], Siriporn Chattipakorn[2], Suthat Fucharoen[6], Nipon Chattipakorn[1,2]

[1]Cardiac Electrophysiology Unit, Department of Physiology; [2]Cardiac Electrophysiology Research and Training Center; [3]Department of Pediatrics; [4]Department of Biochemistry; [5]Department of Internal Medicine, Faculty of Medicine, Chiang Mai University, Chiang Mai, Thailand; [6]Thalassemia Research Center, Institute of Science and Technology for Research and Development, Mahidol University, Bangkok, Thailand

Abstract

Background: Cardiac failure remains the major cause of death in beta-thalassemia major (TM). Reduced heart rate variability (HRV) is associated with a higher risk of arrhythmias after myocardial infarction and heart failure. We evaluated HRV in TM patients and its relationship with hemodynamics and echocardiographic parameters during a 6-month follow-up. *Methods:* Thirty-four TM patients (19 ± 10 yr) and 20 healthy subjects (17 ± 6 yr) were evaluated. Hematologic, biochemical, echocardiographic and HRV parameters were determined at entry and at 6-month follow-up. Time and frequency domain HRV parameters were analyzed from 24-h recorded electrocardiograms. All TM patients received blood transfusion and chelation therapy. *Results:* Both time and frequency domain HRV parameters were markedly reduced in TM patients, compared to the control. The significantly improved HRV was seen in correlation with higher hemoglobin (Hb) level when compared within TM group at different time point. No correlation was seen between HRV and serum ferritin, reactive oxygen species (ROS) and non-transferrin bound iron (NTBI). *Conclusion:* HRV is depressed in TM patients. HRV was significantly correlated with Hb level, suggesting that anemia greatly influences the cardiac autonomic balance.

Key words heart rate variability; thalassemia major; anemia

Correspondence Nipon Chattipakorn MD, PhD, Cardiac Electrophysiology Research and Training Center, Faculty of Medicine, Chiang Mai University, Chiang Mai 50200, Thailand. Tel: +66 53 945329; Fax: +66 53 945368; e-mail: nchattip@med.cmu.ac.th

Accepted for publication 2 July 2009 doi:10.1111/j.1600-0609.2009.01314.x

Cardiac failure remains the major cause of death in patients with transfusion-dependent β-thalassemia (thalassemia major, TM) (1–3). The major complication of long-term red blood cell transfusion is iron deposition, which in the heart causes a functional impairment (4). This cardiac complication due to iron overload can be prevented by intensive iron chelation (4–6). Currently, many available tests, such as serum ferritin level and endomyocardial biopsy, are not definitely representative (7, 8). Furthermore, both endomyocardial and liver biopsies for iron measurement are invasive. Conventional electrocardiography is not helpful since the majority of patients with asymptomatic cardiomyopathy is virtually absent of any abnormal electrocardiogram (ECG), while echocardiographic finding is thought to be late, already indicating poor prognosis in TM patients (9). Although T2-star magnetic resonance (MR-T2*) has been demonstrated to be promising in giving an early diagnosis on iron overload cardiomyopathy (10), its use is currently strictly limited by its availability and cost. Due to this limitations, cardiac T2* is currently not considered as a practical approach for general use in evaluating cardiac iron status in thalassemia patients, particularly for those in the second and third-world countries. Furthermore, current cardiac T2* cannot be used to evaluate the cardiac autonomic disturbances occurring in the heart. For biochemical analysis, non-transferrin-bound iron (NTBI) has been shown to be the good theoretical predictor (11, 12). However, it still remains available only in the research lab and the link between NTBI and cardiac iron/dysfunction has not been established clinically (11, 13, 14). Therefore, a reliable non-invasive, low-cost, and

easily access diagnostic test that can be used to detect an early development of cardiac involvement in this group of patients during the early stage of the disease is needed so that intensive chelation can be properly provided.

Recently, heart rate variability (HRV) has been used to determine the cardiac autonomic function in patients with postmyocardial infarction (15) and heart failure (16), and has been demonstrated as a strong risk predictor in those patients. Despite its clinical significance, there are only a few cross-sectional studies investigating HRV in TM patients (17–20). In the present study, HRV was investigated in TM patients, and the relationships between HRV and hematological and biochemical parameters as well as left ventricular functions were studied during a 6-month follow-up period.

Materials and methods

Study protocol

The study protocol was reviewed and approved by the institutional ethic committee of the Faculty of Medicine, Chiang Mai University. All participants gave written informed consent prior to the study entry. Thirty-four TM patients (14 homozygous beta-thalassemia and 20 Hb E/beta-thalassemia) and 20 healthy subjects were prospectively evaluated. All patients were treated with blood transfusion and desferrioxamine for iron chelation. The inclusion criteria for patient entry into the trial were diagnosed TM patients currently treated with regular blood transfusion and age ≥10 yr. Exclusion criteria were as follows: patients who were lost to follow up; patients taking any antiarrhythmic drug and/or cardiovascular medication that could affect sympatho-vagal balance in the past 3 months; alanine aminotransferase (ALT) >300 U/L; serum creatinine >2 mg/dL; and patients with symptoms and signs of heart disease as evaluated by chest film and ECG. Laboratory profiles, echocardiography as well as 24-h Holter ECG recording for HRV analysis in each patient were collected at the time of entry and at 6-month follow-up. Twenty healthy subjects with matched age (10 males; 17 ± 5 yr) were included as the control group for one-time HRV study. The primary end point of the study was death or ventricular arrhythmias which required intervention during study, and the secondary end point was the ending of a 6-month follow-up.

Heart rate variability measurement

Twenty-four-hour ECG was recorded for HRV determination. The recordings were reviewed and the classification of each beat was manually checked and corrected before the HRV was determined by the analysis software. HRV parameters were categorized into two categories, time domain and frequency domain.

Time-domain HRV parameters determined in the present study were the standard deviation of all normal sinus R-R intervals in the entire 24-h recording (SDNN), the standard deviation of all average normal sinus R-R intervals for all 5-min segment in the 24-h recordings (SDANN), the average of the standard deviations of all R-R intervals for all 5-min segments in the 24-h recordings (ASDNN), and the root mean square of the mean of the squared differences of two consecutive R-R intervals (rMSSD). Frequency-domain HRV parameters including low-frequency power (LF), high-frequency power (HF), and the LF/HF ratio were also determined.

Laboratory profiles

Hemoglobin (Hb), hematocrit (Hct), serum ferritin, plasma NTBI, and the production of reactive oxygen species (ROS) were determined in each patient at the date of entry and at 6-month follow-up.

Quantification of plasma NTBI

Plasma NTBI was evaluated as previously described by Singh *et al.* (21). At the beginning, a small volume of aluminum chloride solution (a final concentration of 200 μM) was added to 450-μL plasma and incubated at room temperature for 1 h. After 50 μL of 800-mM nitrilotriacetic acid (NTA) (a final concentration of 80 mM) solution pH 7.0 was added, the mixture was incubated for 30 min at room temperature to produce a ferric-nitrilotriacetate complex, Fe^{3+}-$(NTA)_2$. Then, the Fe^{3+}-$(NTA)_2$ was separated from plasma proteins by spinning plasma mixture through the membrane filter (30-kDa cut-off, polysulfone type, 0.5-mL capacity) at 12 000 ***g***, 15°C for 45 min. Ultrafiltrate was injected into nonmetallic 50-μL loop and analyzed with the high performance liquid chromatography (HPLC) technique. HPLC requirements were composed of glass analytical column (ChromSep-ODS1, 100 × 3.0 mm, 5 μm) connected with guard column (10× 3.0 mm, 5 μm) and mobile-phase solvent (3 mM CP22 in 19% acetronitrile buffered with 5 mM MOPS pH 7.0). Having been isocratically eluted with the mobile-phase solvent at a flow rate of 1.0 mL/min, NTBI as Fe^{3+}-$(NTA)_2$ was fractionated on the column, then immediately on-column derivatized with CP22 to form a Fe^{3+}-$(CP22)_3$ complex. Resulting orange-colored Fe^{3+}-$(CP22)_3$ product was on-line detected at 450 nm with the SpecMonitor® 2300 flow-cell detector (LDC Milton-Roy Inc., FL, USA). The NTBI peak height was integrated and recorded for further determination of NTBI concentration from the calibration curve. Calibration curve was produced by plotting

obtained peak height values on *y*-axis against iron concentration on *x*-axis. Equation of linear regression line was used to calculate plasma NTBI concentration.

Flow cytometric determination of erythrocyte oxidative stress

The production of ROS was measured using the method previously described (22). Two microliter blood was diluted with 9 mL of Ca^{2+}- and Mg^{2+}-free Dulbecco's phosphate buffered saline (D-PBS) to a concentration of 1 × 106 RBCs/mL, and was incubated with 20-μL DCFH-DA (10 mg/mL in methanol) under 5%CO_2 atmosphere at 37°C for 15 min. The solution was centrifuged at 3000 ***g*** for 15 min at 15°C. RBC pellet was resuspended in 2-mL PBS and centrifuged. Finally, the pellet was resuspended in 1-mL PBS and divided into two cell fractions (500 μL each). The oxidative stress level represented as fluorescence intensity (FI) was determined in the cells with the induction of 3% H_2O_2 (35 μL) by flow cytometry.

Echocardiographic studies

Tissue Doppler and M-mode echocardiography were used to determine cardiac function in all patients. Cardiac chamber was measured by left ventricular end-diastolic dimension (LVEDD) and left ventricular end-systolic dimension (LVESD). Cardiac index (CI), left ventricular ejection fraction (LVEF), and fractional shortening (FS) were used to measure the cardiac function.

Statistical analysis

Numerical data are presented as mean ± standard deviation. Differences between TM patients and the control group were performed using the non-parametric Mann–Whitney *U* test. The Wilcoxon signed rank test was used to test differences between measured parameters at baseline and at follow-up in TM patients. The correlations between the HRV parameters and the hematologic and echocardiographic parameters were determined by Pearson test. A *P* value less than 0.05 was considered statistically significant. Statistical analysis was performed with the use of SPSS version 13.0 for Windows (SPSS Inc., Chicago, IL, USA).

Results

Characteristics of patients are shown in Table 1. There were no significant differences in age and gender between the TM group and the control group. Twenty-eight patients (82%) underwent splenectomy. In the last 12 months prior to the study entry, all patients received blood transfusion (10 ± 6 times) and desferrioxamine for iron chelation. Desferrioxamime was planned to be given as per standard protocol. However, due to problems with availability of infusion equipment and patient compliance, only the minority received proper dose. Fourteen of 34 patients received 30–50 mg/kg/d of desferrioxamine regularly (i.e. >3 times/wk). Mean heart rate of TM patients was significantly higher, whereas Hb and hematocrit (Hct) were significantly lower, compared to the control group. All time-domain HRV parameters (SDNN, SDANN, ASDNN, and rMSSD) were significantly decreased in the TM group, compared to the control group. Frequency-domain HRV parameters, both

Table 1 Demographic, time-domain and frequency-domain HRV parameters of thalassemia major (TM) patients at entry and the control subjects

Parameters	TM group at entry	Control group	*P* value
Number of subjects	34	20	–
Age (yr)	19 ± 10	17 ± 5	NS
Gender			
Male (%)	17 (50)	10 (50)	NS
Female (%)	17 (50)	10 (50)	NS
Splenectomy (%)	28 (82)	–	–
Number of blood transfusion (last 12 months)	10 ± 6	–	–
Heart rate (bpm)	94 ± 11	81 ± 10	0.000
Hemoglobin (g/dL)	6.7 ± 1.4	14.7 ± 1.7	0.000
Hematocrit (%)	21.9 ± 4.7	43.1 ± 4.1	0.000
MCV	73.6 ± 6.2	88.5 ± 4.5	0.000
BSA- normalized O_2 delivery	457 ± 123	461 ± 139	NS
Echocardiographic values			
LVEDD (mm)	49.6 ± 6.1	50.3 ± 5.8	NS
LVESD (mm)	31.2 ± 4.7	30.7 ± 5.0	NS
Cardiac index	5.2 ± 1.0	5.4 ± 1.1	NS
LVEF (%)	63.9 ± 7.6	65.9 ± 8.7	NS
FS (%)	35.8 ± 6.1	36.6 ± 6.8	NS
Cardiac thoracic ratio (%)	53 ± 4	52 ± 4	
Time domain			
SDNN (m s)	92 ± 25	170 ± 51	0.000
SDANN (m s)	85 ± 24	157 ± 57	0.000
ASDNN (m s)	34 ± 11	74 ± 16	0.000
rMSSD (m s)	20 ± 8	53 ± 16	0.000
Frequency domain			
LF (m s^2)	12 ± 4	26 ± 8	0.000
HF (ms^2)	10 ± 5	25 ± 6	0.000
LF/HF ratio	1.3 ± 0.5	1.0 ± 0.3	0.031

SDNN, standard deviation of all normal sinus R-R intervals in the entire 24-h recording; SDANN, standard deviation of all averaged normal sinus R-R intervals for all 5-min segment in the 24-h recordings; ASDNN, average of the standard deviations of all R-R intervals for all 5-min segments in the 24-h recordings; rMSSD, root mean square of the mean of the squared differences of two consecutive R-R intervals; LF, low frequency power; HF, high frequency power.

LF and HF, of TM group were also significantly decreased while LF/HF ratio was significantly increased compared to the control group. Although 10 TM patients with depressed HRV had asymptomatic mild left ventricular hypertrophy (LVH) diagnosed by echocardiography, there was no difference between HRV of TM patients with and without LVH (not shown).

After 6-month follow-up with the same treatment regimen of blood transfusion (6 ± 2 times/6 months) and iron chelation, none had ventricular arrhythmias or died. Although all HRV parameters at 6-month follow-up were significantly decreased compared to the control group, they were significantly improved compared to the HRV at entry (Table 2). For hematologic parameters, Hb level, serum ferritin, and ROS were significantly higher than the levels at entry. The Hct and NTBI levels were slightly increased but did not reach statistical significance, whereas the heart rate was not altered. All measured echocardiographic parameters (LVEDD, LVESD, CI, LVEF, and FS) were not changed at 6-month follow-up, indicating that cardiac function was not deteriorated during the follow-up period.

Table 2 HRV, hematologic, and echocardiographic parameters of TM patients at entry and at 6-month follow-up

Parameters	TM group at entry	TM group at 6-months	*P* value
Hematologic values			
Hemoglobin (g/dL)	6.7 ± 1.4	7.2 ± 1.2	0.023
Hematocrit (%)	21.9 ± 4.7	22.6 ± 4.0	NS
MCV	73.6 ± 6.2	74.1 ± 5.6	NS
Serum ferritin (ng/dL)	4492 ± 2710	5296 ± 3867	0.037
NTBI (μm)	5.1 ± 4.2	5.7 ± 3.6	NS
ROS (FI unit)	16 ± 11	34 ± 14	0.000
BSA-normalized O_2 delivery	457 ± 123	445 ± 92	NS
Echocardiographic values			
LVEDD (mm)	49.6 ± 6.1	49.0 ± 5.8	NS
LVESD (mm)	31.2 ± 4.7	31.7 ± 4.8	NS
Cardiac index	5.2 ± 1.0	5.0 ± 0.9	NS
LVEF (%)	63.9 ± 7.6	62.8 ± 5.7	NS
FS (%)	35.8 ± 6.1	36.1 ± 4.3	NS
Heart rate (bpm)	94 ± 11	95 ± 8	NS
Cardiac thoracic ratio (%)	53 ± 4	53 ± 4	NS
Time domain			
SDNN (m s)	92 ± 25	113 ± 19	0.000
SDANN (m s)	85 ± 24	105 ± 19	0.000
ASDNN (m s)	34 ± 11	43 ± 13	0.003
rMSSD (m s)	20 ± 8	28 ± 15	0.001
Frequency domain			
LF (m s^2)	12 ± 4	14 ± 4	0.023
HF (m s^2)	10 ± 5	14 ± 7	0.002
LF/HF ratio	1.3 ± 0.5	1.2 ± 0.4	0.041

NTBI, non-transferrin-bound iron; ROS, production of reactive oxygen species; LVEF, left ventricular ejection fraction; FS, fractional shortening; LVEDD, left ventricular end-diastolic dimension; LVESD, left ventricular end-systolic dimension.

Table 3 The correlations between HRV parameters and Hb and Hct in TM patients

R	Hemoglobin	Hematocrit
Time domain		
SDNN	0.505*	0.554*
SDANN	0.492*	0.493*
ASDNN	0.527*	0.548*
rMSSD	0.309†	0.300†
Frequency domain		
LF	0.478*	0.506*
HF	0.373†	0.285†

* $P < 0.001$; † $P < 0.05$

SDNN, standard deviation of all normal sinus R-R intervals in the entire 24-h recording; SDANN, standard deviation of all averaged normal sinus R-R intervals for all 5-min segment in the 24-h recordings; ASDNN, average of the standard deviations of all R-R intervals for all 5-min segments in the 24-h recordings; rMSSD, root mean square of the mean of the squared differences of two consecutive R-R intervals; LF, low frequency power; HF, high frequency power.

All improved HRV parameters was found to be significantly correlated with Hb and Hct levels (Table 3). However, there were no correlations between HRV parameters and serum ferritin, NTBI, ROS, O_2 delivery as well as the number of blood transfusion prior to the enrollment. None of the echocardiographic parameters was correlated with HRV.

Discussion

In the present study, the major findings include: (1) all time-domain and frequency-domain HRV parameters are significantly depressed in TM patients while LF/HF ratio was significantly increased, compared to the control and (2) within the TM group, improved HRV parameters were correlated with improved Hb and Hct levels.

Sympatho-vagal imbalance can affect cardiac electrophysiology and may lead to increase mortality due to cardiac autonomic dysfunction (23–28). HRV measurement has been used to assess cardiac autonomic dysfunction in various disorders such as myocardial infarction (29–31), heart failure (32–37), cardiac transplantation (38–40), diabetic neuropathy (41), and HIV infection (42). Numerous studies have confirmed that decreased HRV in the time or frequency domain, measured after myocardial infarction and heart failure is associated with increased risk of mortality (23–28). In TM patients, previous cross-sectional studies have shown that both time-domain and frequency-domain HRV parameters were significantly decreased in patients with TM, and that they had no correlation with any hematologic, biochemical or echocardiographic parameters (18, 19). However, no prospective study has been done to investigate HRV and its relationship to the changes of hematologic values during treatment.

In the present study, we determined for the first time a disturbance of HRV indices with a 6-month follow-up period in TM patients. Consistent with previous cross-sectional studies, all time-domain and frequency-domain HRV parameters were depressed in the TM group at the initial study enrollment, compared to the control. These indices indicated that cardiac autonomic functions, both sympathetic and parasympathetic activities, might be impaired in TM patients. Moreover, sympatho-vagal imbalance which is designated by an increased LF/HF ratio is still observed in the TM group. Since heart rate was increased in TM patients, indicating high sympathetic activity and/or low parasympathetic activity, whereas both LF and HF were depressed, this sympatho-vagal imbalance in the TM group could be mainly due to depressed parasympathetic activity. However, it is premature at this time to conclude that HRV is absolutely 'impaired' in this population since it could represent a normal physiologic adaptation to anemia and that the spectrum of abnormalities observed in the TM patients in the present study might be reproduced in the control population when the Hb and Hct are low.

At 6-month follow-up, Hb was significantly improved in these TM patients. As there was no change in the treatment plan, increased Hb and serum ferritin may have been a trial effect when a transfusion plan was strictly followed as patients were closely monitored. All HRV parameters were also significantly improved. In addition, the LF/HF ratio was decreased, indicating an improvement of sympatho-vagal balance. The finding that heart rate was not changed at 6-month follow-up despite increased Hb, LF, HF, and decreased LF/HF ratio further emphasizes the significant contribution of improved cardiac parasympathetic activity in these TM patients.

In the present study, the production of ROS after blood transfusion was significantly increased during the 6-month follow-up period, indicating oxidative damage. Both NTBI, and echocardiographic parameters (LVEDD, LVESV, CI, LVEF, and FS) were not altered at 6-month follow-up, indicating that they may not be sensitive enough to detect early cardiac disturbance in TM patients with preclinical stage of heart disease. Although there were 10 TM patients diagnosed asymptomatic mild LVH with no clinical sign of heart diseases or cardiac dysfunction, HRV parameters of those with and without mild LVH were not significantly different, indicating that asymptomatic mild LVH may be too mild to affect already depressed HRV in TM patients. Despite this finding, the number of asymptomatic mild LVH included in this study was still small and could be premature for this assumption.

Significant correlations between all HRV parameters, and Hb and Hct levels were found in the present study. However, no correlation between HRV indices and other measured parameters were observed. These findings suggest that blood transfusion therapy not only improved an anemic condition but also mainly increased cardiac parasympathetic activity, represented by an increased HF component. Previous studies in patients with sickle cell anemia and vitamin B-12 deficiency have indicated that chronic anemia may affect the cardiac autonomic dysfunction (43, 44). Similarly, in the present study, improved sympatho-vagal imbalance may be explained by improved anemic condition as seen at 6-month follow-up in TM patients.

It is important to note that the patient population in the present study was significantly undertransfused compared to the European and North American management practices with a mean pre-transfusion Hb level at an average of 2.5 g/dL lower. This disparity could be responsible for the effect of Hb observed in this trial but not others. At the Hb levels observed in the present population, erythropoetic drive was not inhibited and the patients were likely to be hypermetabolic. Furthermore, this degree of anemia could create a chronically elevated cardiac output and possibly responsible for the increased sympatho-vagal tone as well as the LV dilation and LVH observed in some patients in the present study. Also, improved Hb level in this study could be a trial effect, with patients subtly shortening their transfusion intervals (on average) because of closer monitoring. It could also represent improved red cell survival, in which lower levels of circulating free Hb might mediate HRV by affecting NO bioavailability.

Although HRV has been demonstrated in many studies to be a good predictor of mortality, it is possible that the predictive value of depressed HRV can be much different in the TM population than any of the non-anemic disease cohorts where it predicts mortality. Future studies with long-term follow-up are needed to investigate the predictive value of HRV in thalassemia population.

Study limitation

The identification of the amount of iron accumulation in the myocardium was not determined in the present study. Future studies are needed to determine the correlation between HRV parameters and the amount of iron deposit in the heart to warrant its clinical significance. Furthermore, cardiac complication was not observed during a 6-month follow-up period in this study. Therefore, HRV as a predictor of cardiac complication could not be tested. Long-term follow-up is needed to investigate the benefit in risk stratification of HRV. In the present study, many TM patients were under chelated due to the cost and patients' compliances related to chelator administration. Since the use of oral iron chelators was

limited during the study period, all patients in this study received desferrioxamine monotherapy.

Conclusion

In TM patients, HRV was significantly depressed, indicating cardiac autonomic disturbance in these patients. Sympatho-vagal imbalance was markedly improved after Hb level was increased, suggesting that an anemic condition greatly influences cardiac autonomic function in TM patients. Blood transfusion not only maintains the level of Hb, but also reduced HRV disturbance. The improvement of sympatho-vagal imbalance, which is designated by decreased LF/HF ratio, could be mainly due to an enhanced cardiac parasympathetic activity.

Acknowledgements

This work was supported by the Thailand Research Fund grants (NC and SF) and National Research Council Thailand (NC).

References

1. Engle MA. Cardiac involvement in Cooley's anemia. *Ann N Y Acad Sci* 1964;**119**:694–702.
2. Olivieri NF, Nathan DG, MacMillan JH, Wayne AS, Liu PP, McGee A, Martin M, Koren G, Cohen AR. Survival in medically treated patients with homozygous beta-thalassemia. *N Engl J Med* 1994;**331**:574–8.
3. Zurlo MG, De Stefano P, Borgna-Pignatti C, Di Palma A, Piga A, Melevendi C, DiGredorio F, Burattini MG, Terzoli S. Survival and causes of death in thalassaemia major. *Lancet* 1989;**2**:27–30.
4. Olivieri NF. The beta-thalassemias. *N Engl J Med* 1999;**341**:99–109.
5. Borgna-Pignatti C, Rugolotto S, De SP, *et al*. Survival and complications in patients with thalassemia major treated with transfusion and deferoxamine. *Haematologica* 2004;**89**:1187–93.
6. Hoffbrand AV, Cohen A, Hershko C. Role of deferiprone in chelation therapy for transfusional iron overload. *Blood* 2003;**102**:17–24.
7. Fitchett DH, Coltart DJ, Littler WA, Leyland MJ, Trueman T, Gozzard DI, Peters TJ. Cardiac involvement in secondary haemochromatosis: a catheter biopsy study and analysis of myocardium. *Cardiovasc Res* 1980;**14**:719–24.
8. Lee DH, Jacobs DR Jr. Serum markers of stored body iron are not appropriate markers of health effects of iron: a focus on serum ferritin. *Med Hypotheses* 2004;**62**:442–5.
9. Hoffbrand AV. Diagnosing myocardial iron overload. *Eur Heart J* 2001;**22**:2140–1.
10. Anderson LJ, Holden S, Davis B, *et al*. Cardiovascular T2-star (T2*) magnetic resonance for the early diagnosis of myocardial iron overload. *Eur Heart J* 2001;**22**:2171–9.
11. Breuer W, Ermers MJ, Pootrakul P, Abramov A, Hershko C, Cabantchik ZI. Desferrioxamine-chelatable iron, a component of serum non-transferrin-bound iron, used for assessing chelation therapy. *Blood* 2001;**97**:792–8.
12. Hershko C, Link G, Cabantchik I. Pathophysiology of iron overload. *Ann N Y Acad Sci* 1998;**850**:191–201.
13. Grosse R, Lund U, Caruso V, Fischer R, Janka GE, Magnano C, Engelhardt R, Durken M, Nielsen P. Non-transferrin-bound iron during blood transfusion cycles in beta-thalassemia major. *Ann N Y Acad Sci* 2005;**1054**:429–32.
14. Jakeman A, Thompson T, McHattie J, Lehotay DC. Sensitive method for nontransferrin-bound iron quantification by graphite furnace atomic absorption spectrometry. *Clin Biochem* 2001;**34**:43–7.
15. La Rovere MT, Pinna GD, Hohnloser SH, Marcus FI, Mortara A, Nohara R, Bigger JT Jr, Camm AJ, Schwartz PJ. Baroreflex sensitivity and heart rate variability in the identification of patients at risk for life-threatening arrhythmias: implications for clinical trials. *Circulation* 2001;**103**:2072–7.
16. Nolan J, Batin PD, Andrews R, *et al*. Prospective study of heart rate variability and mortality in chronic heart failure: results of the United Kingdom heart failure evaluation and assessment of risk trial (UK-heart). *Circulation* 1998;**98**:1510–6.
17. De Chiara B, Crivellaro W, Sara R, Ruffini L, Parolini M, Fesslova V, Carnelli V, Fiorentini C, Parodi O. Early detection of cardiac dysfunction in thalassemic patients by radionuclide angiography and heart rate variability analysis. *Eur J Haematol* 2005;**74**:517–22.
18. Franzoni F, Galetta F, Di Muro C, Buti G, Pentimone F, Santoro G. Heart rate variability and ventricular late potentials in beta-thalassemia major. *Haematologica* 2004;**89**:233–4.
19. Gurses D, Ulger Z, Levent E, Aydinok Y, Ozyurek AR. Time domain heart rate variability analysis in patients with thalassaemia major. *Acta Cardiol* 2005;**60**:477–81.
20. Veglio F, Melchio R, Rabbia F, Molino P, Genova GC, Martini G, Schiavone D, Piga A, Chiandussi L. Blood pressure and heart rate in young thalassemia major patients. *Am J Hypertens* 1998;**11**:539–47.
21. Singh S, Hider RC, Porter JB. A direct method for quantification of non-transferrin-bound iron. *Anal Biochem* 1990;**186**:320–3.
22. Amer J, Goldfarb A, Fibach E. Flow cytometric measurement of reactive oxygen species production by normal and thalassaemic red blood cells. *Eur J Haematol* 2003;**70**:84–90.
23. Bigger JT Jr, Fleiss JL, Steinman RC, Rolnitzky LM, Kleiger RE, Rottman JN. Frequency domain measures of heart period variability and mortality after myocardial infarction. *Circulation* 1992;**85**:164–71.
24. Vaishnav S, Stevenson R, Marchant B, Lagi K, Ranjadayalan K, Timmis AD. Relation between heart rate

variability early after acute myocardial infarction and long-term mortality. *Am J Cardiol* 1994;**73**:653–7.
25. Copie X, Hnatkova K, Staunton A, Fei L, Camm AJ, Malik M. Predictive power of increased heart rate versus depressed left ventricular ejection fraction and heart rate variability for risk stratification after myocardial infarction. Results of a two-year follow-up study. *J Am Coll Cardiol* 1996;**27**:270–6.
26. Cripps TR, Malik M, Farrell TG, Camm AJ. Prognostic value of reduced heart rate variability after myocardial infarction: clinical evaluation of a new analysis method. *Br Heart J* 1991;**65**:14–9.
27. Mortara A, La Rovere MT, Signorini MG, Pantaleo P, Pinna G, Martinelli L, Ceconi C, Cerutti S, Tavazzi L. Can power spectral analysis of heart rate variability identify a high risk subgroup of congestive heart failure patients with excessive sympathetic activation? A pilot study before and after heart transplantation *Br Heart J* 1994;**71**:422–30.
28. Casolo G, Balli E, Taddei T, Amuhasi J, Gori C. Decreased spontaneous heart rate variability in congestive heart failure. *Am J Cardiol* 1989;**64**:1162–7.
29. Kleiger RE, Miller JP, Bigger JT Jr, Moss AJ. Decreased heart rate variability and its association with increased mortality after acute myocardial infarction. *Am J Cardiol* 1987;**59**:256–62.
30. Malik M, Camm AJ, Janse MJ, Julian DG, Frangin GA, Schwartz PJ. Depressed heart rate variability identifies postinfarction patients who might benefit from prophylactic treatment with amiodarone: a substudy of EMIAT (The European Myocardial Infarct Amiodarone Trial). *J Am Coll Cardiol* 2000;**35**:1263–75.
31. Zuanetti G, Neilson JM, Latini R, Santoro E, Maggioni AP, Ewing DJ. Prognostic significance of heart rate variability in post-myocardial infarction patients in the fibrinolytic era. The GISSI-2 results. Gruppo Italiano per lo Studio della Sopravvivenza nell' Infarto Miocardico. *Circulation* 1996;**94**:432–6.
32. Akyol A, Alper AT, Cakmak N, Hasdemir H, Eksik A, Oguz E, Erdinler I, Ulufer FT, Gurkan K. Long-term effects of cardiac resynchronization therapy on heart rate and heart rate variability. *Tohoku J Exp Med* 2006;**209**:337–46.
33. Gilliam FR III, Singh JP, Mullin CM, McGuire M, Chase KJ. Prognostic value of heart rate variability footprint and standard deviation of average 5-minute intrinsic R-R intervals for mortality in cardiac resynchronization therapy patients. *J Electrocardiol* 2007;**40**:336–42.
34. Gilliam FR III, Kaplan AJ, Black J, Chase KJ, Mullin CM. Changes in heart rate variability, quality of life, and activity in cardiac resynchronization therapy patients: results of the HF-HRV registry. *Pacing Clin Electrophysiol* 2007;**30**:56–64.
35. Piepoli MF, Villani GQ, Corra U, Aschieri D, Rusticali G. Time course of effects of cardiac resynchronization therapy in chronic heart failure: benefits in patients with preserved exercise capacity. *Pacing Clin Electrophysiol* 2008;**31**:701–8.
36. Puglisi A, Gasparini M, Lunati M, *et al*. Persistent atrial fibrillation worsens heart rate variability, activity and heart rate, as shown by a continuous monitoring by implantable biventricular pacemakers in heart failure patients. *J Cardiovasc Electrophysiol* 2008;**19**:693–701.
37. Saul JP, Arai Y, Berger RD, Lilly LS, Colucci WS, Cohen RJ. Assessment of autonomic regulation in chronic congestive heart failure by heart rate spectral analysis. *Am J Cardiol* 1988;**61**:1292–9.
38. Dalla PR, Fuchs A, Bechtold S, Kozlik-Feldmann R, Daebritz S, Netz H. Short-term testing of heart rate variability in heart-transplanted children: equal to 24-h ECG recordings? *Clin Transplant* 2006;**20**:438–42.
39. Pozza RD, Kleinmann A, Bechtold S, Fuchs A, Netz H. Reinnervation after heart transplantation in children: results of short-time heart rate variability testing. *Pediatr Transplant* 2006;**10**:429–33.
40. Havlicekova Z, Jurko A Jr. Heart rate variability changes in children after cardiac transplantation. *Bratisl Lek Listy* 2005;**106**:168–70.
41. Bellavere F, Balzani I, De Masi G, Carraro M, Carenza P, Cobelli C, Thomaseth K. Power spectral analysis of heart-rate variations improves assessment of diabetic cardiac autonomic neuropathy. *Diabetes* 1992;**41**:633–40.
42. Becker K, Gorlach I, Frieling T, Haussinger D. Characterization and natural course of cardiac autonomic nervous dysfunction in HIV-infected patients. *AIDS* 1997;**11**:751–7.
43. Romero Mestre JC, Hernandez A, Agramonte O, Hernandez P. Cardiovascular autonomic dysfunction in sickle cell anemia: a possible risk factor for sudden death? *Clin Auton Res* 1997;**7**:121–5.
44. Sozen AB, Demirel S, Akkaya V, Kudat H, Tukek T, Yeneral M, Ozcan M, Guven O, Korkut F. Autonomic dysfunction in vitamin B12 deficiency: a heart rate variability study. *J Auton Nerv Syst* 1998;**71**:25–7.

Available online at www.sciencedirect.com
ScienceDirect
Nutrition Research 29 (2009) 696 – 704
Nutrition Research
www.nrjournal.com

Cardiac mortality is associated with low levels of omega-3 and omega-6 fatty acids in the heart of cadavers with a history of coronary heart disease

Nipon Chattipakorn[a,b,*], Jongkolnee Settakorn[c], Petnoi Petsophonsakul[a,b], Padiphat Suwannahoi[d], Pasuk Mahakranukrauh[d], Somdet Srichairatanakool[e], Siriporn C. Chattipakorn[b,f]

[a]*Department of Physiology, Cardiac Electrophysiology Unit, Faculty of Medicine, Chiang Mai University, Chiang Mai, 50200 Thailand*
[b]*Cardiac Electrophysiology Research and Training Center, Faculty of Medicine, Chiang Mai University, Chiang Mai, 50200 Thailand*
[c]*Department of Pathology, Faculty of Medicine, Chiang Mai University, Chiang Mai, 50200 Thailand*
[d]*Department of Anatomy, Faculty of Medicine, Chiang Mai University, Chiang Mai, 50200 Thailand*
[e]*Department of Biochemistry, Faculty of Medicine, Chiang Mai University, Chiang Mai, 50200 Thailand*
[f]*Department of Oral Biology, Faculty of Dentistry, Chiang Mai University, Chiang Mai, 50200 Thailand*

Received 27 July 2009; revised 9 September 2009; accepted 21 September 2009

Abstract

The benefits of omega-3 (ie, eicosapentaenoic acid and docosahexaenoic acid [DHA]) and omega-6 (ie, linoleic acid and arachidonic acid [AA]) fatty acids on reducing cardiac mortality are still debated. In this study, we tested the hypothesis that high levels of omega-3 and omega-6 fatty acids in heart tissues are associated with low cardiac mortality in Thai cadavers. One hundred fresh cadavers were examined in this study. The cause of death, history of coronary heart disease (CHD), and fish consumption habits were obtained from death certificates, cadaver medical record profiles, and a questionnaire to a person who lived with the subject before death. In each cadaver, biopsies of cardiac tissues were taken from the interventricular septum for measurement of fatty acid. Of the 100 cadavers (average age, 69 ± 13 years), 60 were men. The frequency of fish consumption was directly associated with omega-3 and omega-6 fatty acids in heart tissues ($P < .01$). History of CHD and cause of death (cardiac vs noncardiac) were not significantly associated with levels of omega-3 or omega-6 fatty acids. However, in cadavers with a history of CHD, high levels of omega-3 and omega-6, particularly DHA and AA, were associated with low cardiac mortality ($P < .05$). Fish consumption is associated with levels of omega-3 and omega-6 fatty acids in heart tissues. Although omega-3 and omega-6 fatty acids are not associated with cardiac mortality in the overall studied population, their low levels (especially DHA and AA) in heart tissues are associated with high cardiac mortality in cadavers with a history of CHD.

Keywords: Cadaver; Omega-3; Omega-6; Fatty acids; Heart; Cardiac mortality
Abbreviations: AA, arachidonic acid; CHD, coronary heart disease; DHA, docosahexaenoic acid; EPA, eicosapentaenoic acid; HPLC, high-performance liquid chromatography; LA, linoleic acid; MMC-FA, methyl-7-methoxycoumarin fatty acid; PUFA, polyunsaturated fatty acids; VT, ventricular tachycardia.

1. Introduction

Cardiovascular mortality is the major health concern in most nations around the world. In the past few decades, diet and food supplements have become an important issue in preventive medicine, particularly in cardiovascular diseases

* Corresponding author. Cardiac Electrophysiology Research and Training Center, Faculty of Medicine, Chiang Mai University, Chiang Mai, Thailand. Tel.: +66 53 945329; fax: +66 53 945368.
E-mail address: nchattip@gmail.com (N. Chattipakorn).

0271-5317/$ – see front matter © 2009 Elsevier Inc. All rights reserved.
doi:10.1016/j.nutres.2009.09.011

[1-5]. A growing body of evidence from both basic and clinical studies has demonstrated that omega-3 long-chain polyunsaturated fatty acids (PUFA) prevent cardiac arrhythmia and reduce cardiovascular mortality [1,3,6-16]. These omega-3 fatty acids, including eicosapentaenoic (EPA; C20:5 omega-3) and docosahexaenoic acid (DHA; C22:6 omega-3), are mainly obtained in the diet from the consumption of fatty fish and fish oils. In the heart, both EPA and DHA are incorporated into the cell membrane of cardiomyocytes.

Previous studies have demonstrated that consumption of food supplements containing omega-3 fatty acid significantly increases the amount of EPA and DHA incorporated into the heart tissue [17-19]. Studies using isolated cardiac myocytes demonstrated that during ischemia EPA and DHA are released from myocardial membrane and exert antiarrhythmic effects by prolonging the refractory periods of cardiac action potentials [20,21]. Clinical studies have also demonstrated an increase of EPA and DHA levels in heart tissues after ingestion of omega-3 supplements and the significance of EPA and DHA in preventing cardiac tachyarrhythmias [17,19].

Unlike omega-3 fatty acids, the cardioprotective roles of omega-6 fatty acids (ie, linoleic acid [LA] and arachidonic acid [AA]) are still debated [22-29]. However, a recent American Heart Association Science Advisory Statement supports the benefits of omega-6 fatty acids in reducing the risk of coronary heart disease (CHD) [30]. Despite these growing bodies of evidence regarding the clinical benefit of omega-3 and omega-6 fatty acids on the heart, information on the significance of the levels of these fatty acids in human heart tissues and their association with mortality is still limited. Furthermore, many studies use food supplements to investigate the role of these long-chained PUFA in reducing cardiovascular mortality and preventing arrhythmia [8,11,16,19,31-33]. The direct association between omega-3 and omega-6 fatty acid levels in human heart tissues and cardiac mortality in the general population without food supplements has never been reported.

Because of a limited source of information regarding the natural levels (ie, without food supplement) of these fatty acids in the heart in the general population and their association with cardiac mortality, it was the intent of this study to directly determine the levels of omega-3 (DHA and EPA) and omega-6 (LA and AA) fatty acids in heart tissues taken from cadavers who died from both cardiac and noncardiac causes. In this study, we tested the hypothesis that the omega-3 and omega-6 fatty acid contents in the heart are associated with fish consumption and that high levels of omega-3 and omega-6 fatty acids in heart tissues are associated with low cardiac mortality. Because it is known that both omega-3 and omega-6 fatty acids are essential in cardiomyocytes and that they exert beneficial effects including arrhythmia prevention and mortality reduction, the direct measurement of omega-3 and omega-6 fatty acids in cardiac tissues would allow us to investigate whether they would have direct association with cardiac mortality. To reach this goal, heart tissues from cadavers were examined. To seek the association between fish consumption and the levels of omega-3 and omega-6 fatty acids in heart tissues, the history of fish consumption habits in each cadaver prior to death was determined. This study also investigated whether cadavers with high levels of omega-3 and omega-6 fatty acids in heart tissues would be less likely to die from cardiac cause as compared with those with low levels of these fatty acids in heart tissues.

2. Methods and materials

2.1. Cadaver selection

This study was approved by the Ethics Committee at the Faculty of Medicine, Chiang Mai University. Consent was obtained from a spouse or close relative of the deceased. Subjects were cadavers who had died within 24 hours of notification. The bodies were immediately frozen and delivered to the Department of Anatomy, Faculty of Medicine, Chiang Mai University. The cadaver's fish consumption habits were obtained from a spouse/close relative who had lived with the subject for at least 6 months before death. The cause of death and history of heart disease for each cadaver were obtained from the death certificate designated by the attending physician who signed the certificate. If additional information was needed, the attending physician was contacted to confirm the definite cause of death. Cases with undetermined cause of death were excluded from the study group.

Cardiac tissues were collected from 100 cadavers. The tissue (approximately 75 mg) was taken from the interventricular septum of fresh cadaveric hearts [17] at the Department of Anatomy and was immediately frozen at −86°C. The interventricular septum was chosen for a region of biopsy because a previous report demonstrated that the level of omega-3 and omega-6 fatty acids in heart tissues biopsied from this region was correlated with the levels of fatty acids supplement [17].

2.2. Extraction of cardiac lipids

Heart tissues were weighed and lyophilized overnight. After lyophilization, saline solution was used to suspend the tissue samples with 10 to 15 seconds of sonication [17]. Lipid extraction was performed using the technique described previously [34]. In brief, total lipid in the heart tissues was extracted with chloroform/methanol (2:1, vol/vol) solvent in a proportion of 1:5 (wt/vol) in a screw-cap tube overnight. The mixture was centrifuged at 3000 rpm, 4°C for 20 minutes to sediment tissue pellet. Chloroform-extractable lipid (upper layer) was transferred to a new test tube and evaporated to dryness under nitrogen gas stream. Before analysis, residue was reconstituted in methanol, and concentrations of PUFA, cholesterol, and triglyceride were measured as described below.

2.3. Determination of PUFA concentrations

2.3.1. Saponification

Lipids extracted from myocardial tissues were dissolved in methanol and saponified with the 10% potassium hydroxide (KOH) solution in methanol (with the help of phenolphthalein as an indicator) or triethylamine at 80°C for 15 minutes [35]. The solvent was evaporated by a rotary evaporator or by blowing down with nitrogen gas, and the residual fatty acid salt was analyzed using the precolumn derivatization high-performance liquid chromatography (precolumn HPLC) technique.

2.3.2. Precolumn HPLC analysis of omega-3 and omega-6 fatty acids

Isopropanol (AnalaR grade), methanol (AnalaR grade), acetonitrile (HPLC grade), and dichlorimethane (AnalaR grade) were purchased from the Merck Chemicals Company (Darmstadt, Germany). Boron trifluoride (14%), butylated hydroxytoluene, methyl acetate, 4-bromomethyl-7-methoxycoumarin, and 18-crown-6 ether were purchased from the Sigma-Aldrich Chemicals Co (St. Louis, Mo). Docosahexaenoic acid, EPA, LA, and AA (Sigma-Aldrich Chemicals Co) were used as reference standards. L-α-phosphatidylcholine diheptadecanoic acid (Sigma-Aldrich Chemicals Co) was used as an internal standard. Butylated hydroxytoluene was added as an antioxidant to all organic solvents at 50 mg/L.

For derivatization, the method was slightly modified from that reported by Wolf and Korf [36,37]. The residual fatty acid salt of tissue extract, internal standard, and dichloromethane were mixed for 15 minutes and evaporated under nitrogen. The derivatizing agent was prepared by mixing 40 μL of solution A (5 mg of Br-MMC in 5 mL dry acetonitrile), 2 μL of solution B (13 mg of 18-crown-6 in 5 mL acetonitrile), and 2 mL acetonitrile. The working derivatizing solution (100 μL) and potassium carbonate (2-4 mg) were then added to the mixture, sonicated rapidly (3 strokes, 30 seconds per stroke), and heated for 15 minutes at 60°C. After cooling, the solution containing methyl-7-methoxycoumarin fatty acid (MMC-FA) derivative was passed through 0.22-μm nylon-membrane filter and analyzed with the HPLC method.

The HPLC system (Waters Corporation Milford, Mass) with 2 dual-piston high-pressure pumps (Waters 600 Controller with a binary gradient device), Rheodyne 7125 manual injector (20-μL loop), and fluorescence detector (Waters 474FL Detector) were used in this study. After 20 μL of sample was injected, the MMC-FA derivatives were adsorbed on the column (NovaPak C18, 7.3% carbon load, 3.9 × 150 mm, 4 μm; Part number WAT036975, Waters Corporation) housed in an oven cabinet (Waters Column Oven) at 30°C. The continuous gradient elution (70%-100% acetonitrile) was performed at a flow rate of 1 mL/min from 0 to 30 minutes. Eluates were monitored online with a fluorescence detector ($\lambda_{excitation}$ 362 nm, $\lambda_{emission}$ 415 nm). Peak area of the eluted fatty acids was recorded and integrated with the Waters Millenium 32 HPLC Software. Persisting fatty acids were identified by comparison with known standard fatty acids and quantified from the curves constructed from different concentrations of EPA, DHA, AA, and LA.

High-performance liquid chromatography was used for fatty acid determination in this study for several reasons. Although gas chromatography/mass spectrometry and gas chromatography/flame ionization detection are commonly used for quantitation of fatty acids [38-40], however, the gas chromatograph was not available. In comparison to a gas chromatograph, HPLC with UV or fluorometric detection is easy to operate and can be used as an alternative way to measure very small amounts of fatty acids. Because fatty acids are nonchromophoric and nonfluorophoric, they were labeled with a fluorogenic 4-bromomethyl-7-methoxycoumarin to produce esters of MMC-FA, which are strongly fluorescent ($\lambda_{excitation}$ 362 nm, $\lambda_{emission}$ 415 nm). The HPLC analysis established by Wolf and Korf [36] can be adapted to very low levels (nanogram range) of fatty acids. In the past decade, simple and highly sensitive HPLC analysis with fluorescent detection has been used for the analysis of fatty acids in many laboratories [41-43], and the results obtained by the HPLC technique have been shown to be similar to those obtained by gas chromatography analysis [44].

In this study, PUFA from the extracts were identified by comparison with known standard fatty acids, and their concentrations were determined from standard curves. The PUFA composition was reported as weight percent of total PUFA, and the levels of omega-3 and omega-6 fatty acid components as well as the cholesterol and triglyceride levels in each specimen were obtained using this method.

2.4. Determination of triglyceride and cholesterol contents in heart tissues

2.4.1. Analysis of triglyceride concentration

Triglycerides assay was based on the enzymatic determination of glycerol using the enzyme glycerol phosphate oxidase after hydrolysis by lipoprotein lipase [45,46]. In principle, triglyceride was hydrolyzed by lipase enzyme to release glycerol and fatty acids. The glycerol was catalyzed by glycerol kinase and then glycerol phosphate oxidase to produce hydrogen peroxide. The hydrogen peroxide was oxidized by peroxidase and gave electron to 4-aminoantipyrin in the presence of phenol to form a red-colored quinoneimine product. In assay procedure, specimen (10 μL) was added to triglyceride enzyme reagent (BioTechnical Co, Bangkok, Thailand) containing lipase, glycerol kinase, glycerol phosphate oxidase/horse-radish peroxidase/*p*-aminoantipyrine (1.0 mL) and incubated at 37°C for 10 minutes. Optical density of the product was measured at 505 nm against reagent blank using a double-beam scanning UV-VIS spectrophotometer (PharmaSpec Model UV-1700, Shimadzu Corporation, Kyoto, Japan). Concentrations of the triglyceride were determined from a calibration curve

constructed from different triglyceride concentrations. The amounts of cardiac triglyceride were calculated and expressed as milligram per gram tissue dry weight.

2.4.2. Analysis of total cholesterol concentration

Estimation of total cholesterol concentrations is based on the method established by Richmond [47]. Cholesterol ester was first hydrolyzed by cholesterol esterase to release unesterified cholesterol and fatty acid. The unesterified cholesterol was then oxidized by cholesterol oxidase to generate cholestynone and hydrogen peroxide. In the presence of peroxidase, *p*-aminoantipyrine, and phenol, the hydrogen peroxide was oxidized to produce red-colored quinoneimine. In the assay procedure, specimen (10 μL) was added to 1.0 mL cholesterol enzyme reagent (Bio-Technical Co) containing cholesterol esterase/cholesterol oxidase/horse-radish peroxidase/*p*-aminoantipyrine and incubated at 37°C for 10 minutes. The optical density of the colored product was measured at 505 nm against reagent blank using a double-beam scanning UV-VIS spectrophotometer (PharmaSpec Model UV-1700, Shimadzu Corporation). Concentrations of the cholesterol were determined from a calibration curve constructed from different cholesterol concentrations. Amounts of cardiac cholesterol were calculated and expressed as milligram per gram tissue dry weight.

2.5. Statistical analyses

Three outcome factors were set as fish consumption habits (≤2 fish-meal/wk vs >2 fish-meal/wk), history of heart disease (with vs without), and causes of death (cardiac vs noncardiac cause). The level of omega-3 and omega-6 fatty acids, triglyceride, and cholesterol in each outcome factor category was compared by 2-sample Wilcoxon rank sum test. Fisher exact and χ^2 tests were used to analyze the difference in gender between the 2 groups. Student *t* test and 2-sample Wilcoxon rank sum tests were used for analyzing the difference in age between the 2 groups [48]. All analyses were performed using Intercooled Stata (version 8.0, Stata Corp, College station, Tex). All measurements were considered to be statistically significant when the $P < .05$.

Table 1
Contents of fatty acids in heart tissues and the fish consumption habits

Fatty acids	≤2 Fish-meal/wk [a]	>2 Fish-meal/wk [b]	*P*
Age			.556 [c]
Mean (SD)	68 (14)	70 (11)	
Median (range)	70 (26-104)	71 (49-97)	
Gender, n (%)			.155 [d]
Male	37 (69)	21 (46)	
Female	17 (31)	25 (54)	
Total measured omega fatty acids [e]			.007 [c]
Mean (SD)	525.3 (322.8)	745.9 (404.0)	
Median (range)	404.8 (57.4-1503.1)	700.5 (148.0-1385.3)	
Omega-3 (EPA + DHA)			.008 [c]
Mean (SD)	96.0 (62.3)	138.7 (84.3)	
Median (range)	84.5 (7.5-330.7)	119.6 (23.9-381.2)	
Omega-6 (AA + LA)			.009 [c]
Mean (SD)	429.3 (279.7)	607.2 (335.2)	
Median (range)	322.3 (49.9-1172.4)	612.3 (35.8-1168.2)	
EPA			.127 [c]
Mean (SD)	4.5 (10.3)	2.5 (6.0)	
Median (range)	0 (0-69.0)	0 (0-32.00)	
DHA			.006 [c]
Mean (SD)	91.6 (62.8)	136.2 (84.0)	
Median (range)	84.5 (5.8-330.7)	115.8 (20.5-349.2)	
AA			.004 [c]
Mean (SD)	240.3 (193.5)	383.9 (245.2)	
Median (range)	168.7 (8.9-824.5)	376.15 (32.3-784.6)	
LA			.178 [c]
Mean (SD)	189.0 (107.7)	223.3 (122.6)	
Median (range)	178.1 (23.0-505.4)	235.6 (0-477.3)	
Triglyceride			.950 [c]
Mean (SD)	1500.8 (186.3)	1495.4 (167.7)	
Median (range)	1466.8 (1134.8-2049.6)	1497 (1193.4-1947.4)	
Cholesterol			.986 [c]
Mean (SD)	1196.4 (233.0)	1188.8 (232.6)	
Median (range)	1136.1 (830.2-1717.0)	1153.0 (688.3-1996.8)	

Parameters with $P < .05$ indicate significant difference between the 2 groups.

[a] n = 54.

[b] n = 46.

[c] Two-sample Wilcoxon rank sum test.

[d] Fisher exact test.

[e] Total measured omega fatty acids: EPA + DHA + AA + LA.

3. Results

3.1. Omega-3 and omega-6 fatty acids in the heart and fish consumption habits

The age and gender were not different between the 2 groups. The total measured omega fatty acids in the heart tissues taken from cadavers who consumed more than 2 fish-meal/wk were significantly higher than those who ate 2 or less fish-meal/wk (Table 1). The levels of both omega-3 (ie, EPA + DHA) and omega-6 (AA + LA) fatty acids in the heart were also significantly higher in the group that consumed fish more frequently. For omega-3 fatty acid levels, the DHA level was significantly higher in those who consumed more than 2 fish-meal/wk. The EPA level, however, was not significantly different between the 2 groups. For omega-6 fatty acid levels, the AA level was significantly higher in those who consumed more than 2 fish-meal/wk. The LA level was not significantly different between the 2 groups. The levels of triglyceride and cholesterol in the heart tissues were not different between the 2 groups. No gender differences were found for the levels of omega-3 and omega-6 fatty acids, as well as the cholesterol and triglyceride levels in heart tissue of cadavers (data not shown).

3.2. Omega-3 and omega-6 fatty acid contents in heart tissues and history of CHD

To seek the relationship between the levels of omega-3 and omega-6 fatty acids in the heart tissues and the history of CHD, cadavers were classified into 2 groups: one with a history of CHD and the other without a history of CHD (Table 2). Age and gender were not different between the 2 groups. Neither omega-3 nor omega-6 levels measured in this study were different between cadavers with a history of CHD and those without CHD. Similarly, the total measured omega fatty acids, triglyceride, and cholesterol were not significantly different between the 2 groups.

3.3. Omega fatty acid contents in heart tissues and cardiac mortality

The association between omega fatty acid levels in heart tissues and cardiac mortality was investigated by dividing cadavers into 2 groups based on the cause of mortality, (ie, cardiac and noncardiac causes; Table 3). Both age and gender were not significantly different between the 2 groups.

Table 2
Fatty acids contents in heart tissues classified by the history of CHD

	No history of CHD [a]	With history of CHD [b]	*P*
Age			.418 [c]
Mean (SD)	68 (14)	71 (11)	
Median (range)	71 (26-104)	74 (51-97)	
Gender, n (%)			.671 [d]
Male	48 (63)	14 (58)	
Female	28 (37)	10 (42)	
Total measured omega fatty acids [e]			.448 [f]
Mean (SD)	616.6 (385.4)	659.0 (355.2)	
Median (range)	575.2 (99.0-1503.1)	671.9 (57.4-1283.7)	
Omega-3 (EPA + DHA)			.122 [f]
Mean (SD)	111.31 (79.0)	129.4 (64.9)	
Median (range)	97.3 (13.6-318.2)	135.55 (7.5-234.2)	
Omega-6 (AA + LA)			.675 [f]
Mean (SD)	505.3 (321.5)	529.6 (311.2)	
Median (range)	478.6 (35.8-1172.4)	532.0 (49.9-1065.1)	
EPA			.707 [f]
Mean (SD)	3.9 (9.4)	2.5 (5.3)	
Median (range)	0 (0-69.1)	0 (0-18.6)	
DHA			.120 [f]
Mean (SD)	107.5 (79.2)	126.8 (65.3)	
Median (range)	94.7 (10.9-349.2)	131.7 (5.8-232.2)	
AA			.859 [f]
Mean (SD)	305.6 (233.3)	308.6 (220.6)	
Median (range)	259.4 (32.3-824.5)	246.0 (8.9-714.5)	
LA			.272 [f]
Mean (SD)	199.7 (177.0)	203.0 (111.3)	
Median (range)	205.5 (0-505.4)	234.5 (23.0-422.9)	
Triglyceride			.465 [f]
Mean (SD)	1507.4 (189.1)	1469.5 (131.3)	
Median (range)	1483.5 (1134.8-2049.6)	1460.9 (1225.4-1761.8)	
Cholesterol			.397 [f]
Mean (SD)	1178.1 (211.8)	1239.9 (285.9)	
Median (range)	1135.5 (688.3-1717.0)	1210.0 (830.2-1996.8)	

Parameters with $P < .05$ indicate significant difference between the 2 groups. None of the determined parameters was significantly different between the 2 groups as indicated by $P > .05$.

[a] n = 76.
[b] n = 24.
[c] Student *t* test.
[d] χ^2 test.
[e] Total measured omega fatty acids: EPA + DHA + AA + LA.
[f] Two-sample Wilcoxon rank sum test.

Table 3
Fatty acids contents in heart tissues classified by causes of death

	Noncardiac mortality [a]	Cardiac mortality [b]	*P*
Age			.926 [c]
Mean (SD)	69 (13)	69 (13)	
Median (range)	71 (26-104)	67 (51-97)	
Gender, n (%)			.526 [d]
Male	54 (61)	8 (73)	
Female	35 (39)	3 (27)	
Total measured omega fatty acids [e]			.381 [c]
Mean (SD)	640.9 (382.7)	512.9 (320.9)	
Median (range)	608.1 (99.0-1503.1)	436.8 (57.4-1097.7)	
Omega-3 (EPA+DHA)			.415 [c]
Mean (SD)	118.0 (76.5)	96.6 (71.3)	
Median (range)	104.8 (13.6-381.2)	71.0 (7.5-234.2)	
Omega-6 (AA + LA)			.293 [c]
Mean (SD)	522.9 (319.6)	416.3 (298.2)	
Median (range)	501.4 (35.8-1172.4)	325.5 (49.9-920.0)	
EPA			.551 [c]
Mean (SD)	3.6 (8.9)	3.4 (6.4)	
Median (range)	0 (0-69.1)	0 (0-18.6)	
DHA			.447 [c]
Mean (SD)	114.4 (77.1)	93.2 (69.1)	
Median (range)	102.9 (10.9-349.2)	71.0 (5.8-215.6)	
AA			.067 [c]
Mean (SD)	320.8 (233.8)	189.3 (149.1)	
Median (range)	272.7 (32.3-824.5)	167.2 (8.9-442.7)	
LA			.620 [c]
Mean (SD)	202.1 (110.7)	227.1 (153.7)	
Median (range)	216.4 (0-505.4)	180.3 (23.0-477.3)	
Triglyceride			.197 [c]
Mean (SD)	1506.0 (182.4)	1436.5 (114.2)	
Median (range)	1503.8 (1134.8-2049.6)	1421.0 (1288.2-1676.7)	
Cholesterol			.250 [c]
Mean (SD)	1182.2 (225.0)	1279.7 (276.9)	
Median (range)	1147.3 (688.3-1996.8)	1424.7 (849.6-1602.3)	

Parameters with $P < .05$ indicate significant difference between the 2 groups. None of the determined parameters was significantly different between the 2 groups as indicated by $P > .05$.

[a] n = 89.
[b] n = 11.
[c] Two-sample Wilcoxon rank sum test.
[d] Fisher exact test.
[e] Total measured omega fatty acids: EPA + DHA + AA + LA.

Both omega-3 and omega-6 fatty acids measured in the heart tissues were not different between cadavers with cardiac mortality and those with noncardiac mortality. The total measured omega fatty acid levels, triglyceride, and cholesterol were also not significantly different between the 2 groups.

3.4. Omega fatty acid contents in heart tissues and the cause of death in cadavers with a history of CHD

In cadavers with a history of heart disease, we sought to determine the association between omega-3 and omega-6 fatty acid contents in the hearts and cardiac mortality in this group (Table 4). Cadavers with a history of heart disease were classified into 2 groups by cause of death (ie, cardiac vs noncardiac mortality). Age and gender were not significantly different between the 2 groups. The total measured omega fatty acid levels in the heart were significantly lower in cadavers in the cardiac mortality group than in the noncardiac mortality group. The levels of omega-3 (EPA + DHA) and omega-6 (AA + LA) fatty acids were also significantly lower in the group with cardiac mortality. Although the EPA level was not different between the 2 groups, the DHA level was significantly lower in cadavers with cardiac mortality. Similar to the DHA level, the AA level in the heart was also significantly lower in the cardiac mortality group. Both triglyceride and cholesterol levels in the heart tissues were not different between the 2 groups.

Table 4
Fatty acids contents in heart tissues in cadavers with heart disease classified by the causes of death

	Cardiac cause [a]	Noncardiac cause [b]	*P*
Age			.591 [c]
Mean (SD)	69 (14)	71 (8)	
Median (range)	67 (51-97)	74 (57-82)	
Gender, n (%)			.678 [d]
Male	6 (67)	8 (53)	
Female	3 (33)	7 (47)	
Total measured omega fatty acids [e]			.016 [c]
Mean (SD)	435.1 (278.3)	793.3 (333.9)	
Median (range)	396.5 (57.4-885.7)	829.1 (265.9-1283.7)	
Omega-3 (EPA + DHA)			.040 [c]
Mean (SD)	92.01 (72.9)	151.8 (49.5)	
Median (range)	71.0 (7.5-234.2)	155.3 (55.3-232.2)	
Omega-6 (AA + LA)			.022 [c]
Mean (SD)	343.0 (265.2)	641.5 (288.2)	
Median (range)	319.0 (49.9-845.8)	656.8 (210.6-1065.1)	
EPA			.070 [c]
Mean (SD)	4.2 (6.9)	1.5 (4.1)	
Median (range)	0.6 (0-18.6)	0 (0-13.4)	
DHA			.034 [c]
Mean (SD)	87.8 (69.9)	150.1 (51.5)	
Median (range)	71.0 (5.8-215.6)	155.3 (46.0-232.2)	
AA			.005 [c]
Mean (SD)	154.6 (134.1)	401.0 (212.8)	
Median (range)	145.2 (8.9-422.9)	400.8 (74.0-714.5)	
LA			.245 [c]
Mean (SD)	188.4 (136.5)	240.5 (92.7)	
Median (range)	151.9 (23.0-422.9)	272.6 (88.1-360.2)	
Triglyceride			.456 [c]
Mean (SD)	1446.9 (124.0)	1483.1 (137.9)	
Median (range)	1435.5 (1288.2-1676.7)	1503.8 (1225.4-1676.7)	
Cholesterol			
Mean (SD)	1283.9 (282.0)	1213.5 (294.7)	
Median (range)	1424.7 (849.6-1602.3)	1189.5 (830.2-1996.8)	.355 [c]

Parameters with $P < .05$ indicate significant difference between the 2 groups.

[a] n = 9.

[b] n = 15.

[c] Two-sample Wilcoxon rank sum test.

[d] Fisher exact test.

[e] Total measured omega fatty acids: EPA + DHA + AA + LA.

4. Discussion

The major findings of this study are as follows: (1) both omega-3 (EPA + DHA) and omega-6 (AA + LA) fatty acids levels in the heart tissues, especially the DHA and AA, are associated with fish consumption and (2) in heart tissues taken from cadavers with CHD, low levels of both omega-3 (EPA + DHA) and omega-6 (AA + LA) in the heart, specifically the DHA and AA, are associated with cardiac mortality.

Epidemiologic studies have reported that there is an association between consumption of fish that is rich in omega-3 fatty acids and cardiovascular disease [1,14,15,49,50]. Basic and clinical studies have also demonstrated the correlation between omega-3 supplements and an increase in omega-3 contents in both plasma and cardiac tissues [17-19]. In this study, the total measured omega fatty acids and the levels of omega-3 (ie, EPA + DHA) and omega-6 (ie, AA + LA) fatty acids in the heart tissues of cadavers are associated with fish consumption habits. However, for the omega-3 fatty acids, only the DHA level in the heart is associated with fish consumption habits. This association is not observed for EPA level in the heart tissues. For omega-6 fatty acids, only the AA level in heart tissues is associated with fish consumption habits. The LA levels are not different between the 2 groups.

A number of studies have demonstrated the significance of omega-3 fatty acid supplements in reducing mortality [1,8,11]. Epidemiologic studies also support these findings [50,51]. For omega-6 fatty acids, there are reports that suggest reducing their intake [22-24,29], reports indicating no significant effects [25-28], and recommending increasing their intake to reduce the risk of CHD [52-55]. Despite this growing body of evidence and controversy, direct association between omega-3 fatty acids content in the heart tissues and cardiac mortality in the general population without food supplements has never been tested.

This study is the first to investigate this relationship. When the cadavers were classified into 2 groups based on the history of CHD, the levels of omega-3 and omega-6 fatty acids in heart tissues were not different between the groups with and without the history of CHD. Similarly, when the cause of mortality was used to classify the sources of heart tissues, no significant difference was found for the omega-3 and omega-6 contents in the hearts between cardiac and noncardiac mortality groups. However, only when cadavers with a history of CHD were categorized into 2 groups using the causes of death, we found that the group with cardiac mortality had lower levels of omega-3 (EPA + DHA) and omega-6 (AA + LA) fatty acids as well as total measured omega fatty acids in the hearts. More importantly, we found that the DHA and AA levels in heart tissues were significantly lower in the cardiac mortality group. All of these findings suggest that both omega-3 and omega-6 contents in the heart may not protect against all-cause mortality. However, the cardiac mortality prevention of omega-3 and omega-6 fatty acids, particularly the DHA and AA levels in the heart, is notably effective only in those who already have pathological hearts.

Raitt et al [56] previously reported that omega-3 supplements in patients with implantable cardioverter defibrillator and with a history of ventricular tachycardia (VT) or ventricular fibrillation do not reduce the risk of VT or ventricular fibrillation, compared with a placebo. In addition, they found that fish oil may be pro-arrhythmic in implantable cardioverter defibrillator patients with a history of VT prior to receiving this supplement. Their findings indicated that the type of arrhythmia is important in determining the beneficial effects of omega-3 fatty acids in the heart [56].

In this study, our findings also indicate that omega-3 fatty acids may be beneficial only in those with underlying heart disease. These findings also suggest that the underlying pathology of the heart is an important parameter in determining whether an omega-3 supplement is beneficial. This hypothesis has recently been elucidated by Ruijter et al, who proposed that omega-3 fatty acids could be either pro- or anti-arrhythmic, depending on the underlying mechanisms of arrhythmias in each individual [57].

In addition to the importance of DHA, our study also indicates a similar importance of AA, an omega-6 fatty acid, in the heart. The association between its low levels and cardiac mortality in cadavers with a history of heart disease suggests that it could play an equally important role to DHA in cardioprotective effects. A recent American Heart Association Science Advisory Statement clearly indicates the cardioprotective benefits of omega-6 fatty acids in reducing the risk of cardiovascular disease [30] and supports our findings.

In the past decades, a number of studies have emphasized the clinical significance of omega-3 fatty acids in preventing arrhythmias and heart disease, as well as reducing mortality [1,14,15,49,50]. The results of this study demonstrate the possibly equal importance of AA, an omega-6 fatty acid, in reducing cardiac mortality. Further studies with a large population are needed to verify the clinical significance of the findings presented in this study.

There are several limitations in this study. First, the population in this study is small, particularly in those with a history of CHD. Second, detailed demographic data such as history of drugs taken, underlying diseases, and history of arrhythmias are not included. In addition, our study was designed to study omega-3 fatty acids, particularly DHA and EPA, and omega-6 fatty acids (ie, AA and LA) in the heart tissues of cadavers. Therefore, other fatty acids were not investigated in this study.

The levels of omega-3 (EPA + DHA) and omega-6 (AA + LA) in the heart are associated with the amount of fish consumption. In cadavers with a history of CHD, these levels are associated with cardiac mortality. These findings indicate that both omega-3 and omega-6 fatty acids, particularly DHA and AA, could be useful in reducing cardiac mortality in those with a history of CHD.

Acknowledgment

This work is supported by grants from the Vedjadusit Foundation, the Faculty of Medicine Endowment Fund, Chiang Mai University, and the Thailand Research Fund RTA 5280006 (NC) and RMU 5180007 (SC).

References

[1] Albert CM, Hennekens CH, O'Donnell CJ, Ajani UA, Carey VJ, Willett WC, et al. Fish consumption and risk of sudden cardiac death. JAMA 1998;279(1):23-8.

[2] Anand RG, Alkadri M, Lavie CJ, Milani RV. The role of fish oil in arrhythmia prevention. J Cardiopulm Rehabil Prev 2008;28(2):92-8.

[3] Ascherio A, Rimm EB, Stampfer MJ, Giovannucci EL, Willett WC. Dietary intake of marine n-3 fatty acids, fish intake, and the risk of coronary disease among men. N Engl J Med 1995;332(15):977-82.

[4] Epstein FH. The relationship of lifestyle to international trends in CHD. Int J Epidemiol 1989;18(3 Suppl 1):S203-9.

[5] Krauss RM, Eckel RH, Howard B, Appel LJ, Daniels SR, Deckelbaum RJ, et al. AHA Dietary Guidelines: revision 2000: a statement for healthcare professionals from the Nutrition Committee of the American Heart Association. Circulation 2000;102(18):2284-99.

[6] Billman GE, Hallaq H, Leaf A. Prevention of ischemia-induced ventricular fibrillation by omega 3 fatty acids. Proc Natl Acad Sci U S A 1994;91:4427-30.

[7] Chattipakorn N, Shinlapawittayatorn K, Sungnoon R, Chattipakorn SC. Effects of n-3 polyunsaturated fatty acid on upper limit of vulnerability shocks. Int J Cardiol 2006;107(3):299-302.

[8] Burr ML, Fehily AM, Gilbert JF, Rogers S, Holliday RM, Sweetnam PM, et al. Effects of changes in fat, fish, and fibre intakes on death and myocardial reinfarction: diet and reinfarction trial (DART). Lancet 1989;2(8666):757-61.

[9] Christensen JH, Korup E, Aaroe J, Toft E, Moller J, Rasmussen K, et al. Fish consumption, n-3 fatty acids in cell membranes, and heart rate variability in survivors of myocardial infarction with left ventricular dysfunction. Am J Cardiol 1997;79(12):1670-3.

[10] Cleland JG, Freemantle N, Kaye G, Nasir M, Velavan P, Lalukota K, et al. Clinical trials update from the American Heart Association meeting: omega-3 fatty acids and arrhythmia risk in patients with an

implantable defibrillator, ACTIV in CHF, VALIANT, the Hanover autologous bone marrow transplantation study, SPORTIF V, ORBIT and PAD and DEFINITE. Eur J Heart Fail 2004;6(1):109-15.
[11] Gissi-Prevenzione Investigators. Dietary supplementation with n_3 polyunsaturated fatty acids and vitamin E after myocardial infarction: results of the GISSI-Prevenzione trial. Lancet 1999;354:447-55.
[12] Siscovick DS, Raghunathan TE, King I, Weinmann S, Wicklund KG, Albright J, et al. Dietary intake and cell membrane levels of long-chain n-3 polyunsaturated fatty acids and the risk of primary cardiac arrest. JAMA 1995;274(17):1363-7.
[13] Wongcharoen W, Chattipakorn N. Antiarrhythmic effects of n-3 polyunsaturated fatty acids. Asia Pac J Clin Nutr 2005;14(4):307-12.
[14] He K, Song Y, Daviglus ML, Liu K, Van Horn L, Dyer AR, et al. Accumulated evidence on fish consumption and coronary heart disease mortality: a meta-analysis of cohort studies. Circulation 2004;109(22): 2705-11.
[15] Daviglus ML, Stamler J, Orencia AJ, Dyer AR, Liu K, Greenland P, et al. Fish consumption and the 30-year risk of fatal myocardial infarction. N Engl J Med 1997;336(15):1046-53.
[16] Berecki G, Den Ruijter HM, Verkerk AO, Schumacher CA, Baartscheer A, Bakker D, et al. Dietary fish oil reduces the incidence of triggered arrhythmias in pig ventricular myocytes. Heart Rhythm 2007;4(11):1452-60.
[17] Harris WS, Sands SA, Windsor SL, Ali HA, Stevens TL, Magalski A, et al. Omega-3 fatty acids in cardiac biopsies from heart transplantation patients: correlation with erythrocytes and response to supplementation. Circulation 2004;110(12):1645-9.
[18] Metcalf RG, James MJ, Gibson RA, Edwards JR, Stubberfield J, Stuklis R, et al. Effects of fish-oil supplementation on myocardial fatty acids in humans. Am J Clin Nutr 2007;85(5):1222-8.
[19] Metcalf RG, Sanders P, James MJ, Cleland LG, Young GD. Effect of dietary n-3 polyunsaturated fatty acids on the inducibility of ventricular tachycardia in patients with ischemic cardiomyopathy. Am J Cardiol 2008;101(6):758-61.
[20] Kang JX, Xiao YF, Leaf A. Free, long-chain, polyunsaturated fatty acids reduce membrane electrical excitability in neonatal rat cardiac myocytes. Proc Natl Acad Sci U S A 1995;92(9):3997-4001.
[21] Kang JX, Leaf A. Prevention and termination of arrhythmias induced by lysophosphatidyl choline and acylcarnitine in neonatal rat cardiac myocytes by free omega-3 polyunsaturated fatty acids. Eur J Pharmacol 1996;297:97-106.
[22] Simopoulos AP. The importance of the omega-6/omega-3 fatty acid ratio in cardiovascular disease and other chronic diseases. Exp Biol Med (Maywood) 2008;233(6):674-88.
[23] Simopoulos AP, Leaf A, Salem Jr N. Essentiality of and recommended dietary intakes for omega-6 and omega-3 fatty acids. Ann Nutr Metab 1999;43(2):127-30.
[24] Hamazaki T, Okuyama H. The Japan Society for Lipid Nutrition recommends to reduce the intake of linoleic acid. A review and critique of the scientific evidence. World Rev Nutr Diet 2003;92:109-32.
[25] Pietinen P, Ascherio A, Korhonen P, Hartman AM, Willett WC, Albanes D, et al. Intake of fatty acids and risk of coronary heart disease in a cohort of Finnish men. The Alpha-Tocopherol, Beta-Carotene Cancer Prevention Study. Am J Epidemiol 1997;145(10):876-87.
[26] Esrey KL, Joseph L, Grover SA. Relationship between dietary intake and coronary heart disease mortality: lipid research clinics prevalence follow-up study. J Clin Epidemiol 1996;49(2):211-6.
[27] McGee DL, Reed DM, Yano K, Kagan A, Tillotson J. Ten-year incidence of coronary heart disease in the Honolulu Heart Program. Relationship to nutrient intake. Am J Epidemiol 1984;119(5):667-76.
[28] Dolecek TA. Epidemiological evidence of relationships between dietary polyunsaturated fatty acids and mortality in the multiple risk factor intervention trial. Proc Soc Exp Biol Med 1992;200(2):177-82.
[29] Sears B. The Omega Rx Zone. The miracle of the new high-dose fish oil. New York: Haper Collins; 2003.
[30] Harris WS, Mozaffarian D, Rimm E, Kris-Etherton P, Rudel LL, Appel LJ, et al. Omega-6 fatty acids and risk for cardiovascular disease. A science advisory from the American Heart Association Nutrition Subcommittee of the Council on Nutrition, Physical Activity, and Metabolism; Council on Cardiovascular Nursing; and Council on Epidemiology and Prevention. Circulation 2009;119(6): 902-7.
[31] Albert CM, Campos H, Stampfer MJ, Ridker PM, Manson JE, Willett WC, et al. Blood levels of long-chain n-3 fatty acids and the risk of sudden death. N Engl J Med 2002;346(15):1113-8.
[32] de Lorgeril M, Salen P, Martin JL, Monjaud I, Delaye J, Mamelle N. Mediterranean diet, traditional risk factors, and the rate of cardiovascular complications after myocardial infarction: final report of the Lyon Diet Heart Study. Circulation 1999;99(6):779-85.
[33] Den Ruijter HM, Berecki G, Verkerk AO, Bakker D, Baartscheer A, Schumacher CA, et al. Acute administration of fish oil inhibits triggered activity in isolated myocytes from rabbits and patients with heart failure. Circulation 2008;117(4):536-44.
[34] Carlson LA. Extraction of lipids from human whole serum and lipoproteins and from rat liver tissue with methylene chloride-methanol: a comparison with extraction with chloroform-methanol. Clin Chim Acta 1985;149(1):89-93.
[35] Ichihara K, Shibahara A, Yamamoto K, Nakayama T. An improved method for rapid analysis of the fatty acids of glycerolipids. Lipids 1996;31(5):535-9.
[36] Wolf JH, Korf J. Automated solid-phase catalyzed pre-column derivatization of fatty acids for reversed-phase high-performance liquid chromatographic analysis with fluorescence detection. J Chromatogr 1988;436(3):437-45.
[37] Wolf JH, Korf J. Improved automated precolumn derivatization reaction of fatty acids with bromomethylmethoxycoumarin as label. J Chromatogr 1990;502(2):423-30.
[38] Kulig CC, Beresford TP, Everson GT. Rapid, accurate, and sensitive fatty acid ethyl ester determination by gas chromatography–mass spectrometry. J Lab Clin Med 2006;147(3):133-8.
[39] Tranchida PQ, Costa R, Donato P, Sciarrone D, Ragonese C, Dugo P, et al. Acquisition of deeper knowledge on the human plasma fatty acid profile exploiting comprehensive 2-D GC. J Sep Sci 2008;31(19): 3347-51.
[40] Zhao DX, Ding ZC, Liu YQ, Huang ZX. Overexpression and purification of single zinc finger peptides of human zinc finger protein ZNF191. Protein Expr Purif 2007;53(1):232-7.
[41] Chung TC, Kou HS, Chao MC, Ou YJ, Wu HL. A simple and sensitive liquid chromatographic method for the analysis of free docosanoic, tetracosanoic and hexacosanoic acids in human plasma as fluorescent derivatives. Anal Chim Acta 2008;611(1):113-8.
[42] Forster L, Schulze EA, Lehr M. High-performance liquid chromatographic assay with fluorescence detection for the evaluation of inhibitors against fatty acid amide hydrolase. Anal Bioanal Chem 2009;394(6):1679-85.
[43] Yano M, Kishida E, Muneyuki Y, Masuzawa Y. Quantitative analysis of ceramide molecular species by high performance liquid chromatography. J Lipid Res 1998;39(10):2091-8.
[44] Ando Y, Haba Y, Soma K, Hiraoka Y, Takatsu T. Rapid preparation of fluorescent 9-anthrylmethyl esters for fatty acid analysis of small amount of triacylglycerols. Lipids 2007;42(10):955-60.
[45] Bucolo G, David H. Quantitative determination of serum triglycerides by the use of enzymes. Clin Chem 1973;19(5):476-82.
[46] Megraw RE, Dunn DE, Biggs HG. Manual and continuous-flow colorimetry of triacylglycerols by a fully enzymic method. Clin Chem 1979;25(2):273-8.
[47] Richmond W. Preparation and properties of a cholesterol oxidase from *Nocardia* sp. and its application to the enzymatic assay of total cholesterol in serum. Clin Chem 1973;19(12):1350-6.
[48] Pagono M, Gauvreau K. Principles of biostatistics. Pacific Grove: Duxbury Press; 2000.
[49] Kromann N, Green A. Epidemiological studies in the Upernavik district, Greenland. Incidence of some chronic diseases 1950-1974. Acta Med Scand 1980;208(5):401-6.

[50] Kagawa Y, Nishizawa M, Suzuki M, Miyatake T, Hamamoto T, Goto K, et al. Eicosapolyenoic acids of serum lipids of Japanese islanders with low incidence of cardiovascular diseases. J Nutr Sci Vitaminol (Tokyo) 1982;28(4):441-53.
[51] Middaugh J. Cardiovascular deaths among Alaskan natives. Am J Public Health 1990;80:282-5.
[52] Djousse L, Pankow JS, Eckfeldt JH, Folsom AR, Hopkins PN, Province MA, et al. Relation between dietary linolenic acid and coronary artery disease in the National Heart, Lung, and Blood Institute Family Heart Study. Am J Clin Nutr 2001;74(5):612-9.
[53] Mozaffarian D, Ascherio A, Hu FB, Stampfer MJ, Willett WC, Siscovick DS, et al. Interplay between different polyunsaturated fatty acids and risk of coronary heart disease in men. Circulation 2005; 111(2):157-64.
[54] Shekelle RB, Shryock AM, Paul O, Lepper M, Stamler J, Liu S, et al. Diet, serum cholesterol, and death from coronary heart disease. The Western Electric study. N Engl J Med 1981;304(2):65-70.
[55] Laaksonen DE, Nyyssonen K, Niskanen L, Rissanen TH, Salonen JT. Prediction of cardiovascular mortality in middle-aged men by dietary and serum linoleic and polyunsaturated fatty acids. Arch Intern Med 2005;165(2):193-9.
[56] Raitt MH, Connor WE, Morris C, Kron J, Halperin B, Chugh SS, et al. Fish oil supplementation and risk of ventricular tachycardia and ventricular fibrillation in patients with implantable defibrillators: a randomized controlled trial. JAMA 2005;293(23):2884-91.
[57] Den Ruijter HM, Berecki G, Opthof T, Verkerk AO, Zock PL, Coronel R. Pro- and antiarrhythmic properties of a diet rich in fish oil. Cardiovasc Res 2007;73(2):316-25.

ELSEVIER

Nutrition 25 (2009) 870–878

NUTRITION

www.nutritionjrnl.com

Basic nutritional investigation

Effects of curcuminoid supplement on cardiac autonomic status in high-fat–induced obese rats

Anchalee Pongchaidecha, Ph.D.[a,c], Narissara Lailerd, Ph.D.[b,c], Warasinee Boonprasert, M.Sc.[a,c], and Nipon Chattipakorn, M.D., Ph.D.[b,c,*]

[a] *Nutrition and Exercise Unit, Department of Physiology, Faculty of Medicine, Chiang Mai University, Chiang Mai, Thailand*
[b] *Cardiac Electrophysiology Unit, Department of Physiology, Faculty of Medicine, Chiang Mai University, Chiang Mai, Thailand*
[c] *Cardiac Electrophysiology Research and Training Center, Faculty of Medicine, Chiang Mai University, Chiang Mai, Thailand*

Manuscript received June 24, 2008; accepted February 12, 2009

Abstract

Objective: Sudden cardiac death in obesity is frequently associated with sympathetic activation due to an elevated plasma free-fatty acid (FFA) level. Curcuminoids, the phenolic yellowish pigments of turmeric, display antioxidative and lipid-lowering activities. We hypothesized that curcuminoids ameliorate cardiac sympathovagal disturbance in high-fat–induced obese rats.

Methods: Male Wistar rats were divided into five groups. A normal-diet control (NDC) group received a normal-fat diet (12% calories as fat) and a high-fat–diet control (HDC) group received a high-fat diet (60% calories as fat) for 12 wk. Three other groups received high-fat diets with curcuminoid supplement at concentrations of 30 mg (HD_{30}), 60 mg (HD_{60}), and 90 mg (HD_{90}) per kilogram of body weight every day for 12 wk. Heart rate variability was determined to assess cardiac autonomic status at weeks 0 and 12.

Results: Body weight, visceral fat mass, plasma FFA, and glucose levels increased significantly in the HDC group compared with the NDC group. Low frequency power in normalized units (LFnu) and the ratio of LF to high-frequency power (HF) in the HDC group were significantly higher, whereas HFnu in the HDC group was significantly lower than in the NDC group. Plasma FFA levels correlated significantly with LFnu and LF/HF ratio. Compared with the HDC group, plasma FFA, glucose levels, LFnu, and LF/HF ratio were significantly decreased in the HF_{30}, HF_{60}, and HF_{90} groups.

Conclusion: Elevated plasma FFA in high-fat–induced obese rats is associated with an increased LF/HF ratio, an expression of sympathovagal disturbance. Curcuminoid supplementation ameliorates cardiac autonomic imbalance in high-fat–fed rats, probably due to its lipid-lowering effect.

Keywords: Curcuminoids; Obesity; Heart rate variability; Sympathovagal disturbance

Introduction

Risk of acute coronary syndrome and other cardiovascular complications has increased along with a growing obesity epidemic. Premature ventricular contractions causing arrhythmia and sudden death also frequently occur in obese people [1]. Although the exact mechanism remains unknown, reports have indicated that obesity raises the risk of cardiovascular diseases partly through its effects on vascular risk factors such as hypertension, dyslipidemia, insulin resistance, glucose intolerance, and type 2 diabetes [2,3].

Hyperlipidemia, particularly increased plasma free fatty acid (FFA) levels, is common in obese subjects [4]. Elevated plasma FFAs are associated with a larger number of ventricular premature complexes in normal subjects and non-ischemic diabetic patients [5]. Although several risk factors may contribute to these events, sympathetic nervous system activation has been proposed as responsible for arrhythmia in obesity [5–7]. Previous studies have demonstrated that portal

This study was supported by grants from the Thailand Research Fund Basic Research Grant (to N.C.), Biomedical Engineering Center (to A.P.), and the Faculty of Medicine, Chiang Mai University, Endowment Fund (to N.L. and A.P.).

*Corresponding author. Tel.:+66-53-945329; fax:+66-53-945368.
E-mail address: nchattip@mail.med.cmu.ac.th (N. Chattipakorn).

0899-9007/09/$ – see front matter
doi:10.1016/j.nut.2009.02.001

fatty acid infusion can stimulate sympathetic nervous system activity [8]. Furthermore, Verwaerde et al. [9] demonstrated that tachycardia induced by acute elevation of plasma FFA concentrations in dogs was mainly caused by impairment of parasympathetic control. These findings indicate the important role of fatty acids in autonomic control.

Currently, analysis of heart rate variability (HRV) is widely used to assess the autonomic nervous system and provides information on risk of cardiovascular diseases and mortality [10,11]. Decreased HRV, an expression of an exaggerated cardiac sympathetic nervous system, is associated with increased cardiovascular mortality [11–13]. Previous studies have demonstrated that elevated plasma FFA levels stimulate cardiac sympathetic nervous activity in healthy subjects [14] and in non–insulin-dependent diabetic (NIDDM) patients [7]. Blood pressure variability and HRV study also show that increased plasma FFAs in rats significantly increases low-frequency power in normalized units (LFnu) and decreases high-frequency power in normalized units (HFnu), causing a significant increase in the LF/HF ratio [15]. This finding indicates that an elevated level of plasma FFA is strongly linked to a reduced vagal component of the cardiac baroreflex and inversely correlated with baroreflex sensitivity.

Curcuminoids, a group of phenolic compounds isolated from the rhizome of the plant *Curcuma longa* Linn., have been reported as an efficient antioxidant, anticarcinogenic, anti-inflammatory, and hypoglycemic agent [16–24]. Curcuminoids exert hypocholesterolemic actions on lipid metabolism [25,26]. Furthermore, dietary curcuminoids have been shown to prevent liver triacylglycerol accumulation and epididymal adipose tissue weight gain and decrease plasma very low-density lipoprotein/triacylglycerol in rats fed a high-fat diet [27]. However, the role of curcuminoids on plasma FFA is not known.

We tested the hypotheses that 1) curcuminoids decrease plasma FFA concentrations of high-fat–induced obese rats and 2) curcuminoids ameliorate cardiac sympathovagal disturbance in obese rats and that this effect is associated with a lipid-lowering action. HRV measurement was employed to assess cardiac autonomic status.

Materials and methods

Animals

Male Wistar rats (100–120 g) from the National Animal Center, Salaya Campus, Mahidol University, Thailand, were housed in the animal facility, where the temperature was maintained at approximately 24–25 °C with 12-h dark/light cycle. The experimental protocol adhered to the Guide for the Care and Use of Animals in compliance with the National Institutes of Health guideline for the care and treatment of animals and followed Faculty of Medicine, Chiang Mai University, standard operating procedures for animal care and research.

Study protocol

Sixty rats were randomly selected and divided into five groups ($n = 12$ each). The normal-diet control (NDC) group received standard rat chow (C.P. Mice Feed Food no. 082; Bangkok, Thailand; energy content 3.8 kcal/g) containing fat for 12% of total energy. The high-fat–diet control (HDC) group consumed a high-fat diet comprised of fat for 60% of total energy with energy content calculated at 5.6 kcal/g [28] (Table 1). The curcuminoid-supplemented groups received a high-fat diet and 30, 60, or 90 mg of curcuminoids per kilogram of body weight (HF_{30}, HF_{60}, HF_{90}). Curcuminoids (Sigma Chemical, St. Louis, MO, USA) were dissolved in a 0.5% tragacanth (Fluka Chemical, Milwaukee, WI, USA) suspension, and a 2% curcuminoid solution was administered daily at different doses (30, 60, or 90 mg/kg body weight) for 12 wk by oral gavage. The NDC and HFC groups were given the same dose of vehicle (0.5% tragacanth suspension). Animals had free access to food and water. Body weight and food intake were recorded daily. Spectral analysis of HRV was performed to determine sympathetic activity before treatment with curcuminoids or vehicle and at week 12. At the end of week 12, animals were fasted overnight and anesthetized deeply. The abdominal cavity was opened following abdominal median line. Blood samples were collected from the right atrium. Samples for assay of glucose were kept on ice in tubes precoated with sodium fluoride. Samples for insulin, FFA, and triacylglycerol assays were taken in tubes with ethylenediaminetetra-acetic acid. Plasma was separated and stored at −70 °C for subsequent biochemical analyses. Visceral fats, including retroperitoneal, epididymal, and perirenal fat pad [29], were removed and weighed.

Measurement of HRV

Cardiac autonomic activity was assessed by spectral analysis of R-R interval variability. Rats were anesthetized with ether for lead insertion and then left conscious for at least 5 min before recording an electrocardiogram [30]. Lead II on the electrocardiogram was recorded continuously for 10 min by Power Lab with chart 5.0 as described previously [31]. During electrocardiographic recording, animals were calm and in a familiar environment without

Table 1
Composition of experiment diets*

	Normal diet		High-fat diet	
	g	%kcal	g	%kcal
Carbohydrate	495.30	51.99	365.00	13.96
Fat	83.70	19.76	310.00	59.16
Protein	269.00	28.23	250.00	26.88
Vitamins–minerals	65.40	0.00	70.00	0.00
Fiber	34.30	0.00	30.00	0.00

* Diet ingredients and nutrient analyses were modified from Srinivasan et al. [28]. Energy per gram (kilocalories per gram): carbohydrate 4, fat 9, and protein 4.

unnecessary noise and movement. Electrocardiographic data were analyzed using MATLAB [31]. R-R interval was determined using peaks of the QRS complex from the electrocardiogram and stored as an interval tachogram. The time domain variables measured were the standard deviation of all R-R intervals and the root mean square of successive difference. Frequency domain analysis, i.e., the power spectra of R-R interval variability, was obtained using the fast Fourier transform algorithm. High frequency (HF ~0.6–3 Hz and varying with respiration), low frequency (LF ~0.2–0.6 Hz), and very LF (≤0.2 Hz) were determined [30,32]. The LF and HF components were expressed in normalized units. Values in normalized unit for LF (LFnu) or HF (HFnu) were obtained by dividing the component by total power minus very LF. The power of the HF component provides an index of cardiac vagal activity [33], whereas the LF component is determined by sympathetic activity with vagal modulation [34]. The LF/HF ratio is considered an index of cardiac sympathetic–parasympathetic tone balance [10].

Determination of insulin resistance (homeostasis model assessment index)

Insulin resistance was assessed by homeostasis model assessment (HOMA) [35], a mathematical model describing the degree of insulin resistance starting from fasting plasma insulin and glucose concentrations. The HOMA index is calculated as follows:

$$\text{HOMA} = \frac{[\text{fasting insulin level}(\mu\text{U/mL}) \times \text{fasting glucose level}(\text{mmol/L})]}{22.5}$$

Analytical procedures

Plasma glucose concentration was determined using a colorimetric assay based on H_2O_2 using a commercially available kit (Biotech). Plasma triacylglycerol and FFA levels were assayed with commercially available kits (Biocode Hycel and Wako). Plasma insulin level was measured by sandwich enzyme-linked immunosorbent assay using a kit (LINCO Research).

Statistical analysis

Data are presented as mean ± standard error. Statistical analyses were carried out using one-way analysis of variance and Fisher's least significant difference test for post hoc testing to identify specific mean differences. Simple correlation analysis was used to determine the relation among plasma parameters and visceral and HRV measurements. Statistical significance was accepted at $P < 0.05$.

Results

Animal characteristics

Initial animal body weight was not different among experimental groups. Body weights in all animals increased significantly after 12 wk. Twelve weeks of high-fat feeding resulted in a significant increase of body weight, accompanied by accumulation of visceral fat in the HDC group compared with the NDC group (Table 2). Analysis of dietary records showed that average daily energy intake over 12 weeks in the HDC group was significantly higher than in the NDC group. These results suggest that high-fat–induced obesity characterized by an increase of body weight with substantial accumulation of visceral fat results from increased energy intake. No significant differences in body weight or visceral fat mass were found among the HDC and HD_{30}, HD_{60}, and HD_{90} groups. Average daily energy intake in the curcuminoid-supplemented groups was also comparable to that in the HDC group, although the value in the HD_{90} group was significantly lower than in the HD_{30} and HD_{60} groups.

Fasting plasma parameters

Plasma FFA levels were significantly higher in the HDC than in the NDC group (Table 3). Furthermore, plasma FFA levels significantly correlated with visceral fat mass ($r = 0.546$; Fig. 1). However, there was no correlation between visceral fat and plasma FFA acid levels after curcuminoid supplementation ($r = 0.020$). Compared with the HDC group, plasma FFA levels were significantly lower in all curcuminoid-supplemented groups. However, decreased plasma FFA levels associated with curcuminoids were not dose dependent. A trend of an increase of plasma triacylglycerol levels was found in the HDC group. A curcuminoid supplement of 90 mg/kg of body weight was associated with a decrease in plasma triacylglycerol levels. Plasma triacylglycerol level was significantly lower in the HD_{90} group than in the HDC, HD_{30}, and HD_{60} groups.

Fasting plasma glucose level was significantly elevated in the HDC group compared with the NDC group. In contrast to fasting hyperglycemia, there was no significant difference between the HDC and NDC groups in fasting plasma insulin levels. Curcuminoid supplements at all doses (30, 60, and 90 mg/kg body weight) significantly lowered fasting plasma glucose concentrations compared with the HDC group but had no effect on plasma insulin levels. No significant differences in HOMA indexes were present among the HDC, NDC, and all curcuminoid-supplemented groups.

Table 2
Effects of curcuminoid supplementation on body weight, visceral fat mass, and energy intake in high-fat–induced obese rats*

	NDC	HDC	HD_{30}	HD_{60}	HD_{90}
Body weight (g)					
Week 0	140.71 ± 8.20	140.71 ± 8.20	139.58 ± 4.94	140.00 ± 5.71	153.91 ± 5.58
Week 12	440.71 ± 10.66†	510.00 ± 18.28†	502.92 ± 17.6†	517.67 ± 16.59†	503.82 ± 10.91†
Visceral fat (g)	26.37 ± 2.11	47.30 ± 3.89‡	46.34 ± 3.52	46.52 ± 3.44	39.97 ± 2.09
Energy intake (kcal/d)	61.63 ± 1.93	102.99 ± 3.51‡	108.89 ± 3.06	107.32 ± 3.73	97.85 ± 3.10§,‖

HD_{30}, high-fat diet + curcuminoid supplementation at 30 mg/kg of body weight; HD_{60}, high-fat diet + curcuminoid supplement at 60 mg/kg of body weight; HD_{90}, high-fat diet + curcuminoid supplement at 90 mg/kg of body weight; HDC, high-fat–diet control; NDC, normal-diet control

* Each value is mean ± SE from 7–12 rats.

† Significantly different from week 0.

‡ Significantly different from NDC group.

§ Significantly different from HD_{30} group.

‖ Significantly different from HD_{60} group ($P < 0.05$).

Heart rate variability

There were no differences in initial values of HRV variables among experimental groups (Table 4). At week 12, LFnu and the LF/HF ratio were significantly higher, whereas HFnu was significantly lower, in the HDC than in the NDC group (Table 5). Compared with the HDC group, LFnu and the LF/HF ratio were significantly lower, whereas HFnu was significantly higher, in the HD_{30}, HD_{60}, and HD_{90} groups. In contrast, neither standard deviation of all R-R intervals nor root mean square of successive difference was affected by high-fat feeding alone or with curcuminoid supplementation. As presented in Table 6, LFnu and the LF/HF ratio significantly correlated with visceral fat mass ($r = 0.650$ and 0.616). Also, significant correlations were noted between plasma FFA levels and LFnu ($r = 0.589$) and the LF/HF ratio ($r = 0.580$), whereas inverse correlations were found between HFnu and visceral fat mass ($r = -0.650$) and plasma FFA levels ($r = -0.589$). However, there were no correlations between HRV with plasma triacylglycerol, plasma glucose, and plasma insulin concentrations.

There was also no correlation between HRV and visceral fat and plasma parameters in NDC rats or HD_{30}, HD_{60}, and HD_{90} rats.

Discussion

The major findings of this study are as follows: 1) an increase of plasma FFA level causes cardiac autonomic disturbance in obesity induced by chronic high-fat feeding, and 2) curcuminoid supplementation effectively decreases plasma FFA levels and improves cardiac autonomic nervous system activity in obesity.

Effects of plasma FFA levels on plasma glucose and insulin in obese rats

The study demonstrates that a high-fat diet causes ventral obesity, as indicated by a significant increase of body weight with substantial accumulation of visceral fat. There is also a significant correlation between visceral fat mass and plasma FFA levels. It has been well recognized that visceral adipose tissue is less responsive to antilipolytic action of insulin but more responsive to lipolytic action of catecholamines compared with subcutaneous adipose tissue [36]. Thus, a significant increase in plasma FFA levels in high-fat–induced obese rats could be due to increased visceral adipocytes with a secondary exaggeration in lipolytic activity. This is consistent with a report showing that an elevated plasma FFA level is common in obese patients with hyperlipidemia [4].

Table 3
Effects of curcuminoid supplementation on fasting plasma parameters and HOMA index in high-fat–induced obese rats*

	NDC	HDC	HD_{30}	HD_{60}	HD_{90}
FFA (mmol/L)	0.38 ± 0.05	0.51 ± 0.04†	0.38 ± 0.03‡	0.36 ± 0.03‡	0.32 ± 0.01‡
TG (mg/dL)	85.14 ± 20.31	110.27 ± 17.37	109.51 ± 8.97	93.76 ± 9.29	56.10 ± 4.42‡,§,‖
Glucose (mg/dL)	132.01 ± 4.62	153.54 ± 4.81†	132.04 ± 5.60‡	134.69 ± 7.12‡	136.18 ± 4.08‡
Insulin (ng/mL)	1.24 ± 0.13	1.35 ± 0.11	1.56 ± 0.61	1.51 ± 0.21	1.40 ± 0.25
HOMA index	11.13 ± 1.35	13.67 ± 1.57	14.41 ± 2.34	14.23 ± 1.67	11.97 ± 2.23

FFA, free fatty acid; HD_{30}, high-fat diet + curcuminoid supplementation at 30 mg/kg of body weight; HD_{60}, high-fat diet + curcuminoid supplement at 60 mg/kg of body weight; HD_{90}, high-fat diet + curcuminoid supplement at 90 mg/kg of body weight; HDC, high-fat–diet control; HOMA, homeostasis model assessment; NDC, normal-diet control; TG, triacylglycerol

* Each value is mean ± SE from 7–12 rats.

† Significantly different from NDC group.

‡ Significantly different from HDC group.

§ Significantly different from HD_{30} group.

‖ Significantly different from HD_{60} group ($P < 0.05$).

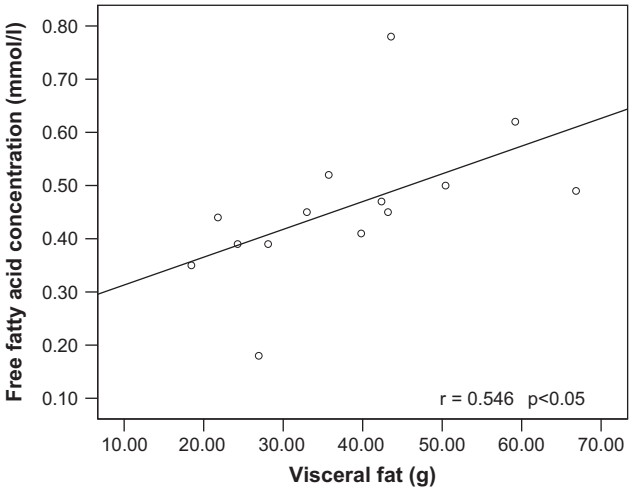

Fig. 1. Correlation between visceral fat and plasma free-fatty acid concentrations in rats receiving a normal diet or a high-fat diet for 12 wk.

In addition, fasting hyperglycemia was noted in high-fat–induced obese rats. An elevated level of plasma FFAs, particularly in obesity, has been shown to play an important role in the overproduction of glucose in the diabetic state [37]. Also, in type 2 diabetic patients, fasting hyperglycemia is caused by an inappropriate increase in hepatic glucose production [38,39], It is most likely that an increase of portal FFAs leads to increased hepatic glucose output [3]. FFAs can also potentially influence hepatic glucose metabolism by several other metabolisms. FFAs have been shown to stimulate gluconeogenesis [40,41] and upregulate the glucose-6-phosphate system. Furthermore, most studies have reported that elevated plasma FFAs impair insulin-induced suppression of endogenous glucose production (i.e., cause hepatic insulin resistance) in normal control subjects or in patients with NIDDM [42,43]. This effect is due to an inhibition of normal insulin suppression of glycogenolysis by FFAs [42]. Moreover, the effect of FFAs in inhibition of insulin-stimulated glucose uptake in skeletal muscle [44,45] should be considered. This effect of FFAs is by the insulin-signaling cascade [46], resulting in inhibition of glucose transporter-4 (GLUT-4) translocation [47] and decreased muscle glycogen synthase activity [48].

Several studies have demonstrated that an increase in hepatic glucose production stimulated by acute elevated plasma FFA levels is antagonized by an FFA-mediated stimulation of insulin secretion [49,50]. Despite elevated plasma FFAs, our study demonstrated no change in fasting plasma insulin levels in high-fat–induced obese rats compared with normal-diet rats, suggesting that its effect on insulin response might be different from the effect caused by acute elevated plasma FFA levels. In this study, elevated plasma FFA levels in high-fat–induced obese rats occurred over months. It has been shown that obese individuals who are genetically predisposed to develop NIDDM may eventually lose their ability to increase insulin secretion in response to chronically elevated plasma FFA levels.

Roles of plasma FFA levels on HRV modulation

Heart rate variability analysis in the present study demonstrated that, in high-fat–induced obese rats, significant increases of LF and the LF/HF ratio were accompanied by significant HF decreases. It is generally considered that the HF component is a marker of the efferent vagal activity to the heart [51]. The interpretation of the LF component is more controversial. Although it was previously proposed as a marker of sympathetic modulation [52] other investigators have suggested that LF represents sympathetic and parasympathetic influences [53]. However, LF in absolute value seems to reflect baroreflex modulation, which is mainly of parasympathetic origin [54], whereas the LF/HF ratio and LFnu are markers of sympathovagal balance [10]. Our findings demonstrated that the impaired cardiac autonomic activity in high-fat–induced obese rats is associated with a reduced vagal contribution and an increased sympathetic contribution to cardiac autonomic control.

A correlation between HRV and visceral fat mass was also observed in this study. LF and the LF/HF ratio significantly correlated with visceral fat mass, whereas HF had a negative correlation with visceral fat mass. These findings indicate the links between central obesity and cardiac autonomic disturbance. An association between

Table 4
Heart rate variability at baseline*

	NDC	HDC	HD_{30}	HD_{60}	HD_{90}
SDNN	2.59 ± 0.42	2.77 ± 0.67	2.89 ± 0.65	2.03 ± 0.43	3.77 ± 0.39
RMSSD	1.82 ± 0.27	2.85 ± 0.89	2.95 ± 1.10	2.60 ± 0.46	2.98 ± 0.48
LFnu	0.16 ± 0.00	0.16 ± 0.01	0.18 ± 0.02	0.15 ± 0.01	0.17 ± 0.01
HFnu	0.84 ± 0.00	0.84 ± 0.01	0.82 ± 0.02	0.85 ± 0.01	0.83 ± 0.01
LF/HF ratio	0.19 ± 0.01	0.20 ± 0.01	0.21 ± 0.03	0.17 ± 0.01	0.20 ± 0.01

HD_{30}, high-fat diet + curcuminoid supplementation at 30 mg/kg of body weight; HD_{60}, high-fat diet + curcuminoid supplement at 60 mg/kg of body weight; HD_{90}, high-fat diet + curcuminoid supplement at 90 mg/kg of body weight; HDC, high-fat–diet control; HFnu, high-frequency power in normalized units; LFnu, low-frequency power in normalized units; NDC, normal-diet control; RMSSD, square root of the mean of the sum of the squares of differences between adjacent R-R intervals; SDNN, standard deviation of all R-R intervals

* Each value is mean ± SE from 7–12 rats.

Table 5
Effect of curcuminoid supplementation on heart rate variability indexes in high-fat–induced obese rats*

	NDC	HDC	HD_{30}	HD_{60}	HD_{90}
SDNN	3.41 ± 0.49	3.91 ± 0.36	4.23 ± 0.62	3.87 ± 0.57	4.11 ± 0.36
RMSSD	2.42 ± 0.25	3.42 ± 0.61	4.11 ± 0.64	3.77 ± 0.82	3.82 ± 0.36
LFnu	0.17 ± 0.01	0.28 ± 0.01†	0.19 ± 0.01‡	0.17 ± 0.01‡	0.18 ± 0.01‡
HFnu	0.83 ± 0.01	0.72 ± 0.01†	0.81 ± 0.01‡	0.83 ± 0.01‡	0.82 ± 0.01‡
LF/HF ratio	0.20 ± 0.01	0.40 ± 0.03†	0.24 ± 0.01‡	0.20 ± 0.01‡	0.21 ± 0.01‡

HD_{30}, high-fat diet + curcuminoid supplementation at 30 mg/kg of body weight; HD_{60}, high-fat diet + curcuminoid supplement at 60 mg/kg of body weight; HD_{90}, high-fat diet + curcuminoid supplement at 90 mg/kg of body weight; HDC, high-fat–diet control; HFnu, high-frequency power in normalized units; LFnu, low-frequency power in normalized units; NDC, normal-diet control; RMSSD, square root of the mean of the sum of the squares of differences between adjacent R-R intervals; SDNN, standard deviation of all R-R intervals

* Each value is mean ± SE from 7–12 rats.

† Significantly different from NDC group.

‡ Significantly different from HDC group ($P < 0.05$).

visceral obesity and impaired cardiac autonomic activity has been previously reported, but findings were inconsistent. A previous HRV study showed that, in postmenopausal obese women, impaired cardiac autonomic activity varied depending on regional body fat distribution [55]. A significant increase of cardiac sympathetic and parasympathetic activity was pronounced in women with combined upper body obesity and visceral obesity. Conversely, Peterson et al. [56] reported depression of sympathetic and parasympathetic activity in healthy men with an increasing percentage of body fat. Significant inverse correlations were found between the percentage of body fat and variation in R-R interval after β-adrenergic blockade, heart rate, and plasma catecholamine concentrations. These inconsistent results were probably due to differences in the subjects and methods used in those studies. However, a report by Zahorska-Markiewicz et al. [57] using 24-h continuous electrocardiographic and Ewing testing in obese women demonstrated that cardiac autonomic disturbance with high-fat–induced obesity is characterized by overactivity of the cardiac sympathetic nervous system with a relative reduction of parasympathetic nervous system activity. These findings are consistent with the results of our study.

Table 6
Correlation between HRV and visceral fat and plasma parameters in rats that consumed normal diets or high-fat diets for 12 wk

	HRV		
	LFnu	HFnu	LF/HF ratio
Visceral fat (g)	0.650†	−0.650†	0.616*
Plasma free fatty acid (mmol/L)	0.589*	−0.589*	0.580*
Plasma triacylglycerol (mg/dL)	−0.168	0.168	−0.173
Plasma glucose (mg/dL)	0.423	−0.423	0.389
Plasma insulin (ng/mL)	−0.423	0.423	−0.442

HFnu, high-frequency power in normalized units; HRV, heart rate variability; LFnu, low-frequency power in normalized units

* $P < 0.05$

† $P < 0.01$.

Effects of curcumioids on plasma FFA, glucose, and insulin

Curcuminoids, the phenolic yellowish pigment of turmeric, are known to benefit human health [16]. The present results demonstrate that the increased plasma FFA levels that developed in high-fat–induced obese rats were significantly countered by administration of curcuminoids. Although the exact mechanism by which curcuminoids decrease lipid levels was not investigated, it has been previously shown that curcumin, the active component of curcuminoids, modulates several important molecular targets, including transcription factors such as peroxisome proliferator-activated receptor-γ (PPAR-γ) [58]. PPARs are known to regulate the gene involved in fatty acid uptake and storage and in inflammatory and glucose homeostasis [59]. Curcumin has been reported to activate PPAR-γ in rat hepatic stellate cells activated by oxidative stress [60], to exhibit PPAR-γ ligand-binding activity in the GAL4-PPAR-γ chimera assay, and to accelerate triacylglycerol accumulation in adipocytes [21]. Curcumin has been shown to dramatically induce expression of the PPAR-γ gene and activate PPAR-γ–inactivated hepatic stellate cells [60]. Therefore, an activation of PPAR-γ could be responsible for a decrease of plasma FFA levels after curcuminoid supplementation in high-fat–fed rats in this study.

The present study also shows that curcuminoid supplementation suppressed an increase in fasting blood glucose in high-fat–induced obese rats. This antihyperglycemic effect of curcuminoids could be an indirect action resulting from a decreased influx of plasma FFAs into the liver, thus lowering hepatic glucose production. However, a previous study using alloxan-induced diabetic rats demonstrated that curcuminoids were effective in controlling blood glucose level and enzymes of glucose metabolism [61]. A study using genetically altered type 2 diabetic mice also indicated that one mechanism responsible for the antihyperglycemic effect of curcuminoids was mediated by PPAR-γ activation. In addition to its effect on lipid metabolism, activation of PPAR-γ has been reported to increase the expression and translocation of the glucose transporters GLUT-1 and -4, thus increasing

glucose uptake into liver and skeletal muscle cells and decreasing plasma glucose levels [62].

Effects of curcuminoids on cardiac autonomic nervous system activity

The novel findings in the present study were that curcuminoid supplementation improved cardiac autonomic disturbance in high-fat–induced obese rats. Although the mechanism responsible for cardiac autonomic activity disturbance in high-fat–induced obesity remains unresolved, the results of a significant correlation between plasma FFA levels and HRV could indicate a strong link between FFAs and cardiac autonomic activity. Elevated plasma FFA levels have been associated with an increase of the ventricular premature complex in non-diabetic [63] and non-ischemic diabetic patients [64]. Also, elevated plasma FFA levels have been reported to stimulate cardiac sympathetic activity in healthy subjects [14] and in NIDDM patients [31]. Paolisso et al. [14] suggested that such a stimulatory effect of FFAs on cardiac sympathetic activity was indirect and mediated in part through an increase in plasma catecholamine concentrations, which in turn stimulated myocardial β_1-receptors. The present results of a negative correlation between plasma FFA levels and the HF component are in agreement with findings demonstrating that elevated plasma FFA levels suppress myocardial vagal tone [15]. It has been suggested that a decrease of parasympathetic counteraction to sympathetic activation results in a shift toward sympathetic dominance [65]. At the cellular level, Shaltout and Abdel-Rahman [15] showed that elevated plasma FFA levels increase caveola sequestration of cardiac muscarinic cholinergic receptors (M_2-mAChR), which result in muscarinic cholinergic receptor inactivation and attenuation of parasympathetic control on the heart. Based on these findings, the effects of curcuminoids were in part related to a decrease of plasma FFA levels, which in turn led to an improved cardiac autonomic disturbance in high-fat–induced obese rats.

A growing body of evidence has demonstrated that curcuminoids are a potent antioxidant [16,23,24,66]. Increased plasma FFA concentrations have been shown to be a pro-oxidant factor [63]. Manzella et al. [67] demonstrated that increased postprandial plasma FFA concentration is associated with an enhanced degree of oxidative stress and of the LF/HF ratio, an index of cardiac sympathovagal balance. It has also been reported that an impaired cardiac autonomic nervous system activity in type 2 diabetes is linked to elevated oxidative stress. This suggests that changes in cardiac sympathovagal balance correlate with the degree of oxidative stress [67]. Although oxidative stress was not determined in the present study, the additional antioxidant effect of curcuminoids cannot be excluded as a potential mechanism to improve cardiac autonomic nervous system activity in the present study. Future studies are needed to determine whether the effects of curcuminoids on cardiac autonomic activity are direct or indirect.

Study limitations

This study demonstrated that curcuminoid supplementation improved cardiac autonomic disturbance in high-fat–induced obese rats and this was associated with decreased plasma FFA levels. One limitation of this study is that the definite cellular mechanism of curcuminoids lowering plasma FFAs was not investigated. Studies at the cellular level are the next step necessary to provide direct evidence to elucidate the mechanism by which curcuminoids decrease plasma FFAs and its clinical significance. Also, serum epinephrine or norepinephrine was not measured in this study. However, previous studies have indicated that plasma catecholamines are an indirect and rather insensitive index of sympathetic activity because most of the norepinephrine secreted from the sympathetic fibers is destroyed or taken up again, and only a minute fraction escapes from the neuroeffector junctions [68–70]. Moreover, previous human studies examining adrenergic activity in obesity by whole-body methods (i.e., urinary excretion or plasma levels/turnover of catecholamines) have demonstrated inconclusive results, with reports of normal, decreased, or increased sympathetic activity [56,71–75], suggesting that serum catecholamines may not be a reliable indicator for sympathetic activity.

Conclusion

The present study demonstrated that cardiac autonomic disturbance in obesity induced by high-fat feeding is associated with elevated plasma FFA levels. Long-term curcuminoid supplementation decreases plasma FFA levels, thus ameliorating cardiac autonomic disturbance in high-fat–induced obesity. Because elevated plasma FFA levels are an important variable affecting cardiac mortality risk, further studies are needed to clarify the nutritional and therapeutic benefits of curcuminoids.

Acknowledgments

The authors thank Ms.Wassana Pratchayasakul for her technical assistance and Dr. Tanat Incharoen for his assistance in HRV analysis.

References

[1] Messerli FH, Nunez BD, Ventura HO, Snyder DW. Overweight and sudden death. Increased ventricular ectopy in cardiopathy of obesity. Arch Intern Med 1987;147:1725–8.

[2] Dustan HP. Obesity and hypertension. Diabetes Care 1991; 14:488–504.

[3] Modan M, Halkin H. Hyperinsulinemia or increased sympathetic drive as links for obesity and hypertension. Diabetes Care 1991;14:470–87.

[4] DeFronzo RA, Ferrannini E. Insulin resistance. A multifaceted syndrome responsible for NIDDM, obesity, hypertension, dyslipidemia, and atherosclerotic cardiovascular disease. Diabetes Care 1991; 14:173–94.

[5] Paolisso G, Gualdiero P, Manzella D, Rizzo MR, Tagliamonte MR, Gambardella A, et al. Association of fasting plasma free fatty acid concentration and frequency of ventricular premature complexes in nonischemic non–insulin-dependent diabetic patients. Am J Cardiol 1997; 80:932–7.
[6] Laederach-Hofmann K, Mussgay L, Ruddel H. Autonomic cardiovascular regulation in obesity. J Endocrinol 2000;164:59–66.
[7] Matsumoto T, Miyawaki C, Ue H, Kanda T, Yoshitake Y, Moritani T. Comparison of thermogenic sympathetic response to food intake between obese and non-obese young women. Obes Res 2001;9:78–85.
[8] Grekin RJ, Vollmer AP, Sider RS. Pressor effects of portal venous oleate infusion. A proposed mechanism for obesity hypertension. Hypertension 1995;26:193–8.
[9] Verwaerde P, Senard JM, Galinier M, Rouge P, Massabuau P, Galitzky J, et al. Changes in short-term variability of blood pressure and heart rate during the development of obesity-associated hypertension in high-fat fed dogs. J Hypertens 1999;17:1135–43.
[10] Chattipakorn N, Incharoen T, Kanlop N, Chattipakorn S. Heart rate variability in myocardial infarction and heart failure. Int J Cardiol 2007; 120:289–96.
[11] Tsuji H, Venditti FJ Jr, Manders ES, Evans JC, Larson MG, Feldman CL, et al. Determinants of heart rate variability. J Am Coll Cardiol 1996;28:1539–46.
[12] Kleiger RE, Miller JP, Bigger JT Jr, Moss AJ. Decreased heart rate variability and its association with increased mortality after acute myocardial infarction. Am J Cardiol 1987;59:256–62.
[13] Tsuji H, Venditti FJ Jr, Manders ES, Evans JC, Larson MG, Feldman CL, et al. Reduced heart rate variability and mortality risk in an elderly cohort. The Framingham Heart Study. Circulation 1994; 90:878–83.
[14] Paolisso G, Manzella D, Rizzo MR, Ragno E, Barbieri M, Varricchio G, et al. Elevated plasma fatty acid concentrations stimulate the cardiac autonomic nervous system in healthy subjects. Am J Clin Nutr 2000;72:723–30.
[15] Shaltout HA, Abdel-Rahman AA. Mechanism of fatty acids induced suppression of cardiovascular reflexes in rats. J Pharmacol Exp Ther 2005;314:1328–37.
[16] Ammon HP, Wahl MA. Pharmacology of Curcuma longa. Planta Med 1991;57:1–7.
[17] Fu Y, Zheng S, Lin J, Ryerse J, Chen A. Curcumin protects the rat liver from CCl4-caused injury and fibrogenesis by attenuating oxidative stress and suppressing inflammation. Mol Pharmacol 2008; 73:399–409.
[18] Jacob A, Wu R, Zhou M, Wang P. Mechanism of the anti-inflammatory effect of curcumin: PPAR-gamma activation. PPAR Res 2007; 2007:89369.
[19] Manjunatha H, Srinivasan K. Hypolipidemic and antioxidant effects of curcumin and capsaicin in high-fat–fed rats. Can J Physiol Pharmacol 2007;85:588–96.
[20] Menon VP, Sudheer AR. Antioxidant and anti-inflammatory properties of curcumin. Adv Exp Med Biol 2007;595:105–25.
[21] Nishiyama T, Mae T, Kishida H, Tsukagawa M, Mimaki Y, Kuroda M, et al. Curcuminoids and sesquiterpenoids in turmeric (Curcuma longa L.) suppress an increase in blood glucose level in type 2 diabetic KK-Ay mice. J Agric Food Chem 2005;53:959–63.
[22] Reyes-Gordillo K, Segovia J, Shibayama M, Vergara P, Moreno MG, Muriel P. Curcumin protects against acute liver damage in the rat by inhibiting NF-kappaB, proinflammatory cytokines production and oxidative stress. Biochim Biophys Acta 2007;1770:989–96.
[23] Chiu J, Khan ZA, Farhangkhoee H, Chakrabarti K. Curcumin prevents diabetes-associated abnormalities in the kidney by inhibiting p300 and nuclear kappa B. Nutrition 2009; in press.
[24] Memis D, Hekimoglu S, Sezer A, Altaner S, Sut N, Usta U. Curcumin attenuates the organ dysfunction caused by endotoxemia in the rat. Nutrition 2008;24:1133–8.
[25] Patil TN, Srinivasan M. Hypocholesteremic effect of curcumin in induced hypercholesteremic rats. Indian J Exp Biol 1971;9:167–9.
[26] Rao DS, Sekhara NC, Satyanarayana MN, Srinivasan M. Effect of curcumin on serum and liver cholesterol levels in the rat. J Nutr 1970; 100:1307–15.
[27] Asai A, Miyazawa T. Dietary curcuminoids prevent high-fat diet–induced lipid accumulation in rat liver and epididymal adipose tissue. J Nutr 2001;131:2932–5.
[28] Srinivasan K, Viswanad B, Asrat L, Kaul CL, Ramarao P. Combination of high-fat diet–fed and low-dose streptozotocin–treated rat: a model for type 2 diabetes and pharmacological screening. Pharmacol Res 2005;52:313–20.
[29] Borst SE, Conover CF. High-fat diet induces increased tissue expression of TNF-alpha. Life Sci 2005;77:2156–65.
[30] Incharoen T, Thephinlap C, Srichairatanakool S, Chattipakorn S, Winichagoon P, Fucharoen S, et al. Heart rate variability in beta-thalassemic mice. Int J Cardiol 2007;121:203–4.
[31] Manzella D, Barbieri M, Rizzo MR, Ragno E, Passariello N, Gambardella A, et al. Role of free fatty acids on cardiac autonomic nervous system in noninsulin-dependent diabetic patients: effects of metabolic control. J Clin Endocrinol Metab 2001;86:2769–74.
[32] Langager AM, Hammerberg BE, Rotella DL, Stauss HM. Very low-frequency blood pressure variability depends on voltage-gated L-type Ca2+ channels in conscious rats. Am J Physiol Heart Circ Physiol 2007;292:H1321–7.
[33] Malik M, Camm AJ. Components of heart rate variability—what they really mean and what we really measure. Am J Cardiol 1993;72:821–2.
[34] Akselrod S, Gordon D, Ubel FA, Shannon DC, Berger AC, Cohen RJ. Power spectrum analysis of heart rate fluctuation: a quantitative probe of beat-to-beat cardiovascular control. Science 1981;213(4504):220–2.
[35] Matthews DR, Hosker JP, Rudenski AS, Naylor BA, Treacher DF, Turner RC. Homeostasis model assessment: insulin resistance and beta-cell function from fasting plasma glucose and insulin concentrations in man. Diabetologia 1985;28:412–9.
[36] Jensen MD, Haymond MW, Rizza RA, Cryer PE, Miles JM. Influence of body fat distribution on free fatty acid metabolism in obesity. J Clin Invest 1989;83:1168–73.
[37] Bergman RN, Ader M. Free fatty acids and pathogenesis of type 2 diabetes mellitus. Trends Endocrinol Metab 2000;11:351–6.
[38] Massillon D, Barzilai N, Hawkins M, Prus-Wertheimer D, Rossetti L. Induction of hepatic glucose-6-phosphatase gene expression by lipid infusion. Diabetes 1997;46:153–7.
[39] Roden M, Ludwig C, Nowotny P, Schneider B, Clodi M, Vierhapper H, et al. Relative hypoleptinemia in patients with type 1 and type 2 diabetes mellitus. Int J Obes Relat Metab Disord 2000;24:976–81.
[40] Chen X, Iqbal N, Boden G. The effects of free fatty acids on gluconeogenesis and glycogenolysis in normal subjects. J Clin Invest 1999; 103:365–72.
[41] Fanelli C, Calderone S, Epifano L, De Vincenzo A, Modarelli F, Pampanelli S, et al. Demonstration of a critical role for free fatty acids in mediating counterregulatory stimulation of gluconeogenesis and suppression of glucose utilization in humans. J Clin Invest 1993;92:1617–22.
[42] Boden G. Effects of free fatty acids on gluconeogenesis and glycogenolysis. Life Sci 2003;72:977–88.
[43] Rigalleau V, Binnert C, Minehira K, Stefanoni N, Schneiter P, Henchoz E, et al. In normal men, free fatty acids reduce peripheral but not splanchnic glucose uptake. Diabetes 2001;50:727–32.
[44] Boden G, Chen X, Ruiz J, White JV, Rossetti L. Mechanisms of fatty acid–induced inhibition of glucose uptake. J Clin Invest 1994; 93:2438–46.
[45] Roden M, Price TB, Perseghin G, Petersen KF, Rothman DL, Cline GW, et al. Mechanism of free fatty acid–induced insulin resistance in humans. J Clin Invest 1996;97:2859–65.
[46] Schmitz-Peiffer C, Browne CL, Oakes ND, Watkinson A, Chisholm DJ, Kraegen EW, et al. Alterations in the expression and cellular localization of protein kinase C isozymes epsilon and theta are

associated with insulin resistance in skeletal muscle of the high-fat–fed rat. Diabetes 1997;46:169–78.
[47] Shulman GI. Cellular mechanisms of insulin resistance. J Clin Invest 2000;106:171–6.
[48] Boden G. Role of fatty acids in the pathogenesis of insulin resistance and NIDDM. Diabetes 1997;46:3–10.
[49] Crespin SR, Greenough WB III, Steinberg D. Stimulation of insulin secretion by long-chain free fatty acids. A direct pancreatic effect. J Clin Invest 1973;52:1979–84.
[50] Goberna R, Tamarit J Jr, Osorio J, Fussganger R, Tamarit J, Pfeiffer EF. Action of B-hydroxy butyrate, acetoacetate and palmitate on the insulin release in the perfused isolated rat pancreas. Horm Metab Res 1974; 6:256–60.
[51] Malik M, Camm AJ. Components of heart rate variability—what they really mean and what we really measure. Am J Cardiol 1993;72:821–2.
[52] Pagani M, Lombardi F, Guzzetti S, Rimoldi O, Furlan R, Pizzinelli P, et al. Power spectral analysis of heart rate and arterial pressure variabilities as a marker of sympatho-vagal interaction in man and conscious dog. Circ Res 1986;59:178–93.
[53] Malliani A, Pagani M, Lombardi F, Cerutti S. Cardiovascular neural regulation explored in the frequency domain. Circulation 1991; 84:482–92.
[54] Grasso R, Schena F, Gulli G, Cevese A. Does low-frequency variability of heart period reflect a specific parasympathetic mechanism? J Auton Nerv Syst 1997;63:30–8.
[55] Gao YY, Lovejoy JC, Sparti A, Bray GA, Keys LK, Partington C. Autonomic activity assessed by heart rate spectral analysis varies with fat distribution in obese women. Obes Res 1996;4:55–63.
[56] Peterson HR, Rothschild M, Weinberg CR, Fell RD, McLeish KR, Pfeifer MA. Body fat and the activity of the autonomic nervous system. N Engl J Med 1988;318:1077–83.
[57] Zahorska-Markiewicz B, Kuagowska E, Kucio C, Klin M. Heart rate variability in obesity. Int J Obes Relat Metab Disord 1993;17:21–3.
[58] Shishodia S, Sethi G, Aggarwal BB. Curcumin: getting back to the roots. Ann N Y Acad Sci 2005;1056:206–17.
[59] Kersten S, Desvergne B, Wahli W. Roles of PPARs in health and disease. Nature 2000;405(6785):421–4.
[60] Xu J, Fu Y, Chen A. Activation of peroxisome proliferator-activated receptor-gamma contributes to the inhibitory effects of curcumin on rat hepatic stellate cell growth. Am J Physiol Gastrointest Liver Physiol 2003;285:G20–30.
[61] Arun N, Nalini N. Efficacy of turmeric on blood sugar and polyol pathway in diabetic albino rats. Plant Foods Hum Nutr 2002;57:41–52.
[62] Kramer D, Shapiro R, Adler A, Bush E, Rondinone CM. Insulin-sensitizing effect of rosiglitazone (BRL-49653) by regulation of glucose transporters in muscle and fat of Zucker rats. Metabolism 2001; 50:1294–300.
[63] Paolisso G, Gualdiero P, Manzella D, Gambardella A, Verza M, Gentile S, et al. Hyperinsulinemia is associated with ventricular premature complexes. Metabolism 1996;45:1248–53.
[64] Boden G, Chen X. Effects of fat on glucose uptake and utilization in patients with non-insulin–dependent diabetes. J Clin Invest 1995;96:1261–8.
[65] Sgoifo A, Koolhaas JM, Musso E, De Boer SF. Different sympathovagal modulation of heart rate during social and nonsocial stress episodes in wild-type rats. Physiol Behav 1999;67:733–8.
[66] Maheshwari RK, Singh AK, Gaddipati J, Srimal RC. Multiple biological activities of curcumin: a short review. Life Sci 2006;78:2081–7.
[67] Manzella D, Grella R, Marfella R, Giugliano D, Paolisso G. Elevated post-prandial free fatty acids are associated with cardiac sympathetic overactivity in Type II diabetic patients. Diabetologia 2002;45:1737–8.
[68] Reisin E, Frohlich ED, Messerli FH, Dreslinski GR, Dunn FG, Jones MM, et al. Cardiovascular changes after weight reduction in obesity hypertension. Ann Intern Med 1983;98:315–9.
[69] Sowers JR, Whitfield LA, Catania RA, Stern N, Tuck ML, Dornfeld L, et al. Role of the sympathetic nervous system in blood pressure maintenance in obesity. J Clin Endocrinol Metab 1982;54:1181–6.
[70] Young JB, Macdonald IA. Sympathoadrenal activity in human obesity: heterogeneity of findings since 1980. Int J Obes Relat Metab Disord 1992;16:959–67.
[71] DeHaven J, Sherwin R, Hendler R, Felig P. Nitrogen and sodium balance and sympathetic-nervous-system activity in obese subjects treated with a low-calorie protein or mixed diet. N Engl J Med 1980;302:477–82.
[72] Jung RT, Shetty PS, James WP, Barrand MA, Callingham BA. Reduced thermogenesis in obesity. Nature 1979;279(5711):322–3.
[73] Landsberg L, Krieger DR. Obesity, metabolism, and the sympathetic nervous system. Am J Hypertens 1989;2(3 pt 2): 125S–32.
[74] Levin BE, Triscari J, Sullivan AC. Defective catecholamine metabolism in peripheral organs of genetically obese Zucker rats. Brain Res 1981;224:353–66.
[75] Young JB, Saville E, Rothwell NJ, Stock MJ, Landsberg L. Effect of diet and cold exposure on norepinephrine turnover in brown adipose tissue of the rat. J Clin Invest 1982;69:1061–71.

CURRENT TOPICS IN NUTRACEUTICAL RESEARCH Vol. 7, No. 1, pp.11-26, 2009
ISSN 1540-7535 print , Copyright © 2009 by New Century Health Publishers, LLC
www.newcenturyhealthpublishers.com

ROLES OF CURCUMIN IN PREVENTING PATHOGENESIS OF ALZHEIMER'S DISEASE

[1,2]Wasana Pratchayasakul, [2]Makhawadee Pongruangporn, [1,2]Nipon Chattipakorn and [2,3]Siriporn Chattipakorn

[1]Department of Physiology and [2]Cardiac Electrophysiology Research and Training Center, Faculty of Medicine; [3]Department of Odontology and Oral Pathology, Faculty of Dentistry, Chiang Mai University, Chiang Mai, Thailand

[Received January 14, 2009; Accepted March 17, 2009]

ABSTRACT: *Curcumin is a yellow-orange powder derived from the rhizome of Curcuma longa Linn. In traditional medicine, curcumin has been used to treat several diseases. Much evidence has shown curcumin's anti-ulcer, anti-cancer, anti-hepatotoxic, anti-viral, accelerated wound healing, cardioprotective, hypoglycemic and anti-inflammatory properties. Recently, several in vitro and in vivo studies have shown that curcumin has various properties which help prevent the pathogenesis of Alzheimer's disease (AD). These effects include anti-amyloid, anti-inflammation, antioxidant, anti-apoptotic and cholesterol lowering properties. These findings suggest the possible benefits of curcumin in AD therapy. In this review, the pathogenesis of, as well as current therapeutic strategies for, AD are presented, and evidence of the role of curcumin in preventing the pathogenetic cascades which underlie AD are discussed.*

KEYWORDS: Alzheimer's disease, Anti-amyloid, Anti-apoptotic, Anti-inflammation, Antioxidant, Cholesterol lowering, Curcumin

Corresponding author: Siriporn Chattipakorn, DDS, PhD, Department of Odontology and Oral Pathology, Faculty of Dentistry, Chiang Mai University, Chiang Mai, 50200, Thailand; Fax: 011-66-53-222-844; Email: s.chat@chiangmai.ac.th

1. ALZHEIMER'S DISEASE

Alzheimer's disease (AD), the most common form of dementia in the elderly, is a progressive neurological disease resulting in irreversible neuronal loss, particularly in the brain regions of the cortex and hippocampus. The clinical hallmarks of AD are progressive impairment in memory, judgment, decision making, orientation to surroundings and language (Brion, 1996). Diagnosis of AD is based on clinical neurological examination. A definite diagnosis can be made only by autopsy, in which the pathological hallmarks of AD are neuronal loss, extracellular senile plaques containing the peptide amyloid-β (Aβ), and neurofibrillary tangles, a hyperphosphorylated form of the microtubular proteins named tau in neurons (Brion, 1996).

Clinical diagnosis of AD is based on criteria developed by the National Institute of Neurologic and Communicative Disorder and Stroke Alzheimer's Disease and Related Disorders Association (NINCDS-ADRDA). Clinical AD can be divided into definite AD with a clinical diagnosis with histological confirmation, probable AD with the typical clinical syndrome without histological confirmation, and possible AD with atypical clinical features but no alternative diagnostic appearance and no histological confirmation. The typical symptoms of AD are memory impairment, deterioration of language, and visuospatial deficits. Motor and sensory abnormalities, gait disturbances and seizures are uncommon symptoms, but they can be seen in the late phases of AD (McKhann et al., 1984).

The prevalence of AD in the United State (US) is approximately 1% among people 65 to 69 years old and this prevalence increases to 40-45% among people aged 95 years and over (Hy and Keller, 2000). In 2000, there were 4.5 million people with AD in the US (Hebert et al., 2003). The number of patients with AD in the US is expected to increase almost threefold, to approximately 13.2 million people, by the year 2050 because of the rapid growth of the older population and the longer lifespan of people (Hebert et al., 2003). The AD population will continue to rise unless new methods of AD prevention are discovered. Since the costs of caring for patients with AD are very high, searches for effective therapeutic interventions are necessary. Fillit and colleagues have shown that effective therapies in the early stages of AD can delay the progression of dementia and may offer economic benefits to patients' families, caregivers and society (Fillit and Hill, 2005).

The most common risk factors for AD are aging and a family history of dementia (Thomas and Bruce, 2005). A family history of dementia suggests that genetics is one factor in the pathogenesis of AD. It has been proposed that AD is associated with gender, level of education and numerous environmental factors (Flirski and Sobow, 2005; Thomas and Bruce, 2005). Moreover, some studies suggest that inflammation may have a significant role in the pathogenesis of AD (Flirski and Sobow, 2005; Brion, 1996; in't Veld et al., 2001). It has been shown that the use of non-steroid anti-inflammatory drugs (NSAIDs) is correlated with a decrease in the prevalence of AD symptoms (Giovannini et al., 2003).

Two possible aspects of the pathogenesis of AD are the genetic aspect and neurotransmitter abnormality in the brain (Bird, 2005; Martin, 1999). Several studies have shown that mutations in at least four genes could be involved in the pathogenesis of AD (Bird, 2005; Dufouil et al., 2005; Lendon et al., 1997). Those four genes are the presenilin 1 gene (PS-1), the presenilin 2 gene (PS-2), Amyloid-β protein precursor (APP) and Apolipoprotein ε4 (APOE). Mutations in PS-1 on chromosome 14, PS-2 on chromosome 1, and APP on chromosome 21 have been shown to be involved in the pathogenesis of most cases of familial early onset of AD (Bird, 2005). The genetics of late-onset AD (LOAD) are more mysterious and the only confirmed risk factor for LOAD remains APOE on chromosome 19 (Bird, 2005; Lendon et al., 1997). The APOE gene is involved in cholesterol transport and has three alleles: ε2, ε3 and ε4. The ε4 allele of APOE shows a strong association with AD in the general population, including sporadic and late-onset familial cases of AD (Strittmatter et al., 1993). Approximately 40% of patients with AD have at least one ε4 allele in plasma whereas this allele appears in about 12% of people without AD (Reiss, 2005; Frisoni et al., 1998). Patients diagnosed with clinical AD have significantly higher expression of the ε4 allele in plasma than control (Kuusisto et al., 1994). However, the absence of the ε4 allele does not eliminate the incidence of AD (Refolo et al., 2000; Wu et al., 2003). Dufouil and colleagues demonstrated that the interaction between the level of cholesterol and APOE genotype might influence the progression of AD (Dufouil et al., 2005).

Apart from the genetic etiology, the AD brain can also be affected by neuronal loss, or by the deposit of extracellular senile plaques containing the peptide Aβ and neurofibrillary tangles. The amyloid-β protein is a small protein produced by APP. The amyloid-β protein is cleaved from APP by enzymes named α, β, and δ-secretase. Normally, the APP is cleaved by α secretase into a 40 amino acid product, $A\beta_{40}$. This product is soluble and cleared from the brain. Mutation in the gene for the APP increased cleavage by β, and δ-secretase to form a longer 42 amino acid, $A\beta_{42}$ (Selkoe, 2000). $A\beta_{42}$ is a fibrillar amorphous form of amyloid-β protein that is toxic to neurons (Gruys, 2004). Diffuse deposits of $A\beta_{42}$ cause the formation of amyloid plaques (Cummings, 2004). The chromosome 21 is duplicated in Down's syndrome (Sommer and Henrigue-Silva, 2008); it has been proposed that excessive doses of the APP gene on chromosome 21 may be responsible for AD in adult Down's syndrome (Wolvetang et al., 2003).

In addition to the genetic etiology in AD pathogenesis, neurotransmitter abnormality, particularly acetylcholine (ACh), is another possible pathogenesis of AD. ACh is the major neurotransmitter required by the cholinergic system for some forms of learning and memory. ACh is produced by the synthetic enzyme cholineacetyltransferase (ChAT) which uses acetyl coenzyme A and choline as substrates for the formation of ACh. After ACh is released into the synaptic cleft, it is metabolized into choline and acetate by two cholinesterase enzymes, acetylcholinesterase (AChE) and butyrylcholinesterase (BuChE) (Ellis, 2005). In an AD brain, the amount of AChE is greater than the amount of BuChE (Ellis, 2005; Perry et al., 1978). However, in the late stages of AD, BuChE activity can increase up to 165% of the normal physiological level (Perry et al., 1978). Up-regulation in levels of AChE and BuChE has been shown to be associated with amyloid plaque deposition (Guillozet et al., 1997). Some evidence suggests that BuChE may accelerate maturation of amyloid plaques which are associated with neuronal degeneration and the severity of AD symptoms (Guillozet et al., 1997). Several studies have also shown that the cognitive deterioration occurring in patients with probable AD is associated with progressive loss of cholinergic neurons and a consequent decline in levels of ACh and ChAT in the temporal lobe, parietal cortex and hippocampus (Guillozet et al., 1997; McKeith, 2002; Tiraboschi et al., 2000; Whitehouse et al., 1981). This evidence has led to the use of AChE inhibitors as a therapeutic drug of choice for AD. Blocking of cholinesterase activity can increase ACh concentration at the central synapses and enhance cholinergic function. Several clinical studies have demonstrated symptomatic improvements in patients treated with cholinesterase inhibitors (Ellis, 2005; Forchetti, 2005; Hebert et al., 2003; Heinrich and Lee, 2004; Lendon et al., 1997).

In addition to these two aspects of AD pathogenesis, there is evidence showing other possible causes of AD, including oxidation and lipid peroxidation, glutamatergic excitotoxicity, inflammation in neurons, and the activation of the apoptotic cell death cascade (Butterfield et al., 2002; Dickson, 2004). This evidence leads investigators to identify new agents for AD treatment including anti-apoptotic agents or glutamatergic N-Methyl-D-aspartate-receptor antagonists (Butterfield et al., 2002; Cummings, 2004).

2. TREATMENT OF ALZHEIMER'S DISEASE

At present, several regimens for AD therapy focus mainly on treatment at target sites along the pathogenetic cascades of AD. The details of the current therapeutic modalities of AD according to its pathogenesis are described below.

2.1 Anti-amyloid treatment for Alzheimer's disease

Vaccination against the amyloid-β protein is considered a new target therapy for AD. Schenk and colleagues reported that immunization with $A\beta_{42}$ in transgenic mice, which express mutated human amyloid precursor protein under the control of platelet-derived growth factor promoter (PDAPP), reduced pre-aggregated amyloid plaques (Schenk et al., 1999), suggesting that $A\beta_{42}$ immunization could be effective in the prevention and treatment of AD. Behavior testing in transgenic mice with a radial arm water maze demonstrated that immunization with $A\beta_{42}$ improved memory (Janus et al., 2000; Morgan et al., 2000). Moreover, it has been shown that the memory improvement in those animals was correlated with the reduction of amyloid burden (Bard et al., 2000; DeMattos et al., 2001).

The first human neuropathological study after $A\beta_{1-42}$ immunization (AN-1792) in patients with AD showed absent or sparse amyloid plaques in their brains, suggesting that immunization with AN-1792 resulted in the clearance of Aβ in patients with AD (Nicoll et al., 2003). However, Orgogozo and colleagues reported that 6% of patients receiving AN-1792 developed meningoencephalitis (Orgogozo et al., 2003). Further

studies are needed to evaluate the efficacy of vaccines and their side effects for safety in clinical use for patients with AD.

2.2 Cholinesterase inhibitor for Alzheimer's disease

Cholinergic innervation of the hippocampus is required for some forms of learning and memory. The degeneration of the cholinergic system is one hallmark of AD pathogenesis. Therefore, it is logical to presume that boosting the level of ACh by enhancing the activity of ChAT and/or inhibiting the activity of AChE may improve cognitive function (Poirier, 2005). Currently, the best-developed approach for cholinergic therapy has been the use of cholinesterase inhibitors, which is still one of the most promising therapies for AD.

It has been proposed that an intervention inhibiting both AChE and BuChE may decrease symptoms of dementia in patients with AD (Ballard, 2002). Several AChE inhibitors such as tacrine, donepezil, rivastigmine and galantamine are approved by the U.S. Food and Drug Administration (FDA) for AD treatment (Ballard, 2002). Galantamine and donepezil are selective and rapidly reversible AChE inhibitors, whereas rivastigmine is slowly reversible and inhibits both AChE and BuChE activity (Camps and Munoz-Torrero, 2002). A one-year clinical study indicated that the cholinesterase inhibitors decreased the rate of decline in cognitive test scores compared with subjects in a placebo group (Ellis, 2005). However, none of these cholinesterase inhibitors has been effective for the treatment of patients with AD in advanced stages (Ellis, 2005). Although cholinesterase inhibitors are safe, they can increase ACh levels throughout the body, resulting in cholinergic side effects, including diarrhea, bradycardia and muscle cramps (Kaduszkiewicz et al., 2005). Currently, the search for new AChE inhibitors with minimal side effects is of interest to many investigators (Chattipakorn et al., 2007; Chi et al., 2007; Ingkaninan et al., 2003; Oh et al., 2004; Wang et al., 2006).

2.3 N-methyl-D-aspartate (NMDA) receptor antagonist for Alzheimer's disease

Over stimulation of the N-methyl-D-aspartate (NMDA) receptor by glutamate, manifested as neuronal excitotoxicity, is implicated as one hallmark of AD (Reisberg et al., 2003). Doody and colleagues investigated the effect of memantine, a non-specific competitive antagonist at the glutamatergic NMDA receptor, in patients with AD and found that memantine monotherapy improved cognitive function in moderate stage patients with AD (Doody et al., 2004). Similarly, Forchetti showed that patients with AD, who received memantine together with routine donepezil therapy, have improved cognitive function and behaviors (Forchetti, 2005). These findings suggest that adjunctive memantine therapy with donepezil is effective for the treatment of moderate to severe AD. These regimens can improve cognition, activity in daily living, global function, behavior, and care dependence (Forchetti, 2005). Only one clinical trial in patients with mild stage AD demonstrated a slower progression of AD symptoms after a 28-week therapeutic course with memantine (Rossom et al., 2004). However, this regimen did not prevent global deterioration from AD (Rossom et al., 2004).

All of these findings suggest that memantine may have beneficial effects in patients with moderate to severe AD, but less effect in mild types of AD. Although the beneficial effects of memantine have been demonstrated, its adverse effects, such as dizziness, constipation, cataracts, nausea, dyspnea, confusion, headache, and urinary incontinence, have been documented (Raina et al., 2008; Rossom et al., 2004).

2.4 Hormone replacement therapy for Alzheimer's disease

Observational and longitudinal studies suggest that estrogen has several neuroprotective properties, such as lowering Aβ formation, enhancing cholinergic function and promoting synaptic plasticity and nerve growth processes (Cummings, 2004; Flirski and Sobow, 2005). These effects of estrogen may attenuate age-associated cognitive impairment or the development of Alzheimer's disease. However, this beneficial effect of estrogen has been demonstrated by only a few randomized clinical trials (Pinkerton and Henderson, 2005; Yoon et al., 2003).

Recently, a randomized open-labeled study showed that the daily life activities of patients with AD significantly improved after estrogen and progesterone replacement therapy and that the improvement was similar to that following tacrine therapy in those patients (Yoon et al., 2003). However, in a prospective placebo-controlled study of combined estrogen-progesterone therapy in asymptomatic postmenopausal women, an increase in the prevalence of dementia was reported (Pinkerton and Henderson, 2005). The discrepancy in results from these two studies may be due to differences in subjects included in each study. Due to this controversy, further investigations on the effects of hormone replacement therapy in patients with AD are warranted to evaluate its efficacy for clinical use.

2.5 Anti-inflammatory agents for Alzheimer's disease

Cultured brain cells are capable of generating inflammatory and immune complements such as inflammatory cytokines, acute phase reactants, and many proteases and protease inhibitors. These molecules appear in association with AD lesions (McGeer and McGeer, 1995). These findings suggest that the pathogenesis of AD is related to the inflammatory process. Therefore, the use of nonsteroidal anti-inflammatory drugs (NSAIDs) may favorably influence the course of the AD.

This suggestion is confirmed by a clinical trial from in't Veld and colleagues in a three-year prospective study of 74 patients and 232 age- and sex-matched controls (in't Veld et al., 1998), demonstrating the correlation between the use of NSAIDs and the prevention of Alzheimer's disease. Similarly, a cohort study of 6989 subjects showed that long-term use of NSAIDs for 24 months might protect against AD (in't Veld et al., 2001) In addition, the administration of NSAIDs (triflusal) for 18 months could slow down the progression of Alzheimer's disease (Gomez-Isla et al., 2008).

In contrast, several studies showed that the use of NSAIDs did not prevent the progression of AD (ADAPT Research Group et al., 2007; Aisen et al., 2003; Arvanitakis et al., 2008; Beard et al., 1998; Kang et al., 2007). Investigators from the Mayo Clinic

found no correlation between the initiation of AD and the use of NSAIDs in the two years preceding the onset of dementia (Beard et al., 1998). Moreover, Aisen and colleagues found that patients with mild to moderate AD who routinely took a selective cyclo-oxygenase (COX) -2 inhibitor (rofecoxib) or low-dose NSAIDs (naproxen) for 1 year did not slow cognitive decline (Aisen et al., 2003). In addition, the administration of naproxen and celecoxib for 1 year did not prevent the progression of AD (ADAPT Research Group et al., 2007). The discrepancy in these results could be due to differences in types of NSAIDs used, times of exposure to NSAIDs, and study designs. Future studies are needed to define the role of NSAIDs in the treatment of AD.

2.6 Cholesterol lowering agents for Alzheimer's disease

A prospective trial surveying 10,000 people over 65 years of age in three big cities, Dijon, Bordeaux and Montpellier, demonstrated that high cholesterol levels in normal subjects were associated with the APOE genotype, which increased the risk of dementia, and that the use of lipid-lowering agents decreased the risk of dementia (Dufouil et al., 2005; Rodriguez et al., 2002). Wolozin and colleagues investigated the effect of cholesterol lowering agents, statins, on the prevalence of AD (Wolozin et al., 2000). Their study showed that patients who regularly took statins, 3-hydroxy-3-methylglutaryl coenzyme A reductase inhibitors, had a lower incidence of AD than patients who took anti-hypertensive drugs (Wolozin et al., 2000). Recently, an *in vitro* study using primary neuron cultures derived from the Tg2576 mouse model of AD showed that anti-hypertensive drugs (propranolol-HCl, nicardipine-HCL and carvedilol) significantly reduce the accumulation of Aβ peptides (Wang et al., 2007). However, future *in vivo* studies are needed to confirm this finding.

2.7 Antioxidants for Alzheimer's disease

Oxidative stress may be a factor in the pathogenesis of AD. Antioxidants have been proposed as being beneficial in protecting the brain from oxidative stress (Prasad et al., 2002). Among those antioxidants, vitamin E, or α-tocopherol, has been shown to play an important role in the treatment of moderate to advanced AD (Sano et al., 1997). Dietary supplementation with vitamin E or C in patients with AD has been shown to slow the progression of AD (Grundman et al., 2002; Masaki et al., 2000; Martin, 2003; Pham and Plakogiannis, 2005). Although there are only a few studies confirming the beneficial effects of antioxidants in AD, vitamin E has been commonly recommended to patients with AD since it is inexpensive. Future large randomized clinical trials are needed to warrant its clinical use.

2.8 Herbal medicine for Alzheimer's disease

Although many drugs for AD therapy are available, the drug of choice has not yet been definitively established. Since current available medicines for AD are very expensive, the search for new drugs is of interest to many investigators. Several drugs commonly used today in the treatment of AD were developed from local and traditional medicine, such as galantamine, an AChE inhibitor which was developed from the alkaloids in "Snowdrop" (Cummings, 2004). Oken and colleagues demonstrated that gingko biloba could significantly improve cognitive function in patients with AD, compared to a placebo (Oken et al., 1998). Furthermore, Kanowski and Hoerr showed that ginkgo biloba could reduce the rate of AD development and help to improve cognitive function in patients with AD as well as in patients with vascular dementia (Kanowski and Hoerr, 2003). However, recent findings showed that ginkgo has no beneficial effects for AD (Dekosky et al., 2008; Birks and Evan, 2009). Recently, Ingkaninan and colleagues have shown *in vitro* that ethanol extracts from Tabernaemontana divaricata root (TDE) at a concentration of 0.1 mg/ml inhibit more than 90% of AChE activity (Ingkaninan et al., 2003). We also have recently shown that TDE acts as a novel reversible neuronal AChE inhibitor in an animal model and could be beneficial in improving learning and memory (Chattipakorn et al., 2007). Currently, curcumin is another commonly used natural product that has been of interest since it has many beneficial effects, and some of those may provide therapeutic effects in AD prevention and treatment.

3. CURCUMIN

Curcumin is a natural product that has various properties, such as antioxidant, anti-inflammatory and cholesterol-lowering properties (Joe et al., 2004). All of these properties of curcumin may help to prevent AD or to prevent the progression of AD. In India, turmeric, a compound that contains a high level of curcumin, is commonly used in food preparation. Epidemiological study has found that India has one of the lowest prevalence of AD in the world (Chandra et al., 2001), suggesting that curcumin may have beneficial effects in AD therapy. The following paragraphs will describe all studies showing the possible role of curcumin in AD.

3.1 Biological and pharmacological properties of curcumin

Curcuma longa Linn., which belongs to the Zingiberaceae family, is a perennial herb that measures up to 1 m in height, with a short stem, and is distributed throughout tropical and subtropical regions of the world, including India and China (Araujo and Leon, 2001).

Curcuma longa Linn. is commonly known as turmeric. It is recognized by different names in different languages worldwide, such as haldi in Hindi, ukon in Japanese and kha min chan in Thai (Goel et al., 2008). Turmeric is widely consumed for a variety of purposes, including use as a dietary spice, known as curry, a dietary pigment and Indian folk medicine for the treatment of various illnesses. Furthermore, it has been used as an anti-inflammatory and anti-microbial agent for more than 1,000 years in South and Southeast Asia (Lodha and Bagga, 2000).

Turmeric is derived from the rhizome of Curcuma longa Linn. and contains polyphenolic yellow pigments known as curcuminoids. The curcuminoids contain 70-75% curcumin (diferuloylmethane), 15-20% demethoxycurcumin and 3% bisdemethoxycurcumin (Aggarwal et al., 2007) (Figure 1). Curcumin is a yellow-orange powder, insoluble in water, ether and aqueous solvents, but it is soluble in organic solvents such as ethanol, dimethylsulfoxide and acetone (Aggarwal et al., 2007). Curcumin was first discovered in 1815 and its chemical name is

1,6-heptadiene-3,5-dione-1,7-bis(4-hydroxy-3-methoxyphenyl)-(1E,6E) or diferuloylmethane (Aggarwal et al., 2007; Goel et al., 2008). The chemical formula of curcumin is $C_{21}H_{20}O_6$ and its molecular weight is 368.38 g/mol.

In traditional medicine, curcumin has been used for the treatment of several diseases such as dementia, cardiovascular diseases, cancer and arthritis (Lodha and Bagga, 2000). In Thailand, curcumin has been used to prevent and relieve rashes, itches, chafing and mosquito bites by topical application on the skin as a natural nonsteroidal anti-inflammatory drug (Aggarwal et al., 2007; Araujo and Leon, 2001; Lodha and Bagga, 2000). Several animal studies have demonstrated curcumin's anti-ulcer (Rafatullah et al., 1990; Swarnakar et al., 2005), anti-cancer (Chen et al., 1996; Cheng et al., 2001; Huang et al., 1994; Li et al., 2002; Lu et al., 1993; Ramachandran and You, 1999; Wu et al., 2000), anti-viral (Li et al., 1993; Mazumder et al., 1995), accelerated wound healing (Sidhu et al., 1998), cardioprotective (Nirmala and Puvanakrishnan, 1996b; Nirmala and Puvanakrishnan, 1996a), hypoglycemic (Arun and Nalini, 2002; Kuroda et al., 2005) and anti-inflammatory effects (Ambegaokar et al., 2003; Joe and Lokesh, 1997; Lal et al., 1999; Lal et al., 2000; Lim et al., 2001). A summary of curcumin's properties is shown in Table 1.

TABLE 1. Summary of curcumin properties

Properties	Studied models / Effective dosage
Anti-ulcer	Rats / 50 mg/kg, p.o.(Rafatullah et al., 1999) ; 40 mg/kg, i.p. (Swarnakar et al., 2005)
Anti-cancer	Cell culture/ 25 μM (Wu et al., 2000); 60 μM (Chen et al., 1996); 20 & 40 μM (Ramachandran and You , 1999) Hamsters / 10 mmol, topical (Li et al., 2002) Mice / 0.5-4.0%, p.o.(Huang et al., 1994); 1, 3 & 10 μM, topical (Lu et al., 1993) Humans / 500-8000 mg/day, p.o.(Cheng et al., 2001)
Anti-viral	Cell culture / 2, 5 & 10μM (Li et al., 1993) ; 40 μM (Mazumder et al., 1995)
Accelerated wound healing	Rats and Guinea pigs / 40 mg/kg, p.o.(Sidhu et al., 1998)
Cardioprotective	Rats / 200 mg/kg, p.o.(Nirmala and Puvanakrishnan , 1996a; 1996b)
Hypoglycemic	Mice / 200 & 1000 mg/ 100 g diet (Kuroda et al., 2005) Rats / 80 mg/kg, p.o.(Arun and Nalini, 2002)
Anti-inflammatory	Cell culture / 4, 5, 10, 15 & 20 μM (Ambegaokar et al., 2003; Joe and Lokesh , 1997) Mice 160 & 5000 ppm, p.o.(Lim et al., 2001), Humans / 375 mg / 3 times/day, p.o.(Lal et al., 1999; Lal et al., 2000)
Anti-amyloid	Cell culture / 0.1-1 μM (Ono et al., 2004) Mice / 160, 500 & 5000 ppm, p.o. (Lim et al., 2001, Yang et al., 2005); 7.5 mg/kg, i.v. (Garcia-Alloza et al., 2007)
Cholesterol-lowering	Mice / 4g/kg, p.o. (Kamal-Eldin et al., 2000)
Antioxidant	Cell culture / 75 & 250 μM (Reddy and Lokesh, 1996), Rats / 30 mg/kg (Reddy and Lokesh, 1996) ; 1g/kg (Wahlstrom and Blennow , 1978); 0.1% (Kaul and Krishnakantha , 1997); 2%, p.o.(Sharma et al., 2001)
Anti-apoptotic	Cell culture / 2.5, 50, 100 & 200 μM (Zhu et al., 2004); 20 & 60 μM (Moos et al., 2004)

FIGURE 1. The composition of turmeric from the rhizome of Curcuma longa Linn.

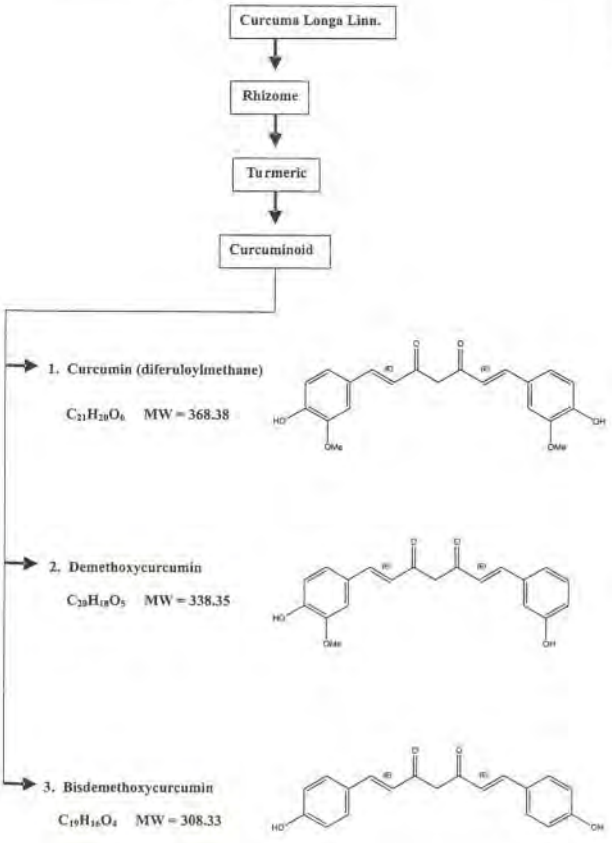

3.2. Possible roles of curcumin in Alzheimer's disease

Strong evidence from several studies suggests that amyloid plaques, oxidative stress, neuronal inflammation, and neuronal apoptosis are involved in the pathogenesis of AD (Cummings, 2004; Kermer and Liman, 2004). Recently, several studies *in vitro* and *in vivo* showed that curcumin has various properties which may possibly prevent the pathogenesis of AD, such as anti-amyloid, anti-inflammation, cholesterol-lowering, antioxidant, and anti-apoptotic properties (Aggarwal et al., 2007; Goel et al., 2008; Joe et al., 2004). The details of these benefits are described in the following sections and summarized in Figure 2.

3.2.1 Anti-amyloid properties of curcumin

Since the accumulation of Aβis one hallmark of the pathogenesis of AD, the destabilization of Aβ would be an attractive therapeutic target for AD treatment. Evidence of curcumin's anti-amyloid properties has been shown in both *in vivo* and *in vitro* studies.

Using fluorescence spectroscopic analysis with thioflavin T and an electron microscope in an *in vitro* study, Ono and colleagues demonstrated that curcumin inhibited Aβ formation, extension and destabilization from $A\beta_{1-40}$ and $A\beta_{1-42}$ in a dose-dependent manner (Ono et al., 2004). This effect of curcumin has been shown to be due to the molecular structure of curcumin, which is potent in Aβ binding (Ringman et al., 2005). Curcumin was

shown to inhibit aggregation as well as disaggregated fibrillar $A\beta_{40}$, indicating that it has favorable stoichiometry for Aβ inhibition (Yang et al., 2005).

Another possible mechanism in the inhibition of Aβ aggregation is related to macrophages. An *in vitro* study showed that AD patients have decreased clearance of amyloid plaques and this defect is related to the decreased phagocytosis of $A\beta_{1-42}$ by the innate immune cells, monocyte or macrophages (Zhang et al., 2006). Zhang and colleagues demonstrated that the Aβ uptake by macrophages was significantly increased after macrophages were treated with curcuminoids, suggesting that curcuminoids may improve immune clearance of amyloid in the AD-affected brain (Zhang et al., 2006).

The effect of curcumin on anti-amyloid formation was also investigated in several animal models of AD, such as the APPswe/PS1dE9 mouse model and the APPSw (Tg2576) mouse model (Garcia-Alloza et al., 2007; Lim et al., 2001; Yang et al., 2005). The study in aged Tg 2576 mice which have Aβ accumulation showed that the administration of curcumin reduced amyloid levels and plaque burden by directly binding to small Aβ species (Lim et al., 2001; Yang et al., 2005). In addition, low dose consumption of dietary curcumin (160 part per million (ppm)) reduced soluble and insoluble Aβ and plaque burden in aged TG 2576 mice (Lim et al., 2001; Ringman et al., 2005; Yang et al., 2005). Recently, a study using multiphoton microscopy and longitudinal imaging to evaluate the real-time effect of systemic curcumin administration on existing Aβ deposits in aged APPswe/PS1dE9 transgenic mice found that curcumin (7.5 mg/kg) reduced plaques and partially restored the altered neurite structure near, and away from, plaques (Garcia-Alloza et al., 2007). These findings suggest that curcumin has beneficial effects in reducing the Aβ accumulation and neurotoxicity along the pathogenic cascade of AD in transgenic mice. Future clinical studies are warranted to evaluate the clinical significance of curcumin.

Apolipoprotein E (APOE) is a plasma protein involved in cholesterol transport (Mahley, 1988). The APOE-knockout mice showed a reduction of amyloid plaques (Bales et al., 1997). Evidence suggests that APOE is one factor involved in the formation of the pathologic form of amyloid plaque in AD because APOE is bound to extracellular senile plaques and to intracellular neurofibrillary tangles (Namba et al., 1991). However, Koistinaho and colleagues showed that APOE could down-regulate APP-induce ischemic susceptibility (Koistinaho et al., 2002). Thus, it is not yet known if APOE is a beneficial or harmful factor in AD. Furthermore, the secretion of APOE requires protein prenylation. It has been shown that monoterpene, curcumin derivative, inhibits the protein prenylation (Chen et al., 1997), which suggest that curcumin should have beneficial effect for AD. However, Cheung and colleagues used dot-blotting and immunoblotting to analyze the effect of curcumin on the level of APOE in a mouse microglial cell line (Cheung et al., 2007). They found that curcumin at physiologically attainable concentrations in the submicromolar to low micromolar ranges can increase the secretion

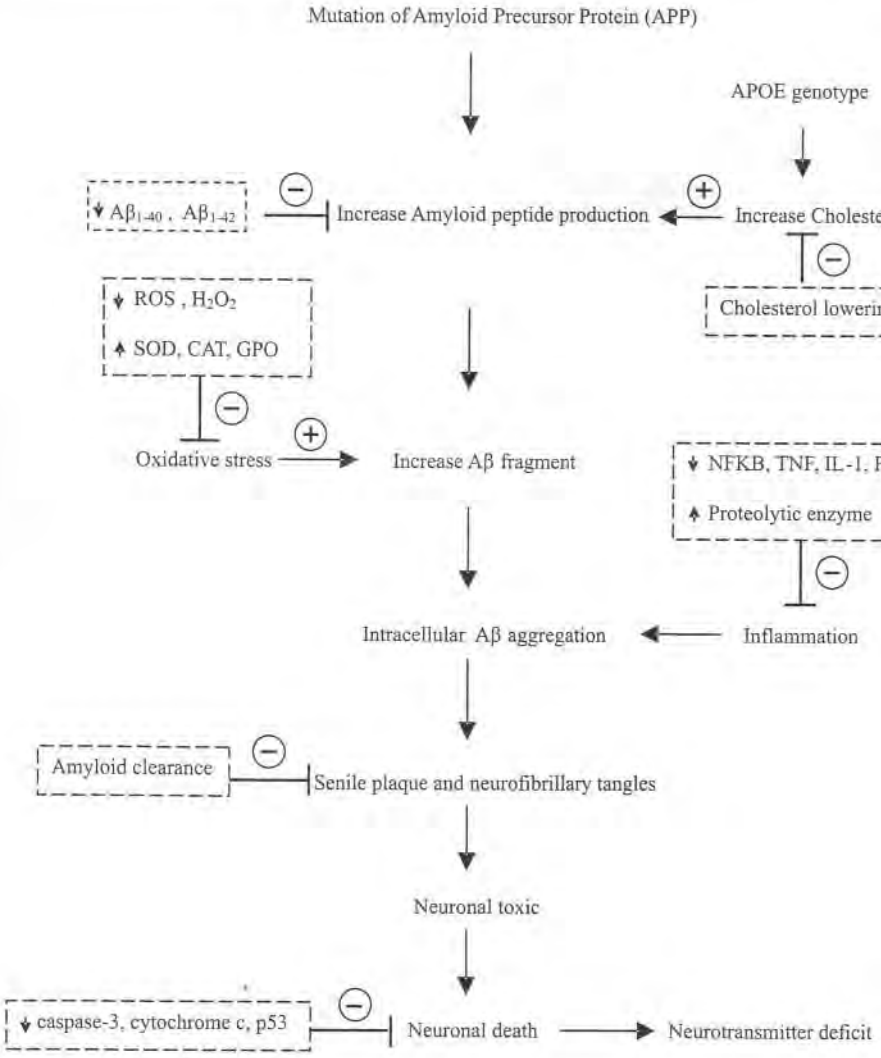

FIGURE 2. Possible roles of curcumin in Alzheimer's disease. The pathogenic cascade of Alzheimer's disease is multifactorial, including genetics, oxidative stress, inflammation, and infection. The possible effect of curcumin, as indicated in the dashed boxes, may interrupt the developing Alzheimer's disease in multiple steps.⊕: Stimulating process, ⊖: Inhibiting process, NFKB: Nuclear factor-kB, TNF: Tumor necrosis factor, IL-1: Interleukin-1, PGE-2: Prostaglandin 2, ROS: Reactive oxygen species, SOD: Superoxide dismutase, CAT: Catalase, GPO: Glutathione peroxidase

of APOE. On the other hand, at concentrations over 6.25 μM, which have been demonstrated to cause cell toxicity, curcumin reduced APOE secretion (Cheung et al., 2007). All of these findings indicate that further investigations regarding the effects of curcumin are needed to warrant its possible role in AD treatment.

3.2.2 Anti-inflammatory properties of curcumin

Several studies have suggested that curcumin has an anti-inflammatory effect similar to that of NSAIDs. Since inflammatory processes, including increased concentrations of cytokines, have been found in the AD-affected brain (Brion, 1996), it is logical to assume that the use of anti-inflammatory drugs, such as NSAIDs, may decrease the risk of AD.

The effect of curcumin on inflammation has been investigated in several cell types such as cancer cells and bone marrow cells (Chan et al., 1998; Lev-Ari et al., 2008). However, its effect on microglials, neuroglia, astrocytes and oligodendrocytes is little known. By using C-6 rat glioma, 2B-clone cells and a mixed colony of both neuroglial cells, Ambegaokar and colleagues found that curcumin inhibits the proliferation of microglia and astrocyte gliosis (Ambegaokar et al., 2003). In addition, Xu and colleagues found that a low dose of curcumin inhibited AP-1 and nuclear factor-kB (NFKB)-mediated transcription of inflammatory cytokines and cyclo-oxygenase-2 (Xu et al., 1997). These findings suggest that curcumin can inhibit inflammation at several levels of the inflammatory process.

The effect of curcumin on the early events in the course of inflammation was investigated in a human monocytic macrophage cell line. It has been demonstrated that curcumin inhibits lipopolysaccharide-induced production of tumor necrosis factor (TNF), interleukin (IL)-1, cyclo-oxygenase, lipoxygenases, prostaglandin E2 and leukotriene in cell lines (Chan, 1995; Kohli and Ali, 2005). Curcumin could also induce the release of proteolytic enzymes such as collagenase, elastase, and hyaluronidase from activated macrophages (Joe and Lokesh, 1997). In Tg2576 mice (Lim et al., 2001), low and high concentrations of curcumin significantly decreased oxidized proteins and interleukin-1 ?, a pro-inflammatory cytokine which is normally elevated in the brains of mice with AD (Lim et al., 2001).

These anti-inflammatory effects of curcumin, as summarized in Table 2, indicate that curcumin exhibits an anti-inflammatory effect similar to that of NSAIDs. The advantage of curcumin over NSAIDs is that it has fewer or no known side effects. As a result, curcumin may be beneficial for the treatment of inflammatory disease, as well as in AD, in which inflammation is an important part of its pathogenetic cascades.

3.2.3 Cholesterol lowering properties of curcumin

It is known that the level of cholesterol is associated with amyloid-β deposits in the brain (Sparks, 1997). In an *in vivo* study, Refolo and colleagues demonstrated that the administration of a cholesterol-lowering drug (BM15.766) in mice for five weeks reduced plasma cholesterol, $A\beta_{1-40}$, and $A\beta_{1-42}$ accumulation in the brain (Refolo et al., 2001). This study suggests that lowering cholesterol by pharmacological treatment may be an effective approach for reducing the risk of developing AD. Similarly, the consumption of curcumin (4 g/kg/day) in mice for four weeks significantly reduced low density lipoprotein and very low density lipoprotein levels in plasma and the total cholesterol level in the liver (Kamal-Eldin et al., 2000). Furthermore, curcumin also inhibited the formation and extension of Aβ and destabilization of $A\beta_{1-40}$ and $A\beta_{1-42}$ in a dose-dependent manner (Ono et al., 2004). All of these findings suggest that curcumin may possibly reduce Aβ-formation similar to BM15.766. However, studies directly investigating the effects of curcumin on cholesterol and Aβ reduction are warranted to evaluate its clinical significance.

3.2.4 Antioxidant properties of curcumin

Oxidative stress plays an important role in the pathogenesis of AD (Brion, 1996; Cummings, 2004). Epidemiological studies demonstrated that consumption of antioxidant agents, such as curcumin, could reduce the risk of AD (Dunsmore et al., 2001; Goel et al., 2008; Lim et al., 2001). The antioxidant mechanism of curcumin is attributed to its unique conjugated structure, which includes two methoxylated phenols and an enol form of β-diketone, and these structures show typical radical-trapping ability as a chain-breaking antioxidant agent (Dunsmore et al., 2001; Goel et al., 2008; Ringman et al., 2005) (Figure 3). It is known that the generation of reactive oxygen species (ROS), H_2O_2 and nitrite radicals can activate macrophages to initiate inflammation (Marriott et al., 2008; Tasaka et al., 2008). Curcumin has been shown to significantly inhibit the generation of these free radicals (Joe and Lokesh, 1997). Dunsmore and colleagues have demonstrated that the antioxidant effect of curcumin could be due to its induction of heat shock protein (Dunsmore et al., 2001), proteins serving as molecular chaperones involved in the protection of cells from various forms of stress (Calabrese et al., 2003).

TABLE 2 . Summary of anti - inflammatory effect of curcumin.

Anti -inflammatory effects	Studied models
Inhibiting nuclear factor -kB (NFKB)	Bone marrow stromal cells (Xu et al., 1997)
Inhibiting tumor necrosis factor (TNF), interleukins (IL)-1, cyclo -oxy genase, lipoxygenases, prostaglandin E2 and leukotriene	Human monocytic macrophage cell lines (Chan, 1995; Kohli and Ali , 2005)
Releasing of proteolytic enzymes such as collagenase, elastase, and hyaluronidase	Rat peritoneal macrophage cells (Joe and Lokesh, 1997)

FIGURE 3. Chemical structural formula of curcumin, which includes two phenolic hydroxyl and beta-diketone groups, these structures show typical radical-trapping ability as a chain-breaking antioxidant agent.

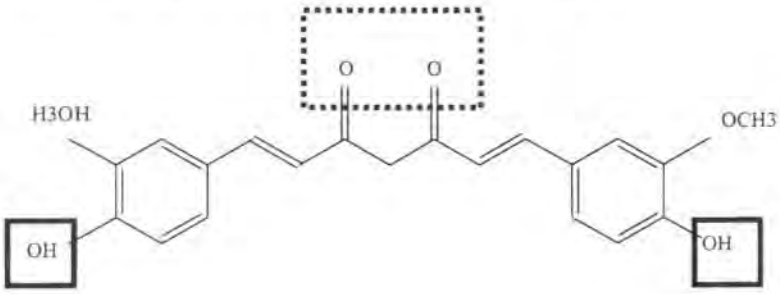

In an *in vivo* study Reddy and Lokesh (Reddy and Lokesh, 1996) demonstrated that the oral administration of 30 mg/kg/day curcumin for 10 days in rats could decrease iron-induced hepatic damage by lowering lipid peroxidation and protecting renal and neural glial cells from oxidative stress. Rats who consumed 0.1% curcumin for three weeks showed the lowering of lipid peroxidation by 12.5-22.6% in the liver, 23.7-24.1% in the kidney, 14.4-18.0% in the spleen, and 16.0-31.4% in the brain (Kaul and Krishnakantha, 1997). Moreover, phenolic substances in curcumin also enhance antioxidative enzymes such as superoxide dismutase (SOD), catalase (CAT), and glutathione peroxidase (GPO) (Sharma et al., 2001; Wahlstrom and Blennow, 1978).

Metals can induce Aβ aggregation and cell toxicity, and are concentrated in the AD-affected brain (Tougu et al., 2008). It has been reported that metal chelation may reduce Aβ aggregation or oxidative neurotoxicity. Desferrioxamine and clioquinol, well-known metal chelators, have been shown to exhibit anti-AD effects (Smith et al., 2007). Baum and Ng found that curcumin has a metal chelating property (Baum and Ng, 2004). They found that curcumin has an affinity for copper, zinc, and iron ions, and binds the redox-active metals iron and copper rather than redox-inactive zinc. Therefore, curcumin might exert a net protective effect against Aβ aggregation via antioxidant activity and metal chelation (Baum and Ng, 2004). Future studies are needed to validate this hypothesis.

All of these antioxidant effects of curcumin, including radical-trapping structure (β-diketone), increased production of heat shock protein, and increased metal chelator properties, indicate that this natural product may be a good anti-oxidant agent that might be beneficial in AD treatment.

3.2.5 Anti-apoptotic properties of curcumin

Apoptosis is a type of cell death process and is involved in both physiological and pathological processes of AD (Flirski and Sobow, 2005). Reactive oxygen species (ROS) or other stimuli can lead to a release of cytochrome C from mitochondria, which can play a key role in caspases' activation of apoptotic signals (Annunziato et al., 2003; Bobba et al., 2004).

Zhu and colleagues investigated the effect of curcumin on apoptosis in primary cortical rat culture and showed that curcumin increases cell viability and decreases cell apoptosis (Zhu et al., 2004). The mechanisms of reduced apoptosis by curcumin include blocking caspase-3, altering the expression of Bcl-2 family protein, lowering reactive oxygen species (ROS), lowering cytochrome C release (Chan, 1995) and disrupting the conformation of p53 (Moos et al., 2004). Since apoptosis is involved in the pathophysiologic process of AD, curcumin may be useful in AD therapy through its anti-apoptotic activity.

4. CLINICAL STUDIES OF CURCUMIN AND AD

Although many *in vivo* and *in vitro* studies confirm the effectiveness of curcumin against AD pathology via multiple pathophysiological cascades, there are currently only a few clinical studies investigating the effects of curcumin in AD.

A controlled randomized clinical trial investigating the effects of curcumin on the lipid profile biomarkers of AD and the cognitive scale in elderly subjects with a six-month follow-up reported that curcumin consumption does not affect serum isoprostane, amyloid-β protein, lipid profile or cognitive scale (Baum et al., 2007; Baum et al., 2008). However, the serum Aβ tended to increase, which might suggest that curcumin disrupts Aβ deposits in brain and the released Aβ then leaves the brain into the serum, where it is detected (Baum et al., 2008). Furthermore, the level of vitamin E was raised in this study, indicating that curcumin possibly slows down AD progression by an antioxidant mechanism (Baum et al., 2008). Currently, there are ongoing clinical trials in patients with mild to moderate AD, investigating the effects of curcumin on changes in the levels of biological markers such as cholesterol level, isoprostanes, alpha-1-anti-chymotrypsin, C-reactive protein, tau, $A\beta_{1\text{-}40}$ and $A\beta_{1\text{-}42}$, and in cognitive scale after 2 or 4 g/day of curcumin consumption for 6-12 months (Kelley and Knopman, 2008; Ringman et al., 2005). This clinical trial is still ongoing; therefore, the results are not yet known. The safety and tolerability of these two different doses of curcumin are also being investigated in these trials (Kelley and Knopman, 2008; Ringman et al., 2005).

In nondemented subjects (Ng et al., 2006), Ng and colleagues reported that subjects who consumed curry occasionally (once or more in six months but less often than once a month), often (once or more a month but less than once a week), or very often (once a week or more, or daily), had significantly better scores on the Mini-Mental State Examination (MMSE), a widely used instrument that provides a global measure of cognitive function, than subjects who never or rarely (never or less than once in 6 months) consumed curry (Ng et al., 2006). These findings suggest that curry consumption may improve cognitive performance in nondemented subjects.

5. SAFETY AND TOXICITY OF CURCUMIN

Studies in animal models have shown that administration of

maximal doses of curcumin (5g/kg) does not have toxic effects (Wahlstrom and Blennow, 1978). Similarly, no toxicity of curcumin has been observed in rats fed 1.2g/kg curcumin for 14 days (Sharma et al., 2001). Also, the safety of curcumin has been confirmed in a clinical study (Chainani-Wu, 2003). Curcumin has been shown to be safe in six clinical trials, in which one trial used 8 g of curcumin per day for three months and the other five trials used 1.125-2.5 g per day (Chainani-Wu, 2003). In addition, curcumin is currently listed as a coloring and flavoring agent in food by the United States Food and Drug Administration (FDA) with only mild adverse side effects, such as gastric irritation and nausea (Abebe, 2002).

Although many studies have shown that curcumin has an anti-cancer property, Frank and colleagues' study did not support this finding. Their study demonstrated that consumption of 0.5% curcumin in Long-Evans Cinnamon (LEC) rats, a model for human Wilson's disease, in which chronic hepatitis and liver tumors develop, did not alter the rate of acute liver failure or the incidence of liver or kidney tumors. The lack of an anti-cancer property of curcumin may be related to enhanced oxidative stress by excess copper in this model (Frank et al., 2003). In addition, Sakano and Kawanishi demonstrated that curcumin could induce DNA fragmentation and base damage in the presence of copper and isozymes of cytochrome p450(CYP) (Sakano and Kawanishi, 2002). This finding indicated that 1-20 mM curcumin may exhibit carcinogenic potential through oxidative DNA damage by its metabolite. Furthermore, curcumin could induce the accumulation of tumor-inducing DNA damage in the colon (Moos et al., 2004). This damage was mediated by inhibiting p53 function, a critical protein in the protection against genomic stress (Moos et al., 2004). Moreover, Yoshino and colleagues demonstrated that 10-20 mM curcumin could act as a pro-oxidant agent in the cell with the presence of transitional metals and may induce DNA damage and apoptotic cell death (Yoshino et al., 2004). In humans, a few studies have shown that curcumin induces allergic dermatitis and urticaria (Hata et al., 1997; Liddle et al., 2006; Swierczynska and Krecisz, 1998). Further *in vivo* and clinical studies are necessary to examine these adverse effects of curcumin.

CONCLUSIONS

Various benefits of curcumin such as anti-amyloid, anti-inflammatory, antioxidant, anti-apoptotic and cholesterol-lowering properties may help to prevent the pathogenesis of AD. Furthermore, due to its low cost with very low or no side effects, curcumin could be a key agent for the development of a new drug for AD. Further clinical trials are required to evaluate its clinical significance in AD treatment.

ACKNOWLEDGMENTS

The authors wish to thank Prof. M. Kevin O'Carroll, Professor Emeritus, University of Mississippi School of Dentistry, USA, and Faculty Consultant, Faculty of Dentistry, Chiang Mai University, Thailand, for his editorial assistance. This work is supported by Thailand Research Fund: TRF-RMU5180007 (SC), TRF-BRG (NC) and Faculty of Medicine Endowment Fund CMU (WP, NC and SC).

REFERENCES

Abebe,W. (2002). Herbal medication: potential for adverse interactions with analgesic drugs. *Journal of Clinical Pharmacy and Therapeutics* **27**, 391-401.

ADAPT Research Group, Lyketsos,C.G., Breitner,J.C., Green,R.C., Martin,B.K., Meinert,C., Piantadosi,S. and Sabbagh,M. (2007). Naproxen and celecoxib do not prevent AD in early results from a randomized controlled trial. *Neurology* **68**, 1800-1808.

Aggarwal,B.B., Sundaram,C., Malani,N. and Ichikawa,H. (2007). Curcumin: the Indian solid gold. *Advances in Experimental Medicine and Biology* **595**, 1-75.

Aisen,P.S., Schafer,K.A., Grundman,M., Pfeiffer,E., Sano,M., Davis,K.L., Farlow,M.R., Jin,S., Thomas,R.G. and Thal,L.J. (2003). Effects of rofecoxib or naproxen vs. placebo on Alzheimer disease progression: a randomized controlled trial. *The Journal of the American Medical Association* **289**, 2819-2826.

Ambegaokar,S.S., Wu,L., Alamshahi,K., Lau,J., Jazayeri,L., Chan,S., Khanna,P., Hsieh,E. and Timiras,P.S. (2003). Curcumin inhibits dose-dependently and time-dependently neuroglial cell proliferation and growth. *Neuro Endocrinology Letters* **24**, 469-473.

Annunziato,L., Amoroso,S., Pannaccione,A., Cataldi,M., Pignataro,G., D'Alessio,A., Sirabella,R., Secondo,A., Sibaud,L. and Di Renzo,G.F. (2003). Apoptosis induced in neuronal cells by oxidative stress: role played by caspases and intracellular calcium ions. *Toxicology Letters* **139**, 125-133.

Araujo,C.C. and Leon,L.L. (2001). Biological activities of Curcuma longa L. *Memórias do Instituto Oswaldo Cruz* **96**, 723-728.

Arun,N. and Nalini,N. (2002). Efficacy of turmeric on blood sugar and polyol pathway in diabetic albino rats. *Plant Foods for Human Nutrition* **57**, 41-52.

Arvanitakis,Z., Grodstein,F., Bienias,J.L., Schneider,J.A., Wilson,R.S., Kelly,J.F., Evans,D.A. and Bennett,D.A. (2008). Relation of NSAIDs to incident AD, change in cognitive function, and AD pathology. *Neurology* **70**, 2219-2225.

Bales,K.R., Verina,T., Dodel,R.C., Du,Y., Altstiel,L., Bender,M., Hyslop,P. and Johnstone,E.M. (1997). Lack of apolipoprotein E dramatically reduces amyloid beta-peptide deposition. *Nature Genetics* **17**, 263-264.

Ballard,C.G. (2002). Advances in the treatment of Alzheimer's disease: benefits of dual cholinesterase inhibition. *European Journal of Neurology* **47**, 64-70.

Bard,F., Cannon,C., Barbour,R., Burke,R.L., Games,D., Grajeda,H., Guido,T., Hu,K., Huang,J., Johnson-Wood,K., Khan,K., Kholodenko,D., Lee,M., Lieberburg,I., Motter,R., Nguyen,M., Soriano,F., Vasquez,N., Weiss,K., Welch,B., Seubert,P., Schenk,D. and Yednock,T. (2000). Peripherally administered antibodies against amyloid beta-peptide enter the central nervous system and reduce pathology in a mouse model of Alzheimer disease. *Nature Medicine* **6**, 916-919.

Baum,L., Cheung,S.K., Mok,V.C., Lam,L.C., Leung,V.P., Hui,E., Ng,C.C., Chow,M., Ho,P.C., Lam,S., Woo,J., Chiu,H.F., Goggins,W., Zee,B., Wong,A., Mok,H., Cheng,W.K., Fong,C., Lee,J.S., Chan,M.H., Szeto,S.S., Lui,V.W., Tsoh,J., Kwok,T.C., Chan,I.H. and Lam,C.W. (2007). Curcumin effects on blood lipid profile in a 6-month human study. *Pharmacological Research* **56**, 509-514.

Baum,L., Lam,C.W., Cheung,S.K., Kwok,T., Lui,V., Tsoh,J., Lam,L., Leung,V., Hui,E., Ng,C., Woo,J., Chiu,H.F., Goggins,W.B., Zee,B.C., Cheng,K.F., Fong,C.Y., Wong,A., Mok,H., Chow,M.S., Ho,P.C., Ip,S.P., Ho,C.S., Yu,X.W., Lai,C.Y., Chan,M.H., Szeto,S., Chan,I.H. and Mok,V. (2008). Six-month randomized, placebo-controlled, double-blind, pilot clinical trial of curcumin in patients with Alzheimer disease. *Journal of Clinical Psychopharmacology* **28**, 110-113.

Baum,L. and Ng,A. (2004). Curcumin interaction with copper and iron suggests one possible mechanism of action in Alzheimer's disease animal models. *Journal of Alzheimer's Disease* **6**, 367-377.

Beard,C.M., Waring,S.C., O'Brien,P.C., Kurland,L.T. and Kokmen,E. (1998). Nonsteroidal anti-inflammatory drug use and Alzheimer's disease: a case-control study in Rochester, Minnesota, 1980 through 1984. *Mayo Clinic Proceedings* **73**, 951-955.

Bird,T.D. (2005). Genetic factors in Alzheimer's disease. *The New England Journal of Medicine* **352**, 862-864.

Birks,J. and Evan,J.G. (2009) Ginkgo biloba for cognitive impairment and dementia. *Cochrance Database of Systematic Reviews*, CD003120.

Bobba,A., Atlante,A., de Bari,L., Passarella,S. and Marra,E. (2004). Apoptosis and cytochrome c release in cerebellar granule cells. *In Vivo* **18**, 335-344.

Brion,J.P. (1996). The neurobiology of Alzheimer's disease. *Acta Clinica Belgica* **51**, 80-90.

Butterfield,D.A., Castegna,A., Lauderback,C.M. and Drake,J. (2002). Evidence that amyloid beta-peptide-induced lipid peroxidation and its sequelae in Alzheimer's disease brain contribute to neuronal death. *Neurobiology of Aging* **23**, 655-664.

Calabrese,V., Scapagnini,G., Colombrita,C., Ravagna,A., Pennisi,G., Giuffrida Stella,A.M., Galli,F. and Butterfield,D.A. (2003). Redox regulation of heat shock protein expression in aging and neurodegenerative disorders associated with oxidative stress: a nutritional approach. *Amino Acids* **25**, 437-444.

Camps,P. and Munoz-Torrero,D. (2002). Cholinergic drugs in pharmacotherapy of Alzheimer's disease. *Mini Reviews in Medicinal Chemistry* **2**, 11-25.

Chainani-Wu,N. (2003). Safety and anti-inflammatory activity of curcumin: a component of tumeric (Curcuma longa). *Journal of Alternative and Complementary Medicine* **9**, 161-168.

Chan,M.M. (1995). Inhibition of tumor necrosis factor by curcumin, a phytochemical. *Biochemical Pharmacology* **49**, 1551-1556.

Chan,M.M., Huang,H.I., Fenton,M.R. and Fong,D. (1998). In vivo inhibition of nitric oxide synthase gene expression by curcumin, a cancer preventive natural product with anti-inflammatory properties. *Biochemical Pharmacology* **55**, 1955-1962.

Chandra,V., Pandav,R., Dodge,H.H., Johnston,J.M., Belle,S.H., DeKosky,S.T. and Ganguli,M. (2001). Incidence of Alzheimer's disease in a rural community in India: the Indo-US study. *Neurology* **57**, 985-989.

Chattipakorn,S., Pongpanparadorn,A., Pratchayasakul,W., Pongchaidacha,A., Ingkaninan,K. and Chattipakorn,N. (2007). Tabernaemontana divaricata extract inhibits neuronal acetylcholinesterase activity in rats. *Journal of Ethnopharmacology* **110**, 61-68.

Chen,X., Hasuma,T., Yano,Y., Yoshimata,T., Morishima,Y., Wang,Y. and Otani,S. (1997). Inhibition of farnesyl protein transferase by monoterpene, curcumin derivatives and gallotannin. *Anticancer Research* **17**, 2555-2564

Chen,Y.C., Kuo,T.C., Lin-Shiau,S.Y. and Lin,J.K. (1996). Induction of HSP70 gene expression by modulation of Ca(+2) ion and cellular p53 protein by curcumin in colorectal carcinoma cells. *Molecular Carcinogenesis* **17**, 224-234.

Cheng,A.L., Hsu,C.H., Lin,J.K., Hsu,M.M., Ho,Y.F., Shen,T.S., Ko,J.Y., Lin,J.T., Lin,B.R., Ming-Shiang,W., Yu,H.S., Jee,S.H., Chen,G.S., Chen,T.M., Chen,C.A., Lai,M.K., Pu,Y.S., Pan,M.H., Wang,Y.J., Tsai,C.C. and Hsieh,C.Y. (2001). Phase I clinical trial of curcumin, a chemopreventive agent, in patients with high-risk or pre-malignant lesions. *Anticancer Research* **21**, 2895-2900.

Cheung,S., Lee,J. and Baum,L. (2007) Polyphenolic compounds curcumin, ferulic acid and tannic acid enhance Apolipoprotein E secretion. *Neuroscience Soc* (Abstract).

Chi,J.F., Niu,J.Z., Xu,S.Q., Li,J., Wang,J.F. and Liu,J.P. (2007).

Treatment of Alzheimer disease: an evidence-based review. *Zhong Xi Yi Jie He Xue Bao* 5, 247-254.

Cummings,J.L. (2004). Alzheimer's disease. *The New England Journal of Medicine* **351**, 56-67.

Dekosky,S.T., Williamson,J.D., Fitzpatrick,A.L., Ives,D.G., Saxton,J.A., Lopez,O.L., Burke,G., Carlson,M.C., Fried,L.P., Kuller,L.H., Robbins,J.A., Tracy,R.P., Woolard,N.F., Dunn,L., Snitz,B.E., Nahin,R.L. and Furberg,C.D. (2008) Ginkgo biloba for prevention of dementia. *The Journal of the American Medical Association* **300**, 2253-2262.

DeMattos,R.B., Bales,K.R., Cummins,D.J., Dodart,J.C., Paul,S.M. and Holtzman,D.M. (2001). Peripheral anti-A beta antibody alters CNS and plasma A beta clearance and decreases brain A beta burden in a mouse model of Alzheimer's disease. *Proceedings of the National Academy of Sciences of the United States of America* **98**, 8850-8855.

Dickson,D.W. (2004). Apoptotic mechanisms in Alzheimer neurofibrillary degeneration: cause or effect. *The Journal of Clinical Investigation* **114**, 23-27.

Doody,R., Wirth,Y., Schmitt,F. and Mobius,H.J. (2004). Specific functional effects of memantine treatment in patients with moderate to severe Alzheimer's disease. *Dementia and Geriatric Cognitive Disorders* **18**, 227-232.

Dufouil,C., Richard,F., Fievet,N., Dartigues,J.F., Ritchie,K., Tzourio,C., Amouyel,P. and Alperovitch,A. (2005). APOE genotype, cholesterol level, lipid-lowering treatment, and dementia: the Three-City Study. *Neurology* **64**, 1531-1538.

Dunsmore,K.E., Chen,P.G. and Wong,H.R. (2001). Curcumin, a medicinal herbal compound capable of inducing the heat shock response. *Critical Care Medicine* **29**, 2199-2204.

Ellis,J.M. (2005). Cholinesterase inhibitors in the treatment of dementia. *The Journal of the American Osteopathic Association* **105**, 145-158.

Fillit,H. and Hill,J. (2005). Economics of dementia and pharmacoeconomics of dementia therapy. *The American Journal of Geriatric Pharmacotherapy* **3**, 39-49.

Flirski,M. and Sobow,T. (2005). Biochemical markers and risk factors of Alzheimer's disease. *Current Alzheimer Research.* **2**, 47-64.

Frank,N., Knauft,J., Amelung,F., Nair,J., Wesch,H. and Bartsch,H. (2003). No prevention of liver and kidney tumors in Long-Evans Cinnamon rats by dietary curcumin, but inhibition at other sites and of metastases. *Mutation Research* **523-524**, 127-135.

Frisoni,G.B., Manfredi,M., Geroldi,G., Binetti, G., Zanetti,O., Bianchetti,A. and Trabucchi, M. (1998). The prevalence of apoE-4 in Alzheimer's disease in age dependent. *Journal of neurology, neurosurgery, and psychiatry* **65**, 103-106.

Forchetti,C.M. (2005). Treating Patients With Moderate to Severe Alzheimer's disease: Implication of Recent pharmacologic studies. *Primary Care Companion to the Journal of Clinical Psychiatry* 7, 155-161.

Garcia-Alloza,M., Borrelli,L.A., Rozkalne,A., Hyman,B.T. and Bacskai,B.J. (2007). Curcumin labels amyloid pathology in vivo, disrupts existing plaques, and partially restores distorted neurites in an Alzheimer mouse model. *Journal of Neurochemistry* **102**, 1095-1104.

Giovannini,M.G., Scali,C., Prosperi,C., Bellucci,A., Pepeu,G. and Casamenti,F. (2003). Experimental brain inflammation and neurodegeneration as model of Alzheimer's disease: protective effects of selective COX-2 inhibitors. *International Journal of Immunopathology and Pharmacology* **16**, 31-40.

Goel,A., Kunnumakkara,A.B. and Aggarwal,B.B. (2008). Curcumin as "Curecumin": From kitchen to clinic. *Biochemical Pharmacology* **75**, 787-809.

Gomez-Isla,T., Blesa,R., Boada,M., Clarimon,J., Del Ser,T., Domenech,G., Ferro,J.M., Gomez-Anson,B., Manubens,J.M., Martinez-Lage,J.M., Munoz,D., Pena-Casanova,J. and Torres,F. (2008). A randomized, double-blind, placebo controlled-trial of triflusal in mild cognitive impairment: the TRIMCI study. *Alzheimer Disease and Associated Disorders* **22**, 21-29.

Grundman,M., Grundman,M. and Delaney,P. (2002). Antioxidant strategies for Alzheimer's disease. *The Proceedings of the Nutrition Society* **61**, 191-202.

Gruys,E. (2004). Protein folding pathology in domestic animals. *Journal of Zhejiang. University Science* 5, 1226-1238.

Guillozet,A.L., Smiley,J.F., Mash,D.C. and Mesulam,M.M. (1997). Butyrylcholinesterase in the life cycle of amyloid plaques. *Annals of Neurology* **42**, 909-918.

Hata,M., Sasaki,E., Ota,M., Fujimoto,K., Yajima,J., Shichida,T. and Honda,M. (1997). Allergic contact dermatitis from curcumin (turmeric). *Contact Dermatitis* **36**, 107-108.

Hebert,L.E., Scherr,P.A., Bienias,J.L., Bennett,D.A. and Evans,D.A. (2003). Alzheimer disease in the US population: prevalence estimates using the 2000 census. *Archives Neurology* **60**, 1119-1122.

Heinrich,M. and Lee,T.H. (2004). Galanthamine from snowdrop—the development of a modern drug against Alzheimer's disease from local Caucasian knowledge. *Journal of Ethnopharmacology* **92**, 147-162.

Huang,M.T., Lou,Y.R., Ma,W., Newmark,H.L., Reuhl,K.R. and Conney,A.H. (1994). Inhibitory effects of dietary curcumin on forestomach, duodenal, and colon carcinogenesis in mice. *Cancer Research* **54**, 5841-5847.

Hy,L.X. and Keller,D.M. (2000). Prevalence of AD among whites: a summary by levels of severity. *Neurology* **55**, 198-204.

in't Veld,B.A., Launer,L.J., Hoes,A.W., Ott,A., Hofman,A., Breteler,M.M. and Stricker,B.H. (1998). NSAIDs and incident Alzheimer's disease. The Rotterdam Study. *Neurobiology of Aging* **19**, 607-611.

in't Veld,B.A., Ruitenberg,A., Hofman,A., Launer,L.J., van Duijn,C.M., Stijnen,T., Breteler,M.M. and Stricker,B.H. (2001). Nonsteroidal antiinflammatory drugs and the risk of Alzheimer's disease. *The New England Journal of Medicine* **345**, 1515-1521.

Ingkaninan,K., Temkitthawon,P., Chuenchom,K., Yuyaem,T. and Thongnoi,W. (2003). Screening for acetylcholinesterase inhibitory activity in plants used in Thai traditional rejuvenating and neurotonic remedies. *Journal of Ethnopharmacology* **89**, 261-264.

Janus,C., Pearson,J., McLaurin,J., Mathews,P.M., Jiang,Y., Schmidt,S.D., Chishti,M.A., Horne,P., Heslin,D., French,J., Mount,H.T., Nixon,R.A., Mercken,M., Bergeron,C., Fraser,P.E., George-Hyslop,P. and Westaway,D. (2000). A beta peptide immunization reduces behavioural impairment and plaques in a model of Alzheimer's disease. *Nature* **408**, 979-982.

Joe,B. and Lokesh,B.R. (1997). Effect of curcumin and capsaicin on arachidonic acid metabolism and lysosomal enzyme secretion by rat peritoneal macrophages. *Lipids* **32**, 1173-1180.

Joe,B., Vijaykumar,M. and Lokesh,B.R. (2004). Biological properties of curcumin-cellular and molecular mechanisms of action. *Critical Reviews in Food Science and Nutrition* **44**, 97-111.

Kaduszkiewicz,H., Zimmermann,T., Beck-Bornholdt,H.P. and van den,B.H. (2005). Cholinesterase inhibitors for patients with Alzheimer's disease: systematic review of randomised clinical trials. *BMJ* **331**, 321-327.

Kamal-Eldin,A., Frank,J., Razdan,A., Tengblad,S., Basu,S. and Vessby,B. (2000). Effects of dietary phenolic compounds on tocopherol, cholesterol, and fatty acids in rats. *Lipids* **35**, 427-435.

Kang,J.H., Cook,N., Manson,J., Buring,J.E. and Grodstein,F. (2007). Low dose aspirin and cognitive function in the women's health study cognitive cohort. *BMJ* **334**, 987.

Kanowski,S. and Hoerr,R. (2003). Ginkgo biloba extract EGb 761 in dementia: intent-to-treat analyses of a 24-week, multi-center, double-blind, placebo-controlled, randomized trial. *Pharmacopsychiatry* **36**, 297-303.

Kaul,S. and Krishnakantha,T.P. (1997). Influence of retinol deficiency and curcumin/turmeric feeding on tissue microsomal membrane lipid peroxidation and fatty acids in rats. *Molecular and Cellular Biochemistry* **175**, 43-48.

Kelley,B.J. and Knopman,D.S. (2008). Alternative medicine and Alzheimer disease. *The Neurologist.* **14**, 299-306.

Kermer,P. and Liman,J. (2004). Neuronal Apoptosis in Neurodegenerative Diseases: From Basic Research to Clinical Application. *Neuro-Degenerative Diseases* **1**, 9-19.

Kohli,K. and Ali,J. (2005). Curcumin: a natural antiinflamatory agent. *Indian Journal of Pharmacology* **37**, 141-147.

Koistinaho,M., Kettunen,M.I., Holtzman,D.M., Kauppinen,R.A., Higgins,L.S. and Koistinaho,J.(2002). Expression of human apolipoprotein E downregulates amyloid precursor protein-induced ischemic susceptibility. *Stroke* **33**, 1905-1910.

Kuroda,M., Mimaki,Y., Nishiyama,T., Mae,T., Kishida,H., Tsukagawa,M., Takahashi,K., Kawada,T., Nakagawa,K. and Kitahara,M. (2005). Hypoglycemic effects of turmeric (Curcuma longa L. Rhizomes) on genetically diabetic KK-Ay mice. *Biological and Pharmaceutical Bulletin* **28**, 937-939.

Kuusisto,J., Koivisto,K., Kervinen,K., Mykkanen,L., Helkala,E.L., Vanhanen,M., Hanninen,T., Pyorala,K., Kesaniemi,Y.A. and Riekkinen,P. (1994). Association of apolipoprotein E phenotypes with late onset Alzheimer's disease: population based study. *BMJ* **309**, 636-638.

Lal,B., Kapoor,A.K., Agrawal,P.K., Asthana,O.P. and Srimal,R.C. (2000). Role of curcumin in idiopathic inflammatory orbital pseudotumours. *Phytotherapy Research* **14**, 443-447.

Lal,B., Kapoor,A.K., Asthana,O.P., Agrawal,P.K., Prasad,R., Kumar,P. and Srimal,R.C. (1999). Efficacy of curcumin in the management of chronic anterior uveitis. *Phytotherapy Research* **13**, 318-322.

Lendon,C.L., Ashall,F. and Goate,A.M. (1997). Exploring the etiology of Alzheimer disease using molecular genetics. *The Journal of the American Medical Association* **277**, 825-831.

Lev-Ari,S., Lichtenberg,D. and Arber,N. (2008). Compositions for treatment of cancer and inflammation. Recent Patents. *Anticancer Drug Discovery* **3**, 55-62.

Li,C.J., Zhang,L.J., Dezube,B.J., Crumpacker,C.S. and Pardee,A.B. (1993). Three inhibitors of type 1 human immunodeficiency virus long terminal repeat-directed gene expression and virus replication. *Proceedings of the National Academy of Sciences of the United States of America* **90**, 1839-1842.

Li,N., Chen,X., Liao,J., Yang,G., Wang,S., Josephson,Y., Han,C., Chen,J., Huang,M.T. and Yang,C.S. (2002). Inhibition of 7,12-dimethylbenz[a]anthracene (DMBA)-induced oral carcinogenesis in hamsters by tea and curcumin. *Carcinogenesis* **23**, 1307-1313.

Liddle,M., Hull,C., Liu,C. and Powell,D. (2006). Contact urticaria from curcumin. *Dermatitis* **17**, 196-197.

Lim,G.P., Chu,T., Yang,F., Beech,W., Frautschy,S.A. and Cole,G.M. (2001). The curry spice curcumin reduces oxidative damage and amyloid pathology in an Alzheimer transgenic mouse. *The Journal of Neuroscience* **21**, 8370-8377.

Lodha,R. and Bagga,A. (2000). Traditional Indian systems of medicine. *Annals of the Academy of Medicine, Singapore* **29**, 37-41.

Lu,Y.P., Chang,R.L., Huang,M.T. and Conney,A.H. (1993). Inhibitory effect of curcumin on 12-O-tetradecanoylphorbol-13-acetate-induced increase in ornithine decarboxylase mRNA in mouse epidermis. *Carcinogenesis* **14**, 293-297.

Mahley,R.W. (1988). Apolipoprotein E: cholesterol transport protein with expanding role in cell biology. *Science* **240**, 622-630.

Marriott,H.M., Jackson,L.E., Wilkinson,T.S., Simpson,A.J., Mitchell,T.J., Buttle,D.J., Cross,S.S., Ince,P.G., Hellewell,P.G., Whyte,M.K. and Dockrell,D.H. (2008). Reactive oxygen species regulate neutrophil recruitment and survival in pneumococcal pneumonia. *American Journal of Respiratory and Critical Care Medicine* **177**, 887-895.

Martin,A. (2003). Antioxidant vitamins E and C and risk of Alzheimer's disease. *Nutrition Reviews* **61**, 69-73.

Martin,J.B. (1999). Molecular basis of the neurodegenerative disorders. *The New England Journal of Medicine* **340**, 1970-1980.

Masaki,K.H., Losonczy,K.G., Izmirlian,G., Foley,D.J., Ross,G.W., Petrovitch,H., Havlik,R. and White,L.R. (2000). Association of vitamin E and C supplement use with cognitive function and dementia in elderly men. *Neurology* **54**, 1265-1272.

Mazumder,A., Raghavan,K., Weinstein,J., Kohn,K.W. and Pommier,Y. (1995). Inhibition of human immunodeficiency virus type-1 integrase by curcumin. *Biochemical Pharmacology* **49**, 1165-1170.

McGeer,P.L. and McGeer,E.G. (1995). The inflammatory response system of brain: implications for therapy of Alzheimer and other neurodegenerative diseases. *Brain Research. Brain Research Reviews* **21**, 195-218.

McKeith,I.G. (2002). Dementia with Lewy bodies. *The British Journal of Psychiatry* **180**, 144-147.

McKhann,G., Drachman,D., Folstein,M., Katzman,R., Price,D., and Stadlan,E.M. (1984). Clinical diagnosis of Alzheimer's disease: report of the NINCDS-ADRDA Work Group under the auspices of Department of Health and Human Services Task Force on Alzheimer's Disease. *Neurology* **34**, 939-944.

Moos,P.J., Edes,K., Mullally,J.E. and Fitzpatrick,F.A. (2004). Curcumin impairs tumor suppressor p53 function in colon cancer cells. *Carcinogenesis* **25**, 1611-1617.

Morgan,D., Diamond,D.M., Gottschall,P.E., Ugen,K.E., Dickey,C., Hardy,J., Duff,K., Jantzen,P., DiCarlo,G., Wilcock,D., Connor,K., Hatcher,J., Hope,C., Gordon,M. and Arendash,G.W. (2000). A beta peptide vaccination prevents memory loss in an animal model of Alzheimer's disease. *Nature* **408**, 982-985.

Namba,Y., Tomonaga,M., Kawasaki,H., Otomo,E. and Ikeda,K. (1991). Apolipoprotein E immunoreactivity in cerebral amyloid deposits and neurofibrillary tangles in Alzheimer's disease and kuru plaque amyloid in Creutzfeldt-Jakob disease. *Brain Research* **541**, 163-166.

Ng,T.P., Chiam,P.C., Lee,T., Chua,H.C., Lim,L. and Kua,E.H. (2006). Curry consumption and cognitive function in the elderly. *American Journal of Epidemiology* **164**, 898-906.

Nicoll,J.A., Wilkinson,D., Holmes,C., Steart,P., Markham,H. and Weller,R.O. (2003). Neuropathology of human Alzheimer disease after immunization with amyloid-beta peptide: a case report. *Nature Medicine* **9**, 448-452.

Nirmala,C. and Puvanakrishnan,R. (1996a). Effect of curcumin on certain lysosomal hydrolases in isoproterenol-induced myocardial infarction in rats. *Biochemical Pharmacology* **51**, 47-51.

Nirmala,C. and Puvanakrishnan,R. (1996b). Protective role of curcumin against isoproterenol induced myocardial infarction in rats. *Molecular and Cellular Biochemistry* **159**, 85-93.

Oh,M.H., Houghton,P.J., Whang,W.K. and Cho,J.H. (2004). Screening of Korean herbal medicines used to improve cognitive function for anti-cholinesterase activity. *Phytomedicine* **11**, 544-548.

Oken,B.S., Storzbach,D.M. and Kaye,J.A. (1998). The efficacy of Ginkgo biloba on cognitive function in Alzheimer disease. *Archives of Neurology* **55**, 1409-1415.

Ono,K., Hasegawa,K., Naiki,H. and Yamada,M. (2004). Curcumin has potent anti-amyloidogenic effects for Alzheimer's beta-amyloid fibrils in vitro. *Journal of Neuroscience Research* **75**, 742-750.

Orgogozo,J.M., Gilman,S., Dartigues,J.F., Laurent,B., Puel,M., Kirby,L.C., Jouanny,P., Dubois,B., Eisner,L., Flitman,S.,

Michel,B.F., Boada,M., Frank,A. and Hock,C. (2003). Subacute meningoencephalitis in a subset of patients with AD after Abeta42 immunization. *Neurology* **61**, 46-54.

Perry,E.K., Tomlinson,B.E., Blessed,G., Bergmann,K., Gibson,P.H. and Perry,R.H. (1978). Correlation of cholinergic abnormalities with senile plaques and mental test scores in senile dementia. *British Medical Journal* **2**, 1457-1459.

Pham,D.Q. and Plakogiannis,R. (2005). Vitamin E supplementation in Alzheimer's disease, Parkinson's disease, tardive dyskinesia, and cataract: Part 2. *The Annals of Pharmacotherapy* **39**, 2065-2072.

Pinkerton,J.V. and Henderson,V.W. (2005). Estrogen and cognition, with a focus on Alzheimer's disease. *Seminars in Reproductive Medicine* **23**, 172-179.

Poirier J. (2005). Evidence that clinical effects of cholinesterase inhibitors are related to potency and targeting of action. *International Journal of Clinical Practice* **118**, 6-19.

Prasad,K.N., Cole,W.C. and Prasad,K.C. (2002). Risk factors for Alzheimer's disease: role of multiple antioxidants, non-steroidal anti-inflammatory and cholinergic agents alone or in combination in prevention and treatment. *Journal of the American College of Nutrition* **21**, 506-522.

Rafatullah,S., Tariq,M., Al Yahya,M.A., Mossa,J.S. and Ageel,A.M. (1990). Evaluation of turmeric (Curcuma longa) for gastric and duodenal antiulcer activity in rats. *Journal of Ethnopharmacology* **29**, 25-34.

Raina,P., Santaguida,P., Ismaila,A., Patterson,C., Cowan,D., Levine,M., Booker,L. and Oremus,M. (2008). Effectiveness of cholinesterase inhibitors and memantine for treating dementia: evidence review for a clinical practice guideline. *Annals of Internal Medicine* **148**, 379-397.

Ramachandran,C. and You,W. (1999). Differential sensitivity of human mammary epithelial and breast carcinoma cell lines to curcumin. *Breast Cancer Research and Treatment* **54**, 269-278.

Reddy,A.C. and Lokesh,B.R. (1996). Effect of curcumin and eugenol on iron-induced hepatic toxicity in rats. *Toxicology* **107**, 39-45.

Refolo,L.M., Malester,B., LaFrancois,J., Bryant-Thomas,T., Wang,R., Tint,G.S., Sambamurti,K., Duff,K. and Pappolla,M.A. (2000). Hypercholesterolemia accelerates the Alzheimer's amyloid pathology in a transgenic mouse model. *Neurobiology of Disease* **7**, 321-331.

Refolo,L.M., Pappolla,M.A., LaFrancois,J., Malester,B., Schmidt,S.D., Thomas-Bryant,T., Tint,G.S., Wang,R., Mercken,M., Petanceska,S.S. and Duff,K.E. (2001). A cholesterol-lowering drug reduces beta-amyloid pathology in a transgenic mouse model of Alzheimer's disease. *Neurobiology of Disease* **8**, 890-899.

Reisberg,B., Doody,R., Stoffler,A., Schmitt,F., Ferris,S. and Mobius,H.J. (2003). Memantine in moderate-to-severe Alzheimer's disease. *The New England Journal of Medicine* **348**, 1333-1341.

Reiss,A.B. (2005). Cholesterol and apolipoprotein E in Alzheimer's disease. *American Journal of Alzheimer's Disease and Other Dementias* **20**, 91-96.

Ringman,J.M., Frautschy,S.A., Cole,G.M., Masterman,D.L. and Cummings,J.L. (2005). A potential role of the curry spice curcumin in Alzheimer's disease. *Current Alzheimer Research* **2**, 131-136.

Rodriguez,E.G., Dodge,H.H., Birzescu,M.A., Stoehr,G.P. and Ganguli,M. (2002). Use of lipid-lowering drugs in older adults with and without dementia: a community-based epidemiological study. *Journal of American Geriatric Society* **50**, 1852-1856.

Rossom,R., Adityanjee and Dysken,M. (2004). Efficacy and tolerability of memantine in the treatment of dementia. *The American Journal of Geriatric Pharmacotherapy* **2**, 303-312.

Sakano,K. and Kawanishi,S. (2002). Metal-mediated DNA damage induced by curcumin in the presence of human cytochrome P450 isozymes. *Archives of Biochemistry and Biophysics* **405**, 223-230.

Sano,M., Ernesto,C., Thomas,R.G., Klauber,M.R., Schafer,K., Grundman,M., Woodbury,P., Growdon,J., Cotman,C.W., Pfeiffer,E., Schneider,L.S. and Thal,L.J. (1997). A controlled trial of selegiline, alpha-tocopherol, or both as treatment for Alzheimer's disease. The Alzheimer's Disease Cooperative Study. *The New England Journal of Medicine* **336**, 1216-1222.

Schenk,D., Barbour,R., Dunn,W., Gordon,G., Grajeda,H., Guido,T., Hu,K., Huang,J., Johnson-Wood,K., Khan,K., Kholodenko,D., Lee,M., Liao,Z., Lieberburg,I., Motter,R., Mutter,L., Soriano,F., Shopp,G., Vasquez,N., Vandevert,C., Walker,S., Wogulis,M., Yednock,T., Games,D. and Seubert,P. (1999). Immunization with amyloid-beta attenuates Alzheimer-disease-like pathology in the PDAPP mouse. *Nature* **400**, 173-177.

Selkoe,D.J. (2000). Toward a comprehensive theory for Alzheimer's disease. Hypothesis: Alzheimer's disease is caused by the cerebral accumulation and cytotoxicity of amyloid beta-protein. *Annals of the New York Academy of Sciences* **924**, 17-25.

Sharma,R.A., Ireson,C.R., Verschoyle,R.D., Hill,K.A., Williams,M.L., Leuratti,C., Manson,M.M., Marnett,L.J.,

Steward,W.P. and Gescher,A. (2001). Effects of dietary curcumin on glutathione S-transferase and malondialdehyde-DNA adducts in rat liver and colon mucosa: relationship with drug levels. *Clinical Cancer Research* **7**, 1452-1458.

Sidhu,G.S., Singh,A.K., Thaloor,D., Banaudha,K.K., Patnaik,G.K., Srimal,R.C. and Maheshwari,R.K. (1998). Enhancement of wound healing by curcumin in animals. *Wound Repair and Regeneration* **6**, 167-177.

Smith,D.G., Cappai,R. and Barnham,K.J. (2007). The redox chemistry of the Alzheimer's disease amyloid beta peptide. *Biochimica et Biophysica Acta* **1768**, 1976-1990.

Sommer,C.A. and Henrique-Silva,F. (2008) Trisomy 21 and Down syndrome: a short review. *Brazilian Journal of Biology* **68**, 447-452.

Sparks,D.L. (1997). Coronary artery disease, hypertension, ApoE, and cholesterol: a link to Alzheimer's disease? *Annals of the New York Academy of Sciences* **826**, 128-146.

Strittmatter,W.J., Saunders,A.M., Schmechel,D., Pericak-Vance,M., Enghild,J., Salvesen,G.S. and Roses,A.D. (1993). Apolipoprotein E: high-avidity binding to beta-amyloid and increased frequency of type 4 allele in late-onset familial Alzheimer disease. *Proceedings of the National Academy of Sciences of the United States of America* **90**, 1977-1981.

Swarnakar,S., Ganguly,K., Kundu,P., Banerjee,A., Maity,P. and Sharma,A.V. (2005). Curcumin regulates expression and activity of matrix metalloproteinases 9 and 2 during prevention and healing of indomethacin-induced gastric ulcer. *The Journal Biological Chemistry* **280**, 9409-9415.

Swierczynska,M.K. and Krecisz,B. (1998). Occupational skin changes in persons working in contact with food spices. *Medycyna Pracy* **49**, 187-190.

Tasaka,S., Amaya,F., Hashimoto,S. and Ishizaka,A. (2008). Roles of oxidants and redox signaling in the pathogenesis of acute respiratory distress syndrome. *Antioxidants and Redox Signaling* **10**, 739-753.

Thomas,D.B and Bruce, L.M. (2005). Harrison's Principles of Internal Medicine, (New York, New York: The McGraw Hill companies).

Tiraboschi,P., Hansen,L.A., Alford,M., Sabbagh,M.N., Schoos,B., Masliah,E., Thal,L.J. and Corey-Bloom,J. (2000). Cholinergic dysfunction in diseases with Lewy bodies. *Neurology* **54**, 407-411.

Tougu,V., Karafin,A. and Palumaa,P. (2008). Binding of zinc(II) and copper(II) to the full-length Alzheimer's amyloid-beta peptide. *Journal of Neurochemistry* **104**, 1249-1259.

Wahlstrom,B. and Blennow,G. (1978). A study on the fate of curcumin in the rat. *Acta pharmacologica et Toxicologica* **43**, 86-92.

Wang,J.N., Ho,L., Humala,N., Hainline,C., Rosendorff,C., Badimon,J., Martinez,P. and Pasinetti,G.M. (2007) Development of anti-hypertensive drugs as ?-amyloid lowering agents for the treatment of alzheimer's disease . *Neuroscience Soc* (Abstract).

Wang,R., Yan,H. and Tang,X.C. (2006). Progress in studies of huperzine A, a natural cholinesterase inhibitor from Chinese herbal medicine. *Acta Pharmacologica Sinica* **27**, 1-26.

Whitehouse,P.J., Price,D.L., Clark,A.W., Coyle,J.T. and DeLong,M.R. (1981). Alzheimer disease: evidence for selective loss of cholinergic neurons in the nucleus basalis. *Annals of Neurology* **10**, 122-126.

Wolozin,B., Kellman,W., Ruosseau,P., Celesia,G.G. and Siegel,G. (2000). Decreased prevalence of Alzheimer disease associated with 3-hydroxy-3-methyglutaryl coenzyme A reductase inhibitors. *Archives of Neurology* **57**, 1439-1443.

Wolvetang,E.W., Bradfield,O.M., Tymms,M., Zavarsek,S., Hatzistavrou,T., Kola,I. and Hertzog,P.J. (2003). The chromosome 21 transcription factor ETS2 transactivates the beta-APP promoter: implications for Down syndrome. *Biochimica et Biophysica Acta* **1628**, 105-110.

Wu,C.W., Liao,P.C., Lin,C., Kuo,C.J., Chen,S.T., Chen,H.I., and Kuo,Y.M. (2003). Brain region-dependent increases in beta-amyloid and apolipoprotein E levels in hypercholesterolemic rabbits. *Journal of Neural Transmission* **110**, 641-649.

Wu,Y., Chen,Y. and He,M. (2000). The influence of curcumin on the cell cycle of HL-60 cells and contrast study. *Journal of Tongji Medical University* **20**, 123-125.

Xu,Y.X., Pindolia,K.R., Janakiraman,N., Chapman,R.A. and Gautam,S.C. (1997). Curcumin inhibits IL1 alpha and TNF-alpha induction of AP-1 and NF-kB DNA-binding activity in bone marrow stromal cells. *Hematopathology and Molecular Hematology* **11**, 49-62.

Yang,F., Lim,G.P., Begum,A.N., Ubeda,O.J., Simmons,M.R., Ambegaokar,S.S., Chen,P.P., Kayed,R., Glabe,C.G., Frautschy,S.A. and Cole,G.M. (2005). Curcumin inhibits formation of amyloid beta oligomers and fibrils, binds plaques, and reduces amyloid in vivo. *The Journal of Biological Chemistry* **280**, 5892-5901.

Yoon,B.K., Kim,D.K., Kang,Y., Kim,J.W., Shin,M.H. and Na,D.L. (2003). Hormone replacement therapy in postmenopausal women with Alzheimer's disease: a randomized, prospective study. *Fertility and Sterility* **79**, 274-280.

Yoshino,M., Haneda,M., Naruse,M., Htay,H.H., Tsubouchi,R., Qiao,S.L., Li,W.H., Murakami,K. and Yokochi,T. (2004). Prooxidant activity of curcumin: copper-dependent formation of 8-hydroxy-2'-deoxyguanosine in DNA and induction of apoptotic cell death. *Toxicology In Vitro* **18**, 783-789.

Zhang,L., Fiala,M., Cashman,J., Sayre,J., Espinosa,A., Mahanian,M., Zaghi,J., Badmaev,V., Graves,M.C., Bernard,G. and Rosenthal,M. (2006). Curcuminoids enhance amyloid-beta uptake by macrophages of Alzheimer's disease patients. *Journal of Alzheimer's Disease* **10**, 1-7.

Zhu,Y.G., Chen,X.C., Chen,Z.Z., Zeng,Y.Q., Shi,G.B., Su,Y.H. and Peng,X. (2004). Curcumin protects mitochondria from oxidative damage and attenuates apoptosis in cortical neurons. *Acta Pharmacologica Sinica* **25**, 1606-1612.